

**Control of differential
petiole growth in
*Arabidopsis thaliana***

ISBN: 978-90-393-5132-1

Layout Roy Marsman

Cover design: Bob Derksen,
Beeldwerk.nl

Printing of this thesis was financially
supported by the J.E. Jurriaanse Stichting

Control of differential petiole growth in *Arabidopsis thaliana*

Regulatie van differentiële bladsteelgroei
in *Arabidopsis thaliana*

(met een samenvatting in het Nederlands)

Proefschrift

ter verkrijging van de graad van doctor aan
de Universiteit Utrecht op gezag van de rector magnificus,
prof. dr. J.C. Stoof., ingevolge het besluit van het college voor
promoties in het openbaar te verdedigen op
woensdag 4 november 2009 des middags te 12.45 uur

door

Martijn van Zanten

geboren op 10 juni 1979 te Utrecht

Promotor:
Prof. dr. L.A.G.J. Voesenek

Co-promotoren:
Dr. A.J.M. Peeters
Dr. F.F. Millenaar

Table of contents

7	Chapter 1	General introduction: On the function and regulation of hyponastic petiole growth
23	Chapter 2	Hyponastic petiole growth in <i>Arabidopsis thaliana</i> : Photocontrol and hormonal regulation
43	Chapter 3	Hormone- and light-mediated regulation of heat-induced hyponastic petiole growth in <i>Arabidopsis thaliana</i>
67	Chapter 4	Abscisic Acid is a positive regulator of low light-induced hyponastic petiole growth in <i>Arabidopsis thaliana</i> and GCR2 controls this independent of ABA
89	Chapter 5	Isolation and characterization of genes involved in <i>Arabidopsis thaliana</i> hyponastic petiole growth
103	Chapter 6	A2-type Cyclins redundantly control hyponastic petiole growth in <i>Arabidopsis thaliana</i> seems independent from the cell cycle and endoreduplication
135	Chapter 7	Natural variation in the hyponastic petiole growth response of <i>Arabidopsis thaliana</i>
169	Chapter 8	<i>PHYTOCHROME B</i> and <i>HISTONE DEACETYLASE 6</i> control light- induced chromatin compaction and contribute to natural variation in <i>Arabidopsis</i> chromatin organization
195	Chapter 9	Low light exposure disrupts chromatin organization in <i>Arabidopsis thaliana</i>
215	Chapter 10	General discussion: On the abiotic control of hyponastic petiole growth and chromatin compaction in <i>Arabidopsis thaliana</i>
232	References	
259	Samenvatting in het Nederlands (Summary in Dutch)	
266	Nawoord	
270	Publications	
271	Curriculum Vitae	
272	Color Supplement	

General introduction

On the function and regulation of hyponastic petiole growth

Martijn van Zanten, Laurentius A.C.J. Voeselek, Anton J.M. Peeters,
Frank F. Millenaar[§]

Plant Ecophysiology, Institute of Environmental Biology, Utrecht University,
Padualaan 8, 3584 CH Utrecht, the Netherlands

Present address:

FFM: De Ruiter Seeds, Leeuwenhoekweg 52, 2660 BB Bergschenhoek,
the Netherlands.

The generalities of plant movements

Charles Darwin described in his book: 'The power of movements in plants' (1880) for the first time in a systematical manner that: 'Apparently every growing part of every plant is continuously circumnutating'. Since then, several types of plant-organ movements have been described.

Plant movements are classified in two general categories; nastic and tropic movements. Tropic movements position organs directionally to a stimulus. Examples are phototropism and gravitropism in which plants bend their stems towards the light or away from the gravitational vector, respectively (Firn & Digby, 1980; Morita & Tasaka, 2004; Lino, 2006).

The direction of a nastic movement is independent of the stimulus direction and can be classified in two major categories; i) those that are induced by an environmental stimulus and ii) movements occurring without a direct external stimulus. Movements without a direct environmental stimulus are often under control of the circadian clock e.g. rhythmic diurnal leaf movements of *Arabidopsis thaliana* (Millar *et al.*, 1995) and the nyctinastic sleep-movements in *Leguminosae* species (Coté, 1995; Kawaguchi, 2003). A clear example of a nastic response that is directly induced by an external stimulus is the collapse of *Mimosa pudica* compound leaves when touched (Coté, 1995).

A distinct type of active leaf repositioning is resource-directed, differential growth-driven, upward (re)orientation of rosette leaves called; hyponastic growth (Kang, 1979). A hyponastic response can decrease the capture of an excessively present resource, and as such minimizes damage. Hyponastic movements are for instance induced as a (photo)-protective mechanism against high light damage in *Salvia brousonetii*, *Phaseolus acutifolius* and *Phaseolus vulgaris* (Yu & Berg, 1994; Fu & Ehleringer, 1989; Abreu & Munné-Bosch, 2008). In contrast, hyponastic growth can be utilized to increase the capture of a resource that is limiting to (parts of) the plant. For example, intra-specific leaf angle variation has been found in several tree species where shaded leaves, low in the canopy, have a more vertical position than in the crown (McMillen & McClendon, 1979) and as such optimize light capture for photosynthesis.

Yet, the same nastic movement might serve both aims. For example, leaf repositioning is adopted by several species to optimize water use efficiency and on the same time serves to prevent against heat-overload (for details on leaf angle ecology see; King 1997; Falster & Westoby, 2002). Similarly, constitutive or induced steep leaf angles in rosette plants result in efficient solar light capture in the morning and winter, whereas it may prevent over-irradiation at midday and during summer.

The present knowledge on the physiological regulation of induced hyponastic movements was mainly obtained by the study of semi-aquatic *Rumex sp.*, subjected to complete submergence or ethylene treatment (Cox *et al.*, 2003; 2004). Interestingly, a typical hyponastic growth response is also induced by ethylene, spectral neutral

low light- and heat treatment in the model plant *Arabidopsis thaliana* (Figure 1.1; Millenaar *et al.*, 2005; Hopkins *et al.*, 2008; Koini *et al.*, 2009). In contrast to heat, leaf movement has also been associated with cold tolerance (Nilsen, 1991) and a prolonged decrease in growth temperature (vernalization) resulted in a modest hyponastic growth response in *Arabidopsis* (Hopkins *et al.*, 2008).

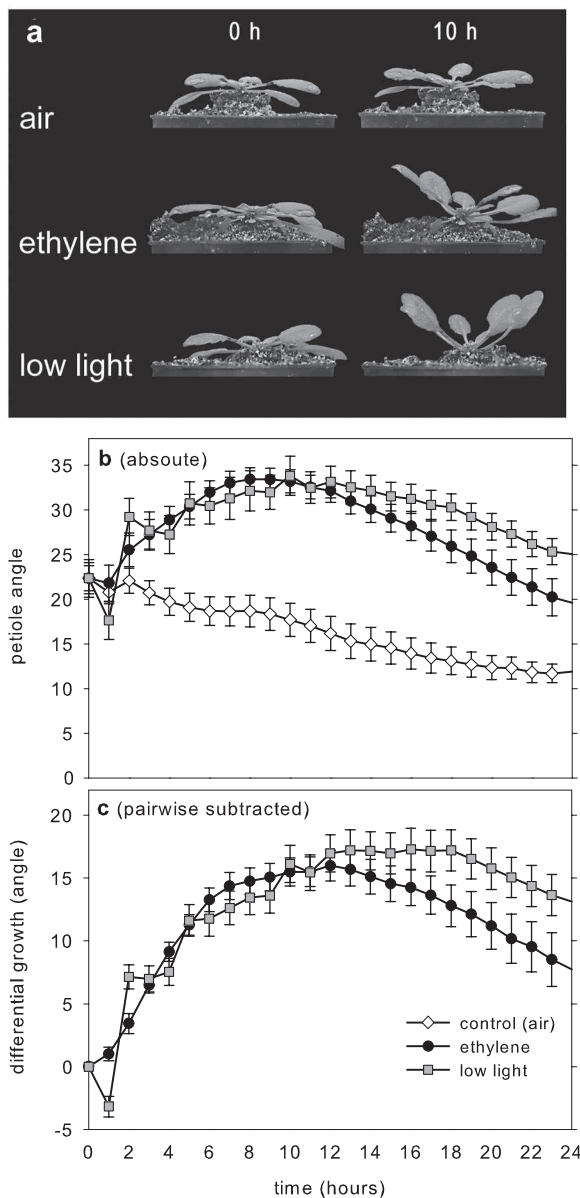


Figure 1.1: Typical hyponastic growth phenotype in *Arabidopsis thaliana* Col-0. a: (See Color Supplement for full color version of this figure). Side view of ethylene ($5 \mu\text{l l}^{-1}$) and low light ($200 \mu\text{mol m}^{-2} \text{s}^{-1}$ to $20 \mu\text{mol m}^{-2} \text{s}^{-1}$) treated plants before ($t=0$ h) and after ($t=10$ h) treatment. Plants kept in control conditions (air; $200 \mu\text{mol m}^{-2} \text{s}^{-1}$) only show modest diurnal leaf movement and leaf angles gradually decline over time due to maturation of the leaves. Note that the orange paint was applied to facilitate quantitative measurement of leaf angle kinetics as shown in panels a & b. b: absolute angles and c: pair wise subtracted petiole angles (Benschop *et al.*, 2007), corrected for diurnal petiole movement in control conditions, upon ethylene (black circles), low light (grey squares) treatment and control (air; white diamonds). Error bars represent SE; $n>12$. Growth conditions, treatments, data acquisition and analysis were as described in Millenaar *et al.* (2005).

In this chapter we summarize the existing knowledge on hyponastic growth in different plant species and discuss the biological functions. By considering the physiological, molecular and genetic regulation, we assess the differences and similarities in hyponastic growth between *Rumex palustris* and *Arabidopsis thaliana*. Finally, an outline and rationale of the research described in this thesis is provided.

Submergence- and shade-induced hyponastic growth as an escape mechanism

Hyponastic growth is triggered by complete submergence in *Rumex palustris* (Voesenek & Blom, 1989; Banga *et al.*, 1997; Cox *et al.*, 2003, Voesenek *et al.*, 2003). When these plants sense flooding, the leaves are tilted until the leaf-blade restores gas exchange by reaching the water table. If the flood water is too deep, hyponastic growth is insufficient to lead to emergence. In these cases petioles subsequently elongate. Notably, this elongation response is only initiated when a critical petiole angle of >50 degrees relative to horizontal is reached (Cox *et al.*, 2003). By this mechanism the plant 'ensures' not to spend energy on shoot elongation when leaves are too horizontal to reach the surface by elongation. This escape strategy is often accompanied by other acclimation processes including; aerenchyma formation, thinner cuticle/cell walls and thinner leaves, to facilitate optimal gas-diffusion (Voesenek *et al.*, 2006; Jackson, 2008).

Hyponastic growth in *Rumex palustris* is notably fast. The lag phase is only 1.5-3 h and the response is completed after 7 h depending on the initial angle (Cox *et al.*, 2003). Other species that show flooding-induced hyponastic growth are: *Ranunculus repens*, *Caltha palustris*, *Leontodon taraxacoides*, *Paspalum dilatatum* and *Rorripa sylvestris* (Ridge, 1987; Grimoldi *et al.*, 1999; Insausti *et al.*, 2001; Stift *et al.*, 2008). Interestingly, submergence-induced hyponastic growth was also observed in the non-wetland plant *Arabidopsis thaliana* (Millenaar *et al.*, 2005).

Hyponastic growth is also part of the shade avoidance syndrome, a suite of traits induced when plants are subjected to diminished light conditions (Smith & Whitelam, 1997; Ballaré, 1999; Vandenbussche *et al.*, 2005; Franklin *et al.*, 2008). Shade-induced leaf inclination may help to optimize photon capture by competitively overgrowing proximal neighbors.

Mechanism of hyponastic growth

Differential growth responses may result from turgor-driven swelling and shrinkage of strategic localized pulvinal motor cells, in for instance *Phaseolus vulgaris* and *Lotus japonicus* (Fu & Ehleringer, 1989; Yu & Berg, 1994; Kawaguchi, 2003; Coté, 1995). Alternatively, differential growth may be initiated by differential, directional cell elongation or differential cell proliferation.

In *R. palustris*, specific elongation of 30 basally located epidermal cells in a confined region at the abaxial side was observed after flooding (Cox *et al.*, 2003). As epidermal cell-layers are assumed to control cell-expansion, but not cell-proliferation, of underlying cell layers and thus may control differential growth (Savaldi-Goldstein 2007, 2008), it was concluded that epidermal elongation should be sufficient to drive the hyponastic response in *R. palustris*. In agreement, a mathematical model

based on this specific cell elongation fully explained the observed hyponastic growth phenotype (Cox *et al.*, 2003). Analogously, specific elongation of basal cells on the abaxial part of the petiole may be responsible for hyponastic growth in the Arabidopsis accession Columbia-0 after ethylene treatment (Figure 1.2). Overall these data suggest that hyponastic growth in Arabidopsis is the result of differential cell elongation rather than cell proliferation, although cell division persists throughout leaf growth in Arabidopsis (Tsuge *et al.*, 1996; Donnelly *et al.*, 1999) and thus cannot completely be ruled out as a factor in hyponastic growth.

Signals triggering shade avoidance-induced hyponastic growth

Typical signals perceived by plants growing in dense canopies include; reduction of the total perceived photosynthetic active radiation (PAR), low blue light photon fluence rates and reduction of the red light to far-red light ratio (R/Fr). Which specific signal or combination of signals is used to adjust leaf angles differs between species. For instance, canopy shade-induced hyponasty in *Impatiens parviflora* can be overcome by supplemental far-red light (Whitelam & Johnson, 1982) and leaf angles of maize (*Zea mays*) declined from vertical in dark to more horizontal under white-, red-, and blue light irradiation, but less to far-red light (Fellner *et al.*, 2003). Hyponasty in tobacco (*Nicotiana tabacum*) is induced by decreased blue light wavelengths, reduced R/Fr ratios and canopy shade (Pierik *et al.* 2003, 2004a, b). *Rumex palustris* shows hyponastic growth upon spectral shade and reduced R/Fr ratios, but not to low PAR levels (Pierik *et al.*, 2005).

Transferring Arabidopsis to darkness induces a quick hyponastic growth response that can be reversed by application of white- or red-, but not by blue light (Hangarter *et al.*, 1997; Mullen *et al.*, 2006). In agreement, newly appearing seedling leaves under red light have a horizontal orientation whereas superimposition of low quantities blue light led to leaf inclination (Inoue *et al.*, 2008).

The level to which Arabidopsis leaves re-adjust to their horizontal position after dark treatment depends on light-intensity (Hangarter *et al.*, 1997). *Vice versa*, spectral neutral reduction of the PAR levels (low light) stimulate a hyponastic growth response in Arabidopsis within a few hours (Figure 1.1; Millenaar *et al.*, 2005) and in agar-grown seedlings within 6 days (Vandenbussche *et al.*, 2003). Spectral shade (low blue + low R/Fr + low PAR) treatment and reduced R/Fr alone also resulted in hyponastic growth (Pierik *et al.*, 2005). In agreement Arabidopsis loss-of-function mutants lacking the red- and far-red light photoreceptor phytochrome B (phyB) are constitutively hyponastic. Additionally, phyA and phyE are implicated in the control of light dependent leaf positioning (Vandenbussche *et al.*, 2003; Mullen *et al.*, 2006).

Signals triggering submergence-induced hyponastic growth

Exchange rates of O₂ and CO₂ between plant and environment, necessary for optimal respiration and photosynthesis, are severely reduced under submerged conditions. This is because gas diffusion is ~10.000 times slower in water compared to air (Armstrong, 1979; Jackson 1985). Other gaseous compounds, such as the phytohormone ethylene accumulate in the plant due to physical entrapment (Banga

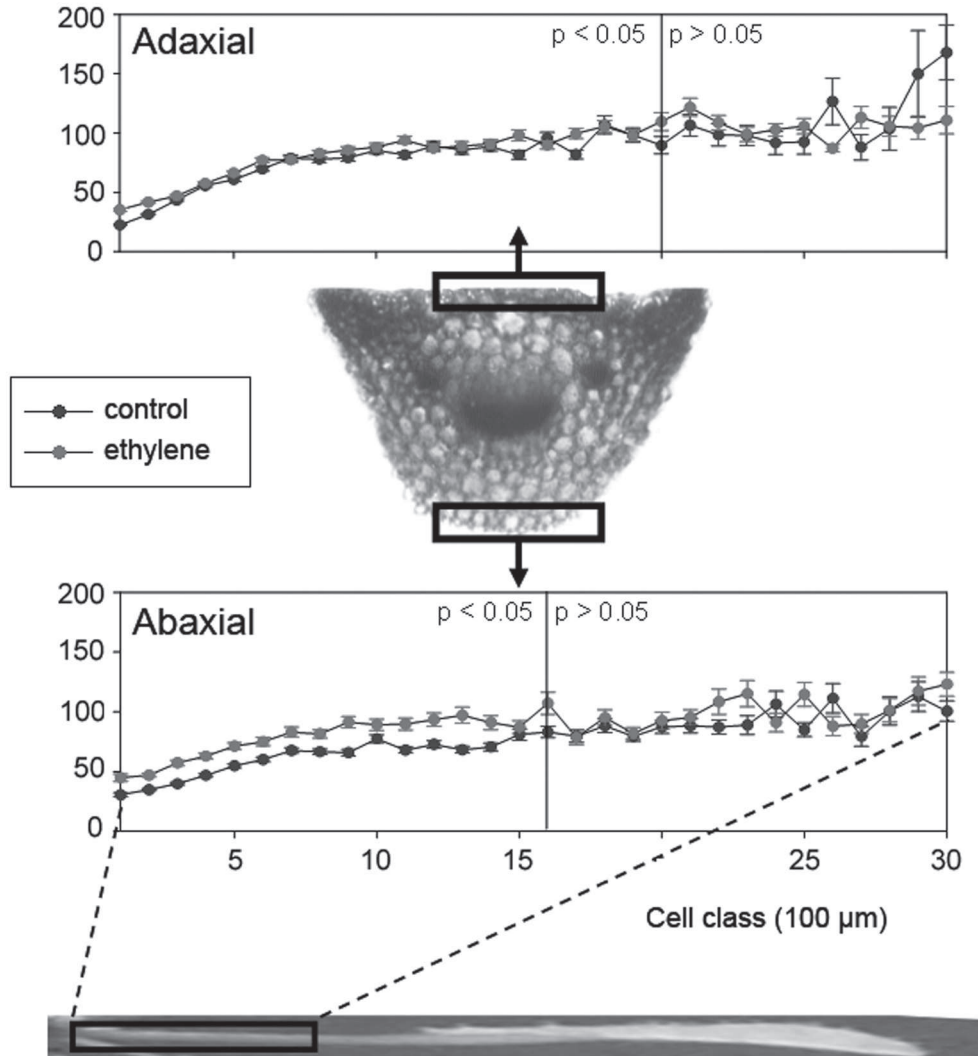


Figure 1.2: Hyponastic growth depends on cell elongation. (See Color Supplement for full color version of this figure). Average cell lengths, per class (100 μm), relative to the basal end of the petiole (see side-view of the petiole) of adaxial and abaxial epidermal Col-0 cells of 5 mm (\pm 1 mm) long petioles (stage 3.7, Boyes *et al.*, 2002). Plants were grown, treated (ethylene; red lines; 5 $\mu\text{l l}^{-1}$ and control; blue lines) as described in Millenaar *et al.* (2005). Error bars represent SE. Vertical lines in the panels mark the class that dissect the classes in majorly significant and majorly non-significant (2-tailed Student's T-test; air compared to ethylene). Epidermal cell layers were stripped from the petiole using a forceps and kept in isotonic solution when measured. A representative, Toluidine-blue stained cross section of a petiole is shown in which the used abaxial and adaxial cell layers are marked. The authors thank; Henri W. Groeneveld & Jop van Rooij for technical assistance with obtaining these data.

et al., 1996; Voeselek et al., 1993; Jackson et al., 2008). Several papers reported that this ethylene accumulation is the key trigger of the various acclimation responses in flood tolerant species including hyponastic growth and non-differential shoot elongation in *Rumex palustris* (Voeselek & Blom, 1989; Banga et al., 1997; Cox et al., 2003). In *Rumex*, a twenty-fold ($0.05 \mu\text{l l}^{-1}$ to $1 \mu\text{l l}^{-1}$) increase in ethylene levels occurs within the first hour post-submergence and eventually $8 \mu\text{l l}^{-1}$ was reached after 16 h of submergence (Banga et al., 1996). This is solely due to physical entrapment, as O_2 dependent ethylene production rates even slightly decreased under water (Voeselek et al., 1993; Banga et al., 1996; Vriezen et al., 1999).

Submergence-induced hyponasty was reduced, but not completely abolished after treatment with the ethylene receptor antagonist 1-methylcyclopropene (1-MCP), whereas 1-MCP abolished ethylene-induced hyponastic growth (Cox et al., 2004). This suggests that other signals too play a role in submergence-induced hyponastic growth. Submergence leads to a quick reduction in O_2 levels in *R. palustris* petiole tissues in stagnant waters (Rijnders et al., 2000). However, in turbid water O_2 levels could be maintained close to ambient 21% due to photosynthesis, oxygen diffusion from the surrounding waters and morphological acclimations e.g. aerenchyma formation and increased specific leaf area and thinner cuticle (Mommer et al., 2004; Voeselek et al., 2006). Yet, hypoxic conditions (reduction from 21% to 3% O_2) sensitized petioles for ethylene and consequently stimulated shoot elongation. This suggests that reduction of O_2 levels could play a role in hyponastic growth induction under certain conditions. CO_2 did not influence petiole elongation rates (Voeselek et al., 1997; Rijnders et al., 2000).

When *Arabidopsis Col-0* plants are subjected to an anoxic environment by replacing flow-trough compressed air in closed cuvettes containing the plants, by a mixture of N_2 and 0.03% CO_2 , but lacking O_2 , a modest increase in leaf angle compared to normoxic (21% O_2) treated control plants was observed (Figure 1.3a). Beyond 13 h, plants could not maintain high leaf angles and showed severe wilting (not shown). Although, the plants were able to photosynthesize and petioles consequently were likely not anoxic in these conditions. This indicates that photosynthetic derived O_2 is not sufficient for respiration demands in the used light conditions. 5% O_2 treatment resulted in a modest increase in petiole angle comparable to the above mentioned 'anoxic' treatment, but now this was maintained for at least 24 h (Figure 1.3b). In the presence of ethylene, 5% O_2 treated plants showed a strongly increased hyponastic growth response (~10 degrees more) compared to ethylene treated plants under normoxic conditions, which was maintained for at least 24 h (Figure 1.3c). These data indicate that O_2 acts additive to ethylene-induced hyponastic growth. This may be due to sensitization of petioles for ethylene under hypoxia and mirrors the observations made in *Rumex palustris* (Voeselek et al., 1997; Rijnders et al., 2000).

Although high ethylene concentrations in general inhibit growth in flooding intolerant species, including *Arabidopsis thaliana* (but see Pierik et al., 2006), treatment with high ethylene ($5 \mu\text{l l}^{-1}$) concentrations induced hyponastic growth to the same extent as complete submergence (Millenaar et al., 2005). This response

was reversible, could be prevented by pre-treatment with the ethylene receptor antagonist 1-MCP and was absent in the ethylene insensitive *etr1-1* mutant. In fact, the only notable difference in response between submergence and ethylene was a delayed induction in submerged plants, which may be explained by the time necessary for ethylene to accumulate to a physiological relevant concentration under flooded conditions.

Ethylene is also associated with (shade)induced hyponastic growth in tobacco (*Nicotiana tabacum*). Low quantities of ethylene triggered hyponasty in this species. Ethylene insensitive tobacco plants exhibited delayed hyponastic growth, stem- and petiole elongation in response to proximal neighbors and failed to induce hyponastic growth under low blue quantities (Pierik *et al.*, 2003, 2004a). A direct role of ethylene in low R/Fr-induced hyponastic growth was absent and thus the delayed ethylene-mediated hyponastic growth in canopies can be attributed to reduced blue light wavelengths (Pierik *et al.*, 2003, 2004a, b). Sorghum (*Sorghum bicolor*) phytochrome b (*phyb*) photoreceptor mutants and stimulated low R/Fr ratios led to increased ethylene production (Finlayson *et al.*, 1998) and Vandenbussche *et al.* (2003) showed that ethylene insensitive mutant seedlings were not able to induce hyponastic growth under low light intensities in agar-grown *Arabidopsis* seedlings.

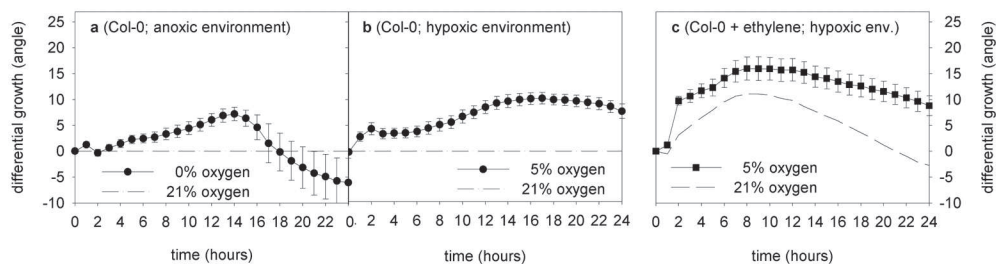


Figure 1.3: Petiole angles of hypoxia and anoxia treated Col-0 plants. Kinetics of petiole movement of **a:** anoxic (0% O₂; circles) and **b:** hypoxic plants (5% O₂; circles) relative to normoxic plants (21% O₂; dash-dotted line). **c:** ethylene (5 μ l l⁻¹) treated plants in hypoxic conditions (circles) compared to the ethylene-induced hyponastic growth response under normoxic conditions (dash-dotted line). Plants were in 200 μ mol m⁻² s⁻¹ photosynthetic active radiation. Growth conditions, treatments, data acquisition and analysis were as described in Millenaar *et al.* (2005). Error bars represent SE; n>12.

The role of hormones in the regulation of hyponastic growth

Decades of research firmly established ethylene as the primary trigger of several submergence-induced physiological and morphological acclimations in plants, including differential petiole growth and non-differential petiole elongation (Kende *et al.*, 1998; Jackson *et al.*, 2008; Voesenek *et al.*, 2003, 2006; Bailey-Serres & Voesenek, 2008). More recently, other phytohormones were described to be involved in the regulation of hyponastic growth.

Auxin and polar auxin transport are important for many differential growth responses (Harper *et al.*, 2000; Friml & Palme, 2002; Friml, 2003). Treatment of *R. palustris* with the auxin efflux carrier inhibitors; naphthylphthalamic acid (NPA) and 2,3,5-triiodobenzoic acid (TIBA), delayed the induction of submergence-induced hyponastic growth by lengthening the lag-phase of the response (Cox *et al.*, 2004). The available data on various auxin related Arabidopsis mutants are not conclusive for the role of auxin in hyponastic growth in this species, as both auxin insensitivity and enhanced auxin activity may confer constitutive hyponastic leaf angles, as is high-lighted by the following examples.

Hyponastic growth induced by decreased light intensities in agar-grown seedlings was less pronounced in several auxin related Arabidopsis mutants (Vandenbussche *et al.*, 2003). Auxin insensitive *massugu1/non-phototropic4/auxin response factor7 (msg1/nph4/arf7)* mutants were constitutively hyponastic (Watahike & Yamamoto, 1997; Harper *et al.*, 2000; Liscum & Briggs 2005; Nakamoto *et al.*, 2006) similar to plants with increased expression levels of IAA CARBOXYL METHYLTRANSFERASE1-DOMINANT (*IAMT1*), which is indicative for high levels of the potent methylated-IAA. Wild type seedlings grown in the presence of the transport inhibitor NPA show hyponastic growth, but also the repressor of *lrx1 (rol1)* mutants, having increased auxin concentrations in cotyledons, induces hyponasty (Ringli *et al.*, 2008). Heat-induced hyponastic growth was abolished in the *phytochrome interacting factor 4 (pif4)* mutant as was increased expression of the auxin marker gene *IAA29* (Koini *et al.*, 2009). A direct functional link between heat-induced hyponastic growth and auxin was however not presented.

Down-regulation of the potato (*Solanum tuberosum*) auxin related Aux/IAA protein; *StIAA2* resulted in petiole hyponasty and the effects were most severe in the shoot-apex, where auxins are primarily produced (Kloosterman *et al.*, 2006). This suggests that auxin suppresses high leaf angles in this species. In agreement, removal of auxin producing main shoots or leaflets of tomato (*Lycopersicon esculentum*) plants induced hyponastic growth in young leaves, likely due to auxin mediated loss of ethylene responses (Kazemi & Kefford *et al.*, 1974). Last, vertical leaf orientation was maintained in the presence of NPA in maize (Fellner *et al.*, 2003). The complexity of the response is underlined by the identification of the Arabidopsis constitutive hyponastic growth mutant; *hyponastic leaves1 (hyl1)* in which TIBA reduced the hyponastic phenotypes whereas NPA on the contrary exaggerates this (Lu & Fedoroff, 2000).

Gibberellin (GA) levels increased after submergence- and ethylene treatment in *Rumex palustris* and petioles showed increased GA sensitivity in respect to elongation growth (Rijnders *et al.*, 1997; Cox *et al.*, 2004). Inhibition of GA biosynthesis using paclobutrazol affected the speed of the hyponastic growth response, but not the lag-phase and maximum angle (Cox *et al.*, 2004). The time frame of GA accumulation was incompatible with the induction of hyponastic growth, which led to the conclusion that response was saturated by endogenous GA levels. Ethylene-induced hyponastic growth, but not stem- and petiole elongation in tobacco required GA, but low R/Fr-induced hyponasty did not (Pierik *et al.*, 2004b).

Abscisic acid (ABA) is a negative regulator of submergence-induced petiole elongation in *Rumex palustris* (Benschop *et al.*, 2005). Similarly, ABA treatment delayed the induction of hyponasty and maximal angles were lower than in control plants (Cox *et al.*, 2004). In accordance, pharmacologic repression of endogenous ABA levels using the ABA biosynthesis inhibitor fluridone, enhanced ethylene- and submergence-induced hyponastic growth.

Upon submergence- and ethylene treatment in *Rumex palustris*, ABA levels in petioles rapidly decline via enhanced turnover to phaseic acid and by inhibition of ABA biosynthesis via repression of the rate limiting 9-cis-epoxycarotenoid dioxygenase (NCED) genes (Benschop *et al.*, 2005). The hereby induced growth responses are likely dependent on ABA-mediated sensitization for, and increased production of, GA, as levels of GA₁ do not increase in submerged plants treated with ABA.

An analogous system was described for submergence intolerant deepwater rice (*Oryza sativa*). The elongation response in this species requires GA and submergence-induced ethylene accumulation results in enhanced GA levels and sensitization (reviewed in Kende *et al.*, 1998). ABA reduced internode elongation and within a few hours after submergence or ethylene treatment ABA levels strongly declined (Hoffmann-Benning & Kende, 1992; Kende *et al.*, 1998). Because this response could be rescued by application of GA, these authors proposed a model in which ethylene-mediated decline of ABA levels led to the sensitization and accumulation of GA during submergence, which subsequently triggers elongation growth.

Application of ABA led to reduced- and fluridone to enhanced ethylene-induced hyponastic growth in *Arabidopsis thaliana* demonstrating that, alike in *Rumex palustris*, ABA is a negative regulator of ethylene-induced hyponastic growth in this species (Benschop *et al.*, 2007). These observations were confirmed using a suite of mutants disturbed in ABA signaling and biosynthesis. Additionally, ABA suppresses the leaf angle independent of ethylene (Mullen *et al.*, 2006; Benschop *et al.*, 2007). In contrast to *R. palustris* and rice, ethylene treatment did however not trigger a reduction in ABA levels in *Arabidopsis*.

The use of *Arabidopsis* in hyponastic growth research

Hyponastic growth has been mainly studied using ecophysiological approaches and is strongly associated with hormone action. Yet, little is known of the molecular mechanisms and signaling routes from environmental perception to functional proteins.

Increasing evidence obtained using the model species *Arabidopsis thaliana*, suggests that well known integrative proteins such as PIF4 (Koini *et al.*, 2009) and endogenous developmental pathways play a role in leaf positioning. In a mutant screen for morphological mutants, four individuals with dominant expression of hyponastic leaves were isolated: *isoginchaku1-D* to *4-D* (*iso1-D* to *iso4-D*; Nakazawa *et al.*, 2003). *Iso1-D* and *Iso2-D* phenotypes are caused by the ectopic expression of ASYMMETRIC LEAVES2 (*AS2*). *Iso3-D* and *Iso4-D* ectopically express the *AS2* homologous gene; LOB DOMAIN-CONTAINING PROTEIN 36 (*LBD36*). In agreement, plants over-expressing *BLADE-ON-PETIOLE1* (*BOP1*) which enhances *AS2* and *LBD36* expression do also show hyponastic leaves (Ha *et al.*, 2007). It may not be surprising that these genes, implicated in the establishment of adaxial-abaxial polarity axes (Xu *et al.*, 2003) have constitutive leaf orientation phenotypes. However, if, and how, these genes are employed in environmentally-induced differential growth responses, including hyponastic growth, remains to be elucidated.

A study using several *Arabidopsis thaliana* accessions from different geographic origins demonstrated that accessions from Southern latitudes have more erect leaves than Northern occurring accessions, when grown under standardized conditions (Hopkins *et al.*, 2008). Considerable natural variation among accessions was also found in initial petiole- and leaf angles and in hyponastic growth response to ethylene treatment (Millenaar *et al.*, 2005).

One notable example of natural variation in induced hyponastic growth needs further attention. Millenaar *et al.* (2005) observed that the accession *Landsberg erecta* has a moderate response to ethylene and submergence when compared to *Col-0*, whereas both accessions had a strong response to low light. This suggests that *Ler* contains the genetic components required for hyponastic growth, but is less able to use ethylene as a signal to induce it (Millenaar *et al.*, 2005).

Indications of the nature of the missing connection between ethylene and hyponastic growth came from a study by Benschop *et al.* (2007). We demonstrated that unlike in *Col-0*, both ABA and fluridone did not affect ethylene-induced hyponastic growth in *Ler* (Figure 1.4). Moreover, ABA insensitive mutants in the *Ler* genetic background restored the responsiveness to ethylene. Thus, although *Ler* is insensitive to ABA in terms of ethylene-induced hyponastic growth; ABA downstream components could relieve this insensitivity. This suggests that *Ler* and *Col-0* are possibly polymorphic in ABA signaling towards induction of hyponastic growth. The identity of this segregating allele between *Ler* and *Col-0* is however not yet clear.

Similar natural genetic variation among accessions exists for many other traits and can be used to isolate and study the molecular components involved (Koornneef *et al.*, 2004; Maloof, 2003). An ongoing Quantitative Trait Loci (QTL) study in our lab, using two Recombinant Inbred Line (RIL) populations (*Col* x *Ler* and Cape Verde Islands-0 x *Ler*), revealed several potential candidate loci for ethylene- and low light-induced hyponastic growth (Snoek & Peeters *et al.*, unpublished). Interestingly,

several QTLs for ethylene and low light-induced hyponastic growth co-localized between treatments and are present in both RIL populations used. This indicates that hyponastic growth is a complex trait and that functional components downstream of ethylene and low light towards hyponastic growth may be shared (Figure 1.4). This hypothesis is validated by the notion that application of low light and ethylene induce hyponasty with highly similar kinetics (Figure 1.1) and that application together does not lead to an exaggerated response (Millenaar *et al.*, 2005). In addition, the expression of 2208 genes changed (998 up; 1118 down) significantly after addition of ethylene and 2354 (1236 up; 1210 down) genes upon low light treatment (Millenaar *et al.*, 2006; Pierik *et al.*, 2005). Combination of the data sets revealed that 453 (165 up; 288 down) genes are regulated by both treatments. This means that 90% of all transcripts that changed upon ethylene or low light are treatment-specific, or alternatively, are not related to differential growth. The ~10% genes in common may be part of an integrated downstream signaling route towards hyponastic growth.

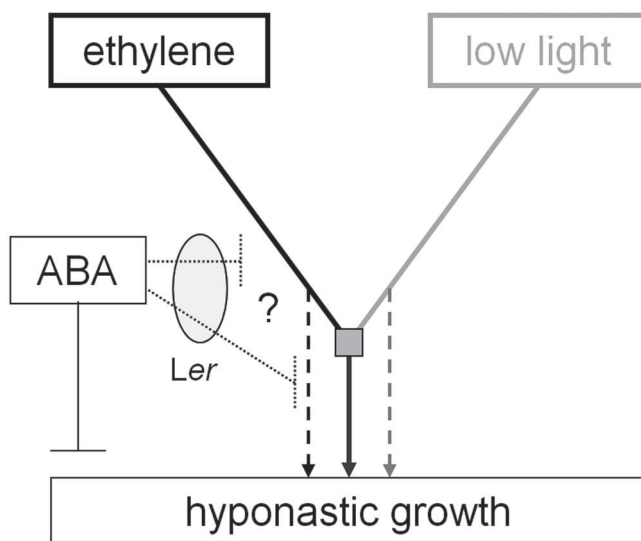


Figure 1.4: Proposed model for hyponastic growth in *Arabidopsis thaliana*. Model based on the observations described in Millenaar *et al.* (2005), Pierik *et al.* (2005) and Benschop *et al.* (2007). Ethylene (black) and low light (grey) induces hyponastic growth with similar kinetics (Figure 1.1), hypothetically by interaction via a shared set of downstream components (square box). It can however not be excluded that ethylene and low light affect petiole angles via unique components (dotted lines). Abscisic acid negatively influences petiole angles independently of ethylene and by inhibiting ethylene-induced hyponastic growth either in the unique ethylene part of the signal transduction, or downstream the putative integration point (dotted lines). A block in ABA mediated repression of ethylene-induced hyponastic growth is present in *Ler* (oval).

Outline thesis

In summary, the data described above indicates that *Arabidopsis thaliana* is a suitable organism to study the genetic and molecular regulation of hyponastic growth responses induced by stimuli from the abiotic environment. Therefore, the available tools, including mutant analyses, forward- and reverse genetics, transcriptomics and quantitative genetics can be employed to investigate aspects of hyponastic growth in detail, using this model species.

In the first part of this thesis (Chapter 1-4) we present the results of several molecular, genetic and physiological approaches with the aim to gain comprehensive understanding of the regulation and mechanisms of the hyponastic growth responses induced by ethylene, low light and heat-treatment in *Arabidopsis thaliana*. The second part describes two unbiased approaches; a forward genetic mutant screen and QTL analysis, to identify novel pathways- and genes controlling hyponastic growth (Chapter 5-7).

In the last part of this work (Chapter 8, 9) we describe that light intensity and light quality controls compaction of nuclear chromatin in *Arabidopsis thaliana* and we present evidence that this is mediated by photoreceptor proteins (phyB, cry2) and HISTONE DEACETYLASE 6.

Chapter 2 describes the low light intensity-induced hyponastic growth response in detail and components of the signal transduction are characterized. Light-spectrum manipulations and mutant analyses indicate that specifically blue light wavelengths can affect petiole movements. Fast induction of hyponasty in low light conditions involves functional cryptochrome 1 (cry1) and cry2, phyA and phyB photoreceptor proteins. Moreover, we show that photosynthesis-derived signals can also induce differential growth. Our experiments demonstrate that low light-induced hyponastic growth is independent of ethylene signaling but requires intact auxin perception and polar auxin transport for response amplitude and maintenance of a high petiole angle. Ethylene-induced hyponastic growth on the contrary, is independent of auxin and polar auxin transport. We conclude that, at least upstream, ethylene and low light signaling pathways towards induction of hyponastic growth are parallel.

Chapter 3 introduces heat (sudden increase in temperature from 20°C to 38°C) as hyponastic growth- inducing factor in *Arabidopsis thaliana*. The kinetics of heat-induced hyponastic growth shows strong resemblance to ethylene- and low light-induced hyponasty. Based on a study of natural variation among accessions, we propose that heat-induced hyponastic growth is likely an adaptive response to optimize photosynthesis. Using pharmacological assays, transcript analysis and mutant analyses we demonstrate that ethylene and the photoreceptor protein phyB are negative regulators of the magnitude of heat-induced hyponasty and that low light, phyA, auxin, auxin transport and ABA are positive regulators of the magnitude of heat-induced hyponastic growth.

Chapter 4 specifically deals with the ABA mediated regulation of low light-induced hyponastic growth. We demonstrate that ABA acts as a positive modulator of low light-induced hyponastic growth, independent of ethylene action. Both low light and ethylene induce transcription of the ABA perception associated protein GPA1, and loss-of-function mutations in this gene repress low light- and ethylene-induced hyponastic growth. Moreover, our results indicate that the reported GPA1 associated GCR2 and the GCR2 LIKE PROTEINS (GCL1 and GLC2) act redundantly as positive regulators of low light-induced hyponasty, independent of ABA action.

Chapter 5 focuses on the methods and general results of a forward genetic approach, employed to identify novel pathways- and genes controlling hyponastic growth. Several activation-tagged lines, which were isolated by screening an 35S CaMV constitutive-promoter-tagged population on initial petiole angles and ethylene-, low light- and heat-induced hyponastic growth, are described and phenotyped. The phenotype of several lines supports the notion that ethylene-, low light- and heat signaling pathways may integrate to induce hyponastic growth.

Chapter 6 contains the detailed analysis of one of the isolated activation tagged lines called; *SEE1-1D*. Our data demonstrates that overexpression of the cell-cycle gene *CYCLINA2;1* explains the enhanced *SEE1-1D* hyponastic growth phenotype to all stimuli, and that the A2-type Cyclin family redundantly controls hyponastic growth. Surprisingly, the control of hyponastic growth is seemingly independent from the proposed roles for A2-type Cyclins in cell cycle-progression and control endoreduplication. Both ethylene and ABA spatially restrict *CYCA2;1* activity to basal petiole tissues, away from more distal tissues. In this way, maintenance of A2-type Cyclin mediated growth in basal tissues and repression of growth in more distal tissues, eventually may result in a differential growth phenotype. We propose a mechanistic model in which Inhibitor of Cyclin-Dependent Kinases/Kip-related proteins (ICK/KRP) proteins function as integrator of ABA and ethylene signals to control hyponastic growth, by inhibition of A2-type Cyclin-Cyclin Dependent Kinases (CDK) complex(es).

Chapter 7 describes natural variation in the hyponastic growth response as induced by ethylene, low light and heat. Assessing hyponasty in 138 natural occurring accessions revealed that the response to these stimuli is probably controlled by a downstream integrated signaling route and that constitutive variation in petiole angles does not interfere with the ability to induce a hyponastic growth response. Utilization of this natural variation in a Quantitative Trait Loci approach revealed several loci involved in controlling petiole angles and hyponastic growth. Subsequent mutant analysis, complementation analysis of both induced mutants in different backgrounds and in naturally occurring mutant accessions, showed that the leucine-rich repeat receptor-like Ser/Thr kinase gene *ERECTA* as an important factor in the control of low light- and ethylene-induced hyponastic growth.

Chapter 8 portrays a novel approach to study plasticity in chromatin organization. By combining microscopic examination, quantitative genetics and analysis of environmental parameters, we show that the level of chromatin compaction among natural *Arabidopsis thaliana* accessions correlates with latitude of origin and depends on local light intensity. Our study provides evidence that the photoreceptor phytochrome B (phyB) and the histone modifier HISTONE DEACETYLASE 6 (HDA6) are positive regulators of global chromatin organization in a light-dependent manner. In addition, HDA6 specifically controls light-mediated chromatin compaction of the Nucleolar Organizing Regions (NORs). We propose that the observed light-controlled plasticity of chromatin plays a role in acclimation and survival of plants in their natural environment.

Chapter 9 demonstrates that reduction of light intensity reversibly induces chromatin de-compaction and that natural variation among *Arabidopsis* accessions exists in the rate of this response. In addition to spectral neutral light, also spectral quality (low blue, low red-to-far red ratio) control chromatin compaction. Data acquired by mutant- and ectopic gene expression analysis, studying natural variation among accessions and protein abundance analysis, all point to cryptochrome 2 as a positive regulator of low light-induced chromatin de-compaction. phytochrome B has contrasting effects on the control of light mediated chromatin compaction between accessions Columbia-0 and Landsberg *erecta* and is a positive regulator of cry2 protein levels.

Chapter 10 provides a synthesis of the key findings and proposes a generic model of induced hyponastic growth in *Arabidopsis thaliana*, as well as perspectives on what future directions to take to elucidate the genetic control of differential petiole growth and light controlled chromatin compaction.

Hyponastic petiole growth in *Arabidopsis thaliana*: Photocontrol and hormonal regulation

Frank F. Millenaar*[§], Martijn van Zanten*, Marjolein C.H. Cox,
Ronald Pierik, Laurentius A.C.J. Voeselek, Anton J.M. Peeters

Plant Ecophysiology, Institute of Environmental Biology, Utrecht University,
Padualaan 8, 3584 CH Utrecht, the Netherlands

* These authors contributed equally to the work

Present address:

FFM: De Ruiter Seeds, Leeuwenhoekweg 52, 2660 BB Bergschenhoek,
the Netherlands.

Adapted from:

- Millenaar FF*, van Zanten M*, Cox MCH, Pierik R, Voeselek LACJ, Peeters AJM. (2009). Differential petiole growth in *Arabidopsis thaliana*: Photocontrol and hormonal regulation. *New Phytologist*. 184: 141-152.
- Van Zanten M, Millenaar FF, Cox MCH, Pierik R, Voeselek LACJ, Peeters AJM. (2009). Auxin perception and polar auxin transport are not always a prerequisite for differential growth. *Plant Signalling & Behaviour*. 4, (9).

Abstract

Environmental challenges such as low light intensity induce a differential growth-driven upward leaf movement (hyponastic growth) in *Arabidopsis thaliana*. However, little is known about the physiological regulation of this response. Here, we studied how low light is perceived and translated into a differential growth response in *Arabidopsis*. We used mutants defective in light, ethylene and auxin signaling and polar auxin transport, as well as chemical inhibitors to analyze the mechanisms of low light-induced differential growth. Our data indicate that photosynthesis-derived signals and blue light-wavelengths affect petiole movements and that rapid induction of hyponasty by low light involves functional cryptochrome 1 and -2, phytochrome A and phytochrome B photoreceptor proteins. The low light response is independent of ethylene signaling. Auxin and polar auxin transport, on the other hand, play a role in low light-induced differential petiole growth but not in ethylene-induced hyponastic growth. We conclude that low light-induced differential petiole growth requires blue light, auxin signaling and polar auxin transport and is at least in part, genetically separate from well characterized ethylene-induced differential growth.

Introduction

Plants must respond rapidly and appropriately to changes in their environment. Among other traits, this can involve reorientation of the growth direction to optimize the position of plant organs relative to limiting resources (Ball, 1969; Kang, 1979). A clear example is the phototropic response in which differential growth directs plant organs towards the light (Firn & Digby, 1980; Hangarter, 1997; Ahmad *et al.*, 1998; Friml *et al.*, 2002). Re-adjustment of leaves to a more vertical position during shade and submergence escape directs leaf growth towards the limiting resources light and air, respectively (Ballaré, 1999; Cox *et al.*, 2003; Pierik *et al.*, 2004b; Millenaar *et al.*, 2005). Often, two responses can be distinguished i) an upward movement (inclination) of petioles, called hyponasty, obtained through differential growth; and ii) enhanced elongation of petioles and/or stems (Voisenek & Blom, 1989; Cox *et al.*, 2003; Pierik *et al.*, 2003, 2004b).

The gaseous plant hormone ethylene is the key trigger for submergence-induced hyponasty in *Arabidopsis thaliana* (Millenaar *et al.*, 2005). Other signals such as vegetation-derived low red/far-red ratio (Pierik *et al.*, 2005), low light intensity (Millenaar *et al.*, 2005; Mullen *et al.*, 2006) and elevated temperatures (Koini *et al.*, 2009) also induce hyponastic growth in *Arabidopsis*. It was shown that ethylene interacts with light quality cues to induce shade avoidance responses, including hyponasty, in tobacco (*Nicotiana tabacum*) (Pierik *et al.*, 2004a). More recently, phytochrome-mediated petiole elongation in *Arabidopsis* was shown to rely on ethylene as well as the phytohormone auxin, and ethylene-induced hypocotyl elongation was suggested to occur through interaction with auxin (Pierik *et al.*, 2009). Auxin and its polar transport

(PAT) are fundamental players in the developmental program, but are also typically associated with differential growth (Lehman *et al.*, 1996; Harper *et al.*, 2000; Friml & Palme 2002; Friml, 2003), and shade avoidance responses (Morelli & Ruberti, 2000; Tao *et al.*, 2008; Pierik *et al.*, 2009). More specifically, auxin plays a role in submergence-induced hyponastic growth in *Rumex palustris* (Cox *et al.*, 2004) and in the regulation of leaf movement in agar-grown *Arabidopsis* seedlings (Vandenbussche *et al.*, 2003). However, it is unknown how low light induces differential growth responses and if this response requires auxin. In the present study, we aim to understand how low light is perceived and how this signal is translated into a hyponastic growth response.

We show that low blue light-photon fluence rate is an important component in low light to establish a rapid induction of hyponastic petiole growth. Cryptochrome 1 (cry1), cry2, phytochrome A (phyA) and phyB are the photoreceptor proteins involved in detecting reduced light intensity. In addition, photosynthesis-derived signals can also induce differential growth. Using mutant analyses, ethylene production measurements and transcript analysis, we demonstrate that low light-induced differential petiole growth does not require ethylene perception and as such is, at least in part, genetically separate from the submergence signaling route towards hyponastic growth. We, furthermore, provide evidence that auxin and polar auxin transport are required to induce a maximal hyponastic growth response and to maintain elevated petiole angles to low light treatment, but does not seem to be a component of ethylene-induced hyponastic growth.

Results

Characterization of low light-induced hyponastic growth

To characterize the *Arabidopsis thaliana* hyponastic growth response to low light conditions, we studied the dose-response relationship between light intensity and petiole angles in Col-0 and *Ler*. Petiole angles decreased gradually with increasing light intensities from 5 to 200 $\mu\text{mol m}^{-2} \text{s}^{-1}$ photosynthetic active radiation (Figure 2.1a). Figure 2.1b demonstrates the kinetics of low light (20 $\mu\text{mol m}^{-2} \text{s}^{-1}$) induced hyponastic growth. In both Col-0 and *Ler* the response starts within 1 h, the angle change per unit time is maximal after approximately 3 h and maximal angles are reached around 10 h (Col-0) or 16 h (*Ler*).

To obtain insight into how low light is sensed, the sensitivity of petioles for different wavelength regions was studied in Col-0. If low blue- or low red-light is important for detection of low light intensity, then low light that is relatively enriched in blue or red should prevent hyponastic growth. The photon fluence rates of blue- (400-500 nm) and red-light (600-700 nm) during the enrichment experiment were made comparable to control light treatment, while total light intensity (400-700 nm) and red/far-red ratio (655-665 nm/725-735 nm) were kept similar (Figure 2.1c, Supporting Information Figure S2.1). After 6 h in blue light-enriched low light, the observed petiole angles (-4.1 ± 1.7 degrees), were significantly ($p < 0.05$) lower than in control

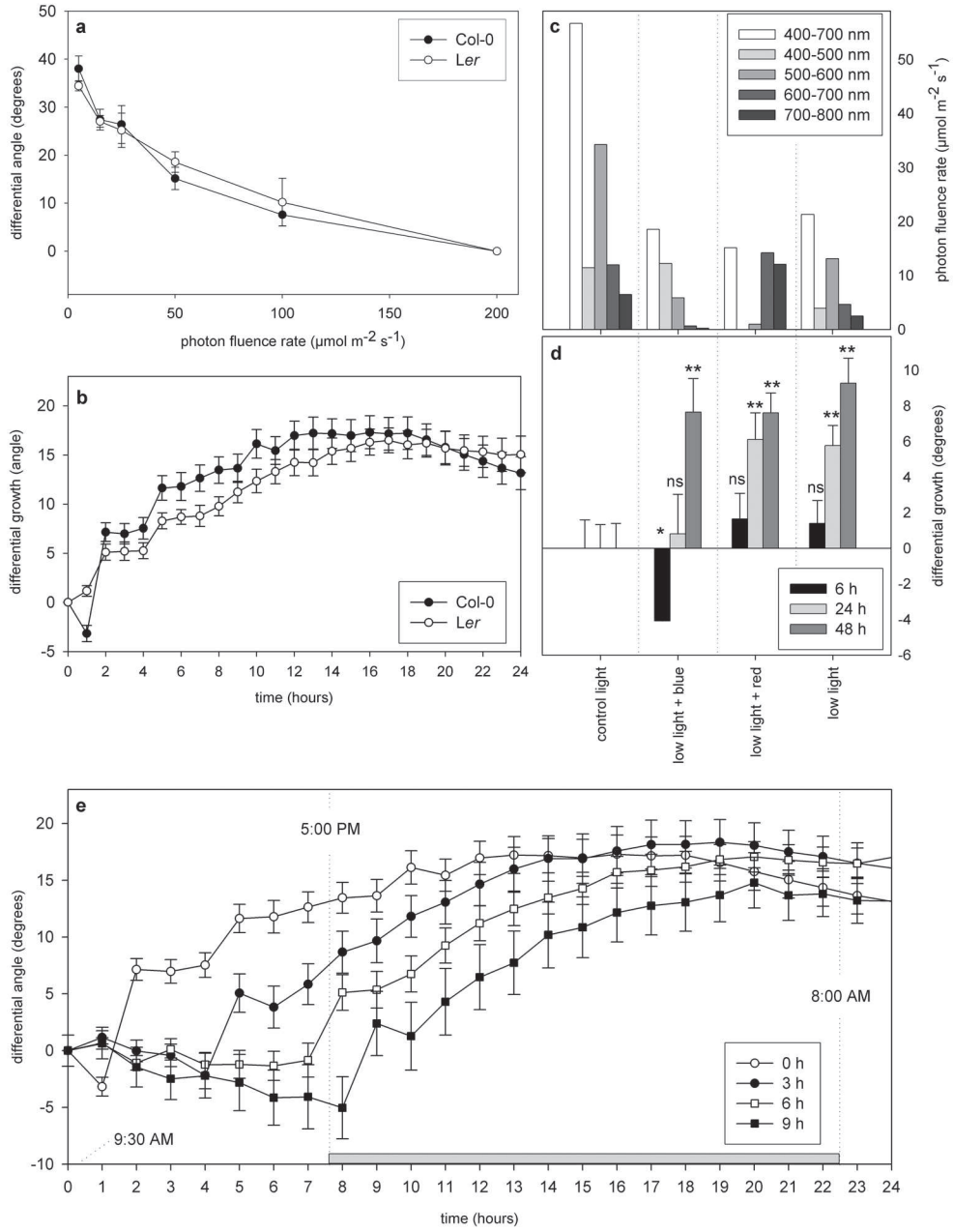


Figure 2.1: Characterization of hyponastic growth upon low light exposure. (See Color Supplement for full color version of this figure) **a:** Photon fluence rate dose-response curve of the accessions Col-0 (closed circles) and *Ler* (open circles), grown at $200 \mu\text{mol m}^{-2} \text{s}^{-1}$ and then treated with the indicated light conditions for 24 h ($n \geq 5$, error bars represent SE). **b:** Effect of low light exposure ($20 \mu\text{mol m}^{-2} \text{s}^{-1}$) on Col-0 (closed circles) and *Ler* (open circles) petiole angle. Depicted angles are pair wise subtracted, which is the difference between the angles of treated and control plants for each time point; $n \geq 8$, error bars represent SE. **c,d:** Effect of enrichment in different wavelength regions in addition to low light treatment, on Col-0 petiole angles. Plants were placed in $60 \mu\text{mol m}^{-2} \text{s}^{-1}$ (control light), $20 \mu\text{mol m}^{-2} \text{s}^{-1}$ (low light), low light enriched in blue (low light + blue) or low light enriched in red (low light + red). The total light intensity ($\mu\text{mol m}^{-2} \text{s}^{-1}$; 400-700 nm) and sum of intensities per nm in various wavelength regions in blue (400-500 nm), green (500-600 nm), red (600-700 nm) and far-red (700-800 nm) are plotted in panel c. The full spectrum is shown in Figure S2.1. Plotted in panel d: are the differential responses. * $p < 0.05$; ** $p < 0.01$, 2-tailed Student's T-test, testing control light against (enriched) low light for each time point. $n \geq 8$, error bars represent SE. **e:** Effect of exposure to low light ($200 \mu\text{mol m}^{-2} \text{s}^{-1}$ to $20 \mu\text{mol m}^{-2} \text{s}^{-1}$) started at different times on the day on Col-0 petiole angles. Note that $t=0$ is 1.5h after start of the photoperiod and corresponds to 9:30 AM. The time of subjective night ($t=9$ h; 5:00 PM) and start of the photoperiod ($t=22.5$ h; 8:00 AM) are depicted as vertical dotted lines. The subjective night period is indicated by a grey bar. Shown angles are pair wise subtracted; $n \geq 12$, error bars represent SE

light conditions (Figure 2.1d). In contrast, red light enrichment did not prevent hyponasty in low light. After prolonged treatment (24 h and 48 h) all low light treatments had induced hyponastic growth, including the one enriched in blue light. Figure 2.1e shows that the time-of-induction of low light does not determine the ability to respond. Even when low light was administered 1.5 h after the start of the subjective night period ($t = 9$ h) a distinct response with normal kinetics, was observed.

Cry1, cry2, phyA and phyB sense low light intensity

To test how low light is perceived, we analyzed photoreceptor mutants. Arabidopsis has four known blue-light photoreceptors: cryptochrome 1 (*cry1*), *cry2*, phototropin 1 (*phot1*) and *phot2* (Lin, 2002 and references therein). The *phot1* and *phot2* mutants and the *phot1 phot2* double mutant showed low light-induced hyponastic growth response similar to wild type, suggesting that phototropins are not involved in this response (Figure 2.2a-c). Also, the *cry1/hy4* and *cry2/fha1* mutants displayed a response similar to wild type (Figure 2.2d, e). Interestingly, the *cry1 cry2* double mutant showed a reduced response to low light (Figure 2.2f), suggesting that cryptochromes are redundantly involved in low light-induced hyponastic growth.

Phytochromes absorb blue, red and far-red light and the *phyA* and *phyB* mutants showed delayed low light-induced hyponastic growth (Figure 2.2g, h). To test involvement of other phytochromes, we examined the phytochrome mutant *long hypocotyl2/genome uncoupled3* that contains reduced levels of phyA-E. The delay in *hy2* for low light-induced hyponastic growth (Figure 2.2i) was comparable to the *phyA* and *phyB* mutants, suggesting that phyC-E are not redundant to phyA and phyB in low light-induced hyponastic growth.

Double combinations of *phyA* with *cry1* or *cry2*, and the *phyA cry1 cry2* triple mutant showed delayed responses similar to *phyA* single or *cry1 cry2* double (Figure 2.2j-l). This suggests that phyA cannot substitute for *cry1* and/or *cry2* in sensing low light intensities.

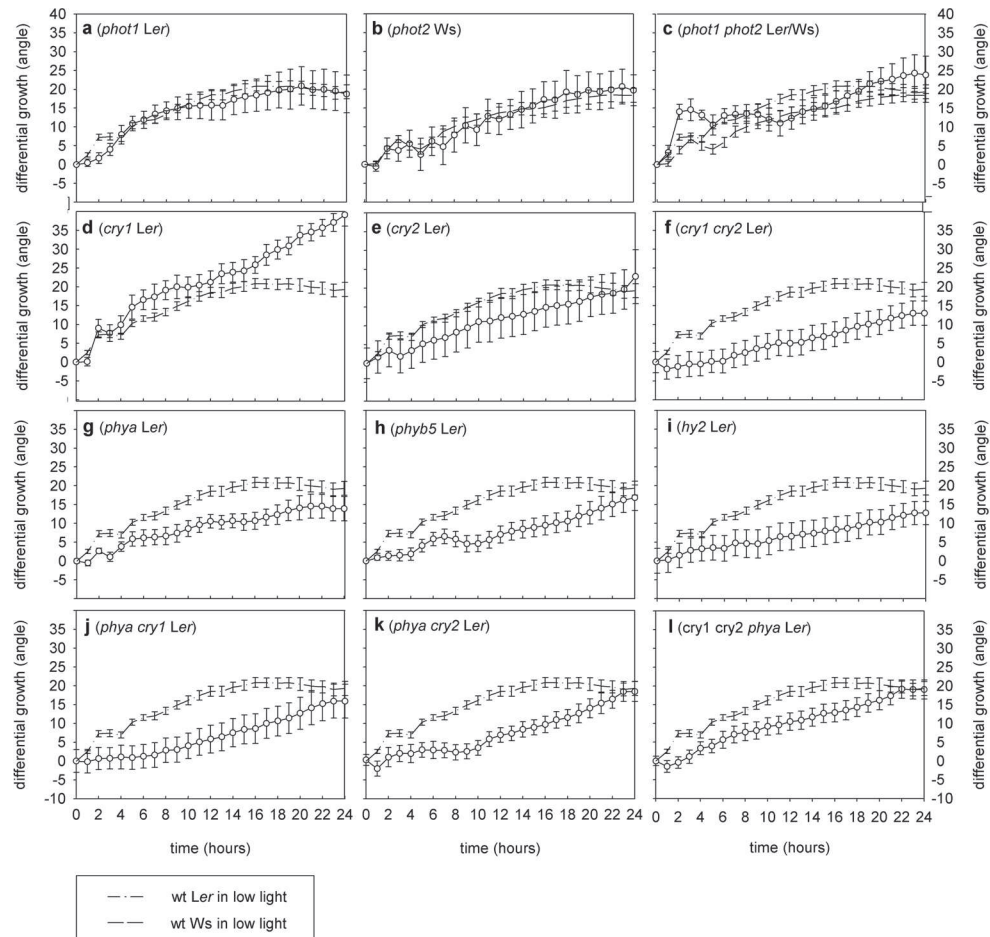


Figure 2.2: Effect of exposure to low light ($20 \mu\text{mol m}^{-2} \text{s}^{-1}$) on petiole angles of *Arabidopsis* light signaling mutants. a-l: Light signaling mutants (open circles), compared to Col-0 wild type response to low light (lines). See legend Figure 2.1 for details; error bars represent SE; $n \geq 12$

After 24 h, all mutants tested responded to low light in a similar manner as wild type. Consequently, there may be additional, unrelated signaling pathways involved in low light-induced differential growth. The photosynthetic machinery can generate light intensity-dependent signals that influence nuclear gene expression. We tested involvement by inhibiting photosynthetic electron transport with 3-(3,4-dichlorophenyl)-1,1-dimethylurea (DCMU). This treatment induced hyponastic growth already in control light conditions (Figure 2.3a). The *executer1* fluorescent (*ex1 flu*) double mutant, disturbed in signaling from the chloroplasts to the nucleus,

showed a clear delay of hyponastic growth in low light (Figure 2.3b). Together, these data suggests that signals derived from the photosynthetic machinery can influence hyponastic growth.

Ethylene perception is not required for low light-induced differential growth

Ethylene induces a hyponastic growth response of which the kinetics are remarkably similar with those for low light-induced hyponasty (Millenaar *et al.*, 2005). It would therefore be well possible that ethylene is a downstream element in low light-induced hyponastic growth.

To test this, we studied low light-induced hyponastic growth in the ethylene insensitive mutants *ethylene insensitive 2 (ein2)*, *ethylene response1-4 (etr1-4)*, *ein4-1* and the constitutive ethylene response mutant; *constitutive triple response (ctr1)*. As expected, none of the tested ethylene insensitive lines showed ethylene-induced hyponastic growth (Figure 2.4a-c). This was also true for *ctr1* (Figure 2.4d) which probably can be explained by saturation of the signal transduction route in this mutant. In sharp contrast to the repressed ethylene-induced response, all lines showed a wild type response to low light (Figure 2.4e-h).

Moreover, ethylene production, measured online using photo acoustic spectroscopy did not significantly change upon low light exposure (Figure 2.4i).

Real-Time RT-PCR experiments showed that the expression of *ACC-oxidase (At1g05010)* and *ETHYLENE RESPONSE SENSOR2 (ERS2)*, serving as ethylene marker genes (Wilkinson *et al.*, 1995; Hua *et al.*, 1998; Vriezen *et al.*, 1999), were as expected strongly induced by ethylene treatment (Figure 2.4j, k), but not at all by low light treatment. The same conclusion could be drawn based on a broader set of ethylene biosynthesis and signal transduction marker genes (Figure S2.2). Together, these data indicate that ethylene is not an essential component in the regulation of low light-induced hyponasty.

Auxin perception and polar auxin transport are required for low light-induced, but not for ethylene-induced hyponastic growth

To test the involvement of auxin transport in low light- and ethylene-induced hyponastic growth, we applied the polar auxin transport (PAT) inhibitor 2,3,5-triiodobenzoic acid (TIBA) to Col-0. Interestingly, inhibitory effects of TIBA on the magnitude of hyponastic growth and on the maintenance (continuation of the high leaf angle after the maximum response magnitude, up to 24 h) were observed in low light (Figure 2.5a). Similarly, albeit stronger, inhibition of low light-induced hyponastic growth was observed after treatment with the auxin transport inhibitor naphthylphthalamic acid (NPA; data not shown). These effects were not due to toxicity of the used chemicals and solvents, as the same treatment had no effect on ethylene-induced hyponastic growth (Figure 2.5b and data not shown).

To further specify the involvement of auxin in low light- and ethylene-induced hyponastic growth, we subsequently tested mutants with disturbed auxin perception or PAT. The TRANSPORT INHIBITOR RESPONSE1 (TIR1) protein is an auxin receptor (Dharmasiri *et al.*, 2005a; Kepinski & Leyser, 2005). The *tir1* mutant

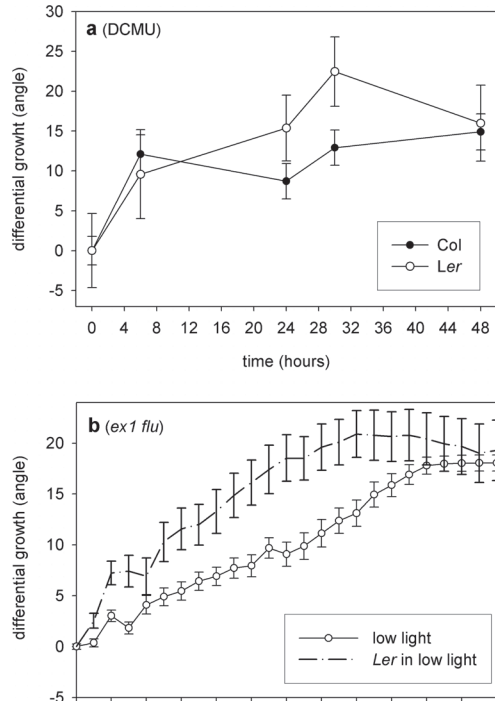
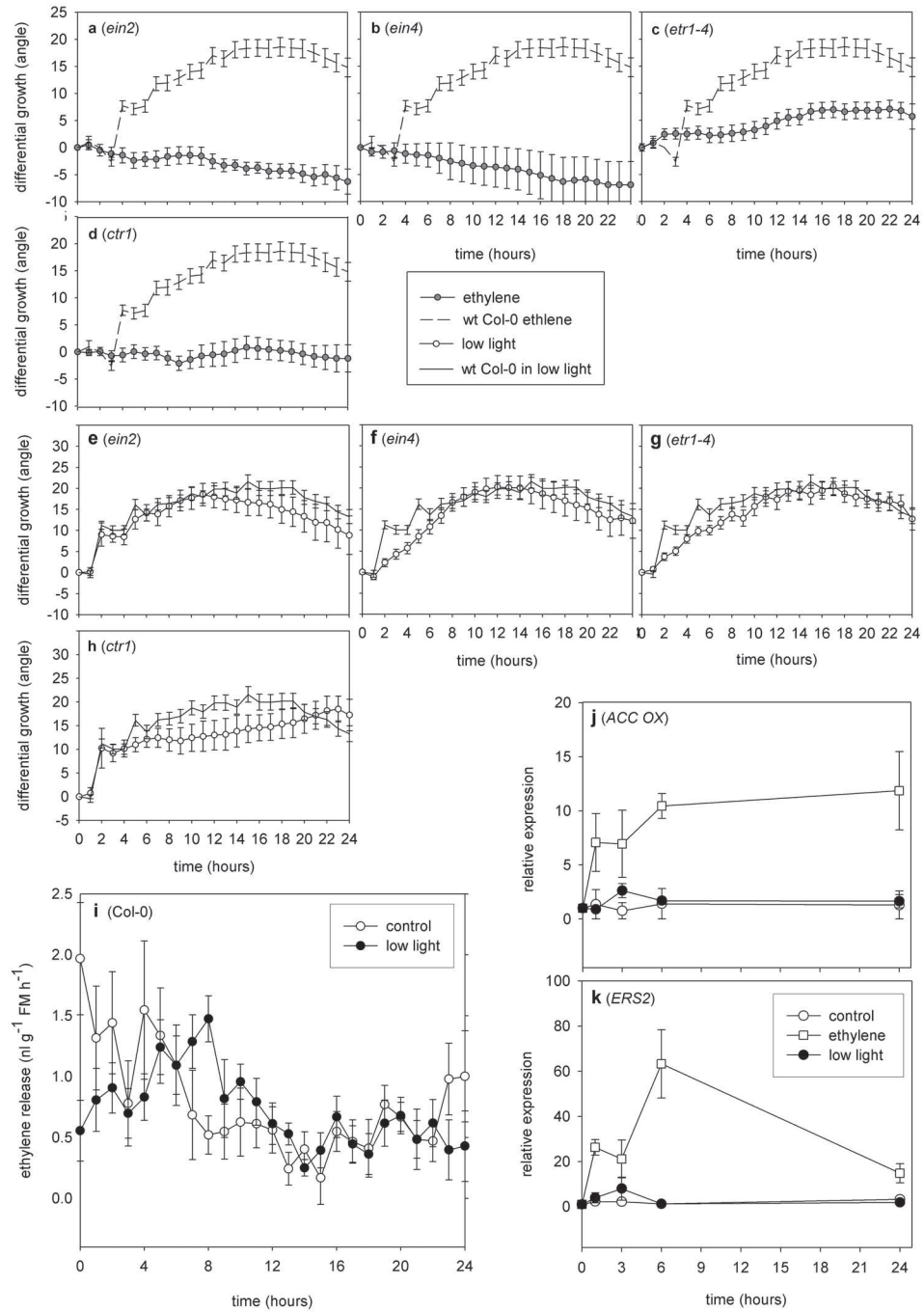


Figure 2.3: Involvement of photosynthesis related signals in hyponastic growth. a: Effect of addition of 10 μM 3-(3,4-dichlorophenyl)-1,1-dimethylurea (DCMU) to Col-0 (closed circles) and Ler (open circles) plants in control light ($200 \mu\text{mol m}^{-2} \text{s}^{-1}$) conditions ($n \geq 5$; error bars represent SE). b: Effect of low light exposure ($20 \mu\text{mol m}^{-2} \text{s}^{-1}$) on petiole angles of the *ex1 flu* mutant (open circles) in a Ler background (line). See legend Figure 2.1 for details; error bars represent SE; $n \geq 12$.

Figure 2.4: Ethylene involvement in low light-induced hyponasty. a-d: Effect of exposure to ethylene ($5 \mu\text{l l}^{-1}$; grey closed circles) and e-i: effect of exposure to low light ($20 \mu\text{mol m}^{-2} \text{s}^{-1}$; open circles) on petiole angles of Arabidopsis ethylene signaling mutants compared to Col-0 wild type response to these stimuli (lines). See legend Figure 2.1 for details; error bars represent SE; $n \geq 12$. i: Ethylene release from Col-0 plants exposed to control (open circles) or low light (closed circles) conditions. $n \geq 3$; error bars represent SE). Real-Time Reverse Transcriptase-PCR of j: *ACO4* (At1g05010) and k: *ERS2* (At1g04310) to ethylene treatment (open squares), low light treatment (closed circles) and control conditions (kept in air and normal light; open circles) in Arabidopsis Col-0 petiole tissue. Expression values for both genes are normalized to 1 at $t=0$ h. $n \geq 3$; error bars represent SE.



in Col showed a comparable low light response as did Col-0 plants treated with TIBA i.e. reduced maximal angle, and angle maintenance defects (Figure 2.5c). Five close *TIR1* homologous F-box proteins are named *AFB1-5*. The *tir1 afb1 afb2 afb3* quadruple mutant had a significantly lower maximal angle and maintenance defects were visible (Figure 2.5d), similar to *tir1*.

The *tir3-1* mutant in Col, in which auxin transport is hampered, and mutants in the auxin efflux-associated proteins, *pin-formed3* (*pin3*) and *pin7* all showed angle maintenance defects similar to TIBA-treated Col plants and *tir1*. *Pin3* and *pin7*, but not *tir3*, were also affected in their maximum angle (Figure 2.5e-g). In agreement with the TIBA treatment (Figure 2.5b), the above mentioned mutants did not have an altered ethylene-induced hyponastic growth (Figure 2.5h-l).

In conclusion, both pharmacological and genetic data demonstrate that auxin perception and PAT are involved in the regulation of the magnitude of low light-induced differential growth as well as the maintenance of elevated petiole angles in low light. Auxin and PAT do not seem to be required for a fast induction of the low light-induced hyponastic growth response. Intriguingly, auxin and PAT are not involved in aspects of ethylene-induced hyponastic growth.

Discussion

Hyponastic growth upon detection of light quality changes is a component of the shade avoidance syndrome, a suite of traits that direct plant growth towards the better lit zones of a vegetation, away from the shade imposed by neighbors (Franklin, 2008). Next to these morphological responses to light quality, reductions in light quantity also induce a variety of acclimations. Shade exposure for example induces strong acclimations at the photosynthetic level, including a reallocation of photosynthetic machinery from the old, shaded, leaves to the younger ones that are higher in the canopy where light conditions are more favorable (Boonman *et al.*, 2006). We propose that the low light-induced hyponastic growth response described here contributes to these shade acclimation responses because it facilitates the exposure of particularly young leaves to less-shaded conditions. This adds light intensity to the palette of signals that induce plant responses to neighbors. We show here that this low light intensity response could be a response to particularly the reduced blue light fluence rate, which has been shown previously to induce shade avoidance responses (Ballaré *et al.*, 1991; Pierik *et al.*, 2004a; Sasidharan *et al.*, 2008).

Interestingly, not only cryptochromes, but also phytochrome A and phytochrome B appear to be involved in the hyponastic growth response to low light. The phytochrome involvement is different from the low blue light-mediated hypocotyl elongation in *Arabidopsis* seedlings that was recently shown to be mediated by cryptochromes 1 and 2 (Pierik *et al.*, 2009) without involvement of phytochromes. It is unlikely that this important role for phytochromes in low light-induced hyponastic growth is due to the red light component in the light treatments since red light-enrichment could not prevent hyponasty. The latter finding differs from a

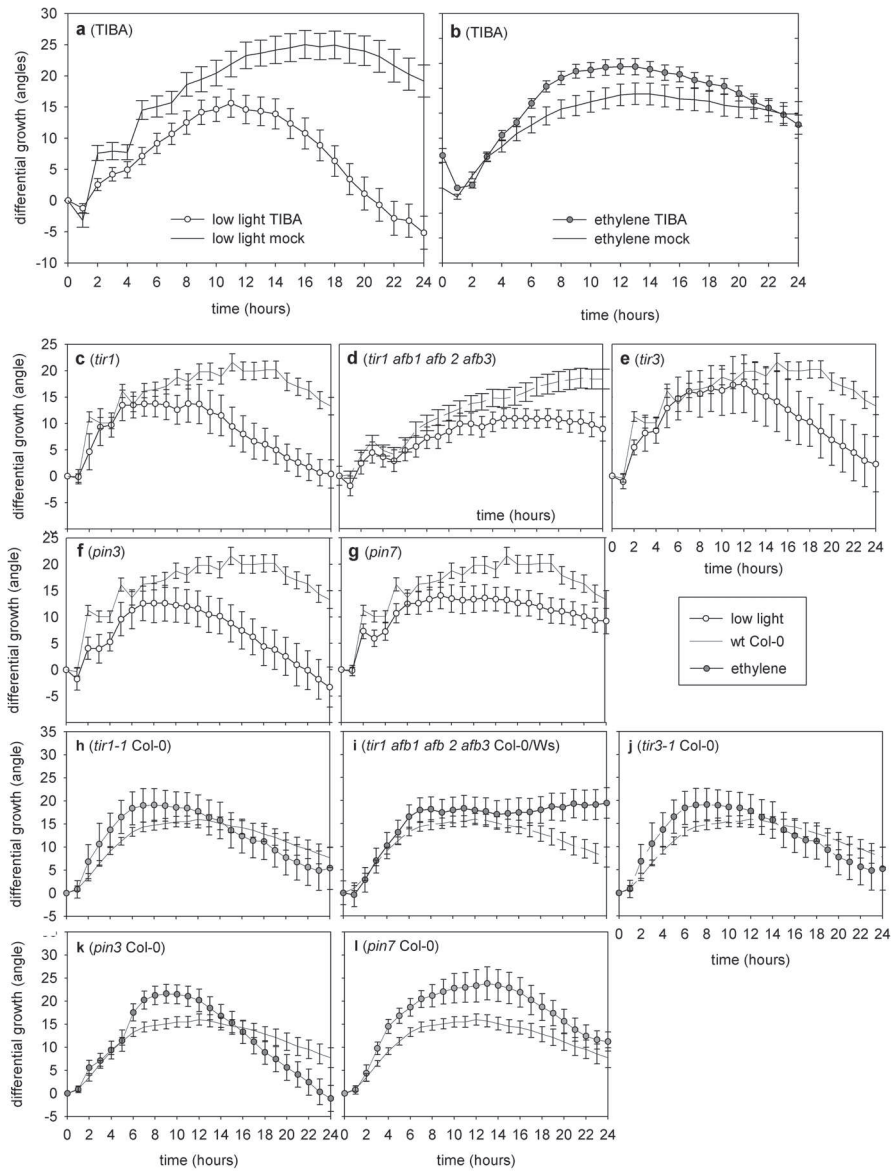


Figure 2.5: Auxin involvement in low light- and ethylene-induced hyponasty. Effect of exposure to a: low light ($20 \mu\text{mol m}^{-2} \text{s}^{-1}$; open circles) or b: ethylene ($5 \mu\text{l l}^{-1}$; grey closed circles) on petiole angles of Arabidopsis Col-0 plants treated with $50 \mu\text{M}$ TIBA (open circles) or a mock solution (line). c-g: Effect of exposure to low light ($20 \mu\text{mol m}^{-2} \text{s}^{-1}$) and h-l: effect of exposure to ethylene ($5 \mu\text{l l}^{-1}$; grey closed circles), on petiole angles of Arabidopsis auxin signaling and polar auxin transport mutants, compared to Col-0 wild type response to these stimuli (lines). See legend Figure 2.1 for details; error bars represent SE; $n \geq 12$.

study on hyponastic growth by Mullen *et al.* (2006) who showed that red light could prevent hyponasty. However, to show this, these authors used a red-light treatment of $100 \mu\text{mol m}^{-2} \text{s}^{-1}$, which is even more than the red light component in our controls. We, therefore, hypothesize that the phytochrome involvement found here, might be through its sensitivity to blue light wavelengths (Whitelam *et al.*, 1993; Neff & Chory, 1998). However, as *phyb* is a constitutively shade avoiding mutant, with constitutively high petiole angles (*phyb-5*: 42.2 ± 1.5 , *Ler*: 31.2 ± 0.5 degrees in control light conditions), we cannot exclude that the reduced response to low light is due to a mechanical constraint and/or saturation of the signaling route caused by this higher initial angle.

Prolonged exposure to low light led to the induction of hyponastic growth, even in combined multiple loss-of-function photoreceptor mutants. Alternative signals might come from the photosynthetic machinery, as it can generate light intensity-dependent signals that influence nuclear gene expression. Possible signals are the redox state of the plastoquinone pool, thioredoxine, oxygen radicals, chlorophyll synthesis and sugar status (Danon & Mayfield 1994; Escoubas *et al.*, 1995; Pfannschmidt *et al.*, 1999; Strand *et al.*, 2003; Geigenberger *et al.*, 2005; Piippo *et al.*, 2006). Indeed, we observed hyponastic growth after addition of the photosynthesis inhibitor DCMU under control light conditions that normally do not induce hyponastic growth (Figure 2.3a). Furthermore, we observed a decreased hyponastic response to low light in the *ex1 flu* mutant (Figure 2.3b), which is disturbed in signaling from the chloroplasts to the nucleus (Wagner *et al.*, 2004; Lee *et al.*, 2007).

Ethylene induces hyponastic growth in *Arabidopsis* and other species (Cox *et al.*, 2003; Pierik *et al.*, 2004a; Millenaar *et al.*, 2005). Interactions between light and ethylene are evident in literature. Low light- and low blue light-induced hyponasty in tobacco are ethylene-dependent (Pierik *et al.*, 2004b) and phytochromes can regulate ethylene production in various species such as *Sorghum* (Finlayson *et al.*, 1998), tobacco (Pierik *et al.*, 2004b) and *Arabidopsis* (Pierik *et al.*, 2009). In dark, ethylene maintains the apical hook in *Arabidopsis* seedlings (Raz & Ecker, 1999), while under continuous red, far-red or blue light the apical hook opens even in the presence of up to $100 \mu\text{l l}^{-1}$ ethylene (Knee *et al.*, 2000). Similarly, the effects of ethylene on hypocotyl length are conditional upon dark versus light conditions (Smalle *et al.*, 1997; Pierik *et al.*, 2006).

Interestingly, multiple lines of evidence indicate that low light-induced differential petiole growth in *Arabidopsis* acts independent of ethylene (Figure 2.4; Figure S2.2). However, downstream of low light and ethylene, the two pathways may still merge. Both signals induce hyponasty with a very similar response kinetics (Millenaar *et al.*, 2005) and low light and ethylene affect the expression of a shared pool of 453 genes (165 up- and 288 down regulated; Pierik *et al.*, 2005). Furthermore, a combined ethylene and low light treatment induced a hyponastic response that is not different from the one induced by either treatment alone (Millenaar *et al.*, 2005) which might indicate that the two pathways saturate shared downstream components. It is thus possible that a basic regulatory machinery, required for petiole movement, that

controls localized growth responses, is regulated by a variety of environmental signals.

The results we present contrast to Vandenbussche *et al.*, (2003) who showed abolishment of low light-induced hyponastic growth in ethylene insensitive mutants. Furthermore, ACC synthase 6 (ACS6) and ACS8 were up-regulated in their shade conditions. This contradicts with our micro-array results that show no change in ACC synthases (Figure S2.2) and with the lack of regulation of ethylene production by low blue light as shown in Pierik *et al.* (2009). In the experiments by Vandenbussche *et al.* (2003) agar-grown seedlings were used and treatment for 6 d was required to observe a change in leaf angle, rather than the very rapid response (within hours) that we describe here. Therefore, these are probably different responses that are based on different mechanisms.

Lowering auxin levels by de-blading leaves of the semi-aquatic species *Rumex palustris*, suggested a stimulatory role for auxin in all aspects of submergence-induced hyponastic growth (Cox *et al.*, 2004). More gentle manipulation of petiolar auxin levels, using the PAT inhibitors TIBA and NPA, demonstrated that auxin and PAT are important in this species for a rapid induction of hyponastic growth, but not for response magnitude and maintenance of elevated petiole angles (Cox *et al.*, 2004). This is exactly opposite to auxin control of low light-induced hyponasty in Arabidopsis. Ethylene is the key trigger of submergence-induced hyponasty in both *Rumex palustris* and in Arabidopsis (Cox *et al.*, 2003; Millenaar *et al.*, 2005). Interestingly, TIBA treatment did not obviously alter aspects of ethylene-induced hyponastic growth in Arabidopsis and the tested auxin signaling- and transport mutants had a close to wild type ethylene-induced hyponastic growth response (Figure 2.5). Together, this suggests that in both species the magnitude and maintenance of hyponastic growth induced by ethylene are not under control of PAT, whereas in Arabidopsis auxin and PAT are important for these hyponastic growth components upon low light exposure. This involvement of auxin and PAT is consistent with its role in light quality-mediated elongation responses. Thus auxin appears to be controlled by both light intensity and light quality and this regulation is functional to both differential petiole growth (Figure 2.5), as well as non-differential elongation of petioles and hypocotyls (Morelli & Ruberti, 2000; Pierik *et al.*, 2009; Tao *et al.*, 2008).

Materials and Methods

Plant material and growth conditions

Three *Arabidopsis thaliana* accessions were used: Columbia-0 (Col-0; N1092), Landsberg erecta (Ler; NW20) and Wassilewskija-2 (Ws-2; N1602). Nottingham Arabidopsis Stock Center (NASC) accession numbers are shown between brackets. The corresponding genes for all mutants used in this study are significantly expressed in Col-0 petioles (Supporting Information Table S2.1). The origin of the mutants for our studies is either from the stock center or from the authors who described these mutants.

The ethylene mutants are all in a Col-0 background: *ein2-1* (N3071; Guzman & Ecker, 1990), *etr1-4* (Chang *et al.*, 1993), *ein4-1* (N8053; Roman *et al.*, 1995), *ctr1* (N8057; Kieber *et al.*, 1993). The photoreceptor mutants are all in Ler background unless stated otherwise: *cry1-1* (*hy4*; Koornneef *et al.*, 1980; Ahmad & Cashmore, 1993), *cry2* (*fha1*; Koornneef *et al.*, 1991; Guo *et al.*, 1998), *cry1 cry2* (*hy4 fha1*; Yanovsky *et al.*, 2000), *ex1-7 flu* (Meskauskiene *et al.*, 2001; Wagner *et al.*, 2004), *hy2* (N68; Koornneef *et al.*, 1980; Kohchi *et al.*, 2001), *phyA-201* (N6219; Nagatani *et al.*, 1993), *phyB-5* (N69; Koornneef *et al.*, 1980); *phyA-201 cry1-1* (Casal & Mazzella, 1998), *phyA-201 cry2* (Mazzella *et al.*, 2001), *phot1-101* (Liscum & Briggs, 1995), *phot2-5* in Ws (Jarillo *et al.*, 2001; Kagawa *et al.*, 2001), *phot1-101 phot2-5* in Ws/Ler (Sakai *et al.*, 2001). The auxin mutants are in a Col-0 background unless stated otherwise: *tir1-1* (N3798; Ruegger *et al.*, 1997), *tir1-1 afb1-1 afb2-1 afb3-1* in Col/Ws (Dharmasiri *et al.*, 2005b), *tir3-1* (Ruegger *et al.*, 1997), *pin3-4* (N9363; Friml *et al.*, 2002) and *pin7-1* (N9365; Friml *et al.*, 2003).

Plants were grown on a fertilized mixture of potting-soil and perlite (1:2) as described in Millenaar *et al.* (2005). Conditions in the growth chamber were: 20°C, 70% (v/v) relative humidity, 9 h photoperiod, 200 $\mu\text{mol m}^{-2} \text{s}^{-1}$ photosynthetic active radiation (PAR). Plants were automatically tap-watered each day to saturation at the start of the photoperiod. For all experiments plants in stage 3.9 according to Boyes *et al.* (2001) were used, which means a vegetative plant with approximate 15 rosette leaves. All experiments started 1.5 h after the start of the photoperiod to minimize variation which could be induced by circadian and diurnal rhythms (Salter *et al.*, 2003). All experiments were repeated at least twice with independent plant batches.

Light manipulation experiments

For low light experiments, the light quantity was reduced by 90% from 200 $\mu\text{mol m}^{-2} \text{s}^{-1}$ to 15 – 20 $\mu\text{mol m}^{-2} \text{s}^{-1}$ (PAR) at the start of the experiment. This was achieved by using a neutral shade cloth that did not change the relative light spectral composition (Figure S2.1) which was verified using a Licor1800 spectroradiometer (Licor, Lincoln, Ne, USA).

Low light was enriched in blue light components or red light components by placing colored filters on top of boxes with forced ventilation to guarantee continuous refreshment of the air (Figure 2.1c, Figure S2.2, Lee filter, Andover, United Kingdom). To filter out all colors but red, a '026 Bright Red' filter was used. To filter out all colors but blue, a '200 Double CT Blue' filter, in combination with a layer of 2 cm 25 g l⁻¹ CuSO₄ · 5 H₂O solution (Merck, Darmstadt, Germany) was used. CuSO₄ removes far-red light and was necessary to maintain a red/far-red ratio similar to the other treatments (data not shown). Because of the low-transparency of some of the filters used, we lowered the control light level in order to have comparable light

intensities. Therefore, the hyponastic growth response was relatively low in this experiment compared to other experiments described.

Ethylene experiments

Ethylene application was as described in Millenaar *et al.* (2005). Pure ethylene (Hoek Loos BV, Schiedam, the Netherlands) and air (70% relative humidity) were mixed using flow meters and controllers (Brooks Instruments BV, Ede, the Netherlands) to generate a concentration of $5 \mu\text{l l}^{-1}$ ethylene. This was flushed continuously through glass cuvettes containing the plants at 75 l h^{-1} , and then vented away. A concentration of $1 \mu\text{l l}^{-1}$ ethylene was reached in the cuvettes after approximately 10 min; $5 \mu\text{l l}^{-1}$ was reached after 40 min. The ethylene concentration was checked regularly on a gas chromatograph (GC955, Synspec, Groningen, the Netherlands), and remained constant for the duration of the experiment. Control cuvettes were flushed with air (70% relative humidity) at the same flow rate.

Ethylene release was measured in real-time on control- and low light-treated Col-0 plants under standard growth chamber conditions. Plants were placed singly in glass cuvettes (1.5 l) that were flushed continuously with ethylene-free air (1 l h^{-1} flow rate) one day prior to the treatment. On the next day, plants were either subjected to standard low light conditions or remained as control. During the measurements, air that had left the cuvettes was led through scrubbers to take out all CO_2 and H_2O and then entered a laser-driven photo acoustic ethylene detector (SensorSense, Nijmegen, the Netherlands) to measure real-time ethylene release from the plants. The ethylene detector signal was corrected for background noise using an empty cuvette and for soil-derived ethylene which was measured from a pot with standard substrate, but no plant. After 24 h, plants were taken out of the cuvettes and weighed. Ethylene production rates were calculated as $\text{nl ethylene g}^{-1} \text{FW h}^{-1}$.

Pharmacological experiments

3-(3,4-dichlorophenyl)-1,1-dimethylurea (DCMU; $10 \mu\text{M}$) and 2,3,5-triiodobenzoic acid (TIBA; $50 \mu\text{M}$) were in 0.1% Tween and 0.01% ethanol. Both were applied by spraying the plants. Mock plants were treated with identical solutions, but lacking the active components. The TIBA pretreatment took place at 66 h, 42 h and 18 h before the start of the experiment.

Computerized digital camera system and image analysis

To measure changes in petiole angle, a custom-built computerized digital camera system was used as described in Millenaar *et al.* (2005). To enable continuous photography, no dark period was included in the 24 h experimental period. Plants were placed singly in glass cuvettes with the petiole of study positioned perpendicular to the axis of the camera. To facilitate the measurements, any leaf that was obscuring the petiole being photographed was removed. Additionally, the petiole was marked at the petiole/lamina junction with drawing ink. These preparations did not influence the response of the petiole (data not shown). Digital photographs were taken every 10 min. The angles of the petioles were measured on these images using a PC-based image analysis system with a custom made macro using the KS400 (Version 3.0) software package (Carl Zeiss Vision, Hallbergmoos, Germany). The petiole angles from the light dose-response curves and light enrichment experiments were measured with ImageJ version 1.35o (<http://rsb.info.nih.gov/ij/>). The petiole angle is defined as the

angle between the horizontal and a line drawn between the ink mark at the petiole/lamina junction and a fixed point at the base of the petiole. To take into account the changes in angle of control plants during the course of the experiments, we did a pair wise subtraction. This is the difference between the angles of treated and control plants for each time point (Benschop *et al.*, 2007). The new standard errors for the differential response were calculated by taking the square root from the summation of the two squared standard errors.

Real-Time RT-PCR

Petioles of Col-0 were harvested and snap frozen in liquid nitrogen. Subsequently, RNA was isolated from these petioles with the RNeasy extraction kit (Qiagen, Valencia, CA, USA). gDNA removal, cDNA synthesis and Real-Time RT-PCR were performed as described by Millenaar *et al.*, (2006). Primer sequences of ACO4 (At1g05010), ERS2 (At1g04310) and ACT2 (reference; At5g09810) were as described in Millenaar *et al.*, (2006). Real-time RT-PCR data were calculated with the comparative C_t method described by Livak & Schmittgen (2001).

Acknowledgments

This work was supported by a PIONIER grant (800.84.470 to LACJV), a VENI grant (86306001 to RP) of the Netherlands organization for scientific research (NWO) and by a NIELS STENSEN grant to FFM. We thank Maarten Terlouw, Yvonne E.M. de Jong-van Berkel, Joke van Elven, for technical assistance, Diederik Keuskamp for comments on the manuscript and our colleagues G.E. Schaller, M. Koornneef, M. Ahmad, C. Lin, K. Apel, Nagatani, J.J. Casal, T. Sakai, J. Friml and M. Estelle who shared mutant lines.

Supporting Information

- **Figure S2.1:** Light spectra of the treatments used in this study.
- **Figure S2.2:** Expression of ethylene biosynthesis and signal transduction genes in Col-0 petiole tissues.
- **Table S2.1:** Arbitrary expression levels in Col-0 petioles of genes studied in this work.

Supporting Information

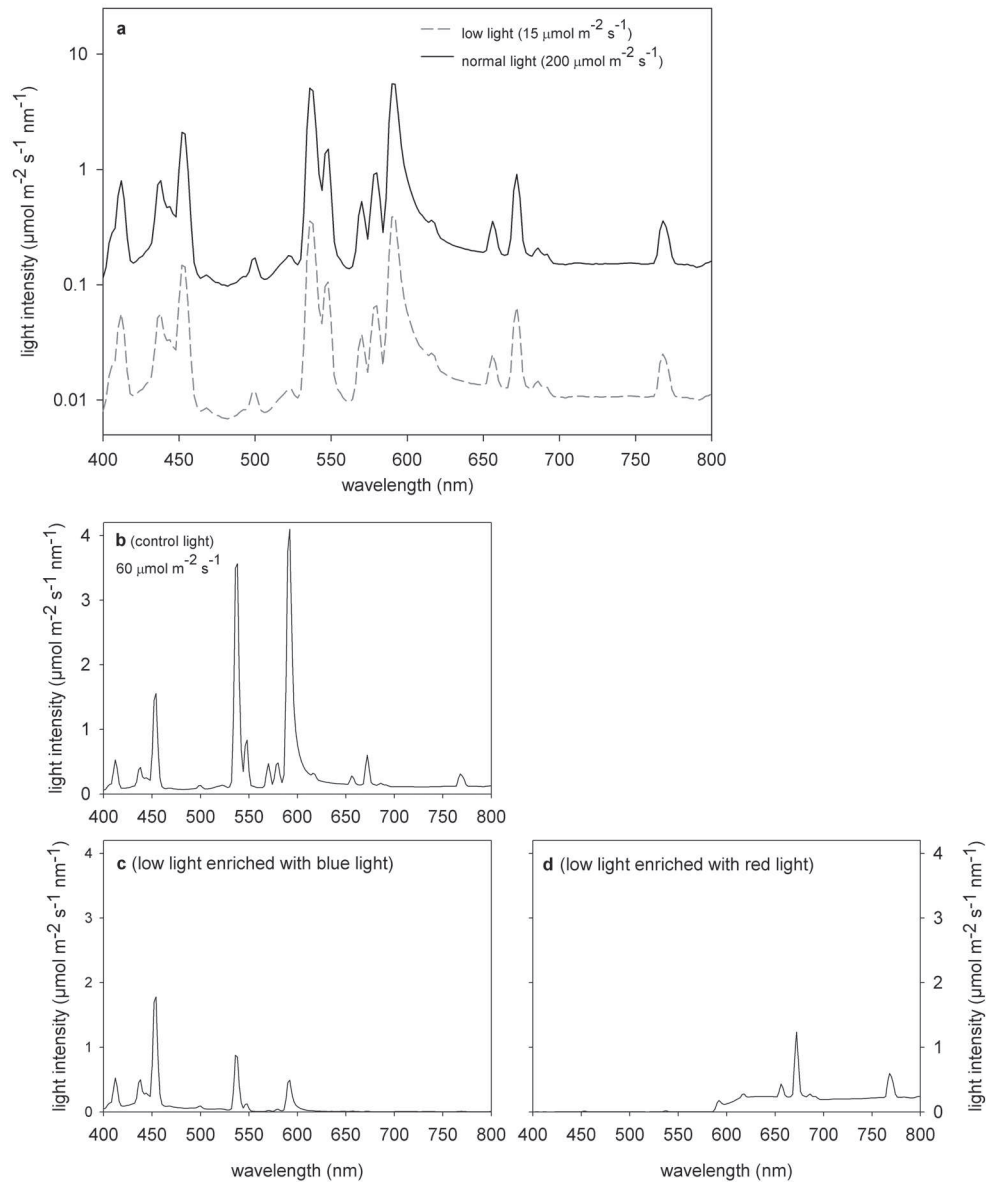


Figure S2.1: Light spectra of the treatments used in this study. a: Spectra (light intensity for each wavelength per nm, in log-scale) of a: control light conditions ($200 \mu\text{mol m}^{-2} \text{s}^{-1}$; lines) and spectral neutral low light intensity treatment ($15 \mu\text{mol m}^{-2} \text{s}^{-1}$; dashed line). b: control light condition used in the light-enrichment experiments ($60 \mu\text{mol m}^{-2} \text{s}^{-1}$). c: low light enriched with blue-light and d: low light enriched with red lightspectra were recorded with a Licor1800 spectro-radiometer (Li-cor, Lincoln, Ne, USA).

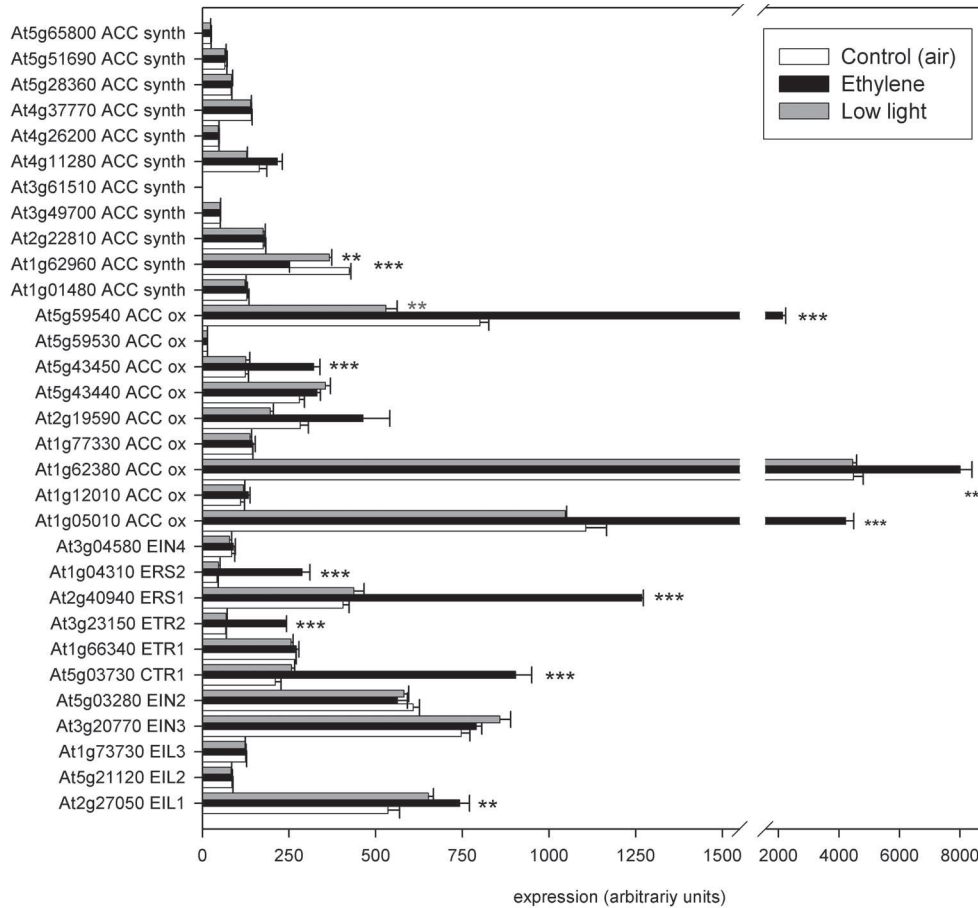


Figure S2.2: Expression of ethylene biosynthesis- and signaltransduction genes in petiole tissues. Expression levels in control conditions (white), upon 3 h ethylene treatment (black; $5 \mu\text{l l}^{-1}$) and low light treatment (grey; $20 \mu\text{mol m}^{-2} \text{s}^{-1}$). ** $p < 0.01$, *** $p < 0.001$, ns = not significant, 2-tailed Student's T-test, $n=3$ and error bars represent SE. The used microarrays were previously described in Millenaar *et al.* (2006) and can be found at: <http://affymetrix.arabidopsis.info/narrays/experimentpage.pl?experimentid=32>. From the Affymetrix microarrays, gene expression was calculated from 11 probe pairs using Robust MultiArrayaverage (RMA) software.

Table S2.1: Arbitrary expression levels in Col-0 petioles of genes studied in this work. AGI identifier, average expression and standard error (SE), of the genes for which mutants have been used in this study, under control conditions ($200 \mu\text{mol m}^{-2} \text{s}^{-1}$). Data was retrieved from Affymetrix microarray data (RMA calculated) as described in Millenaar *et al.* (2006). Details on the used micro arrays are described in Figure S2.2. Expression values of all genes is above the minimum signal intensity (59.2, determined with a RNA spike-in experiments) above which the signal was significantly different from the background.

	AGI code	Average	SE
phot1	At3g45780	2096.40	66.37
phot 2	At5g58140	905.66	42.84
cry1	At4g08920	355.38	0.24
cry2	At1g04400	1205.34	55.22
phyA	At1g09570	412.13	23.96
phyB	At2g18790	427.17	12.74
hy2	At3g09150	109.10	8.05
ex1	At4g33630	388.21	18.66
flu	At3g14110	644.35	27.59
ein2	At5g03280	597.86	15.68
ein4	At3g04580	84.20	9.12
etr1	At1g66340	269.19	2.10
ctr1	At5g03730	210.16	16.79
tir1	At3g62980	450.33	17.34
afb1	At4g03190	430.56	28.57
afb2	At3g26810	469.34	29.54
afb3	At1g12820	348.24	5.79
tir3	At3g02260	556.29	38.03
pin3	At1g70940	665.19	58.95
pin7	At1g23080	650.05	91.98

Hormone- and light-mediated regulation of
heat-induced hyponastic petiole growth in
Arabidopsis thaliana

Martijn van Zanten, Laurentius A.C.J. Voeselek, Anton J.M.
Peeters, Frank F. Millenaar^s

Plant Ecophysiology, Institute of Environmental Biology, Utrecht University,
Padualaan 8, 3584 CH Utrecht, the Netherlands

Present address:

FFM: De Ruiter Seeds, Leeuwenhoekweg 52, 2660 BB Bergschenhoek,
the Netherlands.

Adapted from:

- Van Zanten M, Voeselek LACJ, Peeters AJM, Millenaar FF. (2009). Hormone- and light-mediated regulation of heat-induced differential petiole growth in *Arabidopsis thaliana*. *Plant Physiology*, Online September 9, 2009; 10.1104/pp.109.144386

Abstract

Plants react quickly and profoundly to changes in their environment. A sudden increase in temperature induces for example differential petiole growth driven upward leaf movement (hyponastic growth) in *Arabidopsis thaliana*. We show that accessions that face the strongest fluctuations in diurnal temperature in their natural habitat are least sensitive for heat-induced hyponastic growth. This indicates that heat-induced hyponastic growth is a trait subjected to natural selection. The response is induced with kinetics remarkably similar to ethylene- and low light-induced hyponasty in several accessions. Using pharmacological assays, transcript analysis and mutant analyses, we demonstrate that ethylene and the photoreceptor protein phytochrome B are negative regulators of heat-induced hyponastic growth and that low light, phytochrome A, auxin, polar auxin transport and abscisic acid are positive regulators of heat-induced hyponastic growth. Furthermore, auxin, polar auxin transport, phyA, phyB and cryptochromes are required for a fast induction of the response.

Introduction

Temperature is an important environmental factor that varies over seasons, but also pronouncedly over the day. Supra-optimal temperatures are among the most damaging abiotic factors in crop plants (Mittler *et al.*, 2006; Barnabás *et al.*, 2008) and minor changes in temperature can already have dramatic effects on plants, e.g. fine tuning of several key process in plant development such as germination (Toh *et al.*, 2008), floral transition (Halliday *et al.*, 2003; Balasubramanian *et al.*, 2006a) and circadian clock entrainment and compensation (Samach & Wigge, 2005; Gould *et al.*, 2006; Penfield, 2008).

A study on natural variation of constitutive leaf angles in *Arabidopsis thaliana* accessions originating from different geographic origins revealed that leaves of accessions found on lower latitudes are more erect than from northern accessions (Hopkins *et al.*, 2008). A recent report by Koini and colleagues (2009) showed that a sudden increase in temperature induces an increase in leaf inclination (hyponastic growth), which is controlled by *PHYTOCHROME INTERACTING FACTOR 4* (PIF4).

Hyponastic growth is also associated with shade- and submergence-avoidance and brings leaves towards light and air, respectively (Ballaré, 1999; Cox *et al.*, 2003; Pierik *et al.*, 2004b; Millenaar *et al.*, 2005, 2009; Chapter 2). Accumulation of the gaseous hormone ethylene is the key trigger for the induction of hyponastic growth in submerged plants, including *Arabidopsis thaliana* (Millenaar *et al.*, 2005). Interestingly, reduced light-intensity (low light) triggers a hyponastic growth response with similar kinetics as ethylene (Millenaar *et al.*, 2005). Both genetic and pharmacological data indicated that auxin and polar auxin transport are involved in low light-, but not in ethylene-induced hyponastic growth, whereas the response to low light is ethylene independent (Millenaar *et al.*, 2009; Van Zanten *et al.*, 2009a; Chapter 2). Based on these data, we hypothesized that ethylene and low light induce

differential growth via largely independent routes, but probably share functional components downstream, which explains the phenotypical resemblance.

In this report, we demonstrate that a rapid temperature shift (from 20°C to 38°C), induces hyponastic growth with highly similar kinetics to ethylene- and low light-induced hyponasty. Leaf angles of naturally occurring accessions that face the strongest fluctuations in diurnal temperature in their natural habitat are least sensitive to heat, suggesting that this trait is subject to natural selection. The regulation of this response was studied by a combination of pharmacological experiments, gene-expression studies and mutant analyses. We present evidence that ethylene and phytochrome B are negative regulators, and that low light, phytochrome A, auxin and abscisic acid (ABA) are positive regulators of heat-induced hyponastic growth.

Results

Heat-induced leaf inclination in *Arabidopsis*

To characterize the response of *Arabidopsis thaliana* petioles to elevated temperatures in detail, petiole angles were measured after 7 h exposure to different temperatures, using the standard accessions Columbia-0 (Col-0), Landsberg *erecta* (*Ler*) and Wassilewskija-2 (*Ws-2*). A positive correlation for all accession was found in the temperature range from ~16°C to ~38°C, demonstrating that *Arabidopsis* petioles react with a hyponastic growth response to changes in environmental temperature (Figure 3.1a). Below 16°C none of the tested accessions changed petiole angles and above approximately 30°C, the response of Col-0 and *Ler* reached a plateau whereas *Ws-2* leaf-angles continued to increase.

From this experiment it is not conclusive if petiole angles adjust to the absolute temperature, to the relative change in temperature, or both. Therefore, petiole angles of Col-0 plants that were pre-grown for three weeks at 10°C were measured. In agreement with the results of Hopkins *et al.* (2008), this cold (vernalization) pre-treatment induced a significant increase ($p < 0.001$) in initial petiole angle (35.9 ± 0.6) relative to plants grown at 20°C (25.8 ± 0.4). The dose-response curve was similar regardless the pre-growth temperature, but cold pre-grown plants lost the ability of heat-induced hyponasty at temperatures exceeding ~32°C (Figure 3.1a). Moreover, as cold pre-grown plants showed higher initial angles, the absolute angles of cold pre-grown plants were significantly higher ($p < 0.001$) than in Col-0 grown at 20°C (Figure 3.1b). Overall, these data suggest that over a range of physiological relevant temperatures, *Arabidopsis* positions its petiole relative to the temperature difference between (pre)growth temperature and the new temperature. Regarding the responses of all tested accessions, a shift from 20°C to 38°C induced a strong hyponastic growth response and this is used throughout the experiments.

A time-lapse camera setup (Cox *et al.*, 2003; Millenaar *et al.*, 2005) was employed to monitor the kinetics of heat-induced hyponastic growth. In Col-0, the response starts within 1 h, the angle change per unit time is maximal after approximately 3 h and the maximal angle is reached around 7 h after start of the treatment (Figure 3.1c). Heat-induced hyponastic growth is irreversible once induced, since placing the plants back to control temperature after 3 or 6 h did not alter the maximum response angle (amplitude) at $t = 7$ h. However, plants placed back at control temperature were less able to maintain high leaf angles after the response maximum throughout the experimental period, which resulted in a faster decline of leaf angles after reaching the maximum response.

The amplitude of heat-induced hyponastic growth correlates with the natural diurnal-temperature-range of *Arabidopsis* accessions

To compare heat-induced hyponastic growth with ethylene- and low light-induced hyponastic growth (Millenaar *et al.*, 2005, 2009; Chapter 2), we exposed five frequently used accessions to these three signals (Figure 3.2). Strong similarities in responses were found in Col-0, *Ler* and C24 (Figure 3.2a-c). Elevated temperature

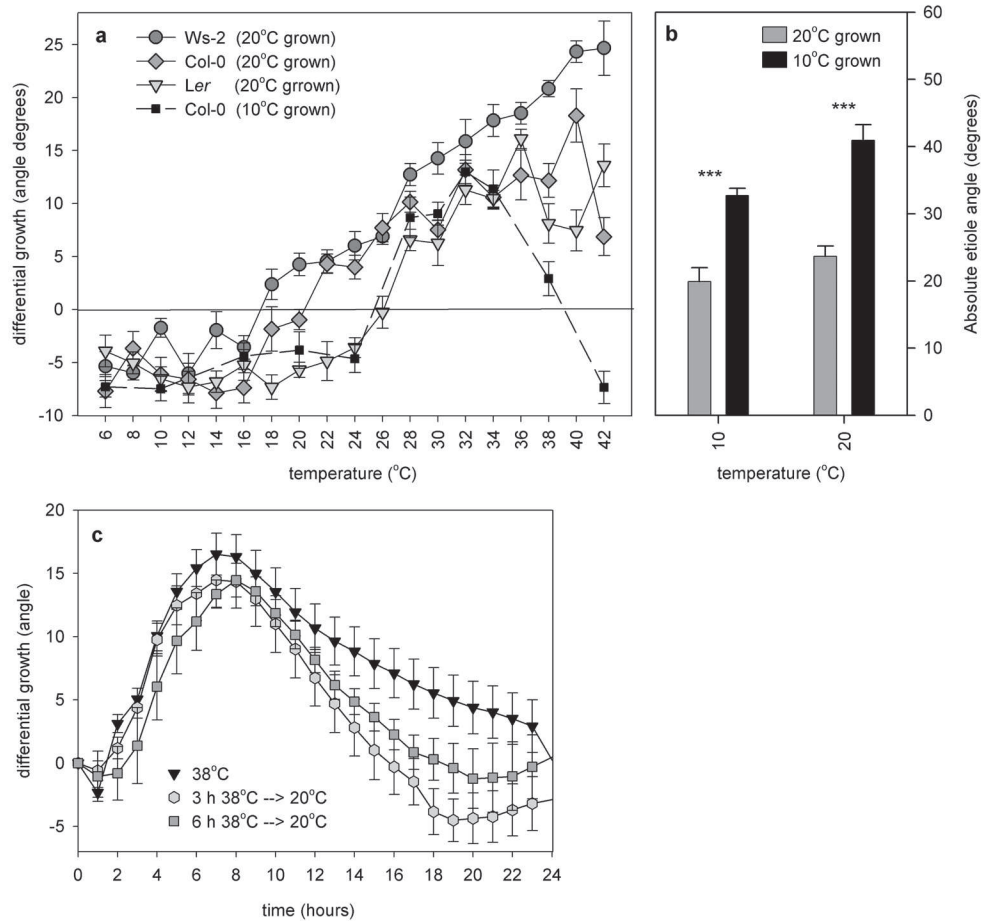


Figure 3.1: Characterization of the hyponastic growth response to different temperatures. **a:** Dose-response relation of temperature and petiole angles after 7 h of treatment with different temperatures, relative to the initial angle. 20°C grown (closed line); Ws-2 (circles), Col-0 (diamonds), *Ler* (triangles) and 10°C pre-grown Col-0 (black squares; dashed line). Angles were pair wise subtracted which is the difference between the angles of treated and control plants for each time point (Benschop *et al.*, 2007). **b:** Absolute (initial) petiole angles of Col-0 pre-grown at 20°C (grey) or at 10°C (black) after 7 h treatment with the indicated temperatures. **c:** Col-0 petiole angles kinetics upon exposure to heat (38°C) for 24 h (triangles) and of reversal from 38°C to 20°C after 3 h (circles) and 6 h (squares). *** $p < 0.001$; 2-tailed Student's T-test. Depicted angles are pair wise subtracted. Error bars represent SE, $n > 10$.

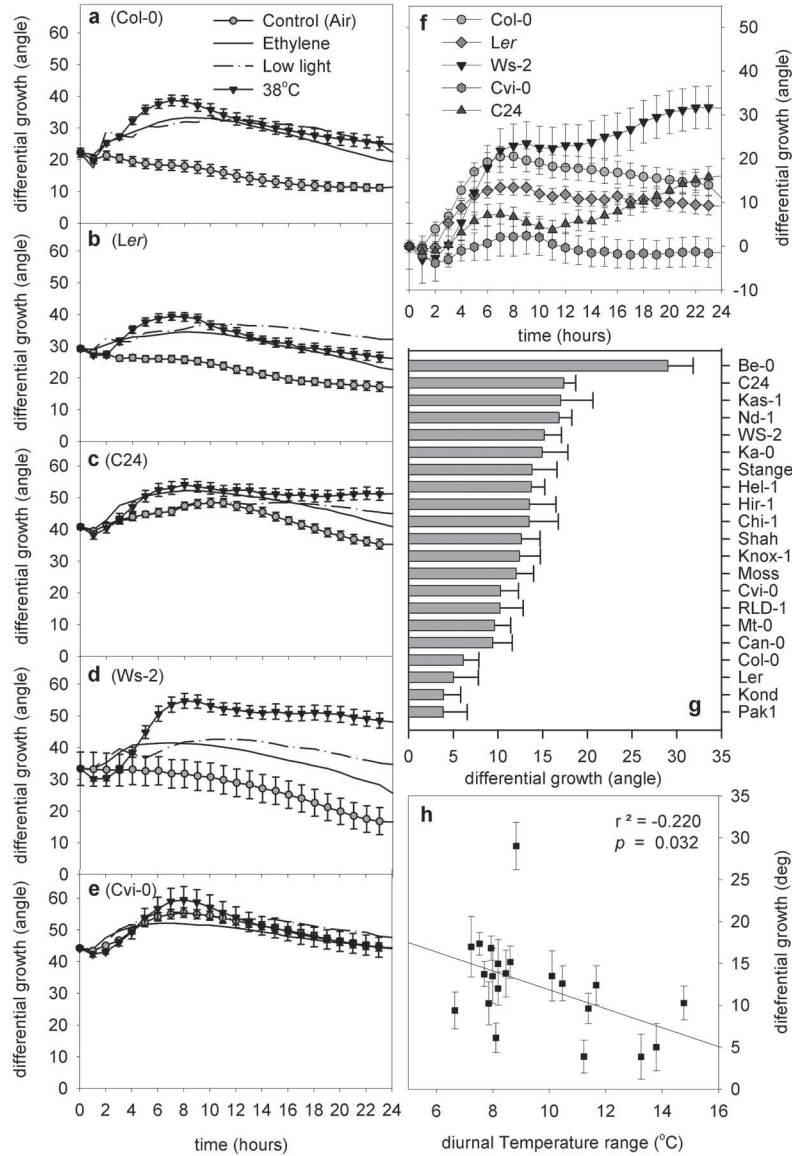


Figure 3.2: Natural variation in heat-induced hyponastic growth. Effect of exposure to air control (grey circles), heat (20°C to 38°C; black triangles), ethylene (5 $\mu\text{l l}^{-1}$; closed lines) and low light (200 $\mu\text{mol m}^{-2} \text{s}^{-1}$ to 20 $\mu\text{mol m}^{-2} \text{s}^{-1}$; dash-dotted line) on a: Col-0; b: Ler; c: C24; d: Ws-2; e: Cvi-0 petiole angles. f: Pair wise subtracted angles of heat-induced hyponastic of the five accessions from panel: a-e. g: Response amplitude after 7 h heat treatment of 21 Arabidopsis accessions. h: Pearson correlation (r^2) between response amplitude from panel g and diurnal temperature-range at the geographical origin of the accessions. The connecting line results from linear regression. Error bars represent SE; $n > 10$.

induced a much stronger response than exposure to ethylene or low light in Ws-2 (Figure 3.2d). Finally, Cape Verde Islands-0 (Cvi-0) lacked a marked response to heat, ethylene and low light, relative to the air-control treatment (Figure 3.2e).

To compare heat-induced hyponastic growth in the five accessions a pair wise subtraction was performed to correct for diurnal and/or circadian petiole movements (Benschop *et al.*, 2007; Figure 3.2f). Cvi-0, which originates from near the equator is a weak responder, whereas C24, originating from the Portuguese accession Coimbra (Schmid *et al.*, 2006) has an intermediate response. On the contrary, Central European accessions; Ler, Col-0 and Ws-2, showed a strong response. These data suggest a correlation between geographic origin and amplitude of heat-induced hyponastic growth. To test this, we extended our study to 21 selected accessions together roughly covering the biogeographical latitudinal distribution range of *Arabidopsis thaliana* (Figure 3.2g; Supporting Information Table S3.1). Considerable variation was observed in the amplitude of the response after 7 h of treatment (less than 5 degrees for Pak-1 to ~30 degrees in Be-0). No significant correlations between amplitude of heat-induced hyponastic growth with latitude, longitude or altitude were found (Supporting Information Figure S3.1), although average temperature itself was strongly negatively correlated to latitude ($r^2 = -0.76$).

Subsequently, we analyzed if local environmental conditions at the collection sites correlated with the amplitude of heat-induced differential growth (Table S3.2). For this aim, mean annual climate data acquired over a 30 years period were examined (New *et al.*, 1999; Table S3.2). A small, but significant, negative correlation ($p=0.032$, $r^2 = -0.22$) was observed between maximum response angles at $t=7$ h after induction and diurnal temperature range, i.e. the differences between maximum and minimum temperature over the day (Figure 3.2h). This might indicate that plants from a location where daily-temperatures are highly fluctuating respond less to heat than plants from relatively temperature stable environments.

Ethylene is a negative regulator of heat-induced hyponastic growth

Because heat-induced hyponastic growth phenocopies ethylene-induced hyponastic growth (Figure 3.2a-c), we hypothesized that ethylene may be a downstream component of heat-induced hyponasty. To test this, we first measured ethylene release upon heat treatment in Col-0. In the first hours after treatment ethylene release tended to decrease relative to the ethylene release during control temperatures and this became significant ($p<0.05$) 3-6 h after the start of the heat treatment (Figure 3.3a).

Transcription of the ethylene biosynthesis gene ACC-oxidase 4 (ACO4) and an ethylene receptor ETHYLENE RESPONSE SENSOR 2 (ERS2) increases in the presence of ethylene (Wilkinson *et al.*, 1995; Hua *et al.*, 1998; Vriezen *et al.*, 1999). We tested expression of these ethylene marker genes in plants subjected to heat. Quantitative RT-PCR analysis (Figure 3.3b, c) did not reveal increase in transcript levels, whereas the heat-inducible positive control marker (Busch *et al.*, 2005); HEAT SHOCK TRANSCRIPTION FACTOR A2 (HSFA2) was strongly up-regulated (Figure 3.3d).

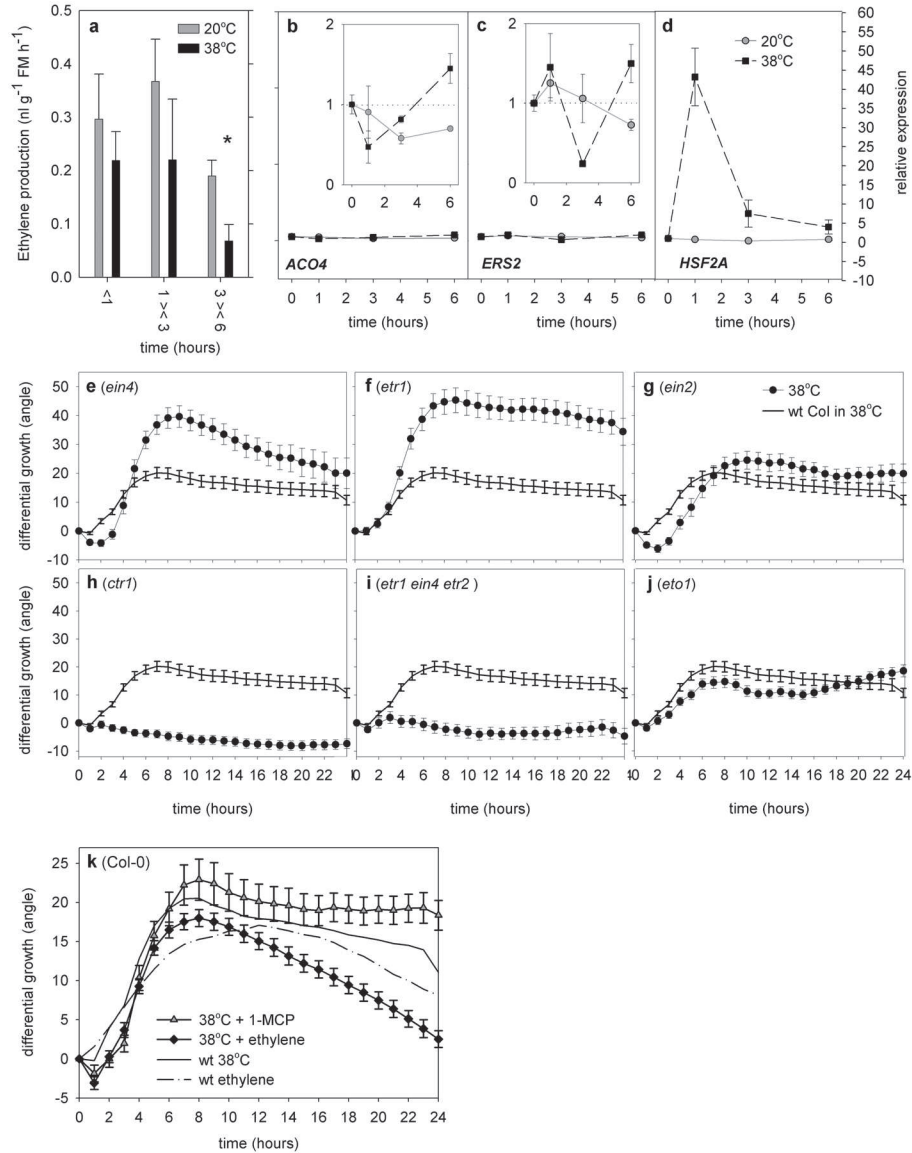


Figure 3.3: Role of ethylene in heat-induced hyponastic growth. a: Ethylene release ($\text{nl g}^{-1} \text{FM h}^{-1}$), from heat treated Col-0 (20°C to 38°C; black) and air control (20°C; grey) at different time windows; $n \geq 7$; * $p < 0.05$, 2-tailed Student's T-test. Real-Time RT-PCR analysis of b: ACC-oxidase 4; c: ERS2; d: HSF2A in air controls (grey circles) and heat treatment (black squares). Expression values are normalized to 1 at $t=0$ h ($n \geq 4$), inset shows close up. e-j: Effect of heat on petiole angles of ethylene insensitive (e-g) mutants, constitutive signaling mutants (h,i) and overproducing mutant (j) (black circles) compared to the wild type response. k: Effect of exposure to heat on Col-0 petiole angles in the presence of ethylene ($5 \mu\text{l l}^{-1}$; black circles) or 1-MCP (grey triangles) compared to plants in heat (black line) or ethylene (dash-dotted line). Angles resulted from pair wise subtraction; $n > 10$. Error bars represent SE.

As a third approach to test ethylene involvement in heat-induced hyponasty, ethylene related mutants were assayed. The ethylene insensitive lines *ethylene insensitive4* (*ein4*) and *ethylene response1* (*etr1*) showed enhanced heat-induced hyponastic growth (Figure 3.3e, f). Enhancement was not observed in *ein2* (Figure 3.3g). A mutant with constitutive ethylene response; *constitutive triple response* (*ctr1*), the triple loss-of-function mutant with a strong constitutive ethylene response phenotype; *etr1 ein4 etr2* and *ethylene overproducer1* (*eto1*; 2.6x more ethylene release than wild-type), all had a marked decrease in amplitude of the response to heat treatment (Figure 3.3h-j). Consistent with a role for ethylene as negative modulator in heat-induced hyponastic growth, pre-treatment with the ethylene receptor antagonist 1-methylcyclopropane (1-MCP) resulted in an enhanced hyponastic growth response to heat (Figure 3.3k). Finally, application of ethylene and heat simultaneously, resulted in a reduced hyponastic growth response compared to heat treatment alone. Particularly, these plants were less able to maintain high leaf angles after the response maximum (Figure 3.3k).

Overall, these data consistently indicate that ethylene is a negative regulator of heat-induced hyponastic growth.

Low light enhances heat-induced hyponastic growth

Plant responses to high temperatures and spectral shade are highly similar (Gray *et al.*, 1998; Halliday *et al.*, 2003; Halliday & Whitelam, 2003; Penfield, 2008). This is perhaps best supported by Koini *et al.* (2009), who showed that responses to high temperature are mediated by *PHYTOCHROME INTERACTION FACTOR 4* (*PIF4*). To test for possible interactions between light and heat signals in hyponastic growth, we applied low light and heat simultaneously to Col-0, and Ler. In both accessions, the combined treatment (heat + low light) resulted in a strong enhancement of hyponastic growth amplitude, as compared to plants subjected to either treatment alone (Figure 3.4a, b). This confirms cross-talk between low light and heat signals in controlling hyponastic growth.

The role of various photoreceptors in heat-induced hyponastic growth was studied with photoreceptor mutants in the Ler genetic background. The *phytochrome a* (*phya*) mutant showed delayed induction of the response, but exhibited a wild type amplitude after 6 h (Figure 3.4c). Interestingly, the response of *phyb* was delayed, but we observed enhanced petiole angles compared to wild type, for the remainder of the experimental period (up to 24 h) (Figure 3.4d). The *phya phyb* double mutant was initially delayed, but indistinguishable from wild type after 24 h (Figure 3.4e). Thus, *phya* appear to antagonize the enhanced response of *phyb* in heat-induced hyponastic growth. To further test if phyB is a negative regulator of heat-induced hyponastic growth, we assayed *phyb9* in Col-0. Interestingly, this mutant had an enhanced response to heat throughout the 24 h experimental period (Figure 3.4f). The response of the chromophore-deficient mutant *long hypocotyl2/genome uncoupled3* (*hy2/gun3*), which has reduced levels of all 5 phytochromes (phyA-E), was similar to the *phya phyb* double mutant (Figure 3.4g). This suggests that phytochromes C-D, are not redundant in this response. Heat-induced hyponastic growth was slightly

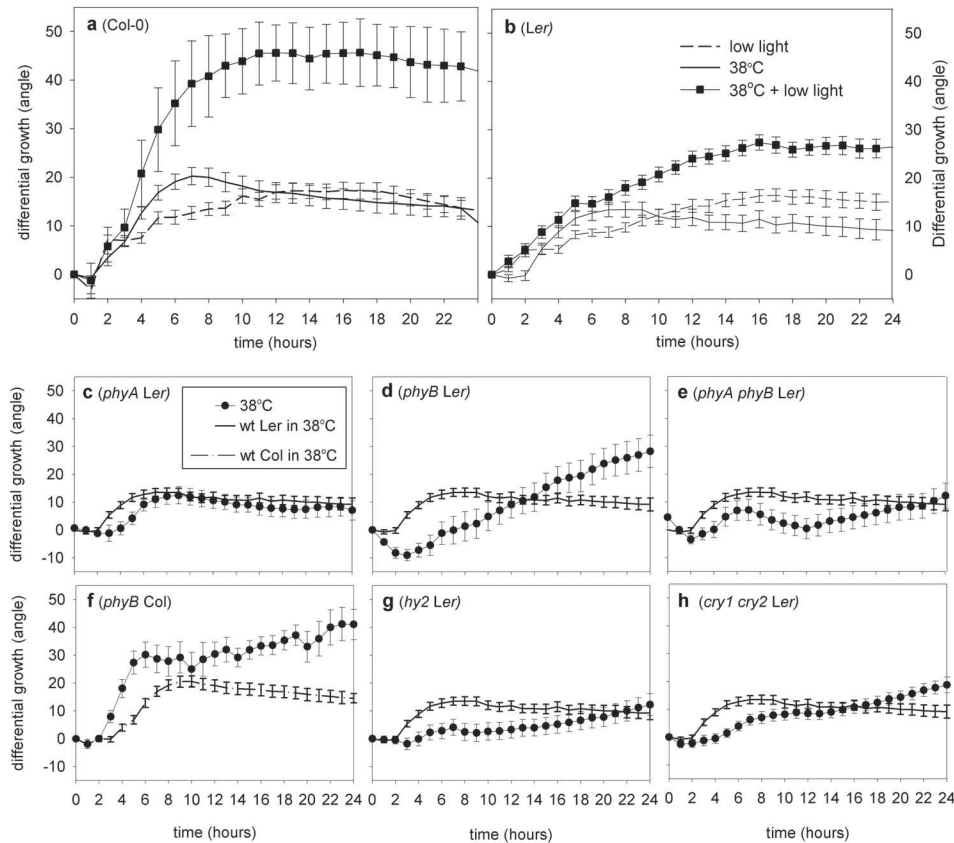


Figure 3.4: Role of light signaling in heat-induced hyponastic growth. Effect of the combination treatment: heat + low light ($38^{\circ}\text{C} + 20 \mu\text{mol m}^{-2} \text{s}^{-1}$; black squares) on petiole angles of **a**: Col-0 and **b**: *Ler*, compared to heat (black line) and low light (dashed line) alone. **c-h**: Effect of heat on petiole angles of photoreceptor mutants (black circles) compared to wild type response (lines). Angles resulted from pair wise subtraction; $n > 10$. Error bars represent SE

delayed in the *cryptochrome 1 cryptochrome 2* (*cry1 cry2*) double mutant (Figure 3.4h) compared to *Ler* wild type, suggesting that these proteins are required for a fast induction of heat-induced hyponastic growth.

In summary, our results demonstrate that *phyA*, *phyB* and cryptochrome photoreceptor proteins are required for proper induction of heat-induced hyponastic growth in *Ler*. *phyB* act as a negative regulator of the response amplitude in both the Col-0 and *Ler* background and loss-of function *phyA* rescues this effect, at least in *Ler*. Notably, the heat-induced hyponastic growth response of *phyb* in both Col-0 and *Ler* mimicked the response of the combination treatment of heat and low light in the respective wild types.

The contrasting effects of ethylene and low light on heat-induced hyponastic growth

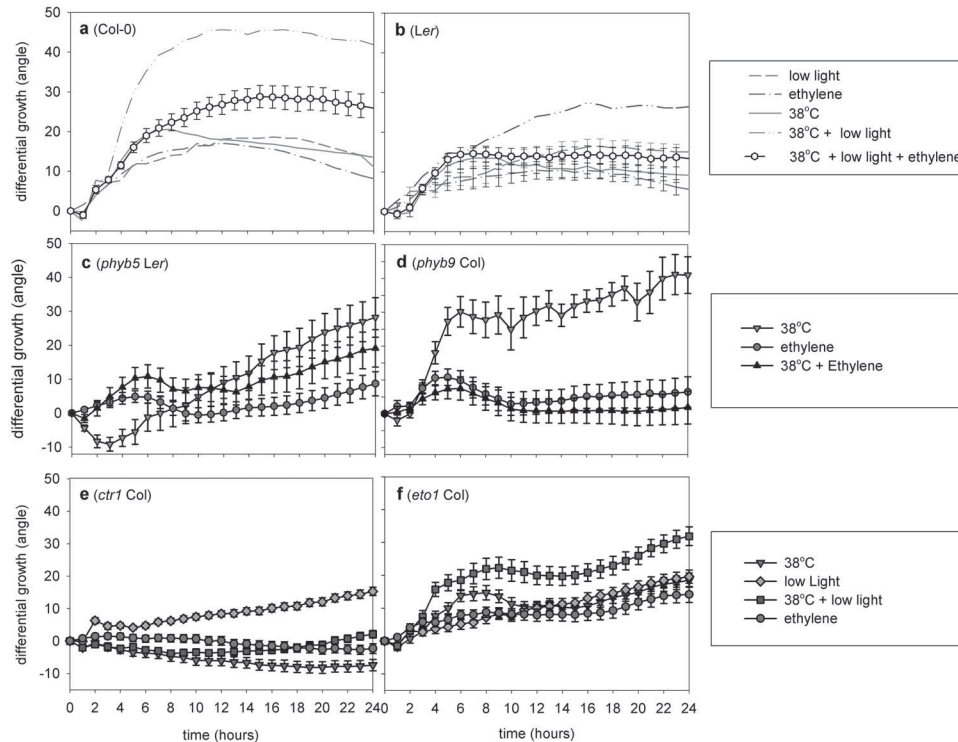


Figure 3.5: Effects of combined treatments on heat-induced hyponastic growth. (See Color Supplement for full color version of this figure) a: Col-0; b: *Ler*; c: *phyb5* (*Ler*); d: *phyb9* (Col-0); e: *ctr1*; f: *eto1*. Plants were treated with: ethylene ($5 \mu\text{l l}^{-1}$; red dash-dotted lines/red circles), low light ($20 \mu\text{mol m}^{-2} \text{s}^{-1}$; grey dashed lines/grey diamonds), heat (38°C ; green line/green triangles down), heat + low light (purple dash double-dotted lines/purple squares), heat + low light + ethylene (yellow circles), heat + ethylene (black triangles up). Angles resulted from pair wise subtraction; $n > 10$. Error bars represent SE.

allowed studying prioritization of the signals. The enhanced hyponastic growth response, as the result of simultaneous application of heat and low light, could be repressed by additional ethylene in Col-0 and *Ler* (Figure 3.5a, b). In agreement, the combinations heat and ethylene, repressed the enhanced amplitude of heat-treated *phyb* in both Col-0 and *Ler*, to a level similar to a single ethylene treatment (Figure 3.5c, d). Similarly, the ethylene overproducer; *eto1-1* (Figure 3.5f) and constitutive ethylene Signaling mutant *ctr1* (Figure 3.5g) lacked any additive effect of simultaneous application of low light and heat. Together, these data suggest that ethylene is a dominant negative signal with respect to heat-induced hyponastic growth.

Auxin Signaling and polar auxin transport are required for heat-induced hyponasty
Auxin and polar auxin transport (PAT) are required for low light-induced hyponastic growth in Arabidopsis (Millenaar *et al.*, 2009; Vandenbussche *et al.*, 2003) and auxin

plays a role in submergence-induced hyponasty in *Rumex palustris* (Cox *et al.*, 2004). Moreover, auxin has been associated earlier with responses to high temperature (Gray *et al.*, 1998, Koini *et al.*, 2009).

To test the involvement of auxin in heat-induced hyponasty, we pharmacologically inhibited the auxin efflux carriers with 2,3,5-Triiodobenzoic acid (TIBA) and naphthylphthalamic acid (NPA). These treatments reduced and abolished heat-induced hyponasty, respectively (Figure 3.6a). This indicates that auxin and PAT are required for heat-induced differential growth. We examined the expression of the auxin activity marker *IAA19/MSG2* (Tatematsu *et al.*, 2004) by quantitative-RT PCR. *IAA19/MSG2* mRNA levels did not change dramatically (<2 times for each time point), although expression is enhanced 3 to 6 h, after initiation of heat treatment compared to controls (Figure 3.6b) suggesting that our heat treatment might enhance auxin activity.

Auxin is perceived by the F-box protein TRANSPORT INHIBITOR RESPONSE1 (TIR1) and AUXIN SIGNALLING F-BOX proteins (AFB; Dharmasiri *et al.*, 2005a, b; Kepinsky & Leyser 2005). The *tir1* mutant showed a delayed response and a slightly reduced amplitude (Figure 3.6c), whereas the quadruple auxin receptor mutant; *tir1 afb1 afb2 afb3* exhibited a similar delay but also a strongly reduced hyponastic growth response amplitude (Figure 3.6d). This suggests that redundancy exists among the TIR/AFB proteins in heat signaling, with respect to hyponastic growth. In agreement with the pharmacological data, auxin efflux carrier mutants *pin-formed7* (*pin7*) and *pin3* showed delayed and abolished responses, respectively (Figure 3.6e, f). Together, these data suggest that auxin signaling and PAT are required for a fast induction and maximum amplitude of heat-induced hyponastic growth.

ABA is a positive regulator of heat-induced hyponastic growth

Abscisic acid (ABA) is a negative regulator of ethylene-induced hyponastic growth in *R. palustris* and *Arabidopsis* (Cox *et al.*, 2004; Benschop *et al.*, 2007). Application of exogenous ABA did not change the hyponastic growth response of the petiole to heat (Figure 3.7a). Application of the ABA biosynthesis inhibitor fluoridon repressed the amplitude of the response. This suggests that ABA is a positive regulator of heat-induced hyponastic growth and that endogenous ABA levels may saturate the response.

ABA INSENSITIVE1 (ABI1) is negative regulator of ABA signaling (Leung *et al.*, 1997; Hoth *et al.*, 2002). We found that *ABI1* expression was modestly enhanced (~2x at 3 h and 6 h) under heat treatment (Figure 3.7b), suggesting that heat may desensitize ABA signaling by enhanced *ABI1* expression. In agreement, the constitutive ABA hypersensitive *era1-2* mutant showed an enhanced heat-induced differential growth response (Figure 3.7c) and several ABA biosynthesis and ABA insensitive mutants (Figure 3.7d, g-i) showed repressed and delayed heat-induced hyponasty. In contrast, *aba2* (Figure 3.7e) exhibited a wild-type response and the amplitude of *aba3* (Figure 3.7f) was slightly enhanced. Overall, our results indicate that ABA and ABA signaling are positive regulators of heat-induced hyponastic growth.

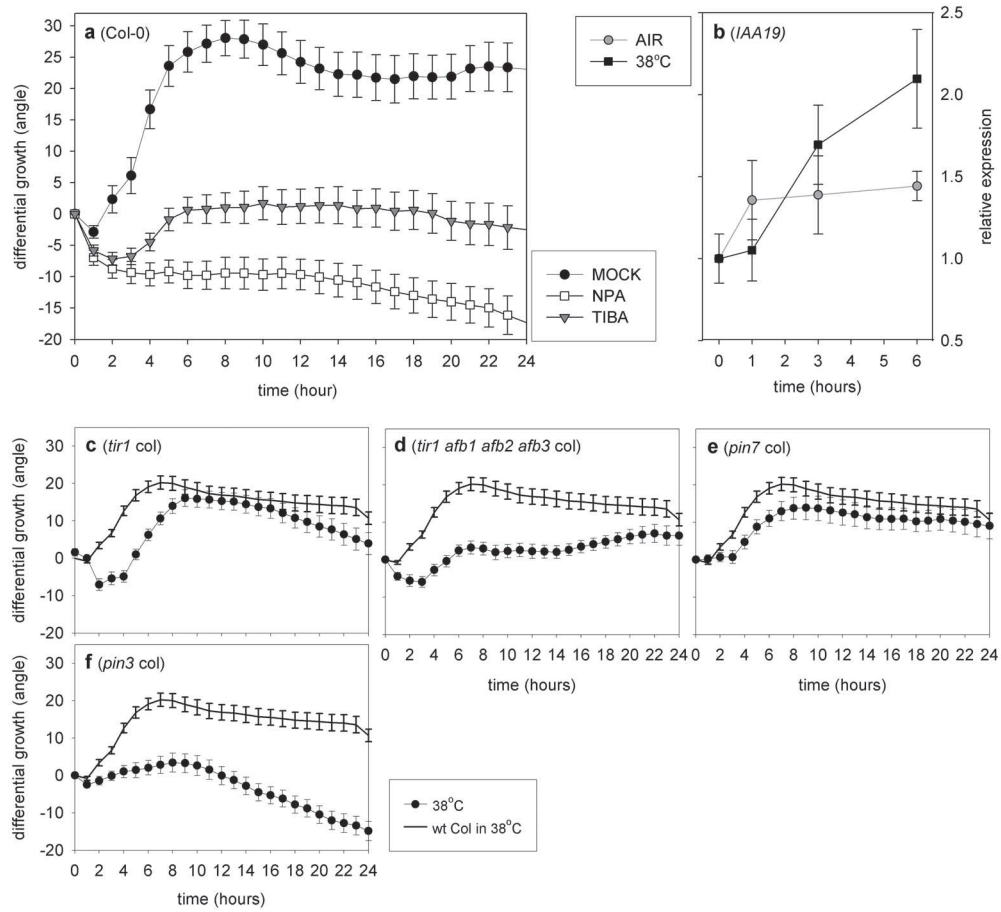


Figure 3.6: Role of auxin and polar auxin transport in heat-induced hyponastic growth a: Effect of heat treatment on Col-0 petiole angles in the presence of TIBA (grey triangles) and NPA (white squares) (both 50 μ mol), compared to mock treated wild type Col-0 (black circles). b: Quantitative Real-Time RT-PCR analysis of IAA19/MSG2 in air controls (grey circles) and heat treatment (black squares). Expression values are normalized to 1 at t=0 h (n \geq 4). c-f: Effect of heat on petiole angles of auxin Signaling and PAT mutants (black circles) compared to the wild type response (black lines). Angles are the result of pair wise subtraction; n \geq 10. Error bars represent SE.

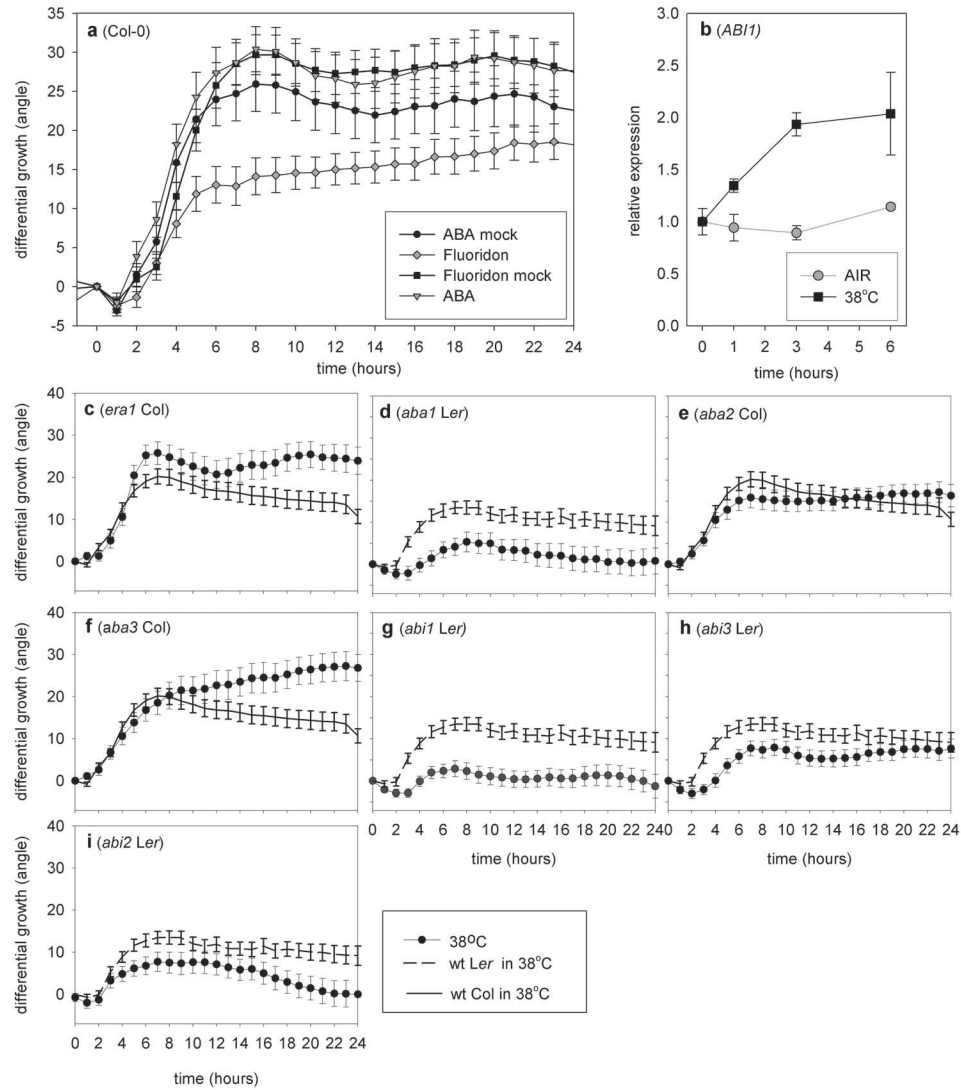


Figure 3.7: Role of ABA in heat-induced hyponastic growth. **a:** Effect of heat treatment on petiole angles of Col-0, treated with 20 μ M ABA (grey triangles) or soil-drained with 100 μ M fluoridon (grey diamonds) compared to their respective mock treatments (ABA; black circles, Fluoridon; black squares). **b:** Real-Time RT-PCR analysis of *ABI1* in control plants in air (grey circles) and upon heat treatment (black squares). Expression values are normalized to 1 at $t=0$ h ($n \geq 4$). **c-j:** Effect of heat on petiole angles of ABA related mutants (black circles) compared to the wild type response (black lines). Angles resulted from pair wise subtraction; $n > 10$. Error bars represent SE.

Discussion

Heat-induced hyponastic growth as an adaptive response

Petiole hyponasty is a resource directed reorientation of plant organs to escape from diminished growth conditions. The response is associated with escape from complete submergence and shade (Cox *et al.*, 2003; Millenaar *et al.*, 2005; Mullen *et al.*, 2006). Here, we studied the kinetics of elevated temperature-induced hyponastic growth in *Arabidopsis thaliana* and showed that petiole angles reversibly adjust, in a dose dependent manner, to changes relative to their growth temperature in a range of physiological relevant temperatures. This is in agreement with Millenaar *et al.* (2005), who found a modest increase in leaf angle when plants were transferred from 20°C to 30°C and with the observations of Koini *et al.* (2009). Notably, the strongest response was observed at ~38°C, after which the responses attenuated. This is in accordance with results of McCabe & Leaver (2000), who showed that a temperature of 38°C is just sub-lethal for Arabidopsis.

Strong natural variation was observed for amplitude of heat-induced hyponastic growth response among natural accessions (Figure 3.2). A latitudinal cline in initial leaf angles was described previously (Hopkins *et al.*, 2008). Yet, the observed high temperature response amplitude was not correlated with latitude. However, heat-response amplitude negatively correlated to diurnal temperature range at the accessions collection sites. Thus, accessions that on average face large daily temperature fluctuations in their natural habitat showed the weakest hyponastic growth response to heat. Tempering hyponastic growth may be adaptive to save resources in a strong fluctuating daily environment, while responding to temperature changes in an otherwise stable temperature environment may potentially bring fitness benefits. Leaf (re)positioning can be explained by functional arguments that steep leaf angles have efficient solar light capture in the morning and winter, whereas it may optimize photosynthesis by avoiding over-irradiation, excess heat-flux and extensive water loss, at midday and during summer (King, 1997; Falster & Westoby, 2003). In agreement, Fu & Ehleringer (1989) showed that heliotropic leaf movements in common bean (*Phaseolus vulgaris*) are controlled by air temperature and that leaves are positioned such that photosynthesis is close to optimal. Moreover, a positive correlation between leaf angles and air temperature has been observed in *P. vulgaris* and *P. acutifolius* (Yu & Berg 1994). Analogously, Gray *et al.* (1998) suggested that in Arabidopsis, heat-induced growth is employed to reposition the photosynthesizing tissues away from heated soil and consequently allow better access to evaporative cooling by moving air. Thus, heat-induced hyponastic growth in Arabidopsis may also be employed for optimization of photosynthesis.

Light Signaling interacts with heat in hyponastic growth

Light- and temperature Signaling are tightly connected (Mazzella *et al.*, 2000, Blazquez *et al.*, 2003; Penfield, 2008; Koini *et al.*, 2009). For example, early flowering of *phyb* mutants is repressed at low growth temperatures (16°C). In contrast, *phyA*,

phyD and phyE, acquire a more prominent functional role at 16°C (Halliday *et al.*, 2003; Halliday & Whitelam, 2003). This cross-talk is response-specific, as the typical, elongated, *phyb* phenotype is temperature independent (Halliday *et al.*, 2003). Moreover, phototropic curvature of Arabidopsis seedlings was delayed by increased temperatures (Orbovic & Poff, 2007).

Accordingly, our study established extensive cross-talk between light- and heat signaling with respect to hyponastic growth. Low light intensity enhanced the amplitude of heat-induced hyponastic growth (Figure 3.4), and this response was mimicked in *phyB* mutants. This is in agreement with the work of Larkindale & Knight (2002), who showed that heat-induced oxidative damage in Arabidopsis, was prevented in the dark. This indicates that oxidative damage to membranes resulted from photo-inhibition of the electron transport chain. Strikingly, a similar inhibition of photosynthesis related electron transport with 3-(3,4-dichlorophenyl)-1,1-dimethylurea (DCMU) induced hyponastic growth in normal light conditions (Millenaar *et al.*, 2009). This supports the notion that heat-induced hyponastic growth may indeed function to optimize photosynthesis and that the photosynthesis associated electron transport chain may be a potential integration point for both signals.

Altogether, our data show that low light sensitizes the plant to heat, resulting in an enhanced hyponastic response, or alternatively, heat desensitizes the plant for light (i.e. sensitizes it for low light) via the photoreceptor proteins. We can not conclusively distinguish between these options.

Hormonal control of heat-induced hyponastic growth

Ethylene action protects against, and facilitates in the repair of, heat-induced oxidative damage and predominantly functions in basal thermotolerance in Arabidopsis. In this respect, ethylene insensitive mutants were more susceptible to heat-induced oxidative damage (Larkindale & Knight, 2002; Larkindale *et al.*, 2005). In agreement with this, our data on ethylene production, insensitive and hypersensitive/overproducing mutants, together with pharmacological data (Figure 3.3), strongly suggests that ethylene is a negative regulator of heat-induced hyponastic growth. In contrast to other ethylene insensitive mutants, *ethylene insensitive 2 (ein2)* however, did not show an enhanced hyponastic phenotype (Figure 3.3). This might be explained by the observation that *ein2* contains enhanced ABA levels (Ghassemian *et al.*, 2000), a factor that we identified as positive modulator of heat-induced hyponastic growth (Figure 3.7).

Ethylene is the pivotal trigger of submergence-induced differential petiole growth in Arabidopsis and others species (Cox *et al.*, 2003; Millenaar *et al.*, 2005; Benschop *et al.*, 2007), but was not required for low light-induced hyponastic growth (Millenaar *et al.*, 2009). The combined (triple) ethylene + low light + heat treatment repressed the cumulative effect of heat and low light on hyponastic growth (Figure 3.5). The combination treatment low light and ethylene did not result in an altered hyponastic growth response (Millenaar *et al.*, 2005). We therefore conclude that the inhibitory effect of ethylene in the triple-combination (heat + low light + ethylene;

Figure 3.5) treatment is due to repression of specifically heat Signaling components, rather than low light specific components.

Altogether, the data suggest that ethylene is a general antagonist of heat effects in Arabidopsis. However, temperature increase (20°C to 29°C) induced hypocotyl elongation independent of ethylene action (Gray *et al.*, 1998). This might implicate that the specific regulation of heat-induced differential growth in hypocotyls differs from the regulation in vegetative adult plants (this study) and seedlings (Larkindale & Knight, 2002; Larkindale *et al.*, 2005), or alternatively, that ethylene is not required *per se* in the response to relatively mild temperature increase used by Gray *et al.* (1998).

Remarkably few studies described the role of auxin in temperature related processes, whereas the roles of auxin and polar auxin transport are relatively well understood in differential growth responses, including hyponasty (Vandenbussche *et al.*, 2003; Cox *et al.*, 2004; Millenaar *et al.*, 2009; Van Zanten *et al.*, 2009a; Chapter 2). Enhanced levels of free auxin have been observed in high temperature treated Arabidopsis hypocotyls (Gray *et al.*, 1998). Furthermore, auxin was required for high temperature-induced hypocotyl elongation. This is in agreement with our pharmacological and mutant analysis showing that auxin is required for heat-induced differential growth. IAA19/MSG2 marker gene expression in petiole tissue tended to increase during 38°C heat treatment, although differences were small. This is consistent with the observations made by Gray *et al.* (1998) and Koini *et al.* (2009), who showed increased expression of the auxin-responsive genes IAA4 and IAA29 in hypocotyls upon heat treatment (29°C and 28°C respectively) and suggests that heat may sensitize the petioles to auxin.

The auxin mediated regulation of heat-induced hyponastic growth shows remarkable parallels with low light-induced hyponastic growth that was also attenuated by TIBA and abolished by NPA treatment (Millenaar *et al.*, 2009; Chapter 2). Moreover, similar to heat- a full induction of low light-induced hyponasty required AFB1, AFB2, AFB3, TIR1, PIN3 and PIN7 (Millenaar *et al.*, 2009).

ABA is involved in the induction of acquired thermotolerance in bromegrass (*Bromus inermis* Leyss), maize (*Zea mays*), creeping Bentgrass (*Agrostis stolonifera*) and Arabidopsis (Robertson *et al.*, 1994; Larkindale & Huang, 1994; Gong *et al.*, 1998; Larkindale & Knight, 2002). Moreover, heat stimulates ABA synthesis in Arabidopsis seeds, which prevents germination at non-optimal temperatures (Toh *et al.*, 2008). In contrast, ABA does not seem to be involved in high temperature-induced hypocotyl elongation (Gray *et al.*, 1998).

ABA is a negative regulator of ethylene-induced hyponastic growth in Arabidopsis (Benschop *et al.*, 2007) and submergence-induced hyponasty in *Rumex palustris* (Cox *et al.*, 2004). In sharp contrast, our data showed that ABA is a positive regulator of heat-induced hyponastic growth (Figure 3.7). However, not all tested ABA related mutants exhibited reduced heat-induced hyponastic growth. *Aba2-1* and *aba3-1* showed a normal, or even slightly exaggerated, heat-induced response, which

might be due to their leaky nature (Léon-Kloosterziel *et al.*, 1996). Nonetheless, these lines also show enhanced ethylene release (LeNoble *et al.*, 2004) and ethylene is a negative regulator of heat-induced hyponastic growth (Figure 3.3). This negative interfere with, and contribute why *aba2* and *aba3* had a close to wild type/exaggerated response. In agreement, *aba2* and *aba3* showed only moderate effects on acquired and basal thermotolerance, relative to *abi1-1* and *abi2-1* (Larkindale *et al.*, 2005). However, the same was true for *aba1* and *abi3*, lines that did show a marked reduced heat-induced hyponastic growth response. Additionally, *aba2-1* and *aba3-1* were affected in ethylene-induced hyponastic growth (Benschop *et al.*, 2007).

Vice versa, *aba1-1* and *abi2-1* did not show an altered response to ethylene, but did show a clear reduced amplitude upon heat treatment and *aba1-1*, *abi1-1*, *abi3-1* and *abi2-1* exhibited an decreased hyponastic response to heat and were unaffected (*aba1-1*, *abi2-1*) or enhanced (*abi1-1*, *abi3-1*) in ethylene (Benschop *et al.*, 2007). Overall, these data suggest that the net effects of ABA on ethylene- and heat-induced hyponastic growth are opposite, and that the ABA-related genetic components employed in the regulation of the response, differ between the treatments.

ABI1 is a negative regulator of ABA Signaling and ethylene-induced hyponastic growth (Benschop *et al.*, 2007). ABI expression was enhanced by ethylene (De Paepe *et al.*, 2004; Benschop *et al.*, 2007) and ABA (Leung *et al.*, 1997; Hoth *et al.*, 2002) application. During heat treatment, ABI1 acts as a positive regulator of differential growth. Yet, ABI1 transcription was enhanced during heat treatment (Figure 3.7b). This suggests that heat modulates (desensitizes) hyponastic growth partly via transcriptional regulation of ABI1.

Conclusions

Regulation of hyponastic growth is complex and different environmental stimuli are integrated in control of differential petiole growth in *Arabidopsis thaliana*. We demonstrated that ethylene act as dominant negative regulator, and auxin and ABA are positive regulators of heat-induced hyponastic growth. Heat and low light act additively on hyponastic growth. Ethylene-induced hyponastic growth is independent from auxin Signaling (Millenaar *et al.*, 2009; Van Zanten *et al.*, 2009a; Chapter 2) and ABA is a negative regulator of ethylene-induced hyponasty (Benschop *et al.*, 2007). In contrast, low light-induced hyponasty depends on auxin and is independent of ethylene Signaling (Millenaar *et al.*, 2009). Thus, factors required for heat-induced hyponastic growth are both overlapping and different from low light and ethylene Signaling towards hyponastic growth.

Nevertheless, the similarities in kinetics suggest that the Signaling routes may converge and affect a similar set of functional components (Millenaar *et al.*, 2009; Chapter 2). Recently, Koini *et al.* (2009) demonstrated that heat-induced hyponasty was abolished in the *phytochrome interaction factor 4* (*pif4*) mutant. PIF4 is required for induction of shade avoidance phenotypes. Active phyB physically interacts with PIF4 and target the protein for degradation, and subsequently inhibits cell elongation (Huq *et al.*, 2002; Lorrain *et al.*, 2008). Accordingly, *phyb* constitutive shade

avoidance phenotypes are abolished in *phyb pif4* double mutants. Heat induces a transient increase in PIF4 levels (Koini *et al.*, 2009). Together, these data facilitate a model in which phyB dependent low light Signaling (Millenaar *et al.*, 2009) and heat Signaling towards hyponastic growth converges on PIF4. Our results suggest that loss-of *phyA* counteracted the enhanced hyponastic growth phenotype of *phyB* (Figure 3.4). In agreement, *phyA* responses do not involve PIF4 action and *phyA* may be dominant over *phyB* in this response (Huq *et al.*, 2002).

Materials and Methods

Plant material and growth conditions

Seeds were from the Nottingham Arabidopsis Stock Centre (NASC accessions numbers between brackets) or were a gift of the author who described the line. All accessions are described in Table S3.1. Ethylene mutants are all in Col-0: *ctr1* (N8075; Kieber *et al.*, 1993), *ein2-1* (N3071; Guzman & Ecker, 1990), *ein4-1* (N8053; Roman *et al.*, 1995), *eto1-1* (N3072; Guzman & Ecker, 1993), *etr1-4* (Chang *et al.*, 1993); *etr1-6 ein4-4 etr2-3* (Hua & Meyerowitz, 1998). Photoreceptor mutants are in *Ler*, unless stated otherwise, *cry1 cry2 (hy4 fha1)*; Yanovsky *et al.*, 2000), *hy2* (N68; Koornneef *et al.*, 1980; Kohchi *et al.*, 2001), *phyA-201* (N6219; Nagatani *et al.*, 1993), *phyA-201 phyb-5* (N6224; Reed *et al.*, 1994), *phyb-9* in Col (Reed *et al.*, 1993). Auxin mutants are in the Col-0 background unless stated otherwise; *pin3-4* (N9363; Friml *et al.*, 2002), *pin7-1* (N9365; Friml *et al.*, 2003), *tir1-1* (N3798; Ruegger *et al.*, 1997), *tir1-1 afb1-1 afb2-1 afb3-1* in Col/Ws (Dharmasiri *et al.*, 2005b). ABA related mutants were in a Col or *Ler* background; *aba2-1* (N156; Leon-Kloosterziel *et al.*, 1996), *aba3-1* (N157; Leon-Kloosterziel *et al.*, 1996), *era1-2* (Cutler *et al.*, 1997), *aba1-1* (N21; Koornneef *et al.*, 1982), *abi1-1* (N22; Koornneef *et al.*, 1984; Leung *et al.*, 1994), *abi2-1* (N23; Koornneef *et al.*, 1984; Leung *et al.*, 1997), *abi3-1* (N24; Koornneef *et al.*, 1982). Plants were grown on a fertilized mixture of potting-soil and perlite (1:2; v/v) as described in Millenaar *et al.* (2005), at: 20°C, unless stated otherwise, 70% (v/v) relative humidity, 9 h photoperiod of 200 $\mu\text{mol m}^{-2} \text{s}^{-1}$ photosynthetic active radiation (PAR). Pots were automatically daily saturated with tap water at the start of the photoperiod.

Treatments

Plants in developmental stage 3.9 (Boyes *et al.*, 2001) were used for all experiments and were transferred to the experimental setups one day before treatment to allow acclimatization. Treatments always started ($t=0$) 1.5 h after photoperiod start, to minimize diurnal and/or circadian effects. Plants used for cold pre-treatment experiments were transferred to a low-temperature (10°C) cabinet, three weeks before treatment, with other conditions similar as described above.

Temperature increase was accomplished by moderating the program of the growth cabinet. 30°C was reached after ~22 minutes; 38°C was reached after ~45 minutes.

Low light was induced by reduction of the light intensities to 15-20 $\mu\text{mol m}^{-2} \text{s}^{-1}$ (PAR) by shading the plants with spectrally neutral shade cloth, which did not influence light quality as checked with a LICOR-1800 spectro-radiometer (LI-COR, Lincoln, NE, USA).

Ethylene was applied in continuous flow-through (75 l h⁻¹), in glass cuvettes containing one

plant each, as described in Millenaar *et al.* (2005) and Benschop *et al.* (2007). Ethylene (Hoek Loos, Schiedam, the Netherlands) and air (70% (v/v) relative humidity) were mixed using flow-meters to generate a concentration of $5 \mu\text{l l}^{-1}$, which is saturating for the hyponastic response (Millenaar *et al.*, 2005). Ethylene concentrations were checked regularly on a gas chromatograph (GC955, Synspec, Groningen, the Netherlands), and remained constant for the duration of the experiment. Control cuvettes were flushed with air (70% (v/v) relative humidity) at the same flow rate.

Pharmacological treatments

Gaseous 1-methylcyclopropene (1-MCP; $1 \mu\text{l l}^{-1}$; 'Ethylbloc' Floralife; Walterboro SC, USA) was applied 3 h prior to treatment as described in Millenaar *et al.* (2005), in the same cuvettes as used for ethylene treatment. 2,3,5-triiodobenzoic acid (TIBA; Duchefa, Haarlem, the Netherlands), Naphthylphalamic acid (NPA; Duchefa) and Absisic acid (ABA; Sigma-Aldrich, Sigma-Aldrich; Zwijndrecht; the Netherlands) were dissolved in MilliQ containing; 0.1% Tween 0.1% DMSO and 0.1% ethanol respectively, to a concentration of $50 \mu\text{M}$ (TIBA, NPA) and $20 \mu\text{M}$ (ABA). These solutions were sprayed on the plants. Fluoridon (Riedel-de Haën, Seelze, Germany) was dissolved in MilliQ containing; 0.1% Tween and 0.07% acetone (0.07%) to $100 \mu\text{M}$ and was applied to the soil, until saturation, to plants saved from watering for two days. All pre-treatments took place 66 h, 42 h and 18 h before the start of the experiment. Control plants (mock) were treated similarly with a pre-treatment solution lacking the active components.

Computerized image analysis of angle kinetics and calculations

Hyponastic growth kinetics measurements were conducted using an automated time-lapse photography setup (Cox *et al.*, 2003; Millenaar *et al.*, 2005; Benschop *et al.*, 2007). Plants were placed singly in glass cuvettes with petioles of study perpendicular to the camera. Leaves that were obscuring the petiole base were removed. Additionally, petioles were marked at the petiole/lamina junction with orange paint (Decofin, Apeldoorn, the Netherlands). These preparations did not influence the responses (data not shown). All conditions were kept to the conditions in the growth chambers until the experiment started.

Pictures of two petioles per plant were taken every 10 min. To enable continuous photography, no dark period was included in the 24 h experimental period. Angles were measured between the orange painted point at the petiole/lamina junction and a fixed basal point of the petiole, compared to the horizontal, by using KS400 (Version 3.0) software package (Carl Zeiss Vision, Hallbergmoos, Germany) and a customized macro. Angles were pair wise subtracted, which is the angle difference between treated and control plants at each time point (Benschop *et al.*, 2007) to correct for diurnal/circadian leaf movements of control plants. New standard errors were calculated by taking the square root from the summation of the two squared standard errors.

Plants used for single time-points angle measurements were manually photographed. Angles were measured using ImageJ; <http://rsb.info.nih.gov/ij>). For all replicate plants, angles of two petioles were averaged prior to further analysis.

Geographic climate data

Geographic parameters of the collection sites of individual accessions were taken from

the Natural Variation in Arabidopsis thaliana (NVAT) website: (<http://dbsgap.versailles.inra.fr/vnat/>), or from authors describing the accessions (Table S3.1). Environmental data of the collection sites (0.5° latitude × 0.5° longitude surface land area plots) of the used accessions were extracted from the *climate baseline data* from the Intergovernmental Panel on Climate Change (IPCC) Data Distribution Centre (DCC) (http://ipcc-ddc.cru.uea.ac.uk/obs/get_30yr_means.html), using a data subtraction tool, kindly provided by I. Wright (Macquarie University, Sydney, Australia). Mean annual data were calculated from monthly averages collected over a 30 years period (1961-1990; New *et al.*, 1999). When no plot existed on the precise location of origin the most nearby plot on the same latitude was used. Correlations were calculated in SPSS-Software 12.01, Chicago, IL, USA version 12 and were statistically compared by a Pearson (2-tailed) test.

Ethylene release

Ethylene release from rosettes was measured as described in Millenaar *et al.* (2005). Whole rosettes of ~300 mg were placed in a syringe. Ethylene was allowed to accumulate in the syringe for 15-20 minutes and subsequently analyzed on a gas chromatograph (GC955, Synspec). This short time frame prevented wound-induced ethylene production, which commenced only after 25 min (data not shown).

Real time Reverse Transcriptase-PCR

Col-0 petioles were snap frozen in liquid nitrogen. RNA was isolated from with the RNeasy extraction kit (Qiagen, Leusden, the Netherlands). gDNA removal, cDNA synthesis and Real-Time RT-PCR were performed as described by Millenaar *et al.*, (2005, 2009). Real-time RT-PCR data were calculated with the comparative C_t method (Livak & Schmittgen, 2001) expressing mRNA values relative to β-Tubulin-6. Primers used are listed in Table S3.3.

Acknowledgements

The authors thank Ronald Pierik (Utrecht University) for comments on the manuscript, Maarten Terlouw (Utrecht University) for technical assistance, Ian Wright (Macquarie University, Sydney, Australia) for software tools and M. Estelle, M. Koornneef, C. Lin, G.E. Schaller and G.C. Whitelam, for sharing mutant lines.

Supporting Information

- **Figure S3.1:** Correlation between amplitude of heat-induced hyponastic growth and geographic parameters.
- **Table S3.1:** Natural variation in response to heat in Arabidopsis accessions.
- **Table S3.2:** Correlations between heat-induced differential petiole growth and geographic and climate data at the collection sites of the used Arabidopsis accessions.
- **Table S3.3:** Primers used for Real-Time RT-PCR in this study.

Supporting Information

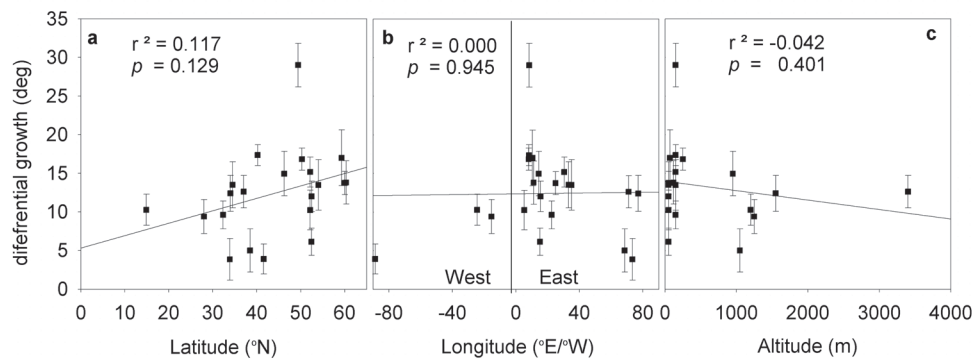


Figure S3.1: Correlation between amplitude of heat-induced hyponastic growth and geographic parameters a: latitude. b: longitude and c: altitude of the collection sites of the individual accessions. Numbers show Pearson correlation (r^2 value) and the significance levels (2-tailed; p value). The connecting line results from linear regression. Error bars represent SE.

Table S3.1: Natural variation in response to heat in *Arabidopsis* accessions. Names, abbreviations, stock numbers (NASC ID), Petiole angle response (0 h–7 h degrees), latitudinal origin (degrees North; °N), longitudinal origin (degrees East(E)/West(W)), altitudinal origin and diurnal temperature range, of 21 *Arabidopsis* accessions. Standard errors of the response never exceeded 3.6 degrees. The latitudes of the collection sites of individual accessions were taken from the Natural Variation in *Arabidopsis thaliana* (VNAT) website: (<http://dbsgap.versailles.inra.fr/vnat/>) unless stated otherwise.

		Stock ID	Reponse 0 h-7 h	Latitude °N	Altitude m	Longitude °E/°W	Diurnal Range °C
Bensheim-0	Be-0	N964	29.0	49.4	150	E8.4	8.8
C24 ^d	C24	N906	17.4	40.2	150	E8.2	7.5
Canary Islands-0 ^a	Can-0	N1064	9.4	28.0	1250	W15.3	6.7
Chisdra-1	Chi-1	N1074	13.5	54.0	150	E35.0	8.0
Columbia-0	Col-0	N1092	6.1	52.4	50	E15.2	8.1
Cape Verde Island-0 ^a	Cvi-0	N902	10.3	14.9	1200	W24.4	14.8
Helsinki-1 ^a	Hel-1	N1222	13.7	60.0	50	E25.0	7.7
Hiroshima-1 ^{a,e}	Hir-1	JW102	13.5	34.5	50	E33.2	10.1
Kärnten-0	Ka-0	N1266	15.0	46.3	950	E14.3	8.2
Kashmir-1	Kas-1	N903	17.0	34.0	70	E77.0	11.7
Knox-10	Knox-1	N22566	12.4	41.6	1550	W88.6	11.2
Kondana-Tady	Kond	N916	3.9	38.5	ND	E68.5	13.8
Landsberg erecta	Ler	NW20	5.0	52.5	1050	E15.5	8.2
Moss ^c	Moss		12.0	59.3	50	E10.4	7.2
Martuba/Cyrenaika-0	Mt-0	N1380	9.6	32.3	150	E22.5	11.4
Niederzenz-1	Nd-1	N1636	16.8	50.3	250	E8.0	7.9
Pakistan-1 ^b	Pak1	JW105	3.9	33.9	ND	E73.4	13.3
RLD-1	RLD-1	N913	10.2	52.2	50	E5.	7.9
Shahdara	Shah	N929	12.6	37.0	3400	E71.0	10.5
Stange ^c	Stange		13.8	60.3	120	E11.1	8.5
Wassilewskija-2	WS-2	N915	15.2	52.1	150	E30.4	8.6

Footnotes:

- a No climate data was available on the 0.5° latitude × 0.5° plots for these locations, therefore average values of nearby plots on the same latitude were used.
- b Geographic characteristics were obtained from El-Lithy et al. (2004), seeds were provided by Maarten Koornneef (Wageningen University, the Netherlands).
- c Geographic characteristics were obtained from Stenøien et al. (2005), seeds were provided by Maarten Koornneef (Wageningen University, the Netherlands).
- d C24 most likely originates from the Portuguese accession; Coimbra (Schmid et al., 2006), we used the Coimbra geographic characteristics (NVAT) in our analysis.
- e Hiroshima-1 was obtained from the Sendai *Arabidopsis* Seed Stock Center (Miyagi University of Education, Japan)

Table S3.2: Correlations between heat-induced hyponastic growth and geographic and climate data at the collection sites of the used *Arabidopsis* accessions.

Environmental parameters presented in this table are mean annual data (of 0.5° latitude × 0.5° longitude land area surface plots), calculated from monthly averages, collected over a 30 years period (1961-1990; New et al., 1999). Total irradiation was converted from W m⁻² to μmol m⁻² s⁻¹ as average for 24 hours using the conversion factor 4.57 for the PAR spectrum (400-700 nm) as described in Jones (1983). Correlations are; 2-tailed Pearson correlation coefficient; ns = non-significant; * *p*<0.05.

	Parameter	Correlation (r ²)	Sign.
Mean Temperature	°C	0.353	ns
Diurnal Range	°C	-0.525	*
Maximum Temperature	°C	-0.325	ns
Minimum Temperature	°C	-0.274	ns
Precipitation	mm day ⁻¹	-0.192	ns
Annual amount of wet days	day	0.117	ns
Vapor pressure	hPa	-0.359	ns
Cloud Coverage	%	0.132	ns
Irradiation	μmol m ⁻² s ⁻¹	0.397	ns

Table S3.3: Primers for Real-Time RT-PCR analysis used in this study. Primers, with AGI codes of the corresponding genes, were custom designed except β-Tubulin-6 (Czechowski et al., 2004) and BLAST searched to confirm uniqueness.

β-Tubulin-6	At5g12250	5'-ATAGCTCCCGAGGTCTCTC-3'
		5'-TCCATCTCGTCCATTGCTTC-3'
ACC-oxidase 4	At1g05010	5'-TATAATCCGGGAAGCGACTC-3'
		5'-GCTTCTTTTCCGATCAGCTC-3'
ERS2	At1g04310	5'-ACGCTTGCCAAAACATTGTA-3'
		5'-TGAGACGCTTTTACCAAAC-3'
IAA19	At3g15540	5'-GGCTTGAGATAACGGAGCTG-3'
		5'-ACCATCTTTCAAGGCCACAC-3'
HFSA2	At2g26150	5'-GTCTCCGTCGTCGTGGTATT-3'
		5'-CGGGAGAATAACTCCGATCA-3'
ABI1	At4g26080.1	5'-TGAAGAAGCGTGTGAGATGG-3'
		5'-CTGTATCGCCAGCTTTGACA-3'

**Abscisic acid is a positive regulator of
low light-induced hyponastic petiole growth in
Arabidopsis thaliana and GCR2 controls this
independent of ABA**

Martijn van Zanten, L. Basten Snoek[§], Laurentius A.C.J. Voesenek,
Anton J.M. Peeters, Frank F. Millenaar[§]

Plant Ecophysiology, Institute of Environmental Biology, Utrecht University,
Padualaan 8, 3584 CH Utrecht, the Netherlands

[§]Present addresses:

FFM: De Ruiter Seeds, Leeuwenhoekweg 52, 2660 BB Bergschenhoek,
the Netherlands.

LBS: Department of Nematology, Wageningen University and Research
Center, Binnenhaven 5, 6709 PD Wageningen, the Netherlands.

Abstract

Upward movement of leaf blades (hyponastic growth), driven by differential petiole growth, is a mechanism used by plants to avoid limited resource availability such as low light levels in dense vegetations. The plant hormone abscisic acid (ABA) is known to antagonize the hyponastic growth response triggered by ethylene in *Arabidopsis thaliana* and is an enhancer of hyponastic growth induced by transferring plants to high temperatures (Chapter 3).

Increasing literature evidence suggests tight connections between light Signaling and ABA. We investigated the role of ABA in low light intensity-triggered hyponastic growth which is phenotypically similar to ethylene- and heat-induced hyponastic growth. Using a combination of pharmacological inhibition of ABA biosynthesis, mutant analysis and transcriptome analysis, we show that ABA acts as a positive modulator of low light-induced hyponastic growth in an ethylene independent manner. Moreover, we demonstrate that the ABA biosynthesis gene *ZEAXANTHIN EPOXIDASE* (*ABA1*) is a positive regulator whereas *ERA1*, *ABA2* and *ABA3* are negative regulators of low light-induced hyponastic growth. The response is, however, independent of other ABA Signaling components such as *ABI1*, *ABI2*, *ABI3* and *ABI5*. Furthermore, we provide evidence that both low light and ethylene induce transcription of the ABA perception associated protein *GPA1*, and that loss-of-function mutations in this gene represses low light- and ethylene-induced hyponastic growth. Moreover, the reported *GPA1* associated *GCR2* and the *GCR2* LIKE PROTEINS (*GCL1* and *GLC2*) act redundantly as positive regulators of low light-induced hyponasty. We demonstrate however that *GCR2* family genes control low light-induced hyponastic growth independent of ABA, as a knock-out mutant lacking the three *GCR2* family gene members, retained sensitive for repression of hyponastic growth by pharmacological inhibition of ABA biosynthesis. These results are in line with accumulative evidence that *GCR2* does not function as an ABA receptor, but do indicate that *GCR2* controls growth responses to light.

Introduction

Light levels are severely affected, in terms of quantity and quality, in developing vegetations and limit plant growth. Some species utilize differential growth of petioles, resulting in leaf inclination (hyponastic growth), as a mechanism to escape from the limiting resources. This response redirects leaves away from for example submergence or shade conditions (Ballaré, 1999; Cox *et al.*, 2003, 2004; Pierik *et al.*, 2004a, 2005; Millenaar *et al.*, 2005). In some species, including semi aquatic *Rumex palustris*, hyponastic growth is followed by non-differential petiole elongation (Voesenek & Blom, 1989; Cox *et al.*, 2003; Pierik *et al.*, 2004a). This mechanism ensures the plant to elongate only if leaves are sufficiently vertical to reach the water-surface or improved light conditions (Cox *et al.*, 2003).

Low light intensity, transfer to complete darkness and transfer to high

temperatures (heat), triggers hyponastic growth in *Arabidopsis thaliana* (Hangarter, 1997; Millenaar *et al.*, 2005; Koini *et al.*, 2009; Chapter 3). Low light conditions are sensed via photosynthesis related signals and by the photoreceptor proteins; cryptochrome1 (*cry1*), *cry2*, phytochrome A (*phyA*) and *phyB* (Millenaar *et al.*, 2009). The phytohormone ethylene, which accumulates in submerged plants, triggers a similar hyponastic growth response in submerged *Arabidopsis thaliana* (Millenaar *et al.*, 2005). Yet, genetic and pharmacological data indicated that the hyponastic growth in response to reduced light intensity is ethylene independent (Millenaar *et al.*, 2009; Chapter 2) and that ethylene is a negative regulator of heat-induced hyponastic growth (Chapter 3). Furthermore, ethylene-induced hyponasty in *Arabidopsis* is independent of auxin and polar auxin transport (Van Zanten *et al.*, 2009a; Chapter 2) whereas the response to low light and heat does require auxin and proper polar auxin transport (Millenaar *et al.*, 2009; Koini *et al.*, 2009; Chapter 2; Chapter 3). This indicates that ethylene, low light and heat induce hyponastic growth via parallel signal transduction routes. Nevertheless, given the similarity in response phenotype, they probably share functional genetic components downstream.

The phytohormone abscisic acid (ABA) is a negative regulator of ethylene-induced hyponastic growth in *Rumex palustris* (Cox *et al.*, 2004), submergence tolerant deepwater rice (*Oryza sativa* L.; Hoffmann-Benning & Kende, 1992) and *Arabidopsis* (Benschop *et al.*, 2007). In contrast, ABA is a positive modulator of heat-induced hyponastic growth (Chapter 3). Increasing evidence in literature indicates that light- and ABA signaling are tightly connected (Wheatherwax *et al.*, 1996; Kozuka *et al.*, 2005; Seo *et al.*, 2006; Mullen *et al.*, 2006; Chen *et al.*, 2008). Thus far, little is known on the functional interactions between light and ABA. In this study we aimed to describe the role of ABA in low light-induced hyponastic growth. Using a combination of pharmacological experiments, mutant analyses and transcriptome analysis, we demonstrate that ABA is a positive modulator of low light-induced differential growth. The reported ABA receptor GCR2 and its reported associated proteins; GPA1, GCL1 and GCL2 do also control hyponastic growth. However, a triple loss-of-function *gcr2 gcl1 gcl2* mutant retains sensitivity to repression of low light-induced hyponastic growth by application of the ABA biosynthesis inhibitor fluridone. We therefore conclude that the GCR2 gene family plays a role in differential growth responses, but does so, likely independent of ABA. This is in line with the accumulating literature evidence sceptical about the role of GCR2 as an ABA receptor.

Results

ABA is a positive modulator of low light-induced hyponastic growth

To evaluate if abscisic acid (ABA) is involved in the regulation of low light-induced hyponastic growth in *Arabidopsis thaliana*, we first assessed if ABA related gene ontology (GO) classes were enriched after 3 h of low light treatment in Columbia-0

(Col-0) petioles (Millenaar *et al.*, 2006). Within the 2792 genes that were significantly ($p < 0.05$) differentially regulated between low light and control conditions, 217 significantly enriched ($p < 0.01$ level) GO classes were identified (Supporting information Table S4.1). Thirteen of these GO classes were hormone related (Table 4.1). Among these were ABA related GO classes, 'response to ABA stimulus' and 'ABA metabolism'. These results suggest that low light modulates the expression of ABA related genes.

To test the functional role of ABA in low light-induced hyponastic growth, we pharmacologically inhibited ABA biosynthesis in Col-0 plants using fluoridon and subsequently monitored the kinetics of low light-induced hyponastic growth in a digital time-lapse camera setup (Cox *et al.*, 2004; Millenaar *et al.*, 2005). Fluoridon treatment reduced the hyponastic growth response during the whole experimental period (Figure 4.1a). We also applied ABA to Col-0 plants and as expected (Benschop *et al.*, 2007) this led to a significantly reduced initial petiole angle in control plants (16.0 ± 1.0 vs. 10.3 ± 0.7 degrees; $p < 0.001$). This pre-treatment did not affect the response to low light, compared to wild type (data not shown). Together, this suggests that ABA is i) a positive modulator of low light-induced hyponastic growth and ii) that endogenous ABA likely saturates the response.

To confirm this, we tested the response to low light in the ABA deficient *aba1-1* mutant, which is mutated in *zeaxanthin epoxidase*, catalyzing an early ABA biosynthesis step. This line showed a reduced response, similar to fluoridon treated plants (Figure 4.1b). In agreement with ABA pre-treatment, the ABA hypersensitive mutant *enhanced response to ABA1-2 (era1-2)* mutant which is disturbed in FARNESYL TRANSFERASE, had a wild type response up to 14 h after induction of low light, but exhibited an enhanced response thereafter (Figure 4.1c).

In contrast to *aba1-1*, petiole angles of two other mutants for factors in the last biosynthetic steps towards ABA; *aba3-1* (mutant for molybdenum cofactor sulfurase) and *aba2-1* (mutant for short-chain dehydrogenase/reductase) were higher than wild type plants after 14 h (Figure 4.2a, b). Additionally, *aba2-1* also showed a tendency of enhanced hyponastic growth relative to wild type during the first 14 h of treatment. The *aba insensitive* mutants *abi1-1*, *abi2*, *abi3-1* and *abi5* did not show altered differential growth under low light conditions (Figure 4.2c-f). Together, these results suggest that ABA is a positive modulator of low light-induced hyponastic growth and that the Signaling requires functional ABA1. In contrast, ABA2, ABA3 and ERA1 are negative regulators of high leaf angle maintenance (angles after 14 h of treatment). Other ABA related genes; ABI1, ABI2, ABI3 and ABI5, seem not to be involved in low light-induced hyponastic growth.

ABA control of low light-induced hyponastic growth is ethylene independent

Ethylene release is enhanced in young vegetative tissues of ABA deficient (*aba2-1*) mutant plants (LeNoble *et al.*, 2004). Moreover, the constitutive ethylene Signaling mutant; *constitutive triple response1 (ctr1)* and the ethylene insensitive *ethylene insensitive2 (ein2)* mutant, respectively enhanced and suppressed *abi1* effects (Beaudoin *et al.*, 2000). Because ethylene triggers hyponastic growth in Arabidopsis

(Millenaar *et al.*, 2005), it is possible that the enhanced hyponastic growth response in low light conditions observed in *aba2-1* and *aba3-1* (Figure 4.2a) is due to ethylene action. To test this, we measured ethylene release of a selection of ABA- biosynthesis, insensitive and hypersensitive mutants in control light conditions (Figure 4.3a, b). In accordance with LeNoble *et al.* (2004), we found a significant ($p < 0.001$) increase in ethylene release in *aba2-1* and in *aba3-1* (Figure 4.3a).

The ABA hypersensitive *era1-2* line released significantly less ($p < 0.01$) ethylene

Table 4.1: Hormone related Gene Ontology (GO) classes of genes that were significantly transcriptional regulated by low light-treatment, compared to air control. GO categories were only considered when a hypergeometric test resulted in $p < 0.01$. 'Regulated' represent the number of genes regulated by low light within a GO group. 'Total' represents the total number of genes within a GO group. Statistical differences are p -values. GO term IDs represents the GO group and were obtained from the GO consortium (www.arabidopsis.org).

ID	GO term ID	ID number	Regulated	Total	Significance (p value)
7	auxin (response to stimulus)	gO:0009733	42	254	<0.01
3	ABA (response to stimulus)	gO:0009737	35	185	<0.01
20	jasmonic acid (response to stimulus)	gO:0009753	23	116	<0.01
12	ethylene (response to stimulus)	gO:0009723	20	101	<0.01
77	salicylic (response to stimulus)	gO:0009751	20	100	<0.01
53	jasmonic acid (biosynthetic process)	gO:0009695	7	23	<0.01
131	brassinosteroid (mediated signaling)	gO:0009742	6	17	<0.01
61	auxin (indoleacetic acid biosynthetic process)	gO:0009684	5	8	<0.001
26	brassinosteroid (biosynthetic process)	gO:0016132	4	12	<0.001
10	auxin (binding)	gO:0010011	3	5	<0.01
31	auxin (efflux transmembrane transporter activity)	gO:0010329	2	4	<0.01
37	ABA (metabolic process)	gO:0009687	2	3	<0.01
69	auxin (basipetal transport)	gO:0010540	2	2	0

compared to wild type plants, whereas *era1-2*, like *aba2-1* and *aba3-1* also displayed enhanced hyponastic growth after 14 h of low light treatment (Figure 4.1c). In contrast, ethylene release in *aba1-1* was similar to wild type, whereas low light-induced hyponasty was repressed in this line (Figure 4.1b). In conclusion, although mutations in some ABA associated genes affect ethylene release, no consistent effect on low light-induced hyponastic growth was observed, suggesting that ABA modulation of low light-induced hyponasty cannot be explained by altered ethylene production. However, we cannot rule out that the enhanced response to low light is due to interference of ethylene in individual lines.

Additionally, out of several tested ABA associated genes, only *ABI1* was identified

to be transcriptional up-regulated by ethylene (Benschop *et al.*, 2007). mRNA levels of *ABI1* were not affected by low light treatment as measured by Real-Time RT-PCR (Figure 4.3c, d). Because the *abi1-1* mutant had wild type levels of ethylene release (Figure 4.3b) and also hyponastic growth induced by low light was unaltered (Figure 4.2c), low light does not seem to desensitize petioles for ABA via *ABI1*. This confirms that low light-induced hyponastic growth is modulated by ABA in an ethylene independent manner and does not involve crosstalk via *ABI1*.

The GCR2 gene family controls differential growth independent of ABA Signaling

To further specify which ABA related genes may modulate low light-induced hyponastic growth, we assessed transcriptional regulation of ABA biosynthesis and catabolism related genes in petiole tissues treated for 3 h with low light (described in Benschop *et al.*, 2007; Table 4.2). Three genes were down regulated in these low light conditions; the 707 family (*CYP707A2*) member *CYTOCHROME P450* (catabolism), the inositol polyphosphate 1-phosphatase: *FIERY1* (*FRY1*) and *ISP5P2*, an inositol-polyphosphate 5-phosphatase (signal transduction). Two genes were significantly up regulated by low light; *ISP5P* member (*ISP5PI*, signal transduction), a Rho-like GTP binding protein 6 (*ROP6/AtRac*, small GTPases, signal transduction). No regulation of *ABI1* was found on these micro-arrays, confirming the results

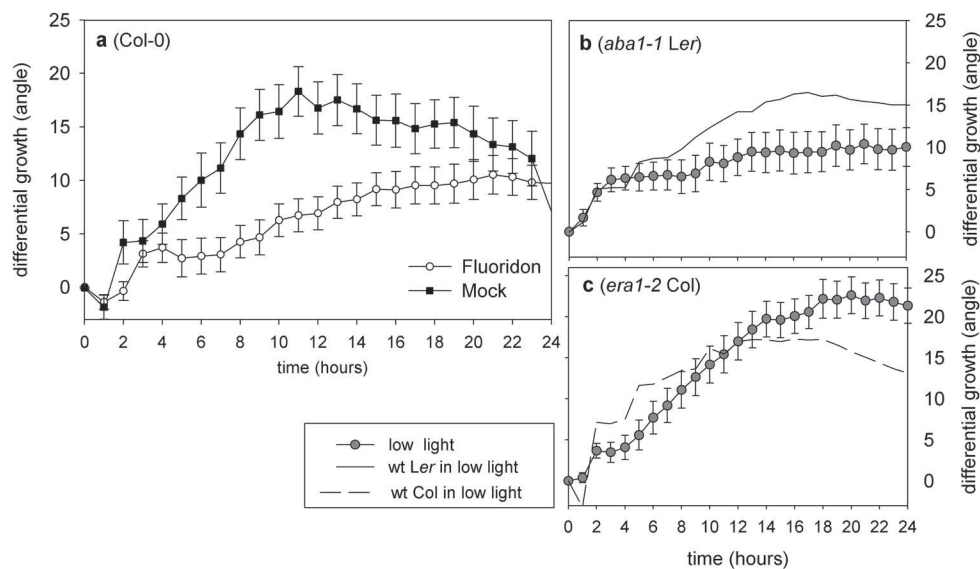


Figure 4.1: Effect of low light on petiole angles of fluoridone treated plants, ABA deficient- and ABA hypersensitive mutants. Response kinetics of plants a: treated with 100 μ M fluoridone (white circles) or mock solution (black square), b: *aba1-1* (grey circles) and *Ler* (closed line), c: *era1-2* (grey circles) and *Col-0* (dashed line), subjected to low light (15-20 μ mol $m^{-2} s^{-1}$). Angles resulted from pair wise subtraction in all cases. Error bars represent SE; $n \geq 10$.

obtained with Real-Time RT-PCR (Figure 4.3c, d).

Next, we assessed transcription of genes involved in ABA perception. Because most of these genes were only recently identified and not incorporated in the work of Benschop *et al.*, (2007), we also assessed if their expression was induced by ethylene (Table 4.3). Interestingly, the ABA receptor; *PYRABACTIN RESISTANT1* (*PYR1*) (Park *et al.*, 2009; Ma *et al.*, 2009) was significantly up-regulated under low light conditions and down-regulated when treated with ethylene treatment. *PYR1-LIKE5* (*PYL5*) and (*PYL8*) showed enhanced transcription after both ethylene and low light treatment. Expression of the G protein alpha-subunit; *GPA1*, was significantly ($p=0.001$) increased by 55% in low light (Table 4.3). Additionally, 3 h of ethylene treatment also resulted in mild, but significant, induction of *GPA1* expression in petiole tissues (Table 4.3). *GPA1* was proposed to physically and genetically interact with the putative G Protein-Coupled Receptor (GPCR); *GCR2*, which was proposed to be an ABA receptor (Liu *et al.*, 2007). However, the ABA binding properties, as well as the annotation as a GPCR are still heavily under debate (Johnston *et al.*, 2007; Guo *et al.*, 2007; Gao *et al.*, 2008; Illingworth *et al.*, 2008; Risk *et al.*, 2009).

Expression of *GCR2*, the *GCR2-LIKE* genes (*GCL1* and *GCL2*; Guo *et al.*, 2008) and the proposed ABA receptors *Mg-chelatase* (*CHLH*) *ABAR* (Shen *et al.*, 2006) and a GPCR-type G protein 2 (*GTG2*; Pandey *et al.*, 2009; *GTG1* was not represented on the micro-

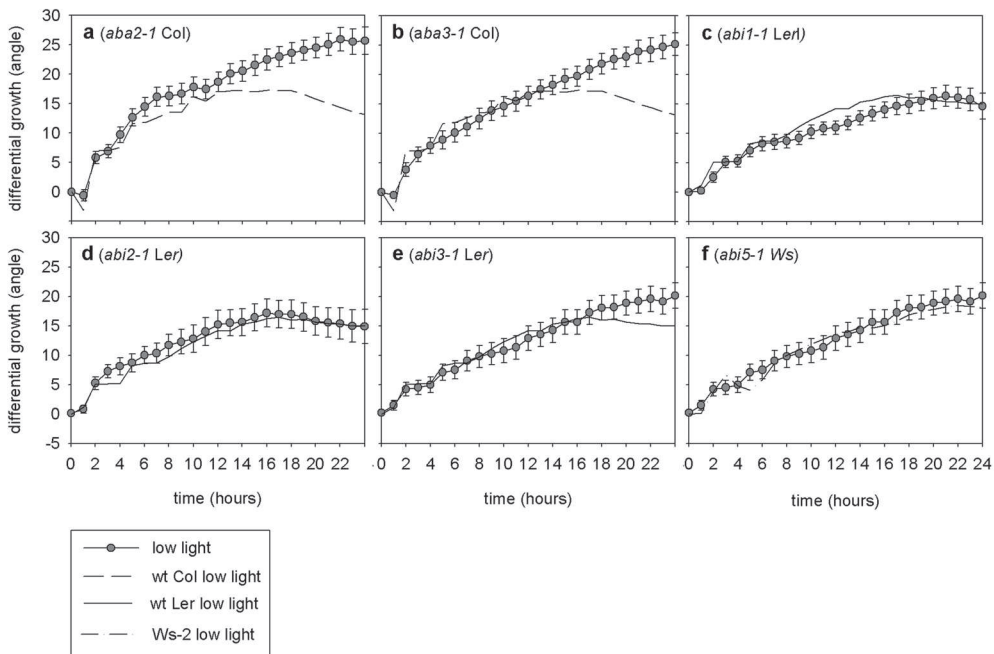


Figure 4.2: Effect of low light on petiole angles of ABA deficient- and ABA insensitive mutants. Response kinetics of a: *aba2-1*, b: *aba3-1*, c: *abi1-1*, d: *abi2-1*, e: *abi3-1* and f: *abi5-1* plants subjected to low light ($15-20 \mu\text{mol m}^{-2} \text{s}^{-1}$; grey circles), compared to their wild types: Col-0 (dashed lines), Ler (closed lines) or Ws (dash-dotted lines). Angles resulted from pair wise subtraction in all cases. Error bars represent SE; $n \geq 10$.

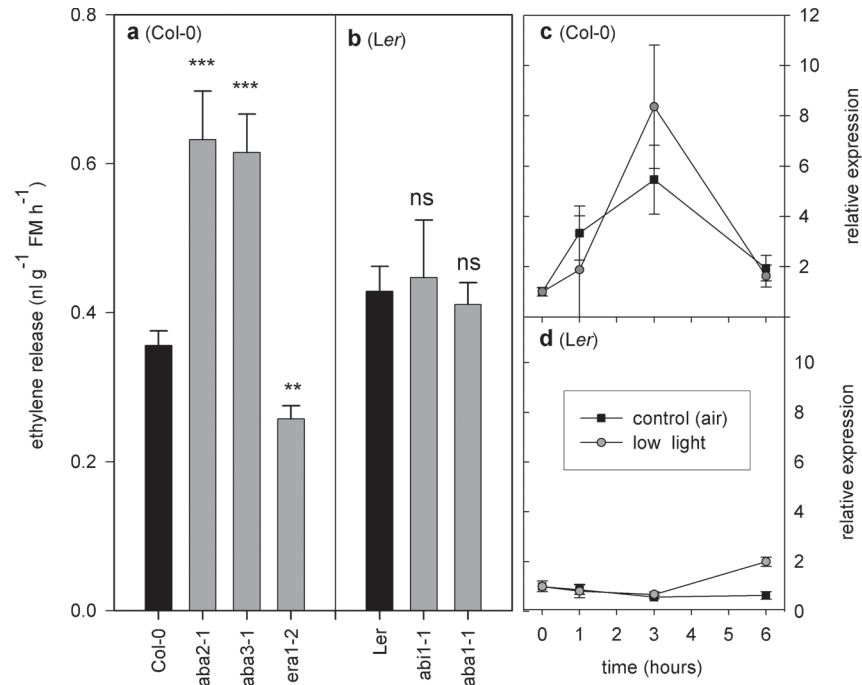


Figure 4.3: Ethylene release of ABA signaling- and biosynthesis mutants and effects of low light on *ABI1* gene expression. a,b: Ethylene release (nl g⁻¹ FM h⁻¹) of ABA related mutants (grey bars), in the a: Col-0 or b: *Ler* genetic background, compared with their wild types (black bars). ** $p < 0.01$, ns = non significant; Students T-test, $n \geq 6$ samples of 3 pooled plants. Kinetics of *ABI1* (At1g72770) gene expression in c: Col-0 and d: *Ler* in air controls (blue) and during low light treatment (grey). Expression values are normalized to 1 at $t = 0$ h. $n \geq 4$ samples of four pooled plants. Error bars represent SE in all panels.

array) were not regulated by low light or ethylene.

Next, we tested the *gpa1-1* and *gpa1-2* mutant alleles (Ullah *et al.*, 2001) for their ability to respond to ethylene and low light treatment. Both alleles showed a reduced hyponastic response to these signals (Figure 4.4a-d). Mutant alleles; *gcr2-2*, *gcr2-4* (Liu *et al.*, 2007; Gao *et al.*, 2007) phenocopied the response of *aba2-1* and *aba3-1* to low light in having a wild type response up to 14 h and an enhanced response thereafter (Figure 4.4e, f). The triple knock-out mutant; *gcr2-4 gcl1-1 gcl2-2* (Guo *et al.*, 2008) was hampered in its response to low light, similar to *aba1-1*, *gpa1-1* and *gpa1-2* (Figure 4.4g). Upon ethylene treatment, *gcr2-2* and to a lesser extent; *gcr2-4*, showed a slightly reduced response magnitude, comparable to the *gpa* mutants (Figure 4.4h, i), whereas the triple mutant had a strongly reduced response (Figure 4.4j).

To test if the hampered response to low light is due to ABA insensitivity of these lines, we measured initial petiole angles and the hyponastic growth response in plants pre-treated with fluroidon. Repressing ABA levels by fluroidon resulted in enhanced initial petiole angles in the absence of hyponastic growth inducing

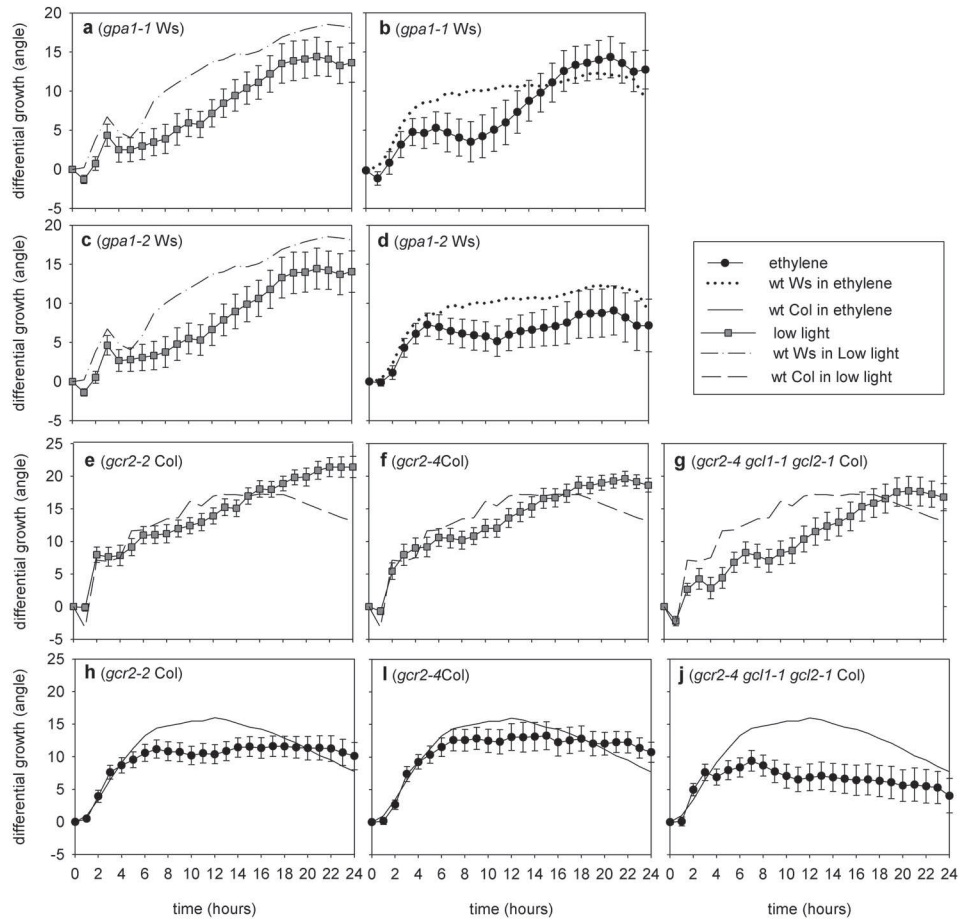


Figure 4.4: Hyponastic growth phenotype of *gcr2* related mutants. Response kinetics of *gpa1* mutants to a,c: low light ($15-20 \mu\text{mol m}^{-2} \text{s}^{-1}$; grey squares) and b,d: ethylene ($5 \mu\text{l l}^{-1}$; black circles) compared to wild type Ws genetic background (ethylene: dotted lines; low light: dash-dotted line). e-g: Response of *gcr2* mutants and *gcr2 gcl1 gcl2* triple mutant to low light and h-j: ethylene, compared to Col-0 wild type (ethylene: closed lines; low light: dashed line). Angles resulted from pair wise subtraction. Error bars represent SE; $n > 10$.

Table 4.2: Transcript levels of genes involved in ABA biosynthesis, catabolism or Signaling in Col-0 petioles subjected to low light for 3 h. Plants treated with air (control) or low light (LL; 15-20 $\mu\text{mol m}^{-2} \text{s}^{-1}$). Transcription values (with standard errors) represent arbitrary expression units derived from Affymetrix ATH1 GeneChips (Millenaar *et al.*, 2006). Three independent biological replicas were obtained per treatment and statistical differences (*p*) were calculated by a 2-tailed Student's T-test. * $p < 0.05$; ** $p < 0.01$; ns = non significant. Gene codes represents AGI codes. Minus sign at % Change column indicates downregulation of the gene. Phospholipases are named according to Qin and Wang (2002). Small GTPases are named according to Yang (2000).

Locus	Gene code	Expression Air	Expression LL	<i>p</i>	% Change
ABA Biosynthesis					
ABA1 (ZEP)	At5g67030	1512 ± 96	1391 ± 89	ns	
NCED1	At3g63520	1321 ± 133	1366 ± 53	ns	
NCED2	At4g18350	45 ± 5	43 ± 2	ns	
NCED3	At3g14440	29 ± 2	31 ± 1	ns	
NCED4	At4g19170	1055 ± 197	855 ± 121	ns	
NCED5	At1g30100	31 ± 2	31 ± 2	ns	
NCED6	At3g24220	49 ± 5	46 ± 3	ns	
NCED9	At1g78390	24 ± 3	24 ± 1	ns	
ABA2	At1g52340	328 ± 19	296 ± 35	ns	
ABA3	At1g16540	45 ± 4	42 ± 6	ns	
AAO3	At2g27150	100 ± 5	93 ± 7	ns	
ABA Catabolism					
CYC707A1	At4g19230	80 ± 14	80 ± 12	ns	
CYC707A2	At2g29090	112 ± 9	83 ± 4	**	-26%
CYC707A3	At5g45340	115 ± 12	149 ± 19	ns	
CYC707A4	At3g19270	46 ± 3	47 ± 4	ns	
ABA Signal Transduction					
ABI1	At4g26080	355 ± 54	371 ± 37	ns	
ABI2	At5g57050	98 ± 7	98 ± 0	ns	
ABI3	At3g24650	52 ± 3	49 ± 2	ns	
ABI4	At2g40220	78 ± 6	82 ± 4	ns	
ABI5	At2g36270	64 ± 5	65 ± 15	ns	
ERA1	At5g40280	174 ± 2	181 ± 8	ns	
EIN2 (ERA3)	At5g03280	608 ± 31	582 ± 24	ns	
FUS3	At3g26790	35 ± 2	34 ± 2	ns	

Control of low light-induced hyponastic growth by ABA

LEC1	At1g21970	53	±	1	53	±	4	ns
FRY1	At5g63980	1408	±	115	753	±	21	*** -47%
HYL1	At1g09700	23	±	1	22	±	0	ns
ABH1	At2g13540	308	±	8	297	±	39	ns
ISP5P1	At1g34120	84	±	2	93	±	3	* 11%
ISP5P2	At4g18010	97	±	4	80	±	4	** -18%
P2C-HA	At1g07430	23	±	2	24	±	3	ns
PP2C	At3g11410	385	±	43	380	±	33	ns
CDPK1	At1g18890	147	±	26	148	±	19	ns
CDPK1a	At1g74740	55	±	7	94	±	28	ns
RAB18	At5g66400	80	±	10	61	±	10	ns
Phospholipases								
PLC1	At5g58670	1014	±	40	941	±	38	ns
PLC2	At3g08510	2764	±	164	3107	±	221	ns
PLDa1	At3g15730	1721	±	233	1357	±	128	ns
PLDa2	At1g52570	160	±	8	161	±	17	ns
PLDa3	At5g25370	144	±	22	136	±	11	ns
PLDa4	At1g55180	110	±	18	102	±	7	ns
PLDb1	At2g42010	124	±	18	114	±	5	ns
PLDb2	At4g00240	37	±	3	38	±	0	ns
Small GTPases								
ROP2	At1g20090	524	±	65	669	±	122	ns
ROP5	At4g35950	455	±	35	392	±	28	ns
ROP6	At4g35020	287	±	32	377	±	14	* 31%
ROP9	At4g28950	90	±	7	83	±	3	ns
ROP10	At3g48040	191	±	21	223	±	12	ns

stimuli (Benschop *et al.*, 2007). The *gcr2-4 gcl1-1 gcl2-2* mutant increased petiole angles significantly ($p < 0.001$), and to the same extent as Col-0, compared to mock treatment (Figure 4.5a). Moreover, low light-induced hyponastic growth could be further repressed by application of fluoridon in *gcr2-4 gcl1-1 gcl2-2* (Figure 4.5b). Together these results suggest that GPA1 and its associated protein GCR2 are positive regulators of both ethylene- and low light-induced hyponastic growth. GCR2 functions redundantly with GCL1 and/or GCL2, as the most dramatic phenotype was observed in the triple knockout mutant. Yet, our results suggest that the hampered response to low light is not due to insensitivity to ABA of the *gcr2-4 gcl1-1 gcl2-2* mutant.

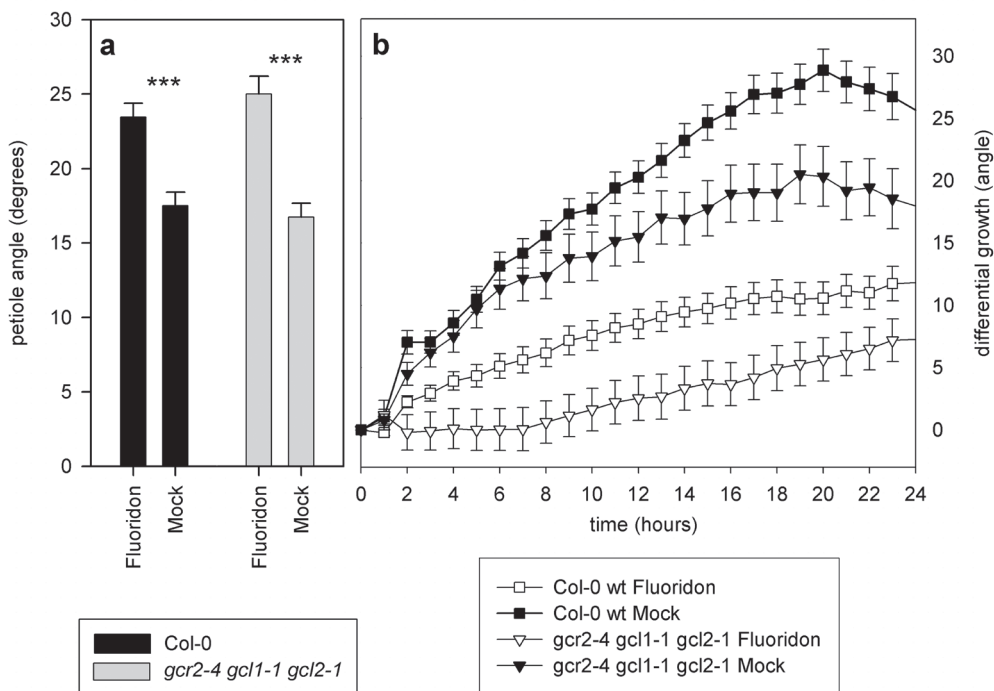


Figure 4.5: GCR2 GCL1 GCL2 control low light-induced hyponastic growth independent of ABA. a: Effect of treatment with fluoridon (100 μM) on initial petiole angles of Col-0 (black) and *gcr2-4 gcl1-1 gcl2-1* (grey). $n > 35$; *** $p < 0.001$, 2-tailed Student's T-test. b: Response of Col-0 (squares) and *gcr2-4 gcl1-1 gcl2-1* (triangles) pre-treated with fluoridon (white symbols) or mock (black symbols), to low light (15-20 $\mu\text{mol m}^{-2} \text{s}^{-1}$). Angles resulted from pair wise subtraction. Error bars represent SE; $n > 20$.

Table 4.3: Transcript levels of genes involved in ABA perception in Col-0 petioles subjected to low light or ethylene for 3 h. Plants treated with air (control), low light (LL; 15-20 $\mu\text{mol m}^{-2} \text{s}^{-1}$) or ethylene (5 $\mu\text{l l}^{-1}$). Values (with standard errors) represent arbitrary expression units derived from Affymetrix ATH1 GeneChips (Millenaar *et al.*, 2006). Three independent biological replicas were obtained per treatment and statistical differences (*p*) were calculated by a 2-tailed Student's T-test. * $p < 0.05$; ** $p < 0.01$; ns = non significant. Gene codes represents AGI codes. Minus sign at % Change column indicates downregulation of the gene

Locus	Gene code	Expression	Expression	Expression	<i>p</i>		% Change	
		Air	LL	ET	LL	ET	LL	ET
FCA	At4g16280	144 ± 9	143 ± 6	150 ± 4	ns	ns		
ABAR / CHLH	At5g13630	5506 ± 406	5430 ± 254	4473 ± 507	ns	ns		
GCR2	At1g52920	54 ± 4	54 ± 1	53 ± 4	ns	ns		
GPA1	At2g26300	159 ± 9	245 ± 17	198 ± 4	**	**	55%	24%
GCL1	At1g52920	54 ± 4	54 ± 1	53 ± 4	ns	ns		
GCL2	At2g20770	128 ± 2	127 ± 14	142 ± 5	ns	ns		
GTG2	At4g27630	81 ± 41	78 ± 17	74 ± 31	ns	ns		
PYR1	At4g17870	595 ± 42	770 ± 63	281 ± 44	***	*	30%	-53%
PYL1	At5g46790	301 ± 52	261 ± 17	214 ± 19	ns	ns		
PYL2	At2g26040	301 ± 52	261 ± 17	214 ± 19	ns	ns		
PYL3	At1g73000	47 ± 3	45 ± 3	44 ± 2	ns	ns		
PYL4	At2g38310	1215 ± 230	1290 ± 146	1529 ± 187	ns	ns		
PYL5	At5g05440	192 ± 17	291 ± 22	499 ± 25	***	**	52%	160%
PYL6	At2g40330	147 ± 14	152 ± 22	164 ± 17	ns	ns		
PYL7	At4g01026	489 ± 11	448 ± 1	512 ± 32	ns	**		5%
PYL9	At1g01360	190 ± 36	213 ± 21	193 ± 40	ns	ns		
PYL8	At5g53160	411 ± 65	596 ± 17	1117 ± 119	**	**	45%	172%
HAB1	At1g72770	229 ± 25	209 ± 19	197 ± 5	ns	ns		

Footnotes: GTG1, PYL10, PYL11, PYL12, PYL13 were not represented on the micro-array. PYR1/PYL13 have been independently identified as 'regulatory component of ABA receptor' (RCAR1 – RCAR14) by Ma *et al.* (2009).

Discussion

The role of ABA in light acclimation

Using transcript analysis, pharmacological inhibition of ABA biosynthesis and mutant analysis, we demonstrated that ABA is a positive modulator of low light-induced differential petiole growth in *Arabidopsis thaliana*. Although ABA and light both are important factors in control of plant development and in response to changing environments, still, little is known on interactions between light and ABA.

Dark-treated *Arabidopsis* plants show substantially increased ABA levels (Wheatherwax *et al.*, 1996) and recently, Chen *et al.* (2008) proposed that the positive transcriptional activator of photomorphogenesis and many light-regulated genes; HYPOCOTYL5 (HY5) integrates light- and ABA signaling during germination and early seedling development. These authors showed that HY5 regulates the expression of ABA-inducible genes, and directly modulates ABA sensitivity by ABA-mediated binding to the ABA-INSENSITIVE5 (ABI5) promoter. Consequently, ectopic expression of ABI5 was able to rescue the reduced ABA sensitivity of *hy5* mutants (Chen *et al.*, 2008). Moreover, light-mediated down-regulation of ABI3, via phytochrome B (phyB), promotes phyA mediated hypocotyl growth (Mazzella *et al.*, 2005). ABA levels in germinating seeds are regulated in a photo-reversible manner via phyB by direct regulation of AtNCED6 transcription and the ABA catabolic gene CYP707A2 (Seo *et al.*, 2006).

The data presented in this chapter, add to these results by demonstrating a functional link between ABA and a response (hyponasty) to low light intensity that is a component of the shade avoidance syndrome. In chapter 2 (Millenaar *et al.*, 2009), we showed that low blue light is the component of low light that controls hyponastic growth responses in *Arabidopsis*. In accordance with our data indicating that ABA is a positive regulator of low light-induced differential growth, Kozuka *et al.*, (2005) demonstrated that leaf blades of ABA-deficient mutants were unable to expand in low blue-light.

More specifically, our results identified novel roles for ABA1, ERA2, ABA2, ABA3, GPA1, GCR2, GCL1 and GCL2 in the modulation of a response (hyponasty) to changing light conditions. Intriguingly, low light-induced hyponastic growth depends on the photoreceptors cryptochrome1 (*cry1*), *cry2*, phyA and phyB, but not on phototropins (*phot1*, *phot2*; Millenaar *et al.*, 2009; Chapter 2). HY5 is part of the signal transduction cascade of phytochromes and cryptochromes, but not of the phototropins (Gyula *et al.*, 2003). Therefore, it is conceivable that in accordance to the observation by Chen *et al.* (2008), HY5 may be a point of cross-talk between perception of low light intensity and ABA modulation of low light-induced hyponasty and possibly also for transcriptional regulation of ABA associated genes (Table 4.1, 4.2). However, as *abi3*, *abi5* and *hy5* mutants all display a wild type hyponastic growth response upon low light-induction (Figure 4.2 and data not shown), probably other, HY5 independent signaling routes, are also involved.

The role of ABA in hyponastic growth is inducer-signal specific.

Three signals, i.e: low light, ethylene and heat, induce a phenotypically similar hyponastic growth response in *Arabidopsis thaliana* (Millenaar *et al.*, 2005, 2009; Koini *et al.*, 2009, Chapter 2, Chapter 3). Nevertheless, we previously concluded that low light-induced hyponastic growth is independent of ethylene action, whereas heat-induced hyponastic growth is repressed by ethylene (Millenaar *et al.*, 2009; Chapter 2; Chapter 3). Moreover, ethylene-induced hyponasty is independent of auxin and polar auxin transport (Van Zanten *et al.*, 2009a; Chapter 2), whereas heat- and low light-induced hyponasty required this (Millenaar *et al.*, 2009; Koini *et al.*,

2009; Chapter 2; Chapter 3). This led to the conclusion that ethylene-, low light- and heat-induced hyponastic growth are brought about via parallel signal transduction routes, but probably shares downstream components. The observation that ABA is a positive regulator of low light-induced hyponastic growth in *Arabidopsis* is in agreement with the role of ABA in heat-induced hyponastic growth (Chapter 3). However, it is in sharp contrast with the results of Benschop *et al.* (2007) and Cox *et al.* (2004), who demonstrated that ABA antagonizes flooding (ethylene)-induced hyponastic growth in *R. palustris* and *Arabidopsis*. On top of this, ABA modulates low light-induced hyponastic growth independent of ethylene action (Figure 4.3). We therefore conclude that ABA modulates hyponastic growth in a response specific manner, upstream of a putative set of shared downstream components.

In agreement with this notion, the role of specific ABA associated genes differed between treatments. Benschop *et al.* (2007) showed that ABA2, ABA3, ABI1, ABI3 and ABI5 are negative regulators and ERA1 is a positive regulator of ethylene-induced hyponastic growth, whereas ABA1 and ABI2 did not influence this response. In the response to heat, ERA1 and ABA3 are negative regulators, ABA1 and ABI1, ABI2 and ABI3 are positive regulators and ABA2 seems not involved (Chapter 3). In low light-induced hyponastic growth; ABA1 is a positive regulator, ERA1, ABA2 and ABA3 are negative regulators and ABI1, ABI2, ABI3 and ABI5 are not involved.

Surprisingly, our results indicated that in *aba1-1* low light-induced hyponastic growth is repressed (Figure 4.1), whereas in *aba2-1* and *aba3-1* a normal phenotype was observed in the first hours, thereafter, the response was even exaggerated (Figure 4.2). This apparent contradiction might be explained by the previous observation that *aba2-1* and *aba3-1* contained reduced, yet still significant amounts of ABA, and double mutant combinations contained lower ABA levels (Leon-Kloosterziel *et al.*, 1996). Therefore, these mutants appear leaky and this might explain why we found a relatively normal response to low light in these lines. Alternatively, as these lines produce significantly ($p < 0.001$) more ethylene than wild-type (LeNoble *et al.*, 2004; Figure 4.3a) the phenotype observed may be caused by ethylene effects rather than low light.

Low light affects expression of ABA related genes

Gene ontology (GO) analysis was employed to search for overrepresented ABA related gene classes in a pool of genes differentially regulated upon 3 h of low light treatment (Table 4.1). This 3 h time point marks the induction of the hyponastic growth response (Millenaar *et al.*, 2005) and was expected to show low light-regulated ABA related genes, if any exists, because in general hyponastic growth associated ABA effects occur fast (Cox *et al.*, 2004; Benschop *et al.*, 2005). Two GO classes; 'Response to ABA stimulus' and 'ABA metabolism' were identified as significantly regulated (Table 4.1). Besides these, five auxin related classes were found. Presence of auxin related classes were expected, given the prominent role of this hormone in the regulation of low light-induced hyponastic growth (Millenaar *et al.*, 2009).

A more dedicated analysis of the ABA related GO classes revealed significant regulation of 6 ABA associated genes (Table 4.2). These included the ABA regulated

CYTOCHROME P450 from the 707 family (CYP707A2) which is involved in the first steps of ABA catabolism. This gene is minimally expressed in mature organs and mainly functions in seed dormancy and germination (Saito *et al.*, 2004; Okamoto *et al.*, 2006). Also *FIERY1* (*FRY1*) is down regulated upon low light treatment. This gene encodes for an inositol polyphosphate 1-phosphatase and is a negative regulator of ABA and stress signaling in Arabidopsis and mutants are ABA hypersensitive (Xiong *et al.*, 2001). Finally, *ISP5P2* which codes for a protein with inositol-polyphosphate 5-phosphatase activity is down regulated under low light conditions. Mutant *isp5p2* is ABA hypersensitive (Gunesekera *et al.*, 2007).

Among the significantly up regulated genes after low light treatment is another *ISP5P* member (*ISP5PI*). However, both *ISP5P* genes may have distinct roles in plants, as ectopic expression of *ISP5PI* resulted in delayed ABA gene expression and ABA insensitivity for stomatal closure (Burnette *et al.*, 2003), but had no effect on ABA mediated seed germination, whereas ectopically expressed *ISP5PII* are insensitive to ABA during germination (Sanchez & Chua, 2001). Another upregulate gene, Rho-like GTP binding protein 6 (*ROP6/AtRac*) negatively regulates ABA responses (Yang 2002; Gu *et al.*, 2004). *ROP6* is essential for ABA mediated stomatal closure (Lemichez *et al.*, 2001) downstream of *ABI1*. It is not clear yet if this gene also exhibits additional pleiotropic ABA effects.

Recently, the isolation of several ABA receptors were reported in Arabidopsis; the Mg-chelatase protein *ABAR/CHLH* (Shen *et al.*, 2006), the G-protein Coupled Receptor2 (*GCR2*; Liu *et al.*, 2007), and the GPCR-type G proteins (*GTG1*, *GTG2*; Pandey *et al.*, 2009). A chemical genetic approach led to the identification of *PYR1* and related *PYL1* to *PYL13* (Park *et al.*, 2009; Ma *et al.*, 2009) as ABA receptors. Intriguingly, *PYR1* was differentially up regulated by low light treatment and down regulated during ethylene treatment (table 4.3). Although highly speculative and correlative, these contrasting effects on transcription may contribute to the explanation why ABA is antagonistically in ethylene-induced hyponasty and agonistically to low light-induced hyponastic growth. In addition, *PYR1* was down-regulated in ethylene and upregulated in low light, whereas *PYL5* and *PYL8* were upregulated in both treatments. Currently, the *pyr/pyl* triple and quadruple ABA insensitive mutant combinations described in Park *et al.* (2009) are being tested in our laboratory for hyponastic growth phenotypes. The *GCR2*, *GTG1* and *GTG2* associated gene; G protein alpha-subunit 1 gene (*GPA1*) showed significant increase in expression after both low light and ethylene treatment (Table 4.3).

Subsequent functional analysis of the *gpa1* mutant alleles revealed a positive function for *GPA1* in controlling hyponastic growth. However, the role of *GPA1* is not restricted to ABA Signaling alone. *GPA1* was previously shown to control a shared signal transduction pathway of both ABA and blue light in seed germination (Warpeha *et al.*, 2007) and mutant *gpa* alleles showed partial de-etiolation in dark, including reduced apical hook formation and short hypocotyls (Ullah *et al.*, 2001). Moreover, *GPA1* is involved in several other Signaling pathways (reviewed in Perfus-Barbeoch *et al.*, 2004), including gibberellin and brassinolide stimulation

of germination and auxin-mediated promotion of lateral root formation. *Gpa* mutants exhibit reduced cell division and analogously, contain fewer, but larger cells which result in longer sepals and pedicels and rounded laminas. Intriguingly, ABA sensitivity in *gpa* mutants differed between responses. For example, *gpa1* mutants displayed hypersensitivity to ABA in germination assays (Ullah *et al.*, 2001, Gao *et al.*, 2007) but were insensitive to ABA in stomatal opening (Liu *et al.*, 2007). In conclusion, it is by no means clear if the effect on hyponastic growth in *gpa1* mutants on ethylene, low light, or both stimuli, are due to disturbed ABA effects.

GCR2 gene family controls differential growth independent of ABA

Liu *et al.*, (2007) claimed that loss-of-function of the ABA binding receptor *gcr2* confers insensitivity for all known ABA responses. This was, however, strongly objected against by several other papers (Guo *et al.*, 2007; Gao *et al.*, 2007; Johnston *et al.*, 2007; Illingworth *et al.*, 2008; Risk *et al.*, 2009). Gao *et al.* (2007) and Guo *et al.*, (2008) observed that GCR2, GCL1 and GCL2 are not required for ABA inhibition of seed germination and early seedling development and moreover, that even the triple mutant in *gcr2 gcl1 gcl2* retained wild-type-like ABA sensitivity. In agreement, Gao and colleagues (2007) could not find evidence that GCR2 is genetically coupled to GPA1, which was initially claimed by Liu and colleagues (2007). GCR2 is also probably not a trans-membrane protein, nor a G protein-coupled receptor (Liu *et al.*, 2007), but is most likely a plant homolog of the bacterial lanthionine synthetases C-like family of proteins (Johnston *et al.*, 2007; Guo *et al.*, 2007; Illingworth *et al.*, 2008). In addition, no evidence of ABA binding to GCR2 was detected in a re-evaluation experiment by Risk and co-workers (2009).

We demonstrated that both GPA and GCR2 family genes control differential petiole growth. As opposed to *gpa1*, to our knowledge, no morphological or response phenotypes were reported previously for *gcr2* mutants, other than the suggested ABA responses (Liu *et al.*, 2007). Three lines of evidence demonstrate that role of the GCR2 family genes on differential growth are independent of ABA and therefore may support the notion that GCR2 is not an ABA receptor. First, we identified ABA as a positive regulator of low light-induced hyponastic growth, whereas ABA is a negative regulator of ethylene-induced hyponastic growth (Benschop *et al.*, 2007). Therefore, if the phenotype of *gcr2 gcl1 gcl2* was ABA mediated, a contrasting effect (enhanced and repressed differential growth respectively) for ethylene and low light could be expected. Secondly, initial petiole angles were as responsive to reduced ABA levels as were wild type plants. Last, the reduced ability to show low light-induced hyponastic growth could be further repressed by pharmacological inhibition of ABA. Therefore, we propose that the GCR2 family control differential petiole growth independent of ABA, via an yet unknown mechanism.

Materials and Methods

Plant material and growth conditions

Seeds were obtained from the Nottingham Arabidopsis Stock Centre (NASC IDs between brackets): Columbia-0 (N1092), Landsberg *erecta* (NW20), Wassilewskija-2 (N915), *aba1-1* (N21; Koornneef *et al.*, 1982), *aba2-1* (N156; Leon-Kloosterziel *et al.*, 1996), *abi1-1* (N22; Koornneef *et al.*, 1984; Leung *et al.*, 1994); *abi2-1* (N23; Koornneef *et al.*, 1984; Leung *et al.*, 1997), *abi3-1* (N24; Koornneef *et al.*, 1982), *abi5-1* (N8105; Finkelstein *et al.*, 1994), *gpa1-1* (N3910; Ullah *et al.*, 2001), *gpa1-2* (N3911 Ullah *et al.*, 2001). *era1-2* (Cutler *et al.*, 1997) was a gift of M. Koornneef (Wageningen University, the Netherlands). *gcr2-2* (Liu *et al.*, 2007), *gcr2-4* and *gcr2-2 gcl1-1 gcl2-1* (Guo *et al.*, 2008), were a kind gift of J-G Chen (University of British Columbia, Canada).

Plants were grown on a fertilized mixture of potting-soil and perlite (1:2; v/v) as described in Millenaar *et al.* (2005) and Benschop *et al.* (2007). Growth room conditions were: 20°C, 70% (v/v) relative humidity, 9 h photoperiod of 200 $\mu\text{mol m}^{-2} \text{s}^{-1}$ photosynthetic active radiation (PAR). Pots were daily automatically saturated with tap water at the start of the photoperiod. Before potting, seeds were stratified for 4 days in dark at 4°C to synchronize germination.

Treatments

Plants at developmental stage 3.9 according to Boyes *et al.* (2001), were used for all experiments. Plants were transferred to the cabinets or cuvettes one day before the experiment to allow acclimatization. Treatments started (t=0) 1.5 h after start of the photoperiod to minimize diurnal and/or circadian effects.

Fluoridon (Riedel-de Haën, Seelze, Germany) was dissolved in MilliQ containing; 0.1% Tween and 0.07% acetone, to 100 μM and was applied to the soil, until saturation, to plants saved for two days from watering. Pretreatment took place 66 h, 42 h and 18 h before the start of the experiment. The mock solution was identical, but lacked fluoridon. This fluoridon pretreatment enhanced the initial angles (Benschop *et al.*, 2007). This feature was used to confirm the effectiveness of the pharmacological treatments (data not shown).

Low light was induced by reduction of the light intensities to 15-20 $\mu\text{mol m}^{-2} \text{s}^{-1}$ (PAR) by shading the plants with spectrally neutral shade cloth. This did not affect light quality as checked with a LICOR-1800 spectro-radiometer (LI-COR, Lincoln, NE, USA; Millenaar *et al.*, 2009; Chapter 2).

Ethylene was applied under standard growth chamber conditions in continuous flow-through at 75 l h^{-1} , in glass cuvettes containing one plant each, as described in Millenaar *et al.* (2005, 2009) and Benschop *et al.* (2007). Ethylene (Hoek Loos, Amsterdam, the Netherlands) and air (70% (v/v) relative humidity) were mixed using flow-meters to generate a concentration of 5 $\mu\text{l l}^{-1}$, which is saturating for the hyponastic response (data not shown). The ethylene concentration was checked regularly on a gas chromatograph (GC955, Synspec, Groningen, the Netherlands), and remained constant for the duration of the experiment. Control cuvettes were flushed with air (70% (v/v) relative humidity) at the same flow rate.

Computerized image analysis of angle kinetics and calculations

Angle kinetics experiments were conducted using an automated time-lapse photography setup (Cox *et al.*, 2003; Millenaar *et al.*, 2005; Benschop *et al.*, 2007). Plants were placed singly in

glass cuvettes with the petiole of study perpendicular to the axis of the camera. To facilitate measurement, leaves that were obscuring the petiole base were removed. Additionally, the petiole was marked at the petiole/lamina junction with orange paint (Decofin Universal; Apeldoorn the Netherlands). These preparations did not influence the response of the petiole (data not shown). The light regime in the cuvettes was kept the same as during the growth period until the experiment started (low light experiments) or throughout the experimental period (ethylene and control experiments). Pictures of two petioles per plant were taken every 10 min. To enable continuous photography, no dark period was included in the 24 h experimental period. Angles were measured between the orange painted point at the petiole/lamina junction and a fixed basal point of the petiole, compared to the horizontal, by using KS400 (Version 3.0) software package (Carl Zeiss Vision, Hallbergmoos, Germany) and a customized macro. Pair wise subtraction was performed to take into account the circadian and/or diurnal variations in petiole angle during the course of the experiments. For this, we calculated the difference between the angles of treated and control plants for each time point (Benschop et al., 2007). Calculation of the new standard error for the differential response was performed by taking the squared root from the summation of the two squared standard errors.

Ethylene release measurements

Ethylene release from rosettes was measured as described in Millenaar *et al.* (2005); Chapter 2; Chapter 3). Whole rosettes of ~300 mg were placed in a syringe. Ethylene was allowed to accumulate in the syringe for 15-20 minutes and subsequently analyzed on a gas chromatograph (GC955, Synspec). This short time frame prevented wound-induced ethylene production, which commenced only after 25 min (data not shown).

Real-Time RT-PCR

Petioles of Col-0 in stage 3.9 according to Boyes *et al.* (2001) were harvested and snap frozen in liquid nitrogen. Subsequently, RNA was isolated from these petioles with the RNeasy extraction kit (Qiagen, Valencia, CA, USA). gDNA removal, cDNA synthesis and Real-Time RT-PCR were performed as described by Millenaar *et al.*, (2006), Benschop *et al.* (2007) with primers: 5'-TGAAGAAGCGTGTGAGATGG-3' and 5'-CTGTATCGCCAGCTTTGACA-3'. Relative mRNA values were calculated using the comparative Ct method described by Livak & Schmittgen (2001), expressing mRNA values of *ABI1* relative to *alpha-Tubulin-6* (5'-ATAGCTCCCCGAGGTCTCTC-3' and 5'-TCCATCTCGTCCATTCCTTC-3').

Acknowledgements

The authors thank Maarten Koornneef and Jin-Gui Chen for providing seed materials and Jin-Gui Chen for comments on a draft of the manuscript.

Supporting Information

- **Table S4.1:** Gene Ontology (GO) classes of genes that were significantly transcriptional regulated by low light-treatment, compared to air control

Supporting Information

Table S4.1: Gene Ontology (GO) classes of genes that were significantly transcriptional regulated by low light-treatment, compared to air control. The depicted genes meet the following criteria: GO categories were only considered when harboring ≥ 5 genes and when a hypergeometric test resulted in $p < 0.01$. Reg = Regulated. This represent the number of genes regulated by low light within a GO group. "Total" represents the total number of genes within a GO group. Statistical differences are p -values. GO term IDs represents the GO group were obtained from the GO consortium (www.arabidopsis.org).

ID	GO term ID	ID number	Reg.	Total	Significance (p value)
63	carbohydrate metabolic process	gO:0005975	60	373	0.004
28	endoplasmic reticulum	gO:0005783	63	278	<0.001
17	plasma membrane	gO:0005886	53	271	<0.001
38	transporter activity	gO:0005215	43	256	0.005
7	response to auxin stimulus	gO:0009733	42	254	0.007
65	protein folding	gO:0006457	56	240	<0.001
1	response to cold	gO:0009409	37	199	0.001
3	response to abscisic acid stimulus	gO:0009737	35	185	0.001
72	hydrolase activity	gO:0016787	33	174	0.002
24	response to salt stress	gO:0009651	39	173	<0.001
13	cytosol	gO:0005829	43	169	<0.001
41	response to oxidative stress	gO:0006979	33	166	0.001
16	plastid	gO:0009536	28	138	0.001
71	heat shock protein binding	gO:0031072	25	136	0.007
70	unfolded protein binding	gO:0051082	24	121	0.003
20	response to jasmonic acid stimulus	gO:0009753	23	116	0.003
4	response to water deprivation	gO:0009414	24	114	0.001
12	response to ethylene stimulus	gO:0009723	20	101	0.005
77	response to salicylic acid stimulus	gO:0009751	20	100	0.005
2	response to heat	gO:0009408	23	97	<0.001
75	thiol-disulfide exchange intermediate activity	gO:0030508	17	80	0.004
15	chloroplast stroma	gO:0009570	15	64	0.002
83	cell redox homeostasis	gO:0045454	15	64	0.002
85	nucleolus	gO:0005730	14	63	0.005
5	response to osmotic stress	gO:0006970	13	59	0.007
44	glycolysis	gO:0006096	18	54	<0.001
84	P-P-bond-hydrolysis-driven protein transmembrane transporter activity	gO:0015450	12	47	0.002
42	toxin catabolic process	gO:0009407	11	47	0.006
49	response to cadmium ion	gO:0046686	11	47	0.006
73	hydrolase activity, acting on glycosyl bonds	gO:0016798	14	41	<0.001
64	vacuolar membrane	gO:0005774	13	41	<0.001
8	response to sucrose stimulus	gO:0009744	9	38	0.010
105	water channel activity	gO:0015250	9	37	0.008
22	circadian rhythm	gO:0007623	11	34	<0.001

Control of low light-induced hyponastic growth by ABA

40	mitochondrial matrix	gO:0005759	8	31	0.007
106	membrane fusion	gO:0006944	8	31	0.007
11	tryptophan biosynthetic process	gO:0000162	9	29	0.001
33	response to red light	gO:0010114	8	28	0.003
18	chlorophyll biosynthetic process	gO:0015995	9	27	0.001
74	amino acid metabolic process	gO:0006520	12	24	<0.001
46	fatty acid beta-oxidation	gO:0006635	7	24	0.004
66	metallopeptidase activity	gO:0008237	7	24	0.004
53	jasmonic acid biosynthetic process	gO:0009695	7	23	0.003
56	cold acclimation	gO:0009631	7	23	0.003
34	response to far red light	gO:0010218	9	22	<0.001
96	autophagy	gO:0006914	7	20	0.001
27	chloroplast outer membrane	gO:0009707	6	20	0.006
39	ER to golgi vesicle-mediated transport	gO:0006888	7	19	0.001
81	glucosinolate biosynthetic process	gO:0019761	7	18	<0.001
104	response to desiccation	gO:0009269	6	18	0.003
120	lactose catabolic process	gO:0005990	6	18	0.003
129	copper ion transport	gO:0006825	6	18	0.003
131	brassinosteroid mediated signaling	gO:0009742	6	17	0.002
103	intra-golgi vesicle-mediated transport	gO:0006891	5	17	0.010
21	response to blue light	gO:0009637	5	15	0.005
93	3-chloroallyl aldehyde dehydrogenase activity	gO:0004028	6	14	<0.001
121	lactose catabolic process via UDP-galactose	gO:0019515	6	14	<0.001
123	sulfate transmembrane transporter activity	gO:0015116	5	14	0.003
150	sulfate assimilation	gO:0000103	7	13	<0.001
122	lactose catabolic process, using glucoside 3-dehydrogenase	gO:0019513	6	13	<0.001
23	phototropism	gO:0009638	5	13	0.002
26	brassinosteroid biosynthetic process	gO:0016132	4	12	0.008
94	malate metabolic process	gO:0006108	4	12	0.008
127	glucose catabolic process to lactate and acetate	gO:0019658	6	11	<0.001
43	gluconeogenesis	gO:0006094	5	11	0.001
100	pentose-phosphate shunt, oxidative branch	gO:0009051	5	11	0.001
128	sulfate transport	gO:0008272	5	11	0.001
52	thylakoid membrane	gO:0042651	4	11	0.005
79	tricarboxylic acid cycle	gO:0006099	4	11	0.005
159	xyloglucan:xyloglucosyl transferase activity	gO:0016762	5	10	<0.001
156	protein tyrosine/serine/threonine phosphatase activity	gO:0008138	4	10	0.003
25	L-ascorbic acid biosynthetic process	gO:0019853	5	9	<0.001
80	malate dehydrogenase activity	gO:0016615	5	9	<0.001
135	chaperone binding	gO:0051087	5	9	<0.001
48	response to mechanical stimulus	gO:0009612	4	9	0.002
88	nucleoside metabolic process	gO:0009116	4	9	0.002
101	glucose catabolic process to D-lactate and ethanol	gO:0019656	4	9	0.002
138	fructose-bisphosphate aldolase activity	gO:0004332	4	9	0.002
61	indoleacetic acid biosynthetic process	gO:0009684	5	8	<0.001
6	nitrate assimilation	gO:0042128	4	8	0.001

57	methionine biosynthetic process	gO:0009086	4	8	0.001
99	pentose-phosphate shunt, non-oxidative branch	gO:0009052	4	8	0.001
149	response to absence of light	gO:0009646	4	8	0.001
32	transcription factor binding	gO:0008134	3	8	0.009
59	starch biosynthetic process	gO:0019252	3	8	0.009
60	oxidoreductase activity	gO:0016709	3	8	0.009
110	L-ascorbate peroxidase activity	gO:0016688	3	8	0.009
124	cellular response to sulfate starvation	gO:0009970	3	8	0.009
142	late endosome	gO:0005770	3	8	0.009
144	UDP-glucosyltransferase activity	gO:0035251	3	8	0.009
164	plant-type vacuole	gO:0000325	3	8	0.009
145	6-phosphofructokinase complex	gO:0005945	4	7	<0.001
146	6-phosphofructokinase activity	gO:0003872	4	7	<0.001
14	aspartate transaminase activity	gO:0004069	3	7	0.005
35	vitamin E biosynthetic process	gO:0010189	3	7	0.005
55	unsaturated fatty acid biosynthetic process	gO:0006636	3	7	0.005
91	leucine biosynthetic process	gO:0009098	3	7	0.005
126	glucose catabolic process to butanediol	gO:0019650	3	7	0.005
157	acyl-CoA oxidase activity	gO:0003997	3	7	0.005
168	cellular response to nitrogen starvation	gO:0006995	4	6	<0.001
29	response to singlet oxygen	gO:0000304	3	6	0.002
45	tryptophan synthase activity	gO:0004834	3	6	0.002
50	response to arsenic	gO:0046685	3	6	0.002
95	cellular carbohydrate metabolic process	gO:0044262	3	6	0.002
102	isopentenyl diphosphate biosynthetic process, mevalonate-independent pathway	gO:0019288	3	6	0.002
107	DNA-3-methyladenine glycosylase I activity	gO:0008725	3	6	0.002
109	glutamate catabolic process to oxaloacetate	gO:0019554	3	6	0.002
111	xylan 1,4-beta-xylosidase activity	gO:0009044	3	6	0.002
115	prephenate dehydratase activity	gO:0004664	3	6	0.002
116	L-phenylalanine biosynthetic process	gO:0009094	3	6	0.002
117	arogenate dehydratase activity	gO:0047769	3	6	0.002
130	glucose-1-phosphate adenyltransferase activity	gO:0008878	3	6	0.002
133	aldehyde dehydrogenase (NAD) activity	gO:0004029	3	6	0.002
141	bile acid:sodium symporter activity	gO:0008508	3	6	0.002
119	flavonol biosynthetic process	gO:0051555	4	5	<0.001
136	SNARE binding	gO:0000149	4	5	<0.001
202	water transport	gO:0006833	4	5	<0.001
10	auxin binding	gO:0010011	3	5	0.001
78	phosphoenolpyruvate carboxylase activity	gO:0008964	3	5	0.001
82	carboxy-lyase activity	gO:0016831	3	5	0.001
139	5-phosphoribose 1-diphosphate biosynthetic process	gO:0006015	3	5	0.001
155	cellular response to water deprivation	gO:0042631	3	5	0.001
167	hydro-lyase activity	gO:0016836	3	5	0.001
197	soluble fraction	gO:0005625	3	5	0.001

Isolation and characterization of genes involved in *Arabidopsis thaliana* hyponastic petiole growth

Martijn van Zanten, Fionn McLoughlin[§], Kerstin Gühl[§],
Laurentius A.C.J. Voesenek, Anton J.M. Peeters,
Frank F. Millenaar[§]

Plant Ecophysiology, Institute of Environmental Biology, Utrecht University,
Padualaan 8, 3584 CH Utrecht, the Netherlands

[§]Present addresses:

FMCL: Section of Plant Physiology, Swammerdam Institute for Life Sciences,
University of Amsterdam, Kruislaan 318, 1098 SM Amsterdam,
the Netherlands.

KG: NSURE BV; Bornsesteeg 59, 6708 PD Wageningen, the Netherlands.

FFM: De Ruiter Seeds, Leeuwenhoekweg 52, 2660 BB Bergschenhoek,
the Netherlands.

Abstract

Hyponastic leaf movement, driven by differential petiole growth, is adopted by several plant species, including *Arabidopsis thaliana*, as a mechanism to escape diminished growth conditions in their abiotic environment. Among the signals that trigger hyponastic growth are the gaseous hormone ethylene, low light intensities and supra-optimal temperatures (heat). Yet, little is known which functional components are involved in the perception, transduction and integration of these signals towards hyponastic growth. Given the similarities in the kinetics of the response induced by these signals, it is hypothesized that downstream the signals converge and operate as a shared set of functional components. We screened a population of activation-tagged lines to isolate novel components involved in hyponastic growth. Eighteen lines with altered initial petiole angle or a different angle after treatment with ethylene and/or low light were isolated by this forward genetic approach and subsequently characterized. Two of these lines, designated *SIMILAR INITIAL ENHANCED ETHYLENE ENHANCED LOW LIGHT ANGLE1* (*SEE1*) and *SEE2* met all criteria to be components in the shared part of the signaling pathway resulting in hyponastic growth. The plant DNA flanking the T-DNA integration locus for both lines was cloned. Yet, for *SEE2* no differentially regulated genes could be isolated. Functional and mechanistic characterization of *SEE1-1D* is described in chapter 6.

Introduction

Upward leaf movement (hyponastic growth), driven by differential petiole growth, is a mechanism exploited by several plant species to outgrow environmental conditions that hamper growth and development (Cox *et al.*, 2003, 2004, Voesenek & Blom, 1989). Several recent studies showed that *Arabidopsis thaliana* is able to induce hyponastic growth (for details see: Chapter 1) upon exposure to ethylene, low light conditions (Millenaar *et al.*, 2005, 2009; Mullen *et al.*, 2006; Chapter 2) and high temperatures (heat) (Millenaar *et al.*, 2005, Koini *et al.*, 2009; Chapter 3). All these signals induce hyponasty within 2 h after start of treatment and the kinetics of the response to these signals are remarkably similar (Figure 5.1). Yet, hormone actions and genetic components involved differ per treatment. For example, mutant- and pharmacological analyses showed that low light-induced hyponastic growth is independent of ethylene action, whereas heat-induced hyponasty is stimulated by this gaseous hormone (Chapter 3). Auxin and polar auxin transport do not seem to play a role in ethylene-induced hyponasty, but are required for the response induced by low light and heat (Millenaar *et al.*, 2009; Van Zanten *et al.*, 2009a Koini *et al.*, 2009; Chapter 2 & 3). ABA antagonizes ethylene-induced hyponastic growth (Benschop *et al.*, 2007) and is a positive regulator of heat- and low light-induced hyponastic growth (Chapter 3 & 4).

Following from these findings, it is reasonable to assume that low light, ethylene

and heat regulate hyponastic growth, at least upstream, through different parallel pathways. Given the remarkable similarities in growth response kinetics (Figure 5.1), we hypothesize however, that downstream the three parallel pathways might merge and operate a shared set of functional hyponastic growth associated genetic components. To test this hypothesis and to isolate novel, previous unanticipated components involved in the perception, transduction and integration of signals towards hyponastic growth in *Arabidopsis*, we conducted a forward genetic screen. In total, 18 lines were isolated from a population of activation tagged plants that showed an altered hyponastic growth response or had a constitutive enhanced or reduced petiole angle phenotype. Two lines; *SIMILAR INITIAL ENHANCED ETHYLENE ENHANCED LOW LIGHT ANGLE1* (*SEE1*) and *SEE2*, met the criteria for being shared downstream components involved in all tested abiotic signals. The plant DNA flanking the T-DNA integration locus of these lines was cloned and further characterized. However, for *SEE2* no differentially regulated genes could be isolated. Mechanistic and functional characterization of *SEE1-1D* is described in detail in chapter 6.

Results and Discussion

Screenings setup

To isolate genetic components involved in *Arabidopsis thaliana* hyponastic growth, we performed a forward genetic screen. To facilitate easy and fast screening, we first checked if *Arabidopsis* Columbia-0 (Col-0) was able to exhibit a normal low light-induced hyponastic growth response when the same plant was treated a day before with ethylene for 6 h and subsequently was allowed to recover overnight. Ethylene-induced hyponastic growth was, as expected, quickly reversed by removing the ethylene source (Millenaar *et al.*, 2005) and this treatment did not interfere with the ability to respond to low light (Figure 5.2).

Using this approach, a population 35S CaMV promoter tagged plants (Weigel *et al.*, 2000) were screened for initial petiole angles and petiole angle after 6 h of ethylene and low light treatment. We chose to screen these gain-of-function lines because of the potential to find dominant or semi-dominant phenotypes (Weigel *et al.*, 2000; Østergaard & Yanofsky, 2004). Therefore, genes may be isolated that belong to multi-gene families which might be missed in traditional loss-of-function screens due to genetic redundancy, or because they confer lethality. On the other hand this approach does not rule out identification of loss-of-function alleles, as the T-DNA tag might integrate in the coding region of a gene or in a regulatory sequence and consequently disrupts gene function. Finally, a comparable approach previously led to the isolation of four dominant gain-of-function mutants with hyponastic leaves (Nakazawa *et al.*, 2003) based on which positive candidates were expected in our screen.

The genetic background of the activation-tagged lines is Columbia-7 (Col-7; Weigel *et al.*, 2000). Col-7 has an identical hyponastic growth response to low light and ethylene as the standard lab accession Col-0 (data not shown). We used Col-0 in all subsequent analyses.

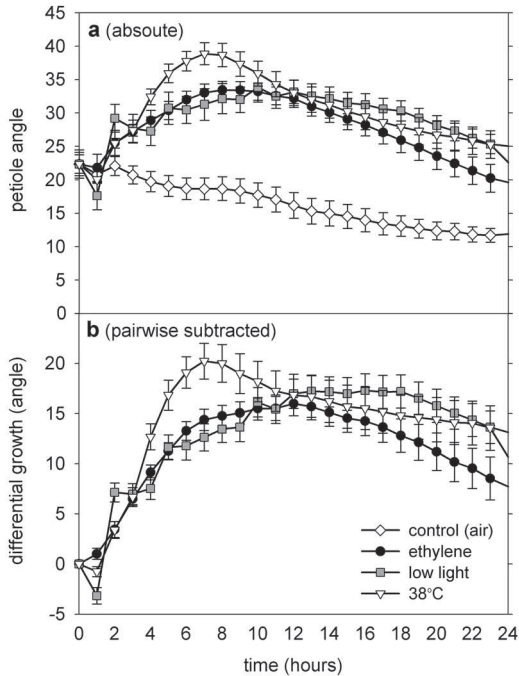


Figure 5.1: *Arabidopsis thaliana* Columbia-0 hyponastic growth response. a: Absolute petiole angles and b: Pair-wise subtracted (Benschop et al., 2007) petiole angles, corrected for diurnal petiole movement in control conditions, upon treatment with ethylene ($5 \mu\text{l l}^{-1}$; black circles), low light ($200 \mu\text{mol m}^{-2} \text{s}^{-1}$ to $20 \mu\text{mol m}^{-2} \text{s}^{-1}$; grey squares) and heat (temperature increase from 20°C to 38°C ; white triangles) and of control plants, left untreated (air; white diamonds). Error bars represent SE; $n > 12$.

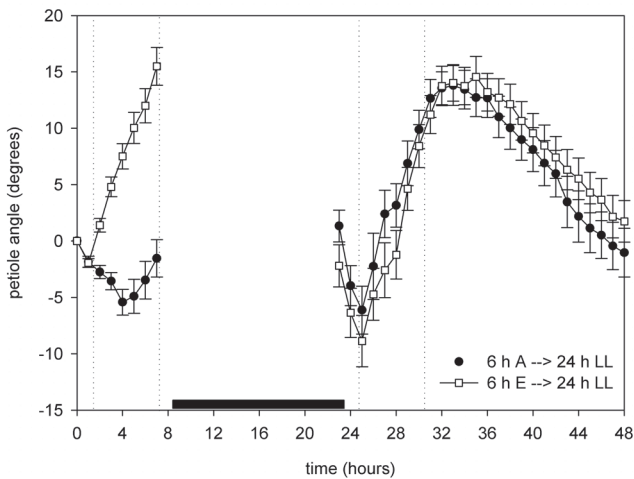


Figure 5.2: Ethylene treatment prior to low light treatment does not affect kinetics of low light-induced hyponastic growth. Columbia-0 plants subjected to 6 h ethylene treatment (E; started at $t=0$ h; $5 \mu\text{l l}^{-1}$; white squares) or air control (black circles), followed the next day by low light treatment (LL; started at $t=24$ h; $20 \mu\text{mol m}^{-2} \text{s}^{-1}$). Petiole angles were normalized to 0 degrees to allow comparison. The dark period is represented by the black horizontal bar. Error bars represent SE; $n > 10$.

Isolation and characterization of candidate lines

Several candidate lines with altered initial petiole angles and/or response angles to ethylene and or low light treatment, compared to Col-0, were isolated (Figure 5.3). After quantification and confirmation of the petiole angle phenotypes, the individual lines/loci were classified and named. We used 'S' for similar, 'D' for decreased and 'E' for enhanced in respective i) initial angle (Figure 5.3a), ii) petiole angle change upon 6 h Ethylene (E) treatment (Figure 5.3b) and iii) petiole angle change upon 6 h Low light (LL) treatment (difference between initial angle and angle after treatment; Figure 5.3c), relative to Col-0 petiole angles. Several types were identified in the screened population (*DDS*, *DDD*, *SDS*, *SSE*, *SDD*, *SEE*, *SDS*, *ESD*, *EDS*, *ESS*; Figure 5.3). Following this, we also quantified the response of these lines to heat treatment (Figure 5.3d). Segregating F₂ progeny, derived from crosses between the candidate lines and Col-0, were tested for BASTA resistance to estimate the amount of T-DNA integrations in each line. For most lines, ~75% of the F₂ progeny showed resistance (Figure 5.4), indicating that those lines contain only one T-DNA insert that can explain the observed petiole angle phenotypes.

However, the used activation tagging lines are prone to head-to-tail insertions (Michael M. Neff, personal communication). Moreover, the instable T-DNA construct might be (partially) silenced in these lines, which often occurs after several propagations (Weigel *et al.*, 2000). Alternatively, silencing might have been partial or the locus has been subject to recombination events (e.g. the BASTA-resistance locus silenced/recombined, but not the 35S enhancers) and also incomplete integrations may occur. Accordingly, *SDD1*, *EDD1*, and *EDD3* did not show any BASTA resistance, whereas these lines had clear petiole angle phenotypes (Figure 5.3). We cannot distinguish if, and which, of the above mentioned processes resulted in the absence of BASTA resistance in these lines, or that the petiole angle phenotypes are caused by insertional mutagenesis in the coding region or regulatory sequences of a gene.

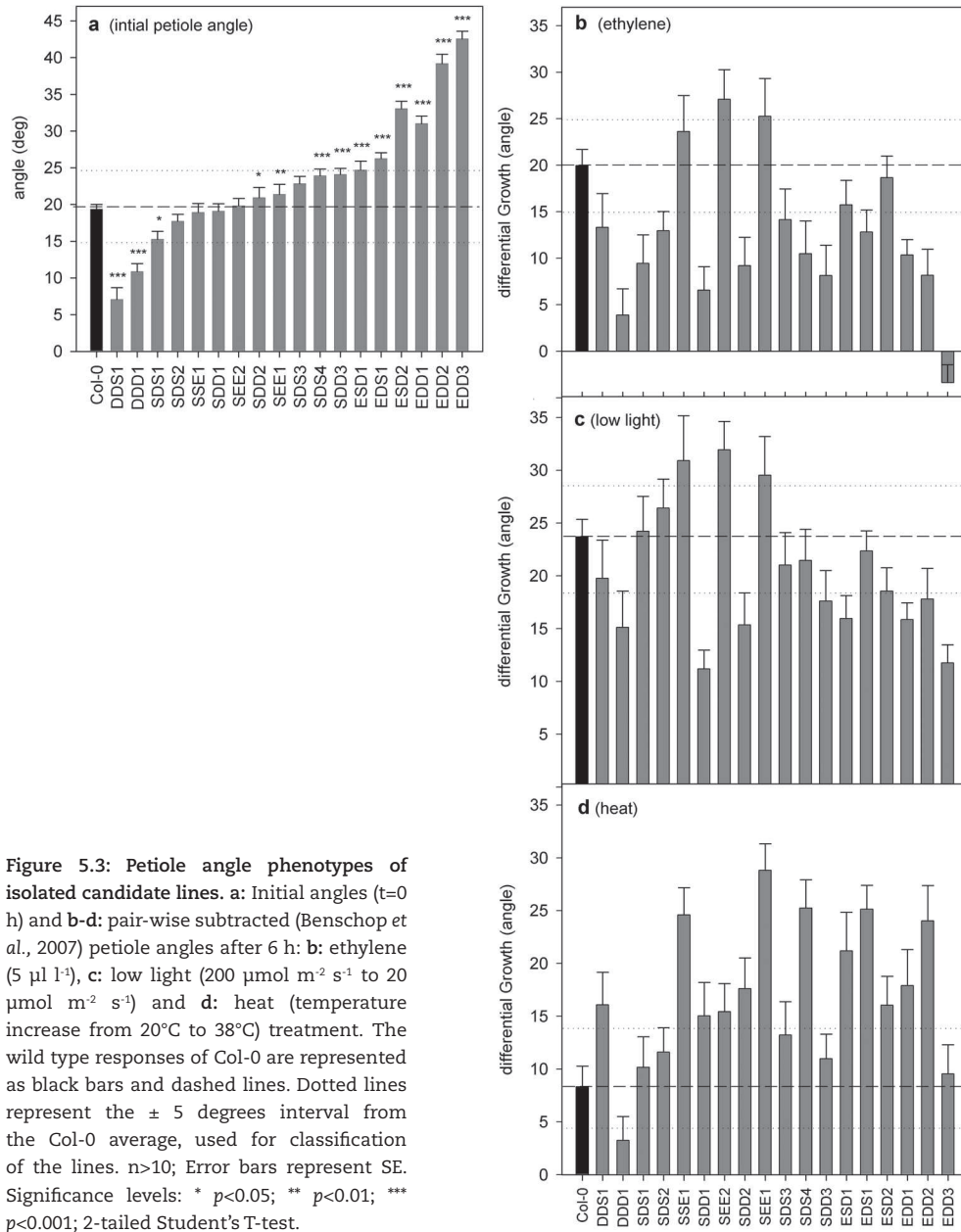


Figure 5.3: Petiole angle phenotypes of isolated candidate lines. a: Initial angles (t=0 h) and b-d: pair-wise subtracted (Benschop *et al.*, 2007) petiole angles after 6 h: b: ethylene ($5 \mu\text{l l}^{-1}$), c: low light ($200 \mu\text{mol m}^{-2} \text{s}^{-1}$ to $20 \mu\text{mol m}^{-2} \text{s}^{-1}$) and d: heat (temperature increase from 20°C to 38°C) treatment. The wild type responses of Col-0 are represented as black bars and dashed lines. Dotted lines represent the ± 5 degrees interval from the Col-0 average, used for classification of the lines. $n > 10$; Error bars represent SE. Significance levels: * $p < 0.05$; ** $p < 0.01$; *** $p < 0.001$; 2-tailed Student's T-test.

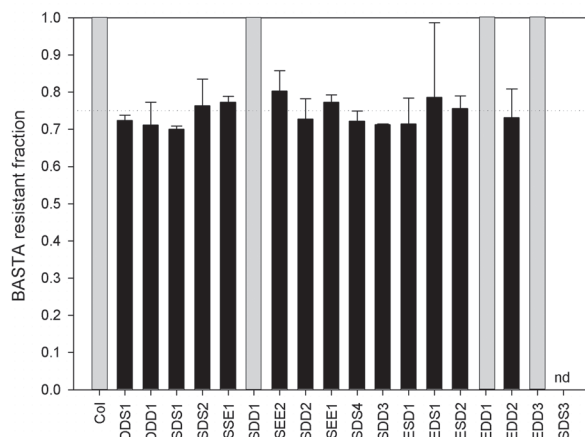


Figure 5.4: BASTA resistance of F2 progeny derived from a cross between candidate lines and sensitive Col-0. Grey bars indicate 100% sensitivity to growth arrest by BASTA whereas black bars indicate the fraction of resistant plants in the screened population. The dotted line represents 75% resistance ratio, expected when only one resistance locus is present in the tested lines. Error bars represent SE. nd; not determined.

To verify the observed petiole angle phenotypes and to study the response in more detail, we monitored the kinetics of hyponastic growth in a selection of the isolated candidate lines upon ethylene-, low light- and heat- treatment using a time-lapse digital camera setup (Cox *et al.*, 2004, Millenaar *et al.*, 2005). This confirmed in all cases the single-time point observations made for ethylene and low light-treatment (Figure 5.5).

DDD1, SDD3 and EDD3 showed a reduced response to all signals throughout the 24 h experimental periods (Figure 5.5a-c, j-l, m-o). Both SEE1 and SEE2 showed an enhanced response over the whole experimental period under ethylene conditions and low light conditions, although in low light they were slightly delayed (Figure 5.5d, e, g, h). In agreement with the single-time point measurements, DDD1 had a reduced response to heat (Figure 5.5c), whereas SEE1, SEE2 had an enhanced response (Figure 5.5f, i). EDD3 and SDD3 had delayed response (Figure 5.5l, o).

Various individual isolated lines exhibited, besides petiole angle phenotypes, morphological phenotypes such as curled leaves (ESD2), low leaf/petiole length ratio typical for shade avoiding plants (EDD2) and broad, flat, leaves (EDD1). For details see Figure 5.6.

We cannot exclude at this point that these morphological phenotypes, and/or the initial petiole angle interacts with the ability to respond to ethylene and low light. Lines representing genes involved in the putative shared downstream route towards hyponastic growth thus ideally have: i) unaltered initial angle, ii) clear response phenotypes to both ethylene and low light, iii) similar, consistent response direction (i.e. enhanced or repressed angle relative to wild type). Based on the initial screen using ethylene and low light, five lines met these criteria: SEE1, SEE2, SDD1, SDD2, and SDD3. However, SDD1 and SDD2 had an exaggerated response to heat (Figure 5.3d) and SDD3 has a delayed response rather than an overall reduced response (Figure 5.5o). Therefore we chose to analyze *SIMILAR INITIAL ENHANCED ETHYLENE ENHANCED LOW LIGHT ANGLE1* (SEE1) and SEE2 further.

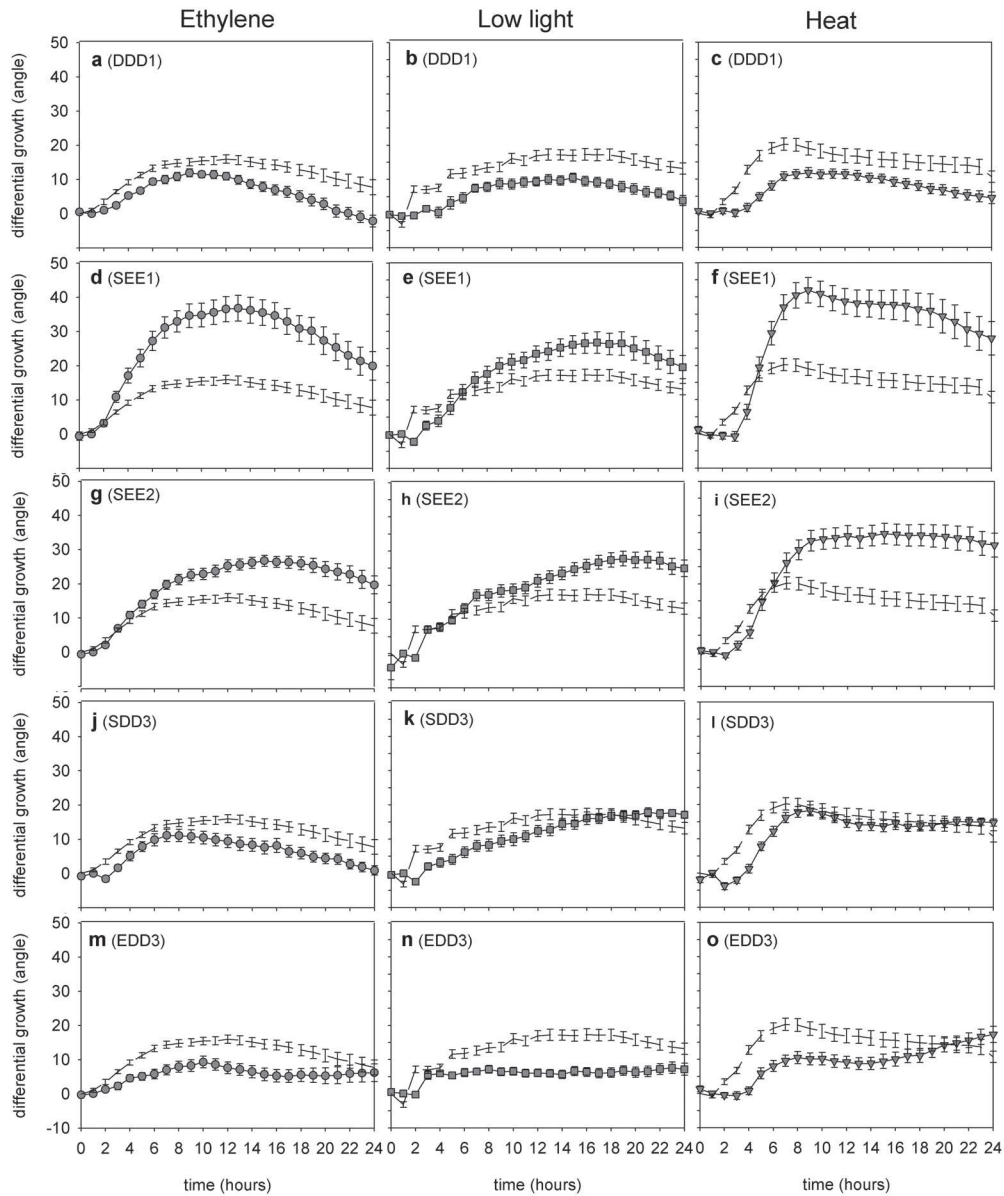


Figure 5.5: Hyponastic petiole growth kinetics of isolated candidate lines. Petiole angle kinetics during treatment with $5 \mu\text{l l}^{-1}$ ethylene (a,d,g,j,m; first column, circles), low light ($200 \mu\text{mol m}^{-2} \text{s}^{-1}$ to $20 \mu\text{mol m}^{-2} \text{s}^{-1}$; b,e,h,k,n; second column, squares) or heat (38°C ; c,f,i,l,o; third column, triangles) compared to Col-0 wild type responses (dashed lines). Angles resulted from pair wise subtraction (Benschop et al., 2007), Error bars represent SE; $n > 10$.

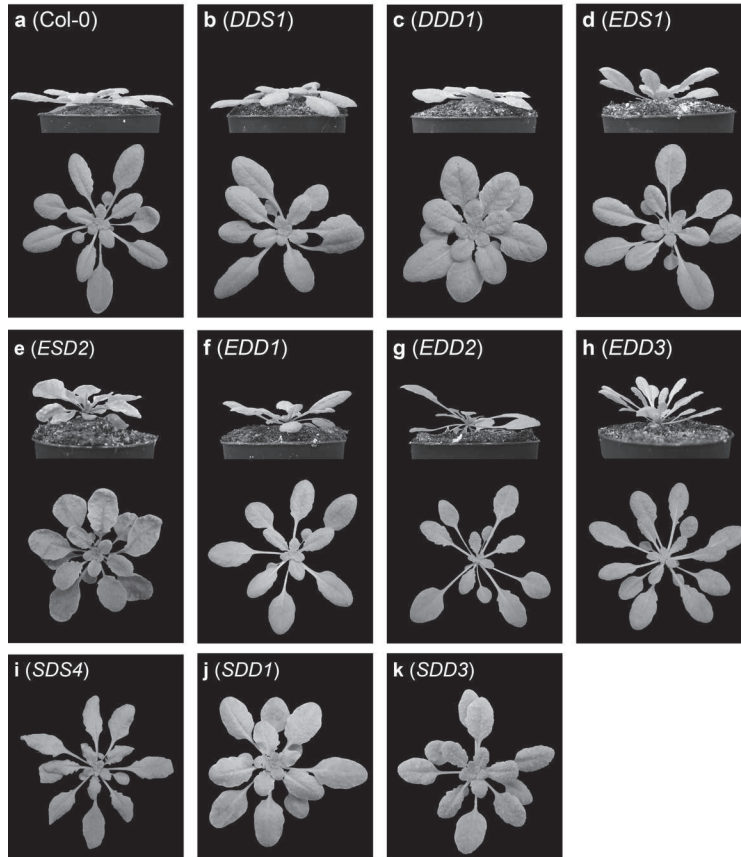


Figure 5.6: Morphology of candidate lines with a visual phenotype. (See Color Supplement for full color version of this figure)

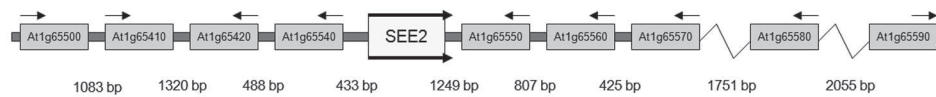


Figure 5.7: Schematic representation of the *SEE2* insertion locus. The T-DNA insertion site is depicted as a large box. Arrows indicate the direction of the multimerized CaMV 35S transcriptional enhancers. Genes in the vicinity are depicted as smaller boxes containing their AGI-codes (For Gene Ontologies of each gene see Table 5.1). Distance in (base pairs (bp)) between adjacent genetic components are depicted below the intergenic regions. The directions of the startcodon are depicted as arrow above the genes. Physical distances of >1500 bp are shown as a break.

Cloning of *SEE1* and *SEE2*

To find the causal genes explaining the *SEE1* and *SEE2* phenotypes, we cloned the T-DNA flanking sequences by Thermal Asymmetric Interlaced-PCR (TAIL-PCR; Liu *et al.*, 1995a, b). The results for *SEE1* are described in Chapter 6.

The T-DNA in *SEE2* was inserted on chromosome 1 (Figure 5.7), in the intergenic region between a calcium-binding EF-HAND family protein (At1g65540) and a XANTHINE/URACIL PERMEASE family protein (At1g65550). Using Micro-array data obtained from Col-0 petioles treated 3 h with ethylene or low light (Millenaar *et al.*, 2006), we first screened for genes, located in the vicinity of the insertion site, that were differentially expressed after ethylene and low light treatments. However, no differentially expressed genes were found. In all isolated lines, described in Weigel *et al.* (2002), the gene directly flanking the T-DNA insertion caused the observed phenotype. The distance between T-DNA insertion point and the over-expressed gene causing the phenotype, was up to 3500 bp (Weigel *et al.*, 2000). We measured transcript abundance of T-DNA border flanking genes by Real-Time Reverse-Transcriptase PCR (Table 5.1). No genes were found with a clear differences in expression in the ~3800 bp region upstream of the *SEE2* integration site (4 genes), nor in the ~7500 bp region downstream (5 genes). However, the ENOYL-COA HYDRATASE/ISOMERASE family protein (At1g65520) and the EF-HAND family protein (At1g65540) were minimally, (respectively 1.9 and 2.2 times), yet significantly ($p < 0.05$) up regulated.

Expression of the XANTHINE/URACIL PERMEASE family protein (At1g65550), directly flanking the tag, and the more upstream putative POLYGALACTURONASE/ECTINASE gene (At1g65570) could not be detected by Real-Time RT-PCR. It remains to be elucidated if one of these genes is causal for the enhanced response in *SEE2* or that an incomplete or silenced secondary insertion(s) influences the phenotype. Nevertheless, we propose that *SEE1* and *SEE2* are general negative regulators of induced hyponastic growth.

Table 5.1: AGI codes, gene ontology (GO) annotation and relative expression (Rel. exp.) of genes flanking the T-DNA insertion site of *SEE2*, compared to Col-0, in control (air) conditions. Data is obtained by Real-time RT-PCR. Significance levels are p -values; * $p < 0.05$; ns = non significant; 2-tailed Student's T-test. Negative signs indicate down regulation compared to Col-0. $n \geq 4$. Error bars represent SE, nd = not detectable.

AGI-code	Gene ontology (GO annotation)	Rel. exp.	SE	p
At1g65500	Unknown protein	1.3 ±	1.2	ns
At1g65510	Unknown protein	1.5 ±	1.3	ns
At1g65520	ENOYL-COA HYDRATASE/ISOMERASE family protein	1.9 ±	1.3	*
At1g65540	Calcium-binding EF HAND family protein	2.2 ±	1.4	*
At1g65550	XANTHINE/URACIL PERMEASE family protein	nd		
At1g65560	Putative ALLYL ALCOHOL DEHYDROGENASE	-1.3 ±	1.2	ns
At1g65570	Putative POLYGALACTURONASE, putative PECTINASE	nd		
At1g65580	ENDONUCLEASE/EXONUCLEASE/PHOSPHATASE family	1.1 ±	1.2	ns
At1g65590	β-HEXOSAMINIDASE activity	1.0 ±	1.1	ns

Materials and Methods

Plant materials and growth conditions

Arabidopsis thaliana activation tagged lines (Weigel *et al.*, 2000; N21991, N23153), Col-7 (N3731) and Col-0 (N1092) were obtained from the Nottingham Arabidopsis Stock Centre (NASC Stock IDs between brackets). Plants were grown on a fertilized mixture of pot-soil and perlite (1:2; v/v) as described previously by Millenaar *et al.* (2005), under the following conditions: 20°C, 70% (v/v) relative humidity, 200 $\mu\text{mol m}^{-2} \text{s}^{-1}$ photosynthetic active radiation (PAR), 9 h short-day photoperiod. Plants were automatically watered to saturation each day, at the start of the photoperiod. Before potting, seeds were stratified in the dark at 4°C for 4 d to synchronize germination.

Treatments and screening

Plants in developmental-stage 3.9 (Boyes *et al.*, 2001) were used for all experiments. In all cases, plants were transferred to the experimental setups (Microclima 1750 growth cabinet (Snijders Scientific, Tilburg, the Netherlands), one day before the experiments to allow acclimatization. All treatments started 1.5 h after the start of the photoperiod to rule out effects of diurnal and circadian leaf movements (Salter *et al.*, 2003).

In total, 17.500 individual Cauliflower Mosaic Virus (CaMV) 35S enhancer (activation) tagged (Weigel *et al.*, 2000) vegetative plants, pooled in batches of approximately 500 plants each, were screened. The plants were visually monitored for i) initial petiole angles, ii) petiole angle after 6 h of ethylene treatment and after overnight recovery iii) the petiole angle after 6 h low light treatment. Given the make-up of the population, screening 17.500 plants theoretically equals screening of 10498 ± 37 unique individual tagged lines. Because each individual line potentially harbors more than a single T-DNA insertion, the total number of screened loci is higher. Lines/loci were named according to their initial angle and response phenotypes (see main text). To be designated to the 'E' or 'D' class, an arbitrary threshold of minimal 5 degrees difference with Col-0 was set. When the lines differed less than 5 degrees with Col-0, they were assigned to the 'S' class.

Ethylene (Hoek Loos, Amsterdam, the Netherlands) was applied to saturating (not shown) concentrations ($1.5 \mu\text{l l}^{-1}$), in continuous flow-through and then vented away. The equilibrium concentration was reached after approximately 1 h, and was regularly checked thereafter on a gas chromatograph (GC955, Synspec, Groningen, the Netherlands).

For petiole kinetics analysis, $5 \mu\text{l l}^{-1}$ ethylene was mixed with humidified air (70% (v/v)) and applied to glass cuvettes containing one plant each, at a flow-rate of 75 l h^{-1} . For more details see: Cox *et al.* (2004); Millenaar *et al.* (2005); Benschop *et al.* (2007).

Low light-induction was accomplished by decreasing photosynthetic activate radiation (PAR) levels from $200 \mu\text{mol m}^{-2} \text{s}^{-1}$ to $20 \mu\text{mol m}^{-2} \text{s}^{-1}$ by covering the plants with spectrally neutral shade cloth. This did not change light quality (checked with a LI-COR 1800 spectro-radiometer (LI-COR, Lincoln, NE, USA). Induction of high temperature was accomplished by moderating the program of the used growth cabinet. The 30°C threshold was reached after 22 minutes; 38°C was reached after 49 minutes.

Petiole angle measurements

Petiole angle kinetics was measured using an automated time-lapse camera system as described by Cox *et al.* (2004); Millenaar *et al.* (2005); Benschop *et al.* (2007). Plants were placed in glass cuvettes with the petiole of study perpendicular to the axis of the camera. To facilitate measurement, leaves that were obscuring the petiole base were removed. This treatment did not affect the petiole angle of the remaining leaves before- and after treatments (Millenaar *et al.*, 2005). Additionally, the petiole was marked at the petiole/lamina junction with orange paint (Decofin Universal; Apeldoorn, the Netherlands). Pictures of two petioles per plant were taken every 10 min. Angles were measured between the marked point at the petiole/lamina junction and a fixed basal point of the petiole, compared to the horizontal, by using KS400 (Version 3.0) software package (Carl Zeiss Vision, Hallbergmoos, Germany) and a custom made macro, developed by Dr. M.Terlou (Utrecht University). For all replicate plants, the two measured petioles were averaged and subjected to further analysis. To enable continuous photography over the 24 h experimental period, no dark period was included during the experiments.

Plants used for measurement of fixed time-points were manually photographed from the side. Angles were measured using the freeware algorithm; ImageJ (<http://rsb.info.nih.gov/ij>) For all replicate plants, the two measured petioles were averaged before they were subjected to further analysis. Statistical significance-levels were determined using a standard 2-tailed Student's t-Test calculated in Microsoft Excell 2003 (Microsoft, Redmond, USA).

To rule out effects of diurnal- and/or circadian effects on petiole movement a pair-wise subtraction (Benschop *et al.*, 2007) was performed, by calculating the difference in angle between treated and control plants at 6 h in the single time-point measurements and for each time point in the petiole angle kinetics measurements. The new standard errors for the differential response were calculated by taking the square root from the summation of the two squared standard errors.

Segregation analysis

Crosses were made between Col-0 as female receiver and pollen from the isolated activation tagged lines, that contain glufosinate ammonium (BASTA)-resistance as selection marker (Weigel *et al.*, 2000). F₁- and self-pollinated F₂ progeny seeds were subjected to BASTA selection on selective agar-plates containing 8 g l⁻¹ plant agar (Duchefa, Brussel, Belgium), 0.22 g l⁻¹ Murashige-Skoog (Duchefa) and 50 µg ml⁻¹ DL-Glufosinate ammonium (BASTA / DL-phosphinotricin; Duchefa). After sawing, seeds were dark stratified at 4°C for 4 days and thereafter placed in the standard growth conditions as above. After three weeks survival ratios were scored. Because BASTA resistance is a dominant trait, it follows from Mendelian segregation analysis that lines with a frequency-distribution; 25% not resistant, 50% heterozygous resistant, 25% homozygous resistant contain only one T-DNA insert that can explain the observed petiole angle phenotypes.

Cloning of T-DNA loci

TAIL-PCR was conducted essentially as described by Liu *et al.* (1995a, b). Genomic-DNA was isolated using Nucleon Phytopure DNA extraction kit, (GE Healthcare/Amersham; Den Bosch, the Netherlands). Integrity of the DNA was checked by specific amplification of Actin (At5g09810) using the primers: 5'-GCATCATCACAAGCATCCTAA-3' and 5'-TTCGTGGTGGTGCCTTTGTT-3'. Subsequent TAIL-PCR was conducted using the degenerate primer: AD2; 5'-

NGTCGASWGANAWGAA-3', TTCWTNTCWSTCGACN; Liu *et al.*,1995a,b) in combination with nested primers from the Left-border: 5'-ATCTAAGCCCCCATTTGGAC-3' (primary PCR); 5'-TAACGCTGCGGACATCTACA-3' (secondary PCR); 5'-CGGACATGAAGCCATTTACA-3' (tertiary PCR). PCR products were separated on agarose-gel and purified using a GFX-spin column (GE Healthcare/Amersham) and subjected to direct sequencing (Macrogen, Seoul, South-Korea) using the tertiary PCR primer.

Real-Time Reverse Transcriptase-PCR

Real-Time RT-PCR was conducted essentially as described by Millenaar *et al.* (2005, 2006). Petioles were harvested and snap-frozen in liquid nitrogen. For one RNA sample eight petioles of four plants were pooled. RNA was isolated using the RNeasy Plant Mini Kit (Qiagen, Leusden, the Netherlands). gDNA was removed using the DNA-Free kit (Ambion, Cambridgeshire, United Kingdom). Superscript III RNase H⁻ Reverse Transcriptase (Invitrogen, Breda, the Netherlands) using Random-Hexamer Primers, was used for cDNA synthesis. Real-Time RT-PCR reactions were performed on MyiQ Single-Color Real-Time PCR Detection System and Software using iQ SYBR Green Supermix Fluorescein (Bio-Rad laboratories, Veenendaal, the Netherlands). The gene specific primers are described in Table 5.2. For At1g65550 and At1g65570 two independent primer combinations were used, which both did not yield detectable product. The sequences were checked for uniqueness by BLAST-search and melt-curves were generated to check if only one product was formed. Relative mRNA values were calculated using the comparative Ct method described by Livak and Schmittgen (2001), expressing mRNA values relative to β -Tubulin-6 (At5g12250, 5'-ATAGCTGCCCGAGGTCCTC-3', 5'-TCCATCTCGTCCATTCTTC-3'; Czechowski *et al.* (2004)).

Acknowledgements

The authors thank Maarten Schippers (National Institute for Public Health and Environment (RIVM), Bilthoven, the Netherlands) for statistical advice on the screenings setup and Michael M. Neff (Washington State University, WA, USA) for advice on the technical aspects of the cloning of the T-DNA loci.

Table 5.2: Forward (F) and reverse (R) gene specific primers used for Real-Time RT-PCR of genes flanking the T-DNA insertion site of SEE2. Note that for At1g65550 and At1g65570 two independent primer combinations were used, which both did not result in detectable product.

AGI-Code		
At1g65500	F	5'-TCACGCTTTCCTCTCAGCTT- ³
	R	5'-GCTGGAGAAGTTCCACATGA- ³
At1g65510	F	5'-TGGGTTCGAAGACATCAACA- ³
	R	5'-CTAGATGCCGGAGTCCACAC- ³
At1g65520	F	5'-GATAGTTCGGCGTGGTTTA- ³
	R	5'-TACCATACGCCGAATCAACA- ³
At1g65540	F	5'-GAAATGGCAAAGGAAGTCCA- ³
	R	5'-CATTCGAAACACCGACTCCT- ³
At1g65550 – a	F	5'-ACTGGGTCAACAGTCTCCT- ³
	R	5'-CACCTCCCATGAGTGGAAGT- ³
At1g65550 – b	F	5'-TTGTGCGAACAATGAGAAGC- ³
	R	5'-GTCCCACTTCAACGCATCTT- ³
At1g65560	F	5'-CTTCGATAACGTGGGTGGAT- ³
	R	5'-TTTGCAAAGACACCATTCCTCA- ³
At1g65570 – a	F	5'-CATCAAAACCGGAGACGATT- ³
	R	5'-TTTGCTAAGCTCCCAATGCT- ³
At1g65570 – b	F	5'-GGCGTGAAAACGTAAGTGT- ³
	R	5'-TCCTGAGAAGGGCAAGAAGA- ³
At1g65580	F	5'-GAGGGTCCACTCGTTACCA- ³
	R	5'-TGGCTTCACAGTTCTGC- ³
At1g65590	F	5'-ACCACTTGACGTGAGCAGTG- ³
	R	5'-TAAGCCATTGGGCTATTTCG- ³

A2-Cyclins redundantly control hyponastic petiole growth in *Arabidopsis thaliana*, seems independent from the cell cycle and endoreduplication

Martijn van Zanten¹, Steffen Vanneste², Ankie M.H. Ammerlaan¹, Fionn McLoughlin^{1§}, Kerstin Gühl^{1§}, Joanna K. Polko¹, Laurentius A.C.J. Voeselek¹, Frank F. Millenaar^{1§}, Tom Beeckman², Anton J.M. Peeters¹

¹ Plant Ecophysiology, Institute of Environmental Biology, Utrecht University, Padualaan 8, 3584 CH Utrecht, the Netherlands

² Department of Plant Systems Biology, Flanders Interuniversity Institute for Biotechnology, Ghent University, Technologiepark 927, B-9052, Ghent, Belgium

§Present addresses:

FMCL: Section of Plant Physiology, Swammerdam Institute for Life Sciences, University of Amsterdam, Kruislaan 318, 1098 SM Amsterdam, the Netherlands.

KG: NSURE BV; Bornsesteeg 59, 6708 PD Wageningen, the Netherlands.

FFM: De Ruiter Seeds, Leeuwenhoekweg 52, 2660 BB Bergschenhoek, the Netherlands.

Abstract

Plants must adjust to changes in their environment to grow and survive. Upward leaf movement (hyponastic growth), induced by differential petiole growth, is an example of a response operated to outgrow unfavorable conditions. Hyponastic growth is induced to a similar extent by different abiotic stimuli, including enhanced ethylene levels, low light intensity and increased temperatures. Despite its functional importance, relatively little is known on the molecular mechanisms that control hyponastic growth. We isolated and characterized an activation-tagged *Arabidopsis thaliana* line; *SIMILAR INITIAL ENHANCED ETHYLENE ENHANCED LOW LIGHT ANGLE1-1D* (*SEE1-1D*), which exhibits an exaggerated hyponastic growth phenotype to several inducing environmental stimuli. We found that ectopic expression of the core cell cycle gene *CYCLINA2;1* was causal to the *SEE1-1D* phenotype. We show that *CYCA2*-mediated control over hyponastic growth may be independent from its predicted function in cell division and/or endoreduplication. Signals from ethylene and ABA converge in a spatial restriction of *CYCA2;1* expression to basal petiole tissues, away from more distal zones. In this way, maintenance of A2-Cyclin mediated growth in basal tissues and repression of growth in more distal tissues may facilitate a differential growth phenotype. Moreover, ABA might fine-tune *CYCA2* activity through induction of cell cycle inhibitory proteins of the Cyclin-Dependent Kinases/Kip-related Protein (ICK/KRP) family.

In the assumption that *CYCA2*s function in complex with Cyclin Dependent Kinases (CDKs) to regulate hyponastic growth, this observation would be consistent with a model in which ABA and ethylene signals become integrated in the regulation of *CYCA2*-CDK activity, through effects on *CYCA2* and *ICK/KRP* expression. Presumably, *CYCA2;1* and *ICK/KRP* proteins are transcriptional controlled by a yet unidentified Ethylene Response Factor(s) (ERFs).

Introduction

Plants must adjust to growth- and reproduction limiting factors in their environment. Among the strategies that plants employ to escape from unfavorable conditions is differential petiole growth-driven upward leaf movement, called hyponastic growth. By tilting the leaves to a more vertical position, plants can avoid complete submergence and shade by restoring contact with the atmosphere and light, respectively (Voeselek & Blom, 1989; Cox *et al.*, 2004; Ballaré, 1999; Pierik *et al.*, 2005). *Arabidopsis thaliana* is able to induce a marked hyponastic growth response upon flooding, which is triggered by endogenous accumulation of the gaseous phytohormone ethylene (Millenaar *et al.*, 2005; Van Zanten *et al.*, 2009a), upon low light intensity (Hangarter *et al.*, 1997; Millenaar *et al.*, 2005, 2009; Mullen *et al.*, 2006) and in response to supra-optimal temperatures (Millenaar *et al.*, 2005; Koini *et al.*, 2009; Chapter 3). Low light-induced hyponastic growth does not require ethylene action (Millenaar *et al.*, 2009; Chapter 2), whereas the response to heat is antagonized

by ethylene (Chapter 3). The abiotic stress hormone abscisic acid (ABA) antagonizes ethylene-induced hyponastic growth and stimulates heat- (Chapter 3) and low light-induced hyponastic growth (Chapter 4). Moreover, ethylene-induced hyponasty does not involve auxin signaling and polar auxin transport (PAT), whereas both heat- and low light-induced hyponasty require functional auxin signaling components and PAT (Millenaar *et al.*, 2009; Van Zanten *et al.*, 2009a; Chapter 2, Chapter 3).

Ethylene, low light and supra-optimal temperatures induce the hyponastic growth response with remarkably similar kinetics (Chapter 2-5). Therefore, we hypothesize that shared functional genetic components may be operated to control hyponastic growth, whereas others probably act in parallel pathways. Although the physiological control of hyponastic growth and its functionality are increasingly understood, little is known of the molecular mechanisms that drive the response. To isolate novel components controlling hyponasty, we followed a forward genetic approach. A population of 35S Cauliflower Mosaic Virus (CaMV)-promotor tagged plants (Weigel *et al.*, 2000) was screened and 18 lines were isolated with altered initial petiole angle phenotypes and/or disturbed hyponastic responses to ethylene, low light or a combination of these treatments (Chapter 5). Among these were two that showed a clear and reproducible enhanced hyponastic growth phenotype to these inducing stimuli, and had a initial petiole angle that was identical to the parental Columbia wild type. These lines were designated SIMILAR INITIAL ENHANCED ETHYLENE ENHANCED LOW LIGHT ANGLE1-1D (*SEE1-1D*) and *SEE2*. The enhanced response to all stimuli suggests that the causal genes explaining the *SEE1-1D* and *SEE2* phenotypes may be central integrators of the different environmental stimuli that promote hyponastic growth. For this reason these lines were subjected to further analysis. The cloning and characterization of *SEE2* is described in more detail in Chapter 5.

Here, we describe the cloning and characterization of *SEE1-1D*. Our data demonstrate that ectopic expression of the core cell cycle gene *CYCLINA2;1* explains the enhanced hyponastic growth phenotype of *SEE1-1D* to all stimuli, and that the A2-Cyclins (*CYCA2s*) control hyponastic growth. Surprisingly, the control of hyponastic growth seems independent from the predicted role for *CYCA2s* in cell cycle regulation and endoreduplication. We provide evidence that both ethylene and ABA restrict *CYCA2;1* activity to the basal petiole tissue region, thereby perhaps maintaining growth in this zone and repressing growth in the distal tissues, resulting in hyponastic growth. Moreover, we found evidence that ICK/KRP proteins (Inhibitor of Cyclin Dependent Kinases/Kip-related proteins) might function as integrators of ABA and ethylene signals to control hyponastic growth, probably via inhibition of *CYCA2*-CDK complexes.

Results

Isolation and cloning of *SEE1-1D*

SIMILAR INITIAL ENHANCED ETHYLENE ENHANCED LOW LIGHT ANGLE1-1D (SEE1-1D) was isolated in a screen of 35S CaMV promoter-tagged Columbia-7 (Col-7) lines (derived from Weigel *et al.*, 2000), for plants displaying initial petiole angle phenotypes and/or altered hyponastic growth response to treatment with ethylene, low light intensity and/or heat. For details on the screenings approach see Chapter 5. *SEE1-1D* had an initial petiole angle (21.4 ± 1.3 degrees), comparable to wild type Col-0 (19.2 ± 0.6 degrees) and exhibited an exaggerated response to 6 h ethylene, low light and heat treatment (Figure 6.1a). These phenotypes were confirmed by quantitative analysis of response kinetics using a time-lapse digital camera setup (Figure 6.1b-d).

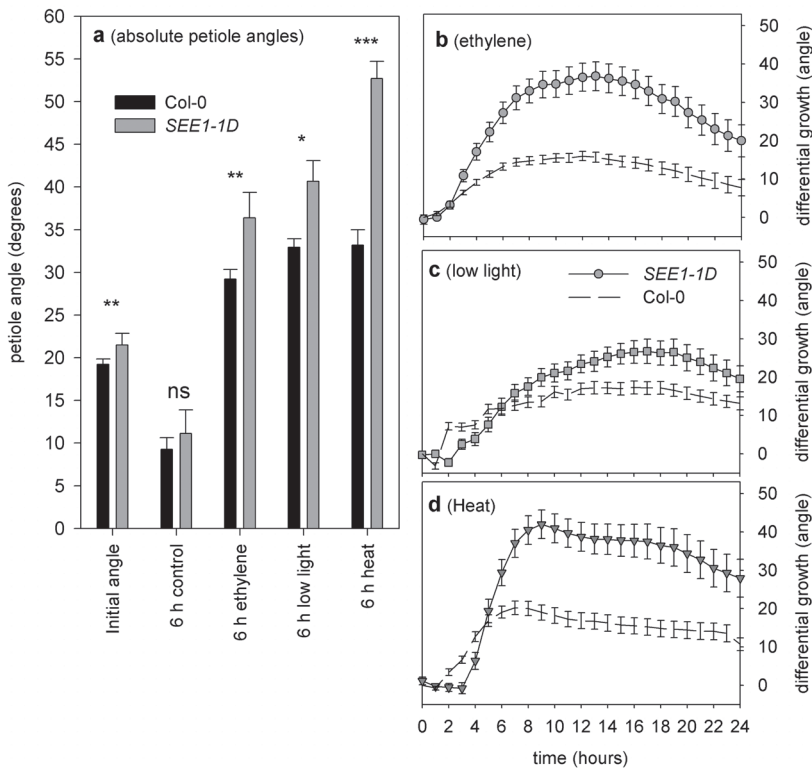


Figure 6.1: Hyponastic growth response of *SEE1-1D*. a: Comparison of initial- and absolute petiole angles after 6 h in control (air) conditions and after 6 h of ethylene ($5 \mu\text{l l}^{-1}$), low light ($200 \mu\text{mol m}^{-2} \text{s}^{-1}$ to $20 \mu\text{mol m}^{-2} \text{s}^{-1}$) and heat (20°C to 38°C) treatment, of *SEE1-1D* (grey bars) and Col-0 (black bars). Significance levels are 2-tailed Student's T-test; ns = non significant, * $p < 0.05$, ** $p < 0.01$, *** $p < 0.001$. b-d: Petiole angle kinetics of *SEE1-1D* compared to Col-0 responses (dashed lines) upon treatment with b: ethylene (circles); c: low light (squares) and d: heat (triangles). Angles resulted from pair wise subtraction (Benschop *et al.*, 2007), Error bars represent SE in all panels; $n > 10$.

BASTA resistance in *SEE1-1D* segregated in a 3:1 ratio in offspring of selfed heterozygous plants, which co-segregated with the phenotypes. This indicates that a single T-DNA integration locus in *SEE1-1D* is responsible for its phenotype (see Figure 5.4). The T-DNA flanking borders were cloned by Thermal Asymmetric Interlaced-PCR (TAIL-PCR; Liu *et al.*, 1995a, b). Sequencing indicated that the T-DNA is inserted on chromosome 5 in the intergenic region between *ETHYLENE RESPONSE FACTOR/APETALA2* (ERF/AP2 transcription factor subfamily B-6; *SHINE3/WAX INDUCER1*) (*SHN/WIN1*; At5g25390, ERF#001; Nakano *et al.*, 2006) and the core cell cycle gene *CYCLINA2;1* (*CYCA2;1*; At5g25380) (Figure 6.2).

Genes causal for the observed phenotypes are often in the direct vicinity of the T-DNA insertion site (Weigel *et al.*, 2000). To identify the most likely effector(s) of the *SEE1-1D* phenotype, transcript levels of the genes within 15 kb up- and downstream of the T-DNA integration site were quantified by Real-Time Reverse-Transcriptase (RT)-PCR. A cluster of five genes surrounding the insertion site (4 downstream and 1 upstream) were markedly up-regulated in *SEE1-1D* in comparison to wild type, including the T-DNA flanking genes; *SHN3/WIN1* and *CYCA2;1* (Table 6.1).

The *SHN3/WIN1* ETHYLENE RESPONSE FACTOR does not control hyponastic growth

Since ETHYLENE RESPONSE FACTORS (ERFs) control many developmental and physiological processes in Arabidopsis, including several ethylene-mediated responses (Nakano *et al.*, 2006), we first tested if *SHN3/WIN1* could be responsible for the enhanced differential petiole growth of *SEE1-1D*. Ectopic expression of *SHN3* in the *Ws* background (Aharoni *et al.*, 2004) did not result in an altered hyponastic growth response upon ethylene, low light or heat treatment (Figure 6.3a-c), nor did ectopic expression of two close homologs (*SHN1*, *SHN2*; Supporting Information Figure S6.1). The typical shiny appearance of *SHN* ectopic expression, due to increased cuticular wax layers (Aharoni *et al.*, 2004) was not observed in *SEE1-1D*. To exclude that appearance of *SHN3* mediated phenotypes depends on the genetic background and that such effects would mask the observation of a hyponastic-growth phenotype, we isolated a line ectopically expressing *SHN3* in the *Col-0* background from a near-complete library of ERF-over-expressing plants (Weiste *et al.*, 2007). Real-Time RT-PCR indicated that *SHN3* was 11.7 ± 0.2 times higher expressed than in *Col-0*, which is comparable to the *SHN3* expression in *SEE1-1D* (19.1 ± 1.5 ; Table 6.1). Indeed, the shiny appearance was found to be accession-dependent, but the hyponastic growth

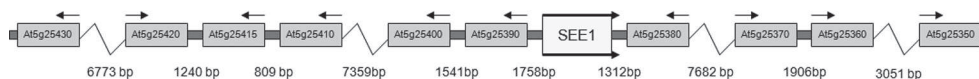


Figure 6.2: Schematic representation of the *SEE1-1D* chromosomal insertion locus. The T-DNA insertion site is depicted as large box. Arrows indicate the direction of the multimerized CaMV 35S transcriptional enhancers. Genes in the vicinity are depicted as smaller boxes with their respective AGI-codes. The direction of the transcription is depicted as arrow above the genes. Length of T-DNA flanking sequences until the start of the coding sequence of the adjacent gene, and physical distances between coding sequences are in base pairs (bp). Physical distance of >2000 bp are shown as break.

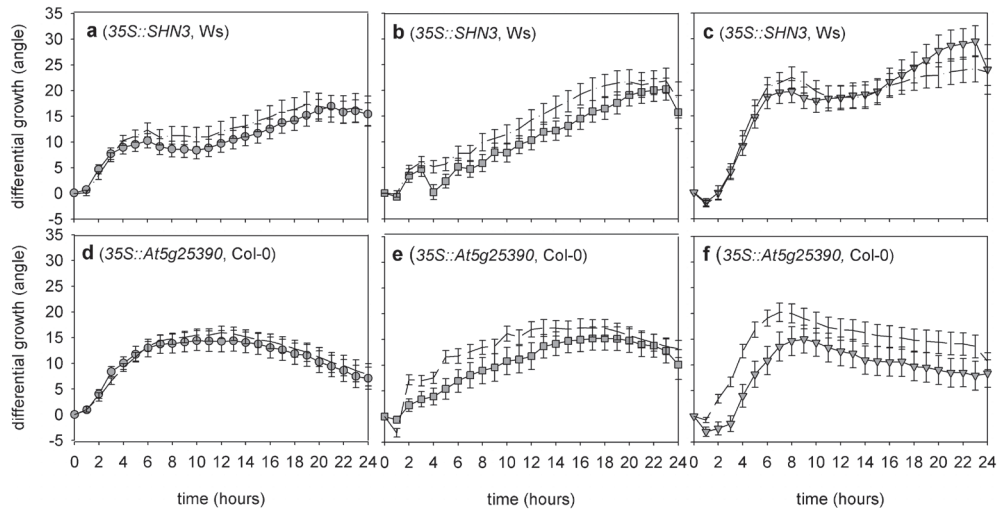


Figure 6.3: Hyponastic growth response of plants ectopically expressing *ERF/AP2 B-6 transcription factor; SHN3/WIN1*. **a-c:** Ectopic expression of *At5g25390/SHN3* in the *Ws-2* (dash-dotted lines) and **d-f:** *Col-0* (dashed lines) background upon: **a,d:** ethylene ($5 \mu\text{l l}^{-1}$; circles), **b,e:** low light ($200 \mu\text{mol m}^{-2} \text{s}^{-1}$ to $20 \mu\text{mol m}^{-2} \text{s}^{-1}$; squares) and **c,f:** heat (20°C to 38°C ; triangles) treatment. Angles resulted from pair wise subtraction, Error bars represent SE; $n > 10$

Table 6.1: Genes with enhanced transcription levels due to the *SEE1-1* T-DNA integration. AGI-codes, gene ontology (GO) annotation and relative expression of genes flanking the T-DNA insertion site of *SEE1-1D*, compared to *Col-0*, in control (air) conditions. Data is obtained by Real-Time RT-PCR. Significance levels are *p*-values; * $p < 0.05$; *** $p < 0.001$; ns = non significant. $n \geq 4$, Error bars represent SE. nd = not detectable.

AGI-code	Gene ontology (GO annotation)	Relative Expression	SE	<i>p</i>
At5g25430	Anion exchange protein family protein	nd		
At5g25420	xanthine/uracil Permease family protein	0.2	± 23.5	ns
At5g25415	Unknown protein	18.5	± 1.6	***
At5g25410	Unknown protein	565.0	± 10.7	*
At5g25400	Phosphate Translocator-related	1043.3	± 1.7	***
At5g25390	<i>ERF/AP2 B-6 transcription factor</i>	19.1	± 1.5	***
At5g25380	<i>CYCA2;1</i>	216.3	± 1.7	***
At5g25370	<i>phospholipase-D α3</i>	1.3	± 1.3	ns
At5g25360	Unknown protein	1.3	± 1.3	ns
At5g25350	<i>EIN3-binding F-box protein 2 (EBF2)</i>	1.6	± 1.3	ns

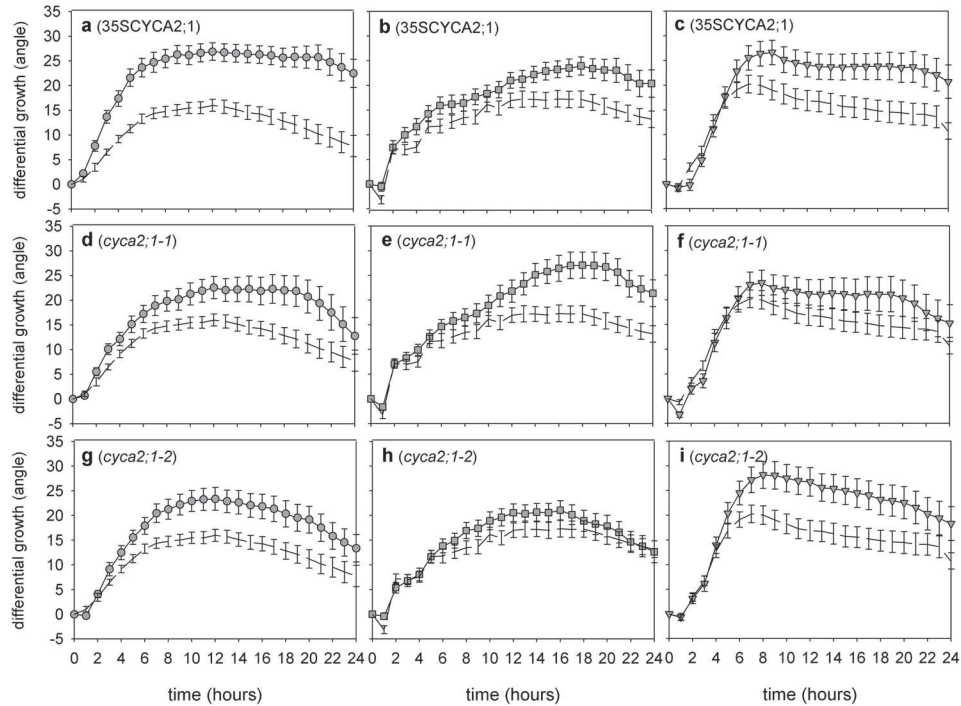


Figure 6.4: Hyponastic growth response of plants misexpressing *CYCA2;1*. a-c: 35S::*CYCA2;1*, d-i: *cyca2;1* loss-of-function alleles in the Col-0 (dashed lines) background upon: a,d,g: ethylene ($5 \mu\text{l l}^{-1}$; circles), b,e,h: low light ($200 \mu\text{mol m}^{-2} \text{s}^{-1}$ to $20 \mu\text{mol m}^{-2} \text{s}^{-1}$; squares) and c,f,i: heat (20°C to 38°C ; triangles) treatment. Angles resulted from pair wise subtraction, Error bars represent SE; $n > 10$.

response kinetics to all three stimuli was identical to wild type in both genetic backgrounds (Figure 6.3d-f). Together these data strongly suggest that the enhanced differential growth phenotype of *SEE1-1D* is not due to ectopic transcription of *SHN3/WIN1*.

A2-Cyclins redundantly control hyponastic growth, downstream of ethylene signaling

To test if the gene *CYCLINA2;1* (*CYCA2;1*; At5g25380), flanking the T-DNA, is responsible for the enhanced petiole angle phenotypes upon ethylene, low light and heat treatment in *SEE1-1D*, we generated plants expressing *CYCA2;1* under control of the constitutive 35S CaMV promoter. Four individual transformants were isolated and enhanced *CYCA2;1* expression in homozygous lines was confirmed by Real-Time RT-PCR (Figure S6.2). Homologous *CYCA2*s were not differentially regulated in these lines (Figure 6.5a).

The hyponastic growth response to ethylene, low light and heat was enhanced in the 35S::*CYCA2;1* lines (Figure 6.4a-c), to comparable levels as *SEE1-1D*, demonstrating

that higher *CYCA2;1* expression explains the amplified hyponastic growth responses observed in *SEE1-1D*.

However, two independent mutant alleles of *cyca2;1* (Yoshizumi *et al.*, 2006) also showed a slightly enhanced hyponastic growth response to ethylene, low light and heat treatment (Figure 6.4d-i). This suggests that loss of *cyca2-1* is compensated for by ectopic compensatory upregulation of other *CYCA2*s (Vandepoele *et al.*, 2002; Pilliteri *et al.*, 2007). We tested this for ethylene-induced hyponasty using the activation-tagged line *INCREASED LEVEL OF POLYPLOIDY1-1D* (*ILP1-1D*), which shows reduced expression of all four *CYCA2* genes (Yoshizumi *et al.*, 2006). Indeed, this line exhibited a reduced hyponastic growth response (Figure 6.5b). As expected, the *ilp1-2* mutant allele (Yoshizumi *et al.*, 2006), with enhanced expression of all *CYCA2*s, shows an enhanced hyponastic response to ethylene treatment (Figure 6.5c). *Cyca2;2-1*,

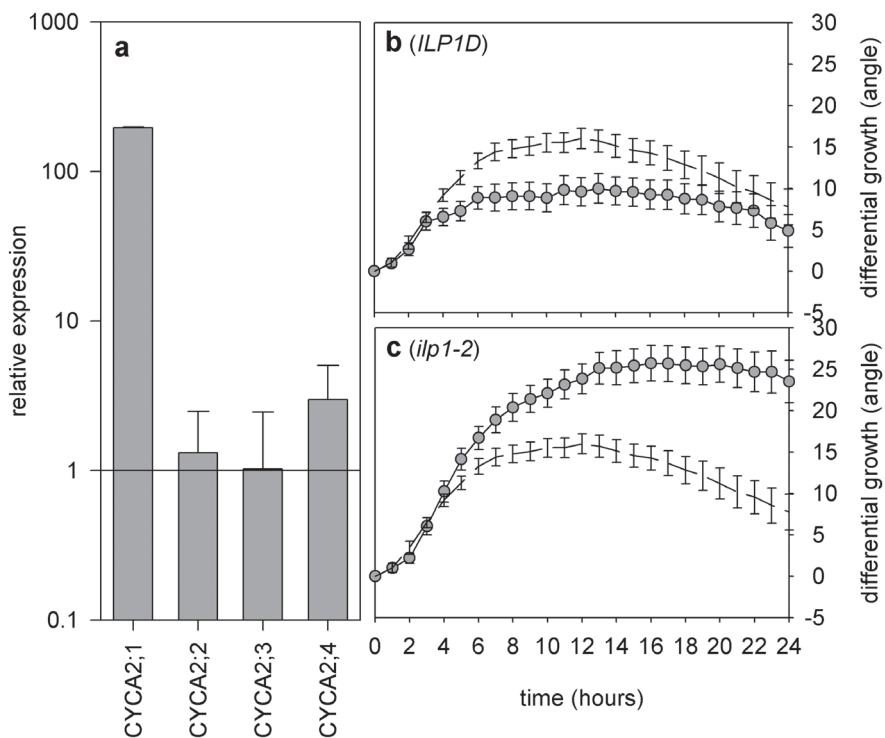


Figure 6.5: Real-Time RT-PCR analysis of A2-Cyclins and hyponastic growth response of plants misexpressing *ILP1*. **a:** Expression of *CYCA2;1* to *CYCA2;4* in *SEE1-1D*, relative to Col-0. Expression values were normalized to 1 for Col-0, $n \geq 4$; Standard errors represent SE. **b,c:** Response kinetics of hyponastic growth of **b:** *ILP1-1D* enhancer tagged line and **c:** *ilp1-2* null-allele (circles), in the Col-0 background (dashed lines), upon ethylene ($5 \mu\text{l l}^{-1}$) treatment. Angles resulted from pair wise subtraction, Error bars represent SE; $n > 10$.

cyca2;3-1 and *cyca2;4-1* insertion mutants did not show an altered hyponastic growth phenotype in response to ethylene (Figure 6.6a-c), whereas several *cyca2* double and triple combinations displayed a reduced ethylene response (Figure 6.6d-l). Double and triple mutants that included *cyca2;1* had a hyponastic growth response less-severe or similar to wild type (Figure 6.6). Thus, genotypes with *cyca2* mutants in addition to *cyca2;1* reverse the enhanced hyponastic growth effects of *cyca2;1* single mutants, underlining the redundancy among A2-type Cyclins in the control of hyponastic growth..

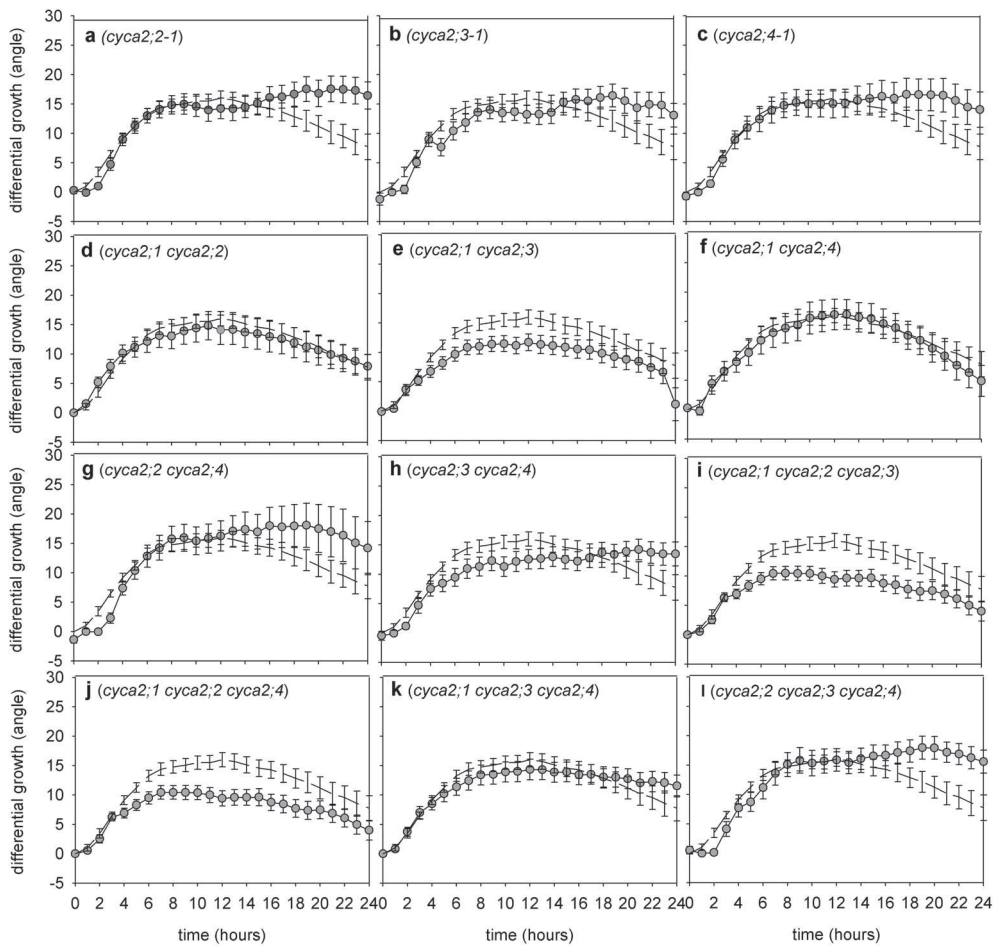


Figure 6.6: Hyponastic growth response of *cyca2* single-, double- and triple mutants alleles. Mutants (circles) and wild Col-0 (dashed lines) upon ethylene ($5 \mu\text{l l}^{-1}$) treatment. Angles resulted from pair wise subtraction, Error bars represent SE; $n > 10$.

Together, these data demonstrate that *CYCA2;1* overexpression is causal to the *SEE1-1D* phenotype. To test if the enhanced hyponastic responses observed in *35S::CYCA2;1* and *cyca2;1* can be explained by altered ethylene sensitivity or production, we monitored the dose-response to ethylene in etiolated seedlings (triple-response assay; Guzman & Ecker, 1990), using the ethylene biosynthetic precursor 1-aminocyclopropane-1-carboxylic acid (ACC). Hypocotyl lengths in *SEE1-1D*, *35S::CYCA2;1* and *cyca2;1-2* were repressed at increasing ACC concentrations to a similar extent as Col-0 (Figure 6.7). Moreover, ethylene release was identical in all tested lines. This indicates that the observed *CYCA2;1*-mediated effects on ethylene-induced hyponastic growth are not caused by secondary ethylene effects and suggests that *CYCA2s* operate downstream of ethylene signaling.

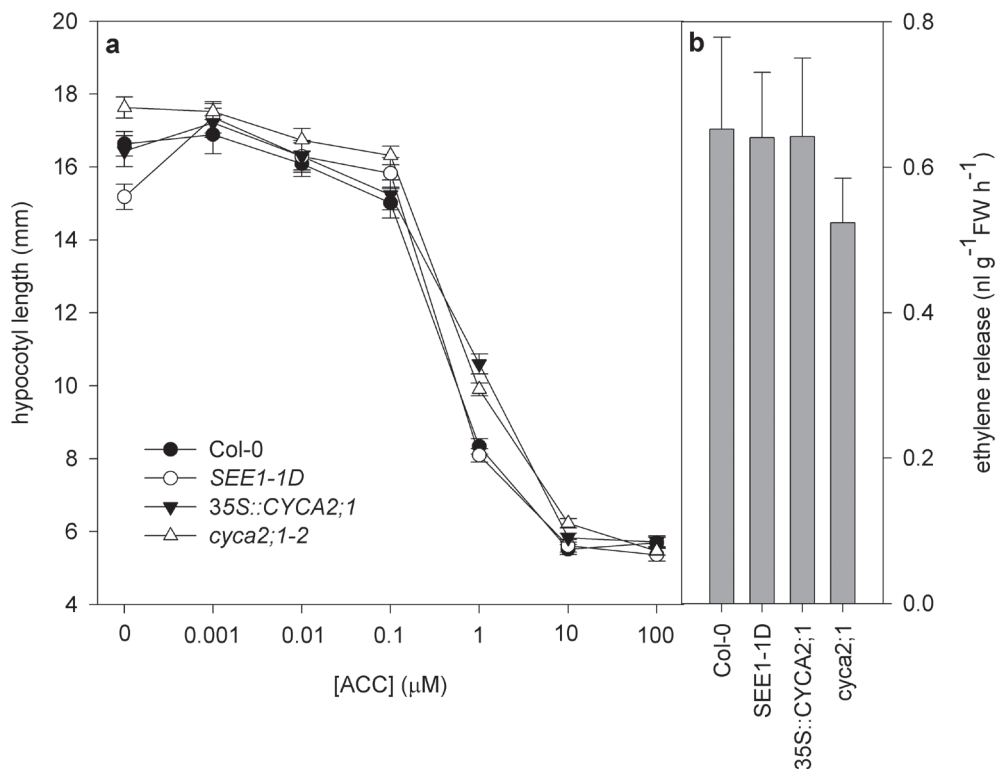


Figure 6.7: Analysis of ethylene production and sensitivity in lines misexpressing *CYCA2;1*. a: Hypocotyl length dose-response curve (triple response assay) of etiolated *SEE1-1D* (open circles), *35S::CYCA2;1* (closed triangles), *cyca2;1-2* (open triangles) and Col-0 wild type (closed circles) seedlings, grown in the presence of various concentrations of the ethylene precursor 1-aminocyclopropane-1-carboxylic acid. $n \geq 22$. b: ethylene release ($\text{nl g}^{-1} \text{FW h}^{-1}$) of Col-0, *SEE1-1D*, *35S::CYCA2;1*, and *cyca2;1*. $n \geq 13$ samples of two pooled vegetative plants each per measurement. Error bars represent SE in both panels.

CYCA2;1 controls ethylene-induced hyponastic growth seemingly independent of the cell cycle and endoreduplication

Current literature supports a role for CYCA2's in cell cycle regulation, more specifically, in controlling the balance between cell division and endoreduplication, a process of consecutive rounds of DNA replication without mitosis (Roudier *et al.*, 2003; Yu *et al.*, 2003; Yoshizumi *et al.*, 2006; Imai *et al.*, 2006; Boudolf *et al.* 2009). Intriguingly, ethylene stimulates endoreduplication in Arabidopsis and Cucumber (*Cucumis sativus*) hypocotyls (Gendrau *et al.*, 1999; Dan *et al.*, 2003). Since ploidy levels are correlated with cell size in many plant species (reviewed in: Sugimoto-Shirasu & Roberts, 2003) and ethylene-induced hyponastic growth is associated with epidermal cell elongation at a confined basal abaxial region of the petiole (Cox *et al.*, 2003; Millenaar *et al.*, 2005; Chapter 1), we hypothesized that ethylene induces hyponastic growth via CYCA2-mediated control of endocycle/mitosis.

Therefore, we analyzed epidermal cell sizes and cell number at the basal abaxial region of the petiole in lines misexpressing CYCA2;1 specifically, or CYCA2s in general (ILP) (Figure 6.8a-n). No apparent differences were observed at the basal abaxial region of the petiole in these lines, suggesting that CYCA2;1-mediated hyponastic growth, is not due to an effect on initial cell number or cell size in the petiole. This was confirmed by quantification of abaxial epidermal cell sizes along the petiole of Col-0 and 35S::CYCA2;1 (Figure 6.8o). In agreement, no differences in transcript levels of mitotic marker genes (Yoshizumi *et al.*, 2006) expressed at specific phases of the cell cycle (Yoshizumi *et al.*, 2006), nor in *ILP1* transcription could be identified between Col-0 and *SEE1-1D* (Figure 6.9). Re-evaluation of petiole tissue derived transcriptome data of 3 h ethylene treated plants (Millenaar *et al.*, 2006) indicated that cell cycle related genes are generally not (strongly) transcriptionally controlled by ethylene (Figure S6.3). Moreover, ethylene did not enhance promoter activity of the mitotic marker gene *CYCLINB1;1* (Figure S6.4).

Ploidy levels, measured by means of flow-cytometry, of basal and distal petiole sections of plants treated for 6 h with ethylene were compared to those of control plants, to determine if ethylene-induced endoreduplication may control hyponastic growth (Figure 6.10a). Ploidy levels were increased after 6 h, equally in the basal and the distal petiole zones, in both ethylene-treated and control plants. Accordingly, a dominant negative *CDKB1;1* overexpressing line, with enhanced ploidy levels and reduced proliferation rate (Boudolf *et al.* 2004), showed a wild type hyponastic growth response to ethylene treatment (Figure 6.10b). Based on these data, we hypothesize that CYCA2;1 controls induced hyponastic growth independent of its role in cell cycle regulation.

Ethylene represses CYCA2 promoter activity in distal- but not in basal petiole tissues

To further study how CYCA2s control hyponastic growth, we assayed promoter activity of individual CYCA2s by histochemical β -glucuronidase (GUS) analysis. All A2-Cyclins were active in meristematic tissues at the rosette center and were mainly, but not exclusively, localized in vascular tissues (Figure 6.11a, b, Figure 6.12; Figure S6.5). This is in agreement with the observation of BursSENS *et al.* (2000) that CYCA2;1

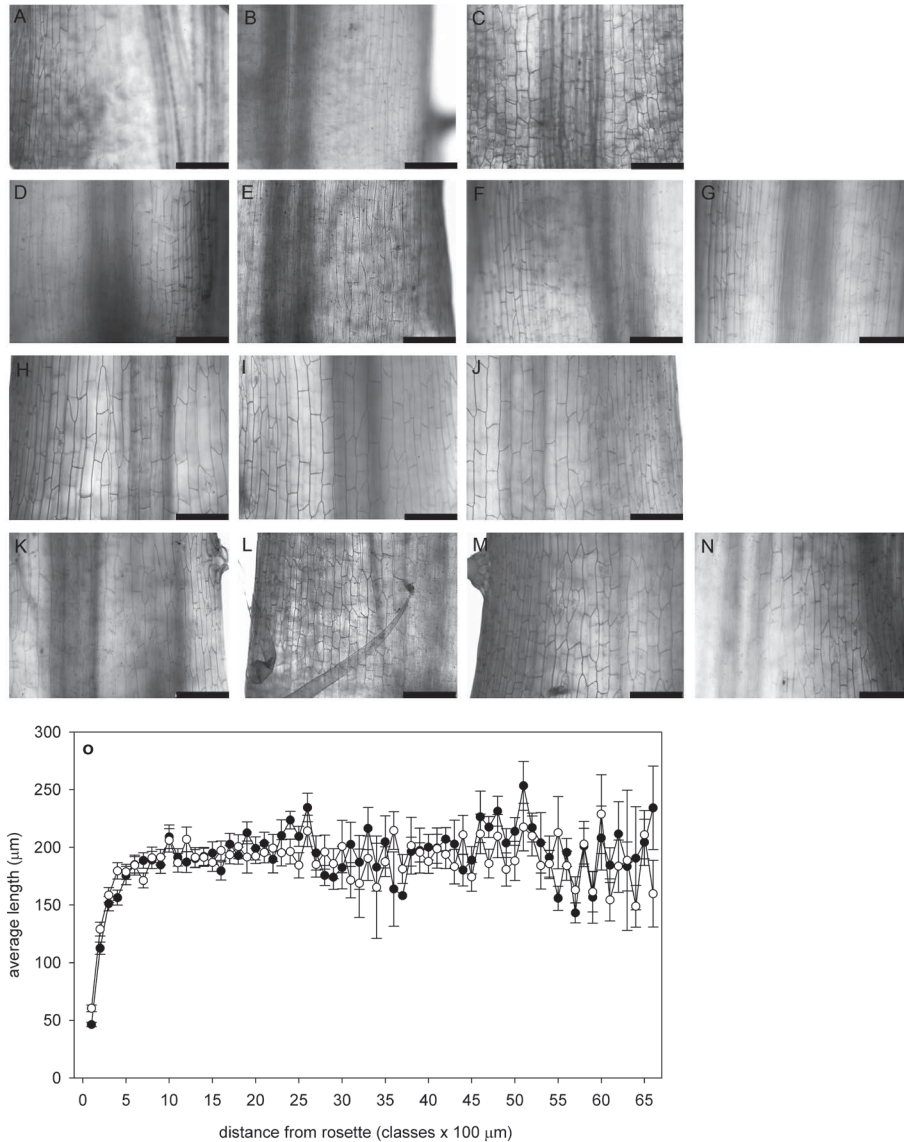


Figure 6.8: Epidermal cell size-analysis of lines misexpressing A2-Cyclins. (See Color Supplement for full color version of this figure). Representative basal sections of **a-g**: abaxial and **h-n**: adaxial side of petioles from: **a,h**: Col-0, **b,i**: *SEE1-1D*, **c,j**: *35S::CYCA2;1*, **d,k**: *cyca2-1*, **e,l**: *cyca2;2*, **f,m**: *ilp1-1*, **g,n**: *ILP1D*. Petioles are Toluidine-blue stained and the middle of each panel is between ~300 and ~400 μm from the basal petiole start, which is well within the zone where epidermal cell elongation drives hyponastic growth (0-1600 μm; see Chapter 1). Scale bars represent 200 μm. **o**: Average cell lengths in classes (100 μm) according to their distance relative to the basal end of the petiole of abaxial epidermal cells of *35S::CYCA2;1* (black circles) and Col-0 wild type (white circles) of a 5 mm (\pm 1 mm) long petioles (stage 3.9, Boyes et al., 2002). Error bars represent SE.

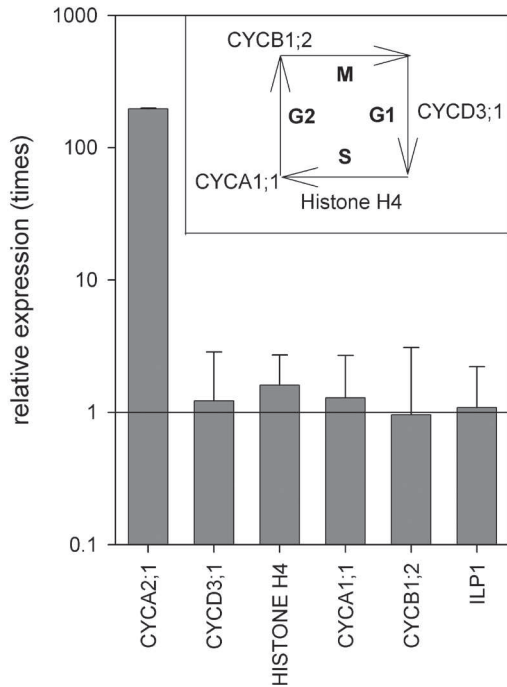


Figure 6.9: Real-Time RT-PCR analysis of cell cycle-marker genes in *SEE1-1D*. Expression of *CYCA2;1* and the markers: *CYCD3;1*, *HISTONE H4*, *CYCA1;1*, *CYCB1;2* (respectively: G1-, S-, G2-, and M-phase-specific; see schematic representation in inset) and *ILP1*, relative to Col-0. Expression values were normalized to 1 for Col-0, $n \geq 4$; Error bars represent SE.

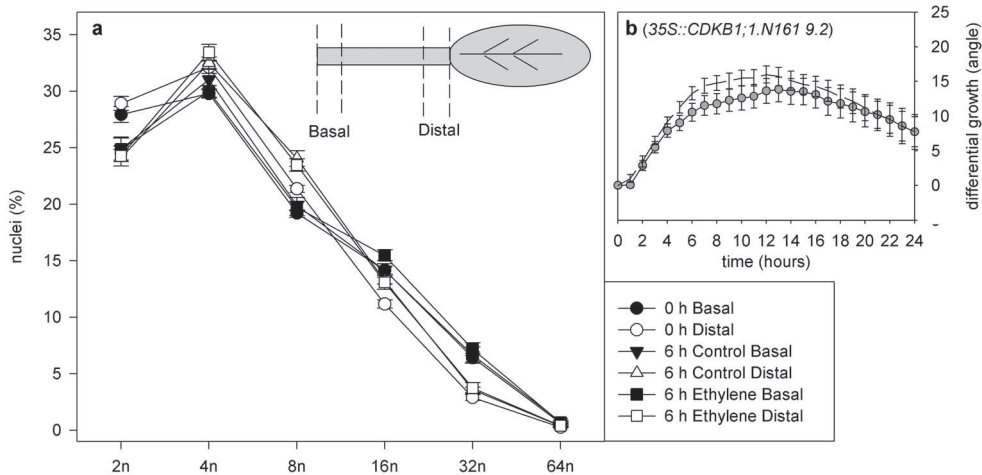


Figure 6.10: Analysis of ethylene effects on endoreduplication. **a:** Fraction (%) of Col-0 nuclei derived from the basal petiole section (1/4 of the petiole length, see inset; black closed symbols) and most distal section (1/4 of the petiole length, see inset; white open symbols), before (0 h; circles) and after 6 h ethylene ($5 \mu\text{l l}^{-1}$; squares) or control (air; triangles) treatment. **b:** hyponastic growth response of *35S::CDKB1;1.N161 9.2* (circles) in the Col-0 background (dashed lines), upon ethylene ($5 \mu\text{l l}^{-1}$) treatment. Angles resulted from pair wise subtraction, Error bars represent SE; $n > 10$.

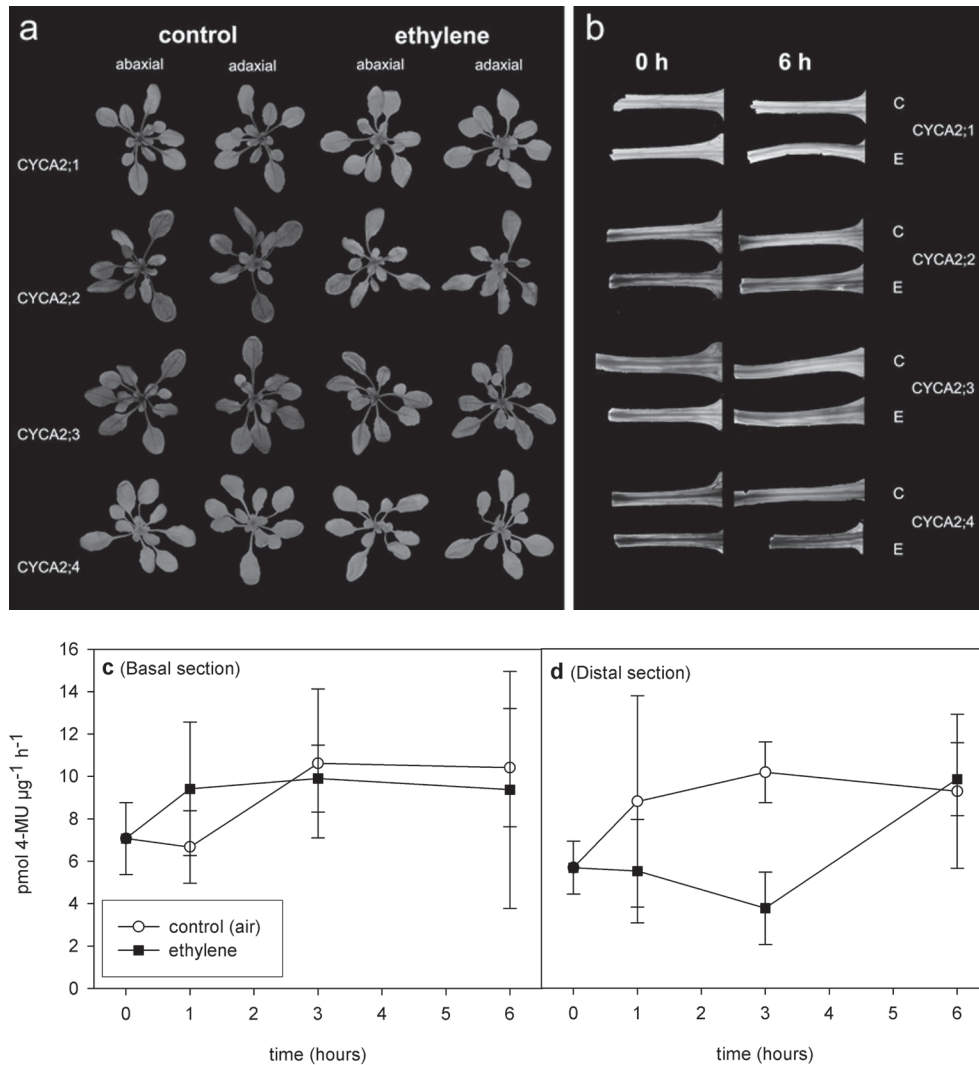


Figure 6.11: Histochemical analysis of A2-Cyclin promoter activity. (See Color Supplement for full color version of this figure). **a:** Plants carrying individual A2-Cyclin family promoters fused to the β -glucuronidase (GUS) reporter gene, treated with ethylene ($1.5 \mu\text{l l}^{-1}$) for 6 h, or kept in control (air) conditions photographed from the adaxial and abaxial side. **b:** typical GUS expression pattern observed in petioles prior (0 h) and after 6 h ethylene (E) treatment and controls (C). **c,d:** Quantification of kinetics of CYCA2;1 promoter activity (pmol 4-MU μg^{-1} protein h^{-1}) in **c:** basal petiole section (see inset figure 6.10) and **d:** distal petiole section, in control (air; white circles) conditions or after ethylene treatment (black squares).

and CYCA2;2 promoter activity predominated in petioles and blades of older leaves (Figure 6.11a). CYCA2;3 was equally active in young and old leaves and petioles. CYCA2;4 was expressed at relatively low levels (Figure 6.11a).

Using the histochemical staining, we observed that CYCA2;1, CYCA2;2, CYCA2;3 and to a lesser extent, CYCA2;4 promoter activity, was repressed in plants treated for 6 h with ethylene (Figure 6.11a). Detailed analysis of petiole tissues indicated that ethylene treatment represses CYCA2 expression predominantly in distal petiole sections (~¾ of the petiole) (Figure 6.11b). This repression was strongest in CYCA2;1 and CYCA2;2 (Figure 6.12) and less evident in CYCA2;3 and CYCA2;4. In sharp contrast, ethylene hardly affected CYCA2 expression in basal petiole tissue (~¼ of the petiole) containing the cells driving hyponastic growth (Cox *et al.*, 2003; Millenaar *et al.*, 2005; Chapter 1) (Figure 6.11b; Figure 6.12). Transverse sections of the histochemically stained petioles indicated that the repressive effects of ethylene were general across the cell types, rather than restricted to specific cells (Figure 6.12).

Quantitative analysis of CYCA2;1 promoter activity in plants sampled at different times during ethylene treatment, using a 4-methylumbelliferyl-glucuronide (MUG) fluorometric assay, confirmed that ethylene repressed CYCA2;1 promoter activity in distal tissues and maintains activity in basal tissue (Figure 6.11c, d). Notably, repression of CYCA2;1 promoter activity was already evident after 1 h of ethylene treatment, coinciding with the induction phase of the hyponastic growth response (Figure 6.1b). After 6 h of ethylene treatment CYCA2;1 promoter activity was indistinguishable from control plants (Figure 6.11d), this roughly co-occurs with reaching maximum petiole angles upon ethylene treatment (Figure 6.1c). However, this re-establishment of distal CYCA2;1 promoter activity after 6 h of ethylene treatment could not be observed with GUS staining (Figure 6.11b).

Together, these data indicate that hyponastic growth may involve asymmetric regulation of CYCA2;1 in the petiole. Moreover, at least for CYCA2;1, this is sufficiently fast to be functional in the induction of ethylene-induced hyponastic growth.

ABA mirrors ethylene effects on CYCA2;1 tissue specification

ABA antagonizes ethylene-induced (hyponastic) growth in several species (Kende *et al.*, 1998; Cox *et al.*, 2004; Benschop *et al.*, 2007). Interestingly, the enhanced ethylene-induced hyponastic growth phenotypes of *SEE1-1D* and *35S::CYCA2;1* mirrors the enhanced ethylene-induced response phenotype of ABA insensitive and ABA biosynthesis mutant alleles and wild type plants pharmacologically treated with the ABA biosynthesis inhibitor; fluoridon (Benschop *et al.*, 2007). Therefore, we studied if CYCA2;1 could function as an integration point for signals derived from ethylene- and ABA-signaling during hyponastic growth responses.

Treatment with ABA and fluoridon reduced, respectively enhanced, initial petiole angles of *35S::CYCA2;1* and *SEE1-1D* in the absence of ethylene, to a similar level as wild type Col-0 (Figure 6.13a; ABA effect was not tested for *SEE1-1D*). This suggests that CYCA2;1 over-expression does not influence general ABA sensitivity.

Subsequently, we tested the effect of application of fluoridon and ABA on the

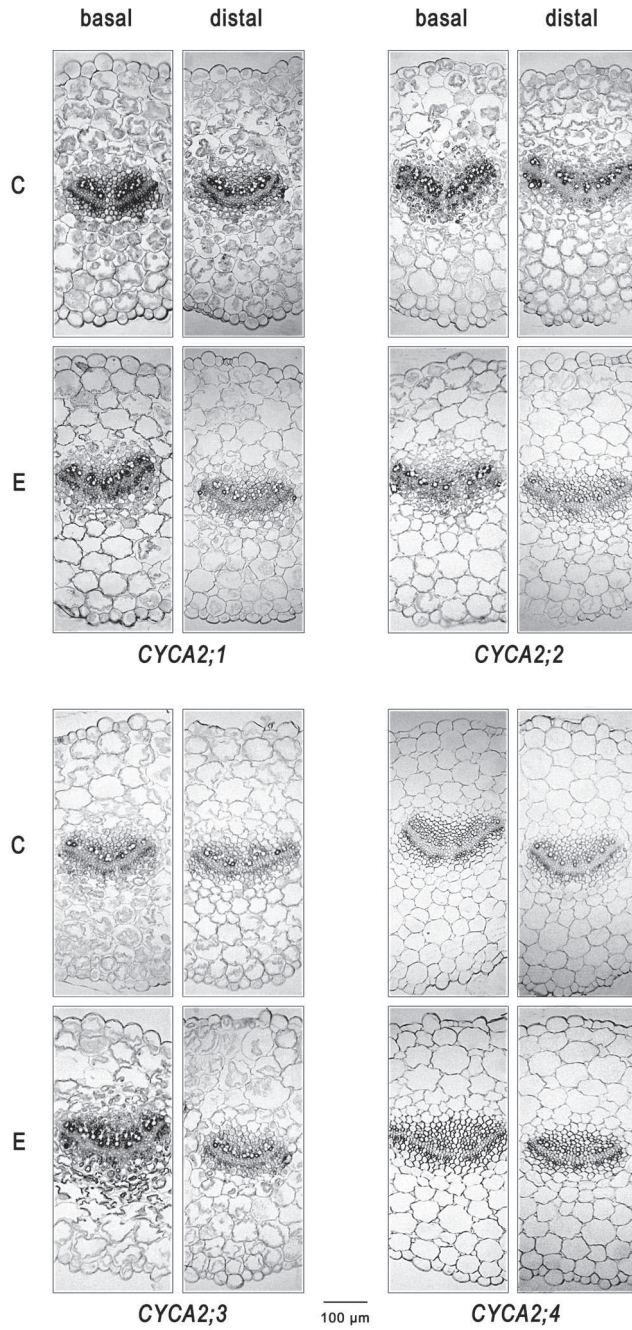


Figure 6.12: Histochemical analysis of A2-Cyclin promoter activity in petioles. (See Color Supplement for full color version of this figure). Transverse sections of basal and distal petiole tissues of plants carrying individual A2-Cyclin family promoters fused to the β -glucuronidase (GUS) reporter gene, treated with ethylene (E; $1.5 \mu\text{l l}^{-1}$) for 6 h, or kept in control (C; air). Scale bar represents 100 μm .

kinetics of ethylene-induced hyponastic growth (Figure 6.13c, d). Fluoridon repressed the enhanced ethylene-induced hyponastic growth response of *SEE1-1D* and *35S::CYCA2;1* (Figure 6.13b), to a level that mirrors the ethylene-induced hyponastic growth response of wild type plants. ABA application abolished ethylene-induced hyponastic growth in both *35S::CYCA2;1* and wild type Col-0.

Together, these data show that both saturation and depletion of ABA in the petioles results in the loss of full ethylene-induced hyponastic growth in the *35S::CYCA2;1* (Figure 6.13c, d) background, suggesting that *CYCA2;1* does modulate ABA sensitivity in the context of ethylene-induced hyponastic growth.

Therefore, we analyzed *CYCA2;1* promoter activity in petiole tissues of plants pretreated with ABA and fluoridon in the presence and absence of ethylene. In the absence of ethylene treatment, ABA restricted *CYCA2* activity to the basal petiole tissues, through repression of *CYCA2;1* promoter activity in distal zones of the petiole mirroring the effect of ethylene (Figure 6.11; Figure 6.14). Application of extra ethylene did not affect this repression. By contrast, reduction of ABA levels by fluoridon treatment did not affect *CYCA2;1* promoter activity before or after ethylene treatment (Figure S6.6).

These results suggest that both ethylene and ABA restrict *CYCA2;1* promoter activity to basal petiole tissues by repressing *CYCA2;1* promoter activity in distal petiole tissue. However, ABA and ethylene have opposite effects on ethylene-induced hyponastic growth (Benschop *et al.*, 2007). Therefore, it is likely that ABA antagonizes ethylene-induced hyponastic growth independent of *CYCA2* action.

***ICK2/KRP2* mediates ABA effects on ethylene-induced hyponastic growth**

Central to the cell cycle regulatory machinery, is the activity of specific kinase complexes consisting of a regulatory CYCLIN subunit and a catalytic subunit, the Cyclin Dependent Kinase (CDK). The specificity, localization, stability and maintenance of these protein complexes is strictly controlled, through interaction with other regulatory proteins, such as Inhibitor of CDK/Kip-Related Proteins (*ICK/KRP*) (Roudier *et al.*, 2000; Verkest *et al.*, 2005; Inzé & De Veylder, 2006; Boudolf *et al.*, 2009). Overexpression of *ICK/KRPs* results in dramatic reductions in CDKA-containing CYC-CDK kinase activity, with associated reduced cell division activity. Interestingly, at least one of the *ICK/KRPs*, *ICK1/KRP1*, was found to be ABA inducible (Wang *et al.*, 1998). Therefore, ABA-induced *ICK/KRPs* might act to repress ethylene-mediated hyponastic growth through inhibition of *CYCA2;1* containing CDK complexes.

Indeed, we found that *ICK2/KRP2* overexpression dramatically reduced ethylene-induced hyponastic growth (Figure 6.13b). Initial petiole angles were affected by pre-treatment with ABA, to a similar extent as wild type, suggesting that general ABA sensitivity was not altered by *ICK2/KRP2* overexpression (Figure 6.13a). However, in contrast to wild type, *SEE1-1D* and *35S::CYCA2;1*, pre-treatment with neither fluoridon nor ABA altered the kinetics of ethylene-induced hyponastic growth of *35S::ICK2/KRP2* (Figure 13c, d). Despite the strong morphological phenotype of *35S::KRP2* (De Veylder *et al.*, 2001), low light and heat stimuli initiated hyponastic growth, although the response was severely delayed, to a similar level as wild type after 24 h (Figure

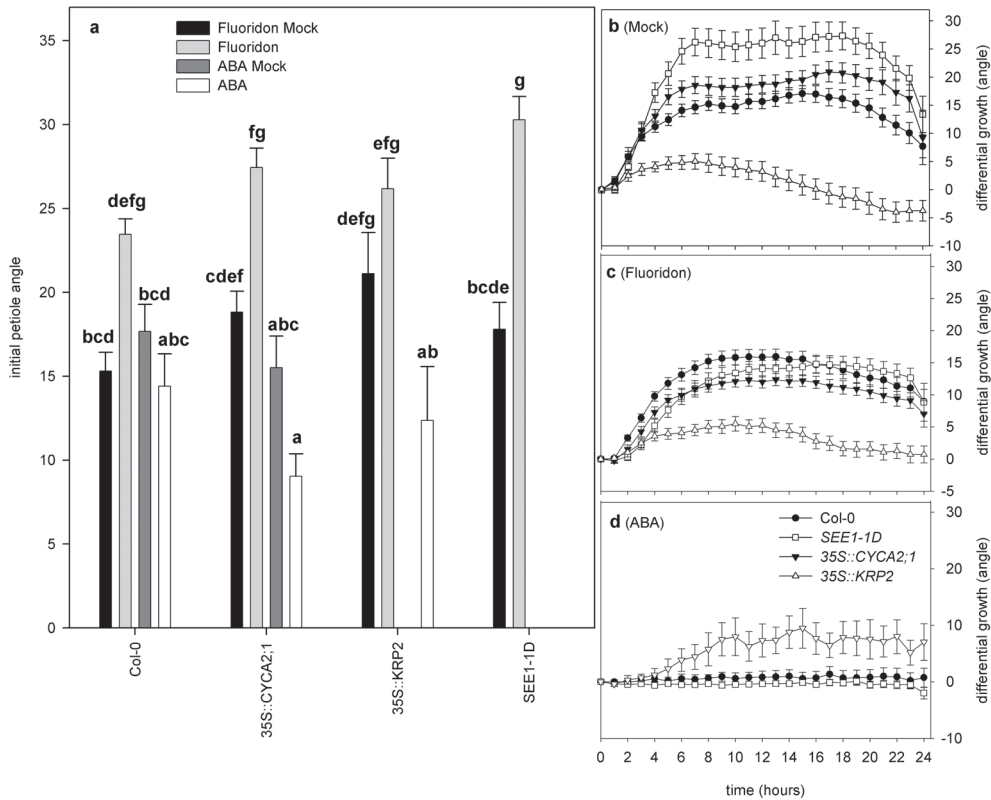


Figure 6.13: ABA control of A2-Cyclin mediated ethylene-induced hyponastic growth. **a:** Initial petiole angles of 35S::CYCA2;1, 35S::KRP2, SEE1-1D and wild Col-0 plants treated with fluoridon (20 μ M; black bars), fluoridon mock (light grey bars), ABA (20 μ M; white bars) and ABA mock (dark grey bars). No overlapping letters indicate a significant difference ($p < 0.05$), multivariate post-hoc ANOVA. **b-d:** Ethylene (5 μ l l⁻¹)-induced hyponastic growth in SEE1-1D (white squares), 35S::CYCA2;1 (grey triangles down), 35S::KRP2 (white triangles up), compared to Col-0 wild type (black circles), of **b:** mock, **c:** fluoridon and **d:** ABA (20 μ M) treated plants (phenotypes in ABA mock-treated plants mirrored those of fluoridon mock and are therefore not shown). Angles resulted from pair wise subtraction, Error bars represent SE; $n > 10$.

S6.7). This indicates that the abolished ethylene-induced hyponastic growth is not due to mechanical constraints.

Taken together, these data support that ICK/KRPs mediate the antagonistic effects of ABA on ethylene-induced hyponastic growth, possibly through repressing CYCA2-CDK activity.

Multiple Ethylene Responsive Elements (EREs) are found in the KRP1 and KRP2 promoters, which predict that these genes are regulated indirectly by ethylene via Ethylene Response Factor (ERF) transcription factors (Richard *et al.*, 2006). In agreement, a small, but significant reduction of KRP1 and a trend of reduction in KRP2 transcription was present after 3 h of ethylene treatment (Figure S6.3). Perhaps

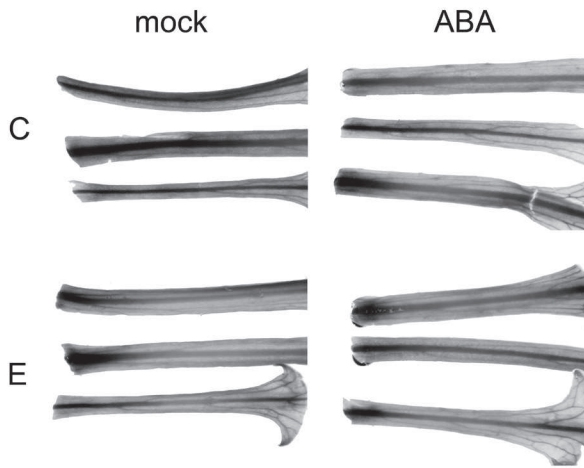


Figure 6.14: Histochemical analysis of *CYCA2;1* promoter activity to ABA treatment. (See Color Supplement for full color version of this figure). Plants carrying the endogenous *CYCA2;1* promoter fused to the β -glucuronidase (GUS) reporter gene pre-treated with mock solution or ABA (20 μ M) kept in control conditions (C) or treated for 6 h with ethylene (1.5 μ l l⁻¹; E) treatment.

this effect is stronger in specific zones (e.g. basal vs. distal), given the dilution effect present, as this analysis was performed on whole petiole tissue. Ethylene release was unaltered in *35S::KRP2* compared to wild type (0.60 \pm 0.03 vs. 0.65 \pm 0.13 nl g⁻¹ FM h⁻¹ respectively). Together, these data suggest that KRP is an integrator of ABA and ethylene signals and controls hyponastic growth, probably by inhibition of A2-Cyclin-CDK complex(es).

Discussion

Hyponastic growth is induced by different environmental stimuli, for example complete submergence (Millenaar *et al.*, 2005), shade (Millenaar *et al.*, 2009; Chapter 2) and heat (Koini *et al.*, 2009; Chapter 3). Given the remarkable similarities in kinetics with which these stimuli induce hyponastic growth, presumably parts of the signal transduction routes are shared. Several activation-tagged lines were isolated and described that confirmed this notion, by showing enhanced or reduced hyponastic growth to all three stimuli (Chapter 5).

One of these activation-tagged lines, *SEE1-1D*, was studied here in greater detail. It was found that the T-DNA had inserted between the AP2/ERF transcription factor *SHN3/WIN1* and the cell cycle regulator *CYCA2;1*. Interestingly, ERFs are known to control several responses to the abiotic environment and mediate responses to several phytohormones, including ethylene and ABA (see Nakano *et al.*, 2006 and references within). Much to our surprise, overexpression of *SHN3/WIN1* could not explain the enhanced hyponastic growth phenotype observed in *SEE1-1D* (Figure 6.3, Figure S6.1). In fact, ectopic expression of this gene in the Col-0 background even slightly reduced hyponastic growth to low light and heat treatment (Figure 6.3).

On the other hand, we demonstrated that the plant specific *CYCA2;1* and other

members of the A2-Cyclin family are positive regulators of induced hyponastic petiole growth to all treatments in *Arabidopsis thaliana* (Figure 6.1, Figure 6.4, Figure 6.6), confirming the existence of an integrated signaling route.

A2-Cyclins seemingly control hyponastic growth independent from cell proliferation

A2-Cyclins are required for cell cycle progression and are regulatory subunits of Cyclin-Dependent Kinase (CDK)-complexes that control the transition from S-to-G2 in *planta* (Roudier *et al.*, 2000, 2004; Inzé & De Veylder, 2006). A2-Cyclins are, among others, required for vascular-differentiation and patterning (Bursens *et al.*, 2000). Through interaction studies and co-overexpression it was shown recently that CYCA2;3 in complex with CDKB1;1, is also involved in G2-to-M transition (Boudolf *et al.*, 2009).

No obvious differences in cell numbers were noted in petioles of plants misregulating CYCA2;1 (Figure 6.8), nor differences in transcription, localization or activity of mitotic-marker genes were found (Figure 6.9; Figure S6.4). In accordance, Yoshizumi *et al.* (2006) demonstrated that modulation of CYCA2 transcripts by ILP1 did not alter cell numbers, whereas loss-of-function- and ectopic expression of ILP1 affected ethylene-induced hyponastic growth (Figure 6.5).

Taken together, this indicates that A2-Cyclins do not control ethylene-induced hyponastic growth by affecting cell proliferation. This is supported by many observations that cell elongation, rather than proliferation drives (differential) growth responses induced by environmental stimuli (Tsukaya, *et al.*, 2000; Cox *et al.*, 2003; Millenaar *et al.* 2005; Vreeburg *et al.*, 2005; Kozuka *et al.*, 2005; Chapter 1). In agreement, CYCA2 transcripts were found in both dividing and non-dividing *Arabidopsis* cells, suggesting that it is not a limiting factor for cell division *per se* (Bursens *et al.*, 2000).

Ethylene and A2-Cyclins may control hyponastic growth independent from endoreduplication

Ethylene stimulates endoreduplication in hypocotyls, a process where cells undergo successive DNA replication cycles (S-phase) without mitosis (Gendreau *et al.*, 1999; Dan *et al.*, 2003). Interestingly, CYCA2s regulate endoreduplication (Bursens *et al.*, 2000; Dewitte & Murray, 2003; Yu *et al.*, 2003; Yoshizumi *et al.*, 2006; Imai *et al.*, 2006; Boudolf *et al.*, 2009). A positive correlation has been reported for cell size and ploidy levels (reviewed in Sugimoto-Shirasu & Roberts, 2003) and lines with reduced CYCA2 transcription often exhibit increased cell sizes in certain tissues (Yoshizumi *et al.*, 2006; Imai *et al.*, 2006; Pilliteri *et al.*, 2007).

We did not observe differences in ploidy levels in petiole sections of 6 h ethylene treated plants (Figure 6.10), suggesting that effects of ethylene on the endocycle and associated increase in cell sizes are not involved in ethylene-induced hyponastic petiole growth. Therefore, it is unlikely that CYCA2;1 controls ethylene-induced hyponastic growth via effects on the endocycle. These results are in agreement with Kozuka *et al.* (2002) who demonstrated that petiole elongation in dark is not correlated with endoreduplication levels in the petiole. In addition, CYCA2;1 is

present in differentiated cells that never undergo endoreduplication, including guard cells (Burssens *et al.*, 2000). Moreover, *Medicago*, CYCA2;2 is not required for endoreduplication (Roudier *et al.*, 2003).

Towards a model for the control of A2-cyclins on hyponastic growth

Arabidopsis thaliana plants ectopically expressing CYCA2;1, and loss-of-function *cyca2;1* mutants, showed enhanced ethylene-induced hyponastic growth (Figure 6.1, Figure 6.4). The reduced hyponastic growth phenotypes of the *ILP1-1D* line, with reduced CYCA2 transcript levels, and of several double- and triple-mutant *cyca2* combinations (Figure 6.4), indicated that the *cyca2;1* phenotype likely can be explained by compensation of other, highly redundant A2-Cyclins (Figure 6.5; Vandepoele *et al.*, 2002; Pillitteri *et al.*, 2007). This is underlined by the observation that the A2-Cyclins quadruple-knockout probably is embryo lethal, as suggested by the severe defects on embryo formation observed in tobacco antisense-CYCA3;2 lines (Yu *et al.*, 2003; Inzé & De Veylder, 2006).

Nevertheless, histochemical data suggested that ethylene treatment restricts CYCA2;1 promoter activity to the basal part of the petiole where hyponastic growth is induced (Figure 6.11). Because CYCA2;1 is a positive regulator of hyponastic growth, this strongly suggests that ethylene controls hyponastic growth by controlling tissue specification of CYCA2;1. A model of the potential mechanism is presented in Figure 6.15 and discussed below.

The CYCA2;1 promoter region contains eight ERF-binding ethylene responsive elements (EREs) (Richard *et al.*, 2006), suggesting that CYCA2;1 repression in distal petiole tissues may be a direct consequence of ethylene action (Figure 6.11). Ethylene release and ethylene sensitivity were unaltered in plants ectopically expressing CYCA2;1 and in *cyca2;1* mutants (Figure 6.7). Together, these lines of evidence confirm that CYCA2;1 acts downstream of ethylene towards hyponastic growth.

We demonstrated that ABA restricts CYCA2;1 promoter activity to basal petiole tissues by repressing activity in distal petiole tissue, similar to ethylene (Figure 6.14). Yet, ABA antagonizes ethylene-induced hyponastic growth (Benschop *et al.*, 2007). CYCA2;1 has only one ABRE ABA-binding cis element, which is not sufficient for ABA-mediated induction of transcription (Skriver *et al.*, 1991; Gómez-Porrás *et al.*, 2007). Thus, ABA effects on CYCA2s are presumably indirect.

The presence of several ERE's in the promoter of *Kip Related Protein2* (*KRP2*) suggests that ethylene controls its transcription by affecting ERF transcription factors (Richard *et al.*, 2006). Indeed, we found that *KRP* (*ICK*) transcription was reduced by ethylene treatment (Figure S6.3). Ectopic expression of *KRP2* inhibits ethylene-induced hyponastic growth (Figure 6.13). Because i) ABA induces expression of the *KRP2* homolog *KRP2* (Wang *et al.*, 1998), ii) pharmacological treatment with ABA and fluoridon did not affect the 35S::*KRP2* ethylene-hyponastic growth phenotype (Figure 6.13b-d), iii) 35S::*KRP2* remained sensitive for alteration of ABA mediated initial petiole angles (Figure 6.13a), iv) reduced ethylene-induced hyponasty is not due to a mechanical constraint in 35S::*KRP2* (Figure S6.7) and v) ethylene release was

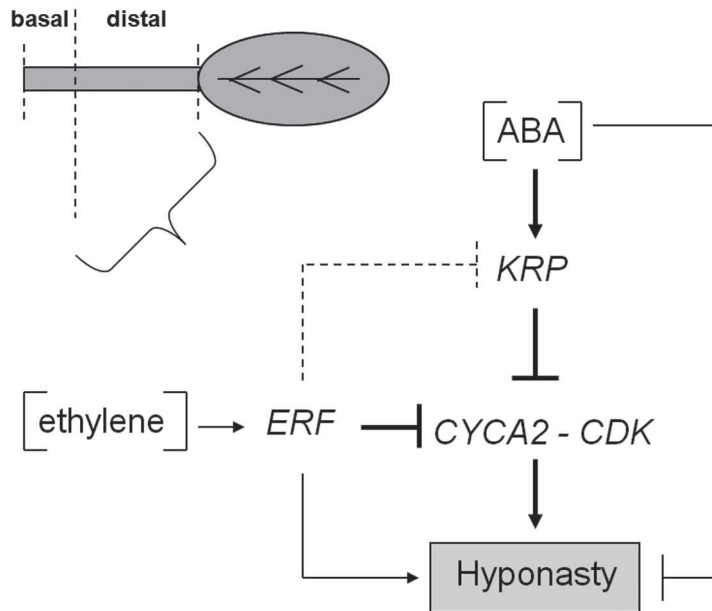


Figure 6.15: Proposed model of the mechanism of A2-Cyclin mediated control of hyponastic growth. A2-Cyclins (CYCA2) control hyponastic petiole growth downstream of ethylene and ABA action. Selective repression of CYCA2 activity by ethylene and ABA, and loss of CYCA2 interaction with its CDKA partner, in distal petiole tissues, but not in the abaxial-basal sections of the petiole, restricts growth in the distal part which may result in a hyponastic growth phenotype due to maintenance of growth in basal petiole sections. Ethylene likely directly controls CYCA2;1 activity via ERF transcription factor(s), whereas KRP2 integrates signals from ABA and ethylene and acts as repressor of the CYCA2-CDK complex. Moreover, both ethylene (positively) and ABA (negatively) control hyponastic growth also independent of KRP-CYCA2-CDK interaction.

unaltered in 35S::KRP2, we propose that KRPs integrate ethylene and ABA signaling towards hyponastic growth.

The sensitivity of 35S::KRP2 for ABA and fluridone to control initial petiole angles and the insensitivity for ethylene-induced hyponastic growth, confirms the observation of Benschop *et al.* (2007) that ABA controls initial petiole angles via a different pathway than the antagonistic effects of ABA on ethylene-induced hyponastic growth. Because of these antagonistic effects and because ABA mirrors ethylene restriction of CYCA2;1 activity to basal petiole tissues, we conclude that ABA has a dual role in controlling hyponastic growth with contrasting effects. Likely, both ethylene and ABA control hyponastic growth via A2-Cyclin tissue specification and via an A2-Cyclin independent route. Requirement of ethylene as a trigger is supported by the observation that neither constitutive expression of CYCA2;1 nor *cyca2;1* mutants exhibit a constitutive hyponastic growth phenotype (altered initial angles). In the preceding chapters we showed that hyponasty is at least controlled by the

phytohormones; ethylene, ABA and auxin (Chapter 1-4). Auxin enhances *CYCA2;1* and *CYCA2;4* expression (Bursens *et al.*, 2000; Himanen *et al.*, 2002; Vanneste *et al.*, 2005) and *CYCA2;2* expression was upregulated by auxin in *Medicago sativa* roots (Roudier *et al.*, 2003). *KRP2* expression is most likely repressed by auxin (Richard *et al.*, 2006). This may explain why auxin and polar auxin transport (PAT) are not involved in ethylene-induced hyponastic growth (Millenaar *et al.*, 2009, Van Zanten *et al.*, 2009a; Chapter 2).

It has been suggested that ectopic *KRP2* expression stabilizes CDKA protein with which A2-Cyclins interact (Roudier *et al.*, 2000; De Veylder *et al.*, 2001; Inzé & De Veylder, 2006). In accordance, recombinant *Medicago truncatula* KRP (KRPMt) differentially inhibited various alfalfa CDK complexes in phosphorylation assays (Pettkó-Szandtner, 2006). Interestingly, recent work of Adachi *et al.* (2009) showed that the CDKA;1 promoter contains a region that directs abaxial side-biased expression, which may be linked to the adaxial/abaxial side specification of leaves. In agreement, both *KRP2* and Arabidopsis *CDKA;1* mRNA's are enriched and co-expressed in the translome of the seedling epidermis (Mustroph & Bailey-Serres, *personal communication*).

Hyponastic growth is specifically induced by elongation growth of a confined zone of cells at the basally located abaxial epidermis cells (Cox *et al.*, 2003; Millenaar *et al.*, 2005; Chapter 1). It is tempting to speculate that abaxial-epidermal localization of CDKA;1 with which A2-Cyclins interact, explains the specificity to the few abaxial cells that eventually drive ethylene-induced hyponastic growth. In such a model *KRP2* integrates ethylene and ABA signals to specify the proximal-distal distribution axis of *CYCA2s* and co-occurrence with CDKA1 would only co-occur in the basal-abaxial zone where elongation is required to induce hyponasty..

Perspectives

Ethylene has dogmatically been associated with growth inhibition in terrestrial plants, including *Arabidopsis thaliana* (for a review see: Pierik *et al.*, 2006). In contrast high-levels of ethylene are assumed to be growth stimulatory in several semi-aquatic plants, thereby driving several escape responses (Voeselek & Blom, 1989, Kende *et al.*, 1998, Cox *et al.*, 2004). In accordance with the role of ethylene as general growth repressor, the data presented in this paper demonstrates that ethylene induces growth inhibition in specific tissues, which consequently drives differential petiole growth. It would be interesting to know if a similar ethylene-mediated tissue specific growth repression mechanism is also associated with escape responses of semi-aquatic species such as *Rumex palustris* and flood intolerant rice varieties. If the proposed Arabidopsis mechanisms involving ethylene, ABA, ERFs, KRPs and A2-Cyclins-CDKs control of hyponastic- and elongation growth is conserved in these species, this would potentially open tremendous potential to use these components as breeding targets for several crop species in which flooding- or heat-tolerance or shade avoidance aspects need to be improved.

Materials and Methods

Plant materials and growth conditions

Arabidopsis thaliana lines were derived from the Nottingham Arabidopsis Stock centre (NASC Stock IDs between brackets) or were a kind gift of the authors who described them. Col-0 wild type (N1092), Activation tagged lines (Weigel *et al.* 2000; N21991, N23153), 35S::KRP2 (De Veylder *et al.*, 2001), 35S::CDKB1;1.N161 line 9.2 (Boudolf *et al.*, 2004), *cyca2-1*, *cyca2-2*, *ilp1-1*, *ilp1-2*, *ILP1-1D* (Yoshizumi *et al.*, 2006), *D-Box-CYCB1;1::GUS* (Colon-Carmona *et al.*, 1999; Wildwater *et al.*, 2005), *CYCA2;1::GUS* (Bursens *et al.*, 2000), 35S::SHN1, 35S::SHN2 and 35S::SHN3 (Aharoni *et al.*, 2004), AtTOTF-Ex ERF ectopic expression library (Weiste *et al.*, 2007).

To generate the 35S::GUS lines, the full-length cDNA and to generate *CYCA2::GUS* the promoter regions 2kb upstream of respective initiation codons, were cloned through GATEWAY technology (Invitrogen, Gaithersburg, MD, USA) in pDONR221 and subcloned into pK2WG7.0 and pKGWFS7.0 respectively (Karimi *et al.*, 2002).

Cyca2 mutants lines were obtained from the SALK- (Alonso *et al.*, 2003) and GABI- (Rosso *et al.*, 2003) T-DNA insertion collections; *cyca2;1-1* (SALK_121077), *cyca2;2-1* (GABI_120D03), *cyca2;3-1* (SALK_092515), *cyca2;4-1* (SALK_070301). For detection of T-DNA inserts left border specific primers were used of the T-DNA insert (LBC1, LB_GABI) in combination with gene-specific primers. All alleles are representative knock-outs. Double and triple combinations were obtained by crossing and subsequently checked by PCR analysis. Reduced root length and root density, reduced leaf sizes and increased epidermal cell size and enhanced endoreduplication levels in the triple mutant combinations confirmed effectiveness of the individual *cyca2* alleles (Vanneste *et al.*, *in preparation*). Isolation of *SEE1-1D* from the 35S CaMV tagged population (Weigel *et al.*, 2000) is described in detail in Chapter 5.

Plants were grown on a fertilized mixture of pot-soil and perlite (1:2; v/v) as described in Millenaar *et al.* (2005), at 20°C, 70% (v/v) relative humidity, 200 $\mu\text{mol m}^{-2} \text{s}^{-1}$ photosynthetic active radiation (PAR), 9 h short-day photoperiod. Plants were automatically watered to saturation each day, at the start of the photoperiod. Before potting, seeds were dark stratified at 4°C for 4 days to synchronize germination.

Cloning of the *SEE1-1D* T-DNA locus

TAIL-PCR was conducted essentially as described by Liu *et al.* (1995a, b). Genomic-DNA was isolated using Nucleon Phytopure DNA extraction kit (GE Healthcare/Amersham; Den Bosch, the Netherlands). Integrity of the DNA was checked by amplification of Actin (At5g09810) using the primers: 5'-GCATCATCACAAAGCATCCTAA-3' and 5'-TTCGTGGTGGTGCGTTTGTT-3'. Subsequent TAIL-PCR was conducted using the degenerate primer: AD2; 5'-NGTCGASWGANAWGAA-3', 5'-TTCWTNTCWSTCGACN-3'; Liu *et al.*, 1995a, b) in combination with nested primers from the Left-border: 5'-ATCTAAGCCCCATTGGAC-3' (primary PCR); 5'-TAACGCTGCGGACATCTACA-3' (secondary PCR); 5'-CGGACATGAAGCCATTTACA-3' (tertiary PCR). PCR products were separated on agarose-gel and excised bands containing DNA purified using a GFX-spin column (GE Healthcare/Amersham) and subjected to direct sequencing (Macrogen, Seoul, South-Korea) using the tertiary PCR primer.

Isolation of 35S::SHN3/WIN1 in Col-0

DNA was isolated (adapted from; Gilmartin & Bowler, 2000) of 200 pooled (5 individuals per pool) plants of set 'IV' of the AtTOTF-Ex ERF ectopic expression library, which contains a mixture of 25 independent 35S CaMV promoter tagged ERF lines, including 35S::SHN3 (At5g25390) (Weiste *et al.*, 2007). Pools were screened for the presence of 35S::SHN3 by standard PCR procedure, using a forward primer designed to span part of the GATEWAY vector T-DNA, the startcodon and a small SHN3 specific sequence (5'-CAGGCTTCATGGTACATTTCG-3') and a SHN3 gene-specific reverse primer (5'-TGAACCGTTCGATTGATGA-3'). Individual plants of pools from which a product of the expected size was obtained were checked with the same primer combination and with vector specific primers that span the recombination sites (5'-GGGGACAAGTTTGTACAAAAAAGCAG-3', 5'-CGTATGGATAACCCCATCAACCAC-3'), to check for the number of inserts. All primer combinations were BLAST-searched against the Arabidopsis genome to check for sequence uniqueness. Lines that contained one insert of the expected size were sequenced using the primer: 5'-CAGGCTTCATGGTACATTTCG-3' (Macrogen, Seoul, South-Korea) to confirm the presence of 35S::SHN3. The confirmed lines were grown on selective agar-plates containing 8 g l⁻¹ plant agar (Duchefa, Haarlem, the Netherlands), 0.22 g l⁻¹ Murashige-Skoog (Duchefa) containing 50 µg ml⁻¹ DL-Glufosinate ammonium (BASTA/DL-phosphinotricin; Duchefa) and scored for survival rates after three weeks, to isolate homozygous lines 35S::SHN3 lines. Thereafter, SHN3 over-expression was determined by Real-Time RT-PCR.

Hormone, light and heat treatments

Plants at developmental-stage 3.9 (Boyes *et al.*, 2001) were used for all experiments. In all cases, plants were transferred to the experimental setups (Microclima 1750 growth cabinet; Snijders Scientific, Tilburg, the Netherlands), one day before the start of the experiments to allow acclimatization. All treatments commenced 1.5 h after the start of the photoperiod to rule out effects of diurnal and circadian leaf movements (Salter *et al.*, 2003).

Ethylene (Hoek Loos, Amsterdam, the Netherlands) was applied to saturating (not shown) concentrations (1.5 µl l⁻¹; except for the hyponastic growth kinetics experiment, see below), in continuous flow-through and then vented away. The equilibrium concentration was reached after approximately 1 h, and was regularly checked by gas chromatograph analysis (GC955, Synspec, Groningen, the Netherlands).

For petiole kinetics analysis, 5 µl l⁻¹ ethylene was mixed with humidified air (70% (v/v) and applied to glass cuvettes containing one plant each at a flow-rate of 75 l h⁻¹. For details see: Cox *et al.* (2004); Millenaar *et al.* (2005); Benschop *et al.* (2007) and Chapters 1-5.

Low light was induced by decreasing PAR-level from 200 µmol m⁻² sec⁻¹ to 20 µmol m⁻² sec⁻¹ by covering the plants with spectrally neutral shade cloth. This did not change light quality (checked with a LI-COR 1800 spectro-radiometer (LI-COR, Lincoln, NE, USA). Induction of high temperature was accomplished by moderating the program of the used growth cabinet. The 30°C threshold was reached after 22 minutes; 38°C was reached after 49 minutes.

Fluoridon (Riedel-de Haën, Seelze, Germany) was dissolved in MilliQ containing; 0.1% TWEEN and 0.07% acetone to 100 µM and was applied to the soil, until saturation, to plants saved from watering for two days. Absisic acid (ABA; Sigma-Aldrich; Zwijndrecht; the Netherlands) was dissolved in MilliQ containing; 0.1% TWEEN and 0.1% ethanol, to a concentration of 20 µM and applied to plants by spraying. Pretreatments took place 66 h, 42 h and 18 h before the start of

the experiment. Mock solutions were identical, but lacked the active components.

Petiole angle measurements

Petiole angle kinetics was measured using an automated time-lapse camera system as described in Cox *et al.* (2004); Millenaar *et al.* (2005); Benschop *et al.*, (2007). Plants were placed in glass cuvettes with the petiole of study perpendicular to the axis of the camera. To facilitate measurement, leaves that were obscuring the petiole base were removed. Additionally, the petiole was marked at the petiole/lamina junction with orange paint (Decofin Universal; Apeldoorn, the Netherlands).

Digital images of two petioles per plant were taken every 10 min. Angles were measured between the marked point at the petiole/lamina junction and a fixed basal point of the petiole, compared to the horizontal, by using KS400 (Version 3.0) software package (Carl Zeiss Vision, Hallbergmoos, Germany) and a custom made macro. To enable continuous photography over the 24 h experimental period, no dark period was included during the experiments.

Plants used for the measurement of fixed time-points were manually photographed from the side. Angles were measured using the freeware algorithm; ImageJ; <http://rsb.info.nih.gov/ij>). For all replicate plants, the two measured petioles were averaged before they were subjected to further analysis. Statistical significance-levels were determined using standard type-2 2-tailed Student's T-Test using Microsoft Excell 2003 (Richmond, VA, USA). Statistical analysis on initial petiole angles was performed by Two-way analysis of variance (ANOVA), with Tukey B post-hoc comparisons (SPSS-Software 12.01, Chicago, IL, USA).

To rule out effects of diurnal- and/or circadian effects on petiole movement pair-wise subtraction (Benschop *et al.*, 2007) by calculating the difference in angle between treated and control plants for each time point was performed on hyponastic growth data. Calculation of the new standard error for the differential response was performed by taking the square root from the summation of the two squared standard errors.

Flow-cytometry

Two petioles of at least two Col-0 plants were harvested per sample, dissected in four segments of equal length and snap frozen in liquid nitrogen. The basal and distal tissue-quarters were ground in 200 μ l nuclei extraction buffer (CyStain UV precise buffer P; Partec, Münster, Germany) and then diluted in a Staining buffer (CyStain UV precise buffer P; Partec) containing DAPI (4',6-diamidino-2-phenylindole). Samples were analyzed on a Cytosflow ML flow-cytometer (Partec).

Real-Time Reverse Transcriptase-PCR

Real-Time RT-PCR was conducted essentially as described in Millenaar *et al.* (2005, 2006). Petioles were harvested and snap-frozen in liquid nitrogen. For one RNA sample eight petioles of four plants were pooled. RNA was isolated using the RNeasy Plant Mini Kit (Qiagen, Leusden, the Netherlands). gDNA was removed using the DNA-Free kit (Ambion, Cambridgeshire, United Kingdom). Superscript III RNase H⁻ Reverse Transcriptase (Invitrogen, Breda, the Netherlands), using Random-Hexamer Primers, was used for cDNA synthesis. Real-Time RT-PCR reactions were performed on MyiQ Single-Color Real-Time PCR Detection System and Software using iQ SYBR Green Supermix Fluorescein (Bio-Rad laboratories, Veenendaal,

the Netherlands). Primers for *SEE1-1D* T-DNA flanking genes are described in Supporting Information Table S6.1. For *CYCA2;1* two independent primer combinations were used, which both did yielded the same expression levels. In all cases, primer sequences were checked for uniqueness by BLAST-search and melt-curves were generated to check if only one product was formed. Primers for A2-Cyclin genes and cycle-specific genes are described in Richard *et al.*, 2001; Mariconti *et al.*, 2002; Yoshizumi *et al.*, 2006). Primers used to test expression of 35S::SHN3: 5'-GGGTCAAAAACGAGTCCAAA-3'; 5'-CGCCATTGATCATCTTCCT-3'. Relative mRNA values were calculated using the comparative cycle threshold (C_t) method described by Livak & Schmittgen (2001), expressing mRNA values relative to β -Tubulin-6 (At5g12250, 5'-ATAGCTCCCCGAGGTCTCTC-3', 5'-TCCATCTCGTCCATTCTTC-3'; Czechowski *et al.* (2004).

Histochemical β -glucuronidase staining and quantification

Harvested tissues were placed briefly in 90% ice-cold acetone and subsequently fixed and vacuum infiltrated with 10 mM MES, 0.3 M mannitol, 0.3% formaldehyde, for 45 min. Tissues were rinsed in 100 mM Buffer (50 mM NaHPO₄ + 50 mM Na₂HPO₄; pH 7.2). The histochemical reaction was performed by incubation in 1 mM X-Gluc (5-bromo-4-chloro-3-indolyl β -D-glucuronide) in DMSO for 24 h at 37°C. The tissues were bleached in ethanol baths with increasing concentrations (5% to 90%), prior to observation.

For quantification of GUS activity, two petioles of at least two Col-0 plants were harvested, dissected in 4 equal-sized segments and snap-frozen in liquid nitrogen. 200 μ l cold extraction buffer (50 mM NaHPO₄ buffer, pH 7.0, 10 mM EDTA, 0.1% Triton X-100, 0.1% sodium lauryl sarcosine, 10 mM β -mercaptoethanol) was added and the samples were shaken for 2 min (25 times per second) in the presence of a tungsten carbide grinding ball. Subsequently, the samples were centrifuged (8000 rcf, 8 min, 4°C) and the supernatant was stored at -80°C. Protein concentrations were measured using the Bradford-analysis based Bio-Rad Protein Assay kit (micro-assay procedure; Biorad).

Enzymatic GUS assay was initialized by adding 20 μ l supernatant to 180 μ l assay buffer (extraction buffer with 1 mM Methyl-Umbelliferyl Glucuronide: MUG). The samples were incubated at 37°C for 24 h. The reaction was stopped by adding 20 μ l of the reaction volume to 180 μ l 0.2 M Na₂CO₃ buffer, in a 96 well ELISA Microplate with F-bottom (Greiner Bio-one, Alphen a/d Rijn, the Netherlands). 4-MU (4-Methyl Umbelliferone) fluorescence was measured using a Fluostar Galaxy reader (BMG Lab tech; de Meern, the Netherlands). 4-MU concentration in the extracts was determined using a standard series of 4-MU concentrations.

Cell wall staining and cell length measurements

For staining, whole petioles were harvested and bleached in 5% (w/v) potassium-hydroxide (KOH) for 3 days and subsequently rinsed with water. The tissues were stained for 2 minutes with Toluidin-blue prior to observation.

To measure epidermal cell lengths, dental paste (Coltene Whaledent, Altstätten, Switzerland) was spread on the epidermis with a brush. After solidification, the dental paste was removed and a solution of polyvinylformaldehyde (Formvar) in 4% (w/w) chloroform was applied to the dental paste segment surface with a brush. After the chloroform had evaporated, the remaining film was removed using cello tape and subsequently microscopically imaged. The obtained pictures were merged and cell lengths were measured using a custom made macro, in KS400 software (Carl Zeiss Vision).

Ethylene release measurements and triple response assays

Sterilized seeds were placed in petri-dishes containing 5 ml of half-strength MS-agar (4 g l⁻¹ plant-agar (Duchefa), 0.22 g l⁻¹ Murashige-Skoog (Duchefa), containing different concentrations of 1-aminocyclopropane-1-carboxylic acid (ACC; Duchefa). Plates were kept 4 days at 4°C in dark. Thereafter, the plates were transferred to 200 μmol m⁻² s⁻¹ light for 4 h, before packing in aluminium-foil. Thereafter the plates were left in darkness for 5 days at 20°C. After 5 days, hypocotyls were photographed and length was measured using ImageJ software. Obtained results were not due to toxic effects of ACC as the ethylene insensitive mutant (*ein2*) had a elongated phenotype at all concentrations (not shown).

Ethylene release from rosettes was performed 1.5 ± 1 h after start of the photoperiod. Measurements were as described in Millenaar *et al.* (2005; 2009) and Chapter 2-4. Whole rosettes of about 300 mg were placed in a syringe with a volume of 1.5 ml. Ethylene was allowed to accumulate in the syringe for 15-20 min, after which the air was analyzed on a gas chromatograph (GC955, Synspec). This short time frame prevented wound-induced ethylene production, which started to accumulate only after 20 min (data not shown).

Acknowledgements

The authors thank; Daan Weits (Utrecht University), Gert van Isterdael (VIB) and Henri W. Groeneveld (Utrecht University) and M. Terlouw (Utrecht University) for excellent technical assistance, Julia Bayley-Serres for comments on the manuscript and Takeshi Yoshizumi and Sari Osato (RIKEN Yokohama research institute, Japan), Asaph Aharoni and Jianxin Shi (Weizmann Institute of science, Israel) and Wolfgang Dröge-Laser (Universität Göttingen; Germany) for kindly sharing plant materials.

Supporting Information

- **Figure S6.1:** Hyponastic growth response of plants ectopically expressing *SHN1* or *SHN2*.
- **Figure S6.2:** Quantitative RT-PCR analysis of *CYCA2;1* expression in independent 35S::*CYCA2;1* transformants and *SEE1-1D*.
- **Figure S6.3:** Expression of cell cycle-related genes upon ethylene treatment in *Arabidopsis thaliana*.
- **Figure S6.3:** Expression of cell cycle-related genes upon ethylene treatment in *Arabidopsis thaliana*.
- **Figure S6.4:** Histochemical analysis of *CyclinB1;1* promoter activity.
- **Figure S6.5:** Spatial localization of A2-Cyclins in petioles.
- **Figure S6.6:** Histochemical analysis of *CYCA2;1* promoter activity to fluoridon treatment.
- **Figure S6.7:** Hyponastic growth response of 35S::*KPR* to low light and heat treatment.
- **Table S6.1:** Primers used for Real-Time RT-PCR.

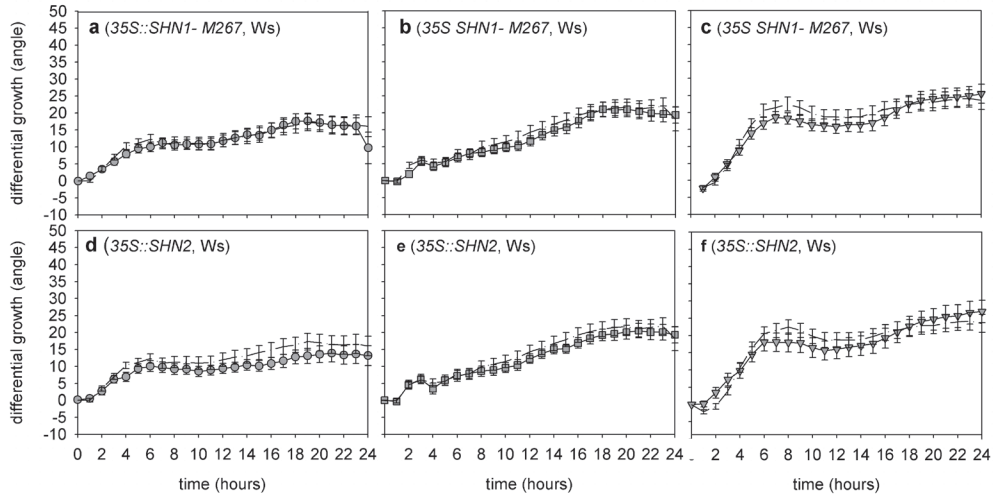


Figure S6.1: Hyponastic growth response of plants ectopically expressing SHN1 or SHN2. a: SHN1 and b: SHN2 in the Ws-2 (dash-dotted lines) background upon ethylene a,d: ($5 \mu\text{l l}^{-1}$; circles), b,e: low light ($200 \mu\text{mol m}^{-2} \text{s}^{-1}$ to $20 \mu\text{mol m}^{-2} \text{s}^{-1}$; squares) and c,f: heat (20°C to 38°C ; triangles) treatment. Angles resulted from pair wise subtraction, Error bars represent SE; $n > 10$.

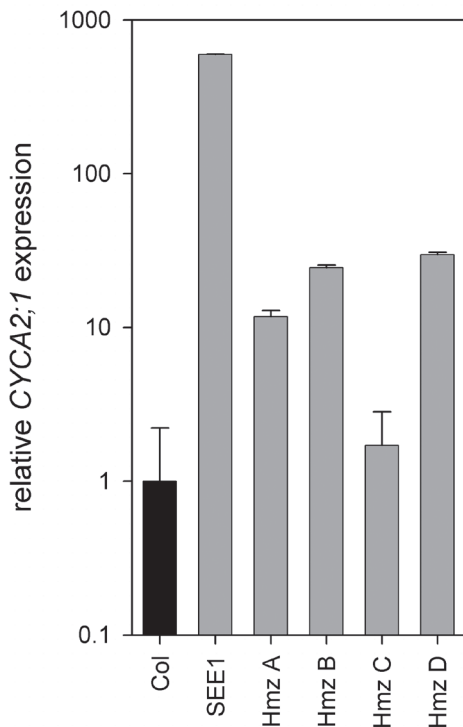


Figure S6.2: Quantitative RT-PCR analysis of CYCA2;1 expression in independent 35S::CYCA2;1 transformants and SEE1-1D. Expression levels were assayed in homozygous plants (grey bars). Expression values were normalized to 1 for Col-0 (black bar), $n \geq 4$; Standard errors represent SE. Transgenic line Himz B was further characterized and is referred to as: 35S::CYCA2;1. Note the logarithmic scale of the X-axis.

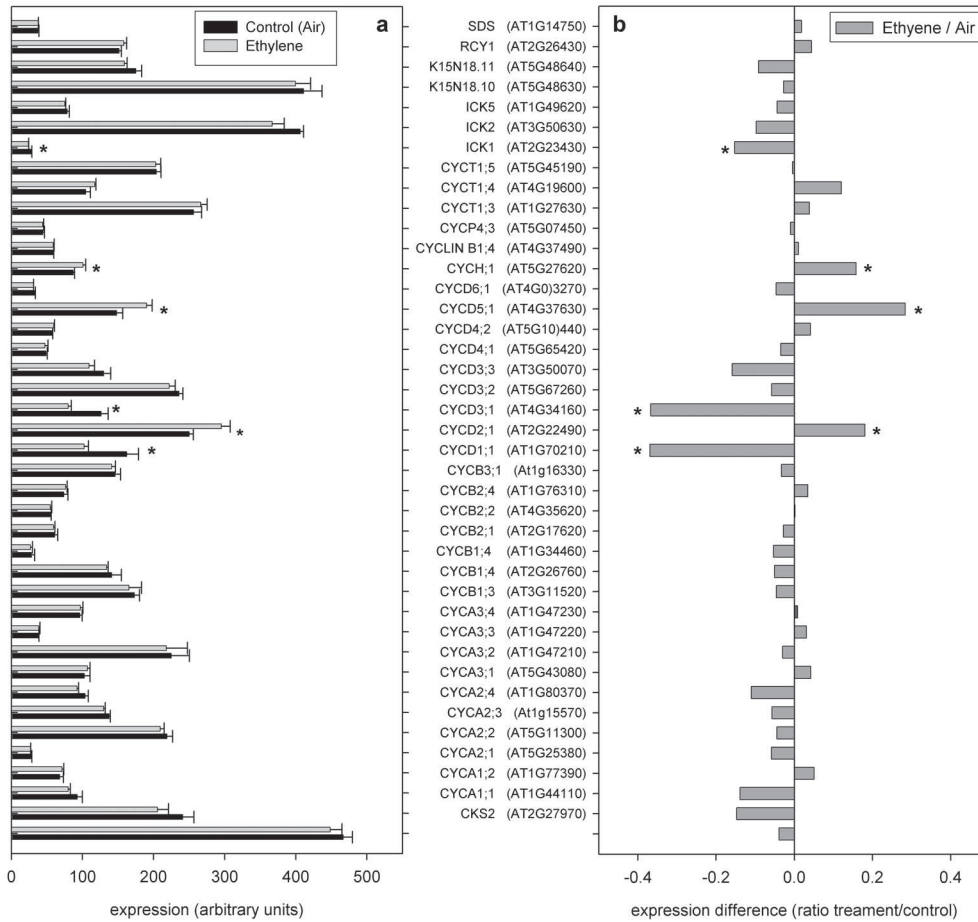


Figure S6.3: Expression of cell cycle-related genes upon ethylene treatment in *Arabidopsis thaliana*. **a:** absolute expression values (in arbitrary units) and **b:** relative expression levels in Col-0 petioles in control conditions (air) or treated with 3 h ethylene ($5 \mu\text{l l}^{-1}$). Micro-arrays (Affymetrix ATH1 chips) and experimental procedures are described in detail in Millenaar *et al.*, (2006). $n=3$ Error bars represent SE. Significant levels are p -values (Student's T-test); * $p<0.05$.

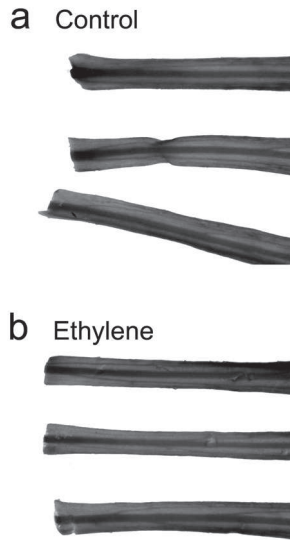


Figure S6.4: Histochemical analysis of CyclinB1;1 promoter activity. (See Color Supplement for full color version of this figure). Histochemical β -glucuronidase (GUS) analysis of plants carrying *D-box-CYCLINB1;1::GUS* in a: control conditions (air) and b: 6 h ethylene ($1.5 \mu\text{l l}^{-1}$) treatment.

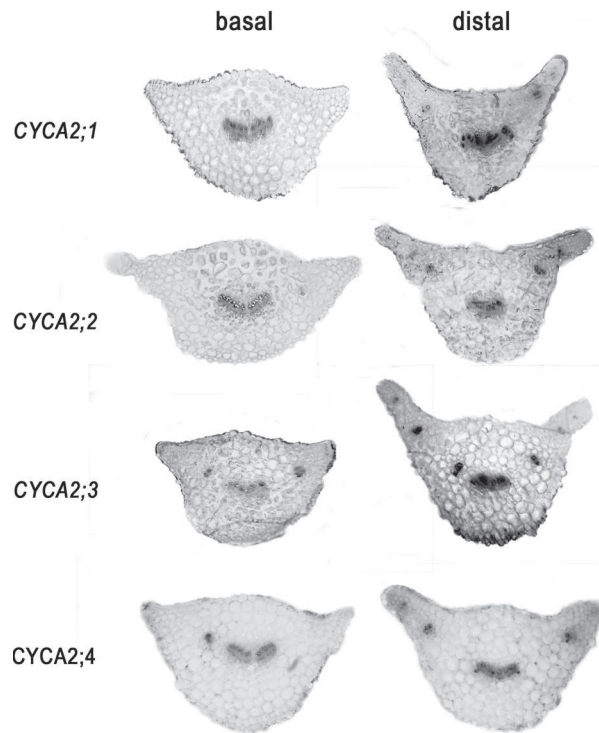


Figure S6.5: Spatial localization of CYCA2s in petioles. (See Color Supplement for full color version of this figure). Histochemical staining of basal and distal transverse sections of petioles in the developmental stage (~1 cm in length as used throughout this study) of plants carrying individual A2-Cyclin family promoters fused to the β -glucuronidase (GUS) reporter gene. Note that these sections are not indicative for quantitative activity.

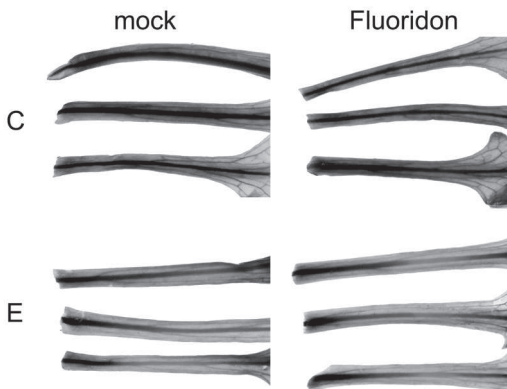


Figure S6.6: Histochemical analysis of CYCA2;1 promoter activity to fluoiron treatment. (See Color Supplement for full color version of this figure). Plants carrying the endogenous *CYCA2;1* promoter fused to the β -glucuronidase (GUS) reporter gene pre-treated with mock solution or fluoiron ($100 \mu\text{M}$) kept in control conditions (C) or treated for 6 h with ethylene ($1.5 \mu\text{l l}^{-1}$; E) treatment.

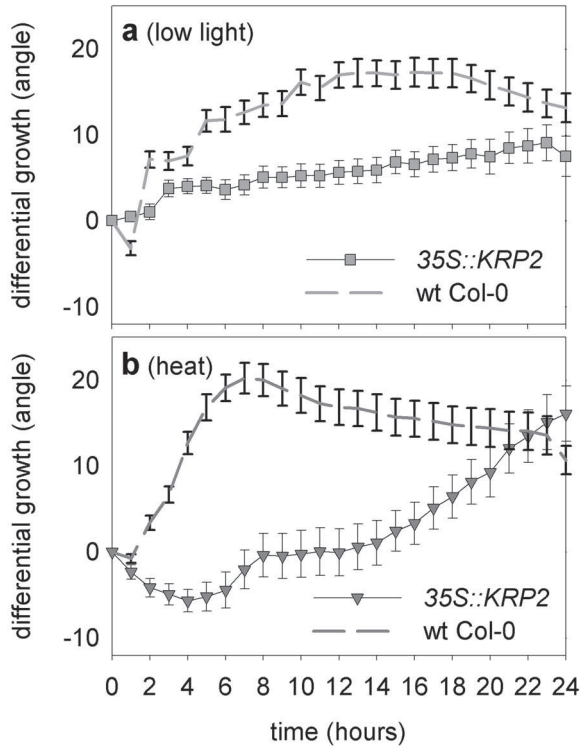


Figure S6.7: Hyponastic growth response of 35S::KRP2 to low light and heat treatment. a: low light ($200 \mu\text{mol m}^{-2} \text{s}^{-1}$ to $20 \mu\text{mol m}^{-2} \text{s}^{-1}$; squares) and b: heat (20°C to 38°C ; triangles) treatment of plants ectopically expressing *ICK2/KRP2*, compared to the wild type response (dashed lines). Angles resulted from pair wise subtraction, Error bars represent SE; $n>10$.

Table S6.1: Primers used for Real-Time RT-PCR. Forward (F) and Reverse (R) gene specific primers, with AGI-code used for Real-Time RT-PCR of genes flanking the T-DNA insertion site of *SEE1-1D*. Note that for At1g65580 two independent primer combinations were used.

AGI-code	
At5g25350	F CTTTCACGGTGTCTGGAAT R GTGGGCAGCTCCTGATAGAG
At5g25360	F AAGCCAAGCGTATCAGAGGA R CAGAGGTTCAATCCGTGGTT
At5g25370	F ATTCAATTTATGCGGCAAGG R CGGTGTAGACGTGGAAGGAT
At5g25380-a	F ATCAGTCCCACCACCAAAA R CCGCGAAATAGTTGGCTAAG
At5g25380-b	F AGCGTGTTGCTAGACCGAGT R TTCTTTACCACCTCGCTTGC
At5g25390	F GGGTCAAAAACGAGTCCAAA R CGCCATTTGATCATCTTCCT
At5g25400	F CCTTGGATGTCTGTGGAGTT R CAGAGGTTTTCCCAACCAAAA
At5g25410	F TGGAGACCCAAAGGAATCAG R TTGGCAAATGTCAAACCTCCA
At5g25415	F CATGAACCAGAGACCAGCAA R GAAGGATCTGAGAGGCAACG
At5g25420	F TGATCGCTTCGGCTTCTTAT R AGCAATCGACAGAGGGCTTA
At5g25430	F CCTATGGCCGGGATATTTTT R CCGCGTCGTAGAAATTCATCT

Natural variation in the hyponastic petiole growth response of *Arabidopsis thaliana*

Martijn van Zanten¹, L. Basten Snoek^{1§}, Evelien van Eck-Stouten², Marcel C.G. Proveniers², Laurentius A.C.J. Voeselek¹, Anton J.M. Peeters¹, Frank F. Millenaar^{1§}

¹ Plant Ecophysiology, Institute of Environmental Biology, Utrecht University, Padualaan 8, 3584 CH Utrecht, the Netherlands

² Molecular Plant Physiology, Institute of Environmental Biology, Utrecht University, Padualaan 8, 3584 CH Utrecht, the Netherlands

§Present addresses:

FFM: De Ruiter Seeds, Leeuwenhoekweg 52, 2660 BB Bergschenhoek, the Netherlands.

LBS: Department of Nematology, Wageningen University and Research Center, Binnenhaven 5, 6709 PD Wageningen, the Netherlands.

Adapted from:

- Van Zanten M, Snoek LB, van Eck-Stouten E, Proveniers MCG, Torii KU, Voeselek LACJ, Peeters AJM, Millenaar FF. Ethylene-induced hyponastic growth in *Arabidopsis thaliana* is controlled by ERECTA. The Plant Journal, Provisionally accepted.

Abstract

Plants can respond quickly and profoundly to changes in their environment. An example is the re-orientation of organs towards limiting resources, which is to improve access to these resources. *Arabidopsis thaliana* is capable of performing differential petiole growth driven upward leaf movement (hyponastic growth) to escape from detrimental conditions and this hyponastic response can be induced by treatment with ethylene, low light intensity and heat.

Variation among natural *Arabidopsis* accessions exists for many traits and can be utilized in quantitative genetic approaches to isolate novel loci controlling those traits. In this report, we studied natural phenotypic variation among *Arabidopsis thaliana* accessions for ethylene-, low light- and heat-induced differential growth, as well as for constitutive petiole angles. We found that hyponastic growth, induced by the different abiotic signals, is probably controlled by a downstream integrated signaling route. Moreover, constitutive variation in petiole angles does not interfere with the ability to induce a hyponastic growth response. Quantitative Trait Loci (QTL) analysis revealed several loci involved in the control of petiole angles and hyponastic growth. By subsequent mutant- and complementation analysis of both induced mutants in different backgrounds and in naturally occurring accessions, we show that the leucine-rich repeat receptor-like Ser/Thr kinase gene *ERECTA*, explains one of the identified major effect QTLs and controls low light- and ethylene-induced hyponastic growth.

Introduction

Plants have to adjust to their environment for optimal growth and survival. An example of a response that evolved to improve access to limiting resources is the re-orientation of organs towards these resources. *Arabidopsis thaliana* can induce differential petiole growth driven upward leaf movement (hyponastic growth) to escape from detrimental conditions. This response has been mainly associated with escape from growth limiting environments including complete submergence, where gaseous ethylene becomes trapped inside the plant due to a diffusion barrier raised by the surrounding water (Millenaar *et al.*, 2005, 2009; Chapter 2), low light intensities (Hangarter, 1997; Millenaar *et al.*, 2005; Mullen *et al.*, 2006; Chapter 2, 4), canopy shade (Ballaré *et al.*, 1999; Pierik *et al.*, 2004b, 2005) and heat (Koini *et al.*, 2009; Chapter 3). Interestingly, these signals induce a hyponastic growth response with remarkable similar kinetics in *Arabidopsis* (Millenaar *et al.*, 2005, 2009; Chapter 2-6). Despite these phenotypic similarities, the hormonal regulation of the response, induced by each environmental factor differs. For example, ethylene-induced hyponastic growth is antagonized by abscisic acid (ABA) (Benschop *et al.*, 2007) whereas ABA is a positive modulator of heat- and low light-induced hyponasty (Chapter 3, 4). Auxin is involved in heat- and low light-induced hyponasty but not in ethylene-induced hyponastic growth (Millenaar *et al.*, 2009; van Zanten *et al.*, 2009a; Chapter 2, 3) and

ethylene does not play a role in low light-induced hyponastic growth (Millenaar *et al.*, 2009; Chapter 2), and antagonizes heat-induced hyponasty (Chapter 3).

Arabidopsis thaliana is native to Europe and Central Asia and is introduced in other parts of the Northern hemisphere (between N 0° and 68°), including North America, Japan and Korea, and at a few places on the Southern hemisphere (Hoffmann 2002, Koornneef *et al.*, 2004). It occurs predominantly, but not exclusively, on disturbed and open sites with loose soils and is found at altitudes up to 4250 m. This wide biogeographical distribution and the variety of environmental conditions to which it has adapted are reflected in extensive genetic variation among accessions (Hoffmann 2002; Koornneef *et al.*, 2004; Nordborg *et al.*, 2005).

Over 1450 accessions are available at the Stock centers (Shindo *et al.*, 2007). Along with the study of induced variation (mutants), assessment of the natural genetic variation by quantitative genetic tools can be utilized to isolate novel genetic components controlling the trait of interest. This ultimately may lead to understanding the molecular basis of adaptation and acclimation (Alonso-Blanco & Koornneef, 2000; Koornneef *et al.*, 2004; Weigel & Nordborg, 2005; Nordborg *et al.*, 2005; Shindo *et al.*, 2007).

Extensive natural variation exists in several species for leaf angles (McMillen & McClendon, 1979; Abreu & Munné-Bosch, 2008; King, 1979; Falster & Westoby, 2003), which is thought to have evolved for optimization of photon capture, water use efficiency and functions against overheating.

Also for *Arabidopsis thaliana* accessions natural phenotypic variation for both constitutive petiole angles and induced hyponastic growth has been described (Millenaar *et al.*, 2005; Hopkins *et al.*, 2008; Chapter 3). However, these studies were based on limited numbers of accessions and were not used to assess the underlying genetic variation. In this report, we surveyed natural phenotypic variation in constitutive petiole angles and for hyponastic growth responses induced by ethylene, low light and heat, in 138 *Arabidopsis thaliana* accessions. Our data indicates that hyponastic growth induced by different abiotic environmental factors is controlled by an integrated signaling route and that constitutive variation in petiole angles does not significantly interfere with the ability to induce a hyponastic growth response. Moreover, Quantitative Trait Loci (QTL) analysis was utilized to identify novel loci controlling hyponastic growth. Subsequent analysis of Near Isogenic Lines (NIL), induced mutants in different genetic backgrounds and complementation analysis of naturally occurring mutant accessions, showed that the leucine-rich repeat receptor-like Ser/Thr kinase gene *ERECTA* (*ER*) explains one of the identified major effect QTLs and controls low light- and ethylene-induced hyponastic growth. Moreover, we demonstrate that these responses are not a consequence of *ER* mediated control of ethylene production or sensitivity.

Results

Extensive natural variation exists in initial petiole angles and induced hyponastic growth among *Arabidopsis thaliana* accessions

To study natural phenotypic variation in petiole angle traits, we measured constitutive petiole angle (initial angle) and induced hyponastic petiole growth after 6 h ethylene, low light and heat treatment, of 138 naturally occurring *Arabidopsis thaliana* accessions (Supporting Information Table S7.1). Initial petiole angles varied across the data-set from 15.3 ± 0.9 degrees (Warschau-1; Wa-1) to 52.0 ± 1.0 degrees (Meloy Ornes) (Figure 7.1). Variation in induced differential petiole growth to 6 h ethylene treatment ranged from strongly hyponastic (39.7 ± 6.4 deg; Niigata) to even epinastic growth (-10.3 ± 2.3 ; Palermo-1; Pa-1) (Figure 7.2a). After 6 h spectral neutral low light conditions (reduction of light intensity by 90%) NG again was identified as the strongest responder (37.8 ± 6.4 deg). Only one accession showed an epinastic response in these conditions (-3.4 ± 3.8 deg; Kyoto) (Figure 7.2b). After 6 h heat treatment (sudden temperature increase from 20°C to 38°C) (Figure 7.2c), Lipovec2-6 (Lp2-6) showed the strongest increase in petiole angle (29.6 ± 3.1) and Billaberget-7 (Bil-7; -11.1 ± 3.0) was the strongest epinastic responder. The Japanese accession Niigata was the third strongest responder to heat (28.5 ± 6.4) and thus, in general, can be regarded the strongest overall responder taking all treatments into account. Intriguingly, another Japanese accession; Kyoto, was the weakest overall responder, as this was the only accession with an epinastic response to all treatments. As expected, we found a significant correlation ($r^2 = 0.80$; $p = 0.01$) between earlier published results on natural variation in ethylene-induced hyponastic growth (Millenaar *et al.*, 2005) and the results presented in Figure 7.2a.

Correlation analysis of petiole angle traits

Because the geographic origin of the accessions (Table S7.1) used in this study roughly spans the biogeographical distribution range of *Arabidopsis thaliana*, we tested for correlations between latitude, longitude and altitude of the individual collection sites on one hand and initial petiole angle (IA) and different aspects of hyponastic growth (see Table 7.1) to ethylene (E), low light (LL) and elevated temperature (Heat; HT) on the other. No significant inter-specific correlations (Pearson 2-tailed) were found (data not shown).

Intra-specific correlation analysis revealed that the initial angles of the accessions across the dataset significantly, strongly positively correlated with the absolute angle after 6 h of all treatments (Table 7.1). Nevertheless, a small, in general negative, trend was observed between initial angle and absolute angles after 6 h control (6 h A) and between initial angle and pair-wise subtracted petiole angles (difference between absolute angles of treated and control plants) after the different treatments. These trends were in most cases not significant, except for the response angle to ethylene and heat (Table 7.1).

Absolute angles after 6 h of a given treatment significantly, positively, correlated with the response window (Response Angle; RA; difference between initial angle

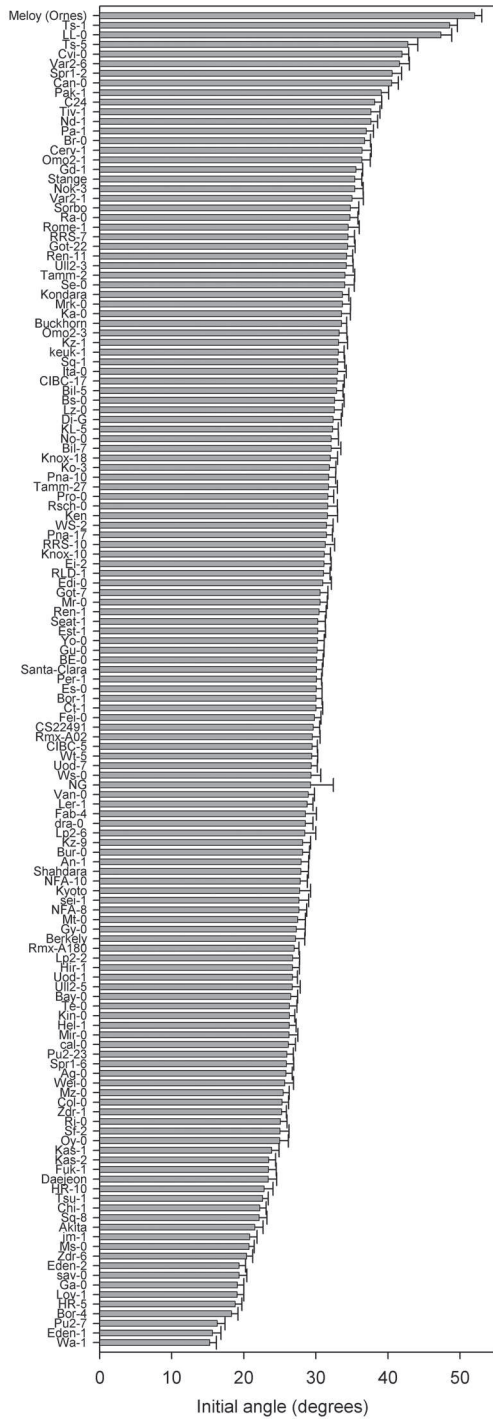


Figure 7.1: Natural variation in initial petiole angles of *Arabidopsis thaliana*. Values represent absolute angles (degrees) relative to the horizontal, at t=0 h of *Arabidopsis thaliana* accessions in control conditions (air; 200 $\mu\text{mol m}^{-2} \text{s}^{-1}$ light).

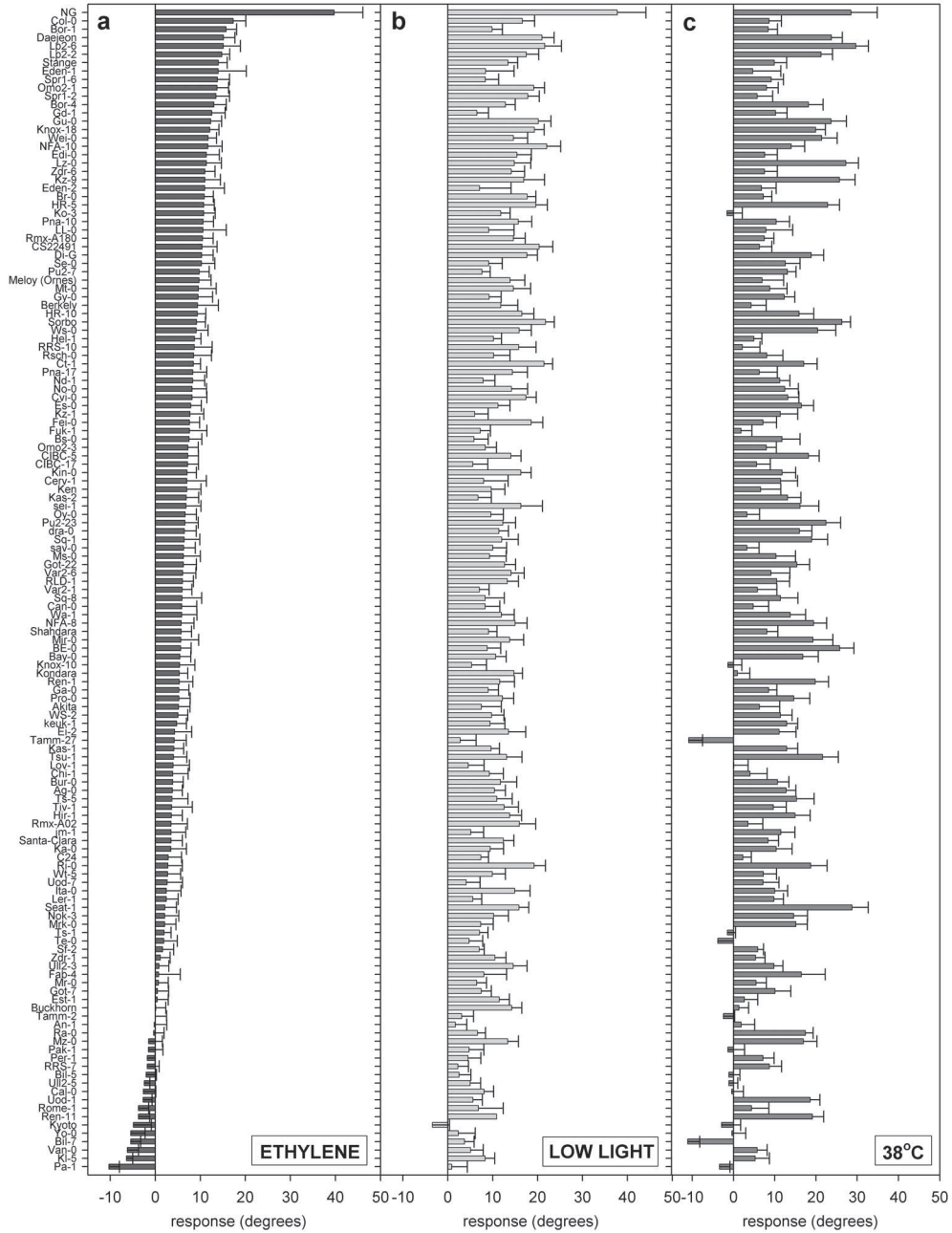


Figure 7.2: Natural variation in induced hyponastic growth of *Arabidopsis thaliana*. Effect of exposure to a: ethylene ($5 \mu\text{l l}^{-1}$), b: low light ($200 \mu\text{mol m}^{-2} \text{s}^{-1}$ to $20 \mu\text{mol m}^{-2} \text{s}^{-1}$) and c: heat (20°C to 38°C) on petiole angles of 138 *Arabidopsis thaliana* accessions. Values are pair wise subtracted. Error bars represent SE; $n=2$ to 15. Note that the values of panel A are sorted by response magnitude.

Table 7.1: Correlation analysis of petiole angle traits. Bivariate relationships between *Arabidopsis thaliana* petiole angle parameters in different hyponastic growth inducing environments.

		Absolute angle after 6 h				Response window				Absolute response			
		Initial angle	6 h A	6 h E	6 h LL	6 h HT	RA A	RA E	RA LL	RA HT	pair wise E	pair wise LL	pair wise HT
Initial angle	P		0.800	0.788	0.870	0.618	-0.050	-0.313	-0.048	-0.170	-0.054	0.059	-0.086
	Sig.		**	**	**	**	ns	**	ns	* (0.047)	ns	ns	ns
6 h A	P	0.800		0.680	0.715	0.525	0.397	-0.093	0.040	-0.028	-0.440	-0.411	-0.376
	Sig.	**		**	**	**	**	ns	ns	ns	**	**	**
6 h E	P	0.788	0.680		0.806	0.566	0.157	0.215	0.150	0.006	0.359	0.137	-0.029
	Sig.	**	**		**	**	ns	* (0.012)	+ (0.08)	ns	**	ns	ns
6 h LL	P	0.870	0.715	0.806		0.687	0.066	-0.049	0.298	0.043	0.076	0.343	0.070
	Sig.	**	**	**		**	ns	0.571	**	ns	ns	**	ns
6 h HT	P	0.618	0.525	0.566	0.687		0.145	-0.031	0.253	0.616	0.025	0.191	0.591
	Sig.	**	**	**	**		+ (0.09)	ns	** (0.003)	**	ns	* (0.025)	**
RA A	P	-0.050	0.397	0.157	0.066	0.145		0.316	0.236	0.281	-0.314	-0.448	-0.219
	Sig.	ns	**	ns	ns	+ (0.09)		**	** (0.005)	** (0.001)	**	**	** (0.01)
RA E	P	-0.313	-0.093	0.215	-0.049	-0.031	0.316		0.308	0.271	0.382	0.062	0.055
	Sig.	**	ns	* (0.012)	ns	ns	**		**	** (0.001)	**	ns	ns
RA LL	P	-0.048	0.040	0.150	0.298	0.253	0.236	0.308		0.339	0.132	0.335	0.238
	Sig.	ns	ns	+ (0.08)	**	** (0.003)	** (0.005)	**		**	ns	**	** (0.005)
RA HT	P	-0.170	-0.028	0.006	0.043	0.616	0.281	0.271	0.339		0.042	0.093	0.697
	Sig.	* (0.047)	ns	ns	ns	**	** (0.001)	** (0.001)	**		ns	ns	**
pair wise E	P	-0.054	-0.440	0.359	0.076	0.025	-0.314	0.382	0.132	0.042		0.691	0.444
	Sig.	ns	**	**	ns	ns	**	**	ns	ns		**	**
pair wise LL	P	0.059	-0.411	0.137	0.343	0.191	-0.448	0.062	0.335	0.093	0.691		0.597
	Sig.	ns	**	ns	**	* (0.025)	**	ns	**	ns	**		**
pair wise HT	P	-0.086	-0.376	-0.029	0.070	0.591	-0.219	0.055	0.238	0.697	0.444	0.597	
	Sig.	ns	**	ns	ns	**	** (0.01)	ns	** (0.005)	**	**	**	

Footnote:

Bivariate correlations coefficients are Pearson (P) 2-tailed, of angle parameters measured in 138 *Arabidopsis thaliana* accessions. Significant (sig.) correlations are in bold; $p < 0.05$ (value between brackets), ** $p < 0.01$ (value between brackets if $p > 0.001$, if lower: not shown). + $p < 0.1$; ns = non significant.

All used parameters for the correlation are petiole angles relative to the horizontal. Initial angle represents absolute petiole angle at $t=0$ h; 6 h indicates the absolute angle after 6 hour of treatment with air control at $200 \mu\text{mol m}^{-2} \text{s}^{-1}$ (A), $1.5 \mu\text{l l}^{-1}$ ethylene (E), low light intensity ($20 \mu\text{mol m}^{-2} \text{s}^{-1}$; LL) or 38°C heat treatment (HT). Response angles represent the relative angle difference between the angle after 6 h of treatment and the initial angle. Pair wise subtracted angles (Benschop et al., 2007) represent the response magnitude, which is the angle at $t=6$ h after treatment relative to the angle of control plants at $t=6$ h (6 h A)

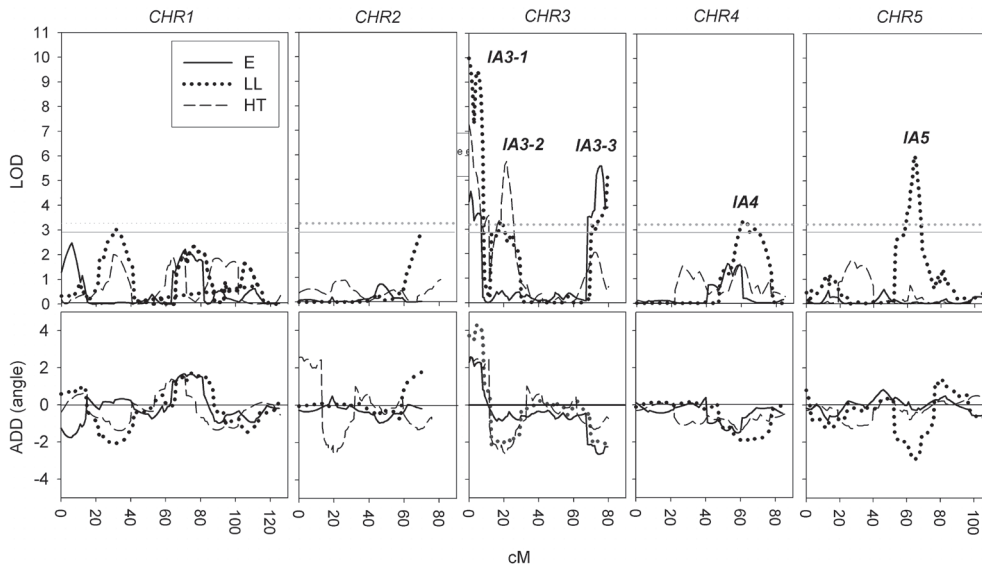


Figure 7.3: Mapping of Initial Angle QTLs. Position of QTLs mapped for initial angles prior to ethylene-, low light- or heat- exposure in the *Ler* x *Cvi-0* RIL population (in centi-Morgan; cM). Upper graphs show the LOD profile of petiole angles per chromosome (CHR). QTL names are near each QTL peak. Solid lines represents the LOD profile of plants preceding ethylene (E) treatment, dotted lines represents the LOD profile of plants preceding low light (LL) treatment and dashed lines represents the LOD profile of plants preceding heat (HT) treatment. The horizontal dashed- and dotted lines mark the 95% confidence thresholds at LOD: 2.92 (E), 2.41 (LL) and 2.85 (HT). The lower graphs show the additive effect (angle) of the *Ler* allele compared to the population average.

and absolute angle after 6 h treatment) and the pair wise subtracted response of the same treatment in all cases. All absolute angles after 6 h treatment, all pair wise subtracted angles after treatment and all response window angles correlated significantly to the same parameter of every other treatment. I.e. plants with on average a strong response/high angle after a given treatment will likely also have a strong response/high angle to one of the other treatments.

Together, these results suggest that initial angles strongly contribute, but not restrict, the absolute angle after treatment. In general, for an individual accession, the ability to respond to a given environment is probably dependent of the genetic make-up of the accession, rather than on the inducing environmental factor.

QTL analysis reveals several signal specific loci controlling hyponastic petiole growth

To identify functional genetic components that control initial petiole angles and induced hyponastic growth, we performed Quantitative Trait Locus (QTL) analysis. For this aim, petiole angles were measured in a population of Recombinant Inbred Lines (RILs) derived from a cross between Cape Verde Islands-0 (*Cvi-0*) and *Landsberg erecta* (*Ler*) (Alonso-Blanco et al., 1998a).

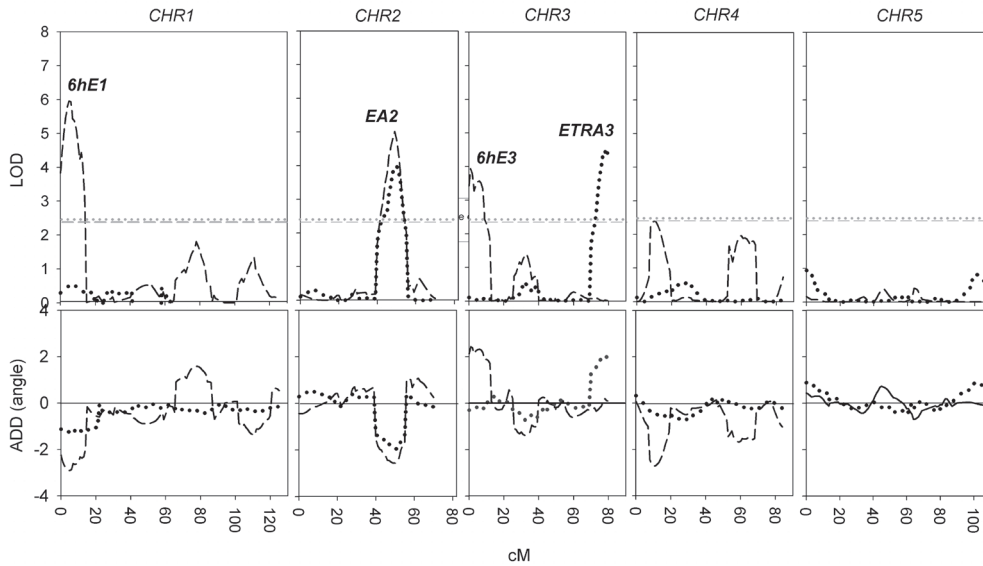


Figure 7.4: QTL mapping of petiole angle traits involved in ethylene-induced hyponastic growth. Position of QTLs mapped for petiole angles after exposure to ethylene (E; $5 \mu\text{l l}^{-1}$) in the *Ler* x *Cvi-0* RIL population (in centi-Morgan; cM). Upper graphs show the LOD profile of petiole angles per chromosome (CHR). QTL names are near each QTL peak. Mapped are: Absolute petiole angles after 6 h of ethylene treatment (6hE; dashed lines) and the difference between initial angle and the absolute angle after 6 h of treatment (Response Angle, ETRA QTL; dotted lines). The horizontal dashed- and dotted lines mark the 95% confidence thresholds at LOD 2.41 and LOD 2.42 of 6hE and ETRA respectively. EA QTL marks the position where a QTL for both traits has been mapped. The lower graphs show the additive effect (angle) of the *Ler* allele compared to the population average.

	BSH (H^2)			LOD threshold		
	E	LL	HT	E	LL	HT
Initial angle	0.43	0.60		2.92	3.28	2.85
6 h angle	0.45	0.49		2.41	2.85	3.35
Response angle	0.50	0.43		2.42	3.07	2.70

Table 7.2: Broad Sense Heritability of initial petiole angles and induced hyponastic growth. Broad Sense Heritability (BSH; H^2) and 1000-permutation calculated Likelihood of odds (LOD) threshold of petiole angles before and after 6 h ethylene (E; $5 \mu\text{l l}^{-1}$), low light (LL; $200 \mu\text{mol m}^{-2} \text{s}^{-1}$ to $20 \mu\text{mol m}^{-2} \text{s}^{-1}$) or heat (HT; 20°C to 38°C) treatments.

Calculation of the broad sense heritability (BSH; H^2) indicated that 43% (IA E) to 60% (IA LL) of the total variation is explained by genetic variation in the RILs (Table 7.2). One (RA LL) to five (IA LL and 6 h HT) QTLs per trait were mapped to be above the permutation calculated Likelihood-of-ODDs (LOD) threshold (Van Ooijen, 1999) (Figure 7.3-7.6; Table 7.3). For most traits, QTLs with both a negative and positive allelic effect were identified, implicating the existence of both positive and negative molecular regulators contributing to the petiole angle phenotype.

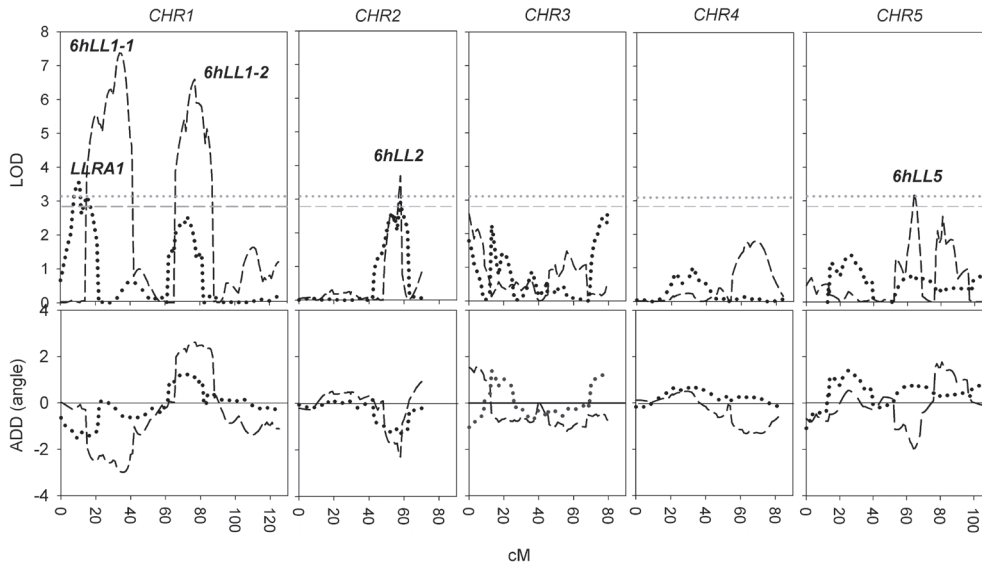


Figure 7.5: QTL mapping of petiole angle traits involved in low light-induced hyponastic growth. Position of QTLs mapped for petiole angles after exposure to low light (LL; PAR reduction of $200 \mu\text{mol m}^{-2} \text{s}^{-1}$ to $20 \mu\text{mol m}^{-2} \text{s}^{-1}$) in the *Ler* x *Cvi-0* RIL population (in centi-Morgan; cM). Upper graph shows the LOD profile of petiole angles per chromosome (CHR). QTL names are near each QTL peak. Mapped are: Absolute petiole angles after 6 h of low light treatment (*6hLL*; dashed lines) and the difference between initial angle and the absolute angle after 6 h of treatment (Response Angle, *LLRA* QTL; dotted lines). The horizontal dashed- and dotted lines mark the 95% confidence thresholds at LOD 2.85 and LOD 3.07 of *6hLL* and *LLRA* respectively. The lower graphs shows the additive effect (angle) of the *Ler* allele compared to the population average.

Because growth conditions prior to ethylene, low light and heat treatments were identical, initial angles were measured independently three times. For this reason, we expected to map largely identical QTLs for IA prior to the treatments. Indeed, one locus; *IA3-1*, at the top of chromosome 3, was mapped for all three treatments (Figure 7.3; Table 7.3). Moreover, *IA3-2* was found for HT and LL and *IA3-3* was mapped for E and LL. All the identified IA QTLs, except *IA3-1*, had a negative *Ler* additive effect. Also, several 6 h absolute angle and RA QTLs co-located (these were designated as ethylene angle QTL; EA, or heat angle QTL; HTA, Figure 7.4-7.6; Table 7.3). Most notable in this respect is *EA2* (Figure 7.4) which showed a negative *Ler* effect for both the absolute angle (6 h) and RA after ethylene treatment. Interestingly, *EA2* co-located with a negative *Ler* effect QTL for absolute angle after 6 h of low light (*6hLL2*) (Figure 7.5; Table 7.3). At this position, also a near-significant QTL peak for *LLRA* was found. Similarly, *6hE1* co-located with *LLRA1* (negative *Ler* effect). On the top of chromosome 3 several QTLs co-locate. At this locus *6hE3* with a similar (positive) *Ler* effect as *IA3-1* was observed and also a QTL for response to heat (*HTRA3-1*) mapped to this position, although this QTL has a negative *Ler* effect. A QTL rich region was found at the bottom of chromosome 3. Not only *IA3-3*, mapped

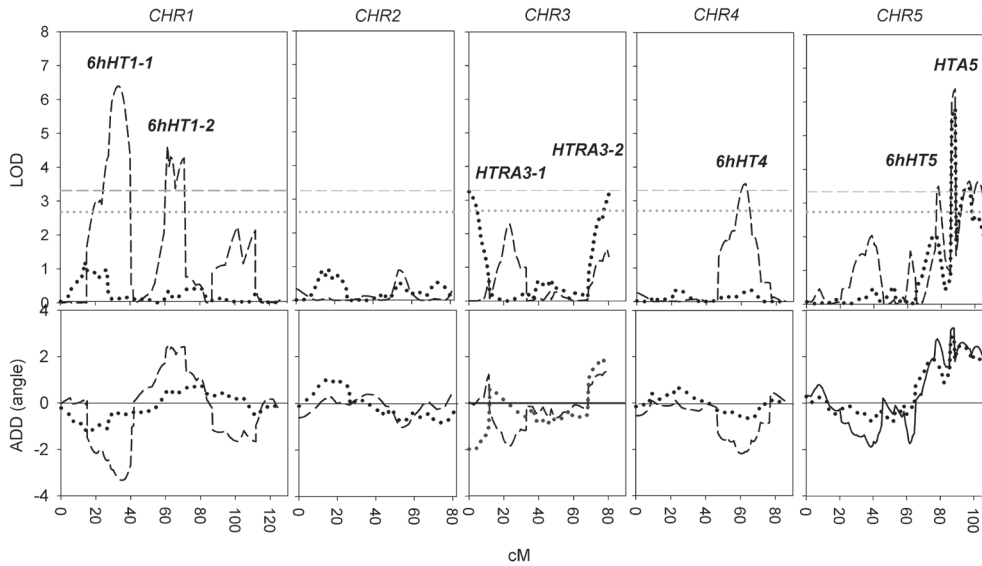


Figure 7.6: QTL mapping of petiole angle traits involved in heat-induced hyponastic growth. Position of QTLs mapped for petiole angles after exposure to heat (HT; 20°C to 38°C temperature increase) in the *Ler* x *Cvi-0* RIL population (in centi-Morgan; cM). Upper graph shows the LOD profile of petiole angles per chromosome (CHR). QTL names are near each QTL peak. Mapped are: Absolute petiole angles after 6 h of heat treatment (*6hHT*; dashed lines) and the difference between initial angle and the absolute angle after 6 h of treatment (Response Angle, *HTRA* QTL; dotted lines). The horizontal dashed- and dotted lines mark the 95% confidence thresholds at LOD 3.35 and LOD 2.70 of *6hHT* and *HTRA* respectively. *HTA* QTL marks the position where a QTL for both traits has been mapped. The lower graphs show the additive effect (angle) of the *Ler* allele compared to the population average.

to this position, but also the positive *Ler* effect QTLs for response to heat (*HTRA3-2*) (Figure 7.6) and to ethylene (*ETRA3*; Figure 7.4).

At the bottom of chromosome 5, positive *Ler* QTLs for *6hHT* and *HTRA* co-located in a sharp peak (*HTA5*). *HTA5* is in the vicinity of the *Ler* positive effect *6hHT5* QTL. Two similar QTLs have been mapped for low light and heat traits on chromosome 1; *6HLL1-1* and *6hHT1-1* (negative *Ler* effect) and *6hHT1-2* and *6HLL1-2* (positive *Ler* effect). However, these QTLs do not strictly co-locate because the LOD peaks are ~16 cM apart. Yet, parts of the QTL area, in a region still above the LOD threshold are shared between both QTLs, indicating that they might map to the same locus. Also, on chromosome 5 the QTLs; *6HLL5* and *IA5* co-locate. Only few trait and treatment specific QTLs have been mapped, (i.e. *6hHT4* and *LLRA1*). No loci could be identified containing response QTLs to all three treatments.

The initial petiole angle and absolute angle after 6 h of ethylene and low light treatment of a heterozygous F1 line, derived from a cross between *Ler* and *Cvi-0*, were intermediate between parental *Ler* and *Cvi-0* (Figure 7.7a-c). This suggests that both accessions lack dominant loci controlling absolute petiole angles. However, the hyponastic growth response of the F1 equaled *Cvi-0* after ethylene treatment

Table 7.3: All QTLs described in this report. QTLs are calculated from the *Ler* x *Cvi-0* RIL population, before and after 6 h of ethylene (E; 5 $\mu\text{l l}^{-1}$), low light (LL; 200 $\mu\text{mol m}^{-2} \text{s}^{-1}$ to 20 $\mu\text{mol m}^{-2} \text{s}^{-1}$) or heat (HT; 20°C to 38°C) treatments. LOD: Likelihood of difference score (bold), Top: position of maximum QTL LOD value (in cM), add: additive effect (*Ler* allele effect difference with mean, in degrees) and R2: explained variance in percentages. The sum of R2 and of the additive effects are depicted in the last row per trait (tot).

	Initial angle (IA)					6 h angle					Response angle (RA)							
	Chr	LOD	Top	add	R2	Chr	LOD	Top	add	R2	Chr	LOD	Top	add	R2			
E	IA3-1	3	4.5	1	2.58	4.55	6hE1	1	6.0	5	-2.92	13.39	EA2	2	4.0	50	-1.95	10.80
	IA3-3	3	5.6	75	-2.64	5.57	EA2	2	5.0	49	-2.56	9.76	ETRA3	3	4.5	80	2.025	11.45
							6hE3	3	3.9	1	2.429	8.37						
	tot				-0.06	10.12	tot				-3.05	31.52	tot				0.079	22.25
LL	IA3-1	3	10.0	0	3.72	15.15	6hLL1-1	1	7.4	34	-2.96	15.91	LLRA	1	3.6	10	-1.49	7.36
	IA3-2	3	3.4	19	-2.08	4.62	6hLL1-2	1	6.6	77	2.61	12.17						
	IA3-3	3	5.3	80	-2.37	7.56	6HL2	2	4.0	59	-2.29	6.71						
	IA4	4	3.4	62	-1.95	4.97	6HL5	5	3.3	64	-1.97	5.49						
	IA5	5	6.0	64	-2.93	8.75												
	tot				-5.61	41.05	tot				-4.61	40.28	tot				-1.49	7.36
HT	IA3-1	3	7.3	0	2.56	13.48	6hHT1-1	1	6.4	33	-3.26	12.52	HTRA3-1	3	3.2	1	-2.01	6.50
	IA3-2	3	5.8	22	-2.59	12.21	6hHT1-2	1	4.6	61	2.46	7.30	HTRA3-2	4	3.2	80	1.94	6.26
							6hHT4	4	3.5	62	-2.13	5.60	HTA5	5	5.8	88	2.87	13.07
							6hHT5	5	3.5	78	2.77	5.42						
							HTA5	5	6.4	88	3.25	12.05						
tot				-0.03	25.69	tot				3.09	42.89	tot				2.80	25.83	

(Figure 7.7d), and equaled *Ler* after low light treatment (Figure 7.7e). Thus, likely *Cvi-0* contains a locus that dominantly controls the response to ethylene, whereas vice versa, *Ler* contains a dominant locus controlling the response to low light.

Evaluation of the complex ethylene- and low light-QTL rich region of chromosome 2

We choose to further characterize the QTL region on chromosome 2, as this was the locus containing most co-locating QTLs among the treatments (*6hE*, *ETRA*; together; *EA2*, *6hLL2* and close-to-significant; *LLRA*). Moreover, these QTLs showed a consistent negative *Ler* effect.

To confirm the *EA2/6hLL2* QTLs, we measured the hyponastic growth response to 6 h ethylene and low light treatment in a Near Isogenic Line (NIL LCN2-7; Keurentjes *et al.*, 2007) containing a single *Cvi-0* introgression, spanning the complete *EA2/6hLL* QTL region (30.3–71.7 cM; outer *Ler* markers at chromosome 2). Unexpectedly, the

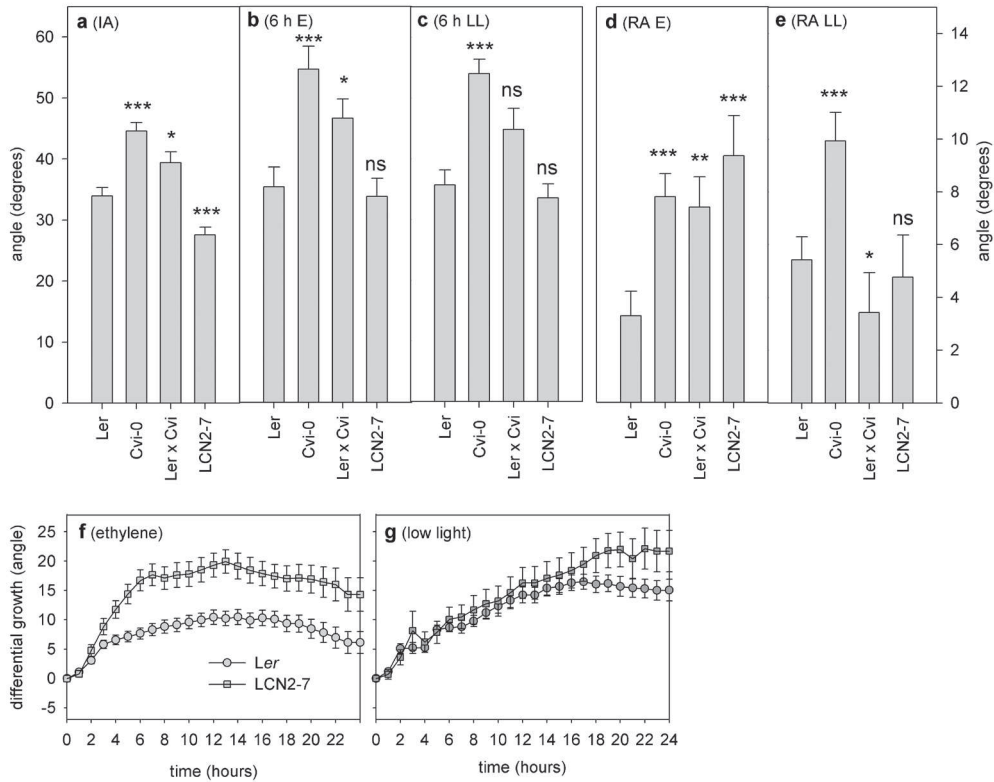


Figure 7.7: Genetic analysis of petiole angle traits in a NIL and in RIL-parents. Absolute petiole angles a: before (initial angle; $t=0$ h) and b: to 6 h of ethylene (E; $5 \mu\text{l l}^{-1}$) or c: to low light (LL; $200 \mu\text{mol m}^{-2} \text{s}^{-1}$ to $20 \mu\text{mol m}^{-2} \text{s}^{-1}$) treatment. d: ethylene and e: low light response angles (RA) to these treatments. Significance levels; * $p<0.05$; ** $p<0.01$; *** $p<0.001$; ns = non significant; 2-tailed Student's T-test, compared to Ler, $n\geq 12$. f: Effect of exposure to ethylene and g: low light on petiole angles of Near Isogenic Line LCN2-7 (squares) and Ler (circles). Values are pair wise subtracted. Error bars represent SE; $n\geq 12$.

initial angle of LCN2-7 was significantly lower than both parental lines ($p<0.001$; Figure 7.7a). The absolute angles, after 6 h ethylene and low light treatment were statistically indistinguishable between Ler and LCN2-7 (Figure 7.7b, c). Yet, the response of LCN2-7 to ethylene was identical to Cvi-0 and to the heterozygous F1 line (Figure 7.7d) and was significantly stronger than Ler ($p<0.001$). The response of LCN2-7 to low light was identical to Ler and the F1 and was significantly lower than the response of Cvi-0 ($p<0.001$). These data were confirmed by analysis of pair wise subtracted response kinetics (Figure 7.7f, g), which corrects for circadian and diurnal influences on leaf movement as well as IA. These data show that the Cvi-0 introgression strongly enhances the response to ethylene (Figure 7.7f) whereas the response to low light remained identical to Ler.

Together, this indicates that the LCN2-7 introgression contains a Cvi-0 locus that was not detected by our QTL analysis, affecting initial petiole angles and is only displayed in the *Ler* isogenic background. The introgression of LCN2-7 confirmed the negative *Ler* effect QTL for ethylene response, but not for absolute angle after ethylene treatment and for low light-induced hyponastic growth.

ERECTA receptor-like kinase controls initial petiole angle and induced hyponastic growth

The *EA2/6hLL2* QTLs mapped to the *ERECTA* (*ER*) locus. *ER* encodes a leucine-rich repeat receptor-like Ser/Thr kinase and has been previously shown to segregate between Landsberg *erecta* and Cvi-0 (Van Zanten *et al.*, 2009b; and references within) and *Ler* carries a null-allele (Torii *et al.*, 1996).

To test if *ER* controls hyponastic growth, we measured initial petiole angles and induced hyponastic growth in *erecta* mutant alleles, in different genetic backgrounds (Torii *et al.*, 1996), and in the original Landsberg wild type line (Lan-0), from which *Ler* was isolated in the sixties of the last century (Redei, 1962).

Lan-0 had a significantly ($p < 0.001$) lower initial petiole angle than *Ler* (Figure 7.8a). To test if this was caused by *er*, we introduced the Col-0 *ER* locus, including the promoter sequences, in *Ler* by transformation (*ER-Ler*). This transgenic line complemented all characteristic plant architectural phenotypes typically attributed to *er*, including the compact rosette appearance (Figure 7.9a-c), reduced plant height,

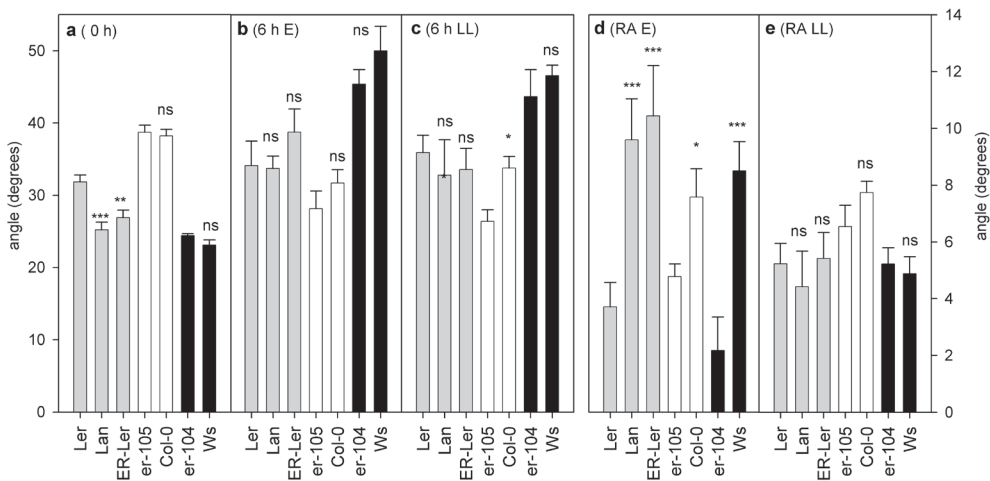


Figure 7.8: Effects of *ER* on initial petiole angles and induced hyponastic growth. a: Initial petiole angle ($t=0$ h), b: absolute angle after 6 h exposure to ethylene ($5 \mu\text{l l}^{-1}$) or c: to low light ($200 \mu\text{mol m}^{-2} \text{s}^{-1}$ to $20 \mu\text{mol m}^{-2} \text{s}^{-1}$). Response angle after d: ethylene and e: low light treatment of *erecta* mutants, their corresponding wild types and a *ER-Ler* complemented transgenic line. Error bars represent SE; $n \geq 8$. Significance levels; * $p < 0.05$; ** $p < 0.01$; *** $p < 0.001$; ns = non significant; 2-tailed Student's T-test.

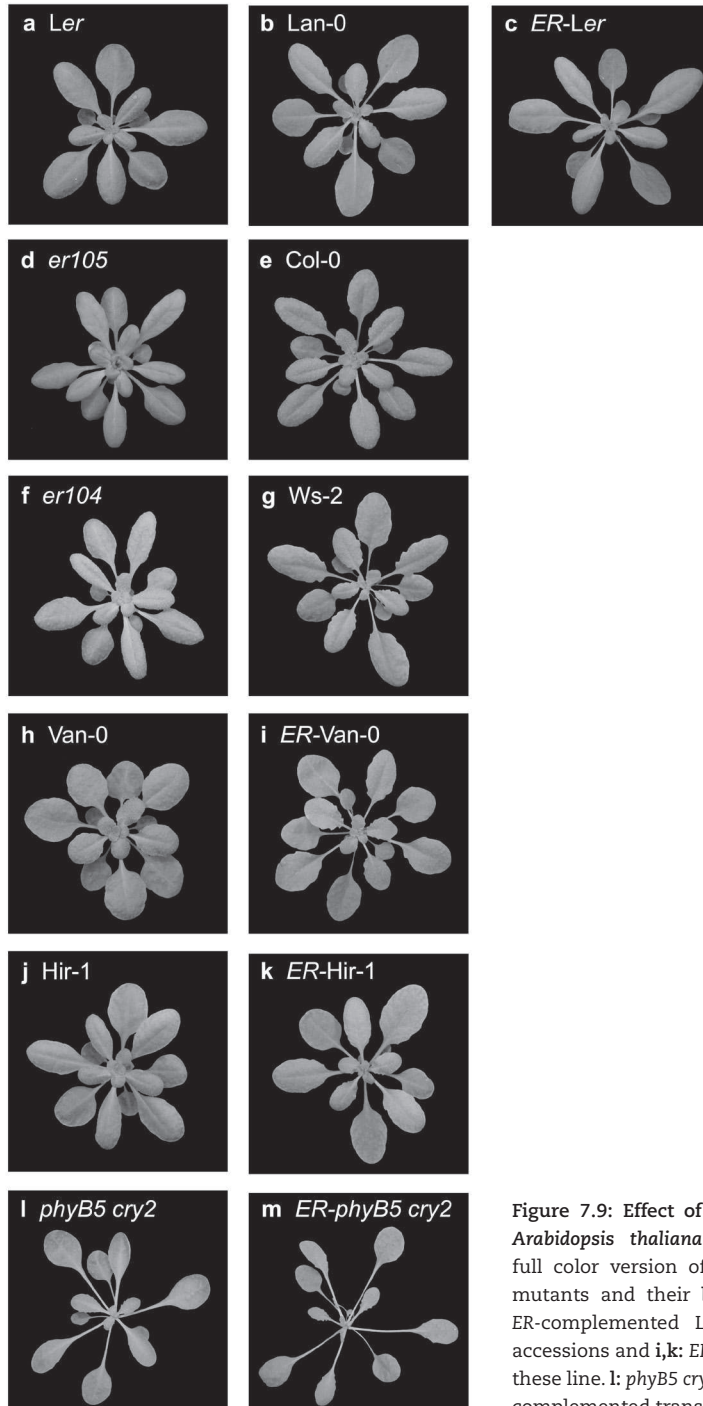


Figure 7.9: Effect of ER on rosette morphology of *Arabidopsis thaliana*. (See Color Supplement for full color version of this figure) **a,d,f**: induced *er* mutants and their **b,e,g**. respective wild types **c**: ER-complemented *Ler*. **h,j**: natural occurring *er* accessions and **i,k**: ER-complemented transgenics of these line. **l**: *phyB5 cry2* mutant and **m**: *phyB5 cry2* ER-complemented transgenic line.

increased inflorescence thickness and decreased silique length (Figure 7.10a-c). Initial petiole angles in *ER-Ler* were significantly ($p < 0.01$) lower than in *Ler* and were indistinguishable from *Lan-0* (Figure 7.8a). Interestingly, no such differences in initial petiole angle could be found between the *er-105* null-allele and its parental line Columbia-0 (*Col-0*) and between *er-104* loss-of-function allele and Wassileskija (*Ws*), although the typical architectural traits attributed to *er* were noticed in these lines (Figure 7.9d-g; Figure 7.10). Several other *er* alleles, isolated in the *Col-0* background (Lease *et al.*, 2001) also showed the significantly reduced initial angle (Figure 7.11a), suggesting that ER mediated control of initial petiole angles is not specific for the Landsberg background and appears allele specific.

No significant differences in absolute angles after 6 h ethylene (Figure 7.8b) or low light (Figure 7.8c) treatment were found between *er* alleles, *ER-Ler* and their respective wild-types, which is in accordance with the observations made on LCN2-7 (Figure 7.7f, g). A notable exception was *er-105* after low light treatment, which had a significantly reduced angle compared to *Col-0* (Figure 7.8c). Moreover, in the broader set of *er* alleles in the *Col-0* background several alleles showed a significantly reduced absolute petiole angle after 6 h of ethylene treatment (Figure 7.11b, c).

The response angles after 6 h of ethylene treatment revealed without exception, that lines carrying functional ER are able to respond stronger to ethylene (Figure 7.7d, Figure 7.8d, 7.11c). Yet, the response to low light was not affected by *er* (Figure 7.7e, Figure 7.8e). These results were confirmed by analysis of the pair wise corrected

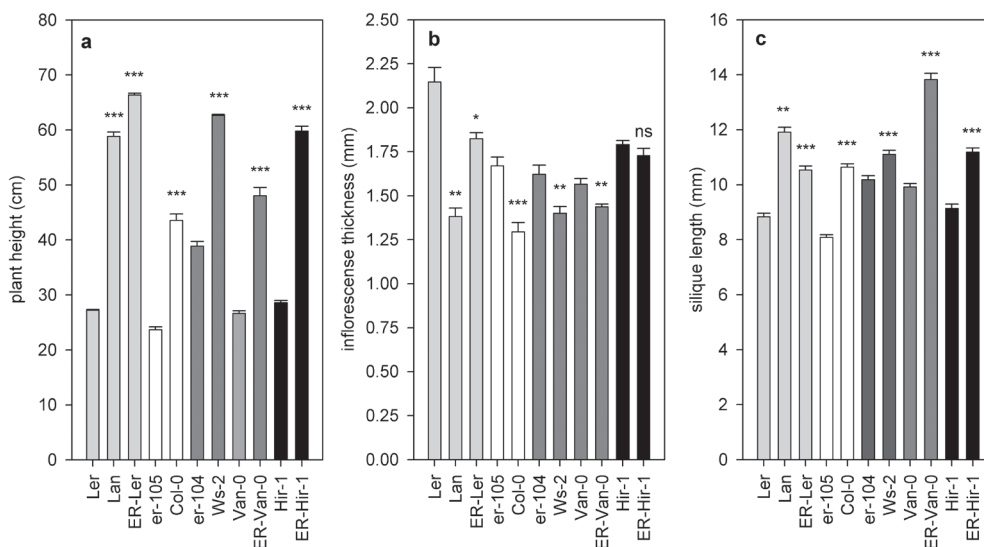


Figure 7.10: Effects of ER on plant architecture. a: plant height, b: inflorescence stem thickness and c: silique length of *er* mutants, *erecta* mutant accessions, corresponding wild types and *ERECTA* (*ER*) complemented transgenic lines. Error bars represent SE, n > 10. Significance levels: * $p < 0.05$; ** $p < 0.01$; *** $p < 0.001$; 2-tailed Student's T-test.

response kinetics. Lan-0 exhibited a stronger response to ethylene throughout the experimental period than Ler (Figure 7.12a), and the ER-Ler response was similar to Lan-0 (Figure 7.12c). In agreement, *er-105* had an attenuated response to ethylene compared to Col-0 (Figure 7.12e). However, kinetic analysis did not reveal any differences between *er-104* and *Ws-2* (Figure 7.12f). In response to low light, Lan-0 was indistinguishable from Ler (Figure 7.12b), whereas ER-Ler did show an enhanced response (Figure 7.12d). Similarly, the response of *er-105* was slightly attenuated compared to Col-0 (Figure 7.12f). *Er-104* however, showed an indistinguishable response low light compared to *Ws-2* (Figure 7.12h).

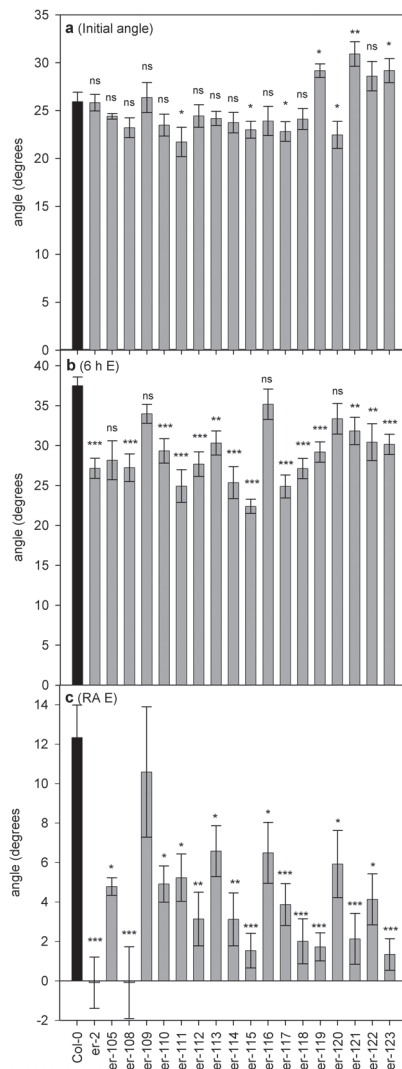


Figure 7.11: Effects of ER on initial petiole angles and induced hyponastic growth of *er*-alleles in Col-0. a: Initial angles (t=0 h) before treatment. b: absolute angles and c: response angles of 6 h exposure to ethylene ($5 \mu\text{l l}^{-1}$) of *erecta* mutants in the Col-0 genetic background. Col-0 wild type is shown as a black bar. Error bars represent SE; $n \geq 4$. Significance levels; * $p < 0.05$; ** $p < 0.01$; *** $p < 0.001$; ns = non significant; 2-tailed Student's T-test.

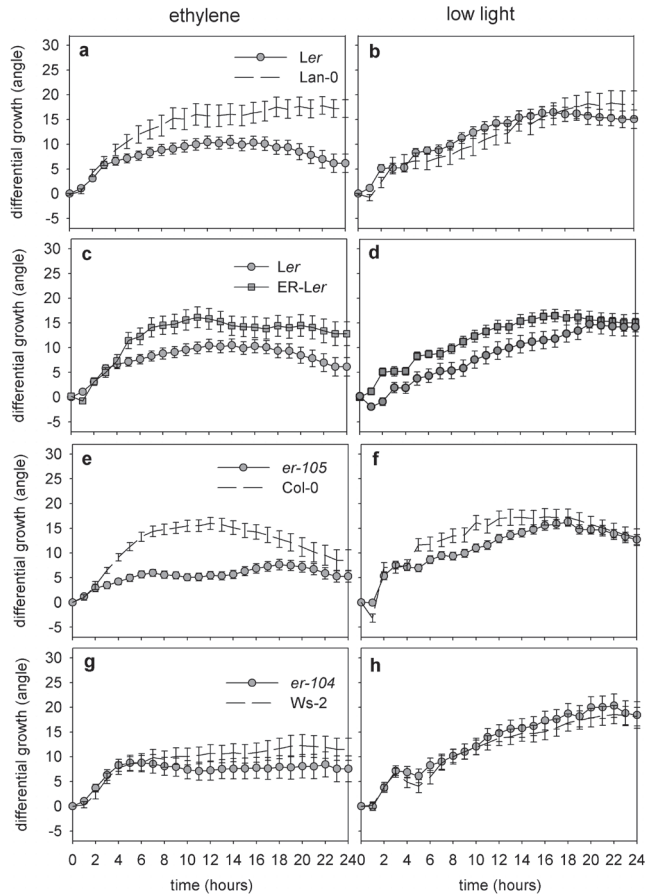


Figure 7.12: ER mediated effects on kinetics of ethylene- and low light-induced hyponastic growth. a,c,e,g: Effect of exposure to ethylene ($5 \mu\text{l l}^{-1}$) and b,d,f,h: low light ($200 \mu\text{mol m}^{-2} \text{s}^{-1}$ to $20 \mu\text{mol m}^{-2} \text{s}^{-1}$) right column on petiole angles of *erecta* mutants (circles), corresponding wild types (dashed lines) and ER-Ler complemented transgenic line (squares). Values are pair wise subtracted. Error bars represent SE; $n \geq 12$.

Next to induced mutations in *er*, at least two natural occurring accessions carry a malfunctioning *er* allele, as shown by allelism tests (Koornneef *et al.*, 2004; Van Zanten *et al.*, 2009b). Indeed, these lines; Hiroshima-1 (Hir-1) and Vancouver-0 (Van-0), had a relatively mild response to ethylene (Figure 7.1a; Van-0 ranked as third weakest responder to ethylene and Hir-1 as 43rd; Ler is 33rd). Moreover, these accessions grouped together with the induced *er* mutations in a randomly selected set of natural accessions with respect to plant height (Supporting Information Figure S7.1). We complemented Hir-1 and Van-0 with the Col-0 ER allele. This restored the typical *er* associated architectural features (Figure 7.9h-k, Figure 7.10) and the ability to induce hyponastic growth upon ethylene treatment (Figure 7.13a, c). Moreover, a mild increased response to low light was observed in Van-0 (Figure 7.13b).

To test if ER is part of the low light signaling route towards hyponastic growth, we transformed the *phyb5 cry2* mutant in the Ler genetic background (Mazzella *et al.*, 2001) with Col-0 ER. This complementation did not restore the ability of *phyb5 cry2*

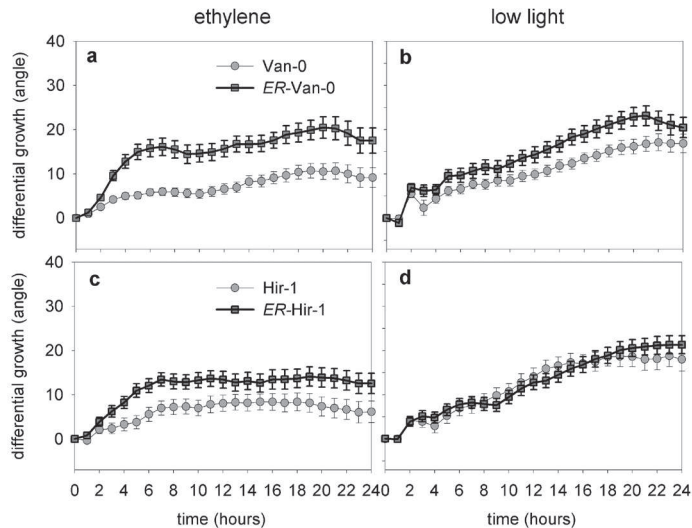


Figure 7.13: Effects of complementation of natural *er* mutant accessions on hyponastic growth. a,c: Effect of exposure to ethylene ($5 \mu\text{l l}^{-1}$) and b,d: low light ($200 \mu\text{mol m}^{-2} \text{s}^{-1}$ to $20 \mu\text{mol m}^{-2} \text{s}^{-1}$) on petiole angles of *erecta* mutant accessions (circles) and *ERECTA* (*ER*) complemented transgenic lines (squares). Values are pair wise subtracted. Error bars represent SE; $n \geq 12$.

to induce hyponastic growth to ethylene nor low light conditions (Figure 7.14a, b). *Phyb cry2* plants have a typical constitutive shade avoidance phenotype, reflected by severely elongated organs, including inflorescence length and siliques length and thin inflorescences (Figure 7.14c-e). Complementation with *ER* had a significant additional effect on these parameters (Figure 7.14c-e). This suggests that *ER* is not an integral part of (low) light signaling.

Taken together, *ERECTA* positively affects initial petiole angle and induced hyponastic growth to both ethylene and low light treatment and likely explains the *EA2* and near-significant *LLTRA* QTLs. Yet, the penetration of the *er* effects are highly dependent on the genetic background and are allele specific. Moreover, *ER* mediated responses to low light occurs independent of phytochrome B and Cryptochrome-2 signaling with respect to hyponastic growth.

Enhanced ethylene production in *Ler* is not controlled by *ERECTA*

It is possible that the observed *er* effects on initial petiole angle and on hyponastic growth are due to indirect effects of *er* on ethylene production or sensitivity. Transcription of several genes encoding early ethylene signal transduction components, as well as of catalytic enzymes in the ethylene biosynthesis route are up-regulated in the presence ethylene (Wilkinson *et al.*, 1995; Hua *et al.*, 1998; Vriezen *et al.*, 1999; Millenaar *et al.*, 2005; 2006; Chapter 2). We compared relative expression data of several ethylene signaling- and biosynthesis genes obtained using microarrays that were hybridized with *Ler* and *Lan-0* derived cDNA from aerial parts of 7 d old plants (Snoek, 2009) and of *Col-0* petioles treated 3 h with air control or ethylene (Millenaar *et al.*, 2006). Indeed, several ethylene-signaling genes were significantly up-regulated in ethylene treated petioles as compared to air control (Figure 7.15a; Millenaar *et al.*, 2006). The same genes were not significantly differentially expressed between *Lan-0* and *Ler*. The only exception was *ERS1* ($p=0.036$) (Figure 7.15c), which

has a slightly higher expression in Lan-0 compared to Ler.

In contrast, several ethylene inducible (Figure 7.15c) ACC-oxidase-family ethylene biosynthesis genes were significantly transcriptionally induced in Ler compared to Lan-0 (Figure 7.15d). In agreement, ethylene release from Ler was significantly ($p < 0.001$) higher than Lan-0 (Figure 7.16a). However, the ER complemented (ER-Ler) line, released ethylene to a similar extent as Ler, thus, significantly ($p < 0.001$) more than Lan-0, suggesting that ER does not control ethylene production, but that an ER independent polymorphism, segregating between Ler and Lan-0 controls the enhanced ethylene production in Ler. In agreement, ethylene release of *er-104* and *er-105* were indifferent from their respective wild-types (Figure 7.16a).

Moderate and high ethylene concentrations inhibit cell elongation of hypocotyls in etiolated seedlings, whereas low and ambient concentrations ethylene stimulates hypocotyl elongation. We used this trait to generate ethylene dose response curves (triple response assay) to assess ethylene sensitivity (Guzman & Ecker, 1990; Hua & Meyerowitz, 1998; Pierik *et al.*, 2006). No differences in ethylene sensitivity were found between Lan-0 and Ler and between Col-0 and *er-105* (Figure 7.16b, c). In contrast, *er-104* showed increased hypocotyl length in the low-range of ethylene as well as at higher ethylene concentrations (Figure 7.16d). This suggests that *er-104* is more sensitive in the low-range (stronger growth induction) and less sensitive in the

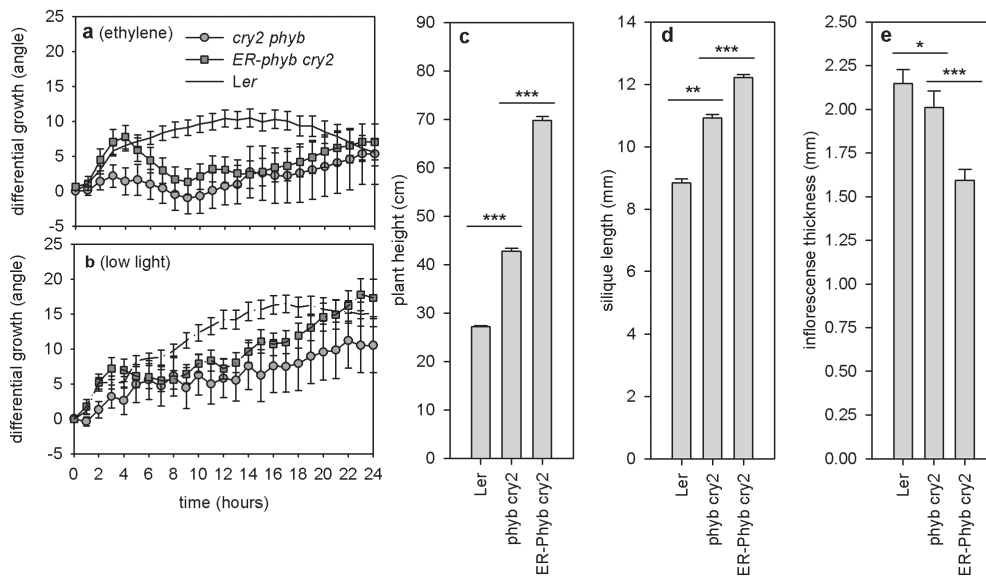


Figure 7.14: Effects of ER on light signaling. a: Effect of exposure to ethylene ($5 \mu\text{l l}^{-1}$) and b: low light ($200 \mu\text{mol m}^{-2} \text{s}^{-1}$ to $20 \mu\text{mol m}^{-2} \text{s}^{-1}$) on petiole angles of *phyb5 cry2* (circles) and ER complemented transgenic ER-*phyb5 cry2* lines (squares), compared to Ler (dashed lines). Values are pair wise subtracted. Error bars represent SE; $n \geq 14$: c: plant height, d: inflorescence stem thickness and e: silique length of Ler, *phyb5 cry2* and ER-*phyb5 cry2*. Error bars represent SE; $n \geq 8$. * $p < 0.05$; ** $p < 0.01$; *** $p < 0.001$; 2-tailed Student's T-test.

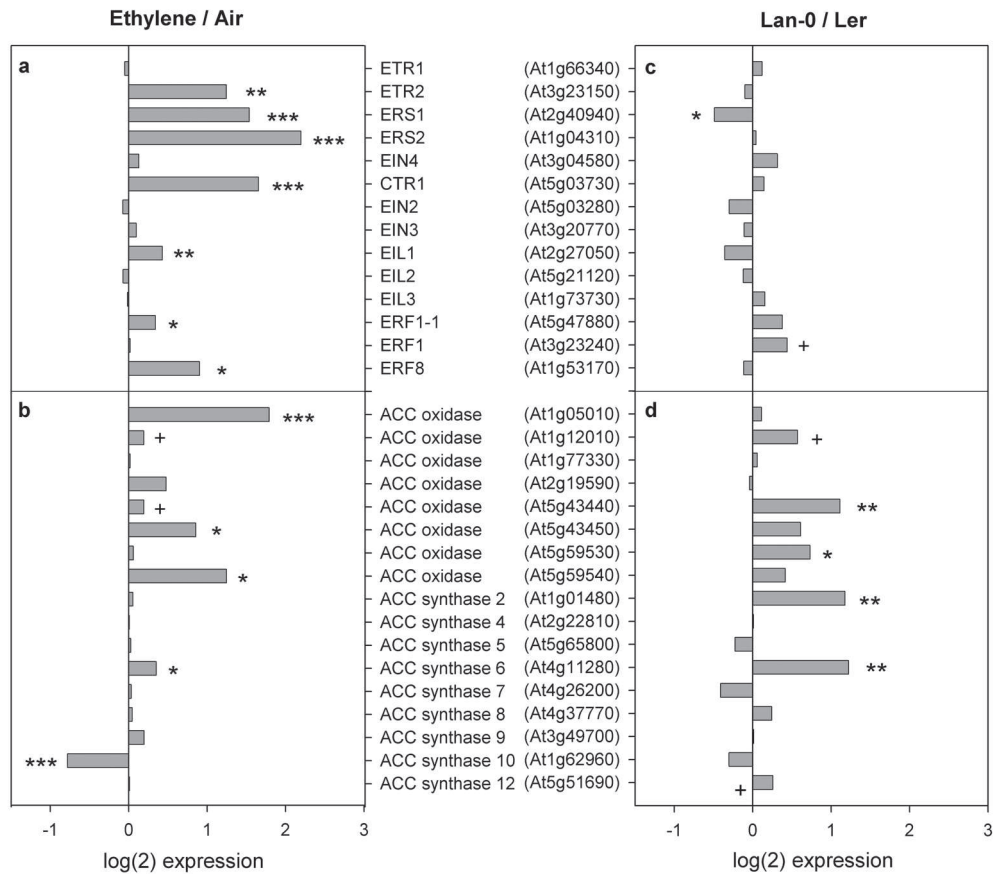


Figure 7.15: Effects of ER on gene transcription of ethylene-related genes. Expression ratio of a,c: ethylene signaling genes and b,d: ethylene biosynthesis genes (AGI codes of the genes used are shown between brackets) between plants treated with a,b: ethylene (5 μ l l⁻¹) compared to air control (ATH1 Affymetrix microarrays, procedures are described in Millenaar *et al.* (2006)) and c,d: Lan-0 compared to Ler (CATMA spotted arrays, procedures are described in Snoek, (2009)). Depicted are Log(2) values of the ratio obtained by dividing raw arbitrary expression data of the respective micro-arrays. Significance levels are a,b: determined by a 2-tailed Student's T-test and c,d: adjusted *p* values; +*p*<0.1; **p*<0.05; ***p*<0.01; ****p*< 0.001.

Together, these data indicates that ER does not control ethylene production and does not have a consistent effect on ethylene sensitivity. It is therefore unlikely that ER-mediated control of ethylene production or sensitivity can explain *er* effects on initial petiole angles and hyponastic growth phenotypes.

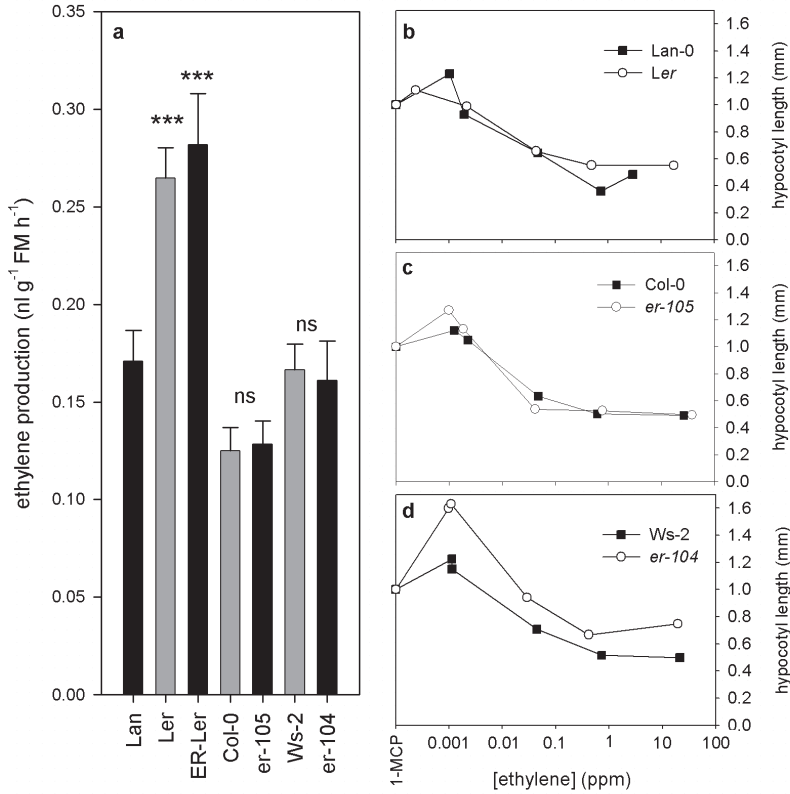


Figure 7.16: Effects of ER on ethylene production and sensitivity. a: Ethylene release (nl g⁻¹ FM h⁻¹) of *erecta* mutants and corresponding wild-types. Significance: *** $p < 0.001$; 2-tailed Student's T-test. Error bars represent SE, $n \geq 14$ samples of three pooled plants each. b-d: Ethylene dose-response curves of hypocotyl growth in etiolated *erecta* mutant- (white circles) and wild type (black squares) seedlings. 1-MCP indicates plants in which ethylene perception was pharmacologically blocked. $n \geq 8$.

Discussion

Natural variation in petiole angles and hyponastic growth

Leaf positioning is considered adaptive for optimization of light-capture, water use efficiency and against heat damage. In nature, constitutive variation in leaf angles is therefore found in many species (King, 1997; Falster & Westoby, 2003 and references within). A study on 21 *Arabidopsis* accessions revealed a latitudinal cline in leaf angles, with accessions from low (Southern) latitudes having more inclined leaves than more Northern occurring accessions (Hopkins *et al.*, 2008). Accordingly, we report considerable natural variation in petiole angles among *Arabidopsis thaliana* accessions. In addition, we present considerable variation in induced leaf repositioning (hyponastic growth) upon ethylene, low light and heat treatment.

In apparent discrepancy with Hopkins *et al.* (2008), this and previous work did not reveal a correlation between geographic parameters and initial petiole angle nor with differential petiole growth driven leaf movement, after treatment with ethylene, low light or heat (Millenaar *et al.*, 2005; Edwards *et al.*, 2005; Chapter 3). Hopkins *et al.* (2008) measured leaf-tip angle instead of the petiole angle used in this study. Control of leaf-tip angle and of petiole angles is spatially separated and the responses of both organs differ depending on the inducing factor (Snoek, 2009). Moreover, the accessions used were collected from diverse environments (Koornneef *et al.*, 2004). When grown in controlled conditions, observed phenotypes likely reflect the difference between the natural environment to which the accessions have adapted and the growth-chamber conditions. Differences in growth regimes may therefore influence these traits.

Various intra-specific correlations were identified between accessions for petiole angle traits before and after treatment with ethylene, low light or heat. Our data indicated that initial petiole angles determine the petiole angle after treatment. However, initial petiole angle does not restrict the ability to respond to different treatments. In general, the extent with which an accession responds to a given treatment depends on the accession, rather than on the inducing factor. It is therefore plausible to assume that the plant may utilize the same genetic components to functionally induce hyponastic growth. Natural genetic variation in downstream components may control the ability of individual accessions to induce differential petiole growth. Yet, the available data suggests that at least upstream, the signaling pathways of the hyponastic growth inducing factors are parallel. For example, low light-induced hyponastic growth is independent of ethylene (Millenaar *et al.*, 2009, Chapter 2) and a combined ethylene and low light treatment induced a hyponastic response that is identical to the response induced by either treatment alone (Millenaar *et al.*, 2005). In contrast, ethylene is a positive modulator of heat-induced hyponastic growth (Chapter 3). Similarly, the phytohormone ABA is a negative regulator of ethylene-induced hyponastic growth (Benschop *et al.*, 2007) and a positive modulator of heat- and low light-induced hyponastic growth (Millenaar *et al.*, 2009; Chapter 3, 4). Auxin controls low light- and heat-induced hyponasty but does not play a role in ethylene-induced hyponastic growth (Millenaar *et al.*, 2009; Van Zanten *et al.*, 2009a; Chapter 2, 3). These results, however, do not exclude merging of the pathways downstream of the observed phytohormonal regulation. Potential candidate genes for a hypothetical shared signaling route have been isolated by a forward genetic approach (Chapter 5, 6). These candidate loci are currently under investigation in our lab.

Quantitative genetic analysis of initial petiole angle control and induced hyponastic growth

Several QTLs were mapped for initial petiole angle and for different aspects of induced hyponastic growth. The notion that several QTLs co-located strengthens the idea that different inducing environments may employ the same genetic components to induce hyponastic growth.

Until present, only few loci have been empirically shown to control leaf movement

in *Arabidopsis thaliana*. Probably best understood in this respect are circadian clock controlled diurnal leaf movements (Millar *et al.*, 1991). Because extensive natural variation has been observed in circadian/diurnal leaf movements among *Arabidopsis* accessions (Swarup *et al.*, 1999; Edwards *et al.*, 2005), it is highly likely that part of the observed variation in initial petiole angles and in induced hyponastic growth phenotypes among the accessions and RILs assessed in this study, are in fact due to circadian effects on petiole angle. In agreement, several previously identified QTLs for circadian leaf movement co-located with QTLs in this study. These include *6hHT5/HTA5*, *6hLL1-1/6hHT1-1* and *EA2/6hLL2* (Swarup *et al.*, 1999). Notably, the *6hLL1-1/6hHT1-1* locus was also identified in more dedicated QTL studies for light control of cotyledon movement (Tseng *et al.*, 2004) and temperature compensation of leaf movement (Edwards *et al.*, 2005). The circadian clock controlled *GIGANTEA* (*GI*) gene, which segregates between *Ler* and *Cvi-0*, was isolated as causal gene in these studies. It is therefore likely that *GI* also explains the *6hLL1-1* and *6hHT1-1* QTLs for absolute petiole angle after low light and heat treatment.

Alleles of the photoreceptor proteins *phyB* and *cry2* also segregate between *Ler* and *Cvi-0*, and explained QTLs for light control of both flowering time and hypocotyl length (El-Assal *et al.*, 2001; Borevitz *et al.*, 2002; Filiault *et al.*, 2008). These proteins control low light and heat-induced hyponastic growth (Millenaar *et al.*, 2009; Chapter 2, Chapter 3; Figure 7.14) and probably ethylene-induced hyponastic growth (Chapter 3; Figure 7.14). The *Cry2* locus is within the QTL interval of *6hE1* and *LLRA1*, and may contribute to these QTLs. The *phyB* locus is located upstream of the *Erecta* locus at 35 cM from the top of the chromosome. No QTLs were identified in this region. Therefore, segregating variation in *phyB* is not likely to contribute significantly to the petiole angle QTLs in this study.

A confounding feature of quantitative genetic studies such as linkage disequilibrium- and association mapping, using large sets of natural occurring accessions, are spurious genotype x environment correlations due to population structure (Nordborg *et al.*, 2005; Nordborg & Weigel, 2008). *Vice versa*, LOD intervals of QTLs mapped in RIL populations based on accessions from divergent populations, such as the here used population derived from Polish Landsberg *erecta* and *Cvi-0* from Cape Verde Islands, often contains many DNA polymorphisms unrelated to the mapped trait. Notably, in the broad screen of accessions, those with in general the strongest (NG) and weakest (Kyoto) hyponastic growth response, both originate from Japan. Therefore, constructing RIL populations based on these accessions would bring additional advantages to the isolation of genetic components involved in the control of petiole angles and hyponastic growth.

***ERECTA* controls ethylene- and low light-induced hyponastic growth**

The *Erecta* locus, encoding a leucine-rich repeat receptor-like Ser/Thr kinase (*ER*), was isolated in several quantitative genetic studies for growth related traits (Van Zanten *et al.*, 2009b), including plant height and leaf morphology (Alonso-Blanco *et al.*, 1999; Pérez-Pérez *et al.*, 2002; Ungerer *et al.*, 2002; El-Lithy *et al.*, 2004), hormone and light responses (Borevitz *et al.*, 2002), resistance to pathogen attack (Godiard *et al.*, 2003;

Llorente *et al.*, 2005), transpiration efficiency (Masle *et al.*, 2005) and epidermal leaf cell size (Tisné *et al.*, 2008).

Detailed analysis of the co-locating *EA2/6hLL2* QTLs using NILs, induced mutants in various genetic backgrounds and complemented natural *er* accessions, all indicated that ER controls ethylene-induced hyponastic growth. Although, ER explains a minor circadian leaf movement QTL (Swarup *et al.*, 1999), circadian clock associated leaf movement does not account for *EA2/6hLL* QTLs, since calculation of pair wise subtracted leaf angles, to correct for circadian movements (Benschop *et al.*, 2007), showed a clear remaining effect of ethylene. Moreover, ER control of petiole angles is not a consequence of modulation of ethylene sensitivity or production. Besides ethylene-induced hyponastic growth, ER also controls initial petiole angle. Yet, in the vicinity of the *Erecta* locus more segregating loci modulating initial petiole angles are to be found, as NIL2-7 (with the Cvi-0 ER allele) has a initial angle that was even lower than *Ler*.

The role of ER in low light-induced hyponastic growth was less pronounced than in ethylene-induced hyponasty. NIL analysis failed to confirm the *6hLL* QTL and introduction of functional ER in the *cry2 phyB* mutant in the *Ler* genetic background could not restore low light-induced hyponastic growth. Moreover, other typical ER associated phenotypes including plant height were enhanced by introducing the Col-0 ER allele, despite that this line already exhibits an elongated phenotype due to the constitutive shade avoiding appearance (Mazella *et al.*, 2001). This suggests that *phyB* and *cry2* control of hyponastic growth and plant architecture does not require ER. Overall, These results are in agreement with the results of Millenaar *et al.* (2005) showing that *Ler* typically has a mild response to ethylene but is well able to induce hyponastic growth to low light intensities.

Nevertheless, mutant *er* did result in decreased low light-induced hyponastic growth in the Col-0 background (*er-105*) and the reverse was observed in *Ler* and Van-0 plants complemented with the Col-0 ER allele. Previously, it was shown that effects of *er* on plant development are weaker/masked in Col-0 *er* mutants compared to *Ler* and that enhanced disease susceptibility against *P. cucumerina*, typically attributed to the *er* mutation in *Ler*, was not detected in the natural *er* accession Van-0 (Llorente *et al.* 2005). Similarly, in sharp contrast to the *er* effects on ethylene-induced hyponastic growth in Col-0, *Ler*, Van-0 and Hir-1, we observed no *er* effects on ethylene-induced hyponastic growth in the strong *er-104* allele (Torii *et al.*, 1996). The trait specific variation in penetration level of *er* phenotypes between genetic backgrounds may be explained by ER mediated effects on genetic canalization/buffering (Hall *et al.*, 2007). Genetic canalization is a process that makes developmental pathways relatively insensitive for environmental 'noise'. As a result of canalization, organisms have stereotyped phenotypes in a range of (micro) environments (Waddington, 1942; Hornstein & Shomron, 2006). In particular, ER affected canalization of rosette leaf number (flowering time) in long day conditions, without interfering with the phenotypic mean (Hall *et al.*, 2007). This observation was confirmed by increased canalization of this trait in *er-105*. In this study, ER promotes, rather than buffers,

the effect of (micro) environmental fluctuation on phenotypic variation in leaf number. One of the consequences of canalization of a developmental pathway is that accumulated polymorphisms do not necessarily lead to phenotypic variation (Waddington, 1942; Hornstein & Shomron, 2006; Hall *et al.*, 2007). Therefore, it is possible that the genetic variation controlling low light-induced hyponastic growth in Lan-0, Ws and Hir-1 is masked by ER through canalization (or vice versa revealed by *er*, in Col-0 and Van-0). Perhaps similar mechanisms would explain why the strong *er-104* allele did not show altered responses to ethylene compared to wild type and why ER mediated control of initial angles was observed between *Ler* and Lan-0/ *ER-Ler* and not between *er-104* and Ws and was allele specific in several Col-0 *er* alleles. Canalization of other typical ER-mediated developmental traits, among others plant height, root- and hypocotyl length, were not affected by ER (Hall *et al.*, 2007; Sangster *et al.*, 2008), suggesting that the canalization potential is trait specific rather than general. Accordingly, in our study all lines carrying a functional ER allele showed increased plant height, excluding genetic background effects.

Only limited data is published on the mechanism of direct ER action. Similarly, ER binding ligands have not yet been isolated. We recently re-analyzed *trans* gene transcription regulation at the *Erecta* locus (Van Zanten *et al.*, 2009a) from a genetical genomics experiment (eQTLs) by Keurentjes *et al.* (2007). Gene Ontology (GO) analysis of these genes revealed overrepresentation of several phytohormone and abiotic environment associated classes (a.o. response to; abscisic acid stimulus, auxin stimulus, ethylene stimulus; wounding; heat), indicating that those GO classes are potentially mediated by ER. *ERECTA* is also required for reducing plant sensitivity to heat stress during adaxial–abaxial polarity formation in leaves and promotes leaf adaxial cell-fate specification (Qi *et al.*, 2004; Xu *et al.*, 2003). In Chapter 1 we described that it is the difference in elongation response of cells at the adaxial opposed to the abaxial side of the petiole that drives hyponastic growth. Heat dependent defects in leaf polarity are however only expressed in *asymmetric leaves-1* (*as1*) and/or *as2* mutants, which might be the reason that we did not identify QTLs for heat-induced hyponastic growth upon heat treatment.

It may not be only coincidence that ER is indirectly associated to such factors, also known to control hyponastic growth (Millenaar *et al.*, 2005, 2009; Benschop *et al.*, 2007; Chapter 2-4). Yet, if, and how ER exerts control on hyponastic growth by modulation one or more of these pathways remains to be studied.

Materials and Methods

Plant material and growth conditions

The origin of all accessions used in this study is described in Table S7.1. The *Ler* x *Cvi-0* recombinant inbred line population (Nottingham Arabidopsis Stock Center no. N22000; Alonso-Blanco *et al.*, 1998a), NIL LCN2-7 (Keurentjes *et al.*, 2007) and Lan-0 (N1298) were a gift from M. Koornneef (Wageningen UR; the Netherlands). *er-104* (Ws), *er-105* (Col) were a gift of Keiko U. Torii (University of Washington, Seattle, USA). *er2* (N3401); *er-108* to *er-123* (N3912-N3927; Lease *et al.*, 2001) were obtained from NASC. *phyB5 cry2* (Mazzella *et al.*, 2001) was a gift from J.J. Casal (University of Buenos Aires, Argentina). The Generated F1 crosses between *Ler* and *Cvi-0* were checked with the SSLP markers polymorphic between *Ler* and *Cvi-0*; NGA128 and NGA162 (Bell & Ecker, 1994) with a standard PCR procedure.

Plants were grown on a mixture of fertilized potting soil and perlite (1:2) as described in Millenaar *et al.* (2005), in: 20°C, 70% (v/v) relative humidity, 9 h short-day photoperiod: 200 $\mu\text{mol m}^{-2} \text{s}^{-1}$ photosynthetic active radiation (PAR). Pots were automatically daily saturated with tap water at the start of the photoperiod. Before potting, seeds were kept 4 days in dark at 4°C to synchronize germination. All plants, except the RILs, were used in developmental stage 3.8-3.9 according to Boyes *et al.* (2001). RILs were measured 25 days after germination which was just before the earliest flowering RILs started to bolt. Although the developmental stages of the RILs were variable due to the inherent mixed genetic make-up of the RIL lines, the extend of hyponastic growth response was robust until a few days after bolting (data not shown) and therefore not interfering with the measurements. In all cases, plants were transferred to an experimental setup, under growth-room conditions, one day prior to the treatment to allow acclimatization. All experiments started 1.5 h after the start of the light period to minimize variation which could be induced by circadian and diurnal rhythms (Salter *et al.*, 2003).

Experimental design

Accessions were selected randomly and grown in several batches, with all accession occurring in at least two separate batches. In total, data of 4 to 15 individuals per accessions, per treatment, were obtained with two petioles measured per plant. For QTL analysis of the ethylene and low light response, 156 individual RILs were used that were randomly divided in 4 groups containing approximately 50 RILs each and 10 RILs were overlapping between the experiments. All experiments were performed twice, on separate batches and in total data of 3 to 12 individuals per RIL line per treatment were obtained. For high temperature QTL analysis, 159 individual RIL lines were randomly selected and grown in several batches, with all individual RILs occurring in at least two separate batches. In total data of 4 to 15 individuals per RIL line were obtained. Means of the individual RILs were used for QTL mapping. The parental lines were measured on a regular basis along with the RILs.

Petiole angle and plant architecture measurements

Plants used for the fixed time-points measurement were manually photographed from the side. Angles were measured using the freeware algorithm; ImageJ; <http://rsb.info.nih.gov/ij>). For all replicate plants, two petioles were measured and the average value was used for further analysis. Outliers outside the 95% confidence interval per line, per treatment, were removed prior to further

analysis. Absolute petiole angles are defined as the angle between the horizontal and the petiole/lamina junction through the base of the petiole in the rosette center. Response petiole angles represent the calculated difference between initial absolute angle and absolute angle reached after 6 h treatment, on the same plants.

To measure petiole angle kinetics, a custom-built computerized digital camera system was used (Millenaar *et al.*, 2005, Cox *et al.*, 2003). To enable continuous photography, no dark period was included in the 24 h experimental period. Plants were placed singly in glass cuvettes with the petioles of study positioned perpendicular to the axis of the camera. Cuvettes were continuously flushed with air (or ethylene if indicated) at a flow rate of 75 l h⁻¹. To facilitate the measurements, any leaf that was obscuring the petiole being photographed was removed. Additionally, the petiole was marked at the petiole/lamina junction with orange paint (Decofin Universal, Apeldoorn, the Netherlands). These preparations did not influence the response of the petiole (data not shown). Digital photographs were taken every 10 min. The angles of the petioles were measured on these digital images using a PC-based image analysis system with a custom made macro using the KS400 (Version 3.0) software package (Carl Zeiss Vision, Germany). To correct for diurnal- and circadian effects on leaf movement (Millar *et al.*, 1991; Salter *et al.*, 2003; data not shown) values of response angles were pair wise subtracted in all cases (Benschop *et al.*, 2007). This was done by calculating the differences between the angles of treated and control plants for each time point. New standard errors for the differential responses were calculated by taking the square root from the summation of the two squared standard errors.

Plant height, stem thickness and silique lengths were measured when the last flower on the plant developed a silique. Plant height was measured from root/shoot junction to inflorescence top. Stem thickness was measured ~1 cm above the root/shoot junction with a caliper and silique lengths were measured from representative pedicles in the top ~10 cm of the main inflorescence stem.

Treatments

All experiments were conducted in growth cabinets (Snijders Scientific B.V, Tilburg, the Netherlands). Low light conditions consisted of a reduction of the light intensity by 90% from 200 $\mu\text{mol m}^{-2} \text{s}^{-1}$ to 15–20 $\mu\text{mol m}^{-2} \text{s}^{-1}$ (PAR) at the start of the experiment (Millenaar *et al.*, 2005). This was achieved by using a shade cloth that did not change the relative light spectral composition, which was checked with a Licor1800 spectroradiometer (Licor, Lincoln, Ne, USA).

Unless stated otherwise, ethylene application was as described in Millenaar *et al.* (2005). Pure ethylene (Hoek Loos BV, Schiedam, the Netherlands) and air (70% relative humidity) were mixed using flow meters and controllers (Brooks Instruments BV, the Netherlands) to generate a concentration of 5 $\mu\text{l l}^{-1}$ ethylene. This was flushed continuously through glass cuvettes containing the plants, with a flow rate of 75 l h⁻¹ and then vented away. For the accession experiments only, pure ethylene was flushed directly into the growth cabinet which generated a concentration of 1.5 $\mu\text{l l}^{-1}$. This concentration saturates the response (data not shown). Ethylene concentration were checked regularly on a gas chromatograph (GC955, Synspec, Groningen, the Netherlands), and remained constant for the duration of the experiment.

Heat treatment (increase from 20°C to 38°C) was accomplished by moderating the program of the used growth cabinet. A temperature of 30°C was reached after ~22 min; 38°C was reached after ~45 minutes.

Data analysis

Frequency distribution of trait-values for QTL analysis was, or came close to a Gaussian distribution (data not shown) and trait values were used in the analyses without mathematical transformation. The genetic map for the *Ler* x *Cvi* RIL population was obtained from the NATURAL website (<http://www.dpw.wau.nl/natural/>). The core maps were used for initial QTL mapping. For fine mapping the available markers were added up to 1 per cM. QTLs were calculated by Composite Interval Mapping (CIM) using the free-ware program QTL Cartographer (Wang *et al.* (2007); <http://statgen.ncsu.edu/qtlcart/WQTLCart.htm>) with a forward and backward regression method and a window size of 7 cM (E+LL) or 10 cM (HT). Genome-wide Likelihood of Odds thresholds (LOD; Van Ooijen, 1999) per trait were estimated in QTL Cartographer using 1000 permutations. QTLs were considered co-locating when the LOD-peaks of individual QTLs from different treatments or traits were 10 cM or less.

Broad sense heritability (BSH) was calculated as part of the between-line variance attributed to the total variance, using variance components of the general linear model procedure Type III ANOVA in SPSS software (12.0.1, SPSS, Chicago, IL, USA), and Excel 2003 (Microsoft, Richmond, VA, USA). Bivariate linear regressions correlation coefficients are Pearson (*P*) 2-tailed and were calculated using a general linear model in SPSS. Statistical comparisons between two lines or treatments were performed by 2-tailed Student's *T*-test (Excel).

Plant transformation

The pKUT196 plasmid vector (Torii *et al.*, 1996) containing the functional Columbia-0 *Erecta* locus, including promoter and terminator was a kind gift of Keiko U. Torii (University of Washington, Seattle, USA). This vector was transformed by electroporation to *Agrobacterium tumefaciens* strain C58C1 (pMP90). Recombinant bacteria were selected using 50 mg/ml spectinomycin (Duchefa; Brussels, Belgium) and the presence of the vector was checked by PCR (not shown). Subsequently plants were transformed by floral-dipping (Clough & Bent, 1998). Selection of T_1 plants was performed on selective agar-plates containing 4 g l⁻¹ plant-agar (Duchefa), 0.22 g l⁻¹ Murahige-Skoog (Duchefa) and 70 mg ml⁻¹ Gentamycin (Duchefa). Gentamycin-resistant T_1 plants were transferred to standard soil and all exhibited the typical ER-associated tall-plant height phenotype. Single seed descendents of the T_1 were re-selected in the T_2 and T_3 generation on gentamycin agar-plates to identify homozygous T_3 lines.

Ethylene release measurements and triple response assays

Ethylene release from rosettes was performed 1.5±1 h after start of the photoperiod. Measurements were as described in Millenaar *et al.* (2005) and Chapter 2-4. Whole rosettes of about 300 mg were placed in a syringe with a volume of 1.5 ml. Ethylene was allowed to accumulate in the syringe for 15-20 min, after which the air was analyzed on a gas chromatograph (GC955, Synspec). This short time frame prevented wound-induced ethylene production, which started to accumulate only after 20 min (data not shown).

For the triple response assay, sterile seeds were placed on half-strength MS-agar-plates containing 4 g l⁻¹ plant-agar (Duchefa), 0.22 g l⁻¹ Murahige-Skoog (Duchefa), placed in air-tight jars and kept 4 days at 4°C in dark. Thereafter, the plates were transferred to 200 µmol m⁻² s⁻¹ light for 6 h. Ethylene was diluted in a dilution series starting from pure ethylene (Hoek Loos BV, Schiedam, the Netherlands) and injected using a syringe, before the jars were packed in aluminium-foil and

left in dark for 5 days at 20°C. After 5 days plants ethylene concentrations were measured using a gas chromatograph (GC955, Synspec) before the plants were photographed. Hypocotyl lengths were measured using ImageJ software. To allow comparison, values were normalized relative to plants in which ethylene perception was blocked by injecting 1 $\mu\text{l l}^{-1}$ 1-methylcyclopropene (1-MCP; 'Ethylbloc' Floralife, Waltherboro SC, USA).

Acknowledgements

We thank Keiko U. Torii (Washington University, Seattle, USA), M. Koornneef and J.J. Keurentjes (Wageningen University, the Netherlands) and J.J. Casal (University of Buenos Aires, Argentina) for kindly sharing plant materials.

Supporting information

- **Figure S7.1** Plant height of several *Arabidopsis thaliana* accessions, natural *er* accessions and induced *er* mutations.
- **Table S7.1** Accessions used in this study.

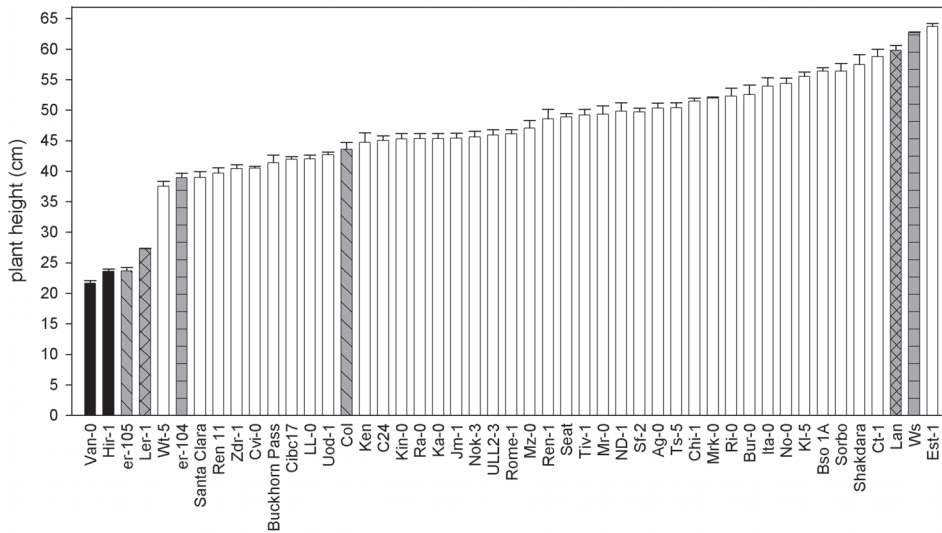


Figure S7.1: Analysis of plant height in accessions and induced *er* mutants. Plant height was measured from root/shoot junction to inflorescence top, and sorted from short to tall of several natural *Arabidopsis thaliana* accessions (white bars), including the natural *er* accessions Van-0 and Hir-1 (black bars) and artificially induced mutations and their wild types (grey bars), *er*-105 and Col-0 (dashed bars), *er*-104 and Ws-2 (horizontal dashed bars), Ler and Lan-0 (hived bars). Error bars represent SE; $n > 10$.

Table S7.1: Accessions used in this study. Names, origin (country), population, altitude (Alt; m), longitude (Long; N=north), latitude (Lat; E= east, W=west) origin and stock center identification numbers of *Arabidopsis thaliana* accession germplasms used in this study.

Accession	Country	Population/region	Alt. ^a	Lat. ^a	Long. ^a	Data from ^b	Stock IDs ^c
Ag-0	France	Argentat	100-200	N45.06	E1.56	INRA	N22630 N901
Akita	Japan	Akita Pref.		N39.43	E40.06	INRA	JW124
An-1	Belgium	Antwerpen; Botanical gardens	1-100	N51.13	E4.25	INRA	N22626 N944
Bay-0	Germany	Bayreuth	300-400	N49.57	E11.35	INRA	N22633 N954
Be-0	Germany	Bensheim-0	100-200	N49.41	E8.37	INRA	N964
Berkeley	USA	Berkeley (CA)		N37.51	E22.15	INRA	N8068
Bil-5	Sweden	Billaberget (Harnosand Area)		N63.19	E18.29	Nordborg	N22578
Bil-7	Sweden	Billaberget (Harnosand Area)		N63.19	E18.29	Nordborg	N22579
Bor-1	Czech Republic	Borky		N49.12	E16.37	Nordborg	N22590
Bor-4	Czech Republic	Borky		N49.12	E16.37	Nordborg	N22591
Br-0	Czech Republic	Brno (Brunn)	100-200	N49.12	E16.37	INRA	N22628 N994
BSO-1a PHW-34	France	Bretigny Sur Orge		N48.36	E2.19	Estimated	N6094
Buckhorn Pass	USA	Buckhorn Pass, Trinity mountains (CA)		N45.75	E20	INRA	N8067
Bur-0	Ireland	Burren	1-100	N53.07	W9.04	INRA	N22656 N1028
C24	Portugal	C24 / Coimbra	100-200	N40.12	W8.25	Nordborg	N22620 N906
cal-0	England	Calver		N53.10	W1.35	Lempe	N1062 N1063
Can-0	Canary Islands	Las Palmas / Mirador	1200-1300	N28.00	W15.30	INRA	N1064
Cerveteri	Italy (Mid/North)	Cerveteri		N42.00	E12.06	El-Lithy	N22523
Chi-1	Russia	Chisdra	100-200	N54.00	E35.00	INRA	N1074
CIBC-17	England	Ascot		N51.25	E0.41	Nordborg	N22603
CIBC-5	England	Ascot		N51.25	E0.41	Nordborg	N22602
Col-0	Poland	Poland Gorzow Wielkopolski (Landsberg/Warthe)		N52,44	E15,15	INRA	N22625 N1092
CS22491	Russia	Konchezero		N61.31	E34.15	Nordborg	N22621
Ct-1	Italy (Sicily))	Catania	1-100	N37.7	E15.06	INRA	N22639 N1094
Cvi-0	Cape Verde Islands	Cape Verde Islands	1200	N16	W24	INRA	N22614 N902
Daejeon	Korea	Daejeon		N36,15	E127.2	Estimated	
Di-G	France	Dijon	400	N48.00	E5.00	Michael	N910
dra-0	Czech Republic	Drahonin	400-500	N49.25	E16.16	INRA	N1116
Eden-1	Sweden	Eden (Harnosand Area)		N62.53	E18.11	Nordborg	N22572
Eden-2	Sweden	Eden (Harnosand Area)		N62.53	E18.11	Nordborg	N22573
Edi-0	Scotland	Edinburgh	1-100	N50.70	W3.13	INRA	N22657 N1122
Ei-2	Germany	Eifel	400-500	N50.15	E6.45	INRA	N22616 N1124
Es-0	Finland	Espoo	1-100	N60.13	E24.40	INRA	N1144

Est-1	Estland	Estonia		N58,30	E25,3	Nordborg	N22629	N1151
Fab-4	Sweden	Faberget (Harnosand Area)		N63.01	E18.19	Nordborg	N22577	
Fei-0	Portugal	St. Maria d. Feiria		N40	W6	Nordborg	N22645	
Fuk-1	Japan	Fukuyama	574	N34	E131	Michael	JW1116	
Ga-0	Germany	Gabelstein	100-200	N50.35	E8.00	INRA	N22634	N1180
Gd-1	Germany	Gudow	1-100	N53.33	E10.46	INRA	N1184	
Got-22	Germany	Göttingen		N51.32	E9.55	Nordborg	N22609	
Got-7	Germany	Göttingen		N51.32	E9.55	Nordborg	N22608	
Gu-0	Germany	Guckingen	100-200	N50.30	E8.00	INRA	N22617	N1212
Gy-0	France	La Miniere	1-100	N48.49	E2.06	INRA	N22631	N1216
Hel-1	Finland	Helsinki	1-100	N60.00	E25.00	INRA	N1222	
Hir-1	Japan	Hiroshima Fukuyama, Hiroshima Pref	1-100	N39.27	E133.22	INRA	N1674	
HR-10	England	HR		N51.25	E0.41	Nordborg	N22597	
HR-5	England	HR		N51.25	E0.41	Nordborg	N22596	
Ita-0	Morocco	Ibel Tazekka	1600-1700	N34.04	W4.12	INRA	N1244	
jm-1	Czech Republic	Jamolice	300-400	N49.04	E16.15	INRA	N1260	
Ka-0	Austria	Karinten	900-1000	N46.25	E14.31	INRA	N1266	
Kas-1	India	Kashmir	1500-1600	N34.00	E76.00	INRA	N22638	N903
Kas-2	India (Kashmir)	Kashmir-2	1580	N35	E77	El-Lithy	N22638	
Kent PHW 230,019	England	Kent		N51	E/W 0	Estimated	N6019	
keuk-1 PHW 230,032	Netherlands	Keukenhof Lisse		N52.10	E4.35	Estimated	N6032	
Kin-0	USA	Kindalville (MI)		N35,58	E83,56	INRA	N22654	N1272
KL-5	Germany	Koln	1-100	N51.00	E07.00	INRA	N1284	
Knox-10	USA	Knoxville (IN)	1-100	N35,58	E83,56	INRA	N22566	
Knox-18	USA	Knoxville (IN)		N41.18	W86.38	Nordborg	N22567	
Ko-3	Denmark	Kopenhagen	50	N55.23	E12.34	Estimated	N1290	JA126
Kondara	Tadjikistan	Khurmatov - Kondana-Tady (Pamiro-Alay)	1000-1100	N38.48	E68.5	INRA	N916	
Kyoto (Kyo-1)	Japan	Kyoto Pref.		N34.58	E35.37	INRA	JW137	
Kz-1	Kazakhstan	Atasu		N49.5	E73.1	Nordborg	N22606	
Kz-9	Kazakhstan	Atasu		N49.5	E73.1	Nordborg	N22607	
Ler-1	Poland	Gorzow Wielkopolski (Landsberg)	1-100	N52.43	E15.13	INRA	N22618	N1642
LL-0	Spain	Llagostera		N41.95	E2.49	Nordborg	N22650	
Lov-1	Sweden	Lovvik (Harnosand Area)		N62.48	E18.15	Nordborg	N22574	
Lp2-2	Czech Republic	Lipovec		N49.22	E16.39	Nordborg	N22594	
Lp2-6	Czech Republic	Lipovec		N49.22	E16.39	Nordborg	N22595	
Lz-0	France	Lezoux (Puy-de-Dome)	400-500	N45.49	E3.22	INRA	N22615	N1354
Meloy (Ornes)	Norway	Ornes / Meloy		N66.47	E13,4	Estimated	Koornneef / Stenoien	
Mir-0	Italy (north)	Miramare / Trieste	100-200	N45.42	E13.42	INRA	N1378	

Natural variation in Arabidopsis hyponastic growth

Mr-0	Italy (north)	Monte / Tosso	1000-1500	N44.30	E9.30	INRA	N22640	N1372
Mrk-0	Germany	Markt / Baden	200-300	N49.54	E9.49	INRA	N22635	N1374
Ms-0	Russia	Moscow	100-200	N55.45	E37.35	INRA	N22655	N905
Mt-0	Libya	Martubad/Cyrenaika	100-200	N32.34	E22.46	INRA	N22642	N1380
Mz-0	Germany	Merzhausen / Ts.	400-500	N50.19	E8.28	INRA	N22636	N1382
Nd-1	Germany	Niederzeuzheim	200-300	N50.28	E8.02	INRA	N1636	
NFA-10	England	NFA		N51.25	E0.41	Nordborg	N22599	
NFA-8	England	NFA		N51.25	E0.41	Nordborg	N22598	
Niigata (NG)	Japan	Niigata Pref.		N37.55	E139.03	INRA	JW125	
No-0	Germany	Nossen	200-300	N51.03	E13.17	INRA	N1394	
Nok-3	Netherlands	Noordwijk		N52,5	E4	INRA	N22643	N1404
Omo2-1	Sweden	Ostra Mocklo (Skane)		N56.12	E15.18	Nordborg	N22584	
Omo2-3	Sweden	Ostra Mocklo (Skane)		N56.12	E15.18	Nordborg	N22585	
Oy-0	Norway	Oystese	1-100	N60.23	E6.13	INRA	N22658	N1436
Pa-1	Italy (south(sicily))	Palermo	1-100	N38.07	E13.22	INRA	N1438	
Pak-1	Pakistan		1500	N33.9	E73.4	Michael	JW105	
Per-1	Russia	Perm		N58.00	E56.15	INRA	N1444	
Pna-10	USA	Benton Harbor (MI)		N41.32	W82.26	Nordborg	N22571	
Pna-17	USA	Benton Harbor (MI)		N41.32	W82.26	Nordborg	N22570	
Pro-0	Spain	Proaza, Asturias		N43.15	W6	Nordborg	N22649	
Pu2-23	Croatia	Prudka		N42.38	E18.07	Nordborg	N22593	
Pu2-7	Croatia	Prudka		N42.38	E18.07	Nordborg	N22592	
Ra-0	France	Randan (Puy-de-Dome)	400-500	N46.01	E3.21	INRA	N22632	N1480
Ren-1	France	Rennes		N48,50	E5,25	Nordborg	N22253	
Ri-0	Canada	Richmond (BC)	1-100	N49.10	W123	INRA	N1492	
RLD-1	Netherlands	RLD	1-100	N52.15	E5.3	INRA	N913	
Rmx-A02	USA	Saint Joseph (MI)		N42.07	W86.29	Nordborg	N22568	
Rmx-A180	USA	Saint Joseph (MI)		N42.07	W86.29	Nordborg	N22569	
Rome-1	Italy (Mid)	Rome-1		N41.9	E12.56	El-Lithy	N22524	
RRS-10	USA	North Liberty (IN)		N41.18	W86.38	Nordborg	N22565	
RRS-7	USA	North Liberty (IN)		N41.32	W82.26	Nordborg	N22624	
Rsch-0	Russia	Rshew / Starize		N56.50	E34.00	INRA	N1490	
Santa Clara	USA	Santa Clara County (CA)		N37.22	W31.58	Estimated	N8069	
sav-0	Czech Republic	Slavice	500-600	N49.49	E12.56	INRA	N1514	
Se-0	Spain	San Eleno	1-100	N41.30	E2.3	INRA	N22646	N1502
Seat-1 (Bg-1)	USA	Seattle (WA)		N47,63	W122,19	Lempe	N22341	
Sei-1	Italy (north)	Seis am Schlern	1200-1300	N46.32	E11.34	INRA	N1504	
Sf-2	Spain	San Feliu	1-100	N41.50	E3.00	INRA	N1516	
Shahdara	Tadjikistan	Shahdara River (Pamir)	3300-3400	N37.29	E71.3	INRA	N929	
Sorbo	Tadjikistan	Khurmatov – Kondana-Tady (Pamiro-Alay)		N38.49	E68.28	INRA	N22653	
Spr1-2	Sweden	Spratteboda (Skane)		N65.32	E14.29	Nordborg	N22582	

Spr1-6	Sweden	Spratteboda (Skane)		N65.32	E14.29	Nordborg	N22583	
Sq-1	England	SQ		N51.25	E0.41	Nordborg	N22600	
Sq-8	England	SQ		N51.25	E0.41	Nordborg	N22601	
Stange	Norway	Strandlykka am Mjøsa-See	30-40	N60.30	E11.14	Stenoien	Koornneef / Stenoien	
Tamm-2	Finland	Tammisari		N59.58	E23.26	Nordborg	N22604	
Tamm-27	Finland	Tammisari		N59.58	E23.26	Nordborg	N22605	
Te-0	Finland	Tenela	1-100	N60.04	E23.18	INRA	N1550	
Tiv-1	Italy (Mid)	Tivoli		N41.57	E12.48	Estimated	N22525	
Ts-1	Spain	Tossa de Mar	1-100	N41.50	E3.00	INRA	N22647	N1552
Ts-5	Spain	Tossa de Mar	1-100	N41.50	E3.00	INRA	N22648	N1558
Tsu-1	Japan	Tsushima	1-100	N34.19	E29.19	INRA	N22641	N1564
Ull2-3	Sweden	Ullstorp		N56.09	E13.46	Nordborg	N22587	
Ull2-5	Sweden	Ullstorp		N56.09	E13.46	Nordborg	N22586	
Uod-1	Austria	Uod (Ottenhof)		N48.07	E14.53	Nordborg	N22612	
Uod-7	Austria	Uod (Ottenhof)		N48.07	E14.53	Nordborg	N22613	
Van-0	Canada	UBC, Vancouver (BC)	1-100	N49.16	W123.07	INRA	N22627	N6884
Var2-1	Sweden	Vårhallarna (Skane)		N55.33	E14.29	Nordborg	N22580	
Var2-6	Sweden	Vårhallarna (Skane)		N55.33	E14.29	Nordborg	N22581	
Wa-1	Poland	Warsaw	100-200	N52.15	E21.00	INRA	N22644	N1586
Wei-0	Switzerland	Weiningen	400-500	N47.25	E8.25	INRA	N22622	N3110
Ws-0	Ukraine	Vasljevici (Wassilewskija / Dnjepr (Bellarus))	100-200	N52.13	E30.38	INRA	N22623	N1602
WS-2	Ukraine	Vasljevici (Wassilewskija / Dnjepr (Bellarus))	100-200	N52.13	E30.38	INRA	N915	
Wt-5	Germany	Wietze		N52.50	E9.50	Nordborg	N22637	
Yo-0	USA	Yosemite National Park (CA)	1400-1500	N37.45	W119.35	INRA	N22624	N1622
Zdr-1	Czech Republic	Zdarec		N49.12	E16.37	Nordborg	N22588	
Zdr-6	Czech Republic	Zdarec		N49.12	E16.37	Nordborg	N22589	

Footnotes:

- ^a Geographical altitude, longitude and latitude of individual accession collection sites is from the indicated publication, by the Institut National de la Recherche Agronomique (INRA) *Natural Variation of Arabidopsis thaliana* website (<http://dbgap.versailles.inra.fr/vnat/>), is an estimated value based on the geographic location of the population/region, or was obtained from literature.
- ^b Abbreviations: Nordborg; Nordborg *et al.* (2005), Stenoien: Stenoien *et al.* (2005); Lempe: Lempe *et al.* (2005), El-Lithy: El-Lithy *et al.* (2004); Michael: Michael *et al.* (2003).
- ^c Seeds were obtained directly via the Nottingham Arabidopsis Stock Centre (<http://arabidopsis.info/>), as set of 96 ecotypes (NASC Stock ID; N22660; Nordborg *et al.*, 2005) or were obtained from the Sendai Arabidopsis Seed Stock Center (SASSC) Miyagi University of Education, Japan (<http://www.brc.riken.jp/lab/epd/Eng/index.shtml>). Others were obtained via M. Koornneef (Wageningen University, the Netherlands).

***Phytochrome B and HISTONE DEACETYLASE 6
control light-induced chromatin compaction in
Arabidopsis thaliana***

Federico Tessadori^{1*§}, Martijn van Zanten^{2*}, Penka Pavlova^{1,3}, Rachel Clifton⁴, Frédéric Pontvianne⁵, L. Basten Snoek^{2§}, Frank F. Millenaar^{2§}, Roeland Kees Schulkes¹, Roel van Driel¹, Laurentius A.C.J. Voeselek², Charles Spillane⁴, Craig S. Pikaard⁵, Paul Fransz¹, Anton J.M. Peeters²

* These authors contributed equally to this work

¹ Nuclear Organization Group, Swammerdam Institute for Life Sciences, University of Amsterdam, Kruislaan 318, 1098 SM Amsterdam, the Netherlands

² Plant Ecophysiology, Institute of Environmental Biology, Utrecht University, Padualaan 8, 3584 CH Utrecht, the Netherlands

³ Laboratory of Genetics, Wageningen University and Research Center, Arboretumlaan 4, 6703 BD Wageningen, the Netherlands

⁴ Genetics & Biotechnology Lab, Department of Biochemistry & Biosciences Institute, University College Cork, Lee Maltings 2.10 Cork, Republic of Ireland

⁵ Biology Department, Washington University, 1 Brookings Drive, St .Louis, Missouri, 63130, United States of America

§ Present addresses:

FT: Cardiac Development and Genetics group, Hubrecht Institute for Developmental Biology and Stem Cell Research, Uppsalalaan 8, 3584 CT Utrecht, the Netherlands; LBS: Department of Nematology, Wageningen University and Research Center, Binnenhaven 5, 6709 PD Wageningen, the Netherlands. FFM: De Ruiter Seeds, Leeuwenhoekweg 52, 2660 BB Bergschenhoek, the Netherlands.

Adapted from:

- Tessadori F*, Van Zanten M*, Pavlova P, Clifton R, Pontvianne F, Snoek LB, Millenaar FF, Schulkes R-K, Van Driel R, Voeselek LACJ, Spillane C, Pikaard CS, Fransz P, Peeters AJM. (2009). PHYTOCHROME B and HISTONE DEACETYLASE 6 control light-induced chromatin compaction in *Arabidopsis thaliana*. *PLoS Genetics*, 5(9): e1000638.

Abstract

Natural genetic variation in *Arabidopsis thaliana* exists for many traits and often reflects acclimation to local environments. Studying natural variation has proven valuable in the characterization of phenotypic traits and in particular, in identifying genetic factors controlling these traits. It has been previously shown that chromatin compaction changes during development and biotic stress. To gain more insight into the genetic control of chromatin compaction, we investigated the nuclear phenotype of 21 selected *Arabidopsis* accessions from different geographic origins and habitats. We show natural variation in chromatin compaction and demonstrate a positive correlation with latitude of geographic origin. The level of compaction appeared to be dependent on light intensity. A novel approach, combining Quantitative Trait Locus (QTL) mapping and microscopic examination pointed at phytochrome B (*phyB*) and HISTONE DEACETYLASE-6 (*HDA6*) as positive regulators of light-controlled chromatin compaction. Indeed, mutant analysis demonstrate that both factors affect global chromatin organization. *HDA6*, in addition, strongly promotes the light-mediated compaction of the Nucleolar Organizing Regions (NORs). The accession Cape Verde Islands-0 (Cvi-0), which shows sequence polymorphism in the *phyB* gene and in the *HDA6* promotor, resembles the *hda6* mutant in having reduced chromatin compaction and decreased methylation levels of DNA and histone H3K9 at the NORs. We provide evidence that chromatin organization is controlled by light intensity. We propose that chromatin plasticity is associated with acclimation of *Arabidopsis* to its environment.

Introduction

Plant phenotypes are the integrated result of developmental programs and plastic responses to the environment. *Arabidopsis thaliana* has a wide biogeographical distribution. Consequently, rich natural (genetic) variation exists among collected accessions (Alonso-Blanco *et al.*, 2005; Hoffmann, 2002; Koornneef *et al.*, 2004; Nordborg *et al.*, 2005), which are acclimated to environmental conditions in their local habitat. Utilization of this natural variation in functional studies has led to a better understanding of the molecular and physiological mechanisms of complex traits such as the acclimation to the light environment (Alonso-Blanco *et al.*, 1998b; Borevitz *et al.*, 2002; Botto & Smith, 2002; El-Din El-Assal *et al.*, 2001; Karlsson *et al.*, 1993; Maloof *et al.*, 2000; 2001).

We recently observed variation in chromatin compaction during floral induction in three *Arabidopsis* accessions (Tessadori *et al.*, 2007a), suggesting the existence of natural genetic variation for chromatin organization. Chromatin folding is an essential process in eukaryotes, which provides differential accessibility of genes and regulatory elements along the linear DNA sequence. At the microscopical level different types of chromatin can be discerned depending on the condensation degree. For example, in *Arabidopsis* nuclei the chromosomes display highly

condensed heterochromatin domains (chromocenters) and less condensed gene-rich euchromatin loops (Fransz *et al.*, 2002; Tessadori *et al.*, 2004). The main component of chromocenters is repetitive DNA which includes long tandemly arranged DNA elements, such as satellite repeats, ribosomal-DNA (rDNA) genes and centromeric sequences. The chromocenters contain epigenetic markers for heterochromatin. Quantification of chromocenter size and intensity has been used to assess chromatin compaction in several studies (Mathieu *et al.*, 2003; Soppe *et al.*, 2002; Tessadori *et al.*, 2004, 2007a, b).

The ensemble of cytogenetically-defined functional parameters constitutes the nuclear phenotype, which is associated with specific transcriptional states (Fransz *et al.*, 2003; Tessadori *et al.*, 2004). The different states of chromatin compaction are accompanied by specific epigenetic markers (Naumann *et al.*, 2005). Methylation of both cytosine and histone H3 lysine 9 occurs in transcriptionally repressed areas, whereas methylation at histone H3K4 and histone acetylation mark regions of gene activity.

Several studies have indicated plasticity in chromatin compaction during development and upon interaction with the environment (Arnholdt-Schmitt, 2004; Madlung & Comai, 2004; Mathieu *et al.*, 2003; Pavet *et al.*, 2006; Tessadori *et al.*, 2004, 2007a, b) (reviewed in: Exner & Hennig, 2008). For example, heterochromatin levels rise during seedling establishment (Mathieu *et al.*, 2003), and the heterochromatin content of young mesophyll cells is lower than in fully differentiated leaves (Tessadori *et al.*, 2004). In addition, Pavet and colleagues (2006) observed severe loosening of chromocenters and hypomethylation upon infection by *Pseudomonas syringae* pv. *Tomato* (Pavet *et al.*, 2006). Recently, it was shown that formation of totipotent protoplasts coincided with a strong reduction of heterochromatin compaction (Tessadori *et al.*, 2007b).

Despite the increasing amount of data showing large-scale reorganization of chromatin domains, we still know very little about the genetic components controlling the plasticity of chromatin. Here, we demonstrate natural variation in chromatin organization in 21 *Arabidopsis thaliana* accessions, originating from different geographic origins. The level of chromatin compaction correlates with latitude of origin and depends on light intensity. We utilized natural variation in a quantitative genetic approach to identify loci affecting chromatin organization. We provide evidence that the photoreceptor phytochrome B (PhyB) and the histone modifier HISTONE DEACETYLASE 6 (HDA6) control light-dependent chromatin organization.

Results

Chromatin compaction correlates with geographic latitude of origin and local irradiation levels

To study natural variation in chromatin compaction, we examined the chromocenter phenotypes of leaf mesophyll cells from 21 accessions originating from a wide variety of natural habitats. We observed large variation in chromocenter size and number between accessions (Figure 8.1). To quantify this variation, we used the heterochromatin index (HX; Tessadori *et al.*, 2007a), which is a measure of the fraction of nuclei with conspicuous chromocenters (i.e. the typical *Landsberg erecta* (*Ler*) phenotype in Figure 8.1a) over the total number of nuclei. The variation in HX ranged from 0.19 (Cape Verde Islands; Cvi-0) to 0.92 (Kondara; Supporting information Table S8.1).

Because the 21 accessions originate from different geographic locations (Figure 8.2a, Table S8.2), we tested if geographic origin correlated with chromatin compaction. We found a significant ($p < 0.001$) inverse correlation ($r^2 = 0.76$) between HX and geographical latitude of origin (Figure 8.2a). Longitude and altitude did not display a significant correlation. Subsequently, we analyzed if local environmental conditions correlated with the chromatin phenotypes. We used mean annual climate parameter data acquired over a 30 years period (Table S8.2; New *et al.*, 1999). Stepwise removing of the least-significant parameters from a multiple-regression analysis, revealed that mean annual irradiation ($p < 0.001$) and annual amount of wet-days ($p = 0.01$) may explain the geographic variation in HX. These parameters also correlated best with latitude (Table S8.2). Although day length is a clear latitude-dependent parameter that affects e.g. flowering time (Shindo *et al.*, 2005; Stinchcombe *et al.*, 2004) and circadian period (Michael *et al.*, 2003), it does not have impact on heterochromatin compaction (data not shown). Apparently, the photon flux density (light intensity) rather than daily quantum input influences chromatin compaction.

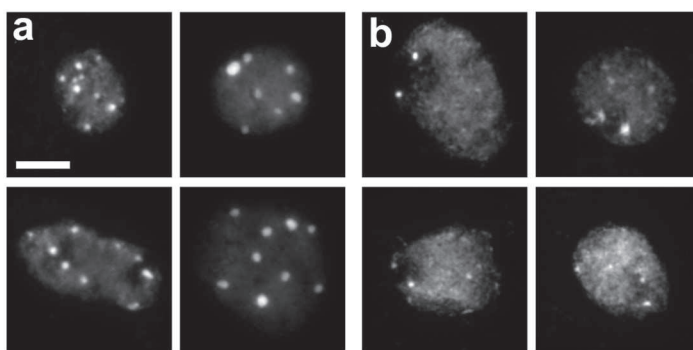


Figure 8.1: *Ler* nuclei display high chromatin compaction and conspicuous chromocenters, in contrast to *Cvi-0*. **a:** *Ler* nuclei have 6-10 conspicuous, round chromocenters. **b:** *Cvi-0* nuclei have fewer and smaller chromocenters. Nuclei are counterstained with DAPI, bar = 5 μm

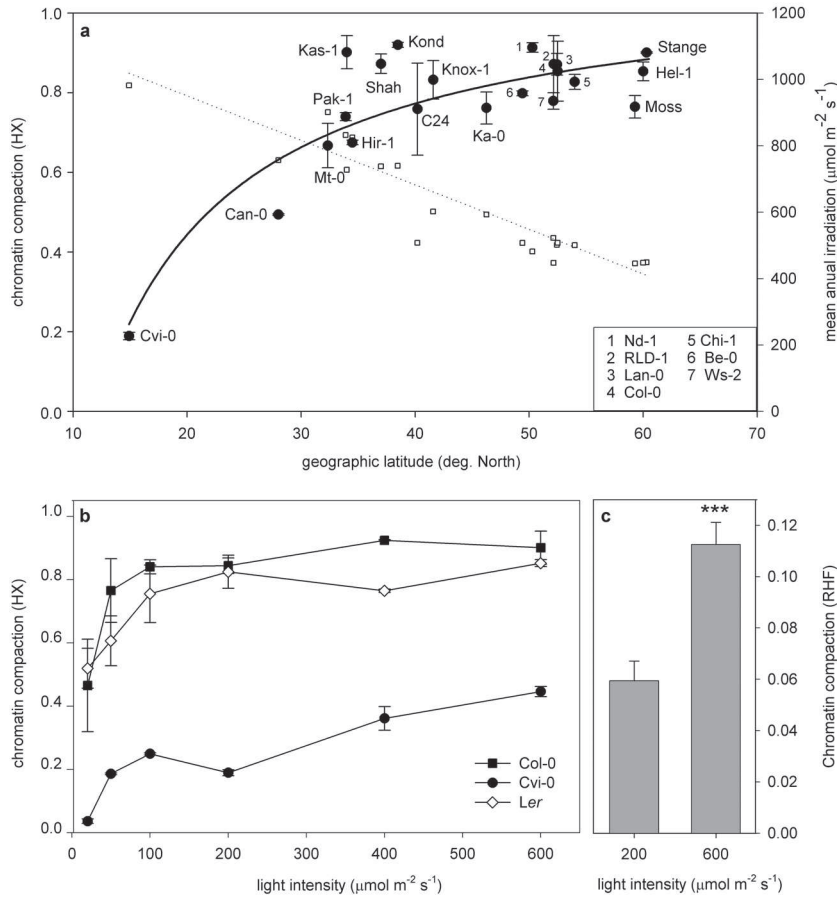


Figure 8.2: Chromatin compaction correlates with latitude of origin and light intensity levels. a: Correlates between chromatin compaction and latitude of origin of 21 accessions. Left Y-axis represents chromatin compaction (HX) of plants grown at a light intensity of $200 \mu\text{mol m}^{-2} \text{s}^{-1}$ in short-day photoperiod (closed round symbols) and right Y-axis represent mean annual irradiation (open squares), on the geographic latitude of collection sites. The best fitted curves are shown (HX; closed line, mean annual irradiation; dotted-line). Inset shows abbreviations of the clustered accessions depicted above in the graph. $n \geq 2$. b: Chromatin compaction of Col-0 (black squares), Ler (white diamonds) and Cvi-0 plants (black circles), grown in different light intensities. $n \geq 2$. c: Relative Heterochromatin Fraction (RHF) of Cvi-0 grown in different light intensities in short-day conditions. $n \geq 30$, *** $p < 0.001$ significance value; 2-tailed Student's T-test, compared to standard conditions ($200 \mu\text{mol m}^{-2} \text{s}^{-1}$). Error bars represent SE in all cases.

To test if light intensity directly influences chromatin organization, we examined the accession with the lowest HX, the sub-tropical accession Cvi-0, together with the commonly used Central-European laboratory accessions, Columbia-0 (Col-0) and Ler at different light intensities. Below $50 \mu\text{mol m}^{-2} \text{s}^{-1}$, these accessions showed a lower HX than under standard conditions (Figure 8.2b). However, above $100 \mu\text{mol m}^{-2} \text{s}^{-1}$ for

Col-0 and $200 \mu\text{mol m}^{-2} \text{s}^{-1}$ for *Ler*, the HX reached a plateau of 0.8-0.9. Strikingly, the HX of *Cvi-0* increased over the entire range of light intensities used. These results confirm that chromocenter compaction depends on light intensity.

In contrast to HX, which assesses variation in chromatin compaction in a population of nuclei, the Relative Heterochromatin Fraction (RHF) reflects the chromocenter compaction per nucleus (Soppe *et al.*, 2002; Tessadori *et al.*, 2004). The positive correlation between light intensity and chromatin compaction in *Cvi-0* was confirmed by RHF measurements (Figure 8.2c). Together, these data indicate that below certain irradiation intensities, light becomes a limiting factor for chromatin compaction. This is reflected by a decrease of the nuclear fraction with conspicuous chromocenters resulting in lower HX. The threshold varies between different accessions and is above $600 \mu\text{mol m}^{-2} \text{s}^{-1}$ for *Cvi-0*.

Altered localization of repeats and epigenetic markers in nuclei of *Cvi-0*

Chromatin compaction at chromocenters involves the condensation of repetitive DNA sequences such as the centromeric repeats, ribosomal genes and transposable elements (Fransz *et al.*, 2003). To find out which sequences remain in the reduced chromocenters of *Cvi-0*, we applied Fluorescence *In Situ* Hybridization (FISH) using probes for the 180 bp centromere repeat, 5S rDNA, 45S rDNA and the BAC F28D6 (Figure 8.3a-c). The latter contains many dispersed repeats such as transposons, which are predominant in pericentric regions (Supporting Information Figure S8.1). The 180 bp centromeric tandem repeats and 45S rDNA subtelomeric region displayed condensed signals at chromocenters (Figure 8.3a, c), similar to Col-0 and *Ler* (Tessadori *et al.*, 2007a,b). In contrast, 5S rDNA and BAC F28D6 signals showed a dispersed pattern (Figure 8.3a, b). This suggests that the loss of chromatin compaction in *Cvi-0* is caused by dislocation of pericentric repeats away from the chromocenters, comparable to the situation observed in gene silencing mutants such as *ddm1* and *met1* (Soppe *et al.*, 2002).

Since chromocenters contain most epigenetic markers for gene silencing (Fransz *et al.*, 2003, 2006), we examined if the epigenetic patterns were affected in *Cvi-0* nuclei (Figure 8.3c-f). Immunolabeling revealed that 5-Methylcytosine (5-MC) is concentrated in chromocenters of Col-0, whereas in *Cvi-0* the 5-MC label is dispersed over the entire nucleus (Figure 8.3c, d), similar to the pericentric repeats. Even the large chromocenters that flank the nucleolus (Figure 8.3c, e) containing the rDNA genes (Nucleolar Organizing Region (NOR) of chromosomes 2 and 4; Fransz, *et al.*, 2002; Jasencakova *et al.*, 2003; Probst *et al.*, 2003) are hypomethylated. Hence, the dispersed 5-MC pattern, supports the FISH results, that low chromatin compaction at chromocenters in *Cvi-0* is due to dispersed repeat regions. Immunostaining of H3K9me2 showed moderate dispersion and a diffuse signal at chromocenters in *Cvi-0*. Interestingly, both 5-MC and H3K9me2 labeling in *Cvi-0* was markedly reduced in the NORs. This is not the case in Col-0 (Figure 8.3d, f), where all chromocenters show distinct H3K9me2 and 5-MC signals. Apparently, the ribosomal genes of *Cvi-0* have decreased levels of both 5-MC and H3K9me2.

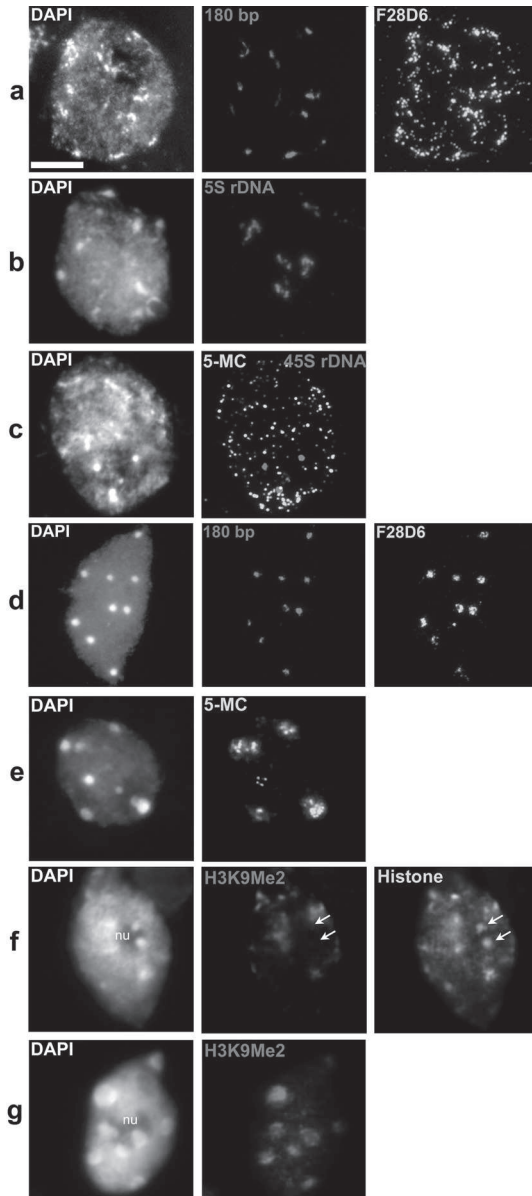


Figure 8.3: Cytogenetic characterization of Cvi-0. (See Color Supplement for full color version of this figure) **a:** FISH signals in Cvi-0 for the centromeric 180 bp (red) and **c:** the subtelomeric 45S rDNA repeats (red) are compact and located at chromocenters. **b:** Signals for the pericentromeric sequences 5S rDNA (red) and **a:** transposon-rich BAC F28D6 (green) are dispersed and outside heterochromatic regions. For comparison, in Col-0 both **d:** the centromeric 180 bp (red) and BAC F28D6 (green) are compact and located at the chromocenters. **c:** Immunolabeling of 5-Methylcytosine (5-MC; green) reveals a dispersed pattern in Cvi-0 compared to the **e:** clustered immunosignals in Col-0. **c:** Note the absence of 5-MC signal on the Cvi-0 45S rDNA sequences (red). **f:** Immunolabeling of H3K9Me2 (red) reveals the absence of this epigenetic mark on NOR chromocenters at the periphery of the nucleolus (arrows) in Cvi-0, while **g:** all chromocenters are marked in Col-0 (red). **f:** Histone immunolabeling on Cvi-0 (green) was carried out as control for histones. Each nucleus was counterstained with DAPI (first column). nu: nucleolus; Bar = 5 μ m.

QTL mapping reveals three loci controlling chromatin compaction

We applied Quantitative Trait Locus (QTL) analysis to map loci controlling light-dependent chromatin compaction. For this aim, RHF was measured in 47 selected *Ler* x Cvi-0 Recombinant Inbred Lines (RILs) (Alonso-Blanco *et al.*, 1998a). We based our analysis on RHF, because this is a composite quantitative trait that combines

nuclear and individual chromocenter size and intensity which is a strong valuation of chromatin compaction in each line.

Heterozygous lines of *Ler* x *Cvi-0* and *Cvi-0* x *Ler* crosses revealed a low RHF, indicating that the *Cvi-0* RHF phenotype is dominant (Figure S8.2). The broad sense heritability (H^2) was 0.4 indicating that 40% of the total variation is explained by genetic differences between the RILs. Three QTLs, designated *Rhf2*, *Rhf4* and *Rhf5*, were above the permutation calculated Likelihood Of Odds (LOD) threshold (Van Ooijen, 2004) of 2.89 (Figure 8.4a). Together these QTLs explained 53.2% of the variation in RHF in the population. No epistasis could be detected between the QTLs (data not shown).

Since *Ler* has a higher RHF than *Cvi-0*, QTLs with a negative allelic effect for *Cvi-0* were anticipated. However, *Rhf4* had a positive *Cvi-0* effect implying the existence of both positive and negative molecular regulators contributing to the average RHF (Figure 8.4b).

To confirm the location and effect of the putative QTLs, we measured the RHF of Near-Isogenic Lines (NIL) covering and flanking the QTL positions. These NILs contain small *Cvi-0* introgressions in the isogenic *Ler* genetic background (Edwards *et al.*, 2005; Keurentjes *et al.*, 2007) (Figure 8.4b). For each QTL, we found one NIL with a

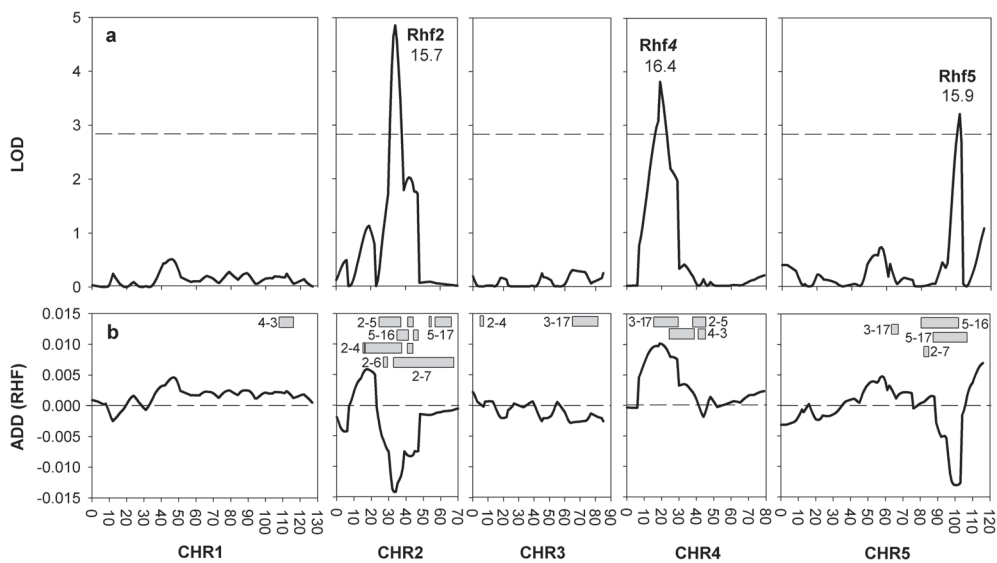


Figure 8.4: QTL analysis reveals three loci explaining the RHF. a: QTL-LOD profile of RHF per chromosome (CHR). The dashed line marks the 95% confidence threshold at LOD 2.89. Percentage explained variance and QTL names are given near each QTL peak. b: Additive effect of the *Cvi-0* allele compared to the population average. Boxes schematically show the positions of the *Cvi-0* introgressions of the NILs used to confirm the QTLs. Numbers depicted are the LCN line-numbers. The average map position of the flanking *Ler* marker and the border *Cvi-0* marker are depicted as cross-over positions.

predicted and significantly different RHF effect (Figure 8.5a). The introgression region in this NIL thus contains a Cvi-0 allele that contributes to the total observed low Cvi-0 RHF. Rhf2 is explained by NIL LCN2-5 (introgression on chromosome 2 between 22 and 27 cM). Surprisingly, LCN2-4 was not significantly different from *Ler* (Figure 8.5a), most likely due to the linked opposite QTL (Figure 8.4) at this locus which may repress the LCN2-4 phenotype. Alternatively, (flanking) positive, additive Cvi-0 alleles that are not detectable by QTL analysis may cause this effect. The Rhf4 region is explained by LCN4-3 and could be assigned, using other NILs, to 35 cM and 50 cM. Similarly, the region for Rhf5 was explained by LCN5-17 and could be restricted to only 3 cM (between 107 and 110 cM). Subsequently, we measured the HX of the two NILs with reduced RHF (LCN2-5 and LCN5-17). Both NILs had a reduced HX compared to *Ler*, confirming the observations found with RHF (Figure 8.5b). When these lines were grown at $600 \mu\text{mol m}^{-2} \text{s}^{-1}$ we observed significantly increased HX values in both lines, compared to plants grown at $200 \mu\text{mol m}^{-2} \text{s}^{-1}$ ($p < 0.001$ for LCN5-17 and $p < 0.01$ for LCN2-5), while the HX of *Ler* remained unchanged. These data indicate that Arabidopsis chromosomes 2 and 5 contain loci (within the introgression of LCN2-5 and LCN5-17, respectively) that are segregating between *Ler* and Cvi-0 accessions and influence chromatin compaction in a light dependent manner.

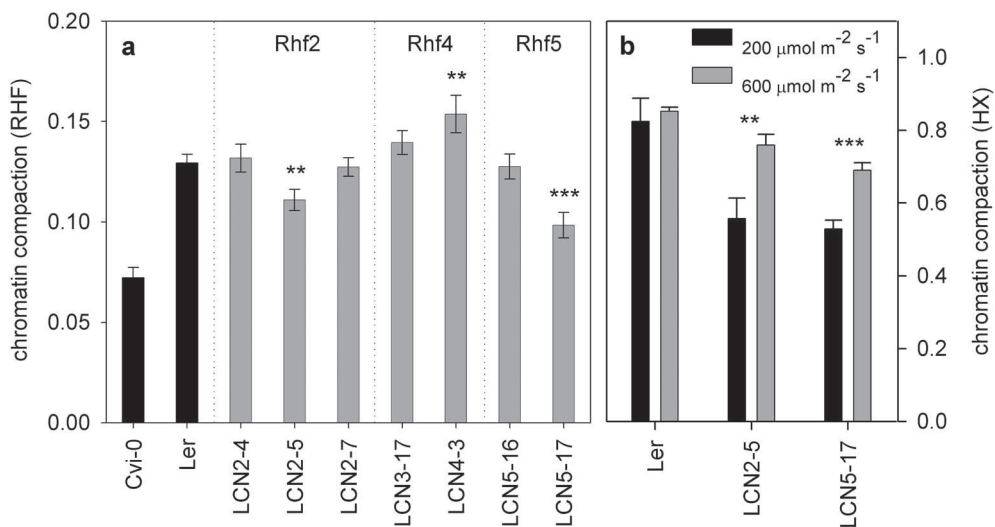


Figure 8.5: Near Isogenic Lines confirm the QTL positions and effects. a: RHF of the NILs with a Cvi-0 introgression in the *Ler* genetic background at the Rhf QTL loci, in control light conditions. The parents used to generate the NILs are in black. NILs are in grey. QTL names are depicted above the NILs; $n > 13$ nuclei. b: HX ($n \geq 2$) of LCN2-5 and 5-17 at 200 - (black bars) and $600 \mu\text{mol m}^{-2} \text{s}^{-1}$ (grey); Error bars represent SE in all cases. ** $p < 0.01$; *** $p < 0.001$ significance value by 2-tailed Student's T-test compared to *Ler* (a) or compared between plants of one genotype grown in $200 \mu\text{mol m}^{-2} \text{s}^{-1}$ compared to the same genotype grown in $600 \mu\text{mol m}^{-2} \text{s}^{-1}$ (b)

Phytochrome B and HISTONE DEACETYLASE 6 are involved in light mediated chromatin compaction

Within the small introgression regions of LCN2-5 and LCN5-17 that contributed to the low RHF of Cvi-0, we selected the photoreceptor *phytochrome B* (*phyB*), and *HISTONE DEACETYLASE-6* (*HDA6*) for further study, based on their annotation as light perception and chromatin component. Although the chromatin remodeler *DDM1* is also located on the introgression region of *Rhf5*, we did not consider this gene, since Cvi-0 has normal overall DNA methylation levels (Riddle & Richards, 2002). The *hda6* (*hda6 sil1/not*; Furner *et al.*, 1998) and the *phyb5* (Koornneef *et al.*, 1980) mutants showed a significantly reduced HX and RHF compared to *Ler* (Figure 8.6; Figure S8.2), indicating that these candidate genes affect chromatin compaction. Moreover, inactivating *PhyB* in a non-invasive manner, by application of low red-to-far red ratio light, mimicking natural canopy shade, did also result in a reduced chromatin compaction (HX; 0.34 ± 0.13), comparable to the *phyb5* effect. A low chromatin compaction has been described before for *hda6* [Probst *et al.*, 2004, Franz *et al.*, 2006], but not for *phyb* alleles.

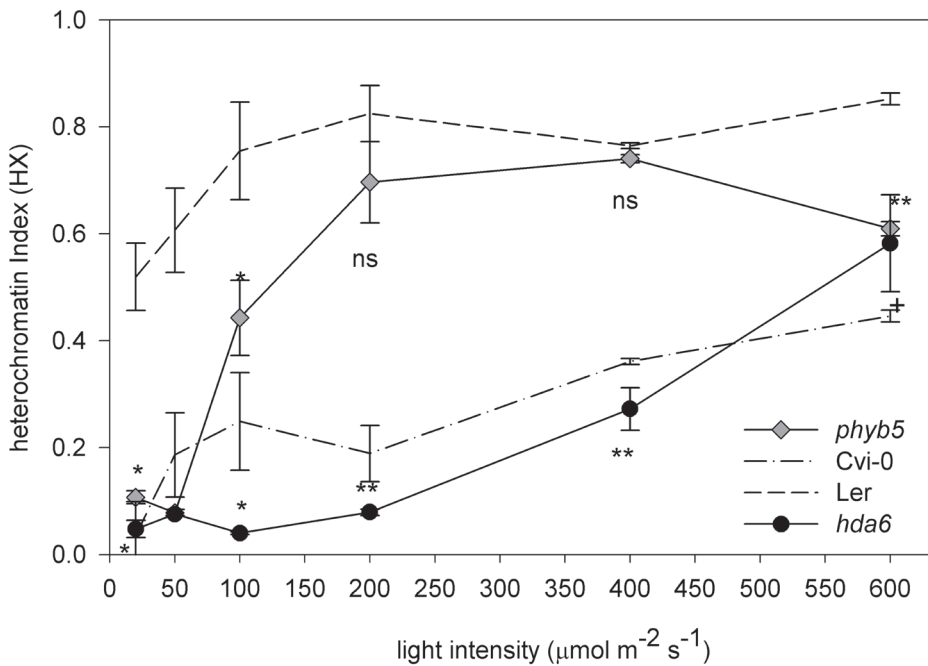


Figure 8.6: Phytochrome B and HISTONE DEACETYLASE-6 are positive regulators of light dependent chromatin compaction. Heterochromatin index of *phyb5* (grey diamonds), *hda6 sil1/not1* (black circles), Cvi-0 (dash-dotted line) and *Ler* (dashed line) grown in different light intensities $n \geq 2$. *** $p < 0.001$; ** $p < 0.01$; * $p < 0.05$; + $p < 0.1$; ns = non significant; significance value; 2-tailed Student's T-test compared to *Ler*. Error bars represent SE in all cases.

Next, we performed complementation analysis (Borevitz & Nordborg, 2003, Mackay, 2001) on F_1 crosses between mutant and wild types. In all cases, F_1 lines from crosses with Cvi-0 showed low RHF levels and were statistically identical to Cvi-0, but never to *Ler* (Figure S8.2), indicating dominance of the Cvi allele(s). However, heterozygous F_1 plants of crosses between *phyB* or *hda6* mutants and *Ler*, in contrast to Cvi-0, showed intermediate levels of RHF (Figure S8.2; significantly different from both Cvi-0 and *Ler*), suggesting that none of these alleles is dominant.

To assay the light dependency of the chromatin compaction phenotypes in *hda6* and *phyb5*, both lines were examined under different light intensities. In general, the mutants displayed a lower HX than wild type *Ler* (Figure 8.6). Similar results were obtained using *phyb9* in the Col-0 background (Figure 8.7). At higher light intensities, the HX increased drastically in both mutants, illustrating the interaction between light intensity and chromatin compaction levels. Interestingly, we observed differences in the response to light intensity between *hda6* and *phyb5*. Up to $200 \mu\text{mol m}^{-2} \text{s}^{-1}$, the chromatin compaction in *phyb5* increased rapidly to values close to *Ler*, whereas in *hda6* the chromatin compaction increased steadily after $200 \mu\text{mol m}^{-2} \text{s}^{-1}$, reminiscent of the pattern of Cvi-0. Thus, PhyB predominantly acts at low light intensity ($<200 \mu\text{mol m}^{-2} \text{s}^{-1}$), whereas HDA6 plays a role throughout the light intensity range. This points to a novel function of the histone modifier HDA6. The data indicate that PhyB and HDA6 are positive controllers of light intensity-mediated chromatin compaction. However, we cannot exclude that other genes underlying the QTLs might also influence chromatin compaction.

Segregating *phyB* alleles contribute to the low chromatin compaction levels of Cvi-0

Recently, polymorphisms have been identified in *PhyB* between *Ler* and Cvi (Filiault *et al.*, 2008). Ectopic over-expression of *PhyB* resulted in increased light sensitivity. However, overexpression of the Cvi allele sensitized the plant less than the *Ler* allele, indicating that the Cvi allele is less able to confer sensitivity to light. We examined chromatin compaction in *phyb9* complemented with $35S::PHYB\text{-Cvi}$ and $35S::PHYB\text{-Ler}$, to test if the same allelic variation accounts for variation in chromatin compaction. Both showed reduced chromatin compaction at $200 \mu\text{mol m}^{-2} \text{s}^{-1}$, indicating that besides light reduction, increased light sensitivity also results in reduction of chromatin compaction (Figure 8.7). The $35S::PHYB\text{-Cvi}$ lines however displayed a non-significant reduction, whereas the *Ler* allele conferred a significant ($p<0.05$) reduction. This confirms the reduced light sensitivity of the Cvi allele as compared to *Ler*.

Among the polymorphisms in *PhyB* segregating between *Ler* and Cvi, five are shared by Cvi and a clade of Spanish accessions (Filiault *et al.*, 2008). At least two of these Spanish accessions; Ts-1 ($HX=0.58 \pm 0.01$) and Se-0 (0.67 ± 0.02) show a low chromatin compaction compared to other European accessions. Together, these data suggest that variation in the *phyB* sequence contributes to variation in chromatin compaction and likely explains the *Rhf2* QTL.

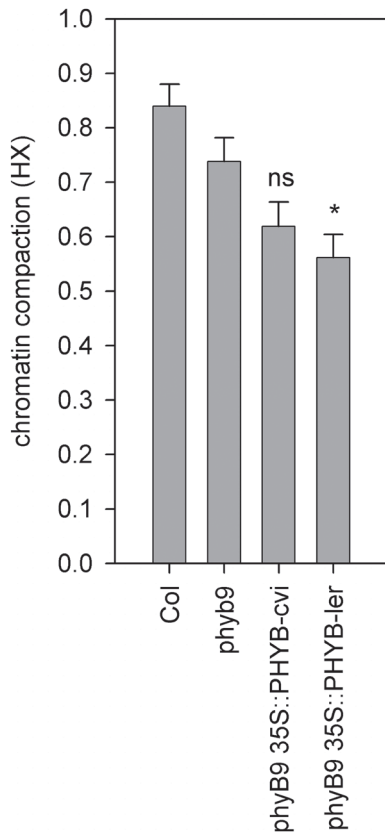


Figure 8.7: Ectopic expression of the *Ler* *phyB* allele, but not the *Cvi-0* allele, reduces chromatin compaction. Heterochromatin index of the *phyb9* mutant in the *Col* genetic background, complemented with gain-of-function *PhyB* alleles from *Cvi-0* or *Ler* (Filiault *et al.*, 2008) at $200 \mu\text{mol m}^{-2} \text{s}^{-1}$. Significance levels are compared to *phyb9* values; * $p < 0.05$; ns = non significant; 2-tailed Student's T-test. Error bars represent SE in all cases.

***Cvi* differs from *Ler* in *HDA6* sequence and resembles *hda6* mutant in chromatin compaction**

No sequence differences were found in the coding region of the *HDA6* alleles in *Ler*, *Cvi-0* and *Col-0*, only in the 5'-UTR and the first intron (Figure 8.8). An intriguing feature was the presence of two base substitutions, each at an identical position in a small 13bp repeat sequence in the 5'-UTR region of *HDA6* in *Cvi-0*. Subsequently, we examined if different *HDA6* mRNA isoforms were produced in *Cvi-0*. Reverse Transcriptase-PCR analysis revealed no evidence for altered expression levels nor for alternative splicing products (data not shown).

To further investigate the cause of the difference in RHF between the *Cvi-0* and *Ler* heterozygotes (Figure S8.2), and to further study *hda6* effects, we dissected the RHF, which is a measure for the whole nucleus, into its components and examined the size of individual chromocenters (Figure 8.9). Small chromocenters are more frequently observed in *Cvi-0* than in *Ler* (Figure 8.9a, b). This is not due to chromocenter association in *Ler*, since the average number of chromocenters per nucleus in *Ler* (8.3) is higher than in *Cvi-0* (5.7). *Cvi-0* lacks the very large chromocenters (>300 area units) (Figure 8.9b), which contain the NORs (Fransz *et al.*, 2002). The fraction of large

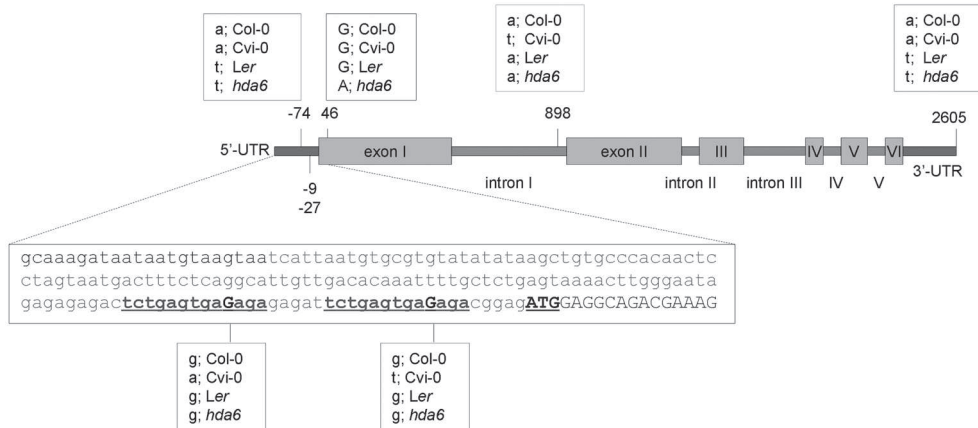


Figure 8.8: Cvi-0 has HDA6 5'-UTR polymorphisms compared to Ler and Col-0. (See Color Supplement for full color version of this figure) a: Schematic representation of the *HDA6* (At5g63110) genomic sequence alignment in; Col-0, Cvi-0, Ler and *hda6 sil1/not*. Untranslated regions (UTR; red), exons (blue boxes) and introns (orange bars) are shown along with the identified polymorphisms in bp relative to the ATG start codon. *Hda6* represents the *hda6 sil1/not* mutant. Sequences were aligned using CLUSTAL W 2.0 multiple sequence alignment and the alignment produced using EMBL EBI tools. The zoom-in box shows the sequence of the *HDA6* 5'-UTR (red) and the start of the first exon (blue, start codon; bold/underlined). The small repeat sequences that harbor the polymorphism in Cvi-0 relative to Col-0 and Ler are shown in green (underlined) and the polymorphism site is shown in dark green. Note a G/A nucleotide substitution at bp 46 in the *hda6 sil1/not* mutant, which results in a predicted amino acid change from glycine (G) to arginine (R) in the *hda6 sil/not* allele, confirming the results of Probst *et al.* (2004). Polymorphisms did not influence histone deacetylase signatures (as found using the NASC genome browser and extracting motifs using the SPRINT Prints view) nor potential miRNA targets, from <http://sundarlab.ucdavis.edu/cgi-bin/mirna/>.

NOR chromocenters increases at higher light intensity (Figure S8.3), suggesting that NOR formation is controlled by light.

Remarkably, *hda6* resembles Cvi-0 in having small NOR chromocenters (Figure 8.9d), suggesting that Cvi-0 has a malfunctional *HDA6* allele. In contrast, the size of NOR chromocenters in *phyb5* equals those in Ler (Figure 8.9a, f), implying that chromatin compaction in this photoreceptor mutant is brought about by a different process than in *hda6*.

Interestingly, the Cvi-0 phenotype with small NOR chromocenters, is dominant in the heterozygous Ler x Cvi-0 (Figure 8.9c), whereas the phenotype for small NOR chromocenters is intermediate (Figure 8.9c vs. 8.9e) in the F₁ Ler x *hda6*. The added parental data (Ler + *hda6*) strongly resembles the distribution of chromocenter size in the heterozygote (Ler x *hda6*) (Figure S8.4). This indicates that half of the chromocenters in the heterozygotes have the wild type appearance and the other half have the *hda6* appearance. This is particularly noticeable for the NOR chromocenters. In contrast, the distribution patterns of Cvi + Ler and the heterozygous Ler x Cvi-0 do not superimpose, pointing to inheritance of chromocenter size.

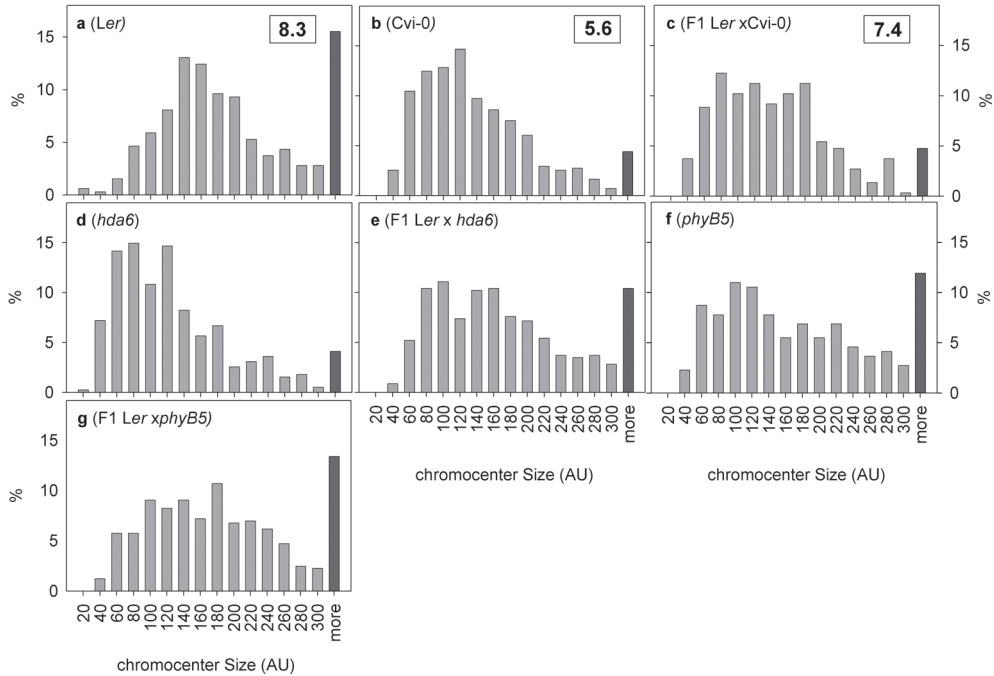


Figure 8.9: NOR chromocenter size is specifically affected in *Cvi-0* and *hda6*. Distribution of size per individual chromocenter in Arbitrary Pixel Units (AU) of F_1 plants derived from crosses between *hda6* and *phyB5* mutants and their parental wild types. Boxed numbers indicate the average number of detectable chromocenters per nucleus. The highest class for both distributions is defined on a 10% cutoff.

Discussion

Natural variation in *Arabidopsis* chromatin compaction reflects latitudinal variation in light intensity

Arabidopsis thaliana is an excellent model plant to study natural variation (Koornneef *et al.*, 2004). Here, we demonstrate latitude dependent variation in chromatin organization, measured in leaf mesophyll nuclei of 21 diverse accessions. Since all accessions were grown under identical conditions, the nuclear phenotype likely reflects the difference in environmental conditions between the growth chamber and the habitats of their origin. Light irradiation at the geographic origin sites turned out to be the best parameter for explaining the observed differences in chromatin compaction. Generally, the more close the habitat is to the equator the higher the light irradiation level to which the plants are exposed. Consequently, in the growth chambers these plants sense low light. The suggested correlation between light response and latitude is in accordance with the observations of Maloof *et al.* (2001) who studied hypocotyl length and demonstrated a correlation between light sensitivity

and latitude of origin. The authors concluded that accessions closer to the equator are less sensitive to light. Accordingly, a high frequency of the phytochrome-C haplotype, that compensates for lower light intensities at high latitudes, was found in Northern accessions (Balasubramanian *et al.*, 2006b). Moreover, it is well known that flowering responses, that is a light controlled trait, correlates with latitude (Lempe *et al.*, 2005). Apparently, natural variation in light sensitivity is reflected in clinal phenotypic variation. Hence, we consider chromatin compaction as a phenotype that reflects light sensitivity. This light-latitude correlation explains why in the most southern accession, Cvi-0, light intensity is a limiting factor for chromatin compaction up to at least $600 \mu\text{mol m}^{-2} \text{s}^{-1}$, whereas in the Central European accessions Col-0 and Ler the threshold is found around $100 \mu\text{mol m}^{-2} \text{s}^{-1}$. We cannot exclude however, that other geographical parameters may have additional effects on chromatin organization. The absence of collected accessions at latitudes between Can-0 and Cvi-0 limited the statistical power. Nevertheless, to our knowledge, this is the first report of a correlation between clinal origin of a plant accession and large-scale nuclear organization.

Light-dependent chromatin compaction requires phyB

Natural variation in chromatin organization was exploited to identify genes affecting light-dependent chromatin organization. We isolated and confirmed QTLs for chromatin compaction, together explaining 53% of the total variation in chromocenter compaction between Ler and Cvi-0. We identified the photoreceptor phyB as a positive regulator of chromatin compaction. PhyB, which locates on QTL Rhf2, was previously identified as a candidate gene explaining a light-related QTL in the same Ler x Cvi-0 RIL population (Borevitz *et al.*, 2002). In addition, sequence polymorphisms in *phyB* between Ler and Cvi-1 has been reported to cause differences in light response (Filiault *et al.*, 2008). A serine-to-threonine substitution in the PAS-A domain appeared to affect hypocotyl length. The same PAS-A allele is also present in a clade of Spanish accessions that show lower chromatin compaction compared to among others, Kondara and Kashmir-1. These accessions do not belong to the 'Spanish' clade, but originate from a similar latitude, supporting the idea that the polymorphism in the PAS domain contributes to the difference in light-dependent chromatin compaction.

A similar polymorphism is present in the PAS-B domain, where an isoleucine in Cvi-0 (Genbank ID; AAW56575) replaces a serine in Col and Ler (AAD08948, AAW56578). Both PAS-A and PAS-B polymorphisms involve serine, which is often subject to phosphorylation for functional conformational changes in phytochromes (Park *et al.*, 2000). The PAS-A/B domain is required for nuclear import into the nucleus (Chen *et al.*, 2005). A serine mutation in the PAS A/B domain may disturb the translocation of PhyB into the nucleus. Once translocated into the nucleus PhyB can physically interact with cryptochrome2 (CRY2) in a light-dependent fashion (Mas *et al.*, 2000). Strikingly, CRY2 has been demonstrated to control chromatin condensation during the floral transition in a light-dependent manner (Tessadori *et al.*, 2007a). These data indicate that Cvi-0 has aberrant PhyB activity which contributes to the reduced chromatin compaction.

Cvi-0 resembles the *hda6* mutant for chromatin organization at the NOR

Similar to Cvi-0, the *hda6* mutant (*sil1/not*) displays a low chromocenter compaction that can be restored at increasing light intensities. HDA6, which locates under the QTL *Rhf5*, is a histone deacetylase, known to control a variety of biological processes such as flowering (Wu *et al.*, 2008), regulation of transcription factors (Tanaka *et al.*, 2008), transcriptional silencing of transgenes and repeats (Aufsatz *et al.*, 2002; Lippman *et al.*, 2003; Murfett *et al.*, 2001; Probst *et al.*, 2004; Rangwala & Richards, 2007; Steimer *et al.*, 2000). A major target of HDA6 activity is the rDNA repeat locus (Probst *et al.*, 2004). Arabidopsis *hda6* mutants display decondensation of NOR chromocenters and reduced rDNA methylation. Moreover, HDA6 is involved in nucleolar dominance (Earley *et al.*, 2006; Pontes & Pikaard, 2008). An RNAi-mediated knock-down of HDA6 in *Arabidopsis suecica*, the natural hybrid between *Arabidopsis thaliana* and *Arabidopsis arenosa*, resulted in reactivation of the silent *A. thaliana* rDNA genes and decondensation of its NOR chromocenters. The process is accompanied by a decrease in rDNA methylation and in dimethylation at histone H3K9. Here we report the same subnuclear features in Cvi-0 with respect to DNA methylation and H3K9 methylation. In addition, reduced DNA methylation has been demonstrated specifically at the rDNA loci in Cvi-0 by Riddle & Richards (2002). This suggests that HDA6 expression or function in Cvi-0 is aberrant. However, we only identified base substitutions in small 13bp repeat sequences of the 5'-UTR region of HDA6 in Cvi-0. It is known from yeast and animals that 5'-UTR sequences may affect protein translation (Beelman & Parker, 1995; Curtis *et al.*, 1995; Pesole *et al.*, 2002). For example, in some forms of breast cancer, the human *BRCA1* gene generates two isoforms due to translation from a first AUG codon and a second, in-frame (Liu *et al.*, 2000). If this accounts for the HDA6 gene in Cvi-0, then the sequence predicts a truncated polypeptide lacking the first 39 amino acids. This region is essential for the catalytic function of HDA6. A substitution at position 16 generated the *hda6 sil1* mutation (Probst *et al.*, 2004). Therefore, a truncated polypeptide lacking this N-terminal region would result in a similar (low chromatin compaction) phenotype.

In contrast, the *hda6-sil1* allele in the heterozygote *Ler* x *hda6* is not dominant and the NOR chromocenter phenotype of both parents is inherited giving rise to an intermediate phenotype for total chromocenter size (see Figure 8.9 and Figure S8.1). Apparently, the presence of a functional *Ler*-derived HDA6 in this heterozygote cannot restore the size of the *hda6*-derived NOR chromocenters. This suggests an epigenetic imprinting factor controlling NOR chromocenter size. This factor may involve DNA methylation, since a similar situation has been reported in the heterozygous methyltransferase mutant, *met1^{+/−}* (Fransz *et al.*, 2003; Soppe *et al.*, 2002). Moreover, HDA6 has been shown to be mechanistically linked to methylation of repetitive DNA (Aufsatz *et al.*, 2002; Fransz *et al.*, 2003; Soppe *et al.*, 2002). In fact, Cvi-0 and HDA6 mutants and knockouts have reduced DNA methylation in NOR genes (Earley *et al.*, 2006; Pontes & Pikaard, 2008; Probst *et al.*, 2004; Riddle & Richards, 2002).

In summary, the analysis of natural variation among *Arabidopsis* accessions revealed a novel link between chromatin organization and light-intensity. In particular,

our data implicate novel roles for the photoreceptor PhyB as positive controller of chromatin organization and for the histone modifier HDA6 in the light signaling pathway towards chromatin compaction. We propose that polymorphisms in the alleles of these genes contribute to natural variation in the nuclear phenotypes among accessions and may function in acclimation to altered light environments on the accessions collection sites.

Materials and Methods

Growth conditions and treatments

Arabidopsis thaliana accessions (Table S8.1), *phyb5* (N69), *Ler* (NW20), *Se-0* (N1502), *Ts-1* (N1552), were obtained from the Nottingham Arabidopsis Stock Centre (NASC) or the Sendai Arabidopsis Seed Stock Center (SASSC), Miyagi University of Education, Japan). Moss and Stange (Stenoien *et al.*, 2005), *Lan-0*, the RILs (Alonso-Blanco *et al.*, 1998a) and NILs (Edwards *et al.*, 2005; Keurentjes *et al.*, 2007) were provided by M. Koornneef (Wageningen University, the Netherlands). The *phyb9* and 35S::PHYB lines (Filiault *et al.*, 2008) were provided by J. Maloof (UC Davis, CA, USA). The *hda6 sil1/not* (Furner *et al.*, 1998) seeds were obtained from Ian Furner (University of Cambridge, UK). Plants were grown as previously described (Millenaar *et al.*, 2005). Unless otherwise stated, the following growth conditions were used: 20°C, 70% (v/v) relative humidity during day and night, 9 h short-day photoperiod of 200 $\mu\text{mol m}^{-2} \text{s}^{-1}$ photosynthetic active radiation (PAR). Twenty-two days old plants, at developmental stage 1.05 to 1.07 (Boyce *et al.*, 2001), were used for all experiments. For all accessions this was well before the floral transition. Reduction of the light intensities below 200 $\mu\text{mol m}^{-2} \text{s}^{-1}$ was accomplished by shading the plants with spectrally neutral shade cloth. The spectral quality was checked with a LICOR-1800 spectro-radiometer (LI-COR, Lincoln, NE, USA).

Sample preparation

Young rosette leaves were harvested 1.5 h after start of the photoperiod to exclude, if any, diurnal and circadian influences, fixed in Carnoy's solution (ethanol/acetic acid 3:1) and stored at -20°C. Each sample consisted of two plants, except in the experiment with transgenic 35S::PHYB lines where each sample contained plants of five individual transformants. Spread preparations were made essentially as described in (Schubert *et al.*, 2001), with a modified enzymatic cell-wall degrading mixture: 0.6% Cellulase R10 (Yakult, Tokyo, Japan), 0.25% Macerozyme R10 (Duchefa, Haarlem, the Netherlands) in 10 mM citrate buffer pH 4.5. Slides were mounted in Vectashield (Vector Laboratories, Burlingame, CA, USA) with 4',6-diamidino-2-phenylindole (DAPI; 2 $\mu\text{g ml}^{-1}$) before observation. For HX calculation, 100-130 nuclei of at least two plants were analyzed.

Measure of Relative Heterochromatin Index (HX) and Heterochromatin Fraction (RHF)

The HX (Tessadori *et al.*, 2007a) was defined as the percentage of nuclei showing high content of compact chromatin (typified by *Ler*; Figure 8.1a), represented by conspicuous chromocenters, as opposed to nuclei with less compact chromatin (typified by *Cvi-0*, Figure 8.1b). For RHF quantification, automated digital analysis of grey-scale images was carried out with *in house* developed macros in ImagePro-Plus (Media Cybernetics, Silver Spring, MD, USA). RHF, defined as

the fluorescence intensity of all DAPI-stained chromocenters relative to the fluorescence of the entire nucleus, was calculated for each sample as described earlier (Soppe *et al.*, 2002; Tessadori *et al.*, 2004). Statistical analysis was performed by Two-way analysis of variance (ANOVA), with Tukey B post hoc comparisons (SPSS-Software 12.01, Chicago, IL, USA;), revealed whether there were significant differences between genotypes.

Geographic climate data

For details on the geographic and environmental data see Table S8.2. Mean annual data (of 0.5° latitude × 0.5° longitude surface land area plots) were calculated from monthly averages collected over a 30 years period (1961-1990; New *et al.*, 1999). We tested (SPSS) whether the obtained data set for all individual environmental variables correlated with the latitude of the collection sites (Table S8.2). If so, these sets were fitted in a linear multivariate data-regression analysis model (SPSS) using the heterochromatin index (HX) as dependent factor. Environmental factors significantly correlating to the variation in HX were found by stepwise removing the least significant (*p*-value) variable each time, starting from the full model, until all remaining factors were significant. Of all temperature-related traits, only the mean temperature was used in the full model because of the high correlations between these traits.

Fluorescence In Situ Hybridization (FISH)

Plasmid pAL1 (Martinez-Zapater *et al.*, 1986) was used to detect the 180 bp centromeric tandem repeat. BAC F28D6 (GenBank accession No. AF147262) obtained from NASC in pBeloBAC-Kan vector was used for the detection of pericentromeric repeats. 5S rDNA was from (Campell *et al.*, 1992), 45S rDNA probe was from (Gerlach & Bedbrook, 1979). FISH experiments were carried out essentially as described in (Schubert *et al.*, 2001). The nuclei were counterstained with DAPI (2 µg ml⁻¹ in Vectashield, Vector Laboratories) prior to observation.

5-Methylcytosine detection

Slide preparations were dried at 60°C for 30 min, treated with RNase A (Roche, Woerden, the Netherlands 10 µg ml⁻¹) for 60 min. at 37°C, rinsed 2x5 min. in PBS, fixed in 1% formaldehyde, dehydrated in successive ethanol baths and air-dried. Denaturation was carried out by adding 50 µl HB50 (50% formamide in 1xSSC) and heating at 80°C for 2 min. The slides were subsequently washed in 70% ice-cold ethanol and dehydrated by successive ethanol baths. Slides were incubated for 1 h in 1% Bovine Serum Albumine (BSA) to prevent aspecific binding and washed 3x5 min in TNT (1 M Tris/HCl; pH=8.0; 1 M NaCl, 0.5% Tween 20). Incubation with the antibody against 5-methylcytosine (Eurogentec, Seraing, Belgium; raised in Mouse, 1:50 in 1% BSA in PBS) was carried out at 37°C for a minimum of 1 h. Detection of the antibody was performed with the same antibodies used for FISH Digoxigenin-labeled probes as described above. The nuclei were counterstained with DAPI (2 µg ml⁻¹ in Vectashield, Vector Laboratories) prior to observation.

Immunolabeling

Leaf nuclei were isolated as previously described (Fransz *et al.*, 2002). Immunolabeling was carried out as described in (Soppe *et al.*, 2002). Primary antibodies were Rabbit anti-dimethyllysine 9 of histone H3 (Ref. No. 07-441; 1:50, Upstate, Lake Placid, NY, USA) and Mouse anti-

histone (Ref. No. 1492519; 1:100, Roche). Slides were incubated with primary antibodies overnight at 4°C. After washing steps with Phosphate-Buffered-Saline (PBS) the slides were detected with antibody Donkey-anti-Rabbit-Cy3 (1:500, Jackson Immunoresearch Laboratories, Soham, UK) for detection in the red channel, or with antibody Donkey-anti-Mouse-FITC (1:200, Jackson Immunoresearch Laboratories) for detection in the green channel, each step at 37°C for 30 min. The nuclei were counterstained with DAPI (2 µg ml⁻¹ in Vectashield, Vector Laboratories) prior to observation.

Image acquisition and processing

Slides were examined with an Olympus BX6000 epifluorescence microscope (Olympus, Tokyo, Japan) coupled to a CCD camera (Coolsnap FX, Photometrics, Tucson, AZ, USA). After acquisition the images were processed, pseudo-colored and merged using Adobe Photoshop software (Adobe, San Jose, CA, USA).

Quantitative trait loci (QTL) analysis

RHF was measured in 3 to 4 weeks old plants of 47 RILs of the *Ler* x *Cvi-0* core-population (Alonso-Blanco *et al.*, 1998a). The RILs, parental lines, and the *Cvi-0* x *Ler* F₁s were grown in a green-house in 16 h light/8 h darkness. These long-day conditions induce the potential for flowering, a trait known to be segregating in the used RIL set (Alonso-Blanco *et al.*, 1998a) and was chosen to synchronize this trait, thereby circumventing interference of floral transition related chromatin reorganization on RHF (Tessadori *et al.*, 2007a). At least 26 nuclei from 2 plants per line were used for RHF measurement.

Outliers beyond the 95% confidence interval per line were removed prior to QTL-mapping. The core-marker map (<http://www.dpw.wau.nl/natural/>) was used for the analysis. QTL-Cartographer algorithm: Composite Interval Mapping (CIM; <http://statgen.ncsu.edu/qtlcart/WQTLCart.htm>) was used, employing the “forward and backward” search method (parameters used: 10cM window; P_{in}: 0.05 P_{out}: 0.05). The threshold value was determined by a 1000 permutation test (95% confidence-interval).

Broad sense heritability was calculated as part of the between-line variance attributed to the total variance, using variance components of the general linear model procedure (SPSS).

NILs were grown in short-day growth chambers, under standard growth-room conditions described above, since no variation in flowering in these lines was expected (Keurentjes *et al.*, 2007). NILs LCN4-3, 5-16 and 5-17 have previously been described as NIL DOG5, NIL 19-2 and NIL 30-2 respectively (Alonso-Blanco *et al.*, 2003; Edwards *et al.*, 2005).

DNA sequencing of HDA6 genomic region

The *HDA6* gene (At5g63110) and flanking regions were PCR amplified from genomic DNA extracted from *Col-0*, *Ler-0*, *Cvi-0* and the *hda6* (*sil1/not*) mutant using Phusion™ High-Fidelity DNA Polymerase (Finnzymes, Espoo, Finland). DNA sequencing of PCR-amplified fragments of the *HDA6* encoding genomic region was performed by Macrogen (Seoul, Korea). Primer pairs used are listed in Table S8.3. Initially, the region encoding *HDA6* was amplified using the primers *HDA6.RPA/HDA6.LPA*, and internal sequencing reactions were performed using primers: *HDA6.LPA*, *HDA6.LPB*, *HDA6.LPC*, *HDA6.RPA*, *HDA6.RPB*, *HDA6.RPC*, *HDA6.RPD*, *HDA6.RPE* and *HDA6.RPF*. To fill gaps in the resulting *HDA6* sequence the amplification and sequencing reactions

were performed using the following primer pairs: HDA6.RPA/HDA6.LP2A, HDA6.RPB/HDA6.LP2B, HDA6.RP2C/HDA6.LP2C and HDA6.RP2D/HDA6.LP2D. The *HDA6* gene was sequenced from three independent plants from each of the three accessions (*Ler-0*, *Cvi-0* and the *hda6* (*sil1/not*)). Sequence are deposited in GenBank data library under accession numbers: EU502909 (*HDA6 Ler-0*), EU502910 (*hda6 Cvi-0*), EU502911 (*hda6* from *sil1/not* mutant).

Acknowledgements

The authors thank M. Koornneef (Wageningen UR, the Netherlands), J. Keurentjes (Wageningen UR, the Netherlands), J. Maloof (UC Davis, CA, USA), I. Furner (University of Cambridge, UK) and I. Wright (Macquarie University, Sydney, Australia) for providing materials or software-tools. We thank M. Koornneef and H. Poorter (Utrecht University, the Netherlands) for discussions on the manuscript.

Supporting information

- **Figure S8.1:** Localization of BAC F28D6 on chromosomes of Col-0
- **Figure S8.2:** The low chromatin compaction of *Cvi-0* is dominant in heterozygotes.
- **Figure S8.3:** High light intensity rescues the formation of NOR chromocenters in *Cvi-0*.
- **Figure S8.4:** The *Cvi-0* NOR phenotype is dominant in crosses.
- **Table S8.1:** Names, abbreviations, stock numbers, and heterochromatin index of 21 *Arabidopsis* accessions used in this study.
- **Table S8.2:** Geographic and environmental parameters on the collection sites of the used *Arabidopsis* accessions and the correlations with HX.
- **Table S8.3:** DNA primers used for PCR amplification of the *HDA6* gene from *Arabidopsis thaliana* genomic DNA.

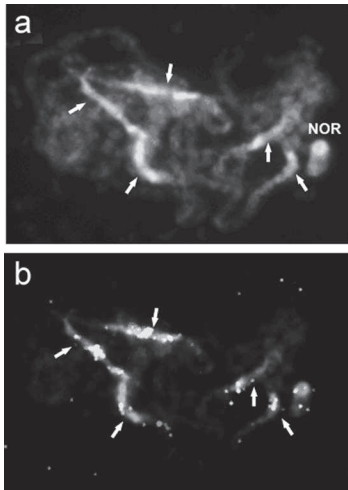


Figure S8.1: Localization of BAC F28D6 on chromosomes of Col-0. (See Color Supplement for full color version of this figure) **a:** DAPI staining and **b:** FISH image of pachytene chromosomes hybridized with a pericentric BAC F28D6 probe showing signals (green) to the pericentric region of all chromosomes in Col-0. Arrows depict centromeres. Red signal indicates euchromatic BAC T1J1 in chromosome arm 4S. NOR = Nucleolar Organizing Region.

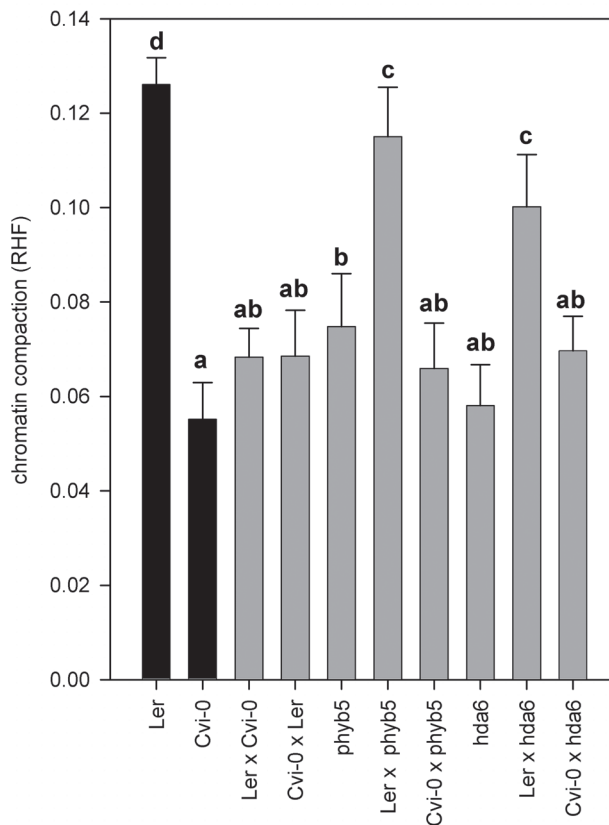


Figure S8.2: The low chromatin compaction of Cvi-0 is dominant in heterozygotes. Chromatin compaction (RHF) of *phyb5* and *hda6* and F_1 progeny from a cross between *hda6* and *phyb5* (grey) and the NIL-parents (black). Error bars represent standard errors. $13 < n < 40$; No overlapping letters indicate a significant difference ($p < 0.05$). Where applicable, crosses were checked with the SSLP markers polymorphic between Ler and Cvi-0; NGA128 and NGA162 (Bell & Ecker, 1994) with a standard PCR procedure.

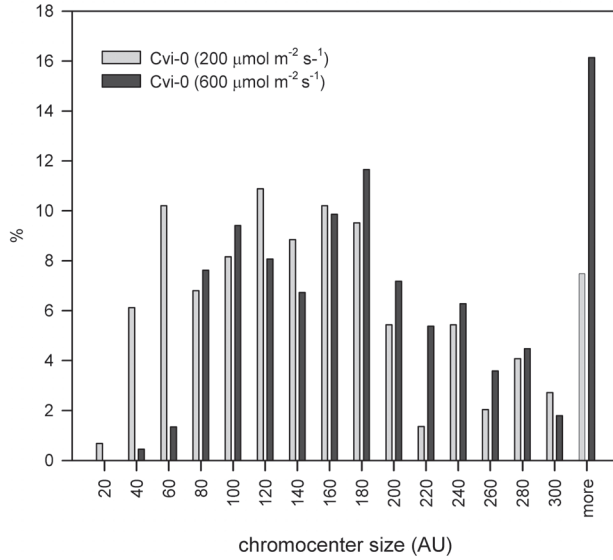


Figure S8.3: High light intensity rescues the formation of NOR chromocenters in Cvi-0.

Distribution of size per individual chromocenter, in Arbitrary Pixel Units (AU) of Cvi-0 plants grown under normal ($200 \mu\text{mol m}^{-2} \text{s}^{-1}$) and high light ($600 \mu\text{mol m}^{-2} \text{s}^{-1}$) conditions. The highest class for both distributions is defined on a 10% cutoff.

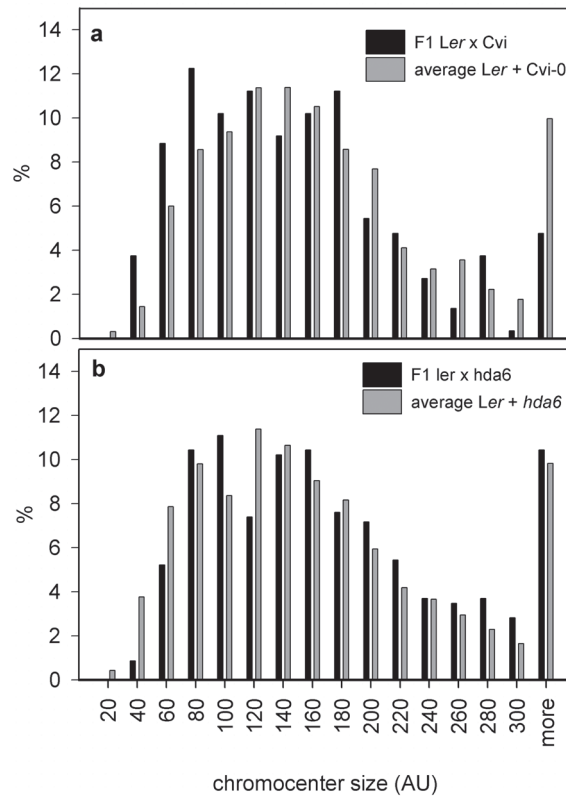


Figure S8.4: The Cvi-0 NOR phenotype is dominant in crosses.

Distribution of sizes per individual chromocenter in Arbitrary Pixel Units (AU) of heterozygous F_1 plants derived from crosses between a: *Ler* x *Cvi-0* and b: *Ler* x *hda6* and combined, superimposed data of the parental individuals. The highest class for both distributions is defined on a 10% cutoff.

Table S8.1: Names, abbreviations, stock numbers and HX of 21 Arabidopsis accessions used in this study. Plants were grown in short-day control conditions ($200 \mu\text{mol m}^{-2} \text{s}^{-1}$). Standard errors never exceeded 0.13.

Name	Abb.	Stock no.	HX
Bensheim-0	Be-0	N964	0.80
C24	C24	N906	0.76
Canary Islands-0	Can-0	N1064	0.49
Cape Verde Island-0	Cvi-0	N902	0.19
Chisdra	Chi-1	N1074	0.83
Columbia-0	Col-0	N1092	0.84
Helsinki-1	Hel-1	N1222	0.85
Hiroshima-1	Hir-1	JSW102	0.68
Moss			0.76
Kärnten-0	Kä-0	N1266	0.76
Kashmir-2	Kas-2	N903	0.90
Knox-10	Knox-10	N22566	0.83
Kondana-Tady	Kond	N916	0.92
Landsberg-0	Lan-0	N1298	0.85
Martuba / Cyrenaika-0	Mt-0	N1380	0.67
Niederzenz-1	Nd-1	N1636	0.91
Pakistan-1	Pak-1	JW105	0.74
RLD	RLD-1	N913	0.87
Shahdara	Shah	N929	0.87
Stange			0.90
Wassilewskija-2	Ws-2	N915	0.78

Seeds were obtained from the Nottingham Arabidopsis Stock Centre (NASC), (<http://arabidopsis.info/>), except accession: Hir-1 and Pak-1, which were obtained from the Sendai Arabidopsis Seed Stock Center (SASSC), Miyagi University of Education, Japan (<http://www.brc.riken.jp/lab/epd/Eng/index.shtml>). Accessions; Lan-0, Moss and Stange (Stenøien et al., 2005) were a gift from M. Koornneef (Wageningen University the Netherlands).

Table S8.2: Geographic and climate parameters on the collection sites of the used *Arabidopsis* accessions and the correlations with HX

The latitudes of the collection sites of individual accessions were taken from the Natural Variation in *Arabidopsis thaliana* (NVAT) website: (<http://dbsgap.versailles.inra.fr/vnat/>) unless stated otherwise.

Environmental data for all collection sites (0.5° latitude \times 0.5° longitude surface land area plots) of the used *Arabidopsis* accessions were extracted from the *climate baseline data* from the Intergovernmental Panel on Climate Change (IPCC) Data Distribution Centre (DDC) (http://ipcc-ddc.cru.uea.ac.uk/obs/get_30yr_means.html), using a data subtraction tool kindly provided by I. Wright (Macquarie University, Sydney, Australia). The data presented in this table is mean annual data that were calculated from monthly averages collected over a 30 years period (1961-1990; New *et al.*, 1999).

Alt = altitude; Long. = longitude; Lat. = latitude; Cloud = cloud coverage; Diurnal = diurnal temperature range; Tmax = maximal temperature; Tmin = minimal temperature; Tmean = average temperature; Prec = precipitation; Irrad. = Irradiation; Vapour = vapor pressure. Wet d = wet day frequency. Corr = correlation with HX

	Alt	Long	Lat	Cloud	diurnal	Tmax	Tmean	Tmin	Prec	Irrad ^f	Vapour	Wet d
	m	$^\circ$ W	$^\circ$ N	%	$^\circ$ C	$^\circ$ C	$^\circ$ C	$^\circ$ C	mm day ⁻¹	$\mu\text{mol.m}^{-2}\text{s}^{-1}$	hPa	day
Be-0	150	8.37	49.41	71.58	8.83	14.58	10.15	5.75	1.89	507.65	9.83	14.46
C24 ^d	150	8.24	40.20	47.75	7.53	19.43	15.65	11.91	1.92	711.00	13.18	8.42
Can-0 ^a	1250	-15.3	28.00	53.83	6.65	19.63	16.28	12.98	1.15	756.71	12.97	8.97
Chi-1	150	35	54.00	69.08	7.99	9.34	5.34	1.34	1.73	500.79	8.13	15.05
Col-0	50	15.15	52.44	68.58	8.11	12.82	8.73	4.69	1.50	501.94	9.39	13.70
Cvi-0 ^a	1200	-24.4	14.90	34.71	14.77	34.76	27.35	19.99	1.16	982.17	18.83	6.30
Hel-1 ^a	50	25	60.00	68.54	7.70	8.41	4.56	0.70	1.79	447.99	7.77	15.18
Hir-1 ^a	50	33.2	34.50	40.67	10.10	23.40	18.33	13.30	1.41	824.89	13.49	6.21
Ka-0	950	14.31	46.25	60.17	8.18	11.97	7.85	3.77	4.62	593.34	8.98	13.89
Kas-1	1550	77	34.00	51.58	11.67	6.35	5.08	-5.33	1.25	752.14	0.58	5.23
Knox-1		-88.63	41.58	63.92	11.23	14.18	8.54	2.94	2.45	602.10	9.55	10.52
Kond	1050	68.5	38.48	49.00	13.79	21.47	14.55	7.67	1.22	739.96	9.33	7.16
Lan-0 ^e	50	15.5	52.50	67.33	8.18	12.83	8.72	4.63	1.46	508.03	9.42	13.66
Moss ^c	70	10.42	59.28	64.33	7.23	9.88	6.23	1.53	2.47	473.00	8.15	15.00
Mt-0	150	22.46	32.34	34.17	11.38	23.99	18.27	12.61	0.97	901.43	14.12	4.62
Nd-1	250	8.02	50.28	73.58	7.93	12.69	8.70	4.74	1.95	481.76	9.17	15.04
Pak-1 ^b		73.4	33.90	38.08	13.25	26.33	19.68	13.08	3.07	832.50	13.65	8.45
RLD-1	50	5.3	52.15	76.25	7.85	13.20	9.26	5.34	2.19	447.48	10.21	15.92
Shah	3400	71	37.00	50.83	10.47	7.21	1.94	-3.28	1.58	738.06	0.28	8.53
Stange ^c	120	11.14	60.30	61.33	8.46	8.38	4.14	-0.08	2.00	449.00	7.22	15.37
Ws-2	150	30.38	52.13	67.08	8.62	11.19	6.88	2.57	1.66	522.50	8.63	13.71
Corr ^g				0.82 ***	-0.68 ***	-0.75 ***	-0.76 ***	-0.64 **	0.26 ns	-0.95 ***	-0.43 ns	0.88 ***

Footnotes:

- ^a No climate data was available on the 0.5° latitude × 0.5° plots for these locations. Therefore average values of surrounding plots were used.
- ^b Geographic characteristics were obtained from El-Lithy *et al.*, (2004).
- ^c Geographic characteristics were obtained from Stenøien *et al.* (2005).
- ^d C24 most likely originates from the Portuguese accession; Coimbra (Schmid *et al.*, 2006). We used the Coimbra geographic characteristics (NVAT) in our analysis.
- ^e We used the original Landsberg wild type accession in our analysis which did not differ in HX and RHF from mutant Landsberg *erecta*.
- ^f Total irradiation was converted from W m⁻² to μmol m⁻² s⁻¹ as average for 24 hours using the conversion factor 4.57 for the PAR spectrum (400-700 nm) as described in Jones (1983).
- ^g Correlation; 2-tailed Pearson correlation coefficient; * $p < 0.05$; ** $p < 0.01$; *** $p < 0.001$; ns = non significant. 2-tailed Pearson correlation coefficient

Table S8.3: DNA primers used for PCR amplification of the HDA6 gene from *Arabidopsis thaliana* genomic DNA.

Primer name	Primer Sequence (5' to 3')
HDA6.LP.A	ATTGCAATCGGTTTTCTTCG
HDA6.LP.B	CCGACATTATCATATGGCAAAA
HDA6.LP.C	ACTCCATCTCCATGGTGGAC
HDA6.LP2A	CAGAGAGATGCCGCTTTCG
HDA6.LP2B	CAGAAGAACATGAAGAAGTTC
HDA6.LP2C	GCAACTGAAGTACAATGACC
HDA6.LP2D	GTTTAGTAACAGCTTCAATGG
HDA6.RP.A	GCTGATTTCCGCTGCTTCTTC
HDA6.RP.B	AGCTGTGCCCACAACCTCCTA
HDA6.RP.C	GGGCTTCACCATGCTAAGAA
HDA6.RP.D	GTCCACCATGGAGATGGAGT
HDA6.RP.E	GGCCAGATTATACGCTTCA
HDA6.RP.F	CTGGAGTGGAAGTGGACTT
HDA6.RP2C	GAGAATGGTTTTCTACATTGC
HDA6.RP2D	GGAACACGTTGCTGGAAC

Low light exposure disrupts chromatin organization in *Arabidopsis thaliana*

Martijn van Zanten^{1*}, Federico Tessadori^{2*§}, Fionn McLoughlin^{1, 2§}, Frank F. Millenaar^{1§}, Roel van Driel², Laurentius A.C.J Voeselek¹, Anton J.M. Peeters¹, Paul Fransz^{2#}

* These authors contributed equally to this work

¹ Plant Ecophysiology, Institute of Environmental Biology, Utrecht University, Padualaan 8, 3584 CH Utrecht, the Netherlands

² Nuclear Organization Group, Swammerdam Institute for Life Sciences, University of Amsterdam, Kruislaan 318, 1098 SM Amsterdam, the Netherlands

§Present addresses:

FT: Cardiac Development and Genetics group, Hubrecht Institute for Developmental Biology and Stem Cell Research, Uppsalalaan 8, 3584 CT Utrecht, the Netherlands.

FMCL: Section of Plant Physiology, Swammerdam Institute for Life Sciences, University of Amsterdam, Kruislaan 318, 1098 SM Amsterdam, the Netherlands.

FFM: De Ruiter Seeds, Leeuwenhoekweg 52, 2660 BB Bergschenhoek, the Netherlands.

Abstract

Development and acclimation processes to the environment are associated with large-scale changes in chromatin compaction in *Arabidopsis thaliana* interphase nuclei. Here, we studied the effects of light signals on chromatin compaction and establish that low light-intensities induce a reversible reduction in chromatin compaction. Next to a reduction in overall light intensity, light quality signals, relevant for natural canopy shade triggers a reduction in chromatin compaction. Data acquired by mutant- and ectopic gene expression analysis, studying natural variation among accessions and by protein abundance analysis, all point to cryptochrome 2 (*cry2*) as a positive regulator of low light-induced chromatin de-compaction. Phytochrome B (*phyB*) has contrasting effects on the control of light mediated-chromatin compaction between accessions Columbia-0 and Landsberg *erecta* and is a positive regulator of *cry2* protein levels. Together, our data indicate that large-scale chromatin compaction is regulated by the light environment.

Introduction

Light plays a crucial role in numerous plant developmental processes including germination, floral transition and senescence (Chen *et al.*, 2004; Sullivan & Deng, 2003). To deal with variable light conditions, such as light intensity, spectral quality, light direction and photoperiod, plants have developed signaling mechanisms involving light-sensitive receptors. Three major photoreceptor families are known in *Arabidopsis thaliana*: phytochromes, cryptochromes and phototropins (reviewed in Sullivan & Deng, 2003; Chen *et al.*, 2004; Franklin *et al.*, 2005; Casal & Yanovsky, 2005; Lorrain *et al.*, 2006). Phytochromes (e.g. *phyA-E*) mainly mediate in red- and far-red light perception, while cryptochromes (*cry1*, *cry2*) and phototropins (*phot1*, *phot2*) are involved in the perception of blue-light and UV-A. *Cry2* is constitutively located in the nucleus (Guo *et al.*, 1999; Kleiner *et al.*, 1999) and is associated with chromatin (Cutler *et al.*, 2000, Yu *et al.*, 2007, 2009). *Cry1* is also present in the nucleus but only during darkness. In response to light *cry1* is exported to the cytosol, where it exerts different activities (Yang *et al.*, 2000; Wu *et al.*, 2007). In contrast to *cry1*, phytochromes are located in the cytosol during darkness and are translocated to the nucleus upon light activation (Chen *et al.*, 2005; Fankhauser & Chen, 2008). Unlike the other photoreceptors, phototropins have not been detected in the nucleus, but reside in the plasma membrane (Sakamoto & Briggs, 2002). The nuclear localization of cryptochromes and phytochromes indicates specific functions related to gene transcription. Indeed, these photoreceptors mediate light-stimulated degradation and stability of several transcription factors (Casal & Yanovsky, 2005, Lorrain *et al.*, 2006; Castillon *et al.*, 2009), leading to modifications in gene expression profiles (Ma *et al.*, 2001). In addition, physical interactions have been demonstrated not only between phytochromes and cryptochromes (Ahmad *et al.*, 1998; Mas *et al.*, 2000), but also between photoreceptors and for example, the E3 ubiquitin ligase, CONSTITUTIVE PHOTOMORPHOGENIC-1 (*COP1*), which plays a role in the degradation of transcription factors (Yi & Deng, 2005).

It is assumed that light-mediated transcriptional control involves chromatin remodeling (Casal, 2005; Lorrain *et al.*, 2006). For example, blue light-activated cry2 releases DEETIOLATED1 (DET1)-mediated inhibition of non-acetylated core histone H2B, permitting transcriptional activation (Benvenuto *et al.*, 2002).

Previously, we demonstrated large-scale reduction of chromatin compaction during floral transition, which is controlled by cry2 (Tessadori *et al.*, 2007a). The phenomenon is photoperiod-independent, since in short day-grown plants the delayed floral transition was accompanied by a similar delay in the reduction of chromatin compaction. Moreover, we found that *phyb* mutants show a constitutively lower level of chromatin compaction under standard light conditions (Chapter 8). Both lines of evidence indicate that light controls large-scale chromatin organization. For both floral transition and light control of chromatin compaction, natural variation among *Arabidopsis* accessions was observed (Tessadori *et al.*, 2007a; Chapter 8). The reduced chromatin compaction resembled the nuclear phenotype of plants facing stress (protoplastization, *Pseudomonas syringae* infection; Pavet *et al.*, 2006; Tessadori *et al.*, 2007b) or progression of development (seedling establishment and leaf maturation; Mathieu *et al.*, 2003; Tessadori *et al.*, 2004). This led to the suggestion that development and responses to the environment are accompanied by large-scale changes in chromatin compaction. Here, we address the question how light induces changes in chromatin compaction.

The *Arabidopsis* interphase nucleus has proven a valuable system to monitor chromatin compaction. Together with specific epigenetic marks (Naumann *et al.*, 2005), the physical condensation state of the genome constitutes the cytologically-defined nuclear phenotype (Fransz *et al.*, 2003; Tessadori *et al.*, 2004). At the microscopic level, different chromatin condensation degrees can be distinguished. For example, chromosomes display highly condensed heterochromatic domains (chromocenters) and less condensed gene-rich euchromatin loops (Fransz *et al.*, 2002; Tessadori *et al.*, 2004). Chromocenters are conspicuous heterochromatin regions that mainly consist of long, tandemly arranged repetitive DNA elements, which include pericentromeric and satellite repeats and ribosomal DNA (rDNA) genes. These regions are typically enriched in repressive markers such as histones H3 dimethylated at lysine 9 (H3K9Me2) and DNA methylation (5-methylcytosine; Fransz *et al.*, 2006).

Here, we demonstrate that low light-intensities induce a reversible reduction in chromatin compaction. Data obtained by mutant and ectopic gene expression analysis, studying natural variation and protein level analysis all point to a general role of cry2 as positive regulator of low light-induced chromatin de-compaction. Additionally, our study highlights a contrasting effect of phytochrome B (phyB) on light-mediated chromatin compaction between the accessions Columbia-0 and Landsberg *erecta*, but, interestingly also establishes phyB as a positive regulator of cry2 protein levels in both accessions. Our data indicate the involvement of large-scale chromatin compaction regulation triggered by a dynamic light environment.

Results

Light intensity controls chromatin compaction in a reversible manner

Interphase nuclei of *Arabidopsis thaliana* can be classified based on the compaction of their (peri)centromeric repeats. Using 4',6-diamidino-2-phenylindole (DAPI), three types of nuclei; “heterochromatin-rich” (type 1) with 6 to 10 conspicuous, round chromocenters; “intermediate” (type 2) containing elongated or irregularly-shaped chromocenters and; “low content” (type 3) with 1 to 3 chromocenters can be identified (Figure 9.1a-c). Fluorescence *in situ* hybridization (FISH), using probes for centromeric repeat sequences and the transposon-rich pericentromeric region supported this classification, as in type 2 nuclei the pericentromeric repeat regions are dispersed, while the centromeric repeats are condensed. In type 3 nuclei we found dispersion of both repeats sequences, which contrasts to type 1 nuclei, where condensation of all repeat regions was observed (Figure 9.1d-f). We used this classification to monitor chromatin compaction dynamics based on the Heterochromatin index (HX) (Tessadori *et al.*, 2007b; Chapter 8). HX is defined as the fraction of type 1 nuclei over the total number of nuclei. The HX in leaf mesophyll nuclei is ~0.85 in the standard laboratory accessions Columbia-0 (Col-0) and Landsberg *erecta* (Ler) under saturating light intensities of 200 $\mu\text{mol m}^{-2} \text{s}^{-1}$ photosynthetic active radiation (PAR). In Col-0 petiole and root cells the HX is lower (0.4% and 0.6% respectively).

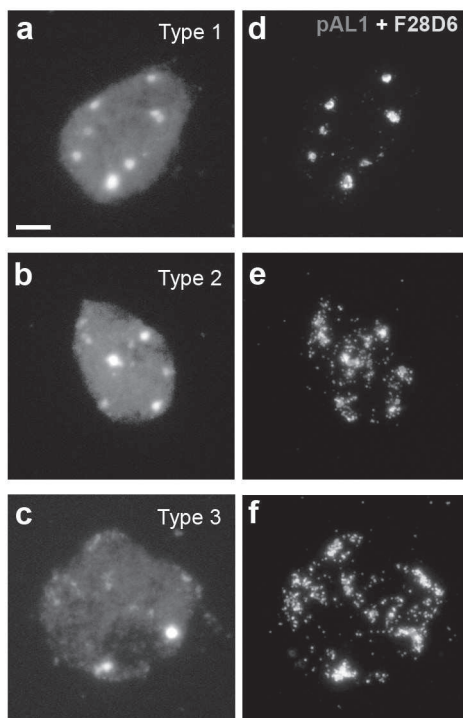


Figure 9.1: Cytogenetic analysis of *Arabidopsis thaliana* Col-0 mesophyll interphase nuclei. (See Color Supplement for full color version of this figure) **a-c:** 4',6-diamidino-2-phenylindole (DAPI) stained nuclei. **a:** type 1 nuclei have 6-10 conspicuous, round chromocenters, **b:** type 2 displays an intermediate phenotype, consisting of elongated chromocenters and irregularly-shaped regions of enhanced DAPI staining, **c:** type 3 nuclei have few and small chromocenters. **d-f:** FISH signals for 180 bp centromeric tandem repeat (pAL1; red signal) and transposon-rich pericentromeric regions (BAC F28D6; green signal). **d:** In type 1 nuclei both probes give a condensed signal localized at chromocenters. **e:** In type 2 nuclei, F28D6 is dispersed, while the 180 bp repeat is still condensed at the chromocenters, illustrating the intermediate state. **f:** In type 3, both centromeric and pericentric sequences are dispersed. Bar = 5 μm .

Previously, we showed that light controls chromatin compaction in *Arabidopsis* (Tessadori *et al.*, 2007a; Chapter 8). To learn how chromatin dynamics is controlled by light, we transferred Col-0 to reduced PAR levels (from 200 $\mu\text{mol m}^{-2} \text{s}^{-1}$ to 15 $\mu\text{mol m}^{-2} \text{s}^{-1}$) without changing the spectral quality (Supporting Information Figure S9.1; Table S9.1). This differs from the conditions in Chapter 8, where plants were grown under constitutive light conditions.

Notably, we observed a gradual decrease of HX over time under low light conditions (4 days; 96 h), whereas under control light conditions HX remained constant (Figure 9.2a). This was confirmed by quantification of chromocenter density, using the Relative Heterochromatic Fraction (RHF; Soppe *et al.*, 2002), that showed a significant ($p < 0.01$) reduction after 96 h of low light treatment (Figure 9.2c). Continuation of low light intensity after 96 h did not lead to a further reduction of HX in Col-0 (Figure 9.2b). During low light-induced chromatin de-compaction, the fraction of type 3 nuclei increased whereas the fraction of type 2 nuclei first showed an increase until ~48 h and then decreased up to 96 h (Figure 9.2a). This suggests that type 2 reflects a transient and true intermediate phenotype.

Remarkably, re-establishment of control light conditions following 96 h of low light treatment, resulted in a gradual increase of the HX to standard levels (Figure 9.2b). Similar observations were made for *Ler*, however, the low light-induced HX reduction was less severe compared to Col-0 (Figure S9.2). Similar to leaf mesophyll nuclei, petioles and roots also showed a HX reduction after 96 h shading (relative reduction; 0.54 and 0.35 respectively), suggesting that the low light signal is transported throughout the plant.

Together, these data demonstrate that low light intensity levels influence chromatin compaction. No significant changes in HX were observed in plants grown in control light conditions, harvested at the beginning and the end of the dark period (night). This suggests that signaling of low light is under control of gating via the circadian clock. Moreover, the HX of plants grown in long day conditions (16 h photoperiod) was not significantly different from the standard short day-grown plants, before and after 96 h of low light treatment (data not shown), suggesting that chromatin compaction is not controlled by photoperiod length. We previously showed reversible HX reduction prior to bolting and floral induction, which was absent in *cry2* mutants (Tessadori *et al.*, 2007a). Therefore, the low light-induced reduction in HX observed here could be associated with (early) floral transition. However, since Col-0 plants showed even delayed flowering after 96 h of low light treatment ($p < 0.001$; appearance of the flower buds; 2.6 days and flower opening 3.1 days later) this is not likely. Similar results were obtained for *Ler*. This is in agreement with Dorn *et al.* (2000), who also observed delayed flowering after shading. This indicates that light-mediated control of chromatin compaction is not *per se* associated with floral transition.

Spectral light quality controls chromatin compaction

In natural conditions, functional signals of shade conditions are an overall reduction in photosynthetic active radiation (PAR), a reduction in the blue-light component and a reduced red-to-far red (R/Fr) ratios (reviewed in Vandenbussche *et al.*, 2005;

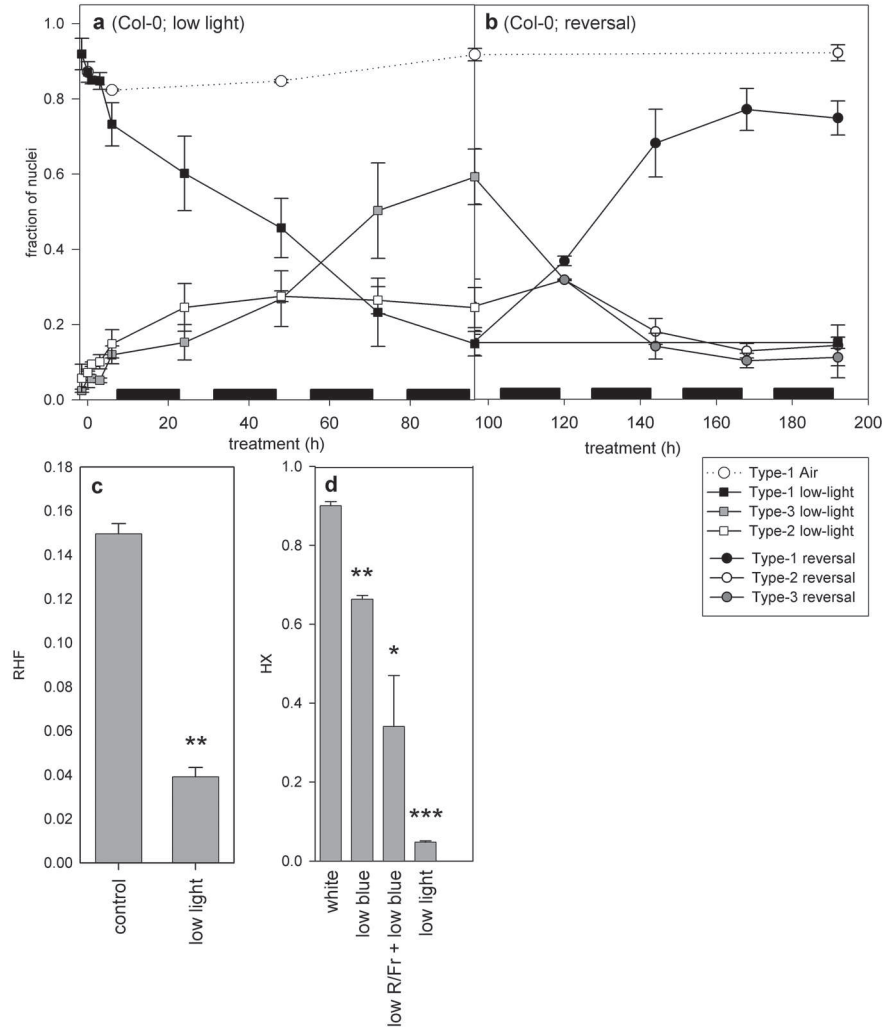


Figure 9.2: Light quantity and -quality controls chromatin compaction. Fraction of type 1, -2 and -3 nuclei (Figure 9.1) in Col-0 during **a**: 4 days (0 h to 96 h) of low light treatment ($200 \mu\text{mol m}^{-2} \text{s}^{-1}$ to $15 \mu\text{mol m}^{-2} \text{s}^{-1}$; squares) and **b**: after return to control light conditions ($200 \mu\text{mol m}^{-2} \text{s}^{-1}$; 96 to 192 h; circles). Plants that were kept in low light conditions during the whole experimental period are shown as black squares and those kept in control light conditions are depicted by white circles and dotted lines. Black horizontal bars indicate the dark periods. $n \geq 2$. **c**: Relative Heterochromatin Fraction (RHF) of Col-0 nuclei exposed to low light intensities ($15 \mu\text{mol m}^{-2} \text{s}^{-1}$) for 96 h in short-day conditions. $n \geq 31$. **d**: HX of Col-0 plants after 96 h treatment with different light-qualities. Conditions were: control filter, indicated as “white light” and correspond to $\sim 100 \mu\text{mol m}^{-2} \text{s}^{-1}$. Low blue-light (yellow filter) and spectral-shade (low- R/Fr + low-blue; green filter). Low light treatment consisted of spectral neutral shading by reducing PAR to $15 \mu\text{mol m}^{-2} \text{s}^{-1}$. $n \geq 3$. For light spectra and wavelength quantification see Figure S9.1 and Table S9.2). Error Bars represent SE in all panels. Significance levels; * $p < 0.05$, ** $p < 0.01$, *** $p < 0.001$, 2-tailed Student’s T-test, compared to control (c) or white light (d).

Franklin, 2008). Our spectral neutral low light treatment reduces the blue-light component and the total PAR, but not the R/Fr ratio (Figure S9.1; Table S9.1). To test the functional importance of blue light wavelengths in the low light response and to test if R/Fr signals can influence chromatin compaction, we dissected the light signal into these different components using colored filters (Figure 9.2d). Total PAR was kept between 90 and 115 $\mu\text{mol m}^{-2} \text{s}^{-1}$, which is sufficient for Col-0 to saturate the HX (Chapter 8). Both low blue (yellow filter) and spectral shade (low blue + low R/Fr; green filter) induced a significant reduction of the HX in Col-0. Since spectral shade led to a stronger reduction than low blue light-shading only, we conclude that both blue light and the R/Fr ratio are important signals controlling chromatin compaction. However, none of these spectral treatments resulted in a reduction in HX as strong as spectral neutral low light, highlighting that perception of total PAR as an important factor in controlling chromatin compaction.

Photoreceptors control chromatin compaction in a genetic background-dependent manner

Because multiple wavelengths influence HX (Figure 9.2d), we considered if and which photoreceptor proteins are involved in the control of chromatin compaction. We evaluated the HX after 96 h of low light treatment in a selection of photoreceptor mutants in the Col-0, *Ler* or *Ws-2* genetic backgrounds. In agreement with the observation in Col-0 (Figure 9.1d), *Ler* and *Ws* wild types also responded to low blue and to spectral shade signals (Figure S9.3).

The relative HX reduction after 96 h low light treatment in *phot1* (*Ler*), *phot2* (*Ws*) mutants and *phot1 phot2* (*Ler/Ws*) double mutant was not significantly different from their wild type backgrounds (Figure 9.3a). This suggests that phototropins are not involved in the response. Low light-mediated HX reduction in cryptochrome mutants (*cry1*, *cry2*) in the Col-0 genetic background, was significantly less ($p < 0.05$ and $p < 0.001$, respectively) than in the wild type (Figure 9.3a). In addition, ectopic expression of *cry2* (driven by the 35S CaMV promoter) resulted in a 19% higher HX after low light treatment (Figure 9.3a). Apparently, cryptochromes are required for low light-induced reduction of chromatin compaction in Col-0 and *Ws-2*. However, we observed no difference in HX reduction in *cry* mutants in a *Ler* background (*cry2* mutant, *cry1 cry2* double mutant; Figure 9.3a). Moreover, the quadruple mutant lacking all dedicated blue light photoreceptors (*cry1 cry2 phot1 phot2*) was not significantly different from wild type *Ler* (Figure 9.3a). This suggests that the effect in *Ler* is masked, because *Ler* is relatively insensitive compared to Col-0 for low light-mediated HX reduction (Figure S9.2). Alternatively, cryptochromes are not involved in the low light-mediated HX reduction in the *Ler* genetic background.

Low light-mediated HX reduction in the *phyb9* mutant in Col-0 was significantly less ($p < 0.001$) than in the wild type (Figure 9.3b). In sharp contrast, *phyb5* and also *phya*, both in the *Ler* genetic background, showed an increase in the chromatin compaction after low light treatment ($p < 0.001$ and $p < 0.05$, respectively; Figure 9.3b). This effect was confirmed by the double *phya phyb* mutant (Figure 9.3b). This suggests that at least phyB has opposite effects in Col-0 and *Ler*. To test for involvement of PhyC-E,

we examined the chromophore-deficient mutant *long hypocotyl2/genome uncoupled3* (*hy2/gun3*) which has reduced levels of active phytochromes (Kohchi *et al.*, 2001). This, and also the quadruple *phy-abde* mutant, showed a mild HX reduction after low light treatment, similar to *Ler* wild type (Figure 9.3b). This suggests that PhyD, PhyE, or both, act antagonistically to PhyA and PhyB. We confirmed this for *phyB* by showing that both *phyb phyd* and *phyb phye* double mutants complemented the enhanced effect of the *phyb* mutant on low light-induced HX reduction, to a level indistinguishable from wild type *Ler* (Figure 9.3b).

The HX increase in the *phyb5* mutant after low light treatment provides a platform to study whether cryptochromes in *Ler* are involved in light mediated control of chromatin compaction. The *cry1 phyb* double mutant had a strong relative HX reduction, comparable to *phyb5* (Figure 9.3c). In contrast, the *cry2 phyb* mutant had a phenotype comparable to *Ler* (Figure 9.3c). Together, these results indicate that *cry2* acts as positive regulator of low light-induced HX reduction in *Ler*, similar to its role in *Col-0* and *Ws*.

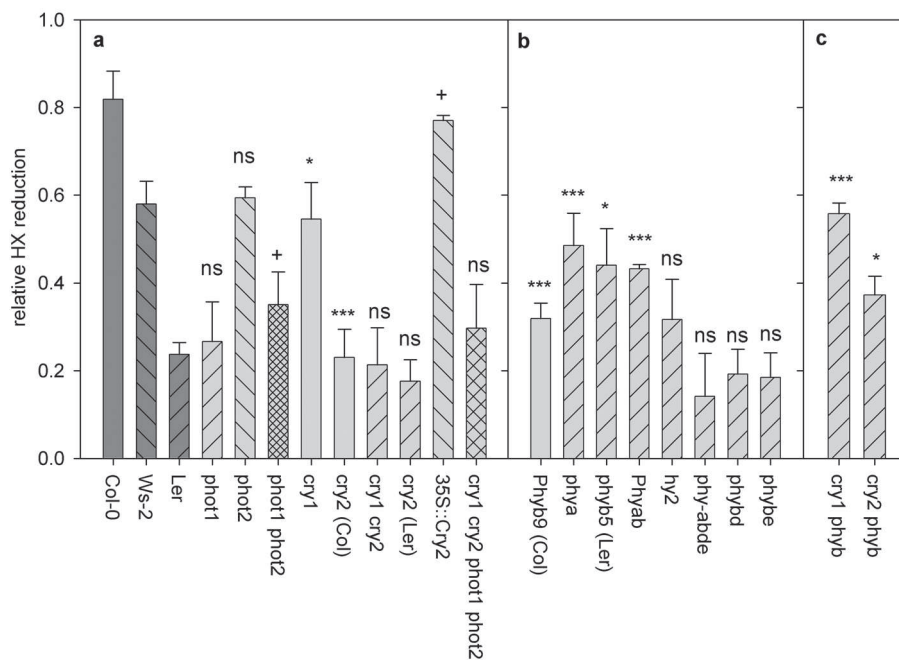


Figure 9.3: Involvement of photoreceptors in low light-induced reduction of chromatin compaction. Relative reduction of HX to 96 h low light treatment ($200 \mu\text{mol m}^{-2} \text{s}^{-1}$ to $15 \mu\text{mol m}^{-2} \text{s}^{-1}$) in **a**: *phototropin* and *cryptochrome* mutants, **b**: *phytochrome* mutants and **c**: *phytochrome b cryptochrome* double mutants. Mutants are in the *Col-0* (bars with no fill), *Ws-2* (back-dashed bars) or *Ler* (forward-dashed bars) genetic background. Mutants in a mixed *Ws/Ler* genetic background have hived bars. Wild type levels of relative HX reduction are shown in panel **a** (dark grey bars). Error Bars represent SE in all panels. $n \geq 2$. Significance levels; ns = non significant, * $p < 0.05$, ** $p < 0.01$, *** $p < 0.001$, 2-tailed Student's T-test, compared to wild types.

CRY2 protein abundance correlates to chromatin compaction

Transient decondensation of chromatin domains during floral transition was absent in *cry2* mutants in both Col-0 and *Ler* genetic background (Tessadori *et al.*, 2007a). Moreover, the natural accession Cape Verde Islands-0 (Cvi-0), which in contrast to Col-0 and *Ler* exhibits stable *cry2* protein levels under short-day conditions (El-Assal *et al.*, 2001), typically shows a low HX compared to other accessions (Chapter 8). Similarly, our analyses demonstrated that *cry2* mutants (in Col-0 and *Ler*) and *cry2* overexpression (in *Ws-2*) prevented and enhanced low light-induced reduction of HX respectively (Figure 9.3a). Together, this implies that incident *cry2* protein levels determine the chromatin compaction state.

We visualized *cry2* protein levels by Western-blot analysis and observed consistently higher *cry2* levels in plants exposed to low light in short day conditions (Figure 9.4a). The enhanced *cry* abundance after 3 h shows that low light enhances or stabilizes *cry2* protein levels over the photoperiod and confirms the existence of a negative correlation between HX and *cry2* abundance. This is consistent with the observation that low light-induced reduction of chromatin compaction is already induced during the first hours after low light application (Figure 9.2a).

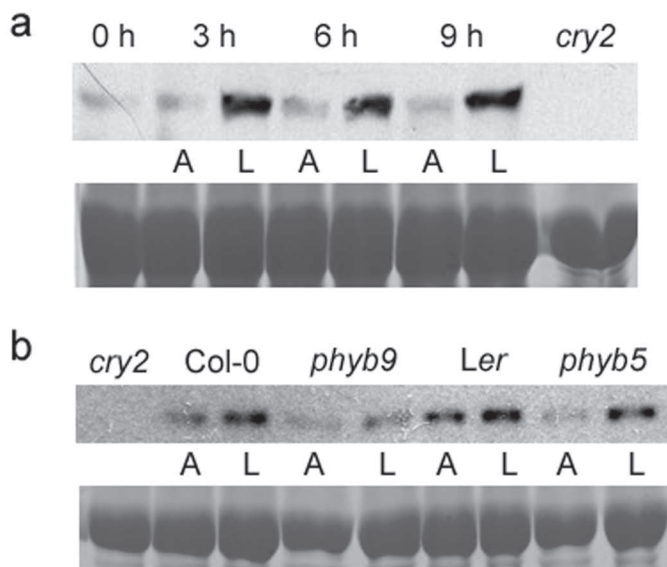


Figure 9.4: Low light treatment enhances *cry2* protein abundance. a.b: Western blot analysis of plants in control light conditions (A: $200 \mu\text{mol m}^{-2} \text{s}^{-1}$) and low light conditions (L: $200 \mu\text{mol m}^{-2} \text{s}^{-1}$ to $15 \mu\text{mol m}^{-2} \text{s}^{-1}$; induced at the start of the photoperiod ($t = -1.5$ h) using *cry2*-antibody (upper lanes) and loading control (Coomassie brilliant blue; lower lanes) a: Col-0 plants sampled at different times during the photoperiod. b: *phyb* mutants in the Col-0 (*phyb9*) and *Ler* (*phyb5*) genetic backgrounds, sampled at $t = 9$ h after low light treatment. Note that in both panels, the absence of a detectable product in the *cry2* (Col-0) mutant indicates correctness of the identified *cry2* protein.

To dissect if cry2 protein concentration can explain the contrasting effects of low light on HX between *phyb* mutants in Col-0 and *Ler* (Figure 9.3b), we examined the cry2 concentration in these mutants. *Phyb* mutants of both accessions showed reduced cry2 levels in control light conditions (Figure 9.4b). In contrast to Col-0, *Ler* did not exhibit a pronounced difference in cry2 protein levels between low- and control light conditions. However, similarly to Col-0 wild type and the *phyb9* mutant (Col-0 background), *phyb5* (*Ler* background) was able to stabilize cry2 protein levels in low light conditions (Figure 9.4b). This indicates that phyB effects on cry2 protein levels may account for the differential phenotypes observed in *phyb9* and *phyb5* mutants in Col-0 and *Ler* and indicates that cry2 and phyB interact in the control of low light-induced chromatin de-compaction.

Natural variation exists in the rate of expression of low light-induced chromatin reduction

Col-0 and *Ler* varied in the ability to show low light-mediated reduction in chromatin compaction (Figure 9.1, Figure S9.2) and in the ability to stabilize cry2 protein levels under low light conditions (Figure 9.4b). This prompted us to examine natural variation in low light-induced reduction of chromatin compaction in a selected set of accessions, for which we previously showed the existence of variation in HX under standard light conditions (Chapter 8).

The relative HX reduction after 96 h of low light varied from ~80% (Col-0) to 7% (Stange) (Figure 9.5; Table S9.2). Even *Cvi-0*, which shows a typical low HX (0.19) in control light conditions (Chapter 8), displayed a strong relative decrease in heterochromatin content. Unlike the HX at control light conditions (Chapter 8), the relative HX reduction after low light treatment did not correlate to geographic or climatologic parameters (data not shown). This suggests that the chromatin response to low light reduction among accessions is at least partially different from the genetic basis of the variation in constitutive HX (Chapter 8). This is confirmed for instance by *hda6* (*Ler* genetic background) which shows a typical HX reduction in low light conditions (relative reduction 0.54) comparable to wild type, despite that its constitutive HX at control light conditions is very low (Probst *et al.*, 2004; Fransz *et al.*, 2006; Chapter 8). To test if the observed variation in HX after 96 h of low light treatment is saturated we assayed the HX after a prolonged period of 192 h (Figure 9.5). After this prolonged treatment all accessions showed a strongly reduced HX, comparable to Col-0 (Figure 9.5). The observed variation in HX after 96 h of low light treatment thus reflects differences in the rate of reduction. This was confirmed by the existence of a significant negative linear-correlation ($r^2 = -0.52$; $p < 0.02$) between remaining type 1 nuclei after 96 h low light treatment and intermediate type 2 nuclei at 96 h, suggesting that the plants after 96 h of low light treatment are still in the process of reduction.

Finally, we tested if cry2 protein levels could account for the observed differences in the rate of low light-induced reduction of chromatin compaction. We did not observe any differences in CRY2 protein levels in control light nor after 96 h of low light treatment between five strong (Col-0, Can-0, Mt-0, Ws-2 and Be-0) and five weak

responding (Stange, Chi-1, Shah, Ka-0, Hel-1) accessions (Figure 9.6). In fact, the only accession that showed a clear stabilization of cry2 in low light was Col-0, indicating that low light-induced reduction of chromatin compaction cannot be explained by variation in the ability to stabilize cry2 under low light-intensity conditions.

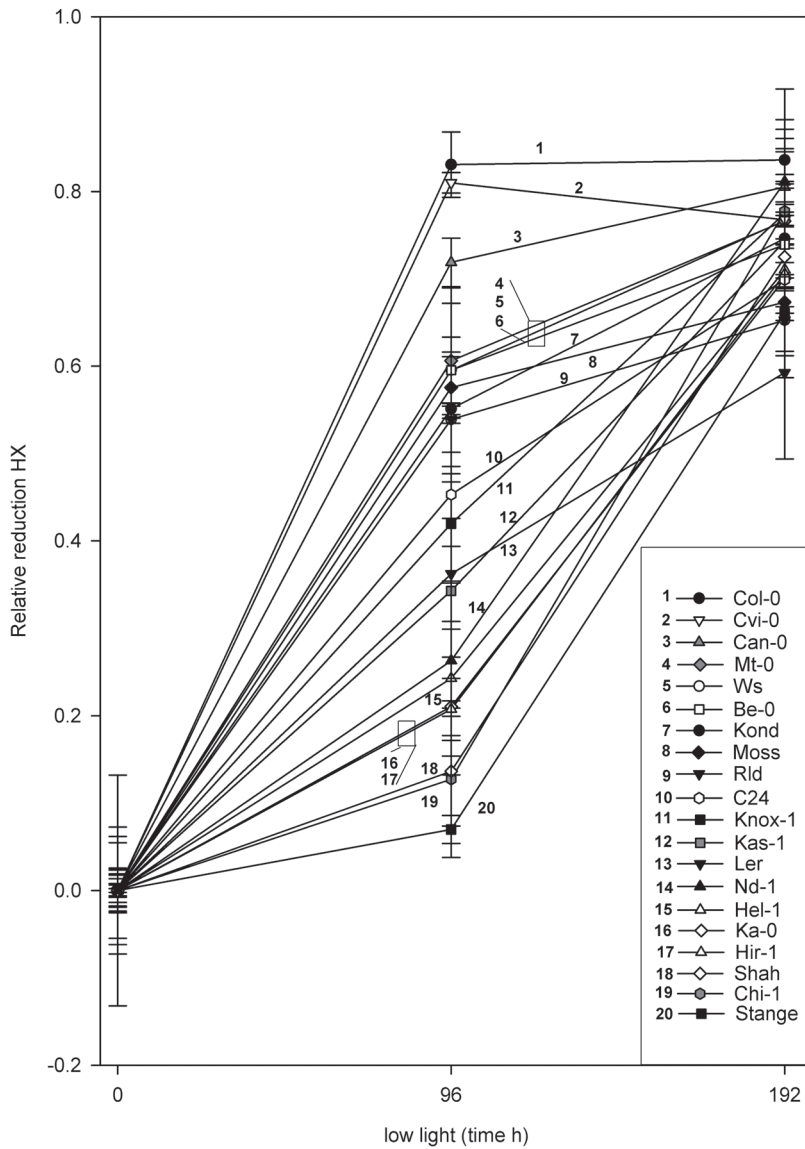


Figure 9.5: Natural variation in the chromatin compaction reduction response to low light treatment. Relative reduction of HX of different *Arabidopsis thaliana* accessions after 96 h and 192 h exposure to low light ($200 \mu\text{mol m}^{-2} \text{s}^{-1}$ to $15 \mu\text{mol m}^{-2} \text{s}^{-1}$). Error bars represent SE, $n \geq 2$.

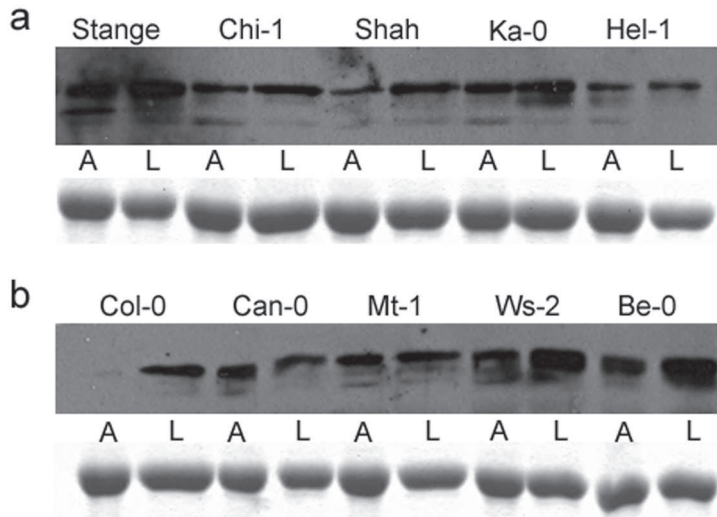


Figure 9.6: Low light treatment enhances cry2 protein abundance specifically in Col-0. Western blot analysis using cry2-antibody (upper lanes) and loading control (Coomassie brilliant blue; lower lanes) of *Arabidopsis thaliana* accessions that had a: mildly reduced chromatin compaction after 96 h low light treatment (Figure 9.5) or b: strong response to 96 h low light conditions (lower panel). “A” indicates control light ($200 \mu\text{mol m}^{-2} \text{s}^{-1}$) and “L” low light conditions ($200 \mu\text{mol m}^{-2} \text{s}^{-1}$ to $15 \mu\text{mol m}^{-2} \text{s}^{-1}$). Low light was applied at the start of the photoperiod ($t = -1.5 \text{ h}$), sampled at $t = 9 \text{ h}$.

Discussion

Many biological processes, such as biotic infestation and development, involve major changes in chromatin organization (Mathieu *et al.*, 2003; Tessadori *et al.*, 2004; 2007a,b; Pavet *et al.*, 2006). Control of light-mediated processes was also proposed to involve chromatin remodeling (Casal, 2005; Lorrain *et al.*, 2006; Tessadori *et al.*, 2007a, Chapter 8). Here, we demonstrate that light reversibly controls chromatin compaction and that the light signals are mediated via the photoreceptor proteins; phyA, phyB, cry1 and cry2.

Cry2 controls light-mediated chromatin compaction

We presented several lines of evidence indicating that cry2 protein abundance controls chromatin compaction. Cry2 has DNA-binding capacities and was demonstrated to decorate mitotic chromosomes (Cutler *et al.*, 2000; Lin & Shalitin, 2003). However, this is not informative of a direct molecular interaction between cry2 and chromatin. Recently, cry2 was shown to regulate transcription of the floral integrator FT via physical interaction with CRYPTOCHROME-INTERACTING BASIC-HELIX-LOOP-HELIX1 (CIB1) (Liu *et al.*, 2008). This transcription factor binds to the G-box of the FT promoter, bringing cry2 activity in connection with chromatin.

A second link between cry2 and chromatin is provided by the interaction of cry2 with the RING finger type E3 ubiquitine ligase (COP1). COP1 represses photomorphogenesis

by targeting light-responsive transcription factors, such as HY5, for proteolysis (Wang *et al.*, 2001; Gyula *et al.*, 2003). Cry2 represses the COP/DET/FUS complex through a physical association with COP1. This interaction between cry2 and the COP/DET/FUS complex is interesting, because DET1 (DEETIOLATED1) was shown to bind non-acetylated core histone H2B, thus maintaining a condensed chromatin state (Benvenuto *et al.*, 2002). Blue light-activated cry2, releases the DET1 block permitting transcriptional activation, which might co-occur with opening of the chromatin as observed under our low light conditions. In cry2 null mutants the cry2-mediated repression of the COP/DET/FUS complex is lost, which is a possible explanation for the absence of chromocenter de-compaction during the low light treatment in this mutant. The role of cry2 in chromatin decondensation may be the same as in photomorphogenesis, where cry2 action is largely restricted to low light conditions (Lin *et al.*, 1998). Accordingly, we observed stabilization of the cry2 protein under low light intensities in short-day conditions, under which cry2 is normally prone to degradation (El-Assal *et al.*, 2001). Additionally, in Chapter 8 we described that Cvi-0 has a constitutive low chromatin compaction under control light conditions. Cry2 in Cvi-0 was shown to be stabilized under short-day photoperiods, compared to Ler (El-Assal *et al.*, 2001), indicating that besides roles for HDA6 and phyB, perhaps cry2 adds to the reduced chromatin compaction phenotype in Cvi-0.

Phytochrome control of chromatin compaction

In Chapter 8, we showed that phyB is a positive regulator of chromatin compaction. Here, we showed by mutant analysis, that phyB also controls chromatin de-compaction to low light intensities. However, the control in Col-0 is opposite to Ler, pointing to the existence of natural allelic variation in phyB signaling with respect to chromatin de-compaction, although no sequence polymorphisms are present between the *phyb* alleles of Col-0 and Ler (Filiault *et al.*, 2008). Loss-of-function mutations in *phyb*, in two independent backgrounds showed that cry2 protein abundance was constitutively reduced in the *phyb* mutant background, indicating that cry2 protein levels are maintained by phyB.

Active cry2 interacts with phyB in specific nuclear speckles (Mas *et al.*, 2000), which may possibly act as “transcriptosomes” (Gyula *et al.*, 2003). Cry2 is rapidly down regulated in blue light (Lin *et al.*, 1998), probably in the same nuclear speckles (Yu *et al.*, 2009). Additionally, COP1 can form nuclear bodies (Wang *et al.*, 2001, Yang *et al.*, 2001) and it has been suggested that cryptochromes, phytochromes and COP1 interact in the nuclear speckles (Yu *et al.*, 2009). This supports our observation that phyB modulates cry2 stability, perhaps by prohibiting cry2 degradation. However, phyB activity cannot solely account for cry2 stabilization, as low light stabilized the remaining cry2 protein in *phyb* mutant backgrounds.

A model for light control of chromatin compaction

The data presented here indicates that low light triggers a reversible reduction of chromatin compaction via cry2 protein stabilization. These data are in agreement with our previous work (Tessadori *et al.*, 2007a), in which we showed that floral

transition-associated reduction in chromatin compaction was absent in the *cry2* mutant background.

Next to this, *phyB* modulates *cry2* protein abundance. We therefore propose that *phyB* affects chromatin compaction via control of *cry2* levels. However, *cry2* is also controlled directly by light, as *cry2* was stabilized by low light intensities independently of *phyB* activity. We cannot exclude that *phyB* has a direct, *cry2*-independent, role in controlling light-mediated chromatin compaction. Mutant analysis indicated that *cry2* is a negative regulator of chromatin compaction in both the Col-0 and *Ler* genetic backgrounds. On the contrary, the data points to natural variation between Col-0 and *Ler* in *phyB* signaling towards chromatin compaction. Based on these data we propose a model on how light-mediated control of chromatin compaction via photoreceptor proteins may be operated (Figure 9.7). We speculate that both *cry2* and *phyB* converge on a Chromatin Protein Complex (CPC) that is functionally responsible for maintenance of chromatin compaction.

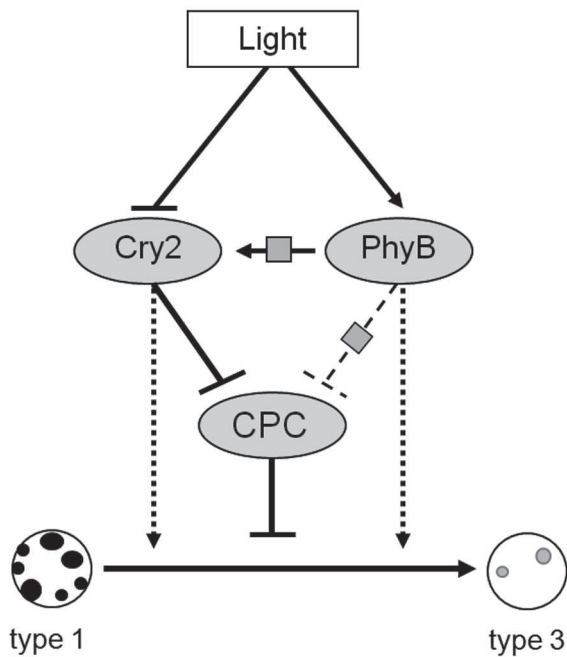


Figure 9.7: A model for light control of chromatin compaction. Light triggers *cry2* degradation, thereby maintaining a condensed chromatin compaction state (type 1 nuclei) via control of a Chromatin associated Protein Complex (CPC) or directly (dashed arrow). *phyB* stabilizes *cry2* protein levels and may have a direct (dashed arrows) effect on chromatin de-compaction (type 1 to type 3), or alternatively, via the same CPC as *cry2* (dashed inhibitory sign). Natural variation in the *phyB* signaling, however, affects the role this photoreceptor has in controlling chromatin compaction (possible points of natural genetic variation are indicated by square boxes).

Materials & Methods

Plant material and growth conditions

The origins of the accessions used are described in Table S9.2. Mutants were either from the Nottingham Arabidopsis Stock Center (NASC) or were a kind gift of authors who described these mutants: *phot1-101* (Liscum & Briggs, 1995), *phot2-5* (Jarillo et al., 2001; Kagawa et al., 2001), *phot1-101 phot2-5* (Ws/Ler; Sakai et al., 2001), *cry1 cry2 phot1 phot2* (in Ws/Ler; Ohgishi et al., 2004), *cry1* (Col; Mockler et al., 1999), *cry2-1* (in Col; Guo et al., 1998), *cry2* (*fha1* in Ler; Koornneef et al., 1991; Guo et al., 1998), *cry1 cry2* (*hy4 fha1* in Ler (Yanovsky et al., 2000), 35S::Cry2 (Lin et al., 1998), *phyb9* (in Col; Reed et al., 1993), *phya201* (N6219; Nagatani et al., 1993), *phyb5* (in Ler; N69; Koornneef et al., 1980), *phya-201 phyb5* (N6224; Reed et al., 1994), *hy2* (N68; Koornneef et al., 1980; Kohchi et al., 2001), *phy-abde* (Franklin et al., 2003), *phyb-1 phyd-2* (Devlin et al., 1999), *phyb phye-1* (Devlin et al., 1998), *phyb5 cry1-1* (Casal & Mazzella, 1998), *phyb5 cry2* (Mazzella et al., 2001).

Plants were grown on a fertilized mixture of potting-soil and perlite (1:2 v/v) as described in Millenaar et al. (2005), at: 20°C; 70% (v/v) relative humidity, 9 h photoperiod of 200 $\mu\text{mol m}^{-2} \text{s}^{-1}$ photosynthetic active radiation (PAR). Pots were daily saturated automatically with tap water at the start of the photoperiod. The long day photoperiod used was 16 h. Twenty-two days old plants, at developmental stage 1.05 to 1.07 (Boyes et al. 2001), were used for all experiments, which is well before the floral transition. Plants used for scoring flowering time were transferred to low light conditions (15 $\mu\text{mol m}^{-2} \text{s}^{-1}$) or long-day regime (16 h photoperiod) 18 d after sowing. After the treatment plants were returned to standard light conditions. Flowering time (number of days) was scored at bolting (appearance of flower buds) and at the time of opening of the first flower.

Light treatment

Plants were transferred to the experimental setups one day before the start of the treatment to allow acclimatization. Treatments always started ($t=0$ h) 1.5 h after photoperiod start, to minimize diurnal and/or circadian effects, except for *cry2* protein level analysis where low light was induced at the start of the photoperiod ($t=-1.5$ h). Reduction of light-intensities consisted of a 90% reduction of the photosynthetic active radiation (PAR; 400-700 nm); from 200 $\mu\text{mol m}^{-2} \text{s}^{-1}$ to 15 $\mu\text{mol m}^{-2} \text{s}^{-1}$ and was accomplished by shading the plants with shade cloth. This did not influence the spectral quality (Figure S9.1; Table S9.1) as checked with a LICOR-1800 spectroradiometer (LI-COR, Lincoln, NE, USA). For colored-filter (Lee filter Andover, United Kingdom) treatments, plants were kept in flow-through aerated boxes, only allowing the filtered top-light to reach the plants. Spectral shade treatment and low-blue were induced by filtering white light through a double layer of Fern-green-filter (Lee filter No. 122) and double layer of yellow filters (Lee filter No. "200 Double CT Blue"), respectively. Both filter treatments also reduced total PAR. Therefore, control plants were shaded with shade cloth to 90 and 115 $\mu\text{mol m}^{-2} \text{s}^{-1}$. For spectra and quantification of wavelength regions of all light treatments used, see Supporting Information Figure S9.1 and Table S9.1.

Sample preparation

Young rosette leaves were harvested, fixed in Carnoy's solution (ethanol/acetic acid 3:1) and stored at -20°C. Each sample consisted of two plants. Spread preparations were made

essentially as described in (Schubert *et al.*, 2001), with a modified enzymatic cell-wall degrading mixture: 0.6% Cellulase R10 (Yakult, Tokyo, Japan), 0.25% Macerozyme R10 (Duchefa, Haarlem, the Netherlands) in 10 mM citrate buffer pH 4.5. Slides were mounted in Vectashield (Vector Laboratories, Burlingame, CA, USA) with 4',6-diamidino-2-phenylindole (DAPI; 2 $\mu\text{g ml}^{-1}$) before observation. For HX calculation, 100-130 nuclei of at least two plants were analyzed.

Measure of Heterochromatin index (HX) and Relative Heterochromatin Fraction (RHF)

HX (Tessadori *et al.*, 2007b) was defined as the percentage of nuclei showing high content of compact chromatin (type 1; Figure 9.1a), represented by conspicuous chromocenters, as opposed to nuclei with less compact chromatin (type 2 or type 3; Figure 9.1a,b). For RHF quantification, automated digital analysis of grey-scale images was carried out with *in house* developed macros in ImagePro-Plus (Media Cybernetics, Silver Spring, MD, USA). RHF, defined as the fluorescence intensity of all DAPI-stained chromocenters relative to the fluorescence of the entire nucleus, was calculated for each sample as described earlier (Soppe *et al.*, 2002; Tessadori *et al.*, 2004). Statistical analysis was 2-tailed Student's T-test.

Fluorescence In Situ Hybridization (FISH)

Plasmid pAL1 (Martinez-Zapater *et al.*, 1986) was used to detect the 180 bp centromeric tandem repeat. BAC F28D6 (GenBank accession No. AF147262) obtained from NASC in pBeloBAC-Kan vector was used for the detection of pericentromeric repeats. 5S rDNA was from (Campbell *et al.*, 1992), 45S rDNA probe was from (Gerlach & Bedbrook, 1979). FISH experiments were carried out essentially as described in (Schubert *et al.*, 2001). The nuclei were counterstained with DAPI (2 $\mu\text{g ml}^{-1}$ in Vectashield, Vector Laboratories) prior to observation. Slides were examined with an Olympus BX6000 epifluorescence microscope (Olympus, Tokyo, Japan) coupled to a CCD camera (Coolsnap FX, Photometrics, Tucson, AZ, USA). After acquisition the images were processed, pseudo-colored and merged using Adobe Photoshop software (Adobe, San Jose, CA, USA).

Western blot analysis

Young Arabidopsis rosette leaves were used. Rosette leaves were snap frozen in liquid nitrogen and stored at -80°C . The plant material was grinded in liquid nitrogen and protein isolation buffer was added (50 mM Tris, pH 7.5, 5 mM EGTA, 5 mM EDTA, 2 mM DTT, 25 mM NaF, 1 mM Na_3VO_4 , 50 mM B-glycerophosphate, complete protease inhibitors (Roche, Mannheim, Germany). The extract was centrifuged for 10 min at 10000 g. Proteins in the supernatant were separated using a 10% acrylamide gel. Goat anti-rabbit conjugated with Horseradish Peroxidase (Amersham) was used to detect the Anti-cry2 and detected by Enhanced Chemiluminescence (Pierce; Rockford, IL, USA). Anti-cry2 polyclonal antibody serum was kindly provided by Margret Ahmad. Loading control was performed using colloidal Coomassie brilliant blue (Sigma-Aldrich, St Louis, MO, USA).

Acknowledgements

We thank J.J. Casal, M. Koornneef, C. Lin, T. Sakai, and G.C. Whitelam, for providing seed of accessions and mutants and Margret Ahmad for kindly sharing the Cry2-Antiserum.

Supporting Information

- **Figure S9.1:** Light spectra of the treatments used in this study.
- **Figure S9.2:** Dynamics of light control of chromatin compaction in *Ler*.
- **Figure S9.3:** HX after 96 h treatment with different light-qualities.
- **Table S9.1.** Quantification of light intensities in specified wavelength regions, and the Red-to-Far red ratio (R/Fr) of the used light treatments.
- **Table S9.2:** Accessions used in this study and quantification of nuclei types.

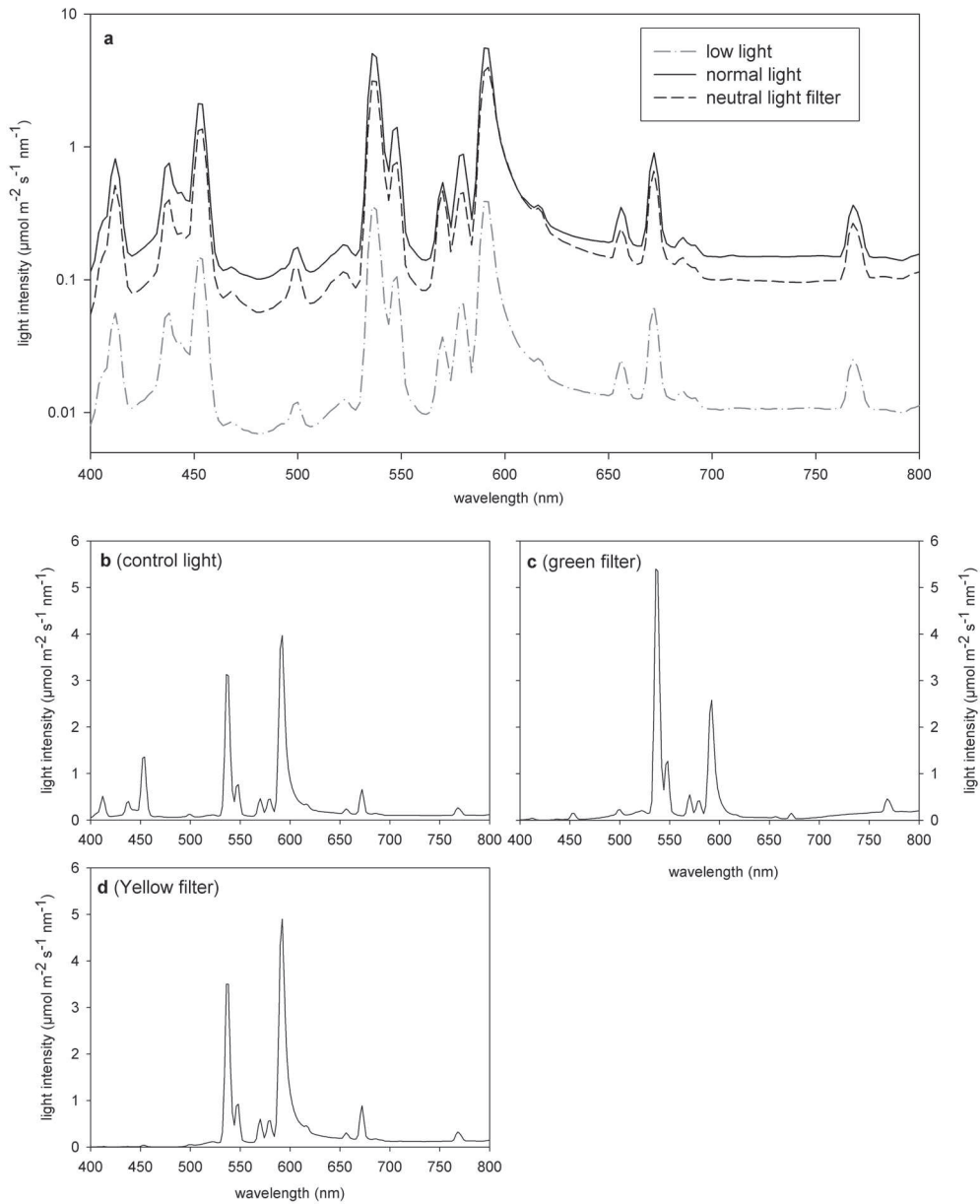


Figure S9.1: Light spectra of the treatments used in this study. Spectra (light intensity for each wavelength per nm, in log-scale) of a: control light conditions ($200 \mu\text{mol m}^{-2} \text{s}^{-1}$; lines), neutral low light treatment ($15 \mu\text{mol m}^{-2} \text{s}^{-1}$; dash-dotted line), and control light conditions of the light quality experiments ($100 \mu\text{mol m}^{-2} \text{s}^{-1}$; dashed line). b: Control light conditions of the light quality experiments ($100 \mu\text{mol m}^{-2} \text{s}^{-1}$), c: green filter treatment and d: yellow filter treatment. Spectra were recorded with a Licor1800 spectro-radiometer (Li-cor, Lincoln, Ne, USA).

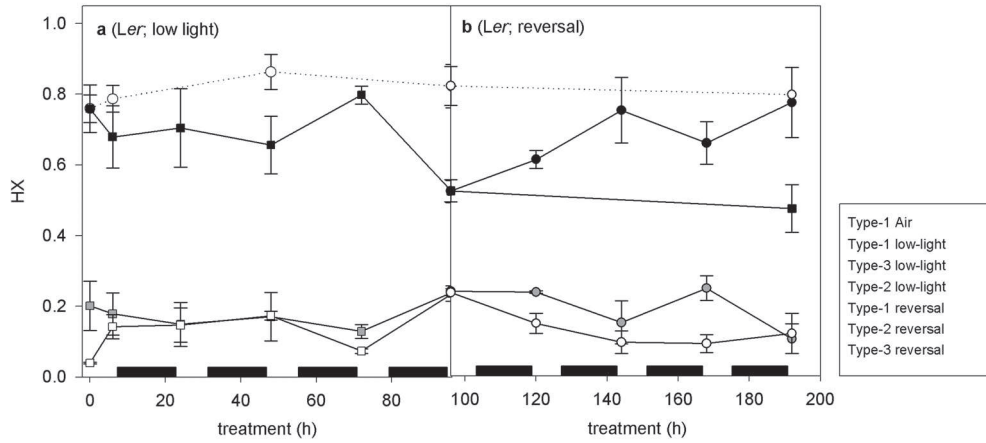


Figure S9.2: Dynamics of light control of chromatin compaction in *Ler*. Fraction of type 1, -2 and -3 nuclei (Figure 9.1) in *Ler* during **a**: 4 days (0 h to 96 h) of low light treatment ($15 \mu\text{mol m}^{-2} \text{s}^{-1}$; squares) and **b**: after reversal to control light conditions ($200 \mu\text{mol m}^{-2} \text{s}^{-1}$; 96 h to 192 h; circles). Plants that were kept in low light conditions during the whole experimental period are shown as black squares and those kept in control light conditions are depicted by white circles and dotted lines. Black horizontal bars indicate the dark periods. $n \geq 2$. Error Bars represent SE in all panels.

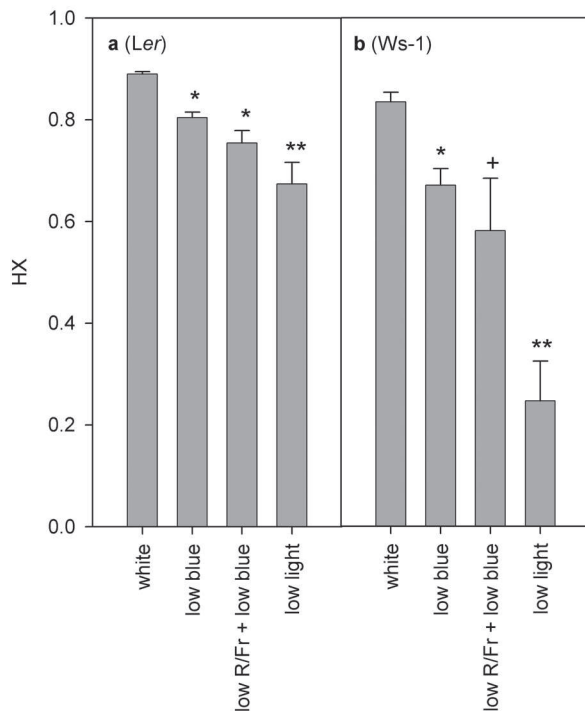


Figure S9.3: HX after 96 h treatment with different light-qualities. **a**: *Ler* and **b**: *Ws-1*. Control conditions are indicated as “white light” and correspond to $100 \mu\text{mol m}^{-2} \text{s}^{-1}$. Low blue-light (yellow filter and spectral-shade (low R/Fr + low-blue; green filter). Low light treatment consisted of spectral neutral shading by reducing PAR from $200 \mu\text{mol m}^{-2} \text{s}^{-1}$ to $15 \mu\text{mol m}^{-2} \text{s}^{-1}$ (grey bar). $n \geq 3$. For light spectra and wavelength quantification see Figure S9.1 and Table S9.1. Error Bars represent SE in all panels. Significance levels; * $p < 0.05$, ** $p < 0.01$, ** $p < 0.001$, 2-tailed Student's T-test, compared to white light.

Table S9.1. Quantification of light intensities in specified wavelength regions, and the Red-to-Far red ratio (R/Fr) of the used light treatments.

	Filter	Blue ^a (400-500 nm)	R/Fr ratio (654-664 nm / 724-734 nm)	PAR (400-700 nm)
Control; 200 $\mu\text{mol m}^{-2} \text{s}^{-1}$		38.2	1.66	200
Low light; 15 $\mu\text{mol m}^{-2} \text{s}^{-1}$	Shade-cloth	2.7 ^a	1.66	15
Control spectral-shade	Shade-cloth	21.3	1.82	115
Spectral-shade	Fern-green	4.7	0.43	90
Low-blue	Yellow	0.9	1.91	115

Footnote: ^a Total photon-flux rates of blue-light in the cryptochrome and phototropin action spectrum: 380–500 nm (Ahmad et al., 2002).

Table S9.2: Accessions used in this study and quantification of nuclei types. Names, abbreviations (abb), stock number IDs and fraction of nuclei per type, in control light conditions (200 $\mu\text{mol m}^{-2} \text{s}^{-1}$) and after 96 h low light treatment (200 $\mu\text{mol m}^{-2} \text{s}^{-1}$ to 15 $\mu\text{mol m}^{-2} \text{s}^{-1}$) of the used *Arabidopsis thaliana* accessions. Standard errors never exceeded 0.13.

Name	Abb.	Stock no	Control			96 h low light		
			type1	type2	type3	type1	type 2	type3
Bensheim-0	Be-0	N964	0.80	0.12	0.08	0.32	0.30	0.38
C24	C24	N906	0.76	0.16	0.08	0.44	0.33	0.24
Canary Islands-0	Can-0	N1064	0.49	0.33	0.17	0.14	0.33	0.53
Cape Verdi Islands-0	Cvi-0	N902	0.19	0.28	0.53	0.04	0.15	0.81
Chisdra	Chi-1	N1074	0.83	0.12	0.05	0.72	0.18	0.10
Columbia-0	Col-0	N1092	0.84	0.09	0.07	0.05	0.08	0.87
Helsinki-1	Hel-1	N1222	0.85	0.09	0.06	0.65	0.20	0.15
Hiroshima	Hir-1	JSW102	0.68	0.26	0.07	0.54	0.26	0.20
Moss			0.76	0.16	0.07	0.32	0.40	0.27
Kärnten-0	Kä-0	N1266	0.76	0.18	0.06	0.60	0.27	0.13
Kashmir-2	Kas-2	N903	0.90	0.07	0.02	0.59	0.21	0.20
Knox-10	Knox-10	N22566	0.83	0.10	0.06	0.48	0.30	0.22
Kondana-Tady	Kond	N916	0.92	0.04	0.04	0.41	0.34	0.24
Landsberg erecta	Ler	NW20	0.82	0.07	0.10	0.52	0.24	0.24
Martuba / Cyrenaika-0	Mt-0	N1380	0.67	0.23	0.10	0.26	0.32	0.42
Niederzenz-1	Nd-1	N1636	0.91	0.02	0.07	0.67	0.15	0.18
Pakistan-1	Pak-1	JW105	0.74	0.15	0.11	0.34	0.34	0.32
RLD-1		N913	0.87	0.08	0.05	0.40	0.33	0.27
Shahdara	Shah	N929	0.87	0.06	0.06	0.75	0.15	0.09
Stange			0.90	0.06	0.04	0.84	0.12	0.04
Wassilewskija-2	Ws-2	N915	0.78	0.12	0.10	0.25	0.30	0.45

Footnote: Seeds were obtained from the Nottingham Arabidopsis Stock Centre (NASC) (<http://arabidopsis.info/>), except accession: Hir-1 and Pak-1, which were obtained from the Sendai Arabidopsis Seed Stock Center (SASSC) Miyagi University of Education, Japan (<http://www.brc.riken.jp/lab/epd/Eng/index.shtml>). Accessions Moss and Stange (Stenoien et al., 2005) were a gift from M. Koornneef (Wageningen University, the Netherlands).

General discussion

On the abiotic control of hyponastic petiole growth and chromatin compaction in *Arabidopsis thaliana*

Martijn van Zanten, Laurentius A.C.J. Voeselek, Frank F. Millenaar[§],
Anton J.M. Peeters

Plant Ecophysiology, Institute of Environmental Biology, Utrecht University,
Padualaan 8, 3584 CH Utrecht, the Netherlands

[§]Present addresses:

FFM: De Ruiter Seeds, Leeuwenhoekweg 52, 2660 BB Bergschenhoek,
the Netherlands.

Plants are sessile organisms that can escape from growth limiting conditions by upward leaf movement (hyponastic growth) driven by differential petiole growth. In this thesis, we described a study that aims to understand how this complex trait is controlled at the molecular genetic and molecular physiological level in *Arabidopsis thaliana*.

The first part of this thesis (Chapters 1-4) has its focus on the identification and evaluation of signaling components involved in the perception and control of hyponastic petiole growth to different environmental stimuli. In addition, we employed unbiased approaches to identify novel, unanticipated pathways- and genes controlling hyponastic growth (Chapter 5-7). Next to our study on differential petiole growth, we show that plants respond to their light environment by dynamic regulation of nuclear chromatin compaction (Chapter 8, Chapter 9).

In this general discussion, we summarize and discuss the major findings and propose a generic model for the control of hyponastic growth in *Arabidopsis*. In addition, we provide perspectives and propose novel directions on how to continue the study of these processes.

Functional significance of induced hyponastic growth in *Arabidopsis thaliana*

The capacity to survive periodic-flooding is an important trait shaping plant distribution and abundance in flood-prone areas (Voeselek et al., 2004). Escape responses including shoot elongation and hyponastic growth, are important in environments with relatively shallow but prolonged floods. In accordance with observations in various species including *Rumex palustris* and deep-water rice (Voeselek & Blom, 1989; Hoffmann-Benning & Kende, 1992; Kende et al., 1998; Jackson et al., 2008), ethylene is the main signal inducing escape responses to flooding. This is also true for hyponastic growth in *Arabidopsis thaliana* (Millenaar et al., 2005). From our results using ethylene insensitive, hypersensitive and overproducing mutants it is clear that an intact ethylene signal transduction pathway is required for ethylene-induced differential growth (Figure 2.4; Table 10.1).

In most *Arabidopsis* accessions, petiole angles do not exceed ~45 degrees after hyponastic growth (Chapter 7), which tilts the leaf tip only a few centimeters above the soil surface. This is insufficient to reach the water-table in many (periodic) floods as these are often much deeper. Moreover, exogenous ethylene application does not induce elongation growth in *Arabidopsis* (Millenaar et al., 2005; Pierik et al., 2009). The functional significance of submergence-induced hyponastic growth in *Arabidopsis* is therefore unclear.

Light intensity is an important determinant for biodiversity in dense vegetations (Hautier et al., 2009). In stands with fierce competition for light, the ability to induce a hyponastic growth response is advantageous, as it helps positioning leaves back into the light (Smith & Whitelam, 1997; Ballaré, 1999; Pierik et al., 2004a, 2005). Canopy shade-induced avoidance responses have received most attention in relation to reduced red-to-far red ratio (R/FR) of light, perceived by the phytochrome photoreceptors (Ballaré, 1999; Franklin, 2008). We showed that the ability to induce

hyponastic growth to spectral neutral low light intensity conditions is also an important signal during shade avoidance (Millenaar *et al.*, 2005, 2009; Pierik *et al.*, 2005; Chapters 2-7).

Given the relative small size of adult *Arabidopsis thaliana* rosettes, it can be considered a weak competitor in macro-vegetations. However, *Arabidopsis thaliana* is an opportunistic species often found on open and disturbed habitats (Koorneef *et al.*, 2004). As such, it likely has to compete for light with other *Arabidopsis* plants immediately after germination or with other small seedlings. The ability to induce hyponasty under shade conditions might therefore increase growth and survival

Table 10.1: Classification of the responses to ethylene, low light and heat, of the mutants used in this study. Response to a stimulus (ethylene; ET, Low light; LL, or heat; HT) were classified as + (enhanced response), - (reduced response), or = similar response compared to wild type. (For detailed kinetics of the hyponastic growth responses of these mutants see chapters 2, 3 & 4). nd = not determined; mutants are in the Col-0, Ler- or Ws-2 genetic background.

		ET	LL	HT			ET	LL	HT		
ABA ^{*1}	<i>aba2-1</i>	Col-0	+	+	=	Auxin	<i>tir-1</i>	Col-0	=	-	-
	<i>aba3-1</i>	Col-0	+	+	+		<i>tir1 afb1 afb2 afb3</i>	Col-0	=	-	-
	<i>aba1-1</i>	Ler	=	-	-		<i>tir3</i>	Col-0	=	-	nd
	<i>abi1-1</i>	Ler	+	=	-		<i>pin3</i>	Col-0	+	-	-
	<i>abi2-1</i>	Ler	=	=	-		<i>pin7</i>	Col-0	+	-	-
	<i>abi3-1</i>	Ler	+	=	-						
	<i>abi5</i>	WS	+	=	nd	Light	<i>phot1</i>	Ler	nd	=	nd
	<i>era1-2</i>	Col-0	-	+	+		<i>phot2</i>	Ws	nd	=	nd
	<i>gpa1-2</i>	Ws	=	-	-		<i>phot1, phot2</i>	Ler/Ws	nd	=	nd
	<i>gcr2-2</i>	Col-0	-	=	nd		<i>cry1</i>	Ler	nd	-	nd
	<i>gcr2-4</i>	Col-0	=	=	nd		<i>cry2</i>	Ler	nd	-	nd
	<i>gcr2-1 gcl1-1 gcl2-2</i>	Col-0	-	-	nd		<i>cry cry2</i>	Ler	nd	-	-
Ethylene	<i>ein2</i>	Col-0	-	=	=	<i>phya</i>	Ler	nd	-	=	
	<i>etr1-4</i>	Col-0	-	=	+	<i>phyb5</i>	Ler	-	-	+	
	<i>ein4</i>	Col-0	-	=	+	<i>phya phyb</i>	Ler	nd	-	-	
	<i>ctr1</i>	Col-0	-	=	-	<i>phyb9</i>	Col	-	nd	+	
	<i>etr1, ein4, etr2</i>	Col-0	nd	nd	-	<i>hy2</i>	Ler	nd	-	-	
	<i>eto1-1</i>	Col-0	-	-	-	<i>phya cry1</i>	Ler	nd	-	nd	
						<i>phya cry2</i>	Ler	nd	-	nd	
						<i>cry1 cry2 phyb</i>	Ler	nd	-	nd	
					<i>ex1 flu1</i>	Ler	nd	-	nd		

Footnote: ^{*1} Results on the role of ABA in ethylene induced hyponastic growth are from Benschop *et al.*, 2007.

under those micro-environmental conditions where *Arabidopsis thaliana* prospers. Leaf positioning directly affects the irradiation flux per unit leaf area, and thereby determines photosynthesis rates (King, 1997; Falster & Westoby, 2003; Hopkins *et al.*, 2008). Accordingly, active leaf movements such as hyponastic growth can optimize photosynthesis rates. Hopkins *et al.* (2008) showed that *Arabidopsis thaliana* accessions from Southern latitudes have more erect leaves than those from Northern latitudes. These authors propose that high leaf angles at low latitudes optimize light capture early in the day and during winter, whereas it would prevent over-irradiation and associated supra-optimal heat flux and water-loss during mid-day and summer, by avoiding direct vertical light on leaf lamina. In our study, we did not find a correlation between initial petiole angles or induced-hyponastic growth, with latitude (Chapter 3, 7). Nevertheless the ability of accessions to induce hyponastic growth to heat correlated to the diurnal temperature range at the site of the accession collection (Figure 3.2), suggesting that the ability of leaf movement may be important to adjust to local temperature environments. Based on this, we suggest that heat-induced hyponastic growth optimizes photosynthesis and might be considered as a (heat)escape mechanism. This is supported by the observation that heat-induced oxidative damage in *Arabidopsis* was prevented in darkness (Larkindale & Knight, 2002), suggesting that this heat damage originates from photo-inhibition of the photosynthesis related electron transport chain. Further support is found in Gray *et al.* (1998) who suggested that heat-induced hypocotyl elongation is employed to reposition the photosynthesizing tissues away from heated soil. This is also in accordance with our observation that pharmacological inhibition of the electron transport chain by DCMU induces hyponastic growth in the absence of stimuli (Figure 2.3). It is tempting to speculate that heat-induced damage to the electron transport chain may play a role in inducing hyponastic growth.

Ethylene is not required for low light-induced hyponastic growth and antagonizes heat-induced hyponastic growth

Given the importance of ethylene as trigger of hyponastic growth during flooding, and because shade and submergence escape strategies are characterized by similar suites of traits including hyponastic growth and fast petiole/stem elongation in many plant species (Smith & Whitelam *et al.*, 1997; Ballaré *et al.*, 1999; Pierik *et al.*, 2005), we expected that low light and heat-induced hyponastic growth might also require ethylene signaling. Several examples in literature show interaction between shade and ethylene action (Finlayson *et al.*, 1998; Raz & Ecker, 1999; Knee *et al.* 2000; Pierik *et al.*, 2003; 2004a). Moreover, low R/Fr induces ethylene production in *Arabidopsis* (Pierik *et al.*, 2009). However, our results demonstrated that low light-induced hyponastic growth occurs independently of ethylene signaling (Figure 2.4; Table 10.1).

Ethylene is involved in basal thermo-tolerance and in protection against- and repair of- heat-induced oxidative damage (Larkindale & Knight, 2002; Larkindale *et al.*, 2005). Heat-induced hyponastic growth is, however, negatively modulated by ethylene action (Figure 3.3). Additionally, heat represses ethylene release (Figure

3.3a), suggesting that heat may modulate ethylene production to control hyponastic growth. Ethylene mediated repression of heat-induced hyponastic growth, can result in an increase of irradiation- and heat-flux per unit leaf area, due to lower leaf angles (see above). We therefore suggest that heat may repress ethylene release to keep-up the leaves and as such regulate heat-flux reaching the blades, and that this advantage balances with the role of ethylene in protection against heat-induced (oxidative) damage.

Petioles of the semi-aquatic plant *Rumex palustris* are sensitized for ethylene under hypoxic conditions that may occur during complete submergence (Voeselek *et al.*, 1997; Rijnders *et al.*, 2000; Mommer *et al.*, 2004). Accordingly, treatment with low-oxygen levels did enhance the responsiveness of petioles to ethylene in *Arabidopsis* (Figure 1.3). Low light and heat stimuli did not result in an enhanced response in low oxygen (not shown), indicating that sensitization of petioles is ethylene specific. However, even petioles of completely submerged *Arabidopsis* in darkness did not reach hypoxic conditions. Endogenous O₂ in submerged petioles equilibrated at approximately 10-15%. In the light O₂ levels remained close to ambient (~21%) demonstrating the importance of underwater photosynthesis (Dyvia & Voeselek *unpublished results*). Similarly, in natural situations flooding does not necessarily result in hypoxia of shoot organs (Mommer *et al.*, 2004; Voeselek *et al.*, 2006).

The role of light perception in hyponastic growth

Light-spectrum manipulations suggested that rapid induction of low light-induced hyponasty is dose-dependent and requires reduction of blue-light wavelengths (Millenaar *et al.*, 2009; Figure 2.1). Accordingly, continuous blue light treatment inhibited shade avoidance-associated petiole elongation in a dose dependent manner (Kozuka *et al.*, 2005). These effects were independent of phytochrome A (phyA) and phyB signaling (Kozuka *et al.*, 2005). In contrast, we showed that cryptochrome 1 (cry1), cry2, phyA and phyB are the photoreceptor proteins involved in detection of reduced light intensity, and all are positive regulators of low light-induced hyponastic growth (Figure 2.2; Table 10.1).

Low blue-treatment alone did not induce petiole elongation (Djakovic-Petrovic *et al.*, 2007; Pierik *et al.*, 2009). Likely, low light-induced differential growth (hyponasty) also requires more signals than low blue light alone. We demonstrated that photosynthesis-derived signals can induce hyponastic growth in the absence of a stimulus (Figure 2.3). Interestingly (as mentioned above), the photosynthesis system may also play a role in heat-induced hyponastic growth, via heat-induced dissipation of excess energy by the electron transport chain. This results in oxidative damage and photo-inhibition (Larkindale *et al.*, 2005; and references herein). Therefore, the photosynthesis system and the electron transport chain may be a point of cross talk between heat and low light signaling. This might explain the strongly enhanced hyponastic growth response when low light and heat are applied simultaneously (Figure 3.4). Application of additional ethylene, rescued this accumulative effect to the level of a single treatment (Figure 3.5). It is tempting to speculate that this is linked to the protective role of this hormone, which prevents and repairs photo-

oxidative damage (Larkindale *et al.*, 2002, 2005).

Besides a role in low light-signaling, *phyA*, *phyB*, *cry1* and *cry2* are also required for proper induction of heat-induced hyponastic growth (Figure 3.4; Table 10.1). *PhyB* is a negative regulator of the response amplitude to heat in both Col-0 and *Ler* background, whereas loss-of-function *phyA* rescues this effect, at least in *Ler*. In agreement with low light-induced hyponasty, both cryptochromes are redundantly required for a fast induction of the response.

These results suggest that interaction between low light and heat Signaling may occur relatively upstream in the signal transduction cascades that leads to hyponastic growth. Literature evidence indicates that light and heat Signaling may integrate at the level of photoreceptors, or photoreceptor-interacting proteins (Halliday *et al.*, 2003; Halliday & Whitelam, 2003; Penfield, 2008). Recently, Koini *et al.* (2009) proposed that high temperature effects on plant architecture, including hyponasty and petiole elongation, require the bHLH transcription regulator PHYTOCHROME INTERACTING FACTOR 4 (PIF4). PIF4 is a negative regulator of *phyB* Signaling and a positive regulator of cell-expansion. Biologically active *phyB* binds and phosphorylates PIF4 and induces its degradation, which consequently represses expression of shade avoidance traits (Huq *et al.*, 2002; Lorrain *et al.*, 2008). Earlier work suggested that some *phyB*-controlled responses, including petiole elongation, are not sensitive to a temperature shift in the *phyB* background, whereas flowering is (Halliday & Whitelam, 2003). Interestingly, *pif4* mutants did not abolish early flowering. This suggests that PIF4 specifically controls heat-mediated responses on plant architecture, independently, but downstream of *phyB* action. Accordingly, our low light treatment did also not induce early flowering (Chapter 9). Therefore, low light and heat Signaling might converge at PIF4 and the observed positive effects on heat-induced hyponastic growth in *phyB* background may be due to stabilised PIF4 acting as positive modulator of hyponasty. Accordingly, *PIF4* transcript was induced by heat (Koini *et al.* 2009). Although not significant, we observed a 21% increase in PIF4 transcript abundance in petioles of plants treated 3 h with low light (Figure 10.1). Perhaps even more intriguing is that 3 h of ethylene strongly down-regulated *PIF4* transcription ($p < 0.01$). This may be in line with the observation that ethylene antagonizes heat-induced hyponasty. It would be informative to assay protein levels of PIF4 under single and combination treatments. Currently, analysis of the hyponastic growth phenotypes of the *pif4-1* loss-of-function mutant is conducted in our laboratory.

Auxin is not always a prerequisite for differential growth

Auxin and polar auxin transport (PAT) are required for many differential growth responses such as phototropism and gravitropism (Harper *et al.*, 2000; Friml & Palme, 2002; Friml, 2003). Our data indicated that low light- and heat-induced hyponastic growth required intact auxin perception and PAT (Millenaar *et al.*, 2009; Figure 2.5, Figure 3.6). Details on involvement of auxin Signaling and PAT differed between these stimuli. Auxin and PAT are required for rapid induction and maximum amplitude of heat-induced hyponastic growth and for amplitude and maintenance

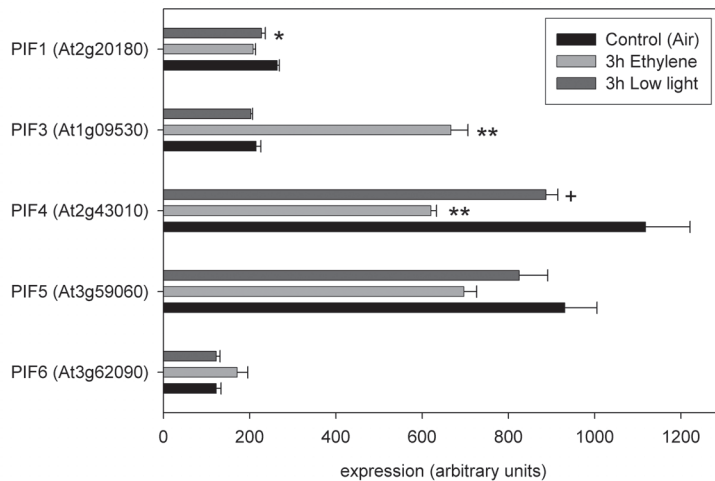


Figure 10.1: Transcriptional regulation of PIF genes to environmental stimuli. Expression levels in Col-0 petioles after 3 h in control conditions, ethylene addition ($5 \mu\text{l l}^{-1}$) or low light ($20 \mu\text{mol m}^{-2} \text{s}^{-1}$). (+ $p < 0.1$, * $p < 0.05$, ** $p < 0.01$; 2-tailed Student's T-test, $n=3$). Error bars represent SE). The used microarrays are described in Millenaar *et al.*, 2006.

of elevated petiole angles during low light-induced hyponasty. These observations are consistent with the available literature. For example, auxin is required for differential and non-differential (elongation) growth of petioles and hypocotyls under altered light intensity and light quality environments (Morelli & Ruberti, 2000; Tao *et al.*, 2008; Pierik *et al.*, 2009). Furthermore, auxin is required for high temperature-induced hypocotyl elongation (Gray *et al.*, 1998) and heat induces transcription of the auxin-responsive genes IAA4 and IAA29, suggesting sensitization of the tissues to auxin (Gray *et al.*, 1998; Koini *et al.*, 2009).

Our data indicated that auxin and PAT are not obligatory for ethylene-induced hyponasty *per se* in Arabidopsis (Van Zanten *et al.*, 2009a; Figure 2.5; Table 10.1). In fact, based on the small exaggerated response amplitude after treatment with the auxin efflux inhibitor naphthylphthalamic acid (NPA) and based on auxin perception- and transport mutants, one might even conclude that auxin antagonizes ethylene-induced hyponasty (Figure 2.5). These results are partly in agreement with observations on *R. palustris*, where pretreatment with NPA resulted in doubling of the lag-phase for hyponastic growth under water, but hardly affected response amplitude (Cox *et al.*, 2004). Together, this indicates that auxin is not always a prerequisite for differential growth responses. Only scattered literature is available showing that this is a more general observation. Harper *et al.* (2000) showed that *NON PHOTOTROPIC4/AUXIN RESPONSE FACTOR 7* (*NPH4/ARF7*) is required for phototropism, but that addition of ethylene can overcome the *nph4/arf7* mutation. Moreover, Jensen *et al.* (1998) showed that the requirement for auxin strongly depends on the environment, as NPA was required for elongation growth in light-grown, but not dark-grown seedlings. This dependency on the environment potentially explains why previous literature data on leaf angles regulation by auxin related-components (see chapter 1 and references within) are not always conclusive.

Is ABA as a central integrator in the induction of hyponastic growth?

Abscisic acid (ABA) is a negative regulator of submergence (ethylene)-induced petiole elongation and delayed the induction of hyponastic growth and reduced response amplitude in *R. palustris* (Cox *et al.*, 2004; Benschop *et al.*, 2005). Upon submergence, ABA levels decline rapidly due to enhanced turnover and inhibition of biosynthesis (Benschop *et al.*, 2005). Analogously, ethylene triggered ABA level decline in flooding intolerant deepwater rice (*Oryza sativa*) and subsequently stimulated rapid elongation growth (Hoffmann-Benning & Kende, 1992; Kende *et al.*, 1998). Genetic and pharmacological evidence indicated that ABA antagonizes ethylene-induced hyponastic growth in *Arabidopsis*, despite that ABA levels remained unaltered after ethylene treatment (Benschop *et al.*, 2007; Table 10.1). Additionally, ABA controls leaf positioning independent of ethylene (Mullen *et al.*, 2006; Benschop *et al.*, 2007). Surprisingly, ABA was identified as a positive regulator of heat- (Figure 3.7; Table 10.1) and low light-induced (Figure 4.1; Table 10.1) hyponastic growth. At least in low light-induced hyponasty, mediation of the response to ABA, seems independent of ethylene signaling (Figure 4.3; Figure 6.14). These results were obtained with ABA insensitive and ABA biosynthesis mutants. The specific effects of these mutants were never consistent throughout the treatments (i.e. enhanced response in ethylene and reduced response in ethylene and low light) and involvement differed among the treatments. Consistent reciprocal results were only obtained using the only available ABA hypersensitive mutant *era1-2* (i.e. reduced response in ethylene and enhanced response in heat and low light) However, next to *era1-2* only *aba3-1* (positive) was involved in controlling hyponastic growth under all treatments. These data strongly suggest that ABA and its associated proteins control environment-induced hyponastic growth, but the treatment specific requirement of ABA related components suggest that ABA is not a central signaling hub towards hyponastic growth.

The signal transduction routes induced by different stimuli integrate towards induction of hyponastic growth

We used three stimuli to induce hyponastic growth in this study: i) application of the phytohormone ethylene, ii) reduction of light intensity and iii) heat treatment. We showed that the kinetics of the hyponastic growth response to these stimuli are highly similar. Therefore, an important hypothesis we aimed to address is whether these apparently unrelated signals utilizes the same set of components to induce hyponastic growth. The data on ethylene, auxin, ABA and light perception (Chapters 1-4), do not conclusively support this assumption by showing consistent effects (see table 10.1 for an overview of the phenotypes of the mutants used in chapter 1-4). This suggests that part of Signaling routes employed are unique for each stimulus. Nevertheless, several lines of evidence point to a shared part of the signal transduction route. First, we have direct evidence based on factors isolated by QTL analysis and a forward genetic approach (ERECTA and A2 type Cyclins; Chapter 6, Chapter 7). Next to ER several other co-locating QTLs shared among the stimuli were found that may harbor central regulators (Chapter 7). Secondly, a correlation study

on hyponastic petiole growth parameters using 138 naturally occurring accessions, demonstrated that an accession that responded relatively strongly to one treatment likely also responds relatively strongly to another (and *vice versa*). This allows the generalization that the magnitude with which an accession respond to the stimuli are linked (Chapter 7). Next to this, overlap in differentially regulated genes was observed using micro-arrays hybridized with petiole derived cDNA of 3 h ethylene- or 3 h low light treated plants. As much as 453 genes were similarly regulated by both ethylene and low light (Pierik *et al.*, 2005; Millenaar *et al.*, 2006). This resulted in a significant correlation ($R=0.353$) when a Spearman rank correlation test on fold change of gene expression (Figure 10.2) was performed. Even stronger correlations were found when data obtained from publicly available microarray data sets on heat-treated plants (Von Koskull-Döring *et al.*, 2007) were compared with those of ethylene- and low light treatment (Figure 10.2). A considerable part of the shared regulated genes between the treatments supports the notion that the pathways may integrate.

We observed that the hyponastic growth inducing signals (ethylene, low light and heat) modify each others effects on petiole angle (Figure 3.5). Light intensity and temperature influences petiole angles in a dose dependent manner (Figure 2.1, Figure 3.1). This was also observed for ethylene, although, this Signaling is saturated already at relatively low concentrations (60 ppb induced 80% of the maximum response amplitude (Polko *et al.*, unpublished data). Therefore, perhaps triggering one Signaling route may influence the sensitivity in which other environmental stimuli

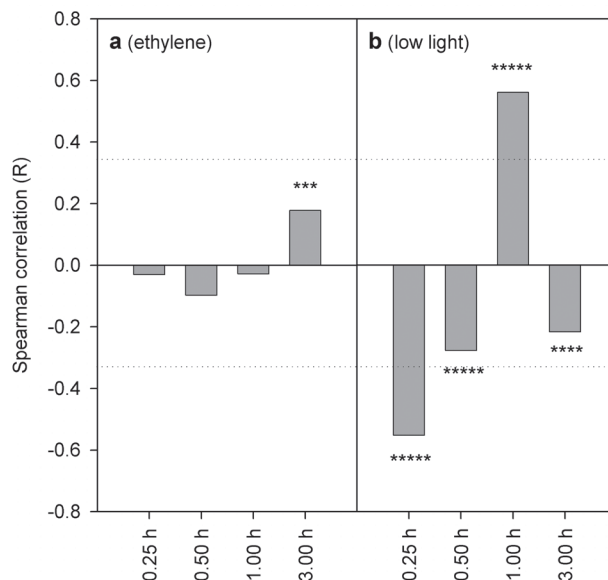


Figure 10.2: Transcriptome meta-analysis of 38°C and ethylene or low light treated plants. Percentage overlap between published microarray data from 18 d old vegetative Col-0 plants (all green parts) treated with 38°C for different periods, compared with the microarray data as described in Millenaar *et al.*, 2006; 2009, separated in **a**: ethylene (3 h) and **b**: low light (3 h) treatment. Dotted lines represent the Spearman rank correlation coefficient (35.3%) between ethylene and low light. Significance levels: *** $p<0.001$, **** $p<0.0001$, ***** $p<0.00001$.

are perceived or affect sensitivity towards hyponastic growth.

The data described in Chapters 1-4 on ethylene, low light and heat control of hyponastic growth are summarized in a working model, constructed on the principle of parsimony (Figure 10.3). It should be noted that this model is only one out of several possibilities and is not the best representation of the complex regulatory network that control of hyponastic growth to environmental stimuli appears to be. For example, this model does not include the findings described in chapter 7 where mapping of several QTLs for initial petiole angles and ethylene-, low light- and heat-induced hyponastic growth is described. Subsequent analysis of a major QTL resulted in the cloning of the segregating Leucine-Rich Repeat Receptor-Like Ser/Thr kinase gene *ERECTA* (*ER*) as controller of ethylene- and low light-induced hyponastic

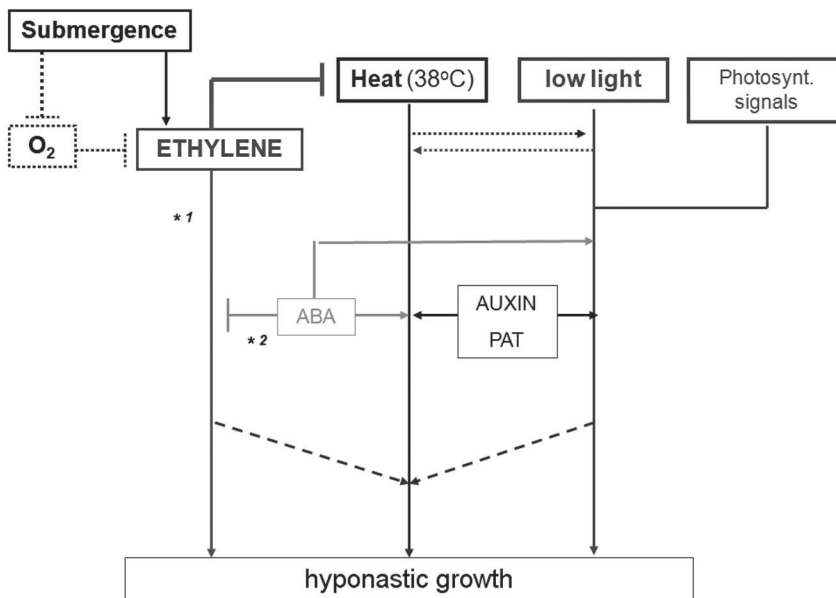


Figure 10.3: Proposed simplified signaling network of ethylene, heat and low light-induced hyponastic petiole growth as described in this thesis. (See Color Supplement for full color version of this figure). Different hyponastic growth inducing signals are color-coded: Submergence/low oxygen (blue), ethylene accumulation (red), Low light/photosynthesis related signals (grey) and heat (green). These signals are modulated by ABA (orange) and auxin (brown). ¹ For ethylene/submergence-induced hyponastic growth see: Millenaar *et al.*, 2005. ² For ABA mediated repression of ethylene-induced hyponasty see Benschop *et al.* (2007). Dotted lines between heat and low light Signaling indicate that we cannot distinguish between the routes. The purple dotted lines at the bottom indicate that we cannot distinguish between continuous parallel pathways of ethylene, heat and low light route towards hyponastic growth or a converged downstream pathway in which the same functional genetic components are utilized by the different signals. The bold inhibition line indicates a dominant ethylene effect over the heat route. Note that order of the signals along the arrows does not necessarily reflect the order of interactions occurring.

growth, downstream of ethylene action.

Moreover, in chapter 5, the results of a forward genetic screen are presented. This approach led to the isolation of several lines with affected initial angles and/or induced hyponastic growth. The observed phenotypes of the isolated activation tagged lines can be used to raise hypotheses to what processes they might be related to. Therefore, these factors can be positioned in the proposed working model (Figure 10.4). However, it is clear that not all isolated lines directly fit this model, underlining the simplified character (Figure 10.4).

SEE1-1 was described in detail (Chapter 6), because it met all criteria to be a downstream integrator (i.e. unaltered initial petiole angle and a marked response to all stimuli, with comparable effects). We demonstrated that ectopic expression of *CYCLINA2;1* most likely causes the enhanced effect on hyponastic growth and concluded that A2-type Cyclins redundantly control this response. A2-type Cyclin-mediated control of hyponastic growth seems independent from the well described role for this gene family in controlling cell cycle-progression and endoreduplication (Chapter 6). As shown in Figure 1.2, described in Chapter 6 and in Cox *et al.* (2003), not cell proliferation, but differential cell elongation at the abaxial-basal side of the petiole drives hyponastic growth. Both ethylene and ABA spatially restrict *CYCA2;1* promoter activity to basal petiole tissues. We expect that maintenance of A2-type Cyclin mediated growth in basal tissues and repression of growth in more distal tissues is related to the differential growth phenotype. We demonstrated that Cyclin-Dependent Kinases/Kip-related proteins (ICK/KRP) function as integrators of ABA and ethylene signals to control hyponastic growth, likely by inhibition of the A2-type Cyclin-Cyclin Dependent Kinase A;1 (CDKA;1) complex.

Intriguingly, *erecta* mutants exhibited reduced A2-type Cyclin transcription, at least during ovule development (Pillitteri *et al.*, 2007). In agreement with the role of A2-type Cyclins as positive controllers of hyponastic growth (Chapter 6), *erecta* mutants consistently had a reduced hyponastic growth response (Chapter 7). This suggests that A2-type Cyclins may be downstream targets of ER. This is supported by the observation that both A2-type Cyclins and ER do not alter ethylene production nor sensitivity, despite that both factors control ethylene-induced hyponastic growth (Figure 6.7, Figure 7.16). Moreover, ER participates in the ASYMMETRIC LEAVES (*AS1*, *AS2*) pathway to promote adaxial leaf identity (Xu *et al.*, 2003). In *as1* or *as2* mutant backgrounds polarity defects were significantly enhanced by application of heat stress. This was only observed in an *er* background, suggesting that ER function is required for reduction of plant heat stress sensitivity during adaxial-abaxial polarity formation in leaves (Qi *et al.*, 2004). Adachi *et al.* (2009), showed that the *CDKA;1* promoter contains a region that directs abaxial side-biased expression of this gene, which links the *CDKA;1* transcription to the adaxial/abaxial side specification of leaves. How ER responds to increasing temperatures and what signaling pathways are involved is not clear yet, but it seems plausible that ER acts upstream of A2-type Cyclins in the control of hyponastic growth, perhaps by affecting polarity

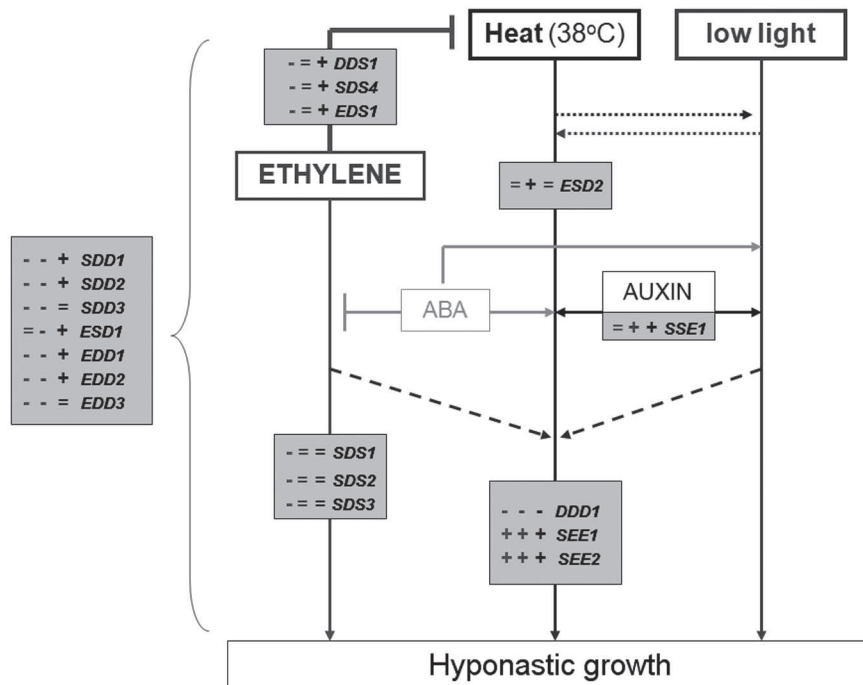


Figure 10.4: Proposed positions where causal factors of the isolated lines from the forward genetic screen fit the model for hyponastic growth. (See Color Supplement for full color version of this figure). Activation tagged candidate lines (Chapter 5) are shown in boxes. The observed phenotypes after treatment are classified as being positive (+) or negative (-) from Col-0 wild type response if the observed angle deviated > 5 degrees from the wild type average, or neutral (=) if not (see also figure 5.3). Response to ethylene is depicted in red (left of the three symbols depicting the phenotype), for low light in grey (middle symbol) or green (right symbol) for heat-induced hyponastic growth. For details on the signaling model see Figure 10.3. Isolated activation tagged lines that does not fit in this model are depicted in separate box outside the accolade.

in a *CYCA2;1-CDKA2;1* related manner. The notion that ER also controls heat-induced hyponastic growth and mutants in the AS1, AS2 pathways have abolished hyponastic growth phenotypes to all stimuli (data not shown) and lines ectopically expressing AS2 have constitutive hyponastic angles (Nakzawa *et al.*, 2003) supports this hypothesis.

In conclusion, several lines of evidence indicate that the signal transduction pathways towards hyponastic growth induced by different environmental stimuli are integrated, but also have parallel, unique parts. We isolated three candidate lines (*DDD1*, *SEE1*, *SEE2*) that fit the criteria to act as downstream integrators and most likely A2-type Cyclins, perhaps controlled by *ERECTA*, are part of the integrated

signaling route towards hyponastic growth. However, based on our data we cannot completely exclude that A2-type Cyclins and/or ER control aspects of hyponastic growth separately in the unique, parallel, parts of the signaling routes to all stimuli. Further dissection of the molecular mechanisms involved in the A2-type Cyclin mediated control of hyponastic growth will clarify this.

Besides *SEE1-1*, we described the cloning of the T-DNA locus of *SEE2* (Chapter 5). However, this line did not show obvious up-regulated genes. The T-DNA insert of *EDD2* was located in the Toll /*Interleukin1 Receptor–Nucleotide Binding Site–Leucine-Rich Repeat (TIR-NBS-LRR)* gene (At5g17880; data not shown). This line was isolated before as *constitutive shade avoidance-1 (csa1)* (Faigon-Sovarna *et al.*, 2008). *CSA1* impairs *phyB* function and in agreement, *EDD2/CSA1*, in Col-0 displayed a strongly enhanced initial petiole angle (Figure 5.5a). Moreover, *EDD2/CSA1* showed, similar to *phyb5* in *Ler* reduced, low light-induced hyponasty (Figures 2.2h, Figure 5.5C), comparable to *phyb5* and *phyb9* (Col-0) enhanced heat-induced hyponasty (Figures 3.4d,f & Figure 5.5d) and reduced ethylene-induced hyponastic growth (Figure 3.4b; Figure 5.5b). The cloning of the causal loci of the remaining 15 lines is currently in progress in our laboratory (Polko & van Zanten, *unpublished results*).

Light control of nuclear chromatin compaction in *Arabidopsis thaliana* is not associated with differential growth responses

In chapters 8 and 9 we showed that light intensity and light quality controls cytogenetically defined chromatin compaction in *Arabidopsis thaliana* interphase nuclei and that this response is controlled by photoreceptors and HISTONE DEACETYLASE 6 (*HDA6*). Moreover, we demonstrated natural variation for these traits among *Arabidopsis* accessions.

The level of chromatin condensation is generally linked to the accessibility of loci for transcription (Tessadori *et al.*, 2004; Jarillo *et al.*, 2009). It is well documented that de-condensation of specific heterochromatic loops of for example *GLABRA2* in non root hair-forming atrichoblasts (Costa & Shaw, 2006) is locally remodeled for this purpose and that epigenetic repression of *Flowering Locus C (FLC)* (Finnegan *et al.*, 2004) is associated with transcriptional activity of the entire locus. Over 10% of *Arabidopsis thaliana* genes are co-expressed in chromosomal domains, which are suggested to facilitate a coordinated, genome-wide response, to the environment (Zhan *et al.*, 2006). Jiao *et al.* (2005) concluded that the expression of ~3000 genes in *Arabidopsis* seedlings are regulated by transferring plants from darkness to white light, which is likely to involve global chromatin-condensation control.

However, with the exception of the Nucleolar Organizing Regions (NORs), we did not observe quantitative changes in epigenetic markers for gene silencing (5-MC and H3K9me2; Figure 8.3) and transcriptional active chromatin (H3K4Me2; data not shown) between Col-0 and Cvi-0. Overall, this suggests that light may control transcription by global chromatin de-condensation, but does not necessarily induce euchromatinization, associated with enhanced transcriptional activity *in stricto sensu*. Accordingly, severe de-compaction during protoplastization was insufficient for transcriptional re-activation of silenced loci (Tessadori *et al.*, 2007b). Therefore, it is

unlikely that the type of global-chromatin compaction control we described here, is operated with the direct purpose of facilitating fast differential growth responses such as low light-induced hyponastic growth. In agreement, hyponasty is induced at a much shorter time frame (within 1 h) than chromatin de-condensation (completion of the response in the fastest responding accession (Col-0) was observed after 96 h). Moreover, prolonged ethylene treatment did not influence chromatin compaction, whereas it does induce hyponasty with similar kinetics as low light and the *hda6* (*sil1/not*) mutant did not show altered hyponastic growth phenotypes to ethylene, low light or heat treatment (data not shown), despite its strongly reduced chromatin compaction (Furner *et al.*, 1998; Fransz *et al.*, 2006). It should however be noted that the third hyponastic growth inducing signal; heat treatment (38°C), does also induce strong chromatin de-compaction (data not shown).

The general notion that the abiotic environment dynamically controls global chromatin compaction was largely unattended so far, but not unexpected, given that few papers described control of chromatin compaction levels by developmental programs and the biotic environment (reviewed in: Exner & Hennig, 2008; Jarillo *et al.*, 2009). Early seedling establishment and leaf maturation for example, are associated with an increase in the heterochromatic fraction (Matthieu *et al.*, 2003; Tessadori *et al.*, 2004). *Vice versa*, floral transition (Tessadori *et al.*, 2007a), protoplastization, callus formation (Tessadori *et al.*, 2007b; Grafi *et al.*, 2007), and pathogen infection (Pavet *et al.*, 2007) induced a reduction of global chromatin compaction. This suggests that the degree of chromatin condensation of Arabidopsis nuclei reflects the developmental (i.e. differentiation) state of the cell. If this was completely true for environmentally controlled chromatin de-compaction, several accessions would undergo a de-differentiation upon substantial low light treatment (Chapter 8) and Cvi-0 should be in an apparent de-differentiated state already at control light conditions (Chapter 9). Overall, the biological function of light control of chromatin compaction remains therefore elusive. Perhaps the best illustration that dynamic control of chromatin compaction might exert some relevance for Arabidopsis in natural stands (Figure 9.2), is the observation that chromatin de-compaction can be triggered by low blue light and low red-to-far-red ratio light, which in contrast to low PAR are specific, light clues during neighbor competition and in closed canopies (Smith & Whitelam, 1997; Vandenbusche *et al.*, 2005; Franklin, 2008)

Perspectives

A major future challenge is to understand how various abiotic stresses are perceived by plants, how the signals are transduced and integrated, which mechanisms they trigger and how this is translated in functional responses. Furthermore, the interconnectivity between different environmental stresses at the physiological and genetic level needs to be acknowledged.

The understanding gained from this will be of great interest to breeders who have to produce high yielding crops to feed a growing and more demanding world-population, on decreasing agronomical acreage. The knowledge will be also of

relevance for the understanding of how plants deal with changes in their natural environment, how this ability has been shaped by evolution and how this will affect plant communities and distribution.

In this work, we demonstrated that *Arabidopsis thaliana* is a very good model to study the molecular physiology of the regulatory mechanisms involved in environmentally induced differential growth and global chromatin organization. We showed that the perception, signal transduction pathways and mechanisms operated to cope with different factors in the abiotic environment are very similar in *Arabidopsis*. Moreover, it becomes increasingly clear that the pathways operated between seemingly unrelated species are often analogous (e.g. hormonal control of submergence escape in rice, *Rumex palustris* and *Arabidopsis*) and thus that results obtained with *Arabidopsis* are translatable and applicable to other species. In this respect, especially the plant-specific APETALA2/ethylene-responsive element binding (AP2/ERF) transcription factor family is promising. So far, 122 members AP2/ERFs have been annotated in *Arabidopsis thaliana* (Nakano et al., 2006). Although the majority of ERFs have not been functionally characterized, it is clear that ERFs are involved in abiotic stress-control and mediate responses to several phytohormones, including ABA and ethylene (see: Nakano et al., (2006) and references within).

Introgression or transformation of the ethylene inducible AP2/ERF *Submergence1A-1* (*Sub1A-1*) into submergence intolerant (elongating) rice (*Oryza sativa* L.) cultivars conferred submergence tolerance to these plants by inducing a quiescence strategy (e.g. restricted growth and energy/carbon conservation). Accordingly, the presence of *Sub1A-1* strongly correlated with submergence tolerance in several accessions, whereas intolerance correlated to complete absence of *Sub1A* or to the presence of the *Sub1-A2* allele (Xu et al., 2006).

The ethylene- and gibberellin (GA)-inducible *Sub1C* gene at the same locus encoding *Sub1A* is associated with elongation growth during submergence; when *Sub1-A1* is present it restricts *Sub1C* transcript accumulation (Xu et al., 2006, Fukao et al., 2006; Fukao & Bailey-Serres, 2008). Moreover *Sub1A-1* enhances transcription of genes involved in ethanolic fermentation and restricts ethylene production by negative feedback regulation. *SUB1A-1* inhibits GA-mediated elongation growth by limiting the proteasome-mediated decline in the DELLA-domain GRAS transcription factor, SLENDERLEAF1 (SLR1) (Fukao & Bailey-Serres, 2008). GA-responsiveness is further limited in rice with *Sub1A-1* through the elevation of the non-DELLA GRAS factor SLR-like 1. Consistent with these observations, *SUB1A-1* represses GA mediated cell expansion and carbohydrate consumption (Fukao et al., 2006; Fukao & Bailey-Serres, 2008). Moreover, *Expansin* genes associated with cell elongation were repressed by *Sub1A-1*. Thus, an ethylene-regulated ERF of rice is responsible for limiting ethylene-induced GA production associated with submergence-induced elongation growth.

In accordance to the growth repression function of *Sub1A* in rice, heterologous expression of the *Sub1-A1* locus in *Arabidopsis* Col-0, repressed ethylene-, and low light- and heat-induced hyponastic growth, whereas *Sub1C* does not affect differential petiole growth to these stimuli and the *Sub1A-1* effects could be rescued

by application of GA (Bailey-Serres & Van Zanten, *unpublished data*).

An exploratory screen of a near-complete library of ERF-over-expressing *Arabidopsis* (Col-0) plants (Weiste *et al.*, 2007; see also chapter 6) resulted in the identification of several lines with an initial petiole angle phenotype or showed induced hyponastic growth phenotypes (either enhanced or repressed) after ethylene and/or low light treatment (Polko & Van Zanten, *unpublished data*). The ERFs that are present in these lines are currently being cloned in our lab and will be studied further. Moreover, ERFs are presumed to be involved in the control of ABA and ethylene mediated effects on KRP-A2-type Cyclin-CDKA control of hyponastic growth (Chapter 7). Together, these data strongly suggest that certain ERFs control hyponastic growth in *Arabidopsis*, and that this control can be either positive or negative.

Knowledge on the mechanisms by which ERFs control hyponastic growth may be used to study this response in other species. For example, it potentially could explain why *Rumex palustris* is able to induce ethylene-mediated hyponastic growth and petiole elongation under complete submergence, whereas the closely related *Rumex acetosa* is unable to connect ethylene accumulation to decrease in ABA levels and therefore lacks the ability to induce hyponasty and shoot elongation (Cox *et al.*, 2004; Benschop *et al.*, 2005).

Not all plant species trigger hyponastic growth upon ethylene/submergence treatment. For example, tomato (*Lycopersicon esculentum*) and Sunflower (*Helianthus annuus*) display epinastic growth when waterlogged (Bradford & Dilley, 1978; Kawase, 1974). Intriguingly, also a considerable part (13%) of the tested natural occurring *Arabidopsis thaliana* accessions showed epinastic growth upon ethylene application. On the whole, ethylene-induced petiole movement in set of screened *Arabidopsis* accessions (Figure 7.2a) showed a continuum in the range between hyponasty and epinasty. This confirms that induced hyponastic growth is multifactorial and that natural genetic variation can be found for many factors controlling this trait. Analogously, considerable variation is observed among accessions in tolerance to complete submergence in the dark (Dyvia & Voesenek, *unpublished data*).

A preliminary study including Palermo-1, the accessions that showed the strongest ethylene-induced epinastic growth (Figure 7.2), indicated that ethylene also inhibited hypocotyl elongation in the light in this accession, whereas these conditions promote hypocotyl elongation in other accessions (Smalle *et al.*, 1997; Keuskamp *et al.*, *unpublished data*). This suggests that at least part of the molecular machinery regulating ethylene hypocotyl elongation in the light may be similar to the components controlling ethylene-regulated hyponastic growth and thus that the latter response may be studied by using hypocotyl assays. For example this system can than be used to perform mutant screens to isolate potential suppressor mutations of ethylene-induced hyponastic growth or can be used in Genome Wide Association mapping (GWA) approaches which in particular requires large sets of accessions to be screened (Nordborg *et al.*, 2005; Nordborg & Weigel, 2008). The isolated components subsequently can be tested in functional approaches for effects on hyponastic growth and may be helpful to explain the natural variation observed between *Arabidopsis*

accessions. Much can be learned by comparing the natural genetic variation in, and mechanistic details of, regulation of hypocotyl elongation in young seedlings with the goal to understand the regulation mechanism and complex genetic networks controlling hyponastic growth induced by different abiotic environmental factors in *Arabidopsis thaliana*. Ultimately, the results obtained using *Arabidopsis thaliana* as a model, might be translatable to more ecological and economically relevant species.

Acknowledgements

The authors thank Julia Bailey-Serres on parts of the manuscript and our collaborators, Federico Tessadori, Paul Fransz, Steffen Vanneste, Tom Beeckman, Basten Snoek, Julia Bailey-Serres and several Plant Ecophysiology group members for sharing unpublished data.

References

- **Abreu ME, Munné-Bosch S.** (2008). Hyponastic leaf growth decreases the photoprotective demand, prevents damage to photosystem II and delays leaf senescence in *Salvia broussonetii* plants. *Physiol Plant.* **134**, 369-379.
- **Adachi S, Nobusawa T, Umeda M.** (2009). Quantitative and cell type-specific transcriptional regulation of A-type cyclin-dependent kinase in *Arabidopsis thaliana*. *Dev Biol.* **329**, 306-314.
- **Aharoni A, Dixit S, Jetter R, Thoenes E, van Arkel G, Pereira A.** (2004). The SHINE clade of AP2 domain transcription factors activates wax biosynthesis, alters cuticle properties, and confers drought tolerance when overexpressed in *Arabidopsis*. *Plant Cell.* **16**, 2463-2480.
- **Ahmad M, Cashmore AR.** (1993). *HY4* gene of *A. thaliana* encodes a protein with characteristics of a blue-light photoreceptor. *Nature.* **366**, 162-166.
- **Ahmad M, Grancher N, Heil M, Black RC, Giovani B, Galland P, Lardemer D.** (2002). Action spectrum for cryptochrome-dependent hypocotyl growth inhibition in *Arabidopsis*. *Plant Physiol.* **129**, 774-785.
- **Ahmad M, Jarillo JA, Smirnova O, Cashmore AR.** (1998a). Cryptochrome blue-light photoreceptors of *Arabidopsis* implicated in phototropism. *Nature.* **392**, 720-723.
- **Ahmad M, Jarillo JA, Smirnova O, Cashmore AR.** (1998b). The CRY1 blue light photoreceptor of *Arabidopsis* interacts with phytochrome A in vitro. *Mol Cell.* **1**, 939-948.
- **Alonso JM, Stepanova AN, Leisse TJ, Kim CJ, Chen H, Shinn P, Stevenson DK, Zimmerman J, Barajas P, Cheuk R, Gadrinab C, Heller C, Jeske A, Koesema E, Meyers CC, Parker H, Prednis L, Ansari Y, Choy N, Deen H, Geralt M, Hazari N, Hom E, Karnes M, Mulholland C, Ndubaku R, Schmidt I, Guzman P, Aguilar-Henonin L, Schmid M, Weigel D, Carter DE, Marchand T, Risseeuw E, Brogden D, Zeko A, Crosby WL, Berry CC, Ecker JR.** (2003). Genome-wide insertional mutagenesis of *Arabidopsis thaliana*. *Science.* **301**, 653-657.
- **Alonso-Blanco C, Peeters AJM, Koornneef M, Lister C, Dean C, van den Bosch N, Pot J, Kuiper MTR.** (1998a). Development of an AFLP based linkage map of Ler, Col and Cvi *Arabidopsis thaliana* ecotypes and construction of a Ler/Cvi recombinant inbred line population. *Plant J.* **14**, 259-271.
- **Alonso-Blanco C, El-Assal SE, Coupland G, Koornneef M.** (1998b). Analysis of natural allelic variation at flowering time loci in the Landsberg erecta and Cape Verde Islands ecotypes of *Arabidopsis thaliana*. *Genetics.* **149**, 749-764.
- **Alonso-Blanco C, Blankestijn-de Vries H, Hanhart CJ, Koornneef M.** (1999). Natural allelic variation at seed size loci in relation to other life history traits of *Arabidopsis thaliana*. *Proc Natl Acad Sci U S A.* **96**, 4710-4717.
- **Alonso-Blanco C, Koornneef M.** (2000). Naturally occurring variation in *Arabidopsis*: an underexploited resource for plant genetics. *Trends Plant Sci.* **5**, 22-29.

- **Alonso-Blanco C, Bentsink L, Hanhart CJ, Blankestijn-de Vries H, Koornneef M.** (2003). Analysis of natural allelic variation at seed dormancy loci of *Arabidopsis thaliana*. *Genetics*. **164**, 711-729.
- **Alonso-Blanco C, Mendez-Vigo B, Koornneef M.** (2005). From phenotypic to molecular polymorphisms involved in naturally occurring variation of plant development. *Int J Dev Biol*. **49**, 717-732.
- **Armstrong W.** (1979). Aeration in higher plants, *Advances in Botanical Research* vol. 7, Academic Press, London, pp. 225-332.
- **Arnholdt-Schmitt B.** (2004). Stress-induced cell reprogramming. A role for global genome regulation? *Plant Physiol*. **136**, 2579-2586.
- **Aufsatz W, Mette MF, van der Winden J, Matzke M, Matzke AJ.** (2002). HDA6, a putative histone deacetylase needed to enhance DNA methylation induced by double-stranded RNA. *EMBO J*. **21**, 6832-6841.
- **Bailey-Serres J, Voeselek LA.** (2008). Flooding stress: acclimations and genetic diversity. *Annu Rev Plant Biol*. **59**, 313-339.
- **Balasubramanian S, Sureshkumar S, Lempe J, Weigel D.** (2006a). Potent induction of *Arabidopsis thaliana* flowering by elevated growth temperature. *PLoS Genet*. **7**, e106.
- **Balasubramanian S, Sureshkumar S, Agrawal M, Michael TP, Wessinger C, Maloof JN, Clark R, Warthmann N, Chory J, Weigel D.** (2006b). The PHYTOCHROME C photoreceptor gene mediates natural variation in flowering and growth responses of *Arabidopsis thaliana*. *Nat Genet*. **38**, 711-715.
- **Ball NG.** (1969). Nastic responses. In Wilkins MB, editor, *The physiology of plant growth and development*. McGraw-Hill, London, pp. 277-300.
- **Ballaré CL, Casal JJ, Kendrick RE.** (1991). Responses of light-grown wild-type and long-hypocotyl mutant cucumber seedlings to natural and simulated shade. *Photochem Photobiol*. **54**, 819-826
- **Ballaré CL,** (1999). Keeping up with the neighbours: phytochrome sensing and other signalling mechanisms. *Trends Plant Sci*. **4**, 97-102.
- **Banga M, Slaa EJ, Blom CWPM, Voeselek LACJ.** (1996). Ethylene biosynthesis and accumulation under drained and submerged conditions: a comparative study of two *Rumex* species. *Plant Physiol*. **112**, 229-237.
- **Banga M, Bögemann GM, Blom CWPM, Voeselek LACJ.** (1997). Flooding resistance of *Rumex* species strongly depends on their response to ethylene: rapid shoot elongation or foliar senescence. *Physiol Plant*. **99**, 415-422.
- **Barnabás B, Jäger K, Fehér A.** (2008). The effect of drought and heat stress on reproductive processes in cereals. *Plant Cell Environ*. **31**, 11-38.
- **Beaudoin N, Serizet C, Gosti F, Giraudat J.** (2000). Interactions between abscisic acid and ethylene signaling cascades. *Plant Cell*. **12**, 1103-1115.
- **Beelman CA, Parker R.** (1995). Degradation of mRNA in eukaryotes. *Cell*. **81**, 179-183.
- **Bell CJ, Ecker JR.** (1994). Assignment of 30 microsatellite loci to the linkage map of

- Arabidopsis*. Genomics. **19**, 137-144.
- Benschop JJ, Jackson MB, Gühl K, Vreeburg RAM, Croker SJ, Peeters AJM, Voesenek LACJ. (2005). Contrasting interactions between ethylene and abscisic acid in *Rumex* species differing in submergence tolerance. *Plant J.* **44**, 756-768.
 - Benschop JJ, Millenaar FF, Smeets ME, van Zanten M, Voesenek LACJ, Peeters AJM. (2007). ABA antagonizes ethylene-induced hyponastic growth in *Arabidopsis*. *Plant Physiol.* **143**, 1013-1023.
 - Benvenuto G, Formiggini F, Laflamme P, Malakhov M, Bowler C. (2002). The photomorphogenesis regulator DET1 binds the amino-terminal tail of histone H2B in a nucleosome context. *Curr Biol.* **12**, 1529-1534.
 - Blázquez MA, Ahn JH, Weigel DA. (2003). Thermosensory pathway controlling flowering time in *Arabidopsis thaliana*. *Nat Genet.* **33**, 168-171.
 - Boonman A, Anten NP, Dueck TA, Jordi WJ, van der Werf A, Voesenek LA, Pons TL (2006). Functional significance of shade-induced leaf senescence in dense canopies: an experimental test using transgenic tobacco. *Am Nat.* **168**, 597-607.
 - Borevitz JO, Maloof JN, Lutes J, Dabi T, Redfern JL, Trainer GT, Werner JD, Asami T, Berry CC, Weigel D, Chory J. (2002). Quantitative trait loci controlling light and hormone response in two accessions of *Arabidopsis thaliana*. *Genetics.* **160**, 683-696.
 - Borevitz JO, Nordborg M. (2003). The Impact of Genomics on the Study of Natural Variation in *Arabidopsis*. *Plant Physiol.* **132**, 718-725.
 - Botto JF, Smith H. (2002). Differential genetic variation in adaptive strategies to a common environmental signal in *Arabidopsis* accessions: phytochrome-mediated shade avoidance. *Plant Cell Environ.* **25**, 53-63.
 - Boudolf V, Lammens T, Boruc J, Van Leene J, Van Den Daele H, Maes S, Van Isterdael G, Russinova E, Kondorosi E, Witters E, De Jaeger G, Inze D, De Veylder L. (2009). CDKB1;1 forms a functional complex with CYCA2;3 to suppress endocycle onset. *Plant Physiol.* **150**, 1482-1493.
 - Boudolf V, Vlieghe K, Beemster GT, Magyar Z, Torres Acosta JA, Maes S, Van Der Schueren E, Inzé D, De Veylder L. (2004). The plant-specific cyclin-dependent kinase CDKB1;1 and transcription factor E2Fa-DPa control the balance of mitotically dividing and endoreduplicating cells in *Arabidopsis*. *Plant Cell.* **16**, 2683-2692.
 - Boyes DC, Zayed AM, Ascenzi R, McCaskill AJ, Hoffman NE, Davis KR, Görlach J. (2001). Growth stage-based phenotypic analysis of *Arabidopsis*: a model for high throughput functional genomics in plants. *Plant Cell.* **13**, 1499-1510.
 - Bradford KJ, Dille DR. (1978). Effects of root anaerobiosis on ethylene production, epinasty, and growth of tomato plants. *Plant Physiol.* **61**, 506-509.
 - Burnette RN, Gunesequera BM, Gillaspay GE. (2003). An *Arabidopsis* inositol 5-phosphatase gain-of-function alters abscisic acid signaling. *Plant Physiol.* **132**, 1011-1019.
 - Burssens S, de Almeida Engler J, Beeckman T, Richard C, Shaul O, Ferreira P, Van

- Montagu M, Inzé D. (2000). Developmental expression of the *Arabidopsis thaliana* CycA2;1 gene. *Planta*. **211**, 623-631.
- Busch W, Wunderlich M, Schoffl F. (2005). Identification of novel heat shock factor-dependent genes and biochemical pathways in *Arabidopsis thaliana*. *Plant J*. **41**, 1-14.
 - Campell BR, Song YG, Posch TE, Cullis CA, Town CD. (1992). Sequence and organization of 5s ribosomal RNA-encoding genes of *Arabidopsis thaliana*. *Gene*. **112**, 225-228.
 - Casal JJ, Mazzella MA. (1998). Conditional synergism between cryptochrome 1 and phytochrome B is shown by the analysis of phyA, phyB, and hy4 simple, double, and triple mutants in *Arabidopsis*. *Plant Physiol*. **118**, 19-25.
 - Casal JJ, Yanovsky MJ (2005). Regulation of gene expression by light. *Int J Dev Biol*. **49**, 501-511.
 - Castillon A, Shen H, Huq E. (2009). Blue light induces degradation of the negative regulator phytochrome interacting factor 1 to promote photomorphogenic development of *Arabidopsis* seedlings. *Genetics*. **182**, 161-171.
 - Chang C, Kwok SF, Bleecker AB, Meyerowitz EM. (1993). *Arabidopsis* ethylene-response gene ETR1: similarity of product to two-component regulators. *Science*. **262**, 539-544.
 - Chen M, Chory J, Fankhauser C. (2004). Light signal transduction in higher plants. *Annu Rev Genet*. **38**, 87-117.
 - Chen M, Tao Y, Lim J, Shaw A, Chory J. (2005). Regulation of phytochrome B nuclear localization through light-dependent unmasking of nuclear-localization signals. *Curr Biol*. **15**, 637-642.
 - Chen H, Zhang J, Neff MM, Hong SW, Zhang H, Deng XW, Xiong L. (2008). Integration of light and abscisic acid signaling during seed germination and early seedling development. *Proc Natl Acad Sci U S A*. **105**, 4495-5000.
 - Clough SJ, Bent AF. (1998). Floral dip: a simplified method for *Agrobacterium*-mediated transformation of *Arabidopsis thaliana*. *Plant J*. **16**, 735-743.
 - Colón-Carmona A, You R, Haimovitch-Gal T, Doerner P. (1999). Technical advance: spatio-temporal analysis of mitotic activity with a labile cyclin-GUS fusion protein. *Plant J*. **20**, 503-508.
 - Costa S, Shaw P. (2006). Chromatin organization and cell fate switch respond to positional information in *Arabidopsis*. *Nature*. **439**, 493-496.
 - Coté GG (1995). Signal transduction in leaf movement. *Plant Physiol*. **109**, 729-734.
 - Cox MCH, Millenaar FF, de Jong van Berkel YEM, Peeters AJM, Voeselek LACJ. (2003). Plant movement; submergence-induced petiole elongation in *Rumex palustris* depends on hyponastic growth. *Plant Physiol*. **132**, 282-291.
 - Cox MCH, Benschop JJ, Vreeburg RAM, Wagemaker CAM, Moritz T, Peeters AJM, Voeselek LACJ. (2004). The roles of ethylene, auxin, abscisic acid, and gibberellin in the hyponastic growth of submerged *Rumex palustris* petioles. *Plant Physiol*. **136**, 2948-2960.

- Curtis D, Lehmann R, Zamore PD. (1995). Translational regulation in development. *Cell*. **81**, 171-178.
- Cutler S, Ghassemian M, Bonetta D, Cooney S, McCourt PA. (1996). protein farnesyl transferase involved in abscisic acid signal transduction in Arabidopsis. *Science*. **273**, 1239-1241.
- Cutler SR, Ehrhardt DW, Griffiths JS, Somerville CR. (2000). Random GFP::cDNA fusions enable visualization of subcellular structures in cells of Arabidopsis at a high frequency. *Proc Natl Acad Sci U S A*. **97**, 3718-3723.
- Czechowski T, Bari RP, Stitt M, Scheible WR, Udvardi MK. (2004). Real-time RT-PCR profiling of over 1400 Arabidopsis transcription factors: unprecedented sensitivity reveals novel root- and shoot-specific genes. *Plant J*. **38**, 366-379.
- Dan H, Imaseki H, Wasteneys GO, Kazama H. (2003). Ethylene stimulates endoreduplication but inhibits cytokinesis in cucumber hypocotyl epidermis. *Plant Physiol*. **133**, 1726-1731.
- Danon A, Mayfield SP. (1994). Light-regulated translation of chloroplast messenger RNAs through redox potential. *Science*. **266**, 1717-1719.
- Darwin C. (1880). *The power of movement in plants*. Clowes, London
- De Paepe A, Vuylsteke M, van Hummelen P, Zabeau M, Van der Straeten D. (2004). Transcriptional profiling by cDNA-AFLP and microarray analysis reveals novel insights into the early response to ethylene in Arabidopsis. *Plant J*. **39**, 537-559.
- De Veylder L, Beeckman T, Beemster GT, Krols L, Terras F, Landrieu I, van der Schueren E, Maes S, Naudts M, Inzé D. (2001). Functional analysis of cyclin-dependent kinase inhibitors of Arabidopsis. *Plant Cell*. **13**, 1653-1668.
- Devlin PF, Patel SR, Whitelam GC. (1998). Phytochrome E influences internode elongation and flowering time in Arabidopsis. *Plant Cell*. **10**, 1479-1487.
- Devlin PF, Robson PRH, Patel SR, Goosey L, Sharrock RA, Whitelam GC. (1999). Phytochrome D acts in the shade-avoidance syndrome in Arabidopsis by controlling elongation and flowering time. *Plant Physiol*. **119**, 909-915.
- Dewitte W, Murray JA. (2003). The plant cell cycle. *Annu Rev Plant Biol*. **54**, 235-264.
- Dharmasiri N, Dharmasiri S, Estelle M. (2005a). The F-box protein TIR1 is an auxin receptor. *Nature*. **435**, 441-445.
- Dharmasiri N, Dharmasiri S, Weijers D, Lechner E, Yamada M, Hobbie L, Ehrismann JS, Jürgens G, Estelle M. (2005b). Plant development is regulated by a family of auxin receptor F box proteins. *Dev Cell*. **9**, 109-119.
- Djakovic-Petrovic T, de Wit M, Voeselek LA, Pierik R. (2007). DELLA protein function in growth responses to canopy signals. *Plant J*. **51**, 117-126
- Donnelly PM, Bonetta D, Tsukaya H, Dengler RE, Dengler NG. (1999). Cell cycling and cell enlargement in developing leaves of Arabidopsis. *Dev Biol*. **215**, 407-419.
- Dorn LA, Hammond-Pyle E, Schmitt J. (2000). Plasticity to cues and resources in Arabidopsis thaliana: Testing for adaptive value and costs. *Evolution*. **54**, 1982-1994.

- Earley K, Lawrence RJ, Pontes O, Reuther R, Enciso AJ, Silva M, Neves N, Gross M, Viegas W, Pikaard CS. (2006). Erasure of histone acetylation by Arabidopsis HDA6 mediates large-scale gene silencing in nucleolar dominance. *Genes Dev.* **20**, 1283-1293.
- Edwards KD, Lynn JR, Gyula P, Nagy F, Millar AJ. (2005). Natural allelic variation in the temperature-compensation mechanisms of the *Arabidopsis thaliana* circadian clock. *Genetics.* **170**, 387-400.
- El-Assal S E-D, Alonso-Blanco C, Peeters AJM, Raz V, Koornneef M. (2001). A QTL for flowering time in Arabidopsis reveals a novel allele of CRY2. *Nat Genet.* **29**, 435-440.
- El-Lithy ME, Clercx EJ, Ruys GJ, Koornneef M, Vreugdenhil D. (2004). Quantitative trait locus analysis of growth-related traits in a new Arabidopsis recombinant inbred population. *Proc Natl Acad Sci U S A.* **135**, 444-458.
- Escoubas JM, Lomas M, Laroche J, Falkowski PG. (1995). Light-intensity regulation of Cab gene-transcription is signaled by the redox state of the plastoquinone pool. *Proc Natl Acad Sci U S A.* **92**, 10237-10241.
- Exner V, Hennig L. (2008). Chromatin rearrangements in development. *Curr Opin Plant Biol.* **11**, 64-69.
- Faigón-Soverna A, Harmon FG, Storani L, Karayekov E, Staneloni RJ, Gassmann W, Más P, Casal JJ, Kay SA, Yanovsky A. (2006). Constitutive shade-avoidance mutant implicates TIR-NBS-LRR proteins in Arabidopsis photomorphogenic development. *Plant Cell.* **18**, 2919-2928.
- Falster DS, Westoby M. (2003). Leaf size and angle vary widely across species: what consequences for light interception? *New Phytol.* **158**, 509-525.
- Fankhauser C, Chen M. (2008). Transposing phytochrome into the nucleus. *Trends Plant Sci.* **13**, 596-601.
- Fellner M, Horton LA, Cocke AE, Stephens NR, Ford ED, Van Volkenburgh E. (2003). Light interacts with auxin during leaf elongation and leaf angle development in young corn seedlings. *Planta.* **216**, 366-376.
- Filiault DL, Wessinger CA, Dinneny JR, Lutes J, Borevitz JO, Weigel D, Chory J, Maloof JN. (2008). Amino acid polymorphisms in Arabidopsis phytochrome B cause differential responses to light. *Proc Natl Acad Sci U S A.* **105**, 3157-3162.
- Finkelstein RR. (1994). Mutations at two new Arabidopsis ABA response loci are similar to the *abi3* mutations. *Plant J.* **5**, 765-771.
- Finlayson SA, Lee I-J, Morgan PW. (1998). Phytochrome B and the regulation of circadian ethylene production in sorghum. *Plant Physiol.* **116**, 17-25.
- Finnegan EJ, Sheldon CC, Jardinaud F, Peacock WJ, Dennis ES. (2004). A cluster of Arabidopsis genes with a coordinate response to an environmental stimulus. *Curr Biol.* **14**, 911-916.
- Firn RD, Digby J. (1980). The establishment of tropic curvatures in plants. *Ann Rev Plant Phys.* **31**, 131-148.
- Franklin KA. (2008). Shade avoidance. *New Phytol.* **179**, 930-944.

- Franklin KA, Larner VS, Whitelam GC. (2005). The signal transducing photoreceptors of plants. *Int J Dev Biol.* **49**, 653-664.
- Franklin KA, Praekelt U, Stoddart WM, Billingham OE, Halliday KJ, Whitelam GC. (2003). Phytochromes B, D, and E act redundantly to control multiple physiological responses in *Arabidopsis*. *Plant Physiol.* **131**, 1340-1346.
- Fransz P, De Jong JH, Lysak M, Castiglione MR, Schubert I. (2002). Interphase chromosomes in *Arabidopsis* are organized as well defined chromocenters from which euchromatin loops emanate. *Proc Natl Acad Sci U S A.* **99**, 14584-14589.
- Fransz P, Soppe W, Schubert I. (2003). Heterochromatin in interphase nuclei of *Arabidopsis thaliana*. *Chromosome Res.* **11**, 227-240.
- Fransz P, Ten Hoopen R, Tessadori F. (2006). Composition and formation of heterochromatin in *Arabidopsis thaliana*. *Chromosome Res.* **14**, 71-82.
- Friml J, Palme K. (2002). Polar auxin transport-old questions and new concepts? *Plant Mol Biol.* **49**, 273-284.
- Friml J, Wisniewska J, Benkova E, Mendgen K, Palme K. (2002). Lateral relocation of auxin efflux regulator PIN3 mediates tropism in *Arabidopsis*. *Nature.* **415**, 806-809.
- Friml J. (2003). Auxin transport - shaping the plant. *Curr Opin Plant Biol.* **6**, 7-12.
- Friml J, Vieten A, Sauer M, Weijers D, Schwarz H, Hamann T, Offringa R, Jürgens G. (2003). Efflux-dependent auxin gradients establish the apical-basal axis of *Arabidopsis*. *Nature.* **426**, 147-153.
- Fu QA, Ehleringer JR. (1989). Heliotropic leaf movements in common beans controlled by air temperature. *Plant Physiol.* **91**, 1162-1167.
- Fukao T, Xu K, Ronald PC, Bailey-Serres J. (2006). A variable cluster of ethylene response factor-like genes regulates metabolic and developmental acclimation responses to submergence in rice. *Plant Cell.* **18**, 2021-2034.
- Fukao T, Bailey-Serres J. (2008). Submergence tolerance conferred by Sub1A is mediated by SLR1 and SLRL1 restriction of gibberellin responses in rice. *Proc Natl Acad Sci U S A.* **105**, 16814-168149.
- Furner IJ, Sheikh MA, Collett CE. (1998). Gene silencing and homology-dependent gene silencing in *Arabidopsis*: genetic modifiers and DNA methylation. *Genetics.* **149**, 651-662.
- Gao Y, Zeng Q, Guo J, Cheng J, Ellis BE, Chen JG. (2007). Genetic characterization reveals no role for the reported ABA receptor, GCR2, in ABA control of seed germination and early seedling development in *Arabidopsis*. *Plant J.* **52**, 1001-1113.
- Geigenberger P, Kolbe A, Tiessen A. (2005). Redox regulation of carbon storage and partitioning in response to light and sugars. *J Exp Bot.* **56**, 1469-1479.
- Gendreau E, Orbovic V, Höfte H, Traas J. (1999). Gibberellin and ethylene control endoreduplication levels in the *Arabidopsis thaliana* hypocotyl. *Planta.* **209**, 513-516.
- Gerlach WL, Bedbrook JR. (1979). Cloning and characterization of ribosomal RNA

- genes from wheat and barley. *Nucleic Acids Res.* **7**, 1869-1885.
- **Ghassemian M, Nambara E, Cutler S, Kawaide H, Kamiya Y, McCourt P.** (2000). Regulation of abscisic acid signaling by the ethylene response pathway in *Arabidopsis*. *Plant Cell.* **12**, 1117-1126.
 - **Gilmartin PM, Bowler C.** editorss. (2002). *Molecular Plant Biology Volume 1*, Oxford. Univ. Press, pp. 112, 113.
 - **Godiard L, Sauviac L, Torii KU, Grenon O, Mangin B, Grimsley NH, Marco Y.** (2003). ERECTA, an LRR receptor-like kinase protein controlling development pleiotropically affects resistance to bacterial wilt. *Plant J.* **36**, 353-365.
 - **Gómez-Porrás JL, Riaño-Pachón DM, Dreyer I, Mayer JE, Mueller-Roeber B.** (2007). Genome-wide analysis of ABA-responsive elements ABRE and CE3 reveals divergent patterns in *Arabidopsis* and rice. *BMC Genomics.* **8**, 260. **Gong M, Li Y-J, Chen SZ.** (1998). Abscisic acid induced thermotolerance in maize seedlings is mediated by Ca^{2+} and associated with antioxidant systems. *J Plant Physiol.* **153**, 488-496.
 - **Gould PD, Locke JC, Larue C, Southern MM, Davis SJ, Hanano S, Moyle R, Milich R, Putterill J, Millar AJ, Hall A.** (2006). The molecular basis of temperature compensation in the *Arabidopsis* circadian clock. *Plant Cell.* **18**, 1177-1187.
 - **Grafi G, Ben-Meir H, Avivi Y, Moshe M, Dahan Y, Zemach A.** (2007). Histone methylation controls telomerase-independent telomere lengthening in cells undergoing dedifferentiation. *Dev Biol.* **306**, 838-846.
 - **Gray WM, Ostin A, Sandberg G, Romano CP, Estelle M.** (1998). High temperature promotes auxin-mediated hypocotyl elongation in *Arabidopsis*. *Proc Natl Acad Sci U S A.* **95**, 7197-7202.
 - **Grimoldi AA, Insausti P, Roitman GG, Soriano A.** (1999). Responses to flooding intensity in *Leontodon taraxacoides*. *New Phytol.* **141**, 119-128.
 - **Gu Y, Wang Z, Yang Z.** (2004). ROP/RAC GTPase: an old new master regulator for plant signaling. *Curr Opin Plant Biol.* **7**, 527-536.
 - **Gunesequera B, Torabinejad J, Robinson J, Gillaspie GE.** (2007). Inositol polyphosphate 5-phosphatases 1 and 2 are required for regulating seedling growth. *Plant Physiol.* **143**, 1408-1417.
 - **Guo HW, Yang WY, Mockler TC, Lin CT.** (1998). Regulation of flowering time by *Arabidopsis* photoreceptors. *Science.* **279**, 1360-1363.
 - **Guo J, Zeng Q, Emami M, Ellis BE, Chen JG.** (2008). The GCR2 gene family is not required for ABA control of seed germination and early seedling development in *Arabidopsis*. *PLoS One.* **3**, e2982.
 - **Guzman P, Ecker JR.** (1990). Exploiting the triple response of *Arabidopsis* to identify ethylene-related mutants. *Plant Cell.* **2**, 513-523.
 - **Gyula N, Schafer E, Nagy F.** (2003). Light perception and signalling in higher plants. *Curr Opin Plant Biol.* **6**, 446-452.
 - **Ha CM, Jun JH, Nam HG, Fletcher JC.** (2007). BLADE-ON-PETIOLE 1 and 2 control *Arabidopsis* lateral organ fate through regulation of LOB domain and adaxial-

- abaxial polarity genes. *Plant Cell*. **19**, 1809-1825.
- **Hall MC, Dworkin I, Ungerer MC, Purugganan M.** (2007). Genetics of microenvironmental canalization in *Arabidopsis thaliana*. *Proc Natl Acad Sci USA*. **104**, 13717-13722.
 - **Halliday KJ, Salter MG, Thingnaes E, Whitelam GC.** (2003). Phytochrome control of flowering is temperature sensitive and correlates with expression of the floral integrator FT. *Plant J*. **33**, 875-885.
 - **Halliday KJ, Whitelam GC.** (2003). Changes in photoperiod or temperature alter the functional relationships between phytochromes and reveal roles for phyD and phyE. *Plant Physiol*. **131**, 1913-1920.
 - **Hangarter RP.** (1997). Gravity, light and plant form. *Plant Cell Environ*. **20**, 796-800.
 - **Harper RM, Stowe-Evans EL, Luesse DR, Muto H, Tatematsu K, Watahiki MK, Yamamoto K, Liscum E.** (2000). The NPH4 Locus encodes the Auxin Response Factor ARF7, a conditional regulator of differential growth in aerial *Arabidopsis* tissue. *Plant Cell*. **12**, 757-770.
 - **Hautier Y, Niklaus PA, Hector A.** (2009). Competition for light causes plant biodiversity loss after eutrophication. *Science*. **324**, 636-638.
 - **Himanen K, Boucheron E, Vanneste S, de Almeida Engler J, Inzé D, Beeckman T.** (2002). Auxin-mediated cell cycle activation during early lateral root initiation. *Plant Cell*. **14**, 2339-2351.
 - **Hoffmann MH.** (2002). Biogeography of *Arabidopsis thaliana* (L.) Heynh. (Brassicaceae). *J. Biogeography*. **29**, 125-134.
 - **Hoffmann-Benning S, Kende H.** (1992). On the role of abscisic-acid and gibberellin in the regulation of growth in rice. *Plant Physiol*. **99**, 1156-1161.
 - **Hopkins R, Schmitt J, Stinchcombe JR.** (2008). A latitudinal cline and response to vernalization in leaf angle and morphology in *Arabidopsis thaliana* (Brassicaceae). *New Phytol*. **179**, 155-164.
 - **Hornstein E, Shomron N.** (2006). Canalization of development by microRNAs. *Nat Genet*. **38**, Suppl, S20-24.
 - **Hoth S, Morgante M, Sanchez JP, Hanafey MK, Tingey SV, Chua NH.** (2002). Genome-wide gene expression profiling in *Arabidopsis thaliana* reveals new targets of abscisic acid and largely impaired gene regulation in the *abi1-1* mutant. *J Cell Sci*. **15**, 4891-4900.
 - **Hua J, Meyerowitz EM.** (1998). Ethylene responses are negatively regulated by a receptor gene family in *Arabidopsis thaliana*. *Cell*. **94**, 261-271.
 - **Hua J, Sakai H, Nourizadeh S, Chen QG, Bleecker AB, Ecker JR, Meyerowitz EM.** (1998). *EIN4* and *ERS2* are members of the putative ethylene receptor gene family in *Arabidopsis*. *Plant Cell*. **10**, 1321-1332.
 - **Huq E, Quail PH.** (2002). PIF4, a phytochrome-interacting bHLH factor, functions as a negative regulator of phytochrome B signaling in *Arabidopsis*. *EMBO J*. **22**, 2441-2550.
 - **Illingworth CJ, Parkes KE, Snell CR, Mullineaux PM, Reynolds CA.** (2008). Criteria

- for confirming sequence periodicity identified by Fourier transform analysis: application to GCR2, a candidate plant GPCR? *Biophys Chem.* **133**, 28-35.
- Imai KK, Ohashi Y, Tsuge T, Yoshizumi T, Matsui M, Oka A, Aoyama T. (2006). The A-type cyclin CYCA2;3 is a key regulator of ploidy levels in Arabidopsis endoreduplication. *Plant Cell.* **18**, 382-396.
 - Inoue S-I, Kinoshita T, Takemiya A, Doi M, Shimazaki K-I. (2008). Leaf positioning of Arabidopsis in response to blue light. *Mol Plant.* **1**, 15-26.
 - Insausti P, Grimoldi AA, Chanton EJ, Vasellati V. (2001). Flooding induces a suite of adaptive plastic responses in the grass *Paspalum dilatatum*. *New Phytol.* **152**, 291-299.
 - Inzé D, De Veylder L. (2006). Cell cycle regulation in plant development. *Annu Rev Genet.* **40**, 77-105.
 - Jackson MB, (1985). Ethylene and the responses of plants to soil waterlogging and submergence. *Ann Rev Plant Phys.* **36**, 145-174.
 - Jackson MB. (2008). Ethylene-promoted elongation: an adaptation to submergence stress. *Ann Bot (Lond).* **101**, 229-248.
 - Jarillo JA, Gabrys H, Capel J, Alonso JM, Ecker JR, Cashmore AR. (2001). Phototropin-related NPL1 controls chloroplast relocation induced by blue light. *Nature.* **410**, 952-954.
 - Jarillo JA, Piñeiro M, Cubas P, Martínez-Zapater JM. (2009). Chromatin remodeling in plant development. *Int. J. Dev. Biol.* In Press doi: 10.1387/ijdb.072460
 - Jasencakova Z, Soppe WJ, Meister A, Gernand D, Turner BM, Schubert I. (2003). Histone modifications in Arabidopsis- high methylation of H3 lysine 9 is dispensable for constitutive heterochromatin. *Plant J.* **33**, 471-480.
 - Jensen PJ, Hangarter RP, Estelle M. (1998). Auxin transport is required for hypocotyl elongation in light-grown but not dark-grown *Arabidopsis*. *Plant Physiol.* **116**, 455-462.
 - Jiao Y, Ma L, Strickland E, Deng XW. (2005). Conservation and divergence of light-regulated genome expression patterns during seedling development in rice and Arabidopsis. *Plant Cell.* **17**, 3239-3256.
 - Johnston CA, Temple BR, Chen JG, Gao Y, Moriyama EN, Jones AM, Siderovski DP, Willard FS. (2007). Comment on "A G protein coupled receptor is a plasma membrane receptor for the plant hormone abscisic acid" *Science.* **318**, 914c.
 - Jones HG. (1983). *Plants and microclimate: a quantitative approach to environmental plant physiology* (Cambridge: Cambridge University Press).
 - Kagawa T, Sakai T, Suetsugu N, Oikawa K, Ishiguro S, Kato T, Tabata S, Okada K, Wada M. (2001). Arabidopsis NPL1: A phototropin homolog controlling the chloroplast high-light avoidance response. *Science.* **291**, 2138-2141.
 - Kang BG. (1979). Epinasty. In: Haupt W, Feinleib ME, editors. *Encyclopedia of Plant Physiology, New Series.* 7. Physiology of Movements. Berlin: Springer-Verlag; pp. 647-667.
 - Karlsson BH, Sills GR, Nienhuis J. (1993). Effects of Photoperiod and Vernalization

- on the Number of Leaves at Flowering in 32 *Arabidopsis thaliana* (Brassicaceae) Ecotypes. *Am J Bot.* **80**, 646-648.
- **Karimi M, Inzé D, Depicker A.** (2002). GATEWAY vectors for Agrobacterium-mediated plant transformation. *Trends Plant Sci.* **7**, 193-195.
 - **Kawaguchi M.** (2003). SLEEPLESS, a gene conferring nyctinastic movement in legume. *J Plant Res.* **116**, 151-154.
 - **Kawase M.** (1974). Role of ethylene in induction of flooding damage in sunflower. *Physiol Plant.* **31**, 29-38.
 - **Kazemi S, Kefford NP.** (1974). Apical correlative effects in leaf epinasty of tomato. *Plant Physiol.* **54**, 512-519.
 - **Kende H, van der Knaap E, Cho HT.** (1998). Deepwater rice: A model plant to study stem elongation. *Plant Physiol.* **118**, 1105-1110.
 - **Kepinski S, Leyser O.** (2005). The Arabidopsis F-box protein TIR1 is an auxin receptor. *Nature.* **435**, 446-451.
 - **Keurentjes JJ, Bentsink L, Alonso-Blanco C, Hanhart CJ, Blankestijn-De Vries H, Effgen S, Vreugdenhil D, Koornneef M.** (2007). Development of a near-isogenic line population of *Arabidopsis thaliana* and comparison of mapping power with a recombinant inbred line population. *Genetics.* **175**, 891-905.
 - **King DA.** (1997). The functional significance of leaf angle in *Eucalyptus*. *Austral J Bot.* **45**, 619-639.
 - **Kleiner O, Kircher S, Harter K, Batschauer A.** (1999). Nuclear localization of the Arabidopsis blue light receptor cryptochrome 2. *Plant J.* **19**, 289-296.
 - **Kloosterman B, Visser RG, Bachem CW.** (2006). Isolation and characterization of a novel potato Auxin/Indole-3-Acetic Acid family member (StIAA2) that is involved in petiole hyponasty and shoot morphogenesis. *Plant Physiol Biochem.* **44**, 766-775.
 - **Knee EM, Hangarter RP, Knee M.** (2000). Interactions of light and ethylene in hypocotyl hook maintenance in *Arabidopsis thaliana* seedlings. *Physiol Plant.* **108**, 208-215.
 - **Kohchi T, Mukougawa K, Frankenberg N, Masuda M, Yokota A, Lagarias JC.** (2001). The Arabidopsis HY2 gene encodes phytochromobilin synthase, a ferredoxin-dependent biliverdin reductase. *Plant Cell.* **13**, 425-436.
 - **Koini MA, Alvey L, Allen T, Tilley CA, Harberd NP, Whitelam GC, Franklin KA.** (2009). High temperature-mediated adaptations in plant architecture require the bHLH transcription factor PIF4. *Curr Biol.* **19**, 408-413.
 - **Koornneef M, Rolff E, Spruitt, C.J.P.** (1980). Genetic control of light-inhibited hypocotyl elongation in *Arabidopsis thaliana* L. Heynh. *Z Pflanzenphysiol.* **100**, 147-160.
 - **Koornneef M, Jorna ML, Brinkhorst-van der Swan DLC, Karssen CM.** (1982). The isolation of abscisic acid (ABA) deficient mutants by selection of induced revertants in non-germinating gibberellin sensitive lines of *Arabidopsis thaliana* (L.) Heynh. *Theor Appl Genet.* **61**, 385-393.

- Koornneef M, Reutling G, Karssen CM. (1984). The isolation and characterization of abscisic acid-insensitive mutants of *Arabidopsis thaliana*. *Physiol Plant*. **61**, 377-383.
- Koornneef M, Hanhart CJ, van der Veen JH. (1991). A genetic and physiological analysis of late flowering mutants in *Arabidopsis thaliana*. *Mol Gen Genet*. **229**, 57-66.
- Koornneef M, Alonso-Blanco C, Vreugdenhil D. (2004). Naturally occurring genetic variation in *Arabidopsis thaliana*. *Annu Rev Plant Biol*. **55**, 141-172.
- Kozuka T, Horiguchi G, Kim GT, Ohgishi M, Sakai T, Tsukaya H. (2005). The different growth responses of the *Arabidopsis thaliana* leaf blade and the petiole during shade avoidance are regulated by photoreceptors and sugar. *Plant Cell Physiol*. **46**, 213-223.
- Larkindale J, Huang BJ. (1994). Thermotolerance and antioxidant systems in *Agrostis stolonifera*: involvement of salicylic acid, abscisic acid, calcium, hydrogen peroxide, and ethylene. *J Plant Physiol*. **161**, 405-413.
- Larkindale J, Knight MR. (2002). Protection against heat stress-induced oxidative damage in *Arabidopsis* involves calcium, abscisic acid, ethylene, and salicylic acid. *Plant Physiol*. **128**, 682-695.
- Larkindale J, Hall JD, Knight MR, Vierling E. (2005). Heat stress phenotypes of *Arabidopsis* mutants implicate multiple signaling pathways in the acquisition of thermotolerance. *Plant Physiol*. **138**, 882-897.
- Lease KA, Lau NY, Schuster RA, Torii KU, Walker JC. (2001). Receptor serine/threonine protein kinases in signalling: analysis of the erecta receptor-like kinase of *Arabidopsis thaliana*. *New Phytol*. **151**, 133-143.
- Lee KP, Kim C, Landgraf F, Apel K. (2007). EXECUTER1- and EXECUTER2-dependent transfer of stress-related signals from the plastid to the nucleus of *Arabidopsis thaliana*. *Proc Natl Acad Sci U S A*. **104**, 10270-10275.
- Lehman A, Black R, Ecker JR. (1996). HOOKLESS1, an ethylene response gene, is required for differential cell elongation in the *Arabidopsis* hypocotyl. *Cell*. **85**, 183-194.
- Lemichez E, Wu Y, Sanchez JP, Mettouchi A, Mathur J, Chua NH. (2001). Inactivation of AtRac1 by abscisic acid is essential for stomatal closure. *Genes Dev*. **15**, 1808-1816.
- Lempe J, Balasubramanian S, Sureshkumar S, Singh A, Schmid M, Weigel D. (2005). Diversity of flowering responses in wild *Arabidopsis thaliana* strains. *PLoS Genet*. **1**, 109-118.
- LeNoble ME, Spollen WG, Sharp RE. (2004). Maintenance of shoot growth by endogenous ABA: genetic assessment of the involvement of ethylene suppression. *J Exp Bot*. **55**, 237-245.
- Léon-Kloosterziel KM, Gil MA, Ruijs GJ, Jacobsen SE, Olszewski NE, Schwartz SH, Zeevaart JA, Koornneef M. (1996). Isolation and characterization of abscisic acid-deficient *Arabidopsis* mutants at two new loci. *Plant J*. **10**, 655-661.

- **Leung J, Bouvier-Durand M, Morris PC, Guerrier D, Chefdor F, Giraudat J.** (1994). Arabidopsis ABA response gene ABI1: features of a calcium-modulated protein phosphatase. *Science*. **264**, 1448-1452.
- **Leung J, Merlot S, Giraudat J.** (1997). The Arabidopsis ABSCISIC ACID INSENSITIVE 2 (ABI2) and ABI1 genes encode redundant protein phosphatases 2C involved in abscisic acid signal transduction. *Plant Cell*. **9**, 759-771.
- **Lin C, Yang H, Guo H, Mockler T, Chen J, Cashmore AR.** (1998). Enhancement of blue-light sensitivity of Arabidopsis seedlings by a blue light receptor cryptochrome 2. *Proc Natl Acad Sci U S A*. **95**, 2686-2690.
- **Lin C.** (2002). Blue light receptors and signal transduction. *Plant Cell*. **14**, 207-225.
- **Lin C, Shalitin D.** (2003). Cryptochrome structure and signal transduction. *Annu Rev Plant Biol*. **54**, 469-496.
- **Lino M.** (2006). Toward understanding the ecological functions of tropisms: interactions among and effects of light on tropisms. *Curr Opin Plant Biol*. **9**, 89-93.
- **Lippman Z, May B, Yordan C, Singer T, Martienssen R.** (2003). Distinct mechanisms determine transposon inheritance and methylation via small interfering RNA and histone modification. *PLoS Biol*. **1**, E67.
- **Liscum E, Briggs WR.** (1995). Mutations in the NPH1 locus of Arabidopsis disrupt the perception of phototropic stimuli. *Plant Cell*. **7**, 473-485.
- **Liu YG, Whittier RF.** (1995a). Thermal asymmetric interlaced PCR: automatable amplification and sequencing of insert end fragments from P1 and YAC clones for chromosome walking. *Genomics*. **25**, 674-681.
- **Liu YG, Mitsukawa N, Oosumi T, Whittier RF.** (1995b). Efficient isolation and mapping of Arabidopsis thaliana T-DNA insert junctions by thermal asymmetric interlaced PCR. *Plant J*. **8**, 457-463.
- **Liu J, Prolla G, Rostagno A, Chiarle R, Feiner H, Inghirami G.** (2000). Initiation of translation from a downstream in-frame AUG codon on BRCA1 can generate the novel isoform protein DeltaBRCA1(17aa). *Oncogene*. **19**, 2767-2773.
- **Liu X, Yue Y, Li B, Nie Y, Li W, Wu WH, Ma LA.** (2007). G protein-coupled receptor is a plasma membrane receptor for the plant hormone abscisic acid. *Science*. **315**, 1712-1716.
- **Liu H, Yu X, Li K, Klejnot J, Yang H, Lisiero D, Lin C.** (2008). Photoexcited CRY2 interacts with CIB1 to regulate transcription and floral initiation in Arabidopsis. *Science*. **322**, 1535-1539.
- **Livak KJ, Schmittgen TD.** (2001). Analysis of relative gene expression data using real-time quantitative PCR and the $2^{-\Delta\Delta CT}$ Method. *Methods*. **25**, 402-408.
- **Llorente F, Alonso-Blanco C, Sánchez-Rodríguez C, Jorda L, Molina A.** (2005). ERECTA receptor-like kinase and heterotrimeric G protein from Arabidopsis are required for resistance to the necrotrophic fungus *Plectosphaerella cucumerina*. *Plant J*. **43**, 165-180.
- **Lorrain S, Genoud T, Fankhauser C.** (2006). Let there be light in the nucleus! *Curr Opin Plant Biol*. **9**, 509-514.

- Lorrain S, Allen T, Duek PD, Whitelam GC, Fankhauser C. (2008). Phytochrome-mediated inhibition of shade avoidance involves degradation of growth-promoting bHLH transcription factors. *Plant J.* **53**, 312-323.
- Lu C, Fedoroff N. (2000). A mutation in the Arabidopsis HYL1 gene encoding a dsRNA binding protein affects responses to abscisic acid, auxin, and cytokinin. *Plant Cell.* **12**, 2351-2366.
- Ma L, Li J, Qu L, Hager J, Chen Z, Zhao H, Deng XW. (2001). Light control of Arabidopsis development entails coordinated regulation of genome expression and cellular pathways. *Plant Cell.* **13**, 2589-2607.
- Ma Y, Szostkiewicz I, Korte A, Moes D, Yang Y, Christmann A, Grill E. (2009). Regulators of PP2C phosphatase activity function as Abscisic Acid sensors. *Science.* **324**, 1064-1068.
- Mackay TFC. (2001). The genetic architecture of quantitative traits. *Annu Rev Genet.* **35**, 303-339.
- Madlung A, Comai L. (2004). The effect of stress on genome regulation and structure. *Ann Bot (Lond).* **94**, 481-495.
- Maloof JN, Borevitz JO, Weigel D, Chory J. (2000). Natural variation in phytochrome signaling. *Semin Cell Dev Biol.* **11**, 523-530.
- Maloof JN, Borevitz JO, Dabi T, Lutes J, Nehring RB, Redfern JL, Trainer GT, Wilson JM, Asami T, Berry CC, Weigel D, Chory J. (2001). Natural variation in light sensitivity of Arabidopsis. *Nat Genet.* **29**, 441-446.
- Maloof JN. (2003). Genomic approaches to analyzing natural variation in Arabidopsis thaliana. *Curr Opin Genet Dev.* **13**, 576-582.
- Mariconti L, Pellegrini B, Cantoni R, Stevens R, Bergounioux C, Cella R, Albani D. (2002). The E2F family of transcription factors from Arabidopsis thaliana. Novel and conserved components of the retinoblastoma/E2F pathway in plants. *J Biol Chem.* **277**, 9911-9919.
- Martinez-Zapater JM, Estelle MA, Somerville CR. (1986). A high repeated DNA sequence in Arabidopsis thaliana. *Mol Gen Genet.* **204**, 417-423.
- Mas P, Devlin PF, Panda S, Kay SA. (2000). Functional interaction of phytochrome B and cryptochrome 2. *Nature.* **408**, 207-211.
- Masle J, Gilmore SR, Farquhar GD. (2005). The ERECTA gene regulates plant transpiration efficiency in Arabidopsis. *Nature.* **436**, 866-870.
- Mathieu O, Jasencakova Z, Vaillant I, Gendrel AV, Colot V, Schubert I, Tourmente S. (2003). Changes in 5S rDNA chromatin organization and transcription during heterochromatin establishment in Arabidopsis. *Plant Cell.* **15**, 2929-2939.
- Mazzella MA, Bertero D, Casal JJ. (2000). Temperature-dependent internode elongation in vegetative plants of Arabidopsis thaliana lacking phytochrome B and cryptochrome 1. *Planta.* **210**, 497-501.
- Mazzella MA, Cerdán PD, Staneloni RJ, Casal JJ. (2001). Hierarchical coupling of phytochromes and cryptochromes reconciles stability and light modulation of Arabidopsis development. *Development.* **12**, 2291-2299.

- **Mazzella MA, Arana MV, Staneloni RJ, Perelman S, Rodriguez Batiller MJ, Muschietti J, Cerdán PD, Chen K, Sánchez RA, Zhu T, Chory J, Casal JJ.** (2005). Phytochrome control of the Arabidopsis transcriptome anticipates seedling exposure to light. *Plant Cell*. **17**, 2507-2516.
- **McCabe PF, Leaver CJ.** (2000). Programmed cell death in cell cultures. *Plant Mol Biol*. **44**, 359-368.
- **McMillen GG, McClendon JH.** (1983). Dependence of photosynthetic rates on leaf density thickness in deciduous woody plants grown in sun and shade. *Plant Physiol*. **72**, 674-678.
- **Meskauskiene R, Nater M, Goslings D, Kessler F, Op den Camp R, Apel K.** (2001). FLU: a negative regulator of chlorophyll biosynthesis in Arabidopsis thaliana. *Proc Natl Acad Sci U S A*. **98**, 12826-12831.
- **Michael TP, Salome PA, Yu HJ, Spencer TR, Sharp EL, McPeck MA, Alonso JM, Ecker JR, McClung CR.** (2003). Enhanced fitness conferred by naturally occurring variation in the circadian clock. *Science*. **302**, 1049-1053.
- **Millar AJ, Kay SA.** (1991). Circadian control of Cab gene transcription and mRNA accumulation in Arabidopsis. *Plant Cell*. **3**, 541-550.
- **Millar AJ, Carré IA, Strayer CA, Chua NH, Kay SA.** (1995). Circadian clock mutants in Arabidopsis identified by luciferase imaging. *Science*. **267**, 1161-1163.
- **Millenaar FF, Cox MC, van Berkel YE, Welschen RA, Pierik R, Voeselek LACJ, Peeters AJM.** (2005). Ethylene-induced differential growth of petioles in Arabidopsis. Analyzing natural variation, response kinetics, and regulation. *Plant Physiol*. **137**, 998-1008.
- **Millenaar FF, Okyere J, May ST, van Zanten M, Voeselek LACJ, Peeters AJM.** (2006). How to decide? Different methods of calculating gene expression from short oligonucleotide array data will give different results. *BMC Bioinformatics*. **7**, 137.
- **Millenaar FF, Van Zanten M, Cox MCH, Pierik R, Voeselek LACJ, Peeters AJM.** (2009). Differential petiole growth in Arabidopsis thaliana: Photocontrol and hormonal regulation. *New Phytol*. Published Online: June 24, 2009. DOI: 10.1111/j.1469-8137.2009.02921.x
- **Mittler R.** (2006). Abiotic stress, the field environment and stress combination. *Trends Plant Sci*. **11**, 15-19.
- **Mockler TC, Guo H, Yang H, Duong H, Lin C.** (1999). Antagonistic actions of Arabidopsis cryptochromes and phytochrome B in the regulation of floral induction. *Development*. **126**, 2073-2082.
- **Mommer L, Pedersen O, Visser EJW.** (2004). Acclimation of a terrestrial plant to submergence facilitates gas exchange underwater. *Plant Cell Environ*. **27**, 1281-1287.
- **Morelli G, Ruberti I.** (2000). Shade avoidance responses. Driving auxin along lateral routes. *Plant Physiol*. **122**, 621-626.
- **Morita MT, Tasaka M.** (2004). Gravity sensing and signaling. *Curr Opin Plant Biol*. **7**, 712-718.

- Mullen JL, Weinig C, Hangarter RP. (2006). Shade avoidance and the regulation of leaf inclination in *Arabidopsis*. *Plant Cell Environ.* **29**, 1099-1106.
- Murfett J, Wang XJ, Hagen G, Guilfoyle TJ. (2001). Identification of *Arabidopsis* histone deacetylase HDA6 mutants that affect transgene expression. *Plant Cell.* **13**, 1047-1061.
- Nagatani A, Reed JW, Chory J. (1993). Isolation and initial characterization of *Arabidopsis* mutants that are deficient in phytochrome A. *Plant Physiol.* **102**, 269-277.
- Nakamoto D, Ikeura A, Asami T, Yamamoto KT. (2006). Inhibition of brassinosteroid biosynthesis by either a dwarf4 mutation or a brassinosteroid biosynthesis inhibitor rescues defects in tropic responses of hypocotyls in the *Arabidopsis* mutant nonphototropic hypocotyl 4. *Plant Physiol.* **141**, 456-464.
- Nakano T, Suzuki K, Fujimura T, Shinshi H. (2006). Genome-wide analysis of the ERF gene family in *Arabidopsis* and rice. *Plant Physiol.* **140**, 411-432.
- Nakazawa M, Ichikawa T, Ishikawa A, Kobayashi H, Tsuhara Y, Kawashima M, Suzuki K, Muto S, Matsui M. (2003). Activation tagging, a novel tool to dissect the functions of a gene family. *Plant J.* **34**, 741-750.
- Naumann K, Fischer A, Hofmann I, Krauss V, Phalke S, Irmeler K, Hause G, Aurich AC, Dorn R, Jenuwein T, Reuter G. (2005). Pivotal role of AtSUVH2 in heterochromatic histone methylation and gene silencing in *Arabidopsis*. *EMBO J.* **24**, 1418-1429.
- Neff MM, Chory J. (1998). Genetic interaction between phytochrome A, phytochrome B and cryptochrome 1 during *Arabidopsis* development. *Plant Physiol.* **118**, 27-36.
- New M, Hulme M, Jones P. (1999). Representing twentieth-century space-time climate variability. Part I: Development of a 1961-90 mean monthly terrestrial climatology. *J Climate.* **12**, 829-856.
- Nilsen ET. (1991). The relationship between freezing tolerance and thermotropic leaf movement in five *Rhododendron* species. *Oecologia.* **87**, 63-71.
- Nordborg M, Hu TT, Ishino Y, Jhaveri J, Toomajian C, Zheng H, Bakker E, Calabrese P, Gladstone J, Goyal R, Jakobsson M, Kim S, Morozov Y, Padhukasahasram B, Plagnol V, Rosenberg NA, Shah C, Wall JD, Wang J, Zhao K, Kalbfleisch T, Schulz V, Kreitman M, Bergelson B. (2005). The Pattern of Polymorphism in *Arabidopsis thaliana*. *PLoS Biol.* **3**, e196.
- Nordborg M, Weigel D. (2008). Next-generation genetics in plants. *Nature.* **456**, 720-733.
- Ohgishi M, Saji K, Okada K, Sakai T. (2004). Functional analysis of each blue light receptor, cry1, cry2, phot1, and phot2, by using combinatorial multiple mutants in *Arabidopsis*. *Proc Natl Acad Sci U S A.* **101**, 2223-2228.
- Okamoto M, Kuwahara A, Seo M, Kushiro T, Asami T, Hirai N, Kamiya Y, Koshiba T, Nambara E. (2006). CYP707A1 and CYP707A2, which encode abscisic acid 8'-hydroxylases, are indispensable for proper control of seed dormancy and

- germination in *Arabidopsis*. *Plant Physiol.* **141**, 97-107.
- **Orbovic V, Poff KL.** (2007). Effect of temperature on growth and phototropism of *Arabidopsis thaliana* seedlings. *J Plant Growth Regul.* **26**, 222-228.
 - **Østergaard L, Yanofsky MF.** (2004). Establishing gene function by mutagenesis in *Arabidopsis thaliana*. *Plant J.* **39**, 682-696.
 - **Pandey S, Nelson DC, Assmann SM.** (2009). Two novel GPCR-type G proteins are abscisic acid receptors in *Arabidopsis*. *Cell.* **136**, 136-148.
 - **Park CM, Bhoo SH, Song PS.** (2000). Inter-domain crosstalk in the phytochrome molecules. *Semin Cell Dev Biol.* **11**, 449-456.
 - **Park SY, Fung P, Nishimura N, Jensen DR, Fujii H, Zhao Y, Lumba S, Santiago J, Rodrigues A, Chow TF, Alfred SE, Bonetta D, Finkelstein R, Provart NJ, Desveaux D, Rodriguez PL, McCourt P, Zhu JK, Schroeder JI, Volkman BF, Cutler SR.** (2009). Abscisic Acid inhibits Type 2C protein phosphatases via the PYR/PYL family of START proteins. *Science.* **324**, 1068-1071.
 - **Pavet V, Quintero C, Cecchini NM, Rosa AL, Alvarez ME.** (2006). *Arabidopsis* displays centromeric DNA hypomethylation and cytological alterations of heterochromatin upon attack by *Pseudomonas syringae*. *Mol Plant Microbe Interact.* **19**, 577-587.
 - **Penfield S.** (2008). Temperature perception and signal transduction in plants. *New Phytol.* **179**, 615-628.
 - **Pérez-Pérez JM, Serrano-Cartagena J, Micol JL.** (2002). Genetic analysis of natural variations in the architecture of *Arabidopsis thaliana* vegetative leaves. *Genetics.* **162**, 893-915.
 - **Perfus-Barbeoch L, Jones AM, Assmann SM.** (2004). Plant heterotrimeric G protein function: insights from *Arabidopsis* and rice mutants. *Curr Opin Plant Biol.* **7**, 719-731.
 - **Pesole G, Liuni S, Grillo G, Licciulli F, Mignone F, Gissi C, Saccone C.** (2002). UTRdb and UTRsite: specialized databases of sequences and functional elements of 5' and 3' untranslated regions of eukaryotic mRNAs. Update 2002. *Nucl. Acids Res.* **30**, 335-340.
 - **Pettkó-Szandtner A, Mészáros T, Horváth GV, Bakó L, Csordás-Tóth E, Blastyák, A, Zhiponova M, Miskolczi P, Dudits D.** (2006). Activation of an alfalfa cyclin-dependent kinase inhibitor by calmodulin-like domain protein kinase. *Plant J.* **46**, 111-123.
 - **Pfannschmidt T, Nilsson A, Allen JF.** (1999). Photosynthetic control of chloroplast gene expression. *Nature.* **397**, 625-628.
 - **Pierik R, Visser EJW, de Kroon H, Voesenek LACJ.** (2003). Ethylene is required in tobacco to successfully compete with proximate neighbours. *Plant Cell Environ.* **26**, 1229-1234.
 - **Pierik R, Whitelam GC, Voesenek LACJ, de Kroon H, Visser EJW.** (2004a). Canopy studies on ethylene-insensitive tobacco identify ethylene as a novel element in blue light and plant-plant signaling. *Plant J.* **38**, 310-319.

- Pierik R, Cuppens ML, Voeselek LA, Visser EJ. (2004b). Interactions between ethylene and gibberellins in phytochrome-mediated shade avoidance responses in tobacco. *Plant Physiol.* **136**, 2928-2936.
- Pierik R, Millenaar FF, Peeters AJM, Voeselek LACJ. (2005). New perspectives in flooding research: the use of shade avoidance and *Arabidopsis thaliana*. *Ann Bot (Lond)*. **96**, 533-540.
- Pierik R, Tholen D, Poorter H, Visser EJ, Voeselek LA. (2006). The Janus face of ethylene: growth inhibition and stimulation. *Trends Plant Sci.* **11**, 176-183.
- Pierik R, Djakovic-Petrovic T, Keuskamp DH, de Wit M, Voeselek LACJ. (2009). Auxin and ethylene regulate elongation responses to neighbour proximity signals independent of GA and DELLA proteins in *Arabidopsis*. *Plant Physiol.* **149**, 1701-1712.
- Piippo M, Allahverdiyeva Y, Paakkarinen V, Suoranta U-M, Battchikova N, Aro E-M. (2006). Chloroplast-mediated regulation of nuclear genes in *Arabidopsis thaliana* in the absence of light stress. *Physiol Genomics.* **25**, 142-152.
- Pillitteri LJ, Bemis SM, Shpak ED, Torii KU. (2007). Haploinsufficiency after successive loss of signaling reveals a role for ERECTA-family genes in *Arabidopsis* ovule development. *Development.* **134**, 3099-3109.
- Pontes O, Pikaard CS. (2008). siRNA and miRNA processing: new functions for Cajal bodies. *Curr Opin Genet Dev.* **18**, 197-203.
- Probst AV, Fagard M, Proux F, Mourrain P, Boutet S, Earley K, Lawrence RJ, Pikaard CS, Murfett J, Furner I, Vaucheret H, Mittelsten-Scheid O. (2004). *Arabidopsis* histone deacetylase HDA6 is required for maintenance of transcriptional gene silencing and determines nuclear organization of rDNA repeats. *Plant Cell.* **16**, 1021-1034.
- Probst AV, Fransz PF, Paszkowski J, Scheid OM. (2003). Two means of transcriptional reactivation within heterochromatin. *Plant J.* **33**, 743-749.
- Qi Y, Sun Y, Xu L, Xu Y, Huang H. (2004). ERECTA is required for protection against heat-stress in the AS1/ AS2 pathway to regulate adaxial-abaxial leaf polarity in *Arabidopsis*. *Planta.* **219**, 270-276.
- Qin C, Wang X. (2002). The *Arabidopsis* phospholipase D family. Characterization of a calcium-independent and phosphatidylcholine-selective PLD zeta 1 with distinct regulatory domains. *Plant Physiol.* **128**, 1057-1068.
- Rangwala SH, Richards EJ. (2007). Differential epigenetic regulation within an *Arabidopsis* retroposon family. *Genetics.* **176**, 151-160.
- Raz V, Ecker JR. (1999). Regulation of differential growth in the apical hook of *Arabidopsis*. *Development.* **126**, 3661-3668.
- Redei GP. (1962). Supervital mutants in *Arabidopsis*. *Genetics.* **47**, 443-460.
- Reed JW, Nagatani A, Elich TD, Fagan M, Chory J. (1994). Phytochrome A and phytochrome B have overlapping but distinct functions in *Arabidopsis* development. *Plant Physiol.* **104**, 1139-1149.
- Reed JW, Nagpal P, Poole DS, Furuya M, Chory J. (1993). Mutations in the gene

- for the red/far-red light receptor phytochrome B alter cell elongation and physiological responses throughout *Arabidopsis* development. *Plant Cell*. **5**, 147-157.
- **Richard C, Granier C, Inzé D, De Veylder L.** (2001). Analysis of cell division parameters and cell cycle gene expression during the cultivation of *Arabidopsis thaliana* cell suspensions. *J Exp Bot*. **52**, 1625-1633.
 - **Richard C, Lescot M, Inze D, De Veylder L.** (2002). Effect of auxin, cytokinin, and sucrose on cell cycle gene expression in *Arabidopsis thaliana* cell suspension cultures. *Plant Tissue Organ Cult*. **69**, 167-176.
 - **Riddle NC, Richards EJ.** (2002). The control of natural variation in cytosine methylation in *Arabidopsis*. *Genetics*. **162**, 355-363.
 - **Ridge I.** (1987). Ethylene and growth control in amphibious species. In Crawford RMM, editor, *Plant Life in Aquatic and Amphibious Habitats*. Blackwell Scientific Publications, Oxford, pp. 53-76.
 - **Rijnders JGHM, Armstrong W, Darwent MJ, Blom CWPM, Voeselek LACJ.** (2000). The role of oxygen in submergence-induced petiole elongation in *Rumex palustris*: in situ measurements of oxygen in petioles of intact plants using micro-electrodes. *New Phytol*. **147**, 497-504.
 - **Rijnders JGHM, Yang Y, Kamiya Y, Takahashi N, Barendse GWM, Blom, CWPM, Voeselek LACJ.** (1997). Ethylene enhances gibberellin levels and petiole sensitivity in flooding-tolerant *Rumex palustris* but not in flooding-intolerant *R. acetosa*. *Planta*. **203**, 20-25
 - **Ringli C, Bigler L, Kuhn BM, Leiber RM, Diet A, Santelia D, Frey B, Pollmann S, Klein M.** (2008). The modified flavonol glycosylation profile in the *Arabidopsis* rol1 mutants results in alterations in plant growth and cell shape formation. *Plant Cell*. **20**, 1470-1481.
 - **Risk JM, Day CL, MacKnight RC.** (2009). Re-evaluation of abscisic acid (ABA) binding assays shows that GCR2 does not bind ABA. *Plant Physiol*. **150**, 6-11.
 - **Robertson AJ, Ishikawa M, Gusta LV, MacKenzie SL.** (1994). Abscisic acid-induced heat tolerance in *Bromus inermis* Leyss cell-suspension cultures. Heat-stable, abscisic acid-responsive polypeptides in combination with sucrose confer enhanced thermostability. *Plant Physiol*. **105**, 181-190.
 - **Roman G, Lubarsky B, Kieber J, Rothenberg M, Ecker J.** (1995). Genetic analysis of ethylene signal transduction in *Arabidopsis thaliana*: Five novel mutant loci integrated into a stress response pathway. *Genetics*. **139**, 1393-1409.
 - **Rosso MG, Li Y, Strizhov N, Reiss B, Dekker K, Weisshaar B.** (2003). An *Arabidopsis thaliana* T-DNA mutagenized population (GABI-Kat) for flanking sequence tag-based reverse genetics. *Plant Mol Biol*. **53**, 247-259.
 - **Roudier F, Fedorova E, Györgyey J, Feher A, Brown S, Kondorosi A, Kondorosi E** (2000). Cell cycle function of a *Medicago sativa* A2-type cyclin interacting with a PSTAIRE-type cyclin-dependent kinase and a retinoblastoma protein. *Plant J*. **23**, 73-83.

- Roudier F, Fedorova E, Lebris M, Lecomte P, Györgyey J, Vaubert D, Horvath G, Abad P, Kondorosi A, Kondorosi E. (2003). The *Medicago* species A2-type cyclin is auxin regulated and involved in meristem formation but dispensable for endoreduplication-associated developmental programs. *Plant Physiol.* **131**, 1091-1103.
- Ruegger M, Dewey E, Hobbie L, Brown D, Bernasconi P, Turner J, Muday G, Estelle M. (1997). Reduced naphthylphthalamic acid binding in the *tir3* mutant of *Arabidopsis* is associated with a reduction in polar auxin transport and diverse morphological defects. *Plant Cell.* **9**, 745-757.
- Saito S, Hirai N, Matsumoto C, Ohigashi H, Ohta D, Sakata K, Mizutani M. (2004). *Arabidopsis* CYP707As encode (+)-abscisic acid 8'-hydroxylase, a key enzyme in the oxidative catabolism of abscisic acid. *Plant Physiol.* **134**, 1439-1449.
- Sakai T, Kagawa T, Kasahara M, Swartz TE, Christie JM, Briggs WR, Wada M, Okada K. (2001). *Arabidopsis* nph1 and npl1: blue light receptors that mediate both phototropism and chloroplast relocation. *Proc. Natl. Acad. Sci. U S A.* **98**, 6969-6974.
- Sakamoto K, Briggs WR. (2002). Cellular and subcellular localization of phototropin 1. *Plant Cell.* **14**, 1723-1735.
- Salter MG, Franklin KA, Whitelam GC. (2003). Gating of the rapid shade avoidance response by the circadian clock in plants. *Nature.* **426**, 680-683.
- Samach A, Wigge PA. (2005). Ambient temperature perception in plants. *Curr Opin Plant Biol.* **8**, 483-486.
- Sanchez JP, Chua NH. (2001). *Arabidopsis* PLC1 is required for secondary responses to abscisic acid signals. *Plant Cell.* **13**, 1143-1154.
- Sangster TA, Salathia N, Undurraga S, Milo R, Schellenberg K, Lindquist S, Queitsch C. (2008). HSP90 affects the expression of genetic variation and developmental stability in quantitative traits. *Proc Natl Acad Sci USA.* **105**, 2963-2968.
- Sasidharan R, Chinnappa CC, Voesenek LA, Pierik R. (2008). The regulation of cell wall extensibility during shade avoidance: a study using two contrasting ecotypes of *Stellaria longipes*. *Plant Physiol.* **148**, 1557-1569.
- Savaldi-Goldstein S, Peto C, Chory J. (2007). The epidermis both drives and restricts plant shoot growth. *Nature.* **446**, 199-202.
- Schmid KJ, Törjék O, Meyer R, Schmuths H, Hoffmann MH, Altmann T. (2006). Evidence for a large-scale population structure of *Arabidopsis thaliana* from genome-wide single nucleotide polymorphism markers. *Theor Appl Genet.* **112**, 1104-1114.
- Schubert I, Fransz PF, Fuchs J, de Jong JH. (2001). Chromosome painting in plants. *Methods Cell Sci.* **23**, 57-69.
- Seo M, Hanada A, Kuwahara A, Endo A, Okamoto M, Yamauchi Y, North H, Marion-Poll A, Sun TP, Koshihara T, Kamiya Y, Yamaguchi S, Nambara E. (2006). Regulation of hormone metabolism in *Arabidopsis* seeds: phytochrome regulation of abscisic acid metabolism and abscisic acid regulation of gibberellin metabolism. *Plant J.*

- 48, 354-366.
- Shen YY, Wang XF, Wu FQ, Du SY, Cao Z, Shang Y, Wang XL, Peng CC, Yu XC, Zhu SY, Fan RC, Xu YH, Zhang DP. (2006). The Mg-chelatase H subunit is an abscisic acid receptor. *Nature*. **443**, 823-826.
 - Shindo C, Aranzana MJ, Lister C, Baxter C, Nicholls C, Nordborg M, Dean C. (2005). Role of FRIGIDA and FLOWERING LOCUS C in determining variation in flowering time of Arabidopsis. *Plant Physiol*. **138**, 1163-1173.
 - Shindo C, Bernasconi G, Hardtke CS. (2007). Natural genetic variation in Arabidopsis: tools, traits and prospects for evolutionary ecology *Ann Bot (Lond)*. **99**, 1043-1054.
 - Skriver K, Olsen FL, Rogers JC, Mundy, J. (1991). Cis-acting DNA elements responsive to gibberellin and its antagonist abscisic acid. *Proc Natl Acad Sci U S A*. **88**, 7266-7270.
 - Smalle J, Haegman M, Kurepa J, Van Montagu M, Straeten DV. (1997). Ethylene can stimulate Arabidopsis hypocotyl elongation in the light. *Proc Natl Acad Sci U S A*. **94**, 2756-2761.
 - Smith H, Whitelam GC. (1997). The shade avoidance syndrome: multiple responses mediated by multiple phytochromes. *Plant Cell Environ*. **20**, 840-844.
 - Snoek LB, (2009). Natural variation in shade and ethylene-induced differential growth and transcription in Arabidopsis. PhD-thesis, Utrecht University, 2009.
 - Soppe WJ, Jasencakova Z, Houben A, Kakutani T, Meister A, Huang MS, Jacobsen SE, Schubert I, Fransz PF. (2002). DNA methylation controls histone H3 lysine 9 methylation and heterochromatin assembly in Arabidopsis. *EMBO J*. **21**, 6549-6559.
 - Sripongpangkul K, Posa GBT, Senadhira DW, Brar D, Huang N, Khush GS, Li ZK (2000). Genes/QTLs affecting flood tolerance in rice. *Theor Appl Genet*. **101**, 1074-1081.
 - Steimer A, Amedeo P, Afsar K, Fransz P, Mittelsten Scheid O, Paszkowski J. (2000). Endogenous targets of transcriptional gene silencing in Arabidopsis. *Plant Cell*. **12**, 1165-1178.
 - Stenøien HK, Fenster CB, Tonteri A, Savolainen O. (2005). Genetic variability in natural populations of *Arabidopsis thaliana* in northern Europe. *Mol Ecol*. **14**, 137-148.
 - Stift M, Luttikhuisen PC, Visser EJ, van Tienderen PH. (2008). Different flooding responses in *Rorippa amphibia* and *Rorippa sylvestris*, and their modes of expression in F1 hybrids. *New Phytol*. **180**, 229-239.
 - Stinchcombe JR, Weinig C, Ungerer M, Olsen, KM, Mays C, Halldorsdottir SS, Purugganan MD, Schmitt J. (2004). A latitudinal cline in flowering time in *Arabidopsis thaliana* modulated by the flowering time gene FRIGIDA. *Proc Natl Acad Sci U S A*. **101**, 4712-4717.
 - Strand Å, Asami T, Alonso J, Ecker JR, Chory J. (2003). Chloroplast to nucleus communication triggered by accumulation of Mg-protoporphyrin IX. *Nature*. **421**,

- 79-83.
- Sugimoto-Shirasu K, Roberts K. (2003). "Big it up": endoreduplication and cell-size control in plants. *Curr Opin Plant Biol.* **6**, 544-553.
 - Sullivan JA, Deng XW. (2003). From seed to seed: the role of photoreceptors in Arabidopsis development. *Dev Biol.* **260**, 289-297.
 - Swarup K, Alonso-Blanco C, Lynn JR, Michaels SD, Amasino RM, Koornneef M, Millar AJ. (1999). Natural allelic variation identifies new genes in the Arabidopsis circadian system. *Plant J.* **20**, 67-77.
 - Tanaka M, Kikuchi A, Kamada H. (2008). The Arabidopsis histone deacetylases HDA6 and HDA19 contribute to the repression of embryonic properties after germination. *Plant Physiol.* **146**, 149-161.
 - Tao Y, Ferrer JL, Ljung K, Pojer F, Hong F, Long JA, Li L, Moreno JE, Bowman ME, Ivans LJ, Cheng Y, Lim J, Zhao Y, Ballaré CL, Sandberg G, Noel JP, Chory J. (2008). Rapid synthesis of auxin via a new tryptophan-dependent pathway is required for shade avoidance in plants. *Cell.* **133**, 164-176.
 - Tatematsu K, Kumagai S, Muto H, Sato A, Watahiki MK, Harper RM, Liscum E, Yamamoto KT. (2004). *MASSUGU2* encodes Aux/IAA19, an auxin-regulated protein that functions together with the transcriptional activator NPH4/ARF7 to regulate differential growth responses of hypocotyl and formation of lateral roots in *Arabidopsis thaliana*. *Plant Cell.* **16**, 379-393.
 - Tessadori F, van Driel R, Fransz P. (2004). Cytogenetics as a tool to study gene regulation. *Trends Plant Sci.* **9**, 147-153.
 - Tessadori F, Schulkes RK, van Driel R, Fransz P. (2007a). Light-regulated large-scale reorganization of chromatin during the floral transition in Arabidopsis. *Plant J.* **50**, 848-857.
 - Tessadori F, Chupeau MC, Chupeau Y, Knip M, Germann S, van Driel R, Fransz P, Gaudin V. (2007b). Large-scale dissociation and sequential reassembly of pericentric heterochromatin in dedifferentiated Arabidopsis cells. *J Cell Sci.* **120**, 1200-1208.
 - Tisné S, Reymond M, Vile D, Fabre J, Dauzat M, Koornneef M, Granier C. (2008). Combined genetic and modelling approaches reveal that epidermal cell area and number in leaves are controlled by leaf and plant developmental processes in Arabidopsis. *Plant Physiol.* **148**, 1117-27.
 - Toh S, Imamura A, Watanabe A, Nakabayashi K, Okamoto M, Jikumaru Y, Hanada A, Aso Y, Ishiyama K, Tamura N, Iuchi S, Kobayashi M, Yamaguchi S, Kamiya Y, Nambara E, Kawakami, N. (2008). High temperature-induced abscisic acid biosynthesis and its role in the inhibition of gibberellin action in Arabidopsis seeds. *Plant Physiol.* **146**, 1368-1385.
 - Torii KU, Mitsukawa N, Oosumi T, Matsuura Y, Yokoyama R, Whittier RF, Komeda Y. (1996). The Arabidopsis *ERECTA* gene encodes a putative receptor protein kinase with extracellular leucine-rich repeats. *Plant Cell.* **8**, 735-746
 - Tseng TS, Salomé PA, McClung CR, Olszewski NE. (2004). *SPINDLY* and *GIGANTEA* interact

- and act in *Arabidopsis thaliana* pathways involved in light responses, flowering, and rhythms in cotyledon movements. *Plant Cell*. **16**, 1550-1563.
- **Tsuge T, Tsukaya H, Uchimiya H.** (1996). Two independent and polarized processes of cell elongation regulate leaf blade expansion in *Arabidopsis thaliana* (L.) Heynh. *Development*. **122**, 1589-1600.
 - **Tsukaya H, Kozuka T, Kim GT.** (2002). Genetic control of petiole length in *Arabidopsis thaliana*. *Plant Cell Physiol*. **43**, 1221-1228.
 - **Ullah H, Chen JG, Young JC, Im KH, Sussman MR, Jones AM.** (2001). Modulation of cell proliferation by heterotrimeric G protein in *Arabidopsis*. *Science*. **292**, 2066-2069.
 - **Ungerer MC, Halldorsdottir SS, Modliszewski JL, Mackay TF, Purugganan MD.** (2002). Quantitative trait loci for inflorescence development in *Arabidopsis thaliana*. *Genetics*. **160**, 1133-1151.
 - **Vandenbussche F, Pierik R, Millenaar FF, Voeselek LA, Van Der Straeten, D.** (2005). Reaching out of the shade. *Curr Opin Plant Biol*. **8**, 462-468.
 - **Vandenbussche F, Vriezen WH, Smalle J, Laarhoven LJJ, Harren FJM, Van Der Straeten D.** (2003). Ethylene and auxin control the *Arabidopsis* response to decreased light intensity. *Plant Physiol*. **133**, 517-527.
 - **Vandenbussche F, Vriezen WH, Smalle J, Laarhoven LJJ, Harren FJM, Van Der Straeten, D.** (2003). Ethylene and auxin control the *Arabidopsis* response to decreased light intensity. *Plant Physiol*. **133**, 517-527.
 - **Vandepoele K, Raes J, De Veylder L, Rouzé P, Rombauts S, Inzé D.** (2002). Genome-wide analysis of core cell cycle genes in *Arabidopsis*. *Plant Cell*. **14**, 903-16.
 - **Vanneste S, De Rybel B, Beemster GT, Ljung K, De Smet I, Van Isterdael G, Naudts M, Iida R, Gruijssem W, Tasaka M, Inzé D, Fukaki H, Beeckman T.** (2005). Cell cycle progression in the pericycle is not sufficient for SOLITARY ROOT/IAA14-mediated lateral root initiation in *Arabidopsis thaliana*. *Plant Cell*. **17**, 3035-3050.
 - **Van Ooijen JW.** (2004). LOD significance thresholds for QTL analysis in experimental populations of diploid species. *Heredity*. **83**, 613-624.
 - **Van Zanten M, Millenaar FF, Cox MCH, Pierik R, Voeselek LACJ, Peeters AJM.** (2009a). Auxin perception and polar auxin transport are not always a prerequisite for differential growth. *Plant Signaling & Behavior*. *Scheduled for publication in 4, issue 9.*
 - **Van Zanten M, Snoek LB, Proveniers MCG, Peeters AJM.** (2009b). The many functions of ERECTA. *Trends Plant Science*. **14**, 214-218.
 - **Verkest A, Manes CL, Vercruyssen S, Maes S, Van Der Schueren E, Beeckman T, Genschik P, Kuiper M, Inzé D, De Veylder L.** (2005). The cyclin-dependent kinase inhibitor KRP2 controls the onset of the endoreduplication cycle during *Arabidopsis* leaf development through inhibition of mitotic CDKA;1 kinase complexes. *Plant Cell*. **17**, 1723-1736.
 - **Voeselek LACJ, Blom CWPM.** (1989). Growth responses of *Rumex* species in relation to submergence and ethylene. *Plant Cell Environ*. **12**, 433-439.

- Voeselek LACJ, Banga M, Their RH, Mudde CM, Harren FJM, Barendse GWM, Blom CWPM. (1993). Submergence-induced ethylene entrapment, and growth of two plant species with contrasting flooding resistances. *Plant Physiol.* **103**, 783-791.
- Voeselek L, Vriezen WH, Smekens M, Huitink F, Bogemann GM, Blom C. (1997). Ethylene sensitivity and response sensor expression in petioles of *Rumex* species at low O₂ and high CO₂ concentrations. *Plant Physiol.* **114**, 1501-1509.
- Voeselek LA, Benschop JJ, Bou J, Cox MC, Groeneveld HW, Millenaar FF, Vreeburg RA, Peeters AJ. (2003). Interactions between plant hormones regulate submergence-induced shoot elongation in the flooding-tolerant dicot *Rumex palustris*. *Ann Bot (Lond)*. **91**, 205-211.
- Voeselek LACJ, Rijnders JHGM, Peeters AJM, Van de Steeg HM, Kroon H. (2004). Plant Hormones regulate fast shoot elongation under water: from genes to communities. *Ecology*. **85**, 16-27.
- Voeselek LA, Colmer TD, Pierik R, Millenaar FF, Peeters AJ. (2006). How plants cope with complete submergence. *New Phytol.* **170**, 213-226.
- Von Koskull-Döring P, Scharf KD, Nover L. (2007). The diversity of plant heat stress transcription factors. *Trends Plant Sci.* **12**, 452-457.
- Vreeburg RA, Benschop JJ, Peeters AJ, Colmer TD, Ammerlaan AH, Staal M, Elzenga TM, Staals RH, Darley CP, McQueen-Mason SJ, Voeselek LA. (2005). Ethylene regulates fast apoplastic acidification and expansin A transcription during submergence-induced petiole elongation in *Rumex palustris*. *Plant J.* **43**, 597-610.
- Vriezen WH, Hulzink R, Mariani C, Voeselek LACJ. (1999). 1-Aminocyclopropane-1-carboxylate oxidase activity limits ethylene biosynthesis in *Rumex palustris* during submergence. *Plant Physiol.* **121**, 189-195.
- Waddington CH. (1942). Canalization of development and the inheritance of acquired characters. *Nature*. **150**, 563-565.
- Wagner D, Przybyla D, Op den Camp R, Kim C, Landgraf F, Lee KP, Würsch M, Laloi C, Nater M, Hideg E, Apel K. (2004). The genetic basis of singlet oxygen-induced stress responses of *Arabidopsis thaliana*. *Science*. **306**, 1183-1185.
- Wang H, Ma LG, Li JM, Zhao HY, Deng XW. (2001). Direct interaction of *Arabidopsis* cryptochromes with COP1 in light control development. *Science*. **294**, 154-158.
- Wang H, Qi Q, Schorr P, Cutler AJ, Crosby WL, Fowke LC. (1998). ICK1, a cyclin-dependent protein kinase inhibitor from *Arabidopsis thaliana* interacts with both Cdc2a and CycD3, and its expression is induced by abscisic acid. *Plant J.* **15**, 501-510.
- Wang S, Basten CJ, Zeng ZB. (2007). Windows QTL Catographer 2.5. Department of Statistics, North Carolina State University, Raleigh, NC, USA.
- Warpeha KM, Upadhyay S, Yeh J, Adamiak J, Hawkins SI, Lapik YR, Anderson MB, Kaufman LS. (2007). The GCR1, GPA1, PRN1, NF-Y signal chain mediates both blue light and abscisic acid responses in *Arabidopsis*. *Plant Physiol.* **143**, 1590-1600.

- **Watahiki MK, Yamamoto KT.** (1997). The massugu1 mutation of *Arabidopsis* identified with failure of auxin-induced growth curvature of hypocotyl confers auxin insensitivity to hypocotyl and leaf. *Plant Physiol.* **115**, 419-426.
- **Weatherwax SC, Ong MS, Degenhardt J, Bray EA, Tobin EM.** (1996). The interaction of light and abscisic acid in the regulation of plant gene expression. *Plant Physiol.* **111**, 363-370.
- **Weigel D, Ahn JH, Blázquez MA, Borevitz JO, Christensen SK, Fankhauser C, Ferrándiz, C, Kardailsky I, Malancharuvil EJ, Neff MM, Nguyen JT, Sato S, Wang ZY, Xia Y, Dixon RA, Harrison MJ, Lamb CJ, Yanofsky MF, Chory J.** (2000). Activation tagging in *Arabidopsis*. *Plant Physiol.* **122**, 1003-1013.
- **Weigel D, Nordborg M.** (2005). Natural variation in *Arabidopsis*. How do we find the causal genes? *Plant Physiol.* **138**, 567-568.
- **Weiste C, Iven T, Fischer U, Oñate-Sánchez L, Dröge-Laser W.** (2007). In planta ORFeome analysis by large-scale over-expression of GATEWAY-compatible cDNA clones: screening of ERF transcription factors involved in abiotic stress defense. *Plant J.* **52**, 382-390.
- **Whitelam GC, Johnson CB.** (1980). Phytochrome control of nitrate reductase activity and anthocyanin synthesis in light-brown *Sinapis alba* (L.). Differential responses of cotyledons and hypocotyls. *New Phytol.* **85**, 475-482.
- **Whitelam GC, Johnson E, Peng J, Carol P, Anderson ML, Cowl JS, Harberd NP.** (1993). Phytochrome A null mutants of *Arabidopsis* display a wild-type phenotype in white light. *Plant Cell.* **5**, 757-768.
- **Wildwater M, Campilho A, Perez-Perez JM, Heidstra R, Blilou I, Korthout H, Chatterjee J, Mariconti L, Gruissem W, Scheres B.** (2005). The RETINOBLASTOMA-RELATED gene regulates stem cell maintenance in *Arabidopsis* roots. *Cell.* **123**, 1337-1349.
- **Wilkinson JQ, Lanahan MB, Yen H-C, Giovannoni JJ, Klee HJ.** (1995). An ethylene-inducible component of signal transduction encoded by Never-ripe. *Science.* **270**, 1807-1809.
- **Wu G, Spalding EP.** (2007). Separate functions for nuclear and cytoplasmic cryptochrome 1 during photomorphogenesis of *Arabidopsis* seedlings. *Proc. Natl. Acad. Sci. U S A.* **104**, 18813-18818.
- **Wu K, Zhang L, Zhou C, Yu CW, Chaikam V.** (2008). HDA6 is required for jasmonate response, senescence and flowering in *Arabidopsis*. *J Exp Bot.* **59**, 225-234.
- **Xiong L, Lee B, Ishitani M, Lee H, Zhang C, Zhu JK.** (2001). FIERY1 encoding an inositol polyphosphate 1-phosphatase is a negative regulator of abscisic acid and stress signaling in *Arabidopsis*. *Genes Dev.* **15**, 1971-1984.
- **Xu L, Xu Y, Dong A, Sun Y, Pi L, Xu Y, Huang H.** (2003). Novel as1 and as2 defects in leaf adaxial-abaxial polarity reveal the requirement for ASYMMETRIC LEAVES1 and 2 and ERECTA functions in specifying leaf adaxial identity. *Development.* **130**, 4097-4107.
- **Xu K, Xu X, Fukao T, Canlas P, Maghirang-Rodriguez R, Heuer S, Ismail AM,**

- Bailey-Serres J, Ronald PC, Mackill DJ. (2006). Sub1A is an ethylene-response-factor-like gene that confers submergence tolerance to rice. *Nature*. **442**, 705-708.
- Yang HQ, Wu YJ, Tang RH, Liu D, Liu Y, Cashmore AR. (2000). The C termini of Arabidopsis cryptochromes mediate a constitutive light response. *Cell*. **103**, 815-827.
 - Yang ZB. (2002). Small GTPases: Versatile signaling switches in plants. *Plant Cell*. **14**, S375- S388.
 - Yanovsky MJ, Mazzella MA, Casal JJ. (2000). Quadruple photoreceptor mutant still keeps track of time. *Curr Biol*. **10**, 1013-1015.
 - Yi C, Deng, XW. (2005). COP1 - from plant photomorphogenesis to mammalian tumorigenesis. *Trends Cell Biol*. **15**, 618-625.
 - Yoshizumi T, Tsumoto Y, Takiguchi T, Nagata N, Yamamoto YY, Kawashima M, Ichikawa T, Nakazawa M, Yamamoto N, Matsui M. (2006). Increased level of polypoidy1, a conserved repressor of CYCLINA2 transcription, controls endoreduplication in Arabidopsis. *Plant Cell*. **18**, 2452-2468.
 - Yu F, Berg VS. (1994). Control of paraheliotropism in two phaseolus species. *Plant Physiol*. **106**, 1567-1573.
 - Yu X, Klejnot J, Zhao X, Shalitin D, Maymon M, Yang H, Lee J, Liu X, Lopez J, Lin L. (2007). Arabidopsis Cryptochrome 2 completes its posttranslational life cycle in the nucleus. *Plant Cell*. **19**, 3146-3156.
 - Yu X, Sayegh R, Maymon M, Warpeha K, Klejnot J, Yang H, Huang J, Lee J, Kaufman L, Lin C. (2009). Formation of nuclear bodies of Arabidopsis CRY2 in response to blue light is associated with its blue light-dependent degradation. *Plant Cell*. **21**, 118-130.
 - Yu Y, Steinmetz A, Meyer D, Brown S, Shen WH. (2003). The tobacco A-type cyclin, Nicta;CYCA3;2, at the nexus of cell division and differentiation. *Plant Cell*. **15**, 2763-2777.
 - Zhan S, Horrocks J, Lukens LN. (2006). Islands of co-expressed neighbouring genes in Arabidopsis thaliana suggest higher-order chromosome domains. *Plant J*. **45**, 347-35

Samenvatting in het Nederlands

(Summary in Dutch)

Zoals alle organismen zijn ook planten in hoge mate afhankelijk van hun omgeving. Voorbeelden zijn licht en koolstofdioxide (CO₂) voor de fotosynthese en zuurstof (O₂) voor de ademhaling. Deze abiotische factoren kunnen onder bepaalde omstandigheden beperkend worden voor de groei van de plant, wanneer zij bijvoorbeeld overschaduw worden door grotere planten (licht), of bij overstroming (lucht en licht). In dit kader is het van essentieel belang dat planten zich kunnen aanpassen aan hun omgeving. Zo kunnen vaak overstroomde uiterwaard planten actief hun bladeren optillen. Hierdoor steken de bladpunten boven het water uit en kan de gasuitwisseling met de atmosfeer voortgezet worden. Analoog hieraan kunnen planten die voorkomen in dichte vegetaties hun bladeren optillen om boven andere planten uit te groeien om zo meer licht op te vangen. Deze opwaartse bladbeweging is dus een ontsnapingsmechanisme en wordt hyponastische groei genoemd. Als hyponastie niet voldoende is om boven de andere planten, dan wel het wateroppervlak uit te komen, zal in bepaalde soorten, waaronder Moeraszuring (*Rumex palustris*) ook de bladsteel strekken (petioolstrekking). Dit strekkingsproces vindt pas plaats als de bladhoek voldoende is toegenomen, zodat de bladeren in het verticale vlak bewegen. Als de bladhoek te laag is zal strekking namelijk niet leiden tot groei in de gewenste richting, weg van de groeibelemerende omgevingsfactoren. Hyponastie is dus een relevant ontsnapingsmechanisme voor planten. Echter, er is nog weinig bekend over hoe de plant veranderingen in zijn omgeving waarneemt en door welke processen vervolgens hyponastie wordt geïnduceerd. Het onderzoek beschreven in dit proefschrift geeft inzicht in deze twee fundamentele vragen.

Om hyponastische groei in detail te begrijpen moet kennis op het niveau van de cellen en van de moleculair processen daarbinnen verkregen worden. Een belangrijke deelvraag in dit onderzoek was dan ook welke genen en eiwitten er betrokken zijn bij dit proces. Veel onderzoek naar hyponastie en bladsteelstrekking is uitgevoerd aan *Rumex palustris*. Deze soort is uitermate geschikt voor onderzoek op het fysiologisch niveau van de hele plant en is intensief gebruikt om de hormonale regulatie van hyponastie en petioolstrekking en de ecologische aspecten van deze processen te bestuderen. Voor moleculair genetisch onderzoek is deze soort minder geschikt. *Rumex palustris* heeft een groot genoom (verzamelnaam voor alle erfelijke informatie binnen een organisme) en is polyploid (meerdere kopieën van elk gen zijn aanwezig in de plant). Tevens is er nog maar weinig genetische en moleculaire informatie beschikbaar. Zo zijn er bijvoorbeeld geen mutanten voorhanden waarin één of meerdere genen niet functioneren. Daardoor is het moeilijk om de betrokkenheid van een gen/eiwit bij een bepaalde respons te identificeren en vervolgens experimenteel

te verifiëren. Tevens is deze plant ook erg weerbarstig voor genetische manipulatie zodat er geen veranderde genen, of genen van andere soorten in de plant gebracht kunnen worden om de uitwerking daarvan te bestuderen. Om deze redenen is het onderzoek uitgevoerd met de Zandraket (*Arabidopsis thaliana*). Een groot voordeel van deze soort is dat het hele genoom bekend is, dat het diploïd is en dat veel laboratoria wereldwijd ermee werken waardoor er veel informatie en zeer veel moleculair genetische technieken voor beschikbaar zijn. Niet onbelangrijk, *Arabidopsis* heeft een duidelijke hyponastische response wanneer het overstromd of overgroeid raakt. In tegenstelling tot *Rumex* is er tijdens overstroming geen strekkingsgroei van de petiolen waarneembaar in *Arabidopsis*.

In **Hoofdstuk 1** van dit proefschrift worden als inleiding de belangrijkste resultaten van eerder onderzoek naar hyponastische groei samengevat. In het bijzonder wordt besproken dat het gasvormig hormoon ethyleen belangrijk is voor inductie van hyponastie in *Arabidopsis* (en andere soorten). Ethyleen wordt continue geproduceerd in de planten. Wanneer deze overstromd raken, accumuleert dit hormoon in de plant en wordt hyponastie geïnduceerd.

Voor het onderzoek maken we gebruik van time-lapse fotografie. Hierdoor is het mogelijk om in groot detail de bladbeweging in de tijd te volgen (kinetiek) van planten die verschillende experimentele behandelingen ondergaan, bijvoorbeeld het toedienen van ethyleen of het beschaduen van planten. Afhankelijk van de specifieke omstandigheden neemt ook de zuurstof concentratie af in overstromde planten. Wij laten zien in Hoofdstuk 1 dat bij een lage zuurstofspanning de hyponastische response tijdens ethyleen behandeling groter is.

Hyponastie is een fysiek proces waarbij slechts een klein deel van de bladsteel betrokken is. In *Rumex* strekken slechts een paar cellen aan de onderkant (abaxiale zijde), dicht bij het begin van de bladsteel (basaal), terwijl alle andere cellen niet reageren. De kracht die hierdoor wordt gegenereerd leidt tot hyponastie. Dit proces heet differentiële groei. Wij laten zien dat analoog aan *Rumex*, ook in *Arabidopsis* hyponastie wordt bewerkstelligd door celstrekking en niet door bijvoorbeeld weefselspecifieke verschillen in het aantal celdeling.

Zoals eerder genoemd, induceert schaduw een vrijwel identieke hyponastische reactie als overstroming of ethyleen begassing. **Hoofdstuk 2** beschrijft hoe een afname van de licht intensiteit wordt waargenomen door *Arabidopsis* en hoe dit signaal wordt vertaald in een differentiële groei respons. Uit de resultaten komt naar voren dat in het bijzonder een afname in de intensiteit van blauwe golflengtes fungeert als belangrijk signaal. Door gebruik te maken van mutanten die 'blind' zijn voor lichtsignalen, tonen wij aan dat de fotoreceptor eiwitten (licht sensoren) Cryptochroom 1 (Cry1), Cry2, Phytochroom A (PhyA) en PhyB nodig zijn voor een snelle en volledige inductie van hyponastische groei. Omdat hyponastie, geïnduceerd door ethyleen en laag licht, zo sterk op elkaar lijkt is het mogelijk dat ethyleen ook een signaal molecuul is in de respons op laag licht. Ethyleen ongevoelige mutanten hebben echter een normale reactie op laag licht en planten die in laag licht staan

produceren niet meer ethyleen. Tevens zijn er geen verschillen waargenomen in de genexpressie van genen die betrokken zijn bij de productie van ethyleen en van genen die ethyleen gevoelig zijn. Daarom concluderen we dat ethyleen niet betrokken is bij de hyponastische respons geïnduceerd door verminderd licht intensiteit.

Een ander hormoon; Auxine dat vaak betrokken is bij differentiële groei processen blijkt zoals verwacht ook betrokken te zijn bij de hyponastische groei response op laag licht, maar verrassend genoeg niet bij ethyleen geïnduceerde hyponastie. Resumerend betekent dit, dat hyponastie geïnduceerd door ethyleen deels anders gereguleerd wordt dan de respons op laag licht. Maar, omdat de kinetiek vrijwel gelijk is, denken we dat een aantal functionele factoren onderdeel zijn van een gezamenlijke signaal transductie route.

In **Hoofdstuk 3** beschrijven we dat naast overstroming (ethyleen) en schaduw, ook een toename van de omgevingstemperatuur een hyponastische groei respons induceert, die qua kinetiek sterk overeenkomt met de respons op ethyleen en laag licht.

Arabidopsis thaliana komt voor op het hele Noordelijk halfrond en natuurlijke populaties zijn aangepast aan lokaal heersende omstandigheden. Deze aanpassingen zijn over het algemeen erfelijk en omdat er van honderden locaties zaden van 'accessies' beschikbaar zijn kan na het bestuderen van een respons (fenotyperen) in verschillende accessies een uitspraak gedaan worden of een eigenschap gevormd is door natuurlijke selectie. Omgekeerd, zijn er verschillende technieken beschikbaar waarmee op basis van het fenotype de onderliggende (veroorzakende) natuurlijke genetische variatie gevonden kan worden en zelfs een uitspraak gedaan kan worden welk gen een bepaalde respons beïnvloedt. Hoe we dit hebben toegepast om nieuwe genen te isoleren die betrokken zijn bij hyponastie wordt beschreven in Hoofdstuk 7. In Hoofdstuk 3 tonen we door analyse van natuurlijke variatie aan dat accessies die in hun natuurlijke omgeving sterke temperatuurswisselingen ondergaan nauwelijks hun bladeren bewegen, terwijl accessies uit meer gematigde locaties een sterke hyponastische respons induceren tijdens hitte behandeling. Dit suggereert dat er natuurlijke selectie op deze respons heeft plaatsgevonden en impliceert dat analoog aan overstroming en schaduw geïnduceerde hyponastie, de respons op hitte als ontsnappingsreactie fungeert, waarschijnlijk om de hitte instraling door de zon te reguleren.

Ook in dit hoofdstuk is naar de regulatie van deze respons gekeken, wederom met mutanten gestoord in verschillende processen, maar ook door gebruik te maken van chemische substanties die deze processen blokkeren dan wel stimuleren. Hieruit bleek dat analoog aan laag licht geïnduceerde groei ook bij hitte geïnduceerde hyponastie ethyleen niet direct betrokken is bij de inductie van de respons. Het is opmerkelijk te constateren dat ethyleen zelfs als remmer (antagonist) werkt. Laag licht werkt additief op hitte geïnduceerde groei en *phyB* mutanten reageren veel sterker op hitte. Analoog aan laag licht, is ook auxine een positieve regulator van hitte geïnduceerde hyponastische groei. Deze resultaten ondersteunen dat hyponastie geïnduceerd door verschillende omgevingssignalen via verschillende,

maar samenhangende routes verloopt.

Uit eerder werk is gebleken dat het plantenhormoon Abscisine zuur (ABA) antagonistisch werkt op ethyleen- en overstroming geïnduceerde groei reacties in zowel *Rumex* als *Arabidopsis*. In hitte geïnduceerde hyponastische groei, maar ook zoals beschreven in **Hoofdstuk 4**, in laag licht geïnduceerde hyponastie is ABA een positieve regulator. Gen expressie analyse suggereerde dat een geassocieerd eiwit (GPA1) van een beschreven ABA receptor; GCR2, wordt gereguleerd door laag licht en ethyleen. Wij hebben aangetoond dat zowel *gpa1* als *gcr2* mutanten een verminderde hyponastische groei vertonen op deze signalen.

Om nieuwe genetische factoren te isoleren die betrokken zijn bij een proces zoals hyponastische groei, is het mogelijk om op grote schaal mutanten te 'analyseren'. Wij hebben gebruik gemaakt van een populatie van planten waarin met behulp van een bacterie op willekeurig plekken in het genoom stukken gemodificeerd DNA (T-DNA) zijn gezet. In dit T-DNA zitten promotoren (regulerend DNA) die genen tot overexpressie brengen. Op de plek waar het T-DNA terecht is gekomen zullen de omliggende genen sterk tot expressie komen. Als dit gen betrokken is bij de controle van een respons, bijvoorbeeld hyponastie, kan de veranderde expressie leiden tot een veranderd (respons) fenotype. Alternatief, als door toeval het T-DNA in een gen is terecht gekomen dan zal het gen niet meer functioneel zijn en is er sprake van een mutant, wat ook tot een (ander) fenotype kan leiden.

Omdat de T-DNAs op willekeurig plaatsen in het genoom terecht komen is het mogelijk om bij benadering het effect van elk gen te bekijken, als er maar genoeg planten worden geanalyseerd. In **Hoofdstuk 5** staat beschreven dat wij 17,500 individuele planten hebben bekeken en hebben gezocht naar planten met een duidelijk andere bladstand zonder behandeling en naar planten met een versterkte, of juist verminderde hyponastische response tijdens ethyleen- en laag licht behandeling. Er zijn 18 lijnen geïdentificeerd die daarna verder zijn gekarakteriseerd.

Een nadeel van een mutantscreen is dat het niet onmiddellijk duidelijk is welk gen dit effect veroorzaakt. Daarvoor moet het gen eerst gekloneerd worden. In **Hoofdstuk 6** beschrijven we de isolatie van het causale gen van één van de geïsoleerde lijnen, *SEE1-1D* genaamd. Deze lijn was in het bijzonder interessant omdat in aanwezigheid ethyleen, laag licht of hitte deze lijn veel sterker reageerde. Na klonering en analyse werd duidelijk dat overexpressie van *CYCLINE-A2;1* (*CYCA2;1*) de versterkte hyponastie van *SEE1-1D* verklaard. Dit is opmerkelijk omdat A2-type CYCLINES tot nu toe alleen beschreven zijn als regulatoren van de celdeling, terwijl hyponastische groei nu juist wordt veroorzaakt door uitsluitend celstrekking. *CYCA2;1* komt in de hele bladsteel tot expressie. Tijdens ethyleen, maar ook ABA behandeling, wordt de expressie van *CYCA2;1* specifiek in de delen van de petiool die niet betrokken zijn bij hyponastie (distaal) geremd. De expressie blijft gehandhaafd in de weefsels die fysiek betrokken zijn bij hyponastie (basaal). We vermoeden daarom dat *CYCA2;1* en de geassocieerde eiwitten groei stimuleren, en dat door de onderdrukking van de expressie van *CYCA2;1* in distale delen van de bladsteel en handhaving van expressie

in basale delen, de hyponastische groei wordt verklaard. Hoe A2-type Cyclines hyponastie mechanistisch controleren is nog niet duidelijk. Omdat overexpressie van CYCA2;1 een versterkte response op alle drie de behandelingen (ethyleen, laag licht en hitte) induceert, concluderen we dat A2-type Cyclines, of geassocieerde eiwitten, mogelijk als moleculaire integratoren dienen van deze signalen richting hyponastische groei.

In **Hoofdstuk 7** analyseren we de natuurlijke variatie in hyponastische groei tussen *Arabidopsis thaliana* accessies, om meer inzicht te krijgen in de respons en om nieuwe regulerende genen te isoleren. Daarvoor hebben we 138 natuurlijke accessies gefenotypeerd op geïnduceerde hyponastie. Er blijkt een continuüm te zijn in de mate van hyponastie en sommige accessies hebben zelfs een epinastische response (neerwaartse bladbeweging) tijdens ethyleen behandeling. Ook is gebleken dat planten die relatief sterk reageren op één van de signalen, over het algemeen ook vaak bovengemiddeld sterk reageren op de andere signalen. Dit is een aanwijzing dat signaal transductie routes van de verschillende omgevingsstimuli richting hyponastische groei genetisch gekoppeld zijn.

Vervolgens hebben we een Quantitative Trait Loci (QTL) analyse uitgevoerd. Dit is een kwantitatief genetische techniek waarbij fenotypische eigenschappen aan moleculaire markers (ankerpunten) op het genoom worden geassocieerd. Op basis van statistiek kunnen dan stukken genoom (loci) worden aangewezen waar naar waarschijnlijkheid een factor(en) liggen die het fenotype controleren (de zogenaamde QTLs). Eén van deze QTLs werd gevonden op het *Erecta* locus, dat vaker naar voren komt in QTL analyse van omgeving- en groei gerelateerde fenotypes. Ook is het bekend dat een mutant voor het *erecta* gen een zeer beperkte hyponastische groei response vertoont tijdens ethyleen behandeling. Daarom hebben we *erecta* verder bestudeerd. Verschillende lijnen van bewijs tonen aan dat dit gen een positieve regulator is van hyponastische groei en dat dit hoogstwaarschijnlijk een algemene regulator van de respons is omdat *ERECTA* de laag licht response beïnvloedt en niet direct de ethyleen productie of gevoeligheid verandert.

Hoofdstuk 8 & 9 beschrijven een separate studie naar de rol van licht in de regulatie van de fysieke compactheid van DNA. Al het dubbelstrengs DNA, dat het genoom vertegenwoordigt, zit met zijn geassocieerde eiwitten (samen chromatine genaamd) in de celkern. Het chromatine is op een ordelijke manier georganiseerd en bestaat uit actieve- (veel genexpressie) en inactieve- en/of genarme gebieden. Deze domeinen worden respectievelijk euchromatine en heterochromatine genoemd. Met een specifieke kleuring kunnen deze gebieden gevisualiseerd worden in geïsoleerde kernen. *Arabidopsis* heeft een relatief simpele kernorganisatie waarin heterochromatische domeinen (de zogenaamde chromocenters) aan de periferie van de kern liggen van waaruit genrijke euchromatische gebieden als 'lussen' ontspringen.

Wij hebben gekeken naar natuurlijke variatie in licht gereguleerde chromatine compactie (de mate van voorkomen van chromocenters). Hieruit kwam naar voren

dat er grote verschillen bestaan tussen accessies. Zo heeft de tropische accessie Cape Verde Islands-0 (Cvi-0) nauwelijks chromocenters, dit in tegenstelling tot accessies uit meer noordelijke delen van de wereld. Uit een statistische analyse bleek dat de aanpassing aan de lokale lichtintensiteit op de verzamelplaatsen van de accessies in belangrijke mate bijdraagt aan de variatie in chromatine compactie. In overeenstemming hiermee leidt een verhoging van de lichtintensiteit tot een verhoogde chromatine compactie in Cvi-0 en omgekeerd leidt een (langdurige) behandeling met laag licht (90% reductie) tot een omkeerbare afname van chromatine compactie in verscheidene accessies, inclusief Cvi-0.

Niet alleen spectraal neutraal laag licht maar ook een verlaagde ratio tussen rood en ver-rood golflengtes induceren chromatine decompactie. Vooral dit laatste signaal is specifiek voor overschaduwning door buurplanten. Daarom concluderen we dat licht gecontroleerde chromatine (de)compactie waarschijnlijk een biologisch relevante respons is voor *Arabidopsis*; de exacte betekenis is echter nog niet duidelijk. Het is aannemelijk dat dit proces niet betrokken is bij differentiële groei zoals hyponastie, omdat dit een veel snellere response is dan laag licht-geïnduceerde chromatine decompactie.

Uit een QTL analyse kwamen drie loci naar voren die een groot deel van de genetische variatie in chromatine compactie tussen Cvi-0 en een Poolse accessie; Landsberg *erecta*, verklaren. Nadere analyses hebben aangetoond dat gensequentie (allelische) verschillen in de fotoreceptor phytochrome B en in het chromatine remodeling-gen; Histon Deacetylase 6 (HDA6) deze QTLs kunnen verklaren. Met behulp van mutanten hebben wij kunnen aantonen dat Phytochrome B belangrijk is voor de laag licht-geïnduceerde chromatine decompactie. Ook het eiwit niveau van Cryptochrome 2 (Cry2) lijkt een belangrijke rol te spelen. Zo zijn Cry2 mutanten veel minder in staat tot licht-geïnduceerde chromatine decompactie en planten die Cry2 tot overexpressie brengen juist beter. Cry2 wordt onder normale omstandigheden snel afgebroken in het licht. Met behulp van eiwitanalyse tonen wij aan dat laag licht de Cry2 eiwitniveaus stabiliseert. In *phyB* mutanten is veel minder Cry2 eiwit aanwezig, wat impliceert dat de rol van PhyB in lichtgeïnduceerde chromatine decompactie verklaard kan worden door een effect van PhyB op de Cry2 eiwit niveaus.

In **Hoofdstuk 10** worden de resultaten van de 9 voorgaande hoofdstukken bediscuseerd. In dit hoofdstuk wordt vooral aandacht besteedt hoe de verschillende omgevingssignalen die hyponastie induceren en de onderliggende processen kunnen worden samengevat in een allesomvattend netwerk of model dat hyponastische groei beschrijft. Het is duidelijk uit het voorgaande dat verschillende hormonale signalen zoals ethyleen, ABA en auxine, maar ook verschillende licht signaleringscomponenten vaak een contrasterend effect hebben. Dit betekent dat hoogstwaarschijnlijk op zijn minst een deel van de signaleringsroutes parallel verlopen. Mede daardoor bleek het niet mogelijk een allesomvattend model op te stellen dat beschrijft hoe hyponastie wordt gereguleerd. Maar, omdat de kinetiek van de hyponastische respons geïnduceerd door de verschillende signalen zeer vergelijkbaar is concluderen we dat minimaal een aantal cruciale regulerende componenten onderdeel zijn van

alle drie de signalering routes. Met andere woorden, de signalen convergeren op factoren die hyponastie reguleren. Deze conclusie wordt ondersteund door onder andere de waarneming dat A2-type Cyclines een vergelijkbaar effect op hyponastie hebben in reactie op alle drie de inducerende factoren, en mogelijk geldt hetzelfde voor ERECTA. Niet in de laatste plaats zijn er nog een aantal mutanten opgepikt in de mutantscreen die een identiek effect hebben op de hyponastische respons in reactie op alle drie de omgevingssignalen. Als laatste stellen we een aantal mogelijke methodes en aanknopingspunten voor vervolg onderzoek voor.

Publications

1. Millenaar FF, Okyere J, May ST, **Van Zanten M**, Voeselek LA, Peeters AJM. (2006). How to decide? Different methods of calculating gene expression from short oligonucleotide array data will give different results. **BMC Bioinformatics**, 15(7): 137.
2. Benschop JJ, Millenaar FF, Smeets ME, **Van Zanten M**, Voeselek LACJ, Peeters AJM. (2007). Abscisic Acid antagonizes ethylene-induced hyponastic growth in *Arabidopsis*. **Plant Physiology**, 143(2): 1013-23.
3. **Van Zanten M**, Snoek LB, Proveniers MCG, Peeters AJM. (2009). The many functions of ERECTA. **Trends in plant science**, 14(4): 214-218.
4. Millenaar FF*, **Van Zanten M***, Cox MCH, Pierik R, Voeselek LACJ, Peeters AJM. (2009). Differential petiole growth in *Arabidopsis thaliana*: Photocontrol and hormonal regulation. **New Phytologist**, 184: 141-152.
5. **Van Zanten M**, Millenaar FF Cox MCH, Pierik R, Voeselek LACJ, Peeters AJM. (2009). Auxin perception and polar auxin transport are not always a prerequisite for differential growth. **Plant Signaling & Behavior**, 4 (9).
6. Tessadori F*, **Van Zanten M***, Pavlova P, Clifton R, Pontvianne F, Snoek LB, Millenaar FF, Schulkes R-K, Van Driel R, Voeselek LACJ, Spillane C, Pikaard CS, Fransz P, Peeters AJM. (2009). PHYTOCHROME B and HISTONE DEACETYLASE 6 control light-induced chromatin compaction in *Arabidopsis thaliana*. **PLoS Genetics**, 5 (9): e1000638
7. **Van Zanten M**, Voeselek LACJ, Peeters AJM, Millenaar FF. (2009). Hormone- and light-mediated regulation of heat-induced differential petiole growth in *Arabidopsis thaliana*. **Plant Physiology**, Online September 9, 2009; 10.1104/pp.109.144386.
8. **Van Zanten M**, Snoek LB, van Eck-Stouten E, Proveniers MCG, Torii KU, Voeselek LACJ, Peeters AJM, Millenaar FF. Ethylene-induced hyponastic growth in *Arabidopsis thaliana* is controlled by ERECTA. **The Plant Journal**, Provisionally accepted.
- Ritsema T*, **van Zanten M***, Leon-Reyes A, Voeselek LACJ, Millenaar FF, Pieterse CMJ, Peeters AJM. Kinome profiling of pathogen defense signals reveals a role for jasmonate and salicylate in light control of hyponastic petiole growth in *Arabidopsis thaliana*. *New Phytologist*. encouraged for resubmission.

* Authors who contributed equally to the work

Curriculum Vitae

Martijn van Zanten was born on June 10, 1979 in Utrecht, the Netherlands. In 1997 he received his Hoger Algemeen Voortgezet Onderwijs (HAVO) diploma at the St. Gregorius College in Utrecht and started in the same year with the study Medical Biotechnology/Molecular Biology at the Utrecht School for professional education (Hogeschool van Utrecht). During this study he did an internship in the Molecular Plant Physiology group at Utrecht University with Dr. M.C.G. Proveniers and Prof. J.C.M. Smeeckens, where he worked on the isolation of genes involved in the biosynthesis of the phytohormone gibberellin in tobacco. After his graduation in 2001 he stayed in this group for a few months to work as technician on the European REGIA (Regulatory Genes Initiative in Arabidopsis) project, with Dr. M. Denekamp. In 2002 he started to study Biology at Utrecht University and performed a research project at the Plant Ecophysiology group with Dr. F.F. Millenaar, Dr. A.J.M. Peeters and Prof. L.A.C.J. Voesenek, where he worked on a project to evaluate and compare different methods for micro-array analysis, and worked on the isolation and characterization of genes involved in the *Arabidopsis thaliana* hyponastic growth response. During this internship, he started to collaborate with Dr. P.F. Fransz and Dr. F. Tessadori of the Nuclear Organization Group at the University of Amsterdam, the Netherlands, to study light control of chromatin compaction. After his graduation in 2004, he was appointed as a PhD student at the Plant Ecophysiology group to continue the study on the molecular physiological and molecular genetic regulation of hyponastic growth. Besides, he continued the collaboration with the UVA. The results of both projects are presented in this thesis. After his graduation he will work as a post-doc at the Max-Planck-Institut für Züchtungsforschung (Plant Breeding) in Cologne, Germany, with Dr. W.J.J. Soppe and Prof. M. Koornneef, to study seed dormancy using cytogenetic approaches.

Color Supplement

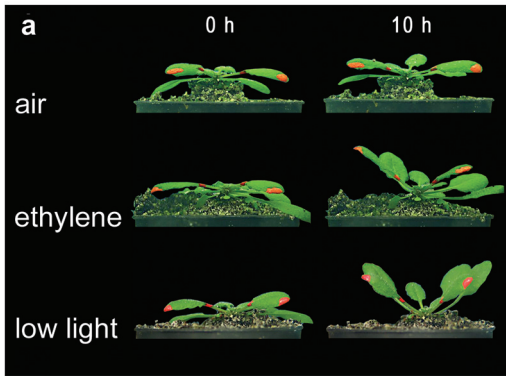


Figure 1.1: Typical hyponastic growth phenotype in *Arabidopsis thaliana* Col-0.

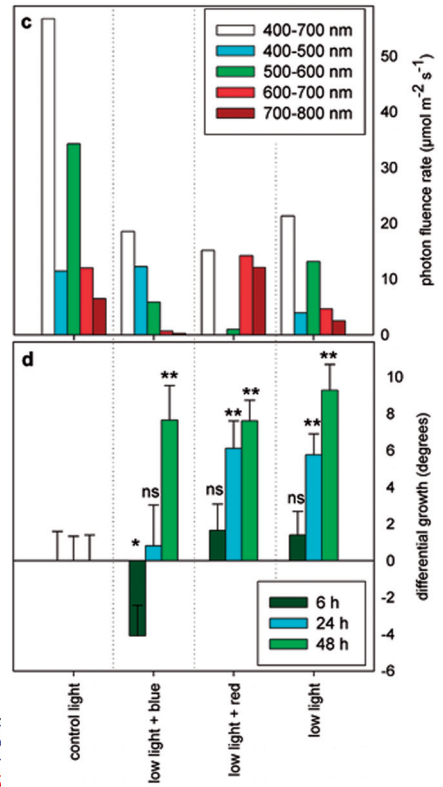


Figure 2.1: Characterization of hyponastic growth upon low light exposure.

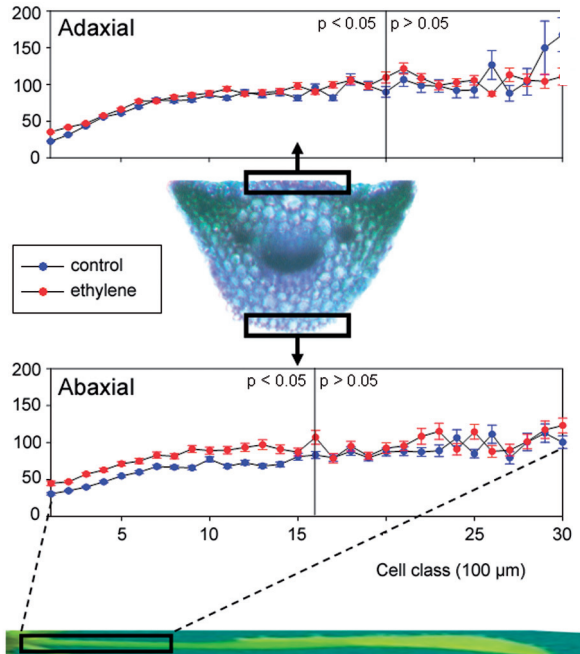


Figure 1.2: Hyponastic growth depends on cell elongation.

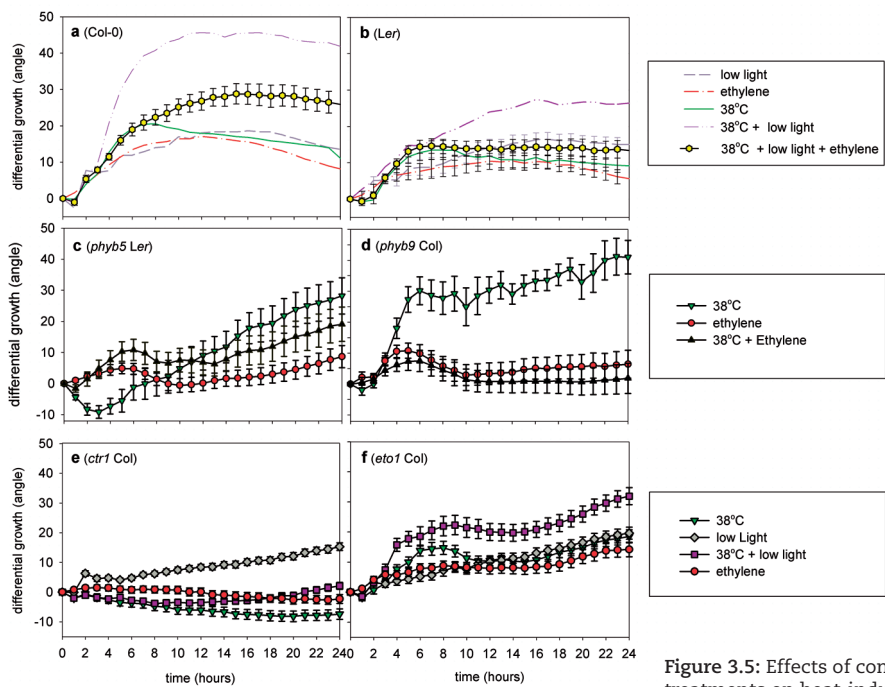


Figure 3.5: Effects of combined treatments on heat-induced hyponastic growth.



Figure 5.6: Morphology of candidate lines with a visual phenotype.

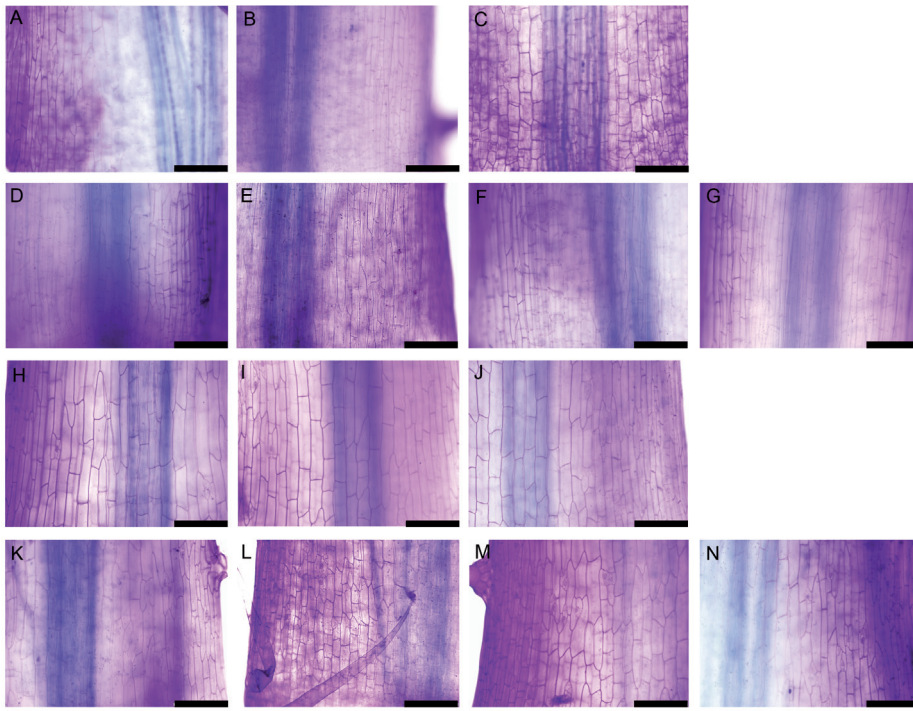


Figure 6.8: Epidermal cell size-analysis of lines misexpressing A2-type Cyclins.

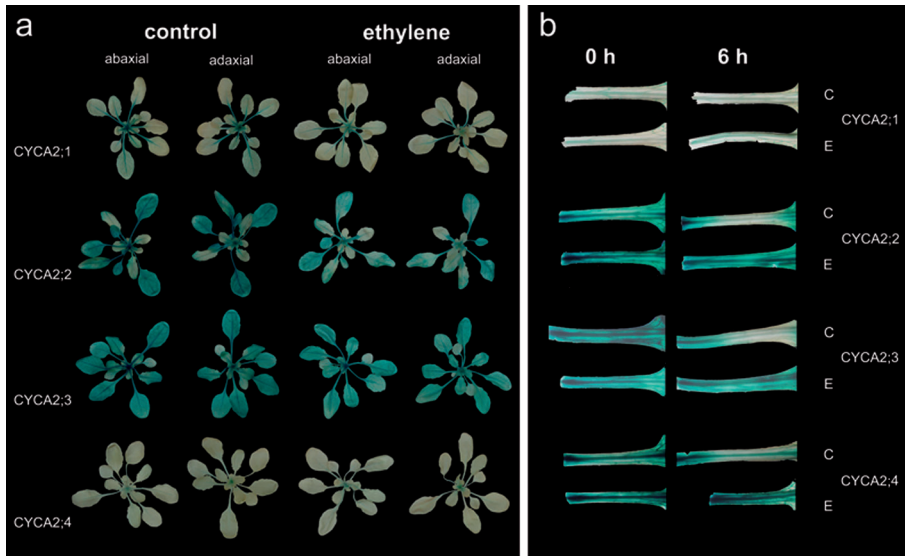


Figure 6.11: Histochemical analysis of A2-type Cyclin promoter activity.

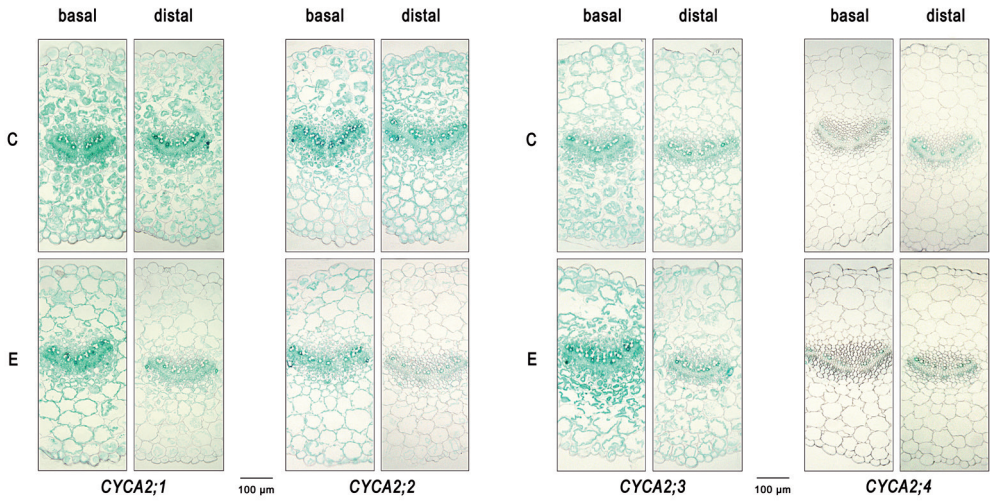


Figure 6.12: Histochemical analysis of A2-type Cyclin promoter activity in petioles.

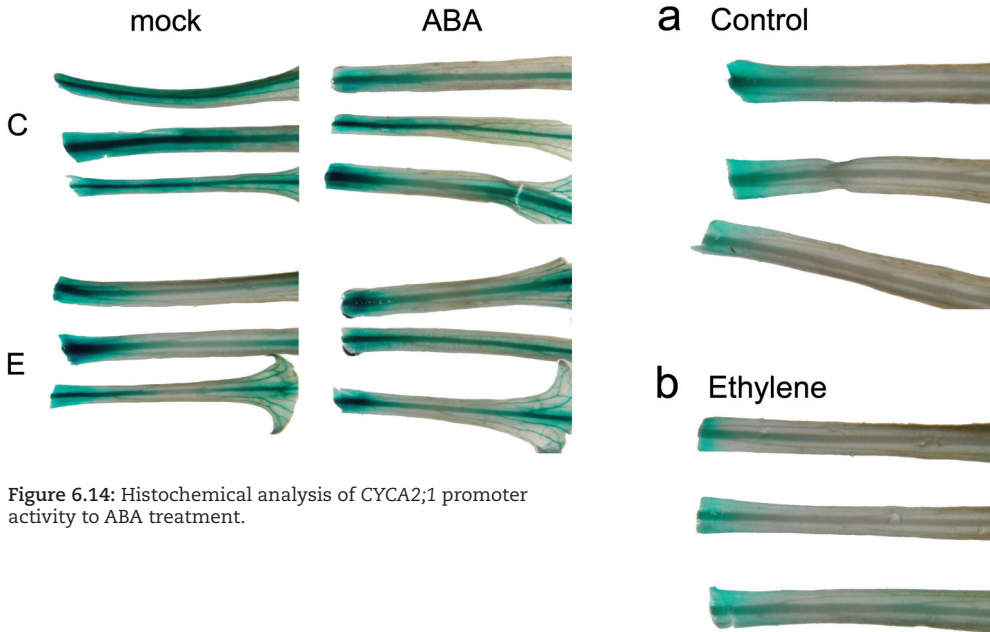


Figure 6.14: Histochemical analysis of CYCA2;1 promoter activity to ABA treatment.

Figure S6.4: Histochemical analysis of CyclinB1;1 promoter activity.

Figure S6.5: Spatial localization of A2-type Cyclins in petioles.

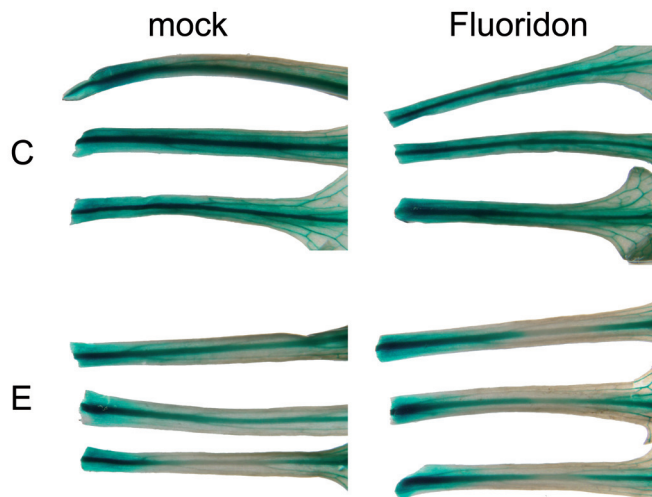
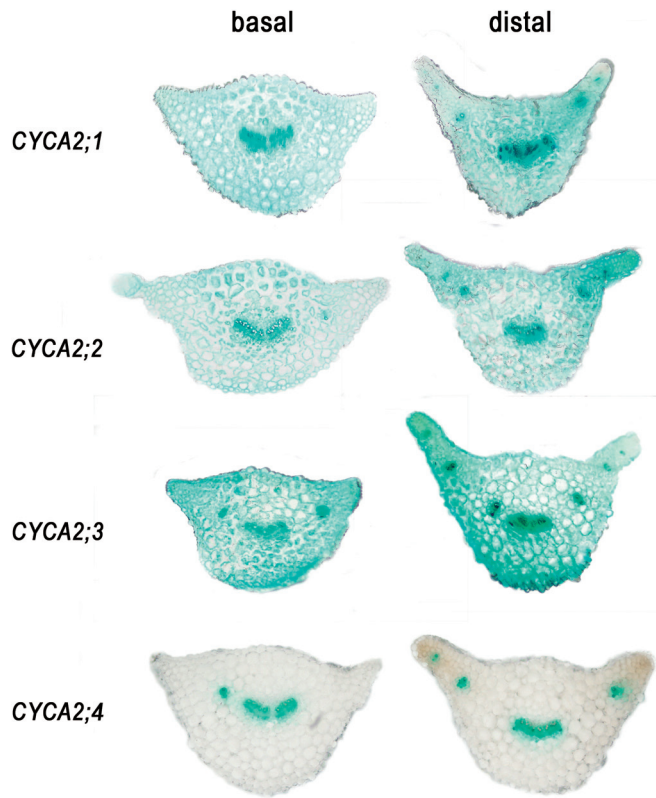


Figure S6.6: Histochemical analysis of CYCA2;1 promoter activity to fluoridon treatment.

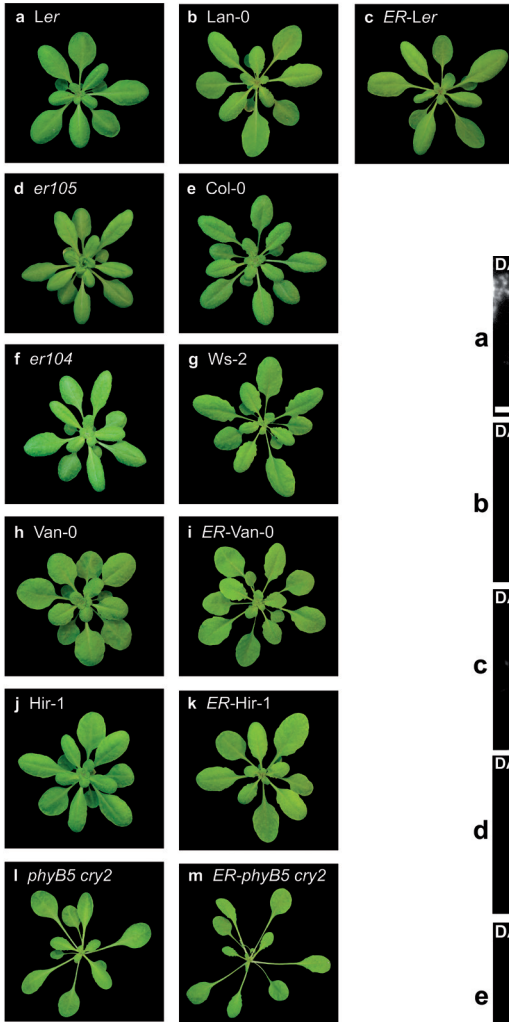


Figure 7.9: Effect of ER on rosette morphology of *Arabidopsis thaliana*.

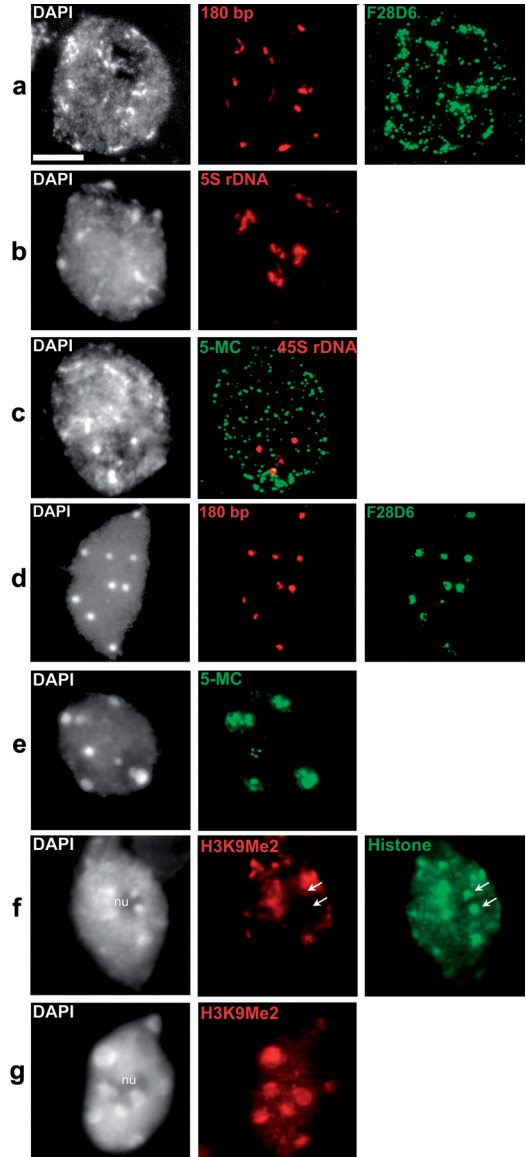


Figure 8.3: Cytogenetic characterization of Cvi-0.

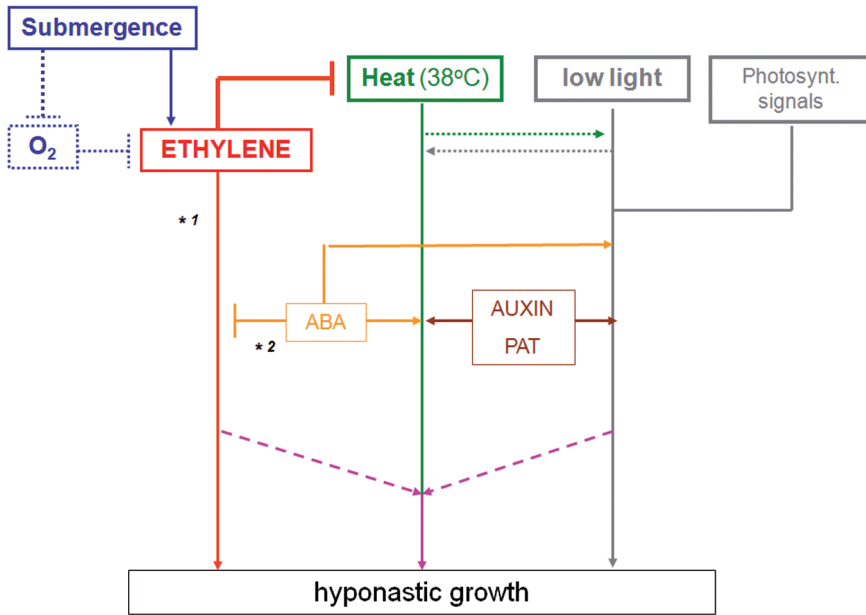


Figure 10.3: Proposed simplified signaling network of ethylene, heat and low light-induced hyponastic petiole growth as described in this thesis.

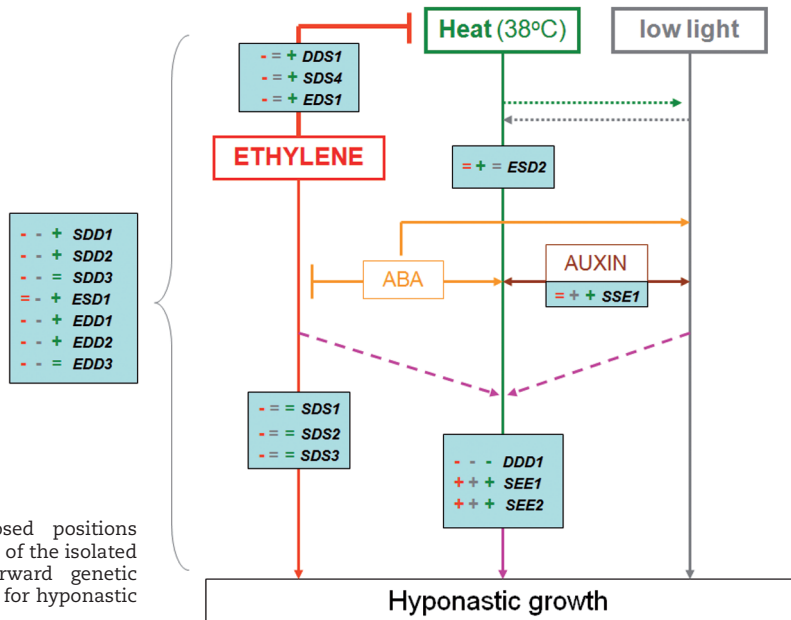


Figure 10.4: Proposed positions where causal factors of the isolated lines from the forward genetic screen fit the model for hyponastic growth.